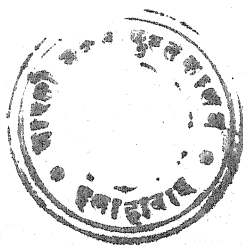# THEORY OF STRUCTURES

THEORY OF

STRUCTURES

BY

S. TIMOSHENKO

Professor of Theoretical and Applied Mechanics
Stanford University

AND

D. H. YOUNG

Associate Professor of Civil Engineering
Stanford University

FIRST EDITION
FIFTH IMPRESSION

THEORY OF STRUCTURES

COPYRIGHT, 1945, BY THE
McGRAW-HILL BOOK COMPANY, INC.

PRINTED IN THE UNITED STATES OF AMERICA

PREFACE

In the preparation of this book, the authors have tried to keep in view the fact that "Theory of Structures" is based on mechanics with which the student is already familiar. Every effort has been made to show him that the methods of analysis used in "Theory of Structures" are only a further development of the general principles of mechanics that he already knows. It is believed that this establishment of a close connection between the teaching of mechanics and structures can be most helpful to the student in understanding the various practical methods of analysis of trusses and frames. In fact, such a complete understanding is necessary for a successful application and adaptation of theoretical knowledge to the solution of various practical problems.

With the above point of view, the first chapter was prepared as an introduction to the "Theory of Structures," in which the basic principles of statics are recapitulated. At the same time the examples of this chapter are chosen to illustrate the adaptation of these principles to the solution of practical problems in the analysis of simple structures.

The second chapter is devoted to the analysis of statically determinate trusses in one plane. Here the generally accepted methods of analysis of plane trusses are discussed in full detail and their application illustrated by examples. The final articles of this chapter develop the general theory of plane trusses and establish the conditions under which a truss can be statically determinate and geometrically rigid. Rapidly developing industry continually brings to the structural engineer new forms of trusses, and it is considered important to give to the younger generation of engineers a broader understanding of the basic properties and functions of truss systems.

The third chapter deals with influence lines. Beginners usually find some difficulty with this subject, and to meet their needs considerable space is given to the discussion of influence lines for beams before the question of influence lines for trusses is taken up. In this connection many examples of both simple and compound beams are discussed in full detail. Here, the fundamental statical principle of virtual displacements can be used to advantage, and several applications of this principle are demonstrated by practical examples. After the discussions of influence lines for beams, the more complex influence diagrams for various trusses can be followed with little difficulty.

The fourth chapter is devoted to the question of formation and analysis of space trusses with hinged joints. Practicing engineers frequently reduce such problems to the analysis of plane trusses, but this is not always possible and it is considered desirable to discuss the general theory of space trusses in some detail. Several general methods of attack for complex space trusses are discussed in the later articles of this chapter, together with completely worked-out examples.

The fifth chapter, like the first, is a recapitulation of general principles of mechanics, in this case preparatory to the analysis of statically indeterminate structures. Here the development of the expressions for strain energy is followed by the establishment of such broad general principles as the principle of least work, the principle of superposition, Castigliano's theorem, and Maxwell's reciprocal theorem. The aim of this chapter is to give a general discussion of principles, together with elementary applications, before methods of analysis of complicated statically indeterminate systems are discussed.

The sixth chapter deals with methods of calculating deflections of trusses. Here will be found developments and applications of the Castigliano and Maxwell-Mohr methods and of the Williot diagram. Methods of fictitious loading are discussed at the end of this chapter.

In the seventh chapter the theory of statically indeterminate trusses is presented. Various methods of computing redundant reactions and forces in redundant members of such trusses are given in detail, together with examples of their application. The construction of influence diagrams for statically indeterminate trusses is also considered at the end of this chapter.

The eighth chapter takes up the question of bending of beams and frames. This chapter begins with a development of the slope-deflection equations for prismatic beams and discusses the application of these equations to the analysis of statically indeterminate beams and continuous beams on many supports. Still further application of these equations is shown in the analysis of frames. Frames both with and without lateral restraint are considered, and it is shown in each case how the equations for computing redundant end moments can be written. Further discussion considers the solution of these equations by methods of successive approximation and illustrates the application of this method of analysis to multiple-story frames. The adaptation of the method of successive approximations to the calculation of secondary stresses in trusses is also presented. The chapter is concluded with a discussion of beams of variable cross section, the corresponding slope-deflection equations being developed and applied to the analysis of continuous beams and frames containing members of variable cross section.

The last chapter contains a treatment of the theory of arches. First, for various shapes of the arch, there is a discussion of the accuracy of the usual arch theory in which the effects of shearing forces and curvature of the arch on deflections are neglected. Thereafter considerable space is given to a discussion of symmetrical arches, the center lines of which coincide with the funicular curves for dead load. In conclusion, non-symmetrical arches and rings are considered.

To facilitate reading of the book by the beginner, two sizes of type have been used. Material printed in small type can be omitted in a first reading. A sufficient number of unsolved examples is included to furnish the student with ample exercise in the solution of problems. Some of these problems are with answers, some without.

In the preparation of this book the senior author's earlier Russian book ("Theory of Structures," by S. Timoshenko, 2d ed., St. Petersburg, 1926) was extensively used. Acknowledgment is also due to Otto Mohr's "Abhandlugen aus dem Gebiete der technischen Mechanik" and H. Müller-Breslau's, "Die graphische Statik der Baukonstruktionen."

In conclusion the authors take this opportunity to express their thanks to Mrs. Evelyn Sarson for her care in typing the manuscript.

<div align="right">

S. Timoshenko,
D. H. Young.

</div>

CONTENTS

CHAPTER IX

NOTATIONS

A cross-sectional area of a member

a, b, c dimensions of a structure

a_1, a_2, a_3 numerical coefficients

B flexural rigidity of a member

C torsional rigidity of a member, constant of integration

d depth, panel distance, elastic center coordinate

E modulus of elasticity in tension or compression

e eccentricity

F force

f sag of a chain, rise of an arch

G modulus of elasticity in shear

H pole distance, horizontal thrust of an arch

h height, moment arm of a force

I moment of inertia

i radius of gyration, general subscript

j number of joints in a structure

k core radius, stiffness factor for a member

l length of a member, span of a beam

m number of members in a structure

M moment of a force, bending moment, end moment

$\mathfrak{M}$ fixed-end moment

$\mathbf{M}$ unbalanced moment at a joint

n any number

N normal force or thrust on a section

o a pole point

O origin of coordinates

p intensity of pressure

P external load

q intensity of distributed load

Q external load

r radius, distribution factor

R reaction

s length of an arc

s_i', s_i'', s_i''' influence numbers for a truss member

S_i axial force in a member

$\mathcal{S}_i$ axial force as for a simple truss

t	temperature change
T	torque or twisting moment
u	strain energy per unit volume
w	intensity of distributed load
u, v, w	displacements corresponding to x, y, z
U	strain energy
U_1	complementary energy
V	shearing force on a section
W	external load, weight
x, y, z	orthogonal coordinates
X, Y, Z	orthogonal projections of a force, redundant quantities
Z	section modulus
y_1, y_2, y_3	influence coefficients
α	coefficient of thermal expansion, shear factor
γ	shearing strain
α, β, γ	angles
$\delta x, \delta y, \delta z$	virtual displacements
Δ	change in length of a member
Δl_i	change in length of a member
$\Delta U, \Delta V, \Delta\Theta$	increments of any quantity
ϵ	unit axial strain
θ	slope at the end of a member
θ, ϕ, ψ	angles
Θ	rotation of a member
λ	haunch-span ratio for beam of variable cross section
ξ, η, ζ	displacements corresponding to x, y, z
ρ	extensibility factor for a member
σ	intensity of normal stress on a section
τ	intensity of shearing stress on a section
φ	haunch factor for a beam of variable cross section
$\overline{OA}, \overline{AB}$, etc.	vector quantities
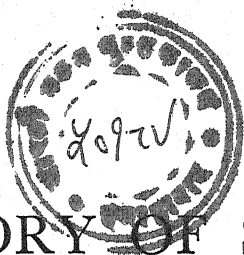
THEORY OF STRUCTURES

CHAPTER I

ELEMENTS OF PLANE STATICS

1. Concurrent Forces in a Plane.—The *theory of structures* is based to a large extent upon the principles of statics with which the student is assumed to be familiar. However, we shall review here some parts of statics that are most useful in the analysis of engineering structures. We begin with the principle of the parallelogram of forces as follows: *Two forces P_1 and P_2, as represented by the vectors $\overline{OA}$ and $\overline{OB}$ in Fig. 1a, are equivalent in action to a single resultant force R obtained as the diagonal $\overline{OC}$ of the parallelogram formed on the given vectors as shown.* The same

Fig. 1.

resultant force can be obtained also from the *triangle of forces* shown in Fig. 1b. This follows from the fact that the triangle ABC in Fig. 1b is identical with the triangle OAC in Fig. 1a.
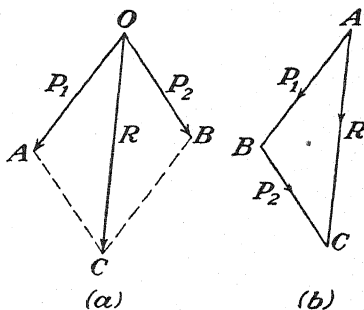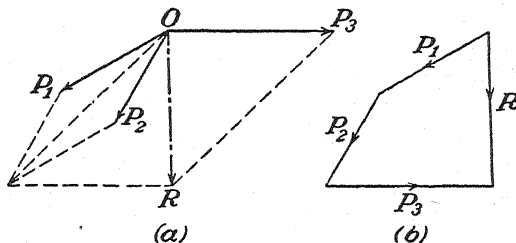
Fig. 2.

If several forces in a plane act at a single point O (Fig. 2a), they can always be reduced to one resultant force which also acts through that point. This resultant force can be found by successive applications of the parallelogram of forces as illustrated in Fig. 2a or as the closing side of the *polygon of forces* constructed as shown in Fig. 2b.

1

If the polygon of forces is closed, the resultant force vanishes and the given forces are in *equilibrium*. Thus if several concurrent forces in a plane are known to be in equilibrium, their free vectors must build a *closed polygon of forces* as shown in Fig. 3.

The above graphical condition of equilibrium is very useful in the analysis of structures. Let us consider, for example, the very simple case of a weight W supported by strings as shown in Fig. 4a. Isolating the ring O as a *free body*, we conclude that it is in equilibrium under the
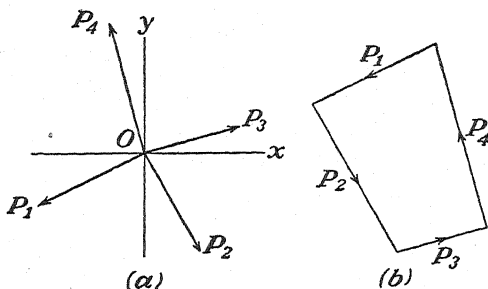
FIG. 3.
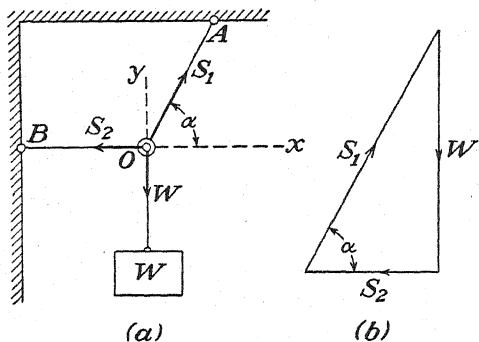
FIG. 4.

action of three forces W, S_1, and S_2 the lines of action of which coincide with the strings and the magnitudes of which represent the *axial forces*, or *tensions*, in these strings. If the magnitude of the weight W is known, the magnitudes of the tensions S_1 and S_2 are found from the closed triangle of forces as shown in Fig. 4b, from which we obtain $S_1 = W \csc \alpha$ and $S_2 = W \cot \alpha$.

From the fact that several concurrent, coplanar forces in equilibrium build a closed polygon (Fig. 3), it follows that the algebraic sums of *projections* of the forces on any system of orthogonal axes x and y in their plane of action must be zero. Thus we arrive at the familiar *equations of equilibrium*,

$$\Sigma X_i = 0, \qquad \Sigma Y_i = 0 \qquad (1)$$

where X_i and Y_i denote, respectively, the projections of any force P on the axes x and y and the summations are understood to include all forces in the system.   These analytical conditions of equilibrium are equivalent to the graphical condition of a closed polygon of forces, but they are sometimes more convenient to use.   Applying the equations of equilibrium to the system shown in Fig. 4a, for example, we obtain

$$S_1 \cos \alpha - S_2 = 0,$$
$$S_1 \sin \alpha - W = 0,$$

from which we find, as before, $S_1 = W \csc \alpha$ and $S_2 = W \cot \alpha$.

The foregoing graphical and analytical conditions of equilibrium are particularly useful in the analysis of pin-connected trusses.   Consider, for example, the truss loaded as shown in Fig. 5a.   The analysis of such a truss entails finding the axial forces induced in the various bars
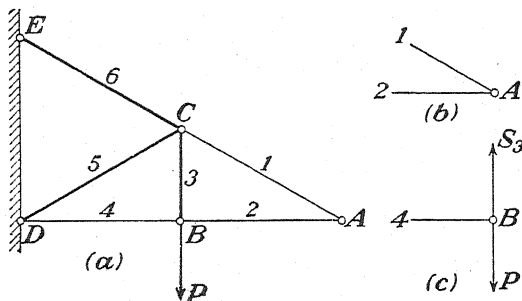
Fig. 5.

by the action of the external load P.   The work can be greatly simplified in this case by noting that some of the bars are inactive, *i.e.*, unstressed. For instance, if we isolate the hinge A as a free body (Fig. 5b), we see at once that the bars 1 and 2 of the truss are inactive, since two forces can be in equilibrium only if they are collinear in action and the axes of these two bars are not collinear.   Having concluded that the bar 2 is inactive, we consider the equilibrium of the hinge B (Fig. 5c), where we find the possibility of three forces in equilibrium, two of which are collinear in action.   Then from the first of Eqs. (1) it follows that the force in bar 4 must be zero, and we conclude that this bar also is inactive. Finally, then, only the bars shown in the figure by heavy lines carry axial forces different from zero.   Considering, further, the equilibrium of hinge B and using the second of Eqs. (1), we conclude that the bar 3 carries a tension equal to the load P.   The axial forces in the bars 5 and 6 can be found by considering the conditions of equilibrium for the hinge C, and this completes the analysis of the truss.

PROBLEMS

1. Find the tensile force S_1 in the member AC and the compressive force S_2 in the member AB of the simple truss shown in Fig. 6.

Ans. $S_1 = P \csc \alpha; \; S_2 = P \cot \alpha.$
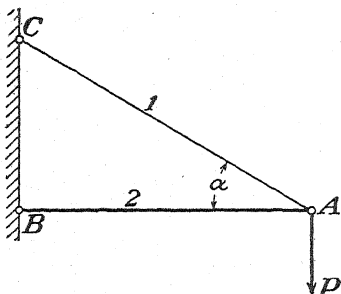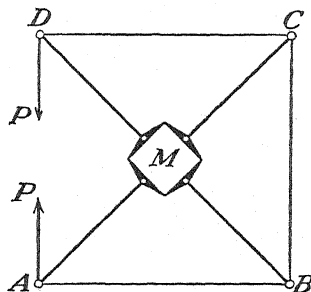
Fig. 6.   Fig. 7.

2. To produce biaxial compression of a concrete cube M, the system of hinged bars shown in Fig. 7 is used.   Find the compressive forces exerted on the faces of the cube if the frame has the form of a square and the inclined bars lie along its diagonals.

Ans. $S = \sqrt{2}\,P.$
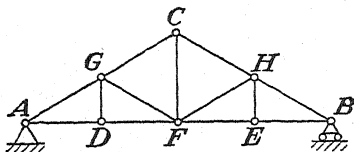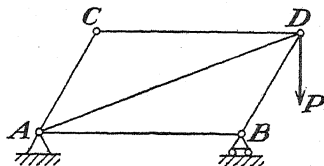
Fig. 8.   Fig. 9.

3. Identify, by inspection, the inactive members of the truss shown in Fig. 8, (a) when there is a vertical load P at F, (b) when the same load is at D.

4. How is the action of the simple truss shown in Fig. 9 affected by changing the direction of the diagonal from AD as shown to BC?

(a)

(b)
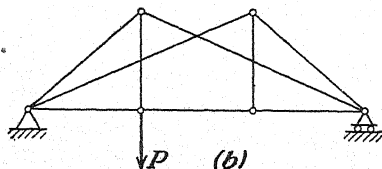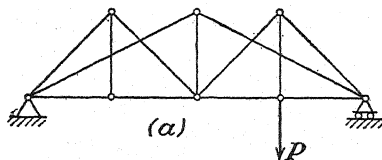
Fig. 10.

5. Distinguish by heavy lines the active members of the two trusses supported and loaded as shown in Fig. 10.

2. Three Forces in Equilibrium.—Three nonparallel forces in a plane can be in equilibrium only if their lines of action meet in one point.   To prove this statement, we refer to Fig. 11, where P and Q are any two forces that intersect at a point O.   Then a third force S can hold these two forces in equilibrium only if it is equal, opposite, and collinear with their resultant R, which, of course, acts through point O.   Hence, the force S also must act through point O as shown.
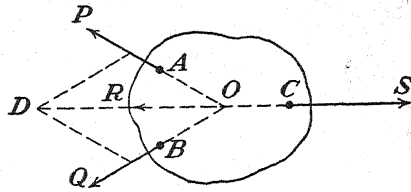
Fig. 11.

The foregoing *theorem of three forces* is very useful in the determination of the *reactions* induced at the points of support of a body or structure under the action of given forces.   Consider, for example, the crane shown in Fig. 12, the mast of which is supported in *bearings* at A and B so that the crane can be rotated around the vertical axis.   Under the action of a vertical load P, the crane exerts pressures on its bearings at A and B, and these *actions* of the crane on its supports induce equal and opposite *reactions* on the crane as shown.   Thus the vertical force P together with the reactions R_a and R_b are three forces in equilibrium.   Neglecting friction in the bearing at B, the reaction R_b must be a horizontal force, and hence the known lines of action of two of the forces (P and R_b) determine the point of concurrence O of the system.   The third force R_a, then, must also pass through point O; and so, by the theorem of three forces, its line of action AO is established.   Knowing the magnitude of the force P, the magnitudes of the reactions R_a and R_b are found from the closed triangle of forces shown in Fig. 12b.   Since this triangle is similar to triangle BAO in Fig. 12a, we obtain $R_a = \frac{5}{4}P$ and $R_b = \frac{3}{4}P$.
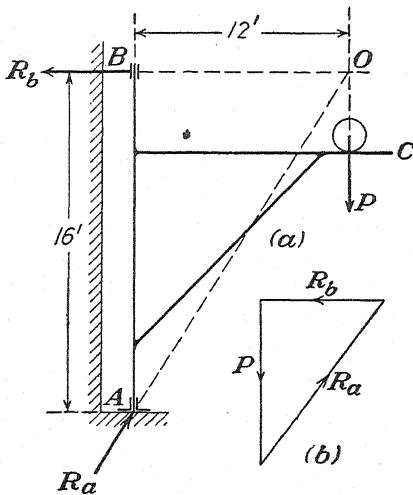
Fig. 12.

As a second example of the application of the theorem of three forces in calculating reactions, let us find the axial forces induced in the hinged bars 1, 2, 3, which support a horizontal beam AB under the action of an applied force P as shown in Fig. 13a.   Replacing the supporting bars by the reactions S_1, S_2, S_3, which they exert on the beam by virtue of the axial forces induced in them, we find ourselves with a system of four

forces (P, S_1, S_2, S_3) in a plane that are in equilibrium. To reduce this system to the case of three forces in equilibrium, we imagine that S_1 and S_2 are replaced temporarily by their resultant R, as yet unknown in direction but evidently acting through point D obtained as the intersection of the known lines of action of S_1 and S_2. Now, instead of four forces, we have the three forces $(P, S_3, \text{ and } R)$ that are in equilibrium.
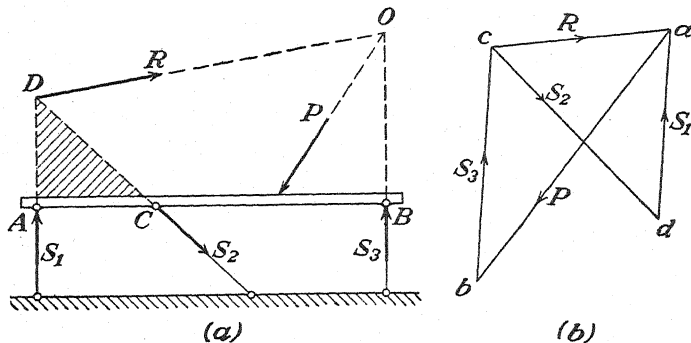
Fig. 13.

The point of concurrence of this system of three forces is evidently point O, obtained as the intersection of the known lines of action of P and S_3. Thus, the line of action DO of the third force R is established as shown, and the closed triangle of forces abc (Fig. 13b) can be constructed. From this construction, the magnitudes of S_3 and R are determined. Finally, knowing the force R, as represented by the vector $\overline{ca}$, we find the magnitudes of S_2 and S_1 by resolving R into the two components $\overline{cd}$ and $\overline{da}$ having the known directions of S_2 and S_1, respectively; and, if all constructions have been made to scale, the three reactions are determined. From the directions of the arrows on the vectors in Fig. 13b, we conclude that the bars 1 and 3 are under compression while the bar 2 carries tension.
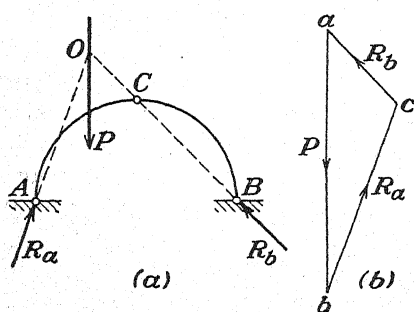
Fig. 14.

A common type of engineering structure is the *three-hinged arch* shown in Fig. 14a. The reactions at the points of support A and B of such a structure under the action of a load P acting as shown can be found by using the theorem of three forces. By virtue of the hinge at the *crown* C, we conclude that the reaction R_b must act along the line BC, which intersects the known line of action of the force P at point O. Thus O is the point of concurrence of the system, and the line of action AO of R_a is established. The magnitudes of the reactions are now found from the closed triangle of forces shown in Fig. 14b.

If, in addition to the load P, there is a load Q on the rib CB, the same procedure can be used. We find first the reactions at A and B due to the load P alone, as above. Then, repeating the same procedure, we find the reactions due to the load Q alone. Thus we shall have two reactions at A and two at B. The resultants of these two forces at each point of support are the desired reactions due to the simultaneous action of P and Q.*

As a last example, let us consider the *compound beam* consisting of two portions AC and BC hinged together at C and supported by four hinged bars as shown in Fig. 15a. To find the axial forces S_1, S_2, S_3, and S_4 induced in the four supporting bars by the action of a load P, we begin with a consideration of the equilibrium of the beam CB, which is acted upon by only three forces. These forces are the two reactions
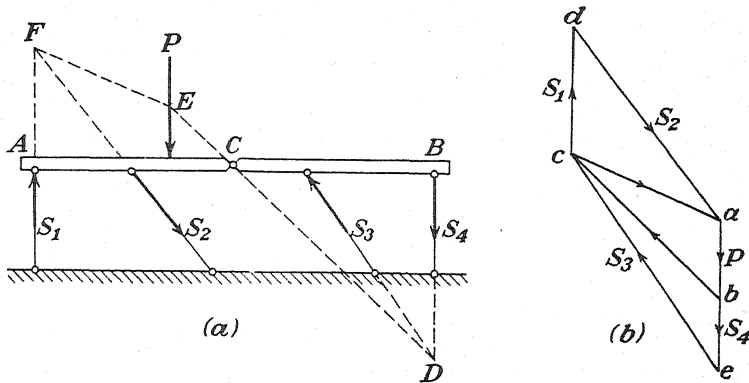
FIG. 15.

S_3 and S_4 together with a force at the hinge C that represents the action of the beam AC on the beam CB. The known lines of action of S_3 and S_4 determine the point of concurrence D of these three forces and hence the line of action CD of the force on the hinge C. The equal and opposite reaction exerted by the beam CB on the beam AC has the same line of action. Hence the beam AC is in the same condition as if it had, in addition to the supporting bars 1 and 2, a third supporting bar along the line CD. With this conclusion in mind, we see that, in considering the equilibrium of the beam AC, we may proceed in exactly the same manner as we did for the beam in Fig. 13. Thus the line of action FE of the resultant of S_1 and S_2 is established, and the closed triangle of forces abc in Fig. 15b can be constructed. The remainder of the solution reduces simply to the resolution of the vectors $\overline{ca}$ and $\overline{bc}$ into their respective components S_1, S_2 and S_4, S_3 as shown in Fig. 15b. Bars 1 and 3 are in compression while 2 and 4 are in tension.

* A more expedient method of handling several forces on the arch is discussed on p. 24.

PROBLEMS

6. Using the theorem of three forces, find the reactions induced at the points of support A and B of the simple beam supported and loaded as shown in Fig. 16.

Ans. $R_a = \frac{1}{3}\sqrt{7}\,P$, $R_b = \frac{2}{3}P$.
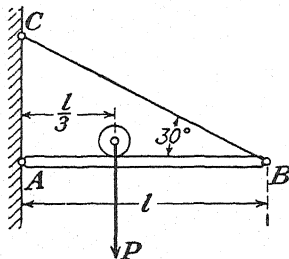
FIG. 16.
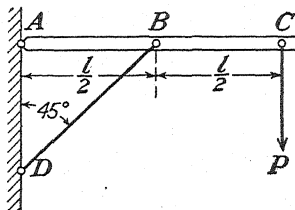
FIG. 17.

7. Find, graphically, the reactions at A and B for the beam shown in Fig. 17.

Ans. $R_a = \sqrt{5}\,P$, $R_b = 2\sqrt{2}\,P$.

8. Find, graphically, the reactions at A and B for the beam shown in Fig. 18.

Ans. $R_a = P$, $R_b = \sqrt{2}\,P$.
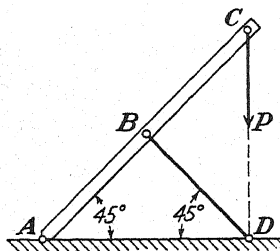
FIG. 18.
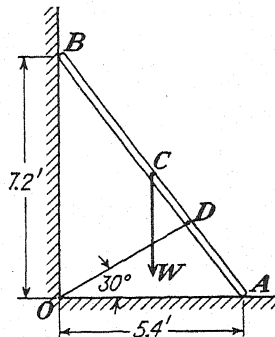
FIG. 19.

9. A prismatic bar AB of weight W rests on a horizontal floor at A and against a vertical wall at B and is kept from falling by a string OD as shown in Fig. 19. Neglecting friction at the points of support, find, graphically, the reactions at A and B and the tension in the string OD.
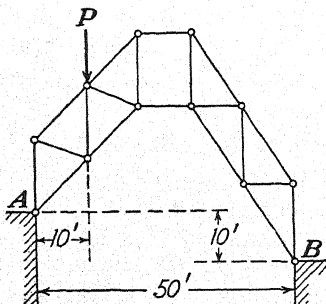
10. Find, graphically, the reactions R_a and R_b induced at the points of support of the compound structure loaded as shown in Fig. 20.

HINT: The reaction at B must be a horizontal force.

3. Equations of Equilibrium.

In general, a system of coplanar forces, the lines of action of which do not intersect in one point, may reduce to (1) *a resultant force,* (2) *a resultant couple,* or (3) *a state of equilibrium.*

FIG. 20.

If the given forces P_1, P_2, P_3, P_4 are such that their free vectors build an *unclosed polygon* as shown in Fig. 21b, the system will always reduce to a resultant force. The magnitude and direction of this resultant are given by the *closing side* $\overline{AE}$ of the polygon of forces, and its line of action is found by the construction illustrated in Fig. 21a.
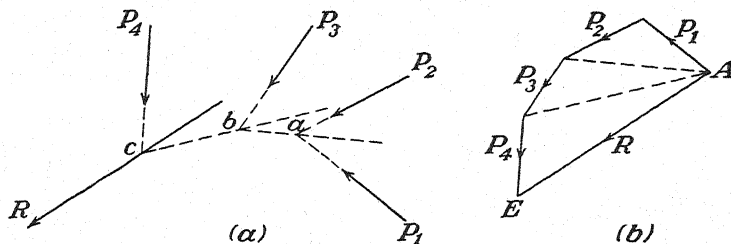
FIG. 21.

If the given forces are such that their free vectors build a *closed polygon* (Fig. 22b), the resultant force vanishes, but there is still the possibility of a resultant couple. In this case, we arbitrarily divide the forces into two groups P_1, P_2, P_3 and P_4, P_5, P_6, having equal and opposite resultants R_1 and R_2 as represented by the vectors $\overline{AD}$ and $\overline{DA}$ in Fig. 22b. Then, proceeding with each of these groups in the same manner
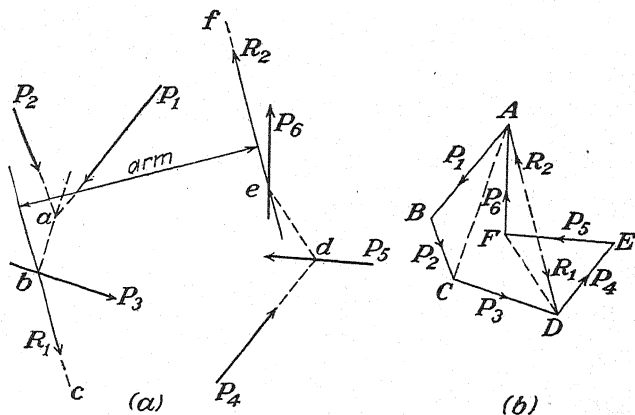
FIG. 22.

as in the preceding case, we find the lines of action bc and ef of their resultants as shown in Fig. 22a, and these two equal and opposite forces represent a resultant couple.

In the particular case where the lines of action of the forces R_1 and R_2 in Fig. 22a are found to coincide, the resultant couple vanishes and the system of forces is in equilibrium. Thus, the conditions of equilibrium for any system of forces in a plane are a closed polygon of forces and a vanishing resultant couple. From the condition of a closed

polygon of forces, we conclude that the algebraic sums of projections of the given forces on any pair of orthogonal axes must be zero. From the condition of a vanishing resultant couple, we conclude, with the help of Varignon's theorem,[1] that the algebraic sum of moments of the given forces with respect to any center in their plane must be zero. These conditions are expressed analytically by the following *equations of equilibrium*,

$$\Sigma X_i = 0, \qquad \Sigma Y_i = 0, \qquad \Sigma M_i = 0, \qquad (2a)$$

where X_i and Y_i are orthogonal projections of any force P_i, and M_i is the moment of the same force with respect to a chosen center. The summations are understood to include all forces of the system.

It can easily be shown that the above conditions of equilibrium can also be expressed by the three moment equations[2]

$$\Sigma M_A = 0, \qquad \Sigma M_B = 0, \qquad \Sigma M_C = 0, \qquad (2b)$$

in which A, B, and C are three arbitrary centers that form a triangle in the plane of action of the forces.

Equations (2) find a wide application in the theory of structures, particularly in the determination of reactions and in the analysis of trusses. As a first example, let us consider the determination of the reactions induced at the points of support of the simple crane ABC loaded as shown in Fig. 23. If we neglect friction in the guide at B, the supports of the crane can be replaced by reactions R_b, X_a, and Y_a, as shown, where X_a and Y_a are horizontal and vertical components of the unknown reaction at A. The system of forces as shown is in equilibrium; and, if point A is used as a moment center, Eqs. (2a) become
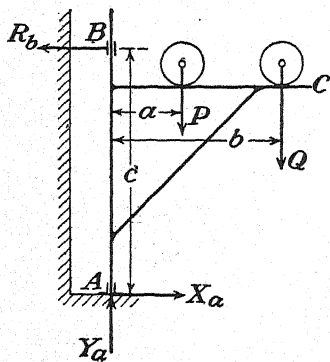
FIG. 23.

$$X_a - R_b = 0,$$
$$Y_a - P - Q = 0,$$
$$R_b c - Pa - Qb = 0.$$

---

[1] The moment of the resultant with respect to any center in the plane of action of the forces is equal to the algebraic sum of the moments of the given forces with respect to the same center. See authors' "Engineering Mechanics." 2d ed., p. 51.

[2] See authors' "Engineering Mechanics," 2d ed., p. 124.

From these equations, we find $X_a = R_b = (Pa/c) + (Qb/c)$ and

$$Y_a = P + Q.$$

As a second example, let us consider the determination of the axial forces induced in the bars 1, 2, and 3 of the simple truss loaded and supported as shown in Fig. 24.   Consider-
ing only the shaded portion BCD of
the truss and replacing the bars 1, 2,
and 3 by the reactions that they exert
upon this portion, we obtain the free-
body diagram as shown.   Here we
have five forces in equilibrium, and the
algebraic sum of their moments with
respect to any center in the plane of the
truss must be zero.   Upon choosing,
successively, the points A, D, and C as
moment centers, Eqs. (2b) become
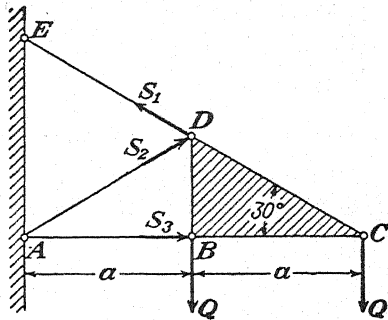
FIG. 24.

$$S_1 a - Qa - 2Qa = 0,$$
$$S_3 a/\sqrt{3} - Qa = 0,$$
$$Qa - S_2 a = 0,$$

and we find $S_1 = 3Q$ (tension), $S_3 = \sqrt{3}\, Q$ (compression), and $S_2 = Q$ (compression).   It should be noted that the moment centers are chosen so as to give us only one unknown in each equation.

PROBLEMS

11. A prismatic bar AE of negligible weight is hinged to a vertical wall at A and supported by a strut BD, as shown in Fig. 25.   Find the reactions induced at A and B through the action of a sphere of weight Q tied by a string CF that is parallel to AE. The radius of the sphere is such that the points B and C are at the same level.
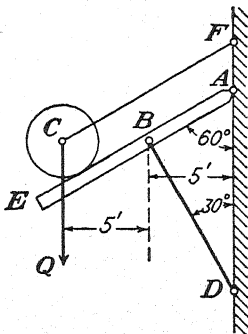
FIG. 25.
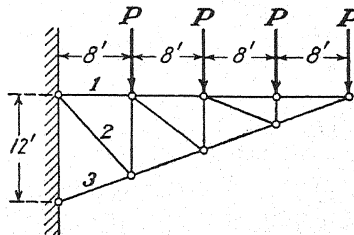
FIG. 26.

12. Find the axial forces induced in the supporting bars 1, 2, and 3 of the simple truss shown in Fig. 26.

13. Evaluate the horizontal and vertical components of the reactions induced at the supports A and B of the compound structure shown in Fig. 27.
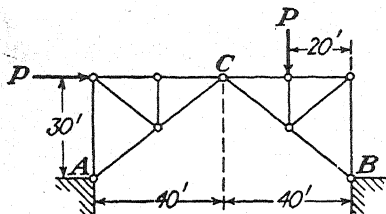
FIG. 27.
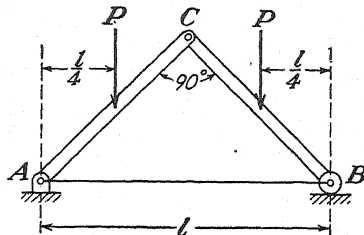
FIG. 28.

14. Determine the tension induced in the tie bar AB of the plane structure supported and loaded as shown in Fig. 28.

15. In Fig. 25, how will the reactions at A and B be changed if the inclined string CF is replaced by a horizontal string CB?

16. In Fig. 16, compute the reactions at A and B by using Eqs. (2a).

17. In Fig. 17, compute the reactions at A and B by using equations of equilibrium.

18. In Fig. 18, compute the reactions at A and B by using equations of equilibrium.

19. In Fig. 19, compute analytically the reactions at A and B and the tension in the string OD.

20. In Fig. 20, compute analytically the horizontal and vertical components of the reactions at A and B.

4. Internal Forces.—In previous articles, we have discussed the determination of external reactions induced at the supports of a rigid body constrained and loaded in one plane. We shall now consider the
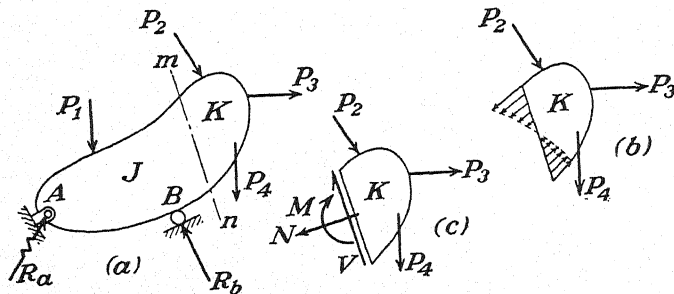
FIG. 29.

internal forces, or *stresses*, that are set up in such a constrained body under the action of applied external forces. Consider, for example, the rigid body supported and loaded in one plane as shown in Fig. 29a. Under the action of the applied loads, reactions R_a and R_b are induced at the supports, and these reactive forces are evaluated in the usual manner by considering the conditions of equilibrium of the entire body. Thus the system of forces external to the body as a whole is completely defined. Now imagine that an arbitrary plane section mn divides the body into

two parts J and K as shown. It is evident that forces of internal constraint must exist between these two parts of the body to hold them together. Such internal forces, of course, always occur in pairs of equal and opposite forces at each point of the body and do not enter into our consideration of the equilibrium of the body as a whole. To bring them under consideration, we isolate one portion K as a free body (Fig. 29b). Then the action of the removed portion J is represented by the forces that its various particles exert on those of the free body K, and in this way the required internal forces are brought under consideration.
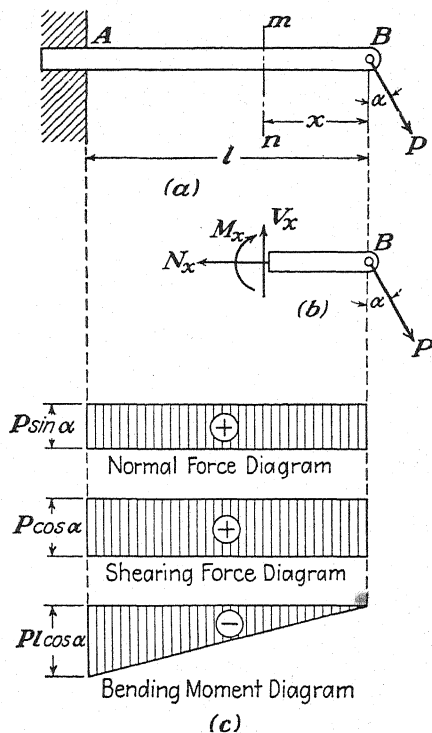
Fig. 30.

Although the actual distribution of these forces over the section may be complicated, it is evident that they must be statically equivalent to the system of forces acting externally on part J and can always be represented by a resultant force R applied at the centroid of the cross section together with a couple of moment M. The force R in turn can be resolved into rectangular components N and V as shown in Fig. 29c. The three quantities N, V, and M on the section mn are called the *normal force*, the *shearing force*, and the *bending moment*, respectively. They are usually considered positive when directed as shown in the figure. In

general, their magnitudes will depend on the position and orientation of the chosen section, but in any case they can be evaluated by the three equations of equilibrium applicable to the free body K.

The simplest and most important class of structures for which we shall wish to investigate the internal forces on various sections are *beams* submitted to transverse loads. Such beams are usually prismatic in form and are constrained and loaded in a plane of symmetry. Under these conditions, we can best define the general state of stress in terms of the internal forces on cross sections that are normal to the axis of the beam. Consider, for example, the cantilever beam AB, loaded as shown in Fig. 30a. Let mn be any normal section defined by its distance x from the free end. Then considering the equilibrium of the free body to the right of this section (Fig. 30b) and using Eqs. (2a), we find

$$N_x = +P \sin \alpha,$$
$$V_x = +P \cos \alpha,$$
$$M_x = -Px \cos \alpha.$$

From these expressions, we see that the normal force N_x and the shearing force V_x are independent of the position of the section along the beam, while the bending moment M_x is proportional to the distance x. The variations in normal force, shearing force, and bending moment along the beam can be represented graphically by the diagrams shown in Fig. 30c, which accordingly are called *normal-force, shearing-force*, and *bending-moment diagrams*.
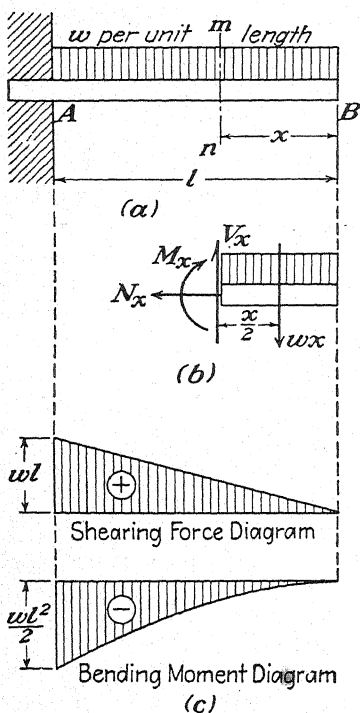
(a)

(b)

Shearing Force Diagram

Bending Moment Diagram

(c)

Fig. 31.

As a second example, consider the same cantilever beam uniformly loaded along its length as shown in Fig. 31a. In this case the expressions for normal force, shearing force, and bending moment on any cross section, defined by its distance x from the free end of the beam, become

$$N_x = 0, \qquad V_x = +wx, \qquad M_x = -\frac{wx^2}{2}.$$

The corresponding diagrams are shown in Fig. 31c.

In the case of curved beams, we may find it convenient to proceed in a slightly different manner. Consider, for example, the cantilever beam that has a circular axis of radius R and is loaded as shown in Fig.

32a. In this case we can most easily define the position of an arbitrary normal cross section by the angular coordinate ϕ measured as shown in
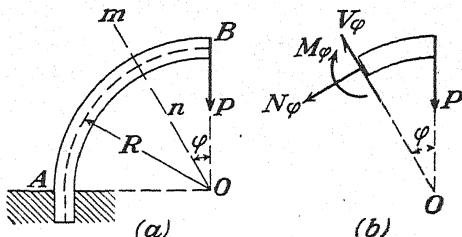
FIG. 32.

the figure. Then, applying Eqs. (2a) to the free body in Fig. 32b, we find

$$N_\varphi = -P \sin \phi, \qquad V_\varphi = +P \cos \phi, \qquad M_\varphi = -PR \sin \phi.$$

As a last example, let us consider the simply supported beam with overhang as shown in Fig. 33a. Under the action of a load uniformly distributed over the span l, the reaction at A is $wl/2$, and the bending moment at any section distance x to the right of this support is

$$M_x = \frac{wl}{2} x - wx \frac{x}{2} = \frac{wx}{2} (l - x).$$

Thus the bending-moment diagram is a parabola with maximum ordinate $wl^2/8$ at mid-span as shown. The free overhang is without internal forces if we neglect the weight of the beam itself.

If the same beam carries a concentrated load P at the free end as shown in Fig. 33b, the reaction at A is Pa/l and the bending moment at any section between A and B is

$$M_x = -\frac{Pa}{l} x_1,$$

where x_1 defines the location of the section as shown. Likewise, for any section distance x_2 to the left of the free end C of the beam, the bending moment is

$$M_x = -Px_2.$$

FIG. 33.

Thus, in this case, the bending-moment diagram is made up of two straight lines having the common maximum ordinate $-Pa$ at the support B as shown.
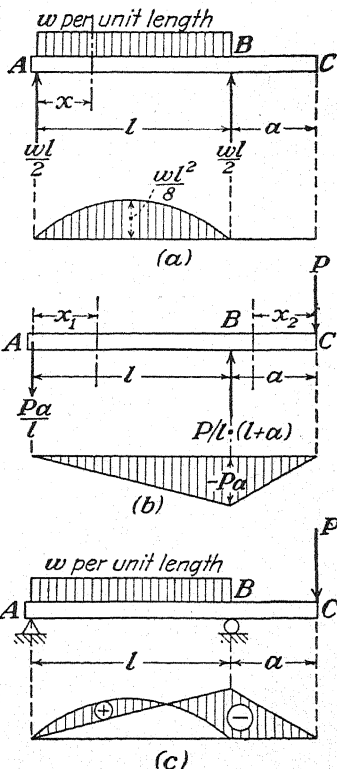
If the beam carries both the distributed load and the concentrated load simultaneously, we obtain the corresponding bending-moment diagram as shown in Fig. 33c simply by superposing the diagrams of Figs. 33a and 33b. The same procedure can be used in the construction of shearing-force and normal-force diagrams.

PROBLEMS

21. Construct shearing-force and bending-moment diagrams for each of the cantilever beams shown in Fig. 34.

(a)

(b)

(c)

Fig. 34.

(a)

(b)

(c)
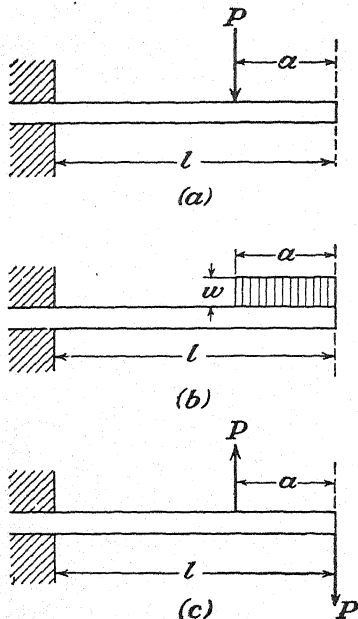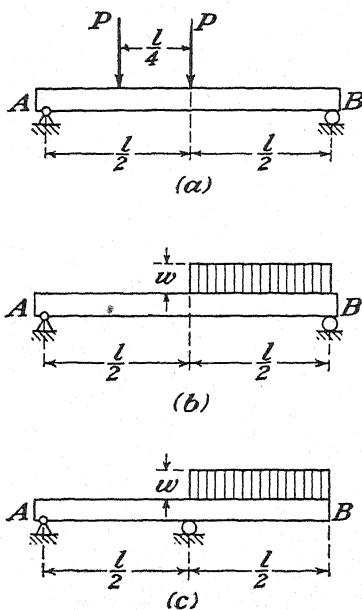
Fig. 35.

22. Construct normal-force, shearing-force, and bending-moment diagrams for each of the beams shown in Figs. 16, 17, 18.

Fig. 36.

23. Construct shearing-force and bending-moment diagrams for each of the simply supported beams shown in Fig. 35.

24. Construct normal-force, shearing-force, and bending-moment diagrams for the bar *BC* of the structure shown in Fig. 28.

25. Prove that the vertical ordinates in Fig. 36 represent the bending moments for corresponding points on the semicircular axis of the three-hinged arch loaded as shown. Evaluate the factor by which each ordinate must be multiplied in order to give the corresponding bending moment. *Ans. P/3.*
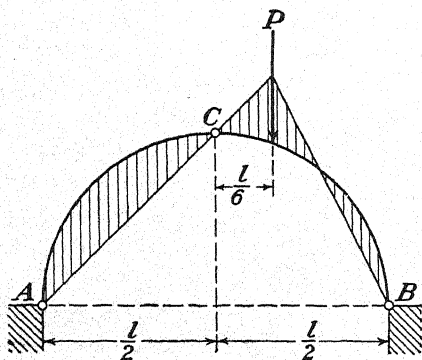
5. The Funicular Polygon.—We shall now develop a general graphical treatment for coplanar forces that has some practical advantages over the analytical treatment discussed in Art. 3. We begin with the very simple case of two forces P and Q as shown in Fig. 37a. As we already know, the closing side $\overline{AC}$ of the polygon of forces (Fig. 37b) gives both the magnitude and the direction of the resultant R, but the position of its line of action remains to be determined. In general, this can be accomplished as follows: In Fig. 37b, we take the arbitrary point O, called a *pole*, and join it by lines 1, 2, and 3 with the apexes of the polygon of forces. These lines are called *rays* and, like the other lines in this figure, may be regarded as free force vectors. Taking, for example, the directions as indicated by the arrows inside the triangle AOB, we may consider the force P as the resultant of the forces 1 and 2. In the same

(a)   (b)
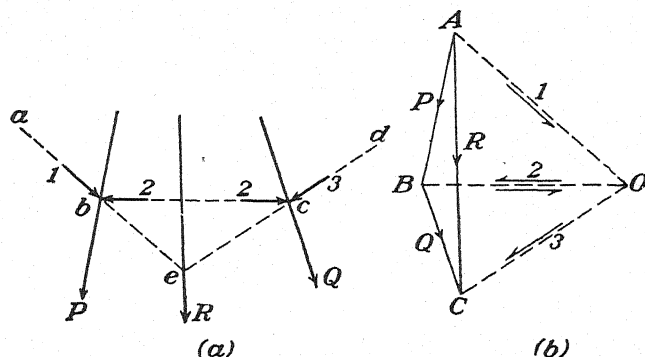
FIG. 37.

manner, the force Q can be considered as the resultant of the forces 2 and 3, the directions of which are indicated by the arrows inside the triangle BOC. Referring now to Fig. 37a, it is evident that the action of the forces P and Q will not be changed if each of them is replaced by its two components indicated in Fig. 37b. These replacements will be made in the following manner: Beginning at any point a in the plane of action of the forces, we draw the line ab parallel to the ray AO. From the point of intersection b of this line with the line of action of the force P, we draw the line bc parallel to the ray BO; and, from the point of intersection c of this line with the line of action of the force Q, we draw the line cd parallel to the ray CO. The polygon $abcd$, obtained in this way, is called a *funicular polygon* for the forces P and Q. The apexes of this polygon are on the lines of action of the given forces, and its sides are parallel to the rays of the polygon of forces. We assume now that at point b the forces 1 and 2, replacing the force P, and at point c the forces 2 and 3, replacing the force Q, are applied as shown in Fig. 37a. Thus the given system of forces P and Q is replaced by a system of four

forces applied at points b and c.   Since the pair of forces 2 acting along
the line bc are equal and opposite, they may be removed from the system
and there remain only the forces 1 and 3, which are equivalent in action
to the given forces P and Q.   The magnitude and direction of the result-
ant of these forces are given by the vector $\overline{AC}$ in Fig. 37b, and a point
on its line of action is given by the point of intersection e of the forces
1 and 3 acting along the first and last sides of the funicular polygon in
Fig. 37a.

   If we imagine a weightless string going along the sides ab, bc, and cd
of the funicular polygon with its ends fixed at a and d, this string will
be in equilibrium under the action of the forces P and Q.   The tensile
forces in the portions ab and bc of the string will be numerically equal to
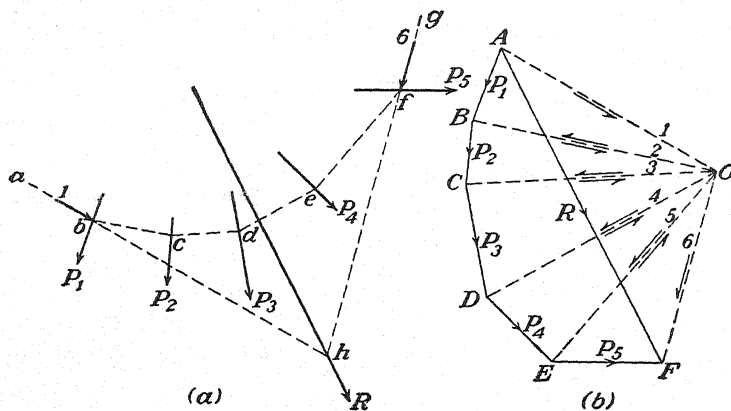
Fig. 38.

the forces 1 and 2, and their actions on the knot at b will balance the force
P.   In the same way the tensile forces in the portions bc and cd of the
string balance the force Q.   This relation between the constructed
polygon $abcd$ and the configuration of equilibrium of a string submitted
to the action of the given forces explains the origin of the name *funicular
polygon*, i.e., string polygon.

   The graphical constructions discussed above are perfectly general
and can be used also in the case of several coplanar forces $P_1 \ldots P_5$ acting
as shown in Fig. 38a.   Again, we begin with the construction of the
polygon of forces $ABCDEF$ (Fig. 38b).   Choosing an arbitrary pole O,
drawing the rays 1, 2, 3, 4, 5, 6, and constructing, in the plane of action
of the forces, the lines ab, bc, ... fg, parallel to these rays, we obtain
the funicular polygon $abcdefg$ as shown.   At the apexes of this polygon,
each of the given forces $P_1 \ldots P_5$ is replaced by its two components as
represented by rays in Fig. 38b.   The forces acting along the sides bc,
cd, de, and ef are pairs of equal and opposite forces in equilibrium and

may be removed from the system.   There remain only the forces 1 and 6 acting at points b and f, which are equivalent to the given forces $P_1 \ldots P_5$.   The magnitude and direction of the resultant of these forces are given by the closing side $\overline{AF}$ of the polygon of forces (Fig. 38b), and a point on its line of action by the intersection h of the first and last sides of the funicular polygon (Fig. 38a).

If the polygon of forces is closed, the possibility of a resultant force vanishes.   In such a case the first and last rays coincide; hence the first and last sides of the funicular polygon become parallel or coincide.   In the first case, the two equal and opposite forces acting along these sides represent a resultant couple.   In the second case they balance each other, and the given system of forces is in equilibrium.   These two cases are illustrated in Fig. 39.   Three given forces P_1, P_2, and P_3 have such magnitudes and directions that their free vectors build a closed polygon (Fig. 39c).   Hence the rays 1 and 4, directed to the beginning of the
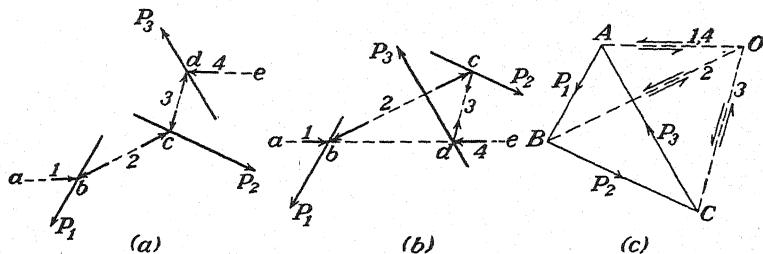
FIG. 39.

first vector $\overline{AB}$ and to the end of the last vector $\overline{CA}$, coincide in one ray OA.

If the given forces have the lines of action shown in Fig. 39a, the first side ab and the last side de of the funicular polygon are parallel but do not coincide.   Hence the unbalanced forces 1 and 4 acting along these sides represent a couple that is the resultant of the given system of forces.

If the given forces $P_1 \ldots P_3$ have the lines of action shown in Fig. 39b, the first and last sides of the funicular polygon coincide and the equal but opposite forces 1 and 4 acting along these coincident sides balance each other.   Hence, in this case, the given system of forces is in equilibrium.

We see that, by using the polygon of forces together with the funicular polygon, the three possibilities for a system of forces in a plane (see page 8) can be investigated entirely by graphical methods.   If the polygon of forces is unclosed, the given system reduces to a resultant force.   If the polygon of forces is closed but the first and last sides of the funicular polygon, which are parallel, do not coincide, the system reduces to a resultant couple.   If the polygon of forces is closed and the first

and last sides of the funicular polygon coincide, *i.e.*, the funicular polygon is closed, also, the system of forces is in equilibrium. Thus the graphical conditions of equilibrium are a closed polygon of forces and a closed funicular polygon.

As an example, let us determine graphically the reactions at the supports A and B of the beam AC loaded as shown in Fig. 40a. Beginning with the load P as represented by the free vector $\overline{AB}$ in Fig. 40b and selecting a pole O, we construct the rays 1 and 2, after which the corresponding sides ab and bc of the funicular polygon can be drawn as shown in Fig. 40a. Then the closing side ac of this polygon determines the direction of the corresponding ray 3 in Fig. 40b, and the reactions R_b and R_a are graphically determined by the vectors $\overline{BC}$ and $\overline{CA}$, respectively. As would be expected, the reaction R_a is directed downward.
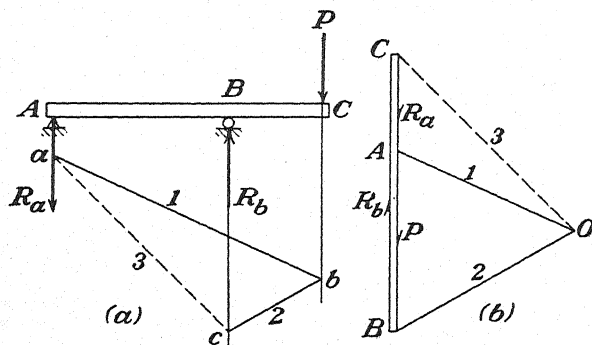
Fig. 40.

As a second example, we take the case of a roof truss ABC supported and loaded as shown in Fig. 41a. Here again, to find the reactions at the supports A and B, we begin with the polygon of forces $ABCDEF$, select a pole O, and draw the rays 1 to 6 as shown in Fig. 41b. Now, in this case, when we come to construct the funicular polygon in Fig. 41a, we note that the hinge A is the only known point on the line of action of R_a. Hence we must start the funicular polygon at this point. Then, since the load P also acts through point A, that side of the funicular polygon corresponding to the ray 1 vanishes. Otherwise, the funicular polygon is constructed in the usual manner and we obtain the closing side Ab as shown. After this, we return to Fig. 41b, where we obtain the apex G of the polygon of forces by the intersection of the ray 7 (parallel to the closing side of the funicular polygon) and the known vertical direction of R_b. The required reactions are now completely determined by the vectors $\overline{FG}$ and $\overline{GA}$ as shown.

PROBLEMS

26. Determine graphically the magnitudes of the reactions R_a and R_b of the simply supported beam loaded as shown in Fig. 35a.   *Ans.* 1.25P, 0.75P.

27. Using the funicular polygon, determine the magnitudes of the reactions at the supports A and B of the structure shown in Fig. 28.   *Ans.* $R_a = R_b = P$.

28. Using the funicular polygon, determine the axial forces in the bars 1, 2, and 3 of the simple truss loaded as shown in Fig. 26.

29. Determine graphically the reactions at the supports A and B of the simple truss shown in Fig. 41a if the hinge A is on rollers while the hinge B is fixed.   Assume $AB = 40$ ft., $\angle CAB = \angle CBA = 15$ deg., $P = 1,000$ lb.

Ans. $R_a = 9,315$ lb., $R_b = 6,465$ lb.
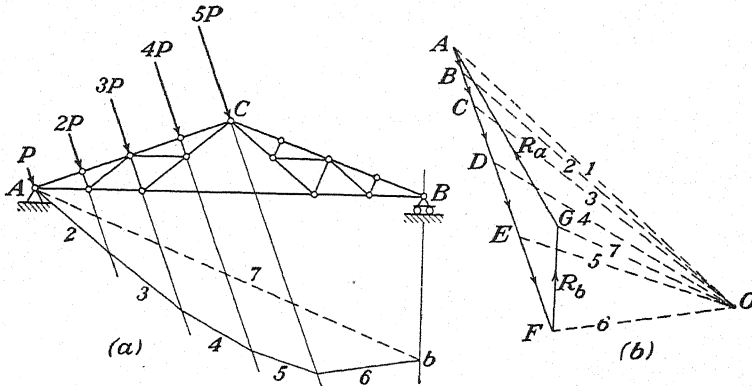
Fig. 41.

30. Determine graphically the axial forces in the bars 1, 2, and 3, which support the beam AB loaded as shown in Fig. 42.

Ans. $S_1 = -1,538$ lb., $S_2 = +1,414$ lb., $S_3 = -1,392$ lb.
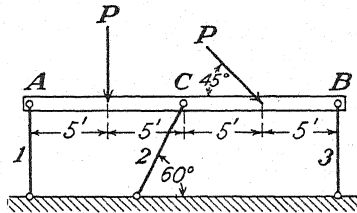
Fig. 42.

6. Applications of the Funicular Polygon.—In the preceding article, we have used the funicular polygon simply as a tool in the graphical composition of forces in a plane and in the evaluation of reactions. We have seen, however, that it possesses a certain physical significance in itself, namely: the configuration of equilibrium of a string under the action of a given system of forces. This concept can be generalized to the extent that we imagine a string capable of sustaining compression as well as tension. Thus, for example, the funicular polygon *abcdef* shown in Fig. 43a may be regarded as a system of hinged bars supported at a and f so as to form an arch that is in equilibrium under the action of the applied forces. Sometimes we need to construct such a funicular polygon to satisfy certain specified conditions such, for example, as

passing through two or three given points. This general problem can be greatly simplified by using the following theorem:

THEOREM: *If, for a given system of forces in a plane, any two funicular polygons are drawn for two different poles O and O', corresponding sides of these polygons will meet in points that lie on a straight line parallel to the line OO' joining the two poles.*
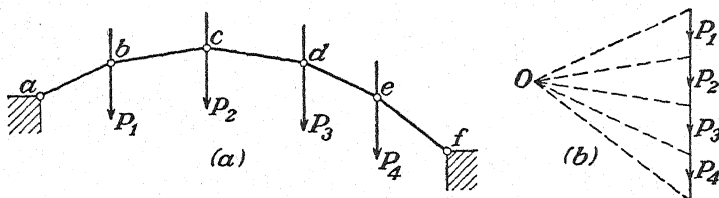
FIG. 43.

This theorem can be proved as follows: Let F_1, F_2, F_3, $\overline{}$ . . . (Fig. 44a) be any system of forces in a plane, and let $ABCDE$ . . . (Fig. 44b) be the corresponding polygon of forces, with O and O' any two arbitrary poles and 1, 2, 3, 4, . . . and 1', 2', 3', 4', . . . the corresponding rays. Then, beginning at any two points a and a' in the plane of action of the forces, two funicular polygons $abcde$ . . . and $a'b'c'd'e'$ . . . corresponding to the poles O and O' can be constructed in the usual manner. Now
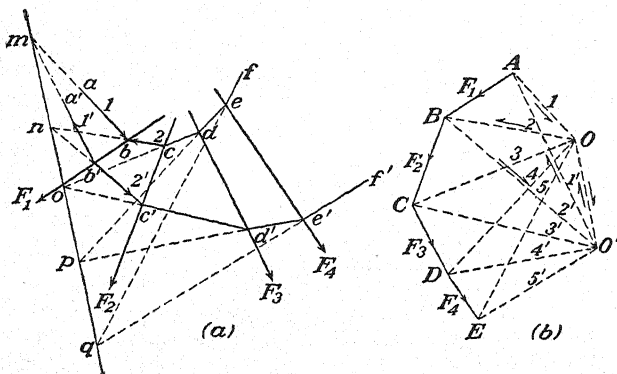
FIG. 44.

it follows from the discussion of Art. 5 that at point b, in Fig. 44a, we can replace the force F_1 by its components 1 and 2 as represented by the vectors $\overline{AO}$ and $\overline{OB}$ in Fig. 44b. In the same way, the forces 2' and 1', represented by the vectors $\overline{BO'}$ and $\overline{O'A}$ (Fig. 44b), when applied at point b' (Fig. 44a), are equivalent to the *equilibrant* of the force F_1. Hence the forces 1, 2, 1', and 2', directed as shown in Fig. 44a, are four forces in equilibrium. From this we conclude that, if at point m in the plane of action of the forces we replace the forces 1' and 1 by their resultant as represented by the vector $\overline{O'O}$ (Fig. 44b) and at point n we

replace the forces 2 and 2′ by their resultant as represented by the vector $\overline{OO'}$ (Fig. 44b), then these two equal and opposite forces are in equilibrium and consequently must be collinear in action. That is, the points of intersection m and n of the corresponding first and second sides of the two funicular polygons lie on a straight line parallel to the line OO' joining the two poles. Applying the same reasoning in connection with the force F_2, we conclude that the intersections n and o of the corresponding second and third sides of the two funicular polygons also lie on a straight line parallel to OO', etc. Hence the points m, n, o, p, q, . . . all lie on one straight line parallel to OO', and the theorem is proved.

FUNICULAR POLYGON THROUGH THREE POINTS.—By the aid of the foregoing theorem, it is possible to construct, for any system of forces in a plane, a funicular polygon three sides of which will pass through three given points in the plane of action of the forces. We begin with the case of two coplanar forces P and Q as shown in Fig. 45a and for which we
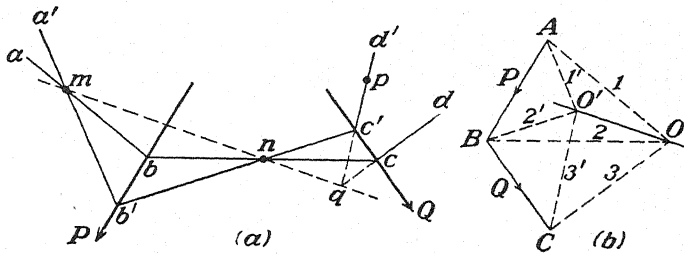
FIG. 45.

wish to construct a funicular polygon whose three sides will pass, respectively, through the given points m, n, and p. We first construct the polygon of forces ABC as shown in Fig. 45b. Then, instead of choosing an arbitrary pole, we first construct two sides ab and bc of a funicular polygon so that these sides do pass through the given points m and n, respectively, as shown in Fig. 45a. The position of the pole O corresponding to the funicular polygon that we have thus started and that we shall call the *trial funicular polygon* can now be found as the intersection of the rays 1 and 2 (Fig. 45b) drawn through the apexes A and B parallel, respectively, to the sides ab and bc of the trial funicular polygon. Having the pole O, we can draw the ray 3, and then the corresponding side cd of the trial funicular polygon can be constructed parallel to this ray as shown in Fig. 45a. In general, this last side of the trial funicular polygon will not pass through the given point p. However, from the trial funicular polygon together with the theorem above, we can easily determine a funicular polygon for the given forces P and Q, the three sides of which will pass through the given points m, n, and p, respectively, and which we shall accordingly refer to as the *true funicular polygon*. To accomplish

this, we note that the first two sides of the trial funicular polygon pass through the given points m and n, respectively, and that the first two sides of the true funicular polygon must also pass through these points. Hence, the straight line mn (Fig. 45a) is the line on which the intersections of corresponding sides of the trial and true funicular polygons must all lie. Prolonging the third side cd of the trial funicular polygon to its intersection q with the line mn, we obtain a point through which the third side of the true funicular polygon must pass. Remembering that the third side of the true funicular polygon must also pass through point p, we have the position of this side $c'd'$ as shown in Fig. 45a. Now through the apex C of the polygon of forces we draw the ray $3'$ parallel to $c'd'$, and through point O we draw a line parallel to the straight line mnq. The intersection of these two lines determines the pole O' for the true
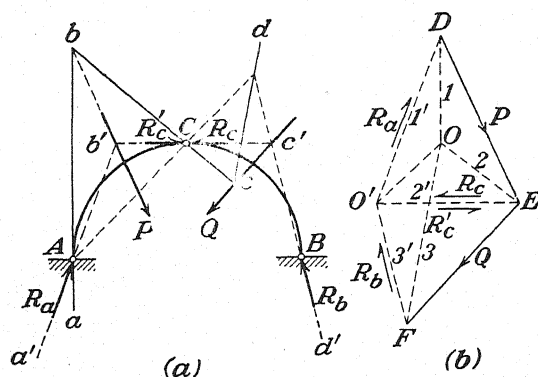
Fig. 46.

funicular polygon. The rays $1'$ and $2'$ can now be drawn and the funicular polygon $a'b'c'd'$ constructed as shown in Fig. 45a. The three sides of this funicular polygon pass, respectively, through the three given points m, n, and p, as desired.

If there are several forces in a plane for which we wish to construct a funicular polygon passing through three given points m, n, and p, we first replace the forces between m and n by their resultant P and the forces between n and p by their resultant Q and then proceed as illustrated in Fig. 45.

The funicular polygon through three given points is of practical value in connection with the determination of the reactions at the supports of a three-hinged arch as shown in Fig. 46a. We first construct, for the applied forces P and Q, a funicular polygon $a'b'c'd'$, the three sides of which pass, respectively, through the centers of the hinges A, C, and B. This construction is carried out as explained above and is completely illustrated in Fig. 46. Obviously, the rays $1'$, $2'$, and $3'$, when con-

sidered as vectors acting as shown in Fig. 46b, represent the reactions R_a, $R_c = R_c'$, and R_b, since, when applied at points A, C, and B, respectively, they fulfill all conditions of equilibrium for the arch as a whole as well as for either portion of it.

PROBLEMS

31. A string ACB of length l hangs between two vertical walls as shown in Fig. 47. Along this string a small pulley C, from which is suspended a load P, can roll without friction. In the particular case where $l = 2a = 4b$, what configuration of equilibrium will the system assume? Make the solution entirely by graphical constructions.

<div style="text-align:right">

Fig. 47.
</div>

Ans. $x = 0.355a$.

32. The hoisting cable of a crane is carried over a series of pulleys a, b, c, d, and e, as shown in Fig. 48a. Using the cable as a funicular polygon for the system of forces that the pulleys exert on the joints of the crane, show that these forces are completely defined by the polygon $ABCDEF$ in Fig. 48b.

33. Determine the proper shape of the top chord $abcdefgh$ of the plane truss shown in Fig. 49 so that, for the given system of loads P, all the diagonal web members will be inactive. What are the corresponding forces in the chord members if $l = 70$ ft. and $k = 18$ ft.?

(a)   (b)
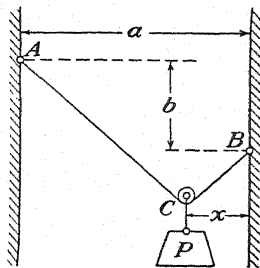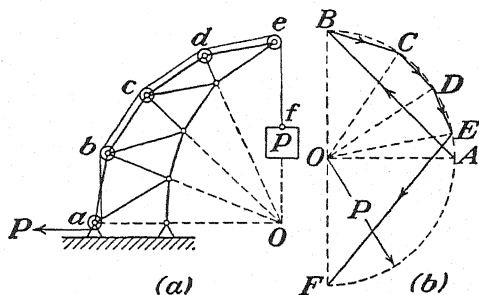
Fig. 48.
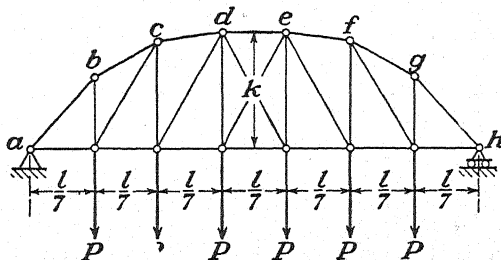
Fig. 49.

34. Construct a funicular polygon through the three points A, C, B, to determine the reactions at the supports of the three-hinged arch with semicircular rib as shown in Fig. 50.   Ans. $R_a = 6{,}880$ lb., $R_b = 8{,}220$ lb.

35. A flexible weightless string is fastened at A, passes over a pulley at D, and carries a load P at its free end as shown in Fig. 51. A stiff bar BC with small rollers at its ends carries weights P and Q as shown and can roll freely along the string.
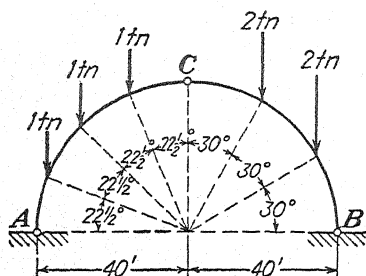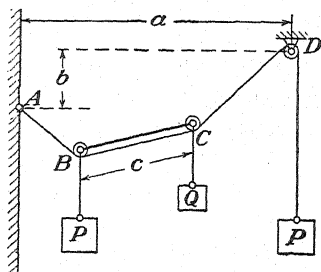
Fig. 50.   Fig. 51.

Neglecting friction, determine the configuration of equilibrium of the system. Numerical data are given as follows: $a = 18$ ft., $b = 4$ ft., $c = 8$ ft., $P = 2Q$. What compressive force S is induced in the bar BC? Make the solution entirely by graphical constructions.   *Ans.* $S = 0.6Q$.

7. Funicular Curves for Distributed Force.—In previous discussions, we have dealt entirely with concentrated forces. Sometimes we need to consider the equilibrium of structures under the action of *distributed force.* Consider, for example, the prismatic beam AB (Fig. 52a), the weight of which is uniformly distributed along its length. Such a distribution of force is completely defined by its *intensity* q, *i.e.*, the weight per unit length of the beam. It is represented graphically by the rectangle $AabB$, which is called a *load diagram.* In a more general case, we may have nonuniformly distributed load along the beam. Here also the distribution of force can be completely defined by a load diagram like that shown in Fig. 52b, where the intensity of load at each point is indicated by the corresponding ordinate.
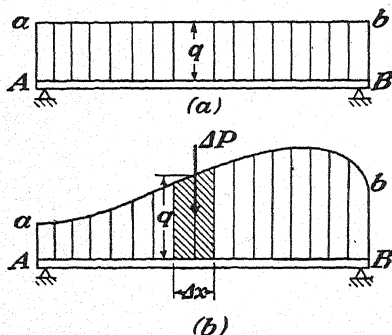
(b)

Fig. 52.

Any given load diagram can always be approximated by a series of trapezoidal elements as shown in Fig. 52b. Then, if q is the average intensity over the length Δx, the corresponding element must represent a force $\Delta P = q \cdot \Delta x$ that acts through the centroid of that element. In this way, we obtain a series of parallel forces the magnitudes of which are represented by the areas of the corresponding trapezoids and the moments of which, with respect to any point, are identical with the corresponding statical moments of those trapezoids. From this it

follows that the resultant force is represented by the total area of the load diagram and acts through its centroid.

We have already seen that any funicular polygon for a system of coplanar forces may be interpreted as a possible configuration of equilibrium of a string fixed at its ends and submitted to the action of the given forces. In the case of continuously distributed force in a plane as discussed above, the corresponding configuration of equilibrium of a string becomes a smooth curve called a *funicular curve*. Physically, we see the manifestation of such a curve in the case of a heavy flexible chain that is fixed at its two ends and otherwise unsupported in the gravity field. This particular curve is called a *catenary*.
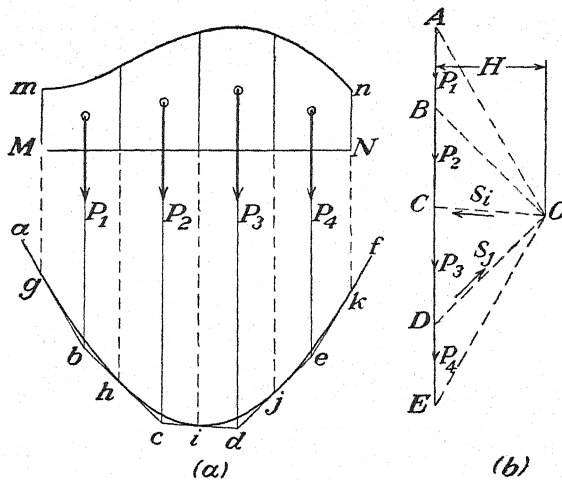
Fig. 53.

Let $MmnN$ (Fig. 53a) be the load diagram for a given distribution of vertical force in a plane. To construct a corresponding funicular curve, we begin by dividing the load diagram into several parts, each small enough so that, without serious error, it may be considered as a trapezoid. Then it follows that each trapezoid represents a vertical force equal in magnitude to the area of that trapezoid and acting through its centroid. We may therefore replace the continuous distribution of force by several vertical forces $P_1, P_2, \ldots$ as shown and construct a funicular polygon *abcdef* for these forces in the usual manner. This done, we inscribe a smooth curve tangent to the sides of the funicular polygon at the points g, h, i, j, and k, and this is the required funicular curve.

From the foregoing discussion it follows that between any funicular curve (Fig. 53a) and the corresponding diagram of forces (Fig. 53b) from which it is derived there exist the following relationships: (1) For every tangent to the string, there is a corresponding parallel ray in the diagram

of forces, the length of which represents the tensile force in the string at the point of tangency. (2) The shortest ray, called the *pole distance* *H*, represents the tension at the vertex of the funicular curve and likewise the horizontal projection of the tension at any other point. (3) For any two points on the funicular curve, rays parallel to the corresponding tangents cut from the *load line* $\overline{AE}$ that portion of the total load which acts between these two points.

Sometimes it is desirable to develop a funicular curve for a given distribution of load analytically rather than graphically. Referring to Fig. 54a, let *MmnN* be a given distribution of force and *abcd* a funicular curve corresponding to the pole *O* as shown in Fig. 54b. On this funicular curve, we choose two adjacent points *b* and *c* as defined
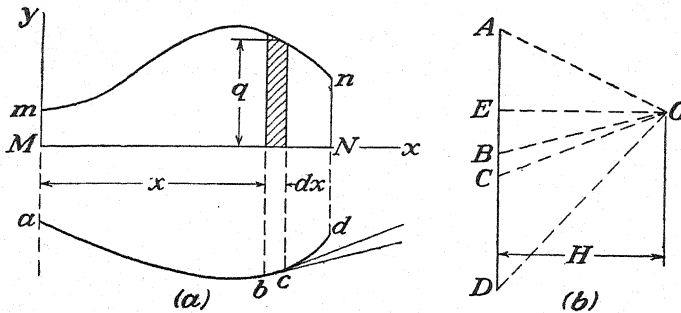
FIG. 54.

by the coordinates x and $x + dx$. The corresponding slopes can be represented by the expressions $\dfrac{dy}{dx}$ and $\dfrac{dy}{dx} + \dfrac{d}{dx}\left(\dfrac{dy}{dx}\right) dx$, respectively. Then from the relationships discussed in the preceding paragraph we have

$$\frac{dy}{dx} = \tan BOE = \frac{BE}{OE}, \qquad (a)$$

$$\frac{dy}{dx} + \frac{d^2y}{dx^2}\, dx = \tan COE = \frac{CE}{OE}. \qquad (b)$$

Subtracting (a) from (b), we obtain

$$\frac{d^2y}{dx^2}\, dx = \frac{BC}{OE} = \frac{q\, dx}{H},$$

which reduces to

$$H\frac{d^2y}{dx^2} = q. \qquad (3)$$

This is the differential equation of a family of funicular curves corresponding to the arbitrary *pole distance H*. For any particular distribution of load as defined by the function q, the corresponding family of curves can be found by integration of this differential equation.

For the particular case of uniformly distributed vertical load, the intensity q is a constant, say q_0, and the solution of Eq. (3) becomes

$$y = \frac{q_0 x^2}{2H} + C_1 x + C_2. \qquad (c)$$

This solution represents a family of parabolas with vertical axis, identical except for position. If we take the vertex c of the parabola as the origin of coordinates, we have

$$(y)_{x=0} = \left(\frac{dy}{dx}\right)_{x=0} = 0$$

This requires $C_1 = C_2 = 0$ in Eq. (c), and we obtain

$$y = \frac{q_0 x^2}{2H}. \tag{d}$$

As a second example, we shall discuss briefly the configuration of equilibrium of a heavy flexible chain supported at a and b as shown in Fig. 55 and hanging freely under
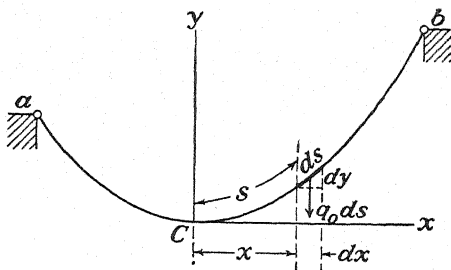
FIG. 55.

its own weight. If q_0 denotes the weight of chain per unit length, we have $q = q_0 ds/dx$ and, for the coordinate axes shown in the figure, Eq. (3) becomes

$$H \frac{d^2 y}{dx^2} = q_0 \sqrt{1 + \left(\frac{dy}{dx}\right)^2}.$$

The solution of this differential equation is

$$y = \frac{H}{q_0} \left[\cosh\left(\frac{q_0 x}{H}\right) - 1 \right], \tag{e}$$

which defines the configuration of equilibrium of the chain. The curve is called a *catenary* and can be constructed easily by using numerical tables for cosh $(q_0 x/H)$. A useful relationship between the coordinate s measured along the curve and its projection x is given by the equation

$$s = \frac{H}{q_0} \sinh \frac{q_0 x}{H}. \tag{f}$$

Verification of this relationship is left as an exercise for the student.

PROBLEMS

36. Prove that if only the first two terms of the power series for cosh $q_0 x/H$ are used in Eq. (e) then this equation of the catenary reduces to the equation of a parabola.

37. A flexible chain 100 ft. long and weighing 500 lb. is freely suspended between equally elevated supports A and B, which are 50 ft. apart. Find the sag f at the middle point C.

38. Referring to Fig. 55, show that the tension in the chain at any point defined by the coordinate x is given by the formula
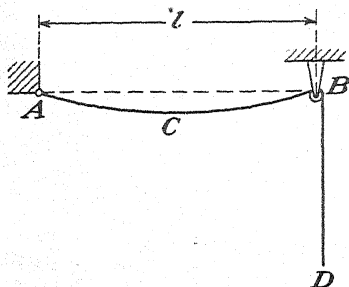
$$S = H \cosh \frac{q_0 x}{H},$$

where H is the tension at C and q_0 is the weight of chain per unit length.

39. Determine the shortest over-all length L of a flexible chain of uniform weight per unit length that can hang in equilibrium as shown in Fig. 56. Neglect friction, and assume that the radius of the pulley at B is very small.

Ans. $L_{\min.} = 1.14l + 0.80l = 1.94l.$

Fig. 56.

40. With reference to the coordinate axes shown in Fig. 57, develop the equation of the curve AOB that will be a funicular curve for the load diagram defined by itself and the line $y = -h$. Let wh be the intensity of load at O.

Ans. $y = h \left(\cosh \sqrt{w/H} \cdot x - 1 \right).$
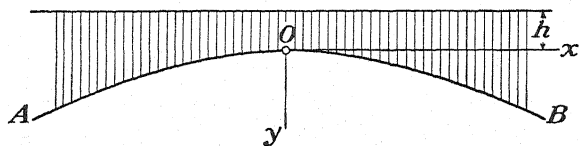
Fig. 57.

8. Graphical Construction of Bending-moment Diagrams.

—In previous articles, we have seen that the funicular polygon for a system of forces in a plane has a variety of practical applications. As a further
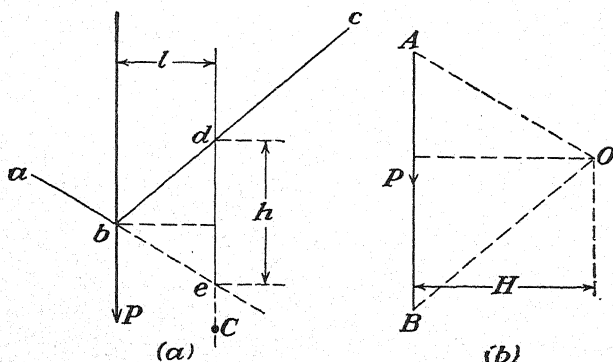
Fig. 58.

application, we shall now show how it can be used in the construction of bending-moment diagrams for transversely loaded beams.

Referring to Fig. 58, let P be a given force for which ab and bc are two adjacent sides of a funicular polygon corresponding to the pole O. Now through any point C (Fig. 58a) let a line be drawn parallel to P so that it

intersects the two sides of the funicular polygon in points d and e as shown. Then the *intercept* h of this line between the two adjacent sides of the funicular polygon, when multiplied by the *pole distance* H (Fig. 58b), represents the moment of the force P with respect to point C. That is,

$$Hh = Pl \qquad (a)$$

where H and P are measured to the scale of force (Fig. 58b) and h and l to the scale of length (Fig. 58a). This follows at once from the fact that triangle bde is similar to triangle OAB, and hence we may write

$$l:h = H:P,$$

which is equivalent to expression (a).

The above conclusion can be used also in the more general case of several parallel forces P_1, P_2, . . . in one plane as shown in Fig. 59. Assume, for example, that. corresponding to the pole O, the funicular

(a)   (b)
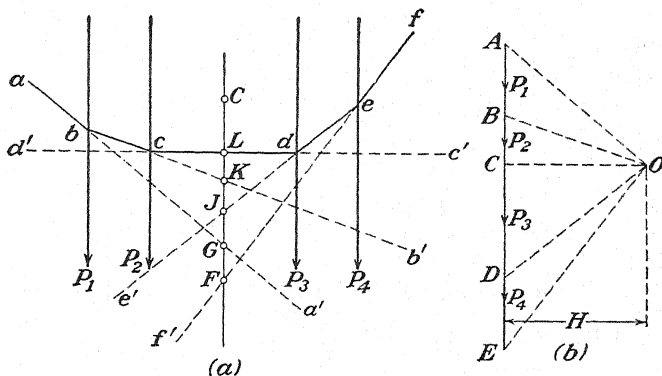
Fig. 59.

polygon $abcdef$ has been constructed in the usual manner. Now through any arbitrary moment center C we draw a line parallel to the lines of action of the given forces. Then the intercept of this line between any two sides of the funicular polygon, when multiplied by the pole distance H, represents the algebraic sum of moments, with respect to point C, of those forces included between the same two sides of the funicular polygon. Thus, for example, to obtain the algebraic sum of moments of all the forces with respect to point C, we take the product of the intercept $\overline{FG}$ and the pole distance H. Again, to obtain the algebraic sum of moments of the forces P_1 and P_2 with respect to point C, we take the intercept $\overline{GL}$ multiplied by H; for the moment of P_4, we take the intercept $\overline{FJ} \times H$, etc. The moment is positive or negative accordingly as the intercept is to the right or to the left of the intersection of the two lines that determine it. All this follows directly from Eq. (a) since the intersection of any two sides of the funicular polygon determines the line of

action of the resultant of those forces included between these two sides
and since the moment of the resultant is always equal to the algebraic
sum of the moments of its components.

Now, referring to Fig. 60, let us again consider a system of parallel
forces P_1, P_2, P_3, and P_4, for which *abcdef* is a funicular polygon cor-
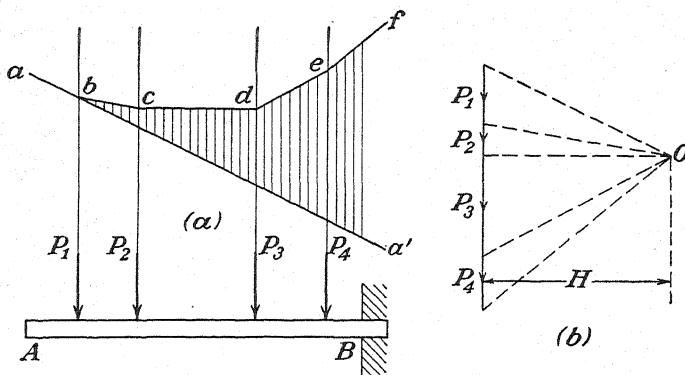
Fig. 60.

responding to the pole O. If, parallel to the lines of action of the forces,
we construct all intercepts between the first side aa' and the remainder
of the funicular polygon as shown, we obtain a *moment diagram*. Any
ordinate of this diagram, when multiplied by the pole distance H, repre-
sents the algebraic sum of moments of those forces to the left of that
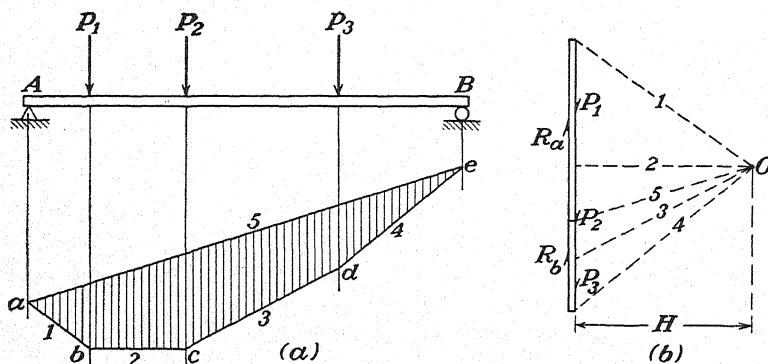
Fig. 61.

ordinate with respect to a point anywhere on the ordinate. This state-
ment follows directly from the discussion in reference to Fig. 59. Now,
in the case of a transversely loaded beam, we know that this idea of the
sum of moments of all forces to one side of a point is of particular value
because it defines the *bending moment* in the beam at that point. Thus,
the diagram shown in Fig. 60 can be considered as a bending-moment

diagram for a cantilever beam AB built in at B and submitted to the action of the forces $P_1 \ldots P_4$ as shown.

As a second example, let us consider the simply supported beam loaded transversely as shown in Fig. 61a. In this case, the closed funicular polygon $abcde$, which has been constructed in the usual manner for the purpose of determining the reactions R_a and R_b, may be used directly as a bending-moment diagram for the beam. It is necessary only to multiply each ordinate of the diagram by the pole distance H to have the corresponding bending moment. This follows from the fact that any ordinate of the diagram is simply the intercept between those two sides of the funicular polygon which intersect on the line of action of the resultant of all forces to one side of the intercept.
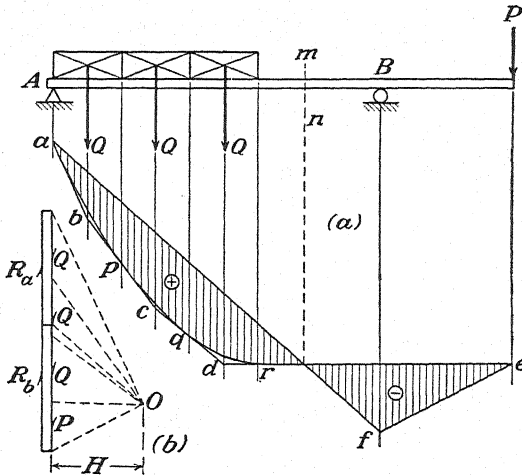
FIG. 62.

In the case of a beam under distributed load, we divide the load diagram into several finite portions as shown in Fig. 62 and then construct the closed funicular polygon $abcdef$ and determine the reactions R_a and R_b in the usual manner. Then, to have a bending-moment diagram for the beam, it is necessary only to inscribe the smooth curve $apqr$ corresponding to the distributed load and take the ordinates as shown. We see that in this case there will be a change in the sign of bending moment as we cross the section mn. As in the previous cases, the ordinates in Fig. 62a must be measured to the scale of length and then multiplied by the pole distance H, measured to the scale of force, before we obtain the true bending moment.

In the preceding examples, we have seen that a funicular polygon constructed for the purpose of determining the reactions at the supports of a beam can also be used as a bending-moment diagram. Sometimes

the situation can be reversed and the fact that such a funicular polygon is a bending-moment diagram can help us in the determination of reactions. Consider, for example, the compound beam shown in Fig. 63a, for which it is desired to determine graphically the reactions at the supports A, B, and D. We begin by constructing in the usual manner the funicular polygon *abcde* for the given loads P_1, P_2, and P_3 as shown. At this stage of the construction the rays 5 and 6 and the corresponding sides *ef* and *fa* of the closed funicular polygon for the entire system are
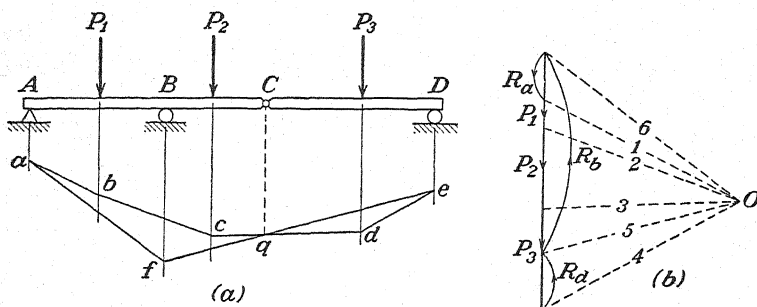
FIG. 63.

missing but the fact that there can be no bending moment in the beam at the hinge C enables us to find them. For, by this condition, we conclude that that side of the closed funicular polygon which is common to R_d and R_b must intersect the established side *cd* on the vertical through the hinge C, that is, at point q. Thus the side *ef* can be drawn, and thence the closing side *fa*. The corresponding rays 5 and 6 determine the reactions as shown.

PROBLEMS

41. For the beam shown in Fig. 64, construct a closed funicular polygon such that the ordinates of the diagram for bending moment thus obtained will be to the scale 1 in. = 1,000 ft.-lb.
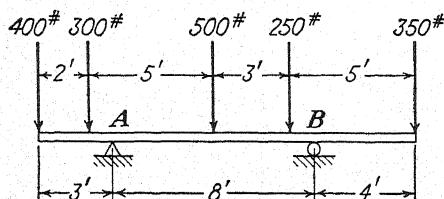
FIG. 64.

42. Prove that the shaded portion of the funicular diagram shown in Fig. 65 represents the bending-moment diagram for the beam AB, while the unshaded portion is the bending-moment diagram for CD.
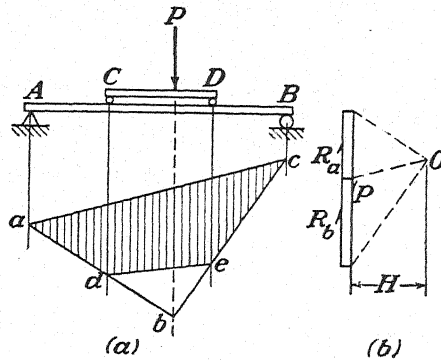
Fig. 65.

43. Construct the bending-moment diagram for the girder AB shown in Fig. 66. The loading is the first locomotive of a standard Cooper's E-60 train (see p. 94).
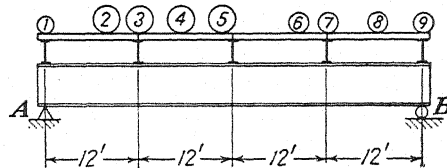
Fig. 66.

44. Determine, by means of a funicular polygon, the reactions at the supports A, B, E, and F of the compound beam loaded as shown in Fig. 67.
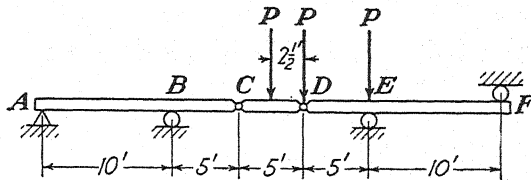
Fig. 67.

45. Referring to the three-hinged arch loaded as shown in Fig. 68, assume that a pole O has been so chosen that the corresponding funicular polygon $abcde$ passes
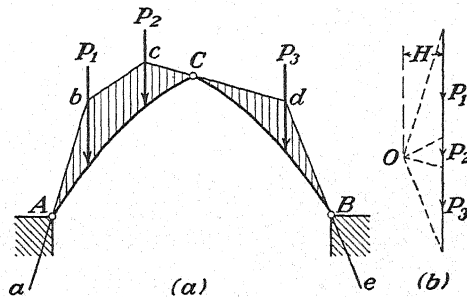
Fig. 68.

through the hinges A, C, and B of the arch as shown. Then prove that any ordinate of the shaded diagram, when multiplied by the pole distance H, represents the corresponding bending moment in the arch rib.

9. Principle of Virtual Displacements.—The various analytical and graphical methods of solution of problems of statics so far considered have been based on the principle of the *parallelogram of forces*. We shall now consider another general principle of statics called the principle of *virtual displacements*. In certain cases, methods of solution based on the latter principle have a decided advantage over any of those previously considered. The principle is perfectly general, but here we shall limit our discussion of its development and application to coplanar systems.
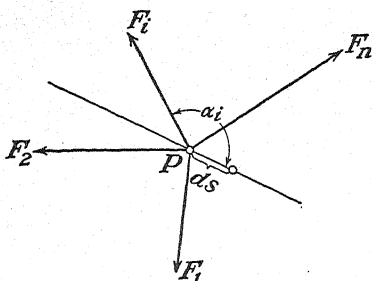
We begin with the case of a single *particle P* under the action of a system of concurrent forces F_1, F_2, . . . F_n in one plane as shown in Fig. 69. Imagine now that this particle is given a small arbitrary displacement ds as shown. Then any force F_i of the system is said to produce *work* on this displacement. This work is defined as the product of the displacement and the projection of the force on the direction of the displacement, *i.e.*, by the expression

$$ds \cdot F_i \cos \alpha_i. \qquad (a)$$

We see, by this definition, that the work will be positive or negative accordingly as the sign of the projection of the force agrees or disagrees with that of the displacement. The *net work* of all the forces, *i.e.*, the algebraic sum of expressions (a), may be written as follows,

$$\sum_{i=1}^{i=n} (ds \cdot F_i \cos \alpha_i) = ds \cdot \sum_{i=1}^{i=n} F_i \cos \alpha_i = ds \cdot R \cos \alpha, \qquad (b)$$

where $R \cos \alpha$ is the projection of the resultant R on the direction of the displacement. From expression (b), we conclude that the net work of the system of forces on any displacement ds of the particle is equal to the work of their resultant on the same displacement. Thus, if the net work of the forces on each of two orthogonal projections dx and dy of the displacement ds is zero, we conclude that the resultant force vanishes and the system is in equilibrium. Conversely, *if a particle is known to be in equilibrium, the algebraic sum of the works of all forces acting upon it must be zero for any arbitrary small displacement of the particle*. This is the principle of *virtual displacements*, or *virtual work* as it is sometimes called.

Fig. 69.

Now let us consider the case of a partially constrained particle, for example, a small bead that can slide along a smooth wire as shown in Fig. 70. In such a case, we distinguish between two kinds of forces acting on the particle; *active forces*, such as F_1, F_2, . . . F_n, and *reactive forces*, such as N, exerted on the bead by the wire. As a condition of equilibrium, we conclude that the algebraic sum of the work of all forces (both active and reactive) on any small dis-

placement of the particle must be zero. Suppose, however, that we agree to restrict such a displacement to one that is consistent with the constraint, *i.e.*, in the direction of the tangent to the wire at P.* Such an imaginary small displacement of the particle is called a *virtual displacement*, *i.e.*, a possible displacement, and it will be denoted by the symbol δs. If the wire is without friction, *i.e.*, an *ideal constraint*, the reactive force N

FIG. 70.

is normal to this virtual displacement δs and does not produce work. Thus, the work of all the forces is identical with the work of the active force alone, and we conclude that, *for any virtual displacement of an ideally constrained particle, the algebraic sum of the works of the active forces alone must be zero.* Reactive forces need not be considered at all.
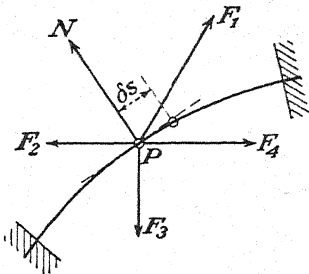
We come finally to the general case of a system of particles. It is in application to such systems that the principle of virtual displacements is of special value. As a specific example of a system of particles, let us consider two blocks A and B that rest on inclined planes and are con-

nected by a flexible but inextensible string overrunning a pulley as shown in Fig. 71. Neglecting friction in the pulley and on the inclined planes, we call this an *ideal system*. Here again we distinguish between active forces such as the weights P and Q and reactive forces such as N_a, N_b, and S. Further, we note that the reactive forces are of two kinds, those external to the system as a whole, like N_a and N_b, and those internal to the system, like the tensile forces S exerted on the particles by the string. A virtual displacement of the system, *i.e.*, a small change in position consistent with the constraints (both external and internal) will be obtained by giving to each particle an imaginary displacement δx along its supporting plane as shown. By virtue of the inextensibility of the
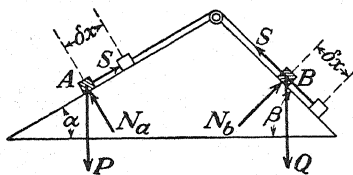
FIG. 71.

* Since the displacement is infinitesimal, an element of the axis of the wire of length ds may be considered as coincident with the tangent at P.

string, these displacements must be equal. Then, if the system is in equilibrium, each particle is in equilibrium, and the algebraic sum of the works of all forces on such a displacement of the system as a whole must vanish. However, the forces N_a and N_b, being normal to the inclined planes along which the particles move, do not produce work and need not be considered. Further, the forces S, being equal in magnitude, produce works of opposite sign, which cancel, and they also can be disregarded. Thus again, *for any virtual displacement of an ideal system of particles in equilibrium, the algebraic sum of the works of the active forces alone must be zero.* Applying this conclusion to the case in hand, we write

$$-P \sin \alpha \cdot \delta x + Q \sin \beta \cdot \delta x = 0,$$

which gives, as a condition of equilibrium of the system,

$$\frac{P}{Q} = \frac{\sin \beta}{\sin \alpha}. \tag{c}$$

To get the above result by the usual equations of equilibrium, we consider each particle separately and write

$$-P \sin \alpha + S = 0,$$
$$Q \sin \beta - S = 0.$$
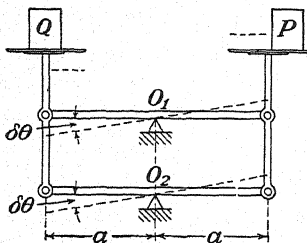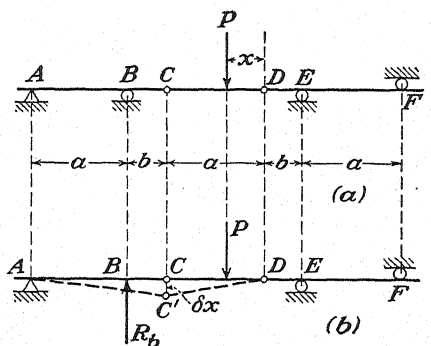
Fig. 72.   Fig. 73.

Then, upon eliminating S between these two equations, condition (c) is obtained. For a more complicated system of several particles, this latter method will require the writing of a number of simultaneous equations of equilibrium, the solution of which can become very complicated. In such cases, the method based on the principle of virtual displacements often proves to be the only practicable one.

The principle can be applied also to any ideally connected system of rigid bodies. Consider, for example, the system of levers arranged as shown in Fig. 72. To find the relation between P and Q for equilibrium, we note that a virtual displacement of the system can be defined by a

small angle of rotation $\delta\theta$ of the horizontal bars. The corresponding displacements of the gravity centers of the weights P and Q are independent of the positions of these bodies on the pans and are always equal. Hence, by the principle of virtual displacements, the weights P and Q must be equal for equilibrium.

Sometimes the principle of virtual displacements can be used to advantage in finding reactions. Consider, for example, the system of connected beams supported and loaded as shown in Fig. 73a. To find the reaction at B, we imagine that the constraint there is replaced by a vertical force R_b as shown in Fig. 73b. In this way we obtain a nonrigid system for which we have the problem of finding the relation between the forces P and R_b for equilibrium. A virtual displacement of the system can be completely defined by a small vertical displacement δx of the hinge C as indicated in the figure. The corresponding equation of virtual work becomes

$$P \cdot \frac{x}{a}\,\delta x - R_b\,\frac{a}{a+b}\,\delta x = 0,$$

and we find $R_b = Px(a+b)/a^2$. The reactions at the other supports can be found in a similar manner. The advantage of the method here lies in the fact that only one reaction need be considered at a time and no consideration need be given to the internal forces of the system. That is, we do not have to take the system apart and consider separate free-body diagrams for each of the beams AC, CD, and DF.

PROBLEMS

46. The platform scales shown in Fig. 74 are so constructed that the ratio P/Q for equilibrium is independent of the position of the load Q on the platform ED. Prove that, for this to be so, we must have $HF/HG = OC/OB$.
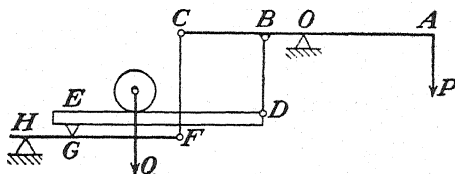
Fig. 74.

47. Using the principle of virtual work, calculate the ratio between the forces P and Q for equilibrium of the ideal system shown in Fig. 75. Each rhombus of the frame has the same dimensions.

Ans. $P/Q = \tfrac{1}{3}$.

48. A compound beam ACB is supported and loaded as shown in Fig. 76. Using the principle of virtual displacements, find the axial forces induced in the vertical bars 1 and 2.

Ans. $S_1 = -P,\ S_2 = +[Pb/(a+b)]$.
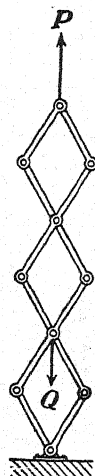
Fig. 75.
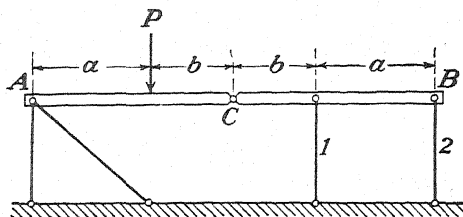
FIG. 76.

49. Calculate the reactions at the supports B, E, and F of the compound beam shown in Fig. 67 by the method of virtual work.

50. Using the principle of virtual displacements, find the horizontal and vertical components of the reactions induced at the supports A and B of the pin-connected frame loaded as shown in Fig. 77.   *Ans.* $X_a = -X_b = \sqrt{3}\,P$, $Y_a = Y_b = 2P$.
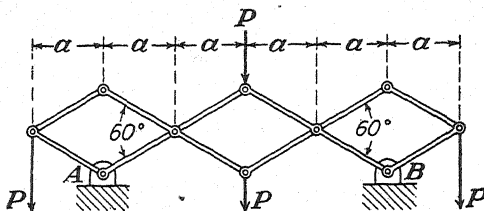
FIG. 77.

10. Virtual-displacement Diagrams.—We have seen that in applying the principle of virtual displacements to any system in equilibrium we need to evaluate a set of
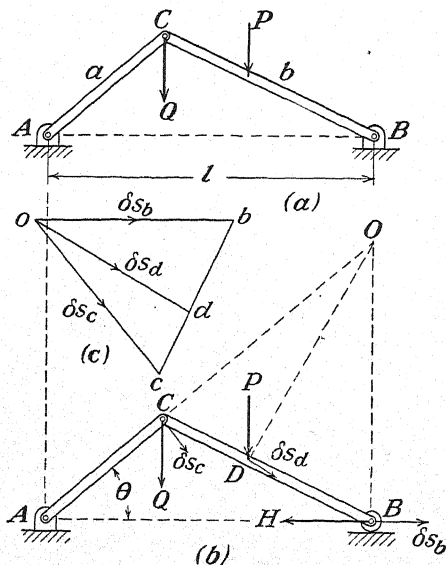
FIG. 78.

compatible displacements of all points of the system to which active forces are applied. Since this purely geometrical problem can sometimes present difficulty, we shall dis-

cuss here a graphical method of determining such displacements that can be used to advantage in the case of any coplanar system having one degree of freedom.

A system is said to have one degree of freedom if its configuration can be completely specified by one coordinate. Consider, for example, the simple frame supported and loaded as shown in Fig. 78a. This system is completely constrained in one plane; but if we remove the horizontal constraint at B and replace it by a force H that will maintain equilibrium, we obtain a system with one degree of freedom as shown in Fig. 78b. The configuration of this system is completely defined by the angular coordinate θ, and a virtual displacement of the system can be defined by a small change $\delta\theta$ in this coordinate. However, in applying the principle of virtual work to the system, we must have, instead of $\delta\theta$, the corresponding linear displacements δs_b, δs_c, and δs_d of the points B, C, and D at which the active forces are applied. The evaluation of the latter displacements can be greatly simplified by introducing the notion of the instantaneous center of rotation of the bar BC. In general, we know that any infinitesimal displacement of a rigid body in a plane can be produced simply by rotating the body around a certain fixed point called the *instantaneous center of rotation*.[1] For the bar BC, we find this point by noting that the end C of the bar must move in a direction perpendicular to AC while the end B moves horizontally. Such motion is equivalent to rotation of the bar about a point O determined by the intersection of a vertical line through B with the prolongation of AC. Owing to such rotation, the point D on the bar moves in the direction perpendicular to OD. Regarding the magnitudes of these displacements, we note that the displacement of point C is $\delta s_c = a\,\delta\theta$. Then, since the displacement of each point on the bar BC is proportional to its distance from point O, we conclude that

$$\left. \begin{aligned} \delta s_c &= a\,\delta\theta, \\ \delta s_b &= \frac{OB}{OC}\,a\,\delta\theta, \\ \delta s_d &= \frac{OD}{OC}\,a\,\delta\theta. \end{aligned} \right\} \qquad (a)$$

Upon using expressions (a), the equation of virtual work becomes

$$-H\frac{OB}{OC}\,a\,\delta\theta + P\cos\,(P,\,\delta s_d)\frac{OD}{OC}\,a\,\delta\theta + Q\cos\theta \cdot a\,\delta\theta = 0,$$

and we find

$$H = \frac{OC}{OB}\,Q\cos\theta + \frac{OD}{OB}\,P\cos\,(P,\,\delta s_d).$$

The ratios OC/OB and OD/OB and the angle $(P,\,\delta s_d)$ between the direction of the force P and the direction of the displacement δs_d can be found from the figure if it is drawn to scale.

If from a pole o (Fig. 78c) we construct vectors $\overline{ob}$, $\overline{od}$, and $\overline{oc}$, representing to a certain scale the displacements δs_b, δs_d, and δs_c respectively, we find that the figure $obdc$, so obtained, is geometrically similar to the figure $OBDC$, since corresponding sides are mutually perpendicular and their lengths are in a constant ratio. This relationship between the two figures holds in all cases of displacement of a body parallel to a plane, and such a figure as $obdc$ is called a *displacement diagram*.

The above-mentioned geometrical similarity being kept in mind, the displacement diagram can be constructed without the necessity of locating the instantaneous center O. For example, assuming an arbitrary length for the vector $\overline{oc}$ and keeping in mind that the vector $\overline{ob}$ is horizontal, we determine point b in the displacement diagram by

---

[1] See authors' "Engineering Mechanics," 2d ed., p. 449.

drawing cb perpendicular to CB. The vector $\overline{od}$ is obtained by taking point d on the line cb such that $cd:bd = CD:BD$. Thus the displacement diagram can be constructed without reference to the instantaneous center O.

By proceeding as above, the displacement diagram can be constructed in more complicated cases, also. Consider, for example, the system shown in Fig. 79a, the configuration of which is completely defined by one coordinate θ. Assuming a small change $\delta\theta$ in this coordinate, the corresponding virtual displacements of all points of the system can be found by constructing a displacement diagram as shown in Fig. 79b. We begin with the vector $\overline{oa}$ perpendicular to O_1A and representing an arbitrary displacement δs_a of the point A. The corresponding displacement δs_b of the point B must be perpendicular to O_2B, and we determine the vector $\overline{ob}$ representing this displacement by constructing ab perpendicular to AB. Next, the vector $\overline{oc}$, representing the displacement δs_c of point C, is determined by choosing point c on the line ab so that $ac:cb = AC:CB$. We are now in a position to consider the displacements of points on the bar CE. Already having the displacement of point C and noting that the point D can move only horizontally, we establish the vector $\overline{od}$ representing δs_d simply by
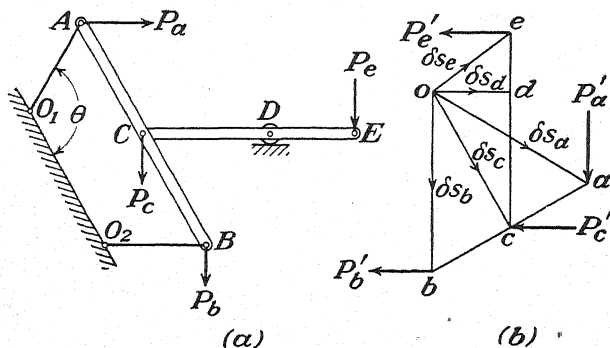
Fig. 79.

making cd perpendicular to CD. Finally, the vector $\overline{oe}$, representing the displacement of point E, is determined by extending the line cd to point e so that $ed:dc = ED:DC$. All displacements necessary for writing the equation of virtual work for the system can now be scaled from this diagram. Denoting by $(P_i, \delta s_i)$ the angle between any force P_i and the displacement δs_i of its point of application, this equation becomes

$$P_a \cos (P_a, \delta s_a) \cdot \delta s_a + P_b \cos (P_b, \delta s_b) \cdot \delta s_b + P_c \cos (P_c, \delta s_c) \cdot \delta s_c$$
$$+ P_e \cos (P_e, \delta s_e) \cdot \delta s_e = 0. \quad (b)$$

Considering the first term in expression (b), representing the work of the force P_a on the virtual displacement δs_a, we see that it can also be interpreted as the moment, with respect to point o, of a fictitious force P_a' applied at point a of the displacement diagram and turned clockwise by 90 deg. from the direction of the true force P_a at A. In the same manner, the other terms in expression (b) can be calculated by taking moments with respect to point o of fictitious forces P_b', P_c', and P_e', applied respectively at points b, c, and e of the displacement diagram as shown. Thus, considering the displacement diagram as a fictitious rigid body hinged to a support at O, it is seen that the equation of virtual work for the system can be interpreted as a moment equation of equilibrium for this figure. When so used, the displacement diagram is called a *Joukowski lever*.

As a specific application of the displacement diagram, we shall now determine the horizontal thrust H for a three-hinged arch loaded as shown in Fig. 80a. We begin by removing the horizontal constraint at B and replacing it by the reactive force H, thus obtaining a system with one degree of freedom as shown in Fig. 80b. In this system, the point C is constrained to move along the arc of a circle with center at A, while point B is constrained to move horizontally. A virtual displacement of the system compatible with its remaining constraints can be defined by giving to point C an infinitesimal displacement δs_c perpendicular to AC and represented by the vector $\overline{oc}$ in the displacement diagram (Fig. 80c). The remainder of this diagram is con-
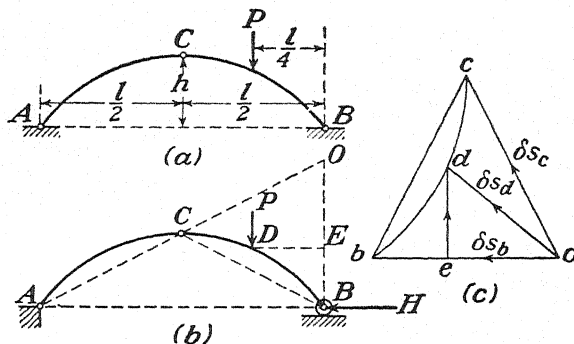
FIG. 80.

structed as explained above by making the figure bcd similar to BCD. The vector $\overline{od}$ then represents the total displacement of the point of application of the load P; and since this is a vertical force, we are interested only in the vertical component of this displacement as given by the vector $\overline{ed}$ in the displacement diagram. Applying now the principle of virtual work, we find

$$H \cdot ob - P \cdot ed = 0,$$

from which

$$H = P\,\frac{ed}{ob}.$$

From the geometric similarity between the displacement diagram obc and the figure OBC, we see that

$$H = P\,\frac{ED}{OB},$$

which, for the particular position of the load P shown in Fig. 80a, becomes

$$H = P\,\frac{l/4}{2h} = \frac{Pl}{8h}.$$

CHAPTER II

STATICALLY DETERMINATE PLANE TRUSSES

11. Simple Trusses.—The plane truss is one of the most important of all structural forms. In general, it may be defined as a system of bars all lying in one plane and joined together at their ends so as to form a rigid framework. Consider, for example, the two simple frames shown in Fig. 81. The rectangular frame, consisting of four bars pinned together
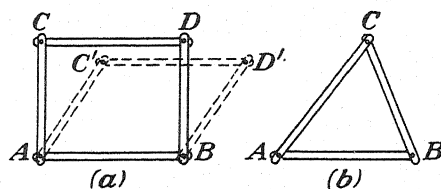
Fig. 81

at their ends as shown in Fig. 81a, obviously is not rigid but can be collapsed as indicated by dotted lines. The same conclusion holds for any other frame composed of more than four bars that are pinned together in the form of a polygon. On the other hand, three bars pinned together at their ends in the form of a *triangle* (Fig. 81b) constitute a rigid frame that cannot be collapsed. That is, neglecting possible small changes
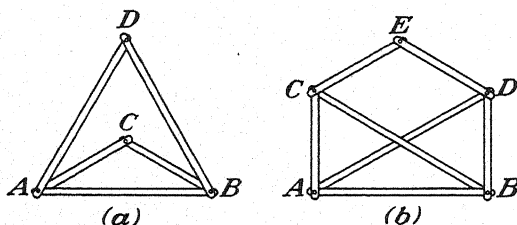
Fig. 82.

in the lengths of the bars, the relative positions of the pins A, B, and C cannot be changed. Thus the triangular frame alone behaves like a rigid body and may be considered as the simplest form of truss.

Beginning with a rigid triangle ABC (Fig. 82a) and attaching to this the bars AD and BD, which are pinned together at D, we obtain the rigid frame $ABCD$. This follows directly from the fact that the rigid triangle ABC together with the bars AD and BD are arranged in triangular form. In the same way, the rigid truss $ABCDE$ shown in Fig. 82b is obtained by

44

adding to the rigid portion $ABCD$ the two bars DE and CE, which are pinned together at E.

Since the procedure above may be continued indefinitely, we conclude that *a rigid plane truss can always be formed by beginning with three bars pinned together at their ends in the form of a triangle and then adding to these two new bars for each new pin.* Any system of bars assembled in accordance with this rule is called a *simple truss.* Figure 83*a*, for example, shows a truss of this kind. The triangle ABC has been taken as a rigid starting unit and the remainder of the joints D, E, F, and G established in alphabetical order, each by the addition of two bars to the existing system.

In Fig. 83*b*, we have a simple truss formed in accordance with a slight variation of the foregoing rule. In this case, instead of starting with a triangle, we begin directly with a rigid foundation (say a vertical wall) and establish the joints of the truss in alphabetical order, each by the addition of two bars to the existing system. This simple truss in Fig. 83*b* differs from that in Fig. 83*a* simply by the fact that it must be considered an integral part of its foundation, whereas the rigidity of the truss in Fig. 83*a* is quite independent of its attachment to any foundation.

Fig. 83.

It can easily be shown that, for each of the two variations of a simple truss as shown in Fig. 83, there must exist a very definite relationship between the number of bars, or *members*, m and the number of pins, or *joints*, j. In the case of the truss in Fig. 83*a*, we note that, exclusive of the starting triangle ABC, which contains three bars and three joints, there are two bars for each joint. Hence, we may write

$$m - 3 = 2(j - 3),$$

from which

$$m = 2j - 3. \tag{4a}$$

In the second case (Fig. 83*b*) the question of the starting triangle is eliminated, and we have simply

$$m = 2j. \tag{4b}$$

In this latter case the points of attachment to the foundation are not to be counted as joints.

In arranging the bars of a truss, the actual form in any situation will depend largely on the structural and architectural functions that
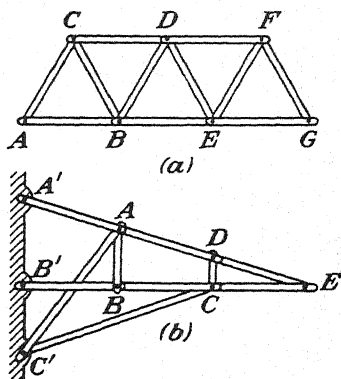
are to be served. There are many standardized forms of trusses for various types of structures, and several examples typical of roof and bridge construction are shown in Fig. 84. For each of these examples, the student should verify the fact that Eq. (4a) regarding the relationship between number of bars m and number of joints j is satisfied. At those
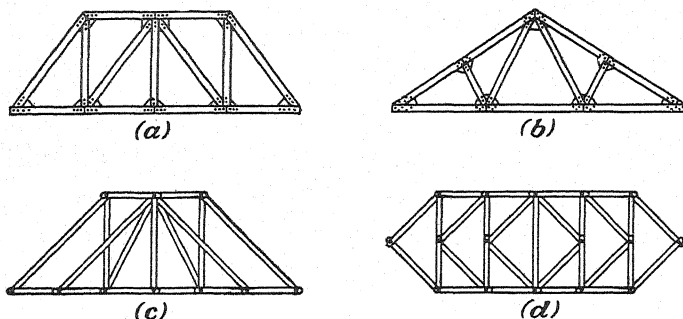
Fig. 84.

intersections where no connections are shown it is understood that the bars pass each other freely; such intersections should not be counted as joints. Welded or riveted joints as shown in (a) and (b) are the most common forms of connection in modern steel structures although pinned joints as shown in (c) and (d) are still to be found.

Essentially the function of every truss is simply that of a large beam to carry loads across an open span. In Fig. 85 we see a very simple low-
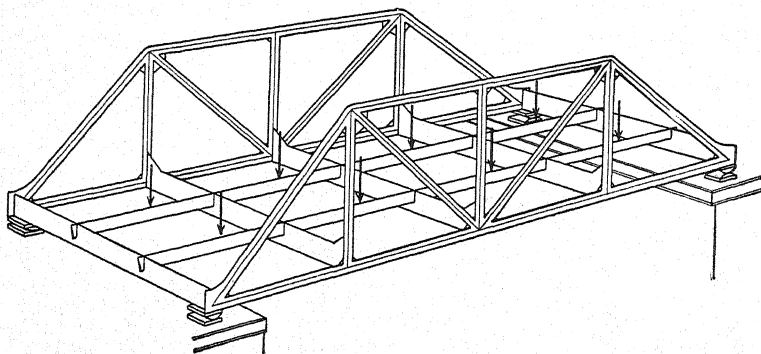
Fig. 85.

truss bridge, which will serve to illustrate this fundamental structural action of a truss. Here we have two identical parallel trusses supported at their ends on piers and carrying between them a floor system to which active loads can be applied. This floor system consists of *crossbeams*, supported between corresponding joints of the trusses, and *stringers*, which in turn are supported on the crossbeams. It is evident from such

construction that all loads applied to the floor of the bridge will be transmitted to the two trusses only at their joints.

Loads applied to the floor of the bridge as well as the weight of the bridge itself produce bending of the trusses principally in their own planes. Such plane bending of a truss is illustrated in Fig. 86*b*. The distortion of the truss as a whole results from slight changes in the lengths of the various members, and in each there is induced a corresponding tension or compression, *i.e.*, an *axial force*. The stress (force per unit area) corresponding to this axial force in any bar is called the *primary stress* in that bar.

In the case of a truss with riveted or welded connections (Fig. 86*c*), bending of the truss as a whole also induces some bending of the individual members due to the rigidity of the joints. Such bending of the bars of a truss superimposes additional bending stresses, which are called

Fig. 86.

secondary stresses; these must be investigated as a separate problem.[1] However, if the bars are carefully arranged so that their center lines meet in one point at each joint, we shall find that the presence of secondary stresses due to the rigidity of the joints does not materially affect the magnitudes of primary stresses. Thus, in calculating the latter, the rigidity of the joints can be ignored and *pinned joints assumed.* In this way we dispose temporarily of the necessity to distinguish between trusses with riveted joints and those with pinned joints.
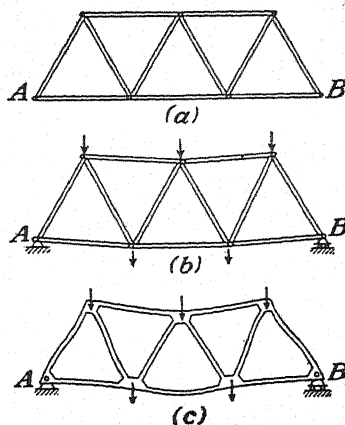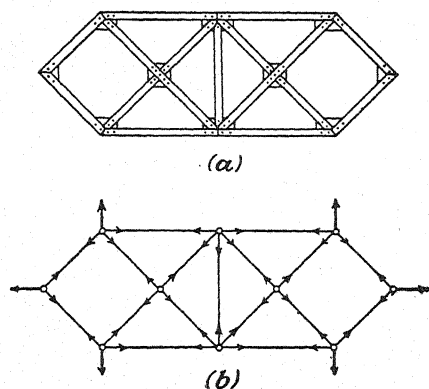
Fig. 87.

Even in the case of a truss that actually does have pinned joints, there will, of course, be some bending of the bars due to their own weights. This bending, however, is usually slight. It is common practice to ignore it and to replace the distributed weight of each bar by two equal concentrated forces on the joints at its ends; *i.e.*, the weight of the truss is assumed to be concentrated in its joints.

[1] See Art. 68, p. 398.

Finally, then, for purposes of analysis, we replace an actual physical truss (Fig. 87a) by a corresponding idealized truss (Fig. 87b) consisting of a system of weightless bars all lying in one plane and joined together at their ends by frictionless hinges to which external forces acting only in the plane of the truss can be applied. Under such idealized conditions, each bar is under simple tension or compression without bending, and consequently the two equal but opposite reactions that it exerts on the pins at its ends are collinear with the axis of the bar. Thus, at each joint of the truss we have in equilibrium a system of concurrent coplanar forces with known lines of action, and a determination of the magnitudes of these internal forces constitutes the analysis of the truss. However, before we can consider general methods of analysis of plane trusses we must first consider the question of support of a truss in its plane and the related problem of determination of reactions induced at such supports.
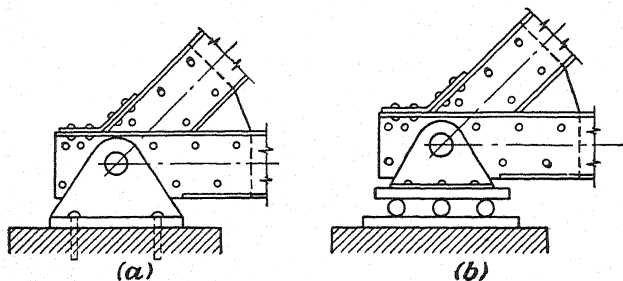
FIG. 88.

12. Reactions.—Any simple truss of the kind shown in Fig. 83b, being formed as an integral part of the foundation, is, of course, completely constrained in its own plane and can hold in equilibrium any system of external loads applied at its joints. However, to complete the constraint in one plane of a simple truss like that in Fig. 83a, we have yet to attach it to a foundation, either by additional bars or by other suitable supports. The most common procedure will be to anchor one point A to the foundation by means of a fixed hinge as shown in Fig. 86c. Such a constraint eliminates all possibility of translation of the truss; there remains only the possibility of rotation around point A. During such rotation, another point B could move only in a direction normal to the line AB. Hence, to complete the constraint of the truss in its own plane it is necessary not to fix the hinge B completely but only to support it on rollers that can move freely in one direction. If this one degree of freedom of the hinge B is incompatible with rotation about A, it follows that such rollers[1] complete the constraint of the truss in its plane.

[1] We assume that these rollers are on a special track that prevents upward as well as downward motion.

Practical means of attaining desired degrees of constraint in the support of actual trusses are shown in Fig. 88. Such details depend very largely on the size, weight, and span of the truss; the sketches shown here are intended to give only a general idea of their design.

Another general method of supporting a truss in its own plane is to attach it to the foundation by means of additional bars like its own members. The simple truss ABC shown in Fig. 89, for example, can be attached to the foundation in this manner by the three bars 1, 2, 3. In general, complete constraint of a truss in one plane can always be attained with three bars so arranged that their axes neither are parallel nor intersect in one point. This may be proved as follows: Imagine first that the truss in Fig. 89 is attached to the foundation by two bars AD and BE that are not parallel. Then points A and B of the truss can move, respectively, in directions normal to the axes of these bars. The result will be equivalent to a rotation of the truss around point G, where the axes of the bars AD and BE intersect. A third bar CF, which constrains point C to move in only one direction not compatible with rotation around point G (which means simply that the axis of the bar CF must not pass through point G), obviously completes the constraint of the truss in its own plane.
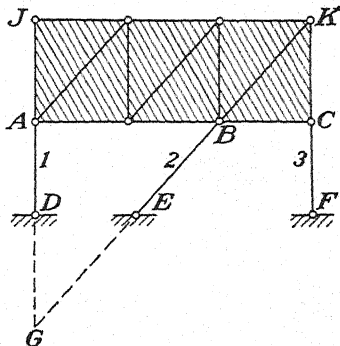
Fig. 89.
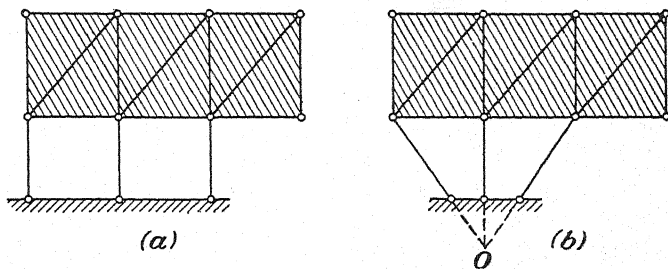
Fig. 90.

In the special case where the truss is supported by three parallel bars (Fig. 90a), it is self-evident that there is freedom for lateral movement and the truss is not completely constrained. In the same way, a truss supported by three bars the axes of which intersect in one point (Fig. 90b) is somewhat free to rotate about this point and is incompletely constrained. Thus, in general, three bars, the axes of which neither are parallel nor intersect in one point, are both necessary and sufficient for the complete constraint of a rigid truss in one plane.

Any supports of a rigid plane truss in excess of those both necessary and sufficient for complete constraint in its own plane are called *redundant supports*. For example, the truss supported by four hinged bars as shown in Fig. 91a is, of course, amply constrained in its plane; but since any one of these bars may be removed without destroying the complete constraint of the truss, any one of them may be considered as a redundant support. Similarly, it is evident that any one of the rollers by which the truss in Fig. 91b is supported may be considered as a redundant support; but not so with the bar *DE*, since without this the truss will be free to move horizontally.

When a simple truss, completely constrained in its own plane, is submitted to the action of a system of forces also in this plane, reactions are
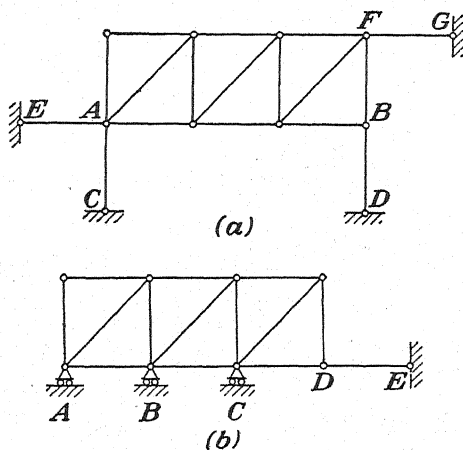
Fig. 91.

developed at the points of support and active forces together with reactive forces constitute a coplanar system of forces in equilibrium. For such a system of forces, we have three conditions of equilibrium as represented by Eqs. 2 (page 10), and hence we can determine not more than three unknown elements pertaining to the system of reactions. This, however, happens to be exactly the number of degrees of constraint required for completely fixing the truss in its plane. Thus, in the case of a simple truss supported in a manner both necessary and sufficient for complete constraint, we conclude that the reactions induced at the supports by any system of applied forces can be completely determined by equations of statics. For this reason, such a system of supports is said to be *statically determinate*. Methods of determining such reactions have already been discussed in Arts. 2, 3, and 5.

If the system of supports of a rigid plane truss involves more than three degrees of constraint, *i.e.*, if there are redundant supports as in

Fig. 91, the three equations of statics will be insufficient for determining the unknowns and the system is said to be *statically indeterminate*. In such a case, the way in which the loads transmitted through the bars of the truss are divided among the several supports depends on the elastic properties of the bars, and the reactions can be determined only by considering these properties.[1]

In special cases like those shown in Fig. 90, a system of supports in one plane, although involving only three degrees of constraint, will also prove to be statically indeterminate. Take, for example, the case shown in Fig. 90*b*, and suppose that the resultant of all active forces applied to the truss is a force which passes through the point *O*. Since the three reactions induced in the supporting bars must also intersect in this point, we have a system of concurrent forces in a plane for which there are only two independent conditions of equilibrium [Eqs. (1), page 2]. Thus the problem is statically indeterminate. On the other hand, if the resultant of all active forces applied to the truss is a couple, or a force that does not pass through point *O*, the situation will be quite different. In this case, if we decide to take point *O* as a moment center, we see at once that it will be necessary to have infinite forces developed in some of the supporting bars since, with zero-moment arms, the reactions exerted on the truss by these bars can in no other way develop a finite moment with respect to point *O* by which to balance the resultant moment of the applied forces. In such case, what actually happens is that the supporting bars deform (elongate or contract) sufficiently to allow the truss to rotate into a new position such that the axes of the three supporting bars no longer intersect in one point. Thus, the final configuration of equilibrium of the system and the corresponding forces developed in the three supporting bars depend on the elastic properties of the system, and we have again a statically indeterminate problem.

PROBLEMS

51. Find the reactions at *A* and *B* for each of the trusses supported and loaded as shown in Fig. 92.
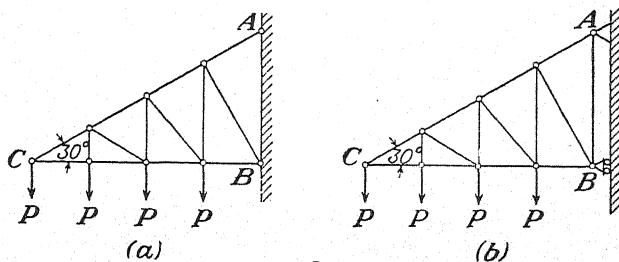
FIG. 92.

[1] This problem is completely discussed in Chap. VII.

52. Find the reactions at A and B for each of the trusses supported and loaded as shown in Fig. 93.
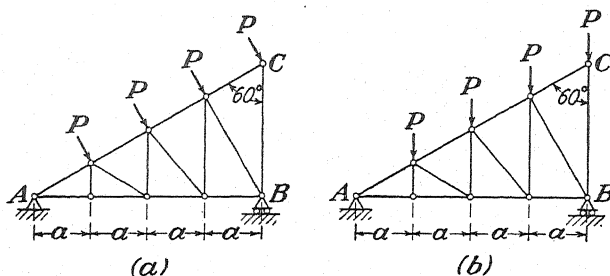
FIG. 93.

53. Find the reactions at A and B of the simple roof truss shown in Fig. 94: (1) when the truss is loaded as shown by the solid vectors and (2) when loaded similarly as shown by the dotted vectors.
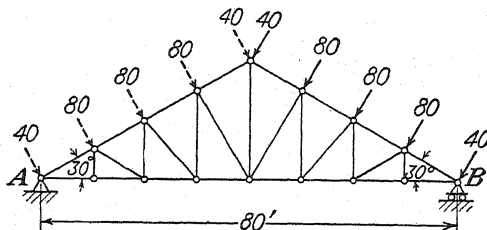
FIG. 94.

54. Find the axial force induced in each of the supporting bars 1, 2, 3, of the truss shown in Fig. 95: (1) when arranged as shown in (a) and (2) when arranged as shown in (b).
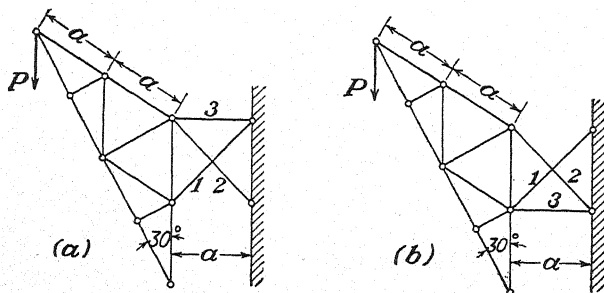
FIG. 95.

Ans. (a) $S_1 = -2.45P$, $S_2 = -3.87P$, $S_3 = +4.46P$; (b) $S_1 = +3.87P$,
$$S_2 = +2.45P, \quad S_3 = -4.46P.$$

55. What axial forces will be induced in the supporting bars of the truss in Fig. 89 by the action of a horizontal force P applied at joint K? Assume $AJ = AD = 12$ ft., $BC = 10$ ft.   *Ans.* $S_1 = 0$, $S_2 = 1.56P$, $S_3 = -1.20P$.

13. Method of Joints.—We shall now consider in detail the analysis of a simple truss ABC supported and loaded as shown in Fig. 96a. Owing to the applied loads P, vertical reactions each equal to $\frac{3}{2}P$ are induced at the supports A and B, and the truss as a whole is in equilibrium under the action of the balanced system of vertical forces shown. As was pointed out in Art. 11, these external loads induce axial forces in the various bars of the truss, and each bar in turn exerts on the hinges at its ends two equal but oppositely directed reactions having for their common line of action the axis of the bar. The magnitude of either of these reactions represents the axial force in the bar; and whether it is directed
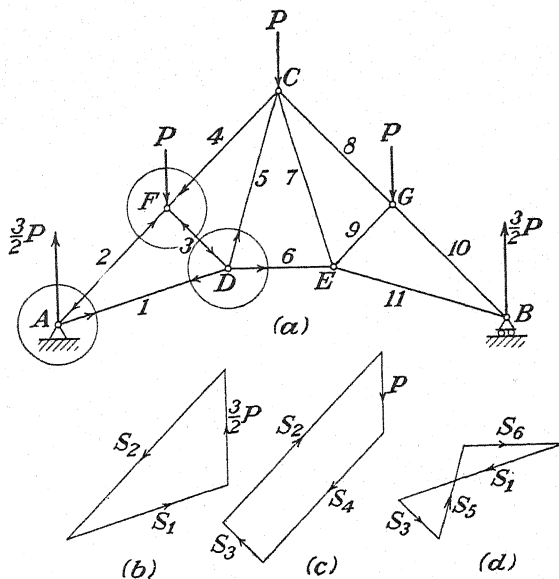
FIG. 96.

away from the hinge or toward it determines, accordingly, whether the bar is in tension or in compression. To avoid confusion in dealing with these internal forces, we shall number each bar of the truss as shown and then denote by S_i the magnitude of axial force in any bar i.

We begin the analysis of the truss in this case by consideration of the equilibrium of the hinge A. Taking this hinge as a free body as indicated by the circle around joint A, we find acting upon it the external reaction $\frac{3}{2}P$, together with the internal reactions S_1 and S_2 exerted, respectively, by the bars 1 and 2. We shall not know at once whether these last two forces should be directed away from the hinge or toward it, but only that their lines of action are represented by the axes of the bars exerting them. From this fact, however, a closed triangle of forces (Fig. 96b) can be constructed and the magnitudes of the forces S_1 and S_2 scaled or cal-

culated from this. Also, from the directions of the arrows, which must follow tail to head around the closed triangle of forces, we see that the bar 1 is in tension while the bar 2 is in compression. Arrows indicating such action can now be placed at A as shown.

We are now in a position to consider the equilibrium of the hinge F. We first replace the bar 2 by its known reaction S_2 directed toward the hinge F. There remain then but two unknown forces at F representing the reactions on this hinge of the bars 3 and 4. Again we do not know which way these last two forces should be directed; but, knowing their lines of action, we can construct the polygon of forces as shown in Fig. 96c. From this closed polygon, the magnitudes of axial force in the bars 3 and 4 can be found as before. In this case, we see from the arrows on
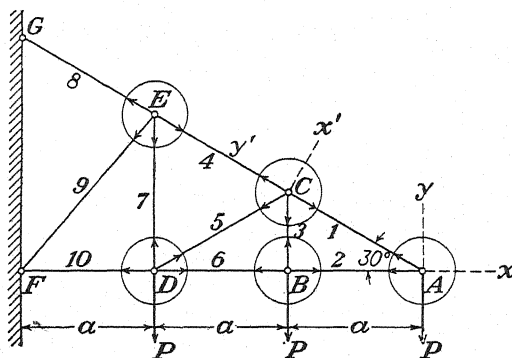
FIG. 97.

the polygon of forces that both bars are in compression, and arrows indicating such action can now be inserted in Fig. 96a.

Proceeding next to a consideration of the hinge D, the reactions exerted on this hinge by the bars 1 and 3 are already known, and again there remain only two bars (5 and 6) for which the axial forces are unknown. The closed polygon of forces for this hinge, from which S_5 and S_6 can be found, is shown in Fig. 96d. This completes the analysis of the truss in this particular case, for, owing to symmetry, it is evident that each bar on the right will carry the same axial force as the corresponding bar on the left.

If desired, the two equations of equilibrium [Eqs. (1), page 2] can be applied successively to the joints of a simple truss instead of constructing the various polygons of forces as was done above. This alternative will usually be preferable in cases where the angles between the bars of the truss are such that the projections of the forces are readily calculated. By way of illustrating this procedure, let us consider the simple truss supported and loaded as shown in Fig. 97. In applying equations of equilibrium in place of the graphical procedure above, it is

convenient to assume at the outset that all bars are in tension as indicated by the reactions directed away from the hinges in the figure. Then, automatically, results with the plus sign will indicate tension, while those with the minus sign will indicate compression. For example, we imagine the hinge A as an isolated free body acted upon by the three forces P, S_1, and S_2 directed as shown. Then, equating to zero the algebraic sums of projections of these forces on the orthogonal axes x and y, we obtain

$$-\frac{\sqrt{3}}{2} S_1 - S_2 = 0,$$

$$-P + \frac{1}{2} S_1 = 0,$$

from which $S_1 = +2P$ and $S_2 = -\sqrt{3}P$. Thus the bar 1 carries a tensile force equal to $2P$, while the bar 2 carries a compressive force equal to $\sqrt{3}\,P$. In using these values in subsequent calculations, the sign should be considered as an integral part of the result.

Upon proceeding to the hinge B and projecting all forces on the same orthogonal axes, the equations of equilibrium become

$$+S_2 - S_6 = 0,$$
$$-P + S_3 = 0.$$

Upon substituting for S_2 its previously determined value $-\sqrt{3}\,P$, these equations yield $S_3 = +P$ and $S_6 = -\sqrt{3}\,P$ (tension and compression, respectively). For the hinge C it will be most convenient to project all forces onto the orthogonal axes x' and y' directed as shown. For such axes, the equations of equilibrium become

$$-\frac{\sqrt{3}}{2} S_3 - \frac{\sqrt{3}}{2} S_5 = 0,$$

$$-S_1 - \frac{1}{2} S_3 + \frac{1}{2} S_5 + S_4 = 0.$$

Using $S_3 = +P$ in the first of these, we find $S_5 = -P$, after which the second equation gives $S_4 = +3\,P$. It is left as an exercise for the student to consider the hinges D and E and complete the analysis of the truss.

The foregoing procedure in the analysis of a simple truss is called the *method of joints*. It always can be applied either graphically or analytically to any truss the bars of which are assembled in accordance with the rule given on page 45, *i.e.*, to any *simple truss*. This follows from the fact that in any such truss there must exist at least one joint (the last one added in accordance with the rule) at which only two bars meet. Hence the axial forces in these two bars can be determined from the two conditions of equilibrium existing for that joint and the two bars

replaced by the reactions that they exert on two other hinges of the truss. Then, again, there must be one joint (the next to the last one established in accordance with the rule) where only two bars with unknown forces will be encountered and these forces can be determined. Thus, by considering the joints of the truss one by one in the reverse order from which they were established, we shall find at each joint only two bars with unknown forces, and the analysis proceeds without difficulty. It must be pointed out, of course, that it will often be necessary to determine the external reactions at the points of support as a separate problem before the analysis of the truss proper can be commenced.

PROBLEMS

56. Determine the axial force in each bar of the simple truss supported and loaded as shown in Fig. 92a.

57. Make a complete analysis of each of the simple trusses supported and loaded as shown in Fig. 93.

58. Referring to the roof truss shown in Fig. 94, make a complete analysis for each of the indicated conditions of loading.

59. Make a complete analysis, by the method of joints, of the simple truss shown in Fig. 98. All inclined bars are at 45 deg. with the horizontal.
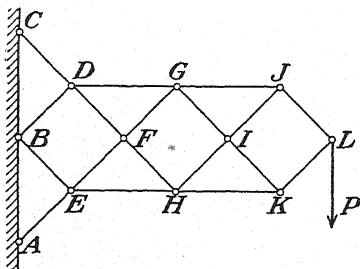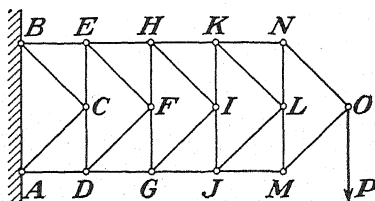
Fig. 98.　　　　　　　　　　　　Fig. 99.

60. Make a complete analysis, by the method of joints, of the K-truss shown in Fig. 99. The inclined bars are at 45 deg. with the horizontal, and the panel distances are uniform.

14. Maxwell Diagrams.—Referring to Fig. 96, in which the analysis of a truss has been made by constructing a separate force polygon for each hinge, we note that each axial-force vector appears in two different force polygons. To avoid this duplication of vectors, the separate polygons of forces, under certain conditions, can be superimposed to form one composite diagram called a *Maxwell diagram* for the truss. For example, the three polygons of forces shown in Fig. 96, when superimposed, make the composite diagram shown in Fig. 100b. Such superposition is desirable since it reduces the amount of necessary construction and also makes a more compact record of the final results. However, in order to avoid duplication of any vector the constructions must be carried out in a definite manner, which we shall now consider.

We begin with the simplest case of a triangular frame ABC, which is in equilibrium under the action of three external forces P, Q, and R acting in the plane of the triangle as shown in Fig. 101a.   These three forces,
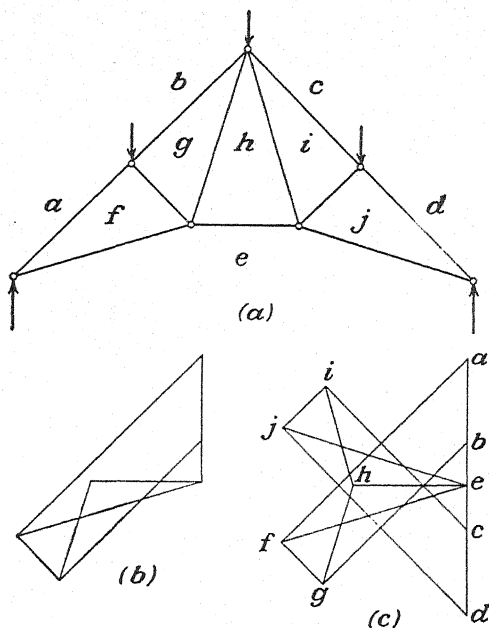
Fig. 100.

being in equilibrium, must intersect in one point D, and their free vectors must build a closed triangle abc as shown in Fig. 101b.   This done, a closed triangle of forces for each hinge can be superimposed directly on this triangle as shown.   For example, the vectors $\overline{ab}$, $\overline{bd}$, and $\overline{da}$ directed in accordance with the arrows inside the $\triangle abd$ represent the forces that are in equilibrium at the hinge A.   Similarly, $\triangle bcd$ and $\triangle cad$ with vectors directed in accordance with the inside arrows are closed triangles of forces for the hinges B and C, respectively.   Thus, in Fig. 101b, all triangles of forces are compactly superimposed, and no vector is duplicated.   This will be possible only if each polygon of forces has its vectors assembled in the same order by which the forces that they represent are encountered in going around the corresponding hinge consistently in one direction (either clockwise or counterclockwise).   We may note now that the basic triangle abc assembles the external forces in the order PQR obtained by going around the truss in a clockwise direction.   Thus, in the construction of the remaining force polygons that are superimposed on the $\triangle abc$, we must go around each hinge in a clockwise direction and take the forces in the order in which they are so encountered.   Only by this consistent procedure can we avoid duplication of some vectors.   For

example, if we go clockwise around the hinges B and C but counter-clockwise around the hinge A, we obtain the composite diagram shown in Fig. 101c, in which there is duplication of the vectors $\overline{bd}$ and $\overline{da}$.

A study of the diagrams in Figs. 101a and 101b shows that they bear a definite relationship to each other. In order to define this relationship
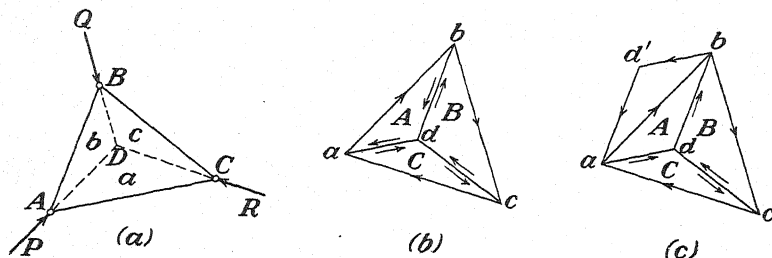
Fig. 101.

between the two figures, let us visualize each one as the plane projection of a four-faced polyhedron. The polyhedron in Fig. 101a, for example, has the faces ABD, ACD, BCD, and ABC, which we designate, respectively, by the lower-case letters a, b, c, d, and the vertexes, A, B, C, D. Similarly, the polyhedron in Fig. 101b has the faces abd, acd, bcd, and abc, designated by A, B, C, D, and the vertexes a, b, c, d. Thus, for each face of the polyhedron in Fig. 101a, there is a corresponding vertex to the one in Fig. 101b, for each vertex of the first, a corresponding face to the second, and their edges are mutually parallel and equal in number. Two such polyhedrons are said to be *reciprocal*, and the two plane figures representing their projections on a common plane are called *reciprocal figures*. It follows at once from such reciprocity that, if forces represented in magnitude by the lines of one such plane figure are made to act between the extremities of the corresponding lines of the reciprocal figure, then the points of the reciprocal figure will all be in equilibrium under the action of these forces. This follows from the fact that the forces meeting in any one point of the second figure are proportional to the sides of a closed polygon in the first figure. . This observation was made in 1864 by Clerk Maxwell in discussing the significance of reciprocal figures to problems of statics.[1] Because Maxwell was the first to point out the reciprocity between the diagrams like those in Fig. 101, the composite vector diagram is called a *Maxwell diagram* for the truss. For the truss in Fig. 100a, the complete Maxwell diagram is shown in Fig. 100c. In a more complex case of this kind it is practically impossible to visualize the corresponding polyhedrons, but this is of no consequence so long as the two diagrams fulfill the requirements of reciprocal figures.

[1] See CLERK MAXWELL, On Reciprocal Figures and Diagrams of Forces, *Phil. Mag.*, vol. 26, p. 250, 1864.

In the construction and use of Maxwell diagrams for the analysis of trusses, a system of notations called *Bow's notation* is convenient. In this system the spaces between the lines of action of the forces acting on the joints of the truss are each given a lower-case letter. Then any force is correspondingly designated by the letters of the two spaces separated by its line of action. Consider, for example, the simple truss supported and loaded as shown in Fig. 102a. In accordance with Bow's system, we letter the spaces between the five external forces a, b, c, d, e and those between the bars of the truss f, g, h, as shown. Thus, reading clockwise around the truss, we refer to the first load P on the left as $\overline{ab}$, the second as $\overline{bc}$, the external reaction at C as $\overline{de}$, etc. Likewise, the reaction of the
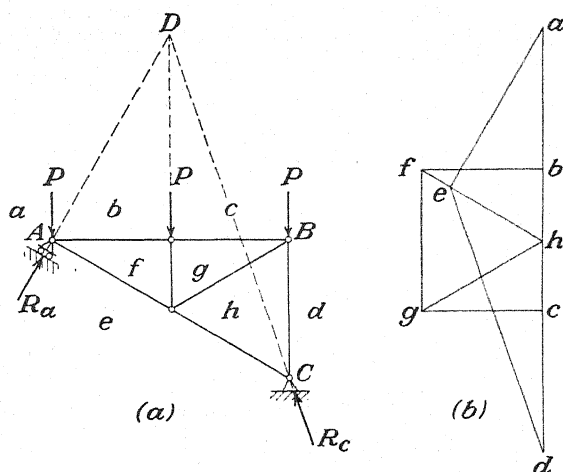
Fig. 102.

vertical bar on the hinge C is $\overline{hd}$; that of the horizontal bar on the hinge A is $\overline{bf}$; etc.

We are now ready to consider the construction of a Maxwell diagram (Fig. 102b), which begins with a closed polygon $abcde$ for the balanced system of forces external to the truss. With this basic polygon, the reciprocal diagram is completed simply by drawing through each of its vertexes lines parallel to all those which bound the corresponding space in the truss diagram. For example, through points b and e, we draw horizontal and inclined lines parallel, respectively, to AB and AC of the truss. Since these two lines also help to bound space f, their intersection determines the vertex f of the reciprocal diagram. Then, through points f and c, we draw vertical and horizontal lines, respectively, and their intersection determines the vertex g of the diagram. Finally, through points g and e, we draw the inclined lines whose intersection h on the line ad determine the final vertex, and the diagram is completed. The student

will do well to identify in this diagram the separate polygon of forces for each hinge of the truss.

Bow's notation is particularly advantageous when we come to decide whether a given bar of the truss is in tension or in compression. Let us consider, for example, the force in the bar BC that is represented in magnitude by the length of the line hd in the Maxwell diagram. Going around the hinge B in a clockwise direction, the reaction that this bar exerts on the hinge will be read as dh. Now, in the Maxwell diagram, the vector $\overline{dh}$ is directed upward, indicating pressure on the hinge B, and we conclude that the bar BC is in compression. If, instead, we choose to consider the reaction of this same bar on the hinge C, then, reading clockwise around C, we have hd instead of dh and in the Maxwell diagram the vector $\overline{hd}$ is directed downward, indicating pressure on C and consequently compression, as before.

PROBLEMS

61. Construct a Maxwell diagram for the truss shown in Fig. 103, and determine from it the axial force in each bar.
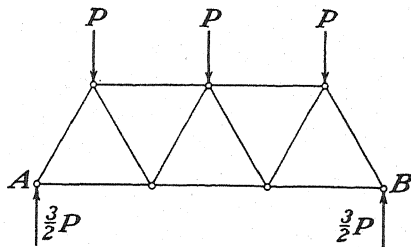
Fig. 103.

62. Construct a Maxwell diagram for the truss shown in Fig. 104, and determine from it the axial force in each bar.
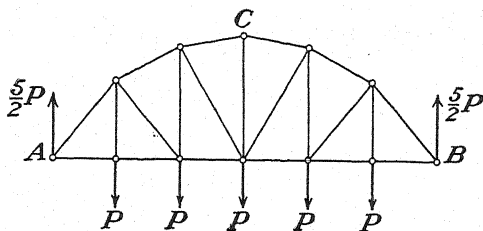
Fig. 104.

63. Construct a Maxwell diagram for the truss shown in Fig. 105, and determine from it the axial force in each bar.
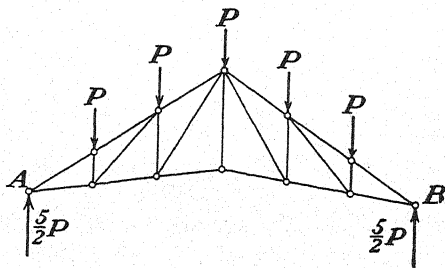
Fig. 105.

64. Construct a Maxwell diagram for the truss shown in Fig. 106, and determine from it the axial force in each bar.
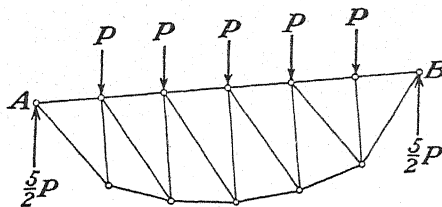
FIG. 106.

65. Construct a Maxwell diagram for the truss shown in Fig. 107, and determine from it the axial force in each bar.
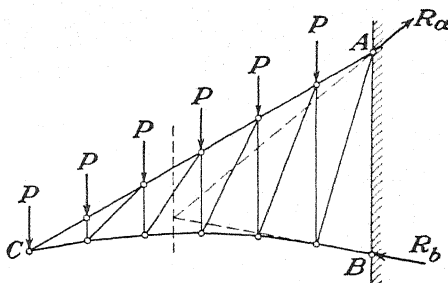
FIG. 107.

66. Construct a Maxwell diagram for the truss shown in Fig. 92b, and determine from it the axial force in each bar.

67. Construct a Maxwell diagram for each of the trusses shown in Fig. 93, and determine from the diagrams the axial forces in the various bars.

68. Construct a Maxwell diagram for each of the trusses shown in Fig. 95, and determine from the diagrams the axial forces in the various bars.

69. Construct a Maxwell diagram for the truss shown in Fig. 98.

70. Construct a Maxwell diagram for the truss shown in Fig. 99.

15. Method of Sections.—We shall now consider another method of analysis of trusses, the use of which makes it possible to determine the axial force in some chosen bar without going through successive considerations of the equilibrium of all hinges as was done in the two preceding articles. Referring to the truss shown in Fig. 108a, let us assume that it is required to determine the axial forces in the bars 10, 11, and 12, due to the loading shown. Instead of considering the equilibrium of the hinges A, H, B, I, C, and J in succession, as would be necessary by the method of joints, we imagine that a section mn cuts the truss into two parts and then consider the conditions of equilibrium of the part to the left of this section (Fig. 108b). Acting upon this free body we have the vertical reaction at A, three vertical loads P, and the three unknown forces S_{10}, S_{11}, and S_{12}, representing the axial forces in the bars that were

cut by the section mn. The directions of these forces must, of course, coincide with the axes of the bars so that only their magnitudes remain unknown. Thus we obtain altogether a system of coplanar forces in equilibrium, and Eqs. (2) (page 10) can be employed to determine the magnitudes of the three unknown forces. For example, equating to zero the algebraic sum of moments of all forces with respect to point D, we obtain

$$-S_{10} \cdot h + P \cdot a + P \cdot 2a + P \cdot 3a - \tfrac{7}{2}P \cdot 3a = 0,$$

from which $S_{10} = -9Pa/2h$. The negative sign, of course, indicates compression instead of tension as assumed. In a similar manner, by
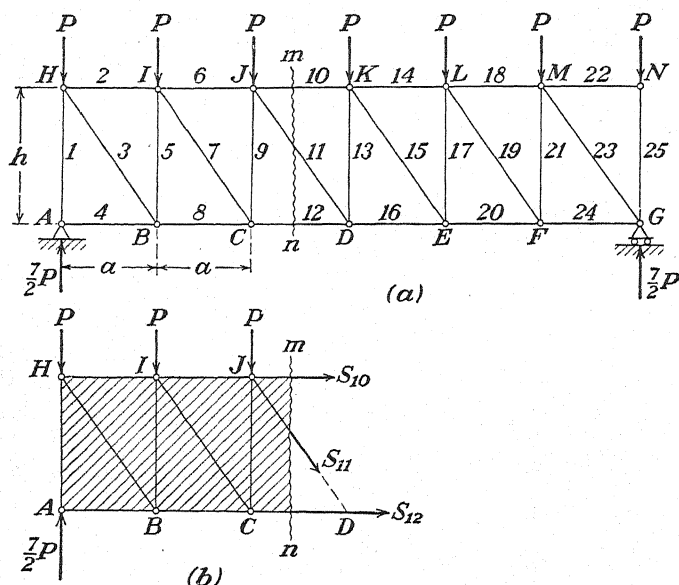
Fig. 108.

taking point J as a moment center, we find $S_{12} = +4Pa/h$. S_{11} can be evaluated most readily by equating to zero the algebraic sum of projections of all forces on a vertical axis. Thus we obtain

$$\frac{7}{2}P - 3P - S_{11} \cdot \frac{h}{\sqrt{a^2 + h^2}} = 0,$$

from which $S_{11} = +P\sqrt{a^2 + h^2}/2h$.

The foregoing procedure in the analysis of trusses is called the *method of sections*. It consists, essentially, in the isolation of a portion of the truss by a section so chosen as to cause those internal forces which we wish to evaluate to appear as external forces on the isolated free body. By this procedure, we usually obtain the general case of a coplanar

system of forces in equilibrium, and Eqs. (2) can always be used in evaluating the unknowns as was done above. The success or failure of the method rests entirely upon the choice of section. In general, a section should cut only three bars, since only three unknowns can be determined from three equations of equilibrium. However, there are occasional exceptions to this rule, some of which are illustrated below.

Sometimes, in order to obtain the desired results, it may be necessary to make more than one section or to use the method of sections in conjunction with the method of joints. Suppose, for example, that it is
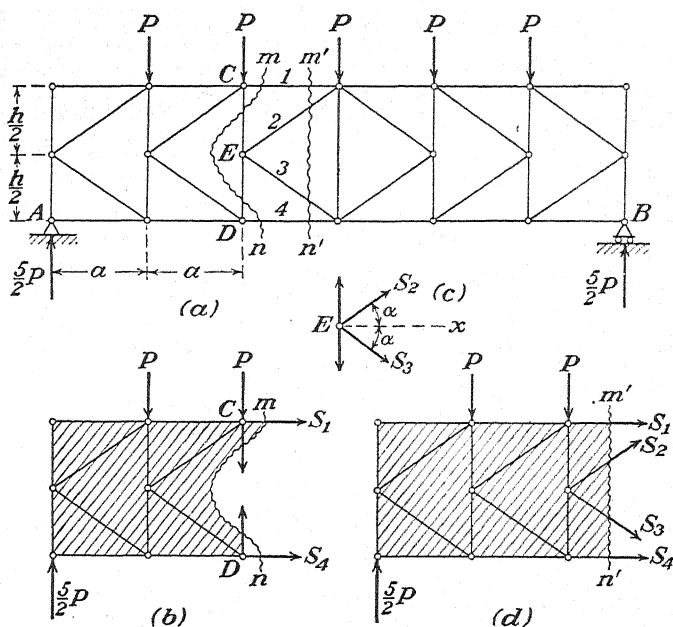
FIG. 109.

required to find the axial force in each of the bars 1, 2, 3, 4 of the simple K-truss shown in Fig. 109a. To accomplish this, we consider two sections and one joint as indicated by the free-body diagrams (b), (c), and (d). Beginning with Fig. 109b and using points D and C successively as moment centers, we obtain $S_1 = -4Pa/h$ and $S_4 = +4Pa/h$. Then, considering the equilibrium of the hinge E (Fig. 109c) and projecting all forces onto a horizontal x-axis, we conclude that the forces in the bars 2 and 3 must be of equal magnitude but opposite sign, i.e., $S_2 = -S_3$. Keeping this condition in mind and proceeding to Fig. 109d, we have only to project all forces onto a vertical axis to find $S_3 = -S_2 = \frac{1}{4}P \csc \alpha$.

It is sometimes advantageous to be able to employ the method of sections in a purely graphical manner; this can be done with very little

trouble. By way of illustration, we take the truss shown in Fig. 110*a* and assume that we wish to evaluate graphically the axial forces in the bars 1, 2, and 3. Then as a first step we consider the equilibrium of the entire truss and make the polygon of forces (Fig. 110*b*) and the corresponding funicular polygon (Fig. 110*c*) from which we find the reactions at the supports A and B as shown. This done, we isolate that portion of the truss to the left of the section *mn* and consider its conditions of equilibrium. It will be remembered from the discussion of Art. 8 that the resultant of all external forces to the left of section *mn* is a vertical force R acting through the intersection q of the sides 3 and 9 of the funicular polygon as shown. This follows from the fact that the rays 9 and 3 in Fig. 110*b* are components of R and must intersect on its line of action. Since the internal forces S_1, S_2, and S_3 must hold the force
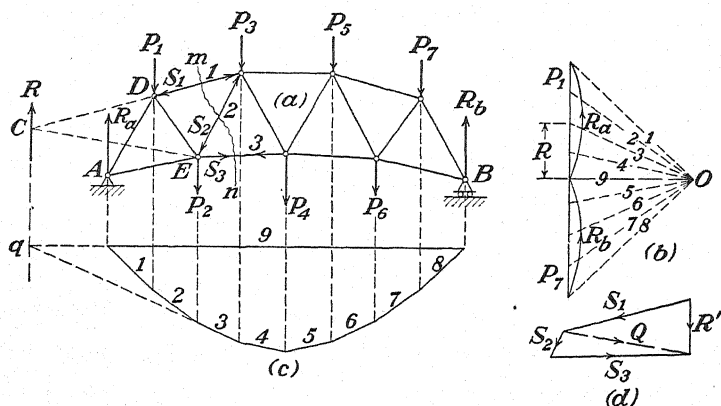
Fig. 110.

R in equilibrium, we see that our problem is simply one of resolution of a given force R' (the equilibrant of R) into three components having specified lines of action (the axes of the bars 1, 2, and 3). This is a completely determinate problem and may be carried out graphically as follows: In Fig. 110*a*, we extend the line of action of S_1 to its intersection C with the resultant force R. At this point the equilibrant of R can be resolved into two components acting along the lines CD and CE, respectively, and having the magnitudes S_1 and Q as shown in Fig. 110*d*. Then, in turn, the force Q can be transmitted to point E and there resolved into components S_2 and S_3 coinciding with the axes of the bars 2 and 3. Finally, ignoring the force Q, we have in Fig. 110*d* the closed polygon of forces for that portion of the truss to the left of *mn*.

Sometimes the analysis of a truss can be made in a very simple manner by considering it as a beam and using conventional bending-moment and shearing-force diagrams as discussed in Art. 4. Consider, for example,

the simple truss with parallel top and bottom chords loaded as shown in Fig. 111a. Making a vertical section mn and writing equations of equilibrium for that portion of the truss to the left of this section, we obtain

$$S_1 = -\frac{R_a \cdot 4a - P_1 \cdot 2a}{h}, \qquad (a)$$

$$S_2 = +\frac{R_a - P_1}{\sin \alpha}, \qquad (b)$$

$$S_3 = +\frac{R_a \cdot 3a - P_1 \cdot a}{h}. \qquad (c)$$

An examination of these equations now shows that the numerators represent, respectively, the bending moment at point E, the shearing force at
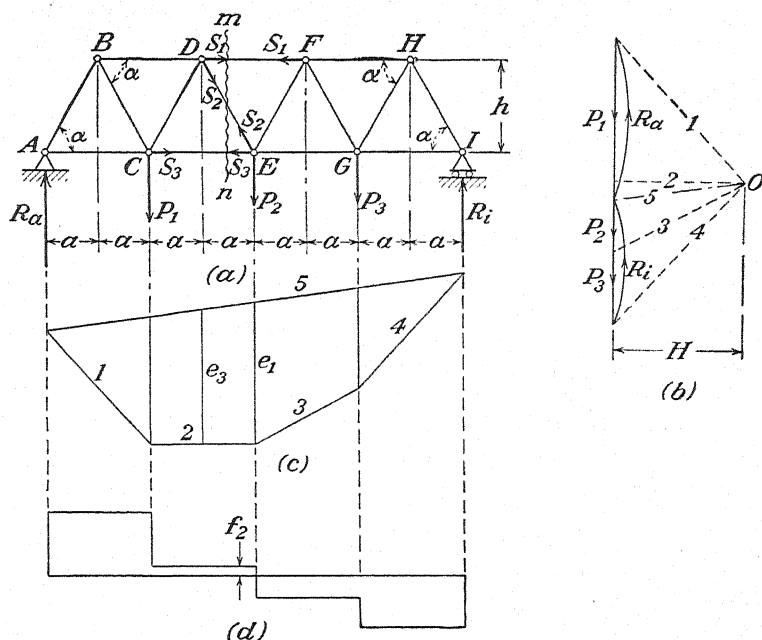
FIG. 111.

the section mn, and the bending moment at point D, when we consider the truss as a beam. The corresponding axial forces S_1, S_2, and S_3 are seen to be proportional to these quantities. Since similar conclusions may be reached for any section other than mn, we conclude that a bending-moment diagram and a shearing-force diagram are all that are needed for a complete analysis of the truss.

In such cases it is expedient to work graphically. First, we determine the reactions as shown in Fig. 111b and thereby we obtain the desired bending-moment diagram as represented by the closed funicular polygon

in Fig. 111c. A shearing-force diagram (Fig. 111d) can always be constructed without difficulty. As was shown in Art. 8, the bending moment for any point on the truss is obtained simply by multiplying the corresponding ordinate of the closed funicular polygon by the pole distance H. Thus, for example, the ordinate e_1 (Fig. 111c) when multiplied by H (Fig. 111b) gives the bending moment with respect to point E, *i.e.*, the numerator of expression (a). We conclude then that the force H when multiplied by the factor e_1/h gives directly the axial force S_1. Similarly, the force H multiplied by e_3/h gives the axial force S_3, etc. We obtain the force S_2 simply by multiplying the ordinate f_2 of the shearing-force diagram by the factor csc α.
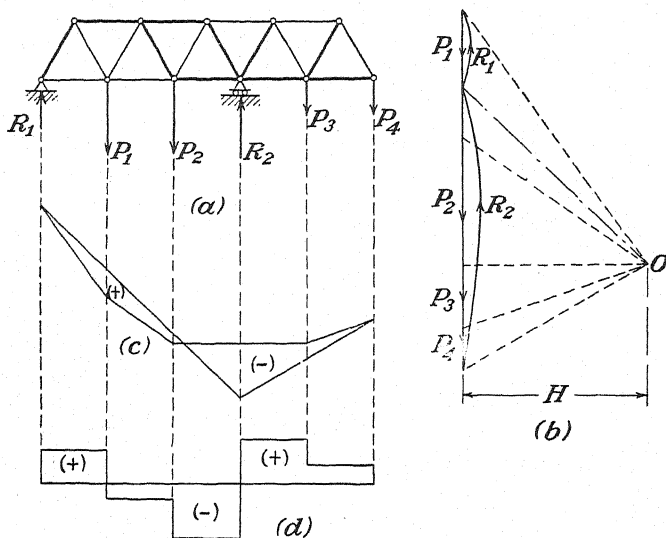
Fig. 112.

The bending-moment and the shearing-force diagrams for a truss are sometimes helpful in distinguishing between tension and compression members. In general, for trusses with parallel chords, it may be observed that, for positive bending moment, top chord members will be in compression and bottom chord members in tension like the extreme fibers of a beam. For negative bending moment, these conditions are simply reversed. For positive shear, web members sloping down to the right will be in tension, and those sloping up to the right will be in compression. For negative shear, these conditions also are reversed. An example, illustrating the foregoing remarks, is shown in Fig. 112. Here compression members are shown by heavy lines and tension members by fine lines. With the aid of the bending-moment and shearing-force diagrams shown below the truss, the student should verify these results for himself.

Another example is shown in Fig. 113. For a uniform loading of this truss, we see from the shearing-force diagram (Fig. 113b) that for the arrangement of web members shown in Fig. 113a we shall have tension in each diagonal and compression in each vertical, whereas, for the arrangement shown in Fig. 113c, these conditions will be reversed. For a steel truss, the arrangement in Fig. 113a is better because the short
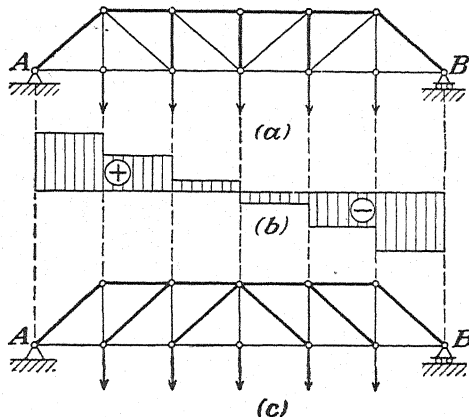
Fig. 113.

verticals can carry compression more efficiently than the longer diagonals, which may have a tendency to buckle. On the other hand, for a wooden truss, with respect to which the question of buckling is not likely to be significant, the arrangement of web members in Fig. 113c is ideal, especially if steel rods are used for the verticals.

PROBLEMS

71. Referring to Fig. 108 and using the method of sections, find the axial forces in the bars 2, 5, and 8. Assume $P = 10,000$ lb., $a = 9$ ft., $h = 12$ ft.
$$Ans. \quad S_2 = -1.875P, \ S_5 = -2.5P, \ S_8 = +1.875P.$$

72. Using the method of sections, compute the axial forces in the bars 1, 2, and 3 of the truss shown in Fig. 114. *Ans.* $S_1 = +2.25P, \ S_2 = -0.75P, \ S_3 = -2.25P.$
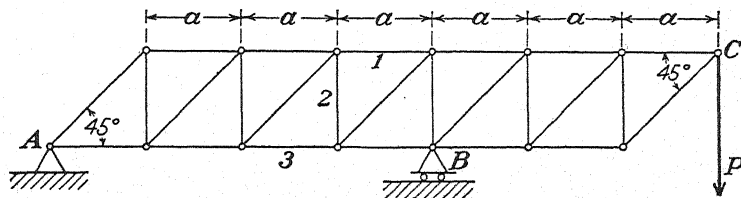
Fig. 114.

73. Construct bending-moment and shearing-force diagrams for the truss in Fig. 114, and distinguish between tension and compression members accordingly.

74. Make a complete analysis of the tower in Fig. 115 by the method of sections.
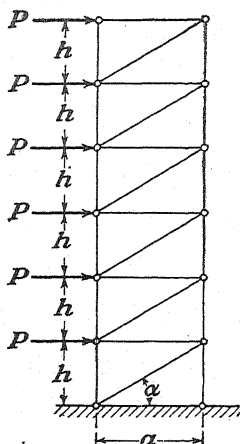
FIG. 115.

75. Using the method of sections, make a complete analysis of the truss in Fig. 103. All triangles are equilateral.

76. Referring to Fig. 116, prove that the axial force in the nth vertical from the free end is $S_i = -[(n-1)/2]P$.
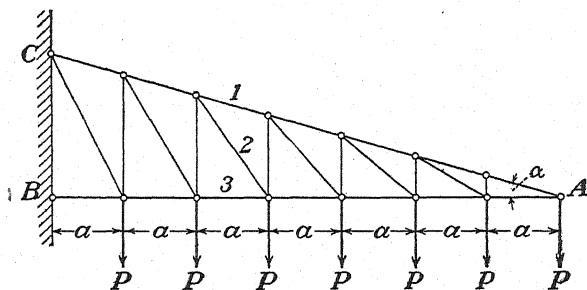
FIG. 116.

77. Analyze the truss in Fig. 99 by the method of joints and sections combined. The panel distances are uniform, and all inclined bars are at 45 deg. with the horizontal.

78. Referring to the tower in Fig. 115, show that the tension in the left-hand vertical of the nth panel from the top is $S_i = n(n-1)(Ph/2a)$.
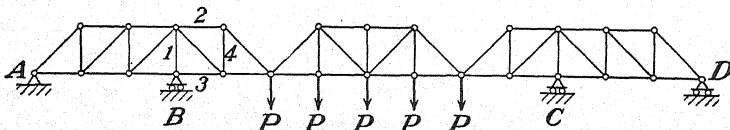
FIG. 117.

79. With the aid of bending-moment and shearing-force diagrams, distinguish between tension and compression members in the bridge loaded as shown in Fig. 117.

80. With the aid of bending-moment and shearing-force diagrams, distinguish between tension and compression members for the two trusses in Fig. 118.
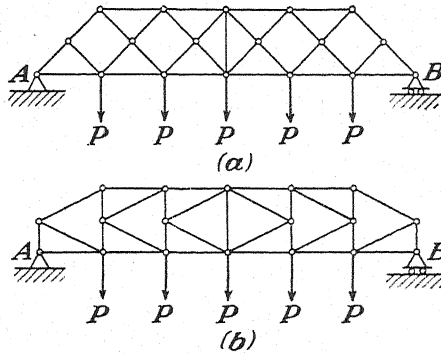
FIG. 118.

16. Compound Trusses.—In preceding articles we have considered only simple trusses formed in accordance with the rule given on page 45. Another kind of plane truss, called a *compound truss*, can be formed by interconnecting two or more simple trusses in accordance with the requirements for complete constraint of a rigid body in one plane (see page 49). The trusses in Fig. 119, for example, are of this kind. In
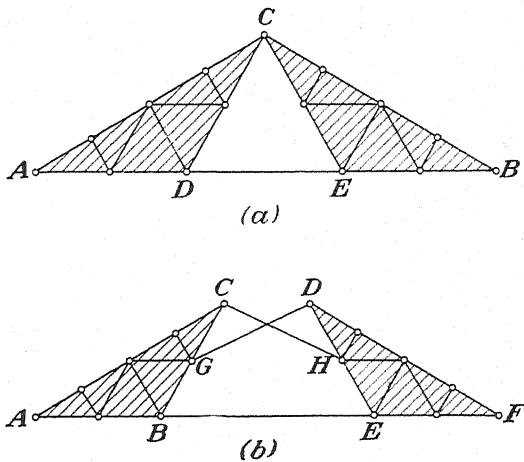
FIG. 119.

Fig. 119*a* two simple trusses *ADC* and *CEB* (shaded in the figure) are hinged together at *C* and otherwise interconnected by the bar *DE*. Likewise, in Fig. 119*b*, the same two simple trusses are interconnected by three bars so arranged that their axes neither are parallel nor intersect in one point. Although such interconnection of two simple trusses always makes a rigid and statically determinate system, it frequently

happens that such a truss cannot be completely analyzed by the method of joints alone.

Consider, for example, the compound truss shown in Fig. 120a, which consists of two shaded simple trusses hinged together at C and also connected by a bar DE. As a first step in the analysis of this truss, we determine the external reactions at A and B as shown in Fig. 120b. This done, we can find the axial forces in the bars 1, 2, 3, 4, without difficulty by the method of joints, but beyond this no progress can be made by this method because there is no joint where we encounter less than three unknown internal forces. Thus the shaded portion $DFCGE$ (Fig. 120b) does not lend itself to analysis by the method of joints, and
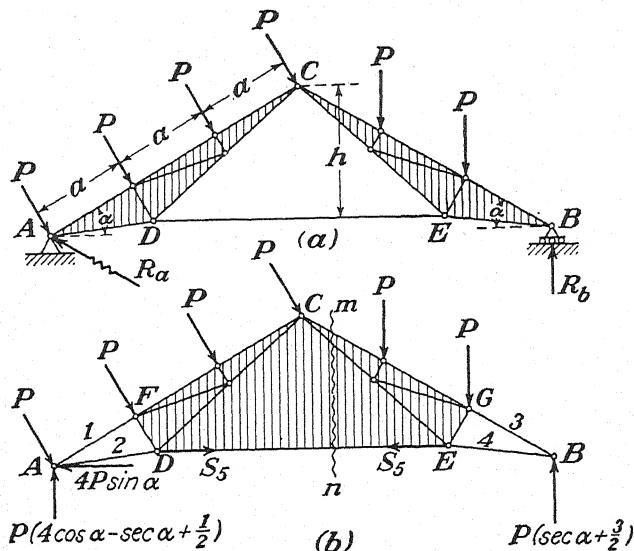
FIG. 120.

to proceed further we must resort to the method of sections. Making a section mn as shown and considering the equilibrium of that portion of the truss to the right of this section, we take C as a moment center and write

$$(P \sec \alpha + \tfrac{3}{2}P)3a \cos \alpha - Pa \cos \alpha - 2Pa \cos \alpha - S_5 \cdot h = 0,$$

from which $S_5 = +(3Pa/h)(1 + \tfrac{1}{2}\cos \alpha)$. As soon as S_5 is known, the analysis may be completed by the method of joints without further difficulty.

If we undertake to construct a Maxwell diagram for this truss loaded as shown in Fig. 121a, we shall, of course, encounter the same difficulty. As soon as the constructions indicated by heavy lines in Fig. 121c have been completed, we shall be unable to finish the reciprocal figure in the

usual manner. Consequently, to proceed further, we introduce the section mn as shown and complete the polygon of forces $efghi5e$ for that portion of the truss to the right of this section.   These constructions, indicated by dotted lines, are carried out as explained in connection with Fig. 110 (see page 64) and serve to establish the apex 5 of our reciprocal diagram.   Point 5 having been established, the remainder of the diagram as indicated by fine lines can be constructed in the usual manner without further difficulty.
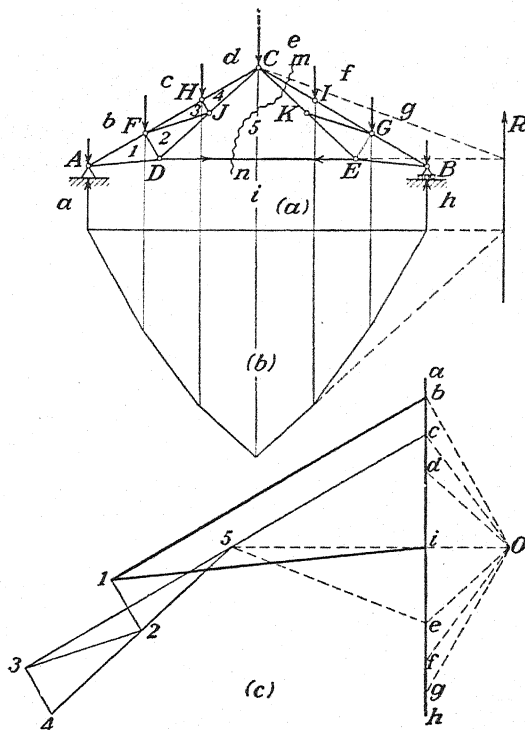
FIG. 121.

In Fig. 122a we have a compound truss for which the method of joints fails at the very beginning because there is no joint to which less than three bars are attached.   It also appears at first glance that there is no possibility of using the method of sections since we cannot make any section that cuts only three bars that do not meet in one point.   However, if we note that the truss consists essentially of two triangles AEF and BCD, which are interconnected by three bars that neither are parallel nor intersect in one point, we see at once how to proceed with the analysis. After the external reactions at A and B have been found as shown, we isolate the triangle BCD as shown in Fig. 122b.   In this way we obtain

a statically determinate system of coplanar forces in equilibrium and by using Eqs. (2) (page 10) can find the three unknown forces S_1, S_2, and

Fig. 122.

S_3 without difficulty. As soon as these forces are known, the remainder of the analysis can be made by the method of joints.

Another method of forming a compound truss, different from those considered above, is illustrated in Fig. 123. Here we have several simple trusses (shaded in the figure) that together with single bars are arranged in accordance with the rule for assembling the bars of a simple truss. It is obvious that any such arrangement of bars and simple trusses must constitute a rigid and statically determinate system. However, such compound trusses usually require special methods of analysis. We have already seen that compound trusses like those in Fig. 119 cannot be completely analyzed by the method of joints alone but that it is necessary to employ also the method of sections. Similarly, for a compound truss like that shown in Fig. 123, it may happen that the method of joints and the method of sections, even when used in conjunction, will
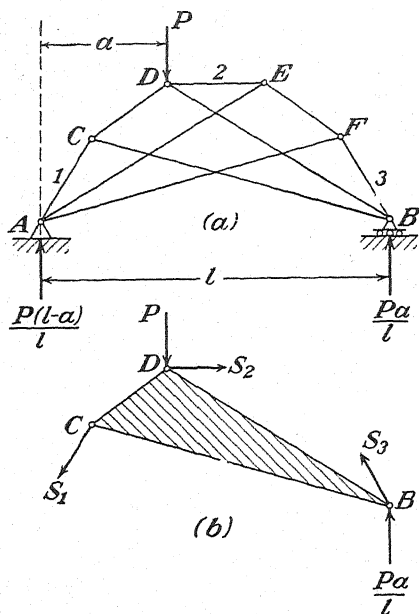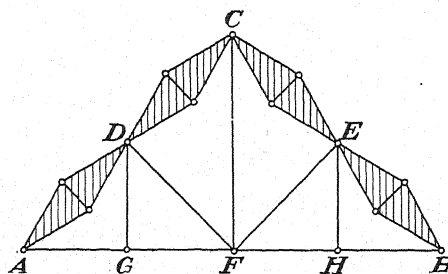
Fig. 123.

be inadequate for a complete analysis. A general method of analysis applicable to all such cases will now be considered.

Referring to Fig. 123, we note that the simple truss elements in this system really serve two functions. They act as single bars in the main truss, and at the same time they function as *secondary trusses* to transfer their own loads to the joints at their ends. By separating these two

functions, we always can make a complete analysis of the system without difficulty. In Fig. 124a, for example, suppose that ADE is a portion of a truss that has within it a secondary truss CE as shown. In the analysis of this system then, we first replace the secondary truss by a fictitious bar CE and the system of loads P_1, P_2, . . . acting upon it by a stati-cally equivalent system consisting of two parallel forces R_1 and R_2 at C and E as shown in Fig. 124b.[1] These substitutions will not affect any of the bars outside the secondary truss, and we may now proceed with the analysis of the main truss by any of the methods already discussed, thereby obtaining the axial force S in the fictitious bar. Now, from a study of Fig. 124b, it is evident that the forces shown at the hinges C and E must represent completely the ac-tion of the secondary truss on the remainder of the system. Hence, by reversing these forces, we obtain the reactions for the secondary truss as shown in Fig. 124c and can now make a complete analysis of this system. If there are other secondary trusses within the main truss, they may be handled in the same manner.
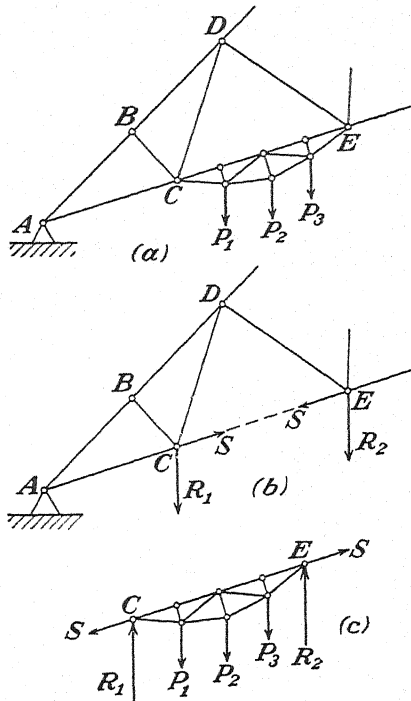
Fig. 124.

A specific application of the foregoing procedure is illustrated in Fig. 125, in which we have a roof truss with secondary trusses for top chord members. We begin our analysis by replacing the actual system of loads (Fig. 125a) by the statically equivalent system shown in Fig. 125b. This leaves the secondary trusses free from all loads so that they function simply as single bars, and we obtain a simple truss as shown. A Maxwell diagram for this system, from which the axial forces in all major members can be scaled, is shown in Fig. 125c. Thus we are ready to consider the secondary trusses. Taking AF as a typical example, we see that the external forces can be broken down into two balanced systems, (1) the loads P together with their vertical reactions at A and F and (2) the equal, opposite, and collinear forces S_1 found from the Maxwell diagram in Fig. 125c. Under the action of this latter system,

---

[1] Any coplanar system of forces can always be resolved into two parallel com-ponents applied at two given points in their plane of action.

only the top chord members will be active, and we already have the corresponding axial force in this chord from Fig. 125c. Hence, in the remaining analysis of the secondary truss, we ignore the forces S_1 and make a Maxwell diagram for the vertical loading only, as shown in Fig. 125e. To obtain the total force in any bar of the compound truss (Fig.
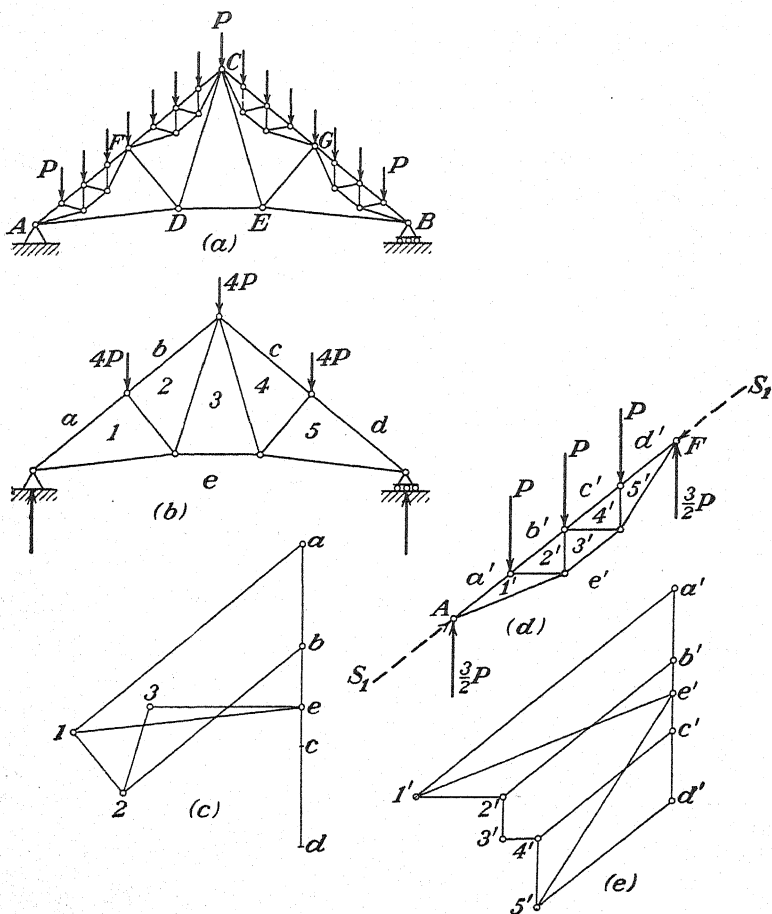
Fig. 125.

125a) we simply superimpose the results from the two separate Maxwell diagrams.

The foregoing method of analysis of a compound truss is sometimes useful even in cases where it is not strictly necessary. Consider, for example, the truss shown in Fig. 126a. Although not necessary in this case, the notion of secondary-truss action can be used to advantage. Proceeding on this basis, we regard ABC, loaded as shown in Fig. 126b,

as the basic truss. Superimposed upon this are the two secondary trusses ADE and BDF, loaded as shown in Fig. 126c. Each of these secondary trusses again can be regarded as consisting of a main truss ADE (Fig. 126d) that has within it two smaller trusses as shown in
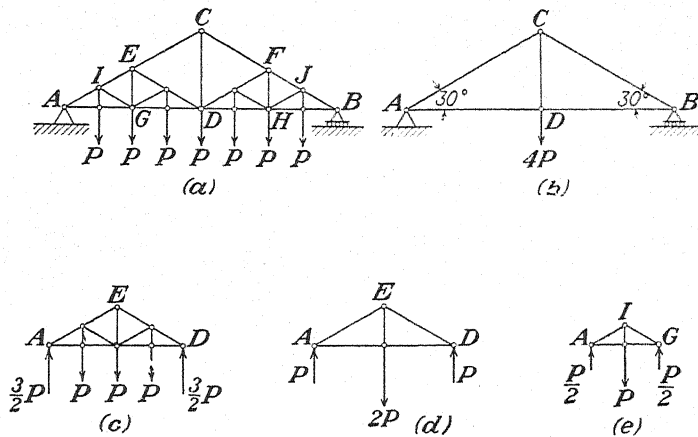
Fig. 126.

Fig. 126e. Finally, then, by making a simple analysis by inspection of each of the trusses in (b), (d), and (e) and superimposing the results, we obtain a complete analysis of the compound truss in (a).

PROBLEMS

81. Make a complete analysis of the compound truss shown in Fig. 127. The triangles ABC and DEF are equilateral.
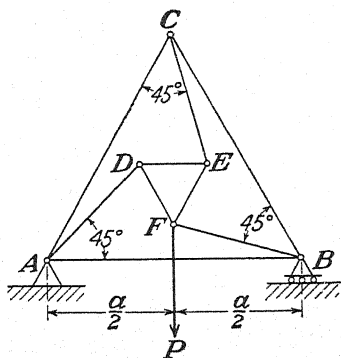
Fig. 127.
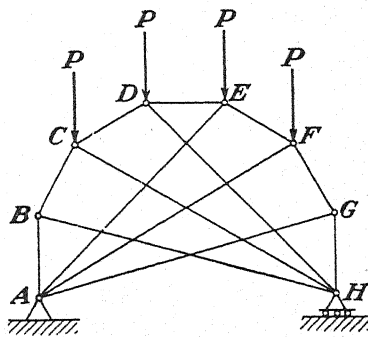
Fig. 128.

82. Make a complete analysis of the compound truss shown in Fig. 128. $ABCDEFGH$ is a portion of a regular duodecagon.

83. Make a complete analysis of the compound truss shown in Fig. 129.   Assume $P = 10$ kip.
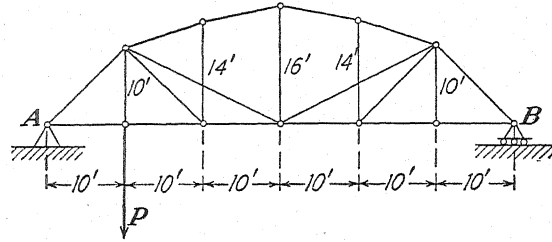
FIG. 129.

84. Make a complete analysis of the compound truss shown in Fig. 130a, and compare with that in Fig. 130b.
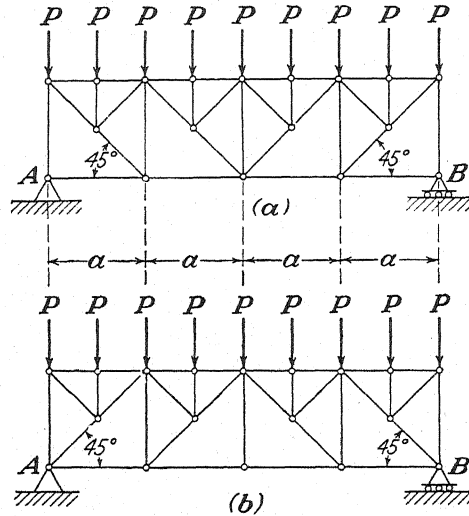
FIG. 130.

85. Make a complete analysis of the compound truss shown in Fig. 130b, and compare with that in Fig. 130a.

17. General Theory of Plane Trusses.—We return now to the general problem of assembling a system of bars in one plane so as to form a rigid truss.   In Art. 11 we have already seen that this can be done in two ways.   In one case we begin with three bars pinned together at their ends in the form of a triangle and attach each joint thereafter by means of two additional bars.   By this procedure we obtain a simple truss (Fig. 83a) for which there will always exist, between the number of members m and the number of joints j, the relationship

$$m = 2j - 3. \tag{4a}$$

The rigidity of such a truss is, of course, entirely independent of any attachment to a foundation. In another case, we begin directly with a foundation and establish each joint by means of two intersecting bars as shown in Fig. 83*b*. In this way, we obtain a simple truss the rigidity of which depends on its interconnection with points of the foundation and for which, instead of Eq. (4*a*), we have

$$m = 2j. \tag{4b}$$

As we have already seen in Art. 12, any simple truss of the first kind requires, for the completion of its constraint in one plane, three additional bars or their equivalent, while for any simple truss of the second kind the constraint is already complete. Thus in either case we come finally to the same conclusion: namely, for the complete constraint of *j*-pins in one plane we must interconnect them between themselves and the foundation by $m = 2j$ bars or equivalent constraints.

A great variety of plane trusses satisfying the foregoing general requirement of rigidity can be obtained by variously rearranging the bars of a simple truss in such a way that neither the total number of bars nor the total number of joints is changed. Consider, for example, the simple truss shown in Fig. 131*a*. Regarding this as a system of two simple trusses that are interconnected by three bars that neither are parallel nor intersect in one point, we conclude that we can substitute

Fig. 131

for the bar *CF* a bar *BH* and obtain the rigid truss shown in Fig. 131*b*. By this substitution we change neither the number of bars nor the number of joints, but we now have a compound truss instead of a simple truss.

As a second example, consider the simple truss shown in Fig. 132*a*. Replacing the bar *CG* by a bar *AD*, we obtain the truss shown in Fig. 132*b*. This arrangement of bars and external constraints still satisfies the relationship $m = 2j$ but otherwise fails to fulfill either the definition of a simple truss or that of a compound truss. Such a system is called a *complex truss*.
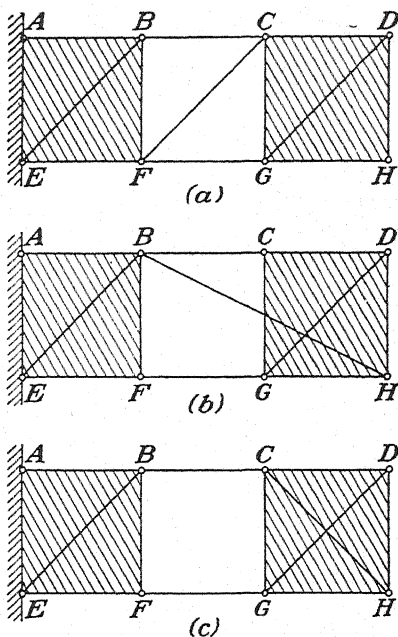
It must not be concluded from the foregoing discussion that we can indiscriminately interconnect $2j$ bars with j joints and expect to obtain a rigid system. That is, the condition $m = 2j$ is not alone a complete criterion of rigidity. Consider again, for example, the simple truss shown in Fig. 131a. If we remove the diagonal FC from the middle panel, we destroy the rigidity of the system and introduce the possibility of relative translation between the two rigid shaded portions. A bar BH as shown in Fig. 131b prevents such distortion and is therefore a legitimate substitute for the bar FC. In fact, as already noted, we now have a compound truss. On the other hand, if we replace the bar FC by a second diagonal CH in the end panel, as shown in Fig. 131c, we do not restore the rigidity of the truss; there is still the same freedom for relative translation between the two shaded portions. Thus, notwithstanding the fact that $m = 2j$, the system in Fig. 131c is not a rigid one. Accordingly, we conclude that we must modify our criterion of rigidity and say that $2j$ bars are necessary and, when properly arranged, sufficient for the rigid interconnection between themselves and the foundation of j joints in one plane.
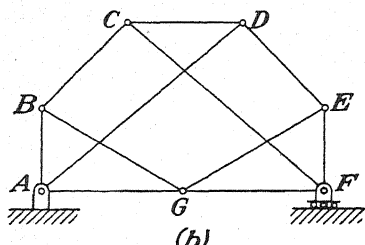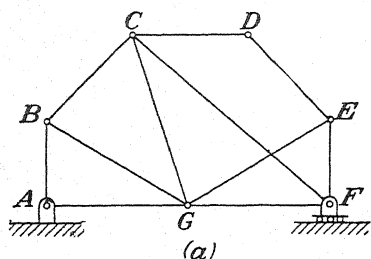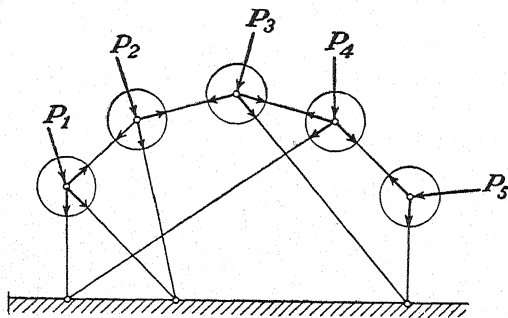
Fig. 132.

Fig. 133.

We shall now consider a further significance of the relationship $m = 2j$. In Fig. 133, we take any completely constrained plane truss (simple, compound, or complex) comprised of m bars and j joints and load it in its own plane and at the joints only as shown. Then, to make a complete analysis of the truss, we must determine the axial force in each of the m

bars.   Replacing each bar by the two equal but opposite reactions that it exerts on the pins at its ends, we obtain j systems of concurrent coplanar forces for each of which there exist two conditions of equilibrium [Eqs. (1), page 2].   Hence we have altogether $2j$ simultaneous equations involving m unknown axial forces; and we see that, if $m = 2j$, there are exactly as many unknowns as there are equations of statics.   Thus, in all but exceptional cases to be considered later, these equations give a definite solution to our problem.   For this reason any completely constrained plane truss that satisfies the condition $m = 2j$ is said to be *statically determinate*.   That is, the axial forces in the bars can be found from equations of statics alone; it is unnecessary to take account of the elastic deformations throughout the system.   Consider, for example, the system shown in Fig. 134a, for which $m = 2j$.   Under the action of a load P applied as shown, we see that the bars AC and AD are inactive, while BC and BD carry, respectively, tension and compression the mag-
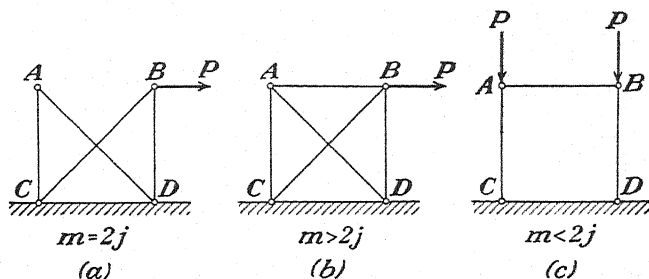
Fig. 134.

nitudes of which can be found from statical considerations of the hinge B. Owing to these internal forces BC will be slightly elongated, while BD will be shortened; consequently the joint B moves slightly downward and to the right, while the joint A remains stationary.   Thus the distance AB is greater after loading than before; but this small elastic distortion of the system does not affect the internal forces, and we need take no account of it.

If $m > 2j$, there will, of course, be more unknown axial forces than there are independent equations of statics and these equations fail to yield a unique solution.   Accordingly, the truss is said to be *statically indeterminate*.   Such a case is shown in Fig. 134b, which is identical with Fig. 134a except for the extra bar AB.   In this case, owing to the presence of the bar AB, the joint B cannot move relative to the joint A, as before, without stretching the bar AB and thus inducing some movement of A, also.   Thus part of the load P will be transmitted to the joint A, and the bars AC and AD also become active.   The way in which P is divided between B and A in this case depends on the relative rigidities of the bars.

...

For example, if AB is very flexible in comparison with the other four bars, then most of the load will be carried at B; in the extreme case where AB has no rigidity, all the load is carried at B as in Fig. 134a. On the other hand, if AB is relatively very rigid, it will remain practically constant in length and A and B will have to move about the same amount. Accordingly, the load will be about equally divided between these two joints. Thus we see that when a truss is statically indeterminate ($m > 2j$) the distribution of internal forces depends on the elastic deformations throughout the system and, to make an analysis, these deformations must be taken into account.[1]

If $m < 2j$ (Fig. 134c), the system is not rigid and can be in equilibrium only under certain conditions of external loading. That is, since there are more equations of statics than unknown axial forces, it follows that these equations will determine the unknowns and, in addition, impose certain limitations on the system of external loads. In Fig. 134c, for example, we can have equilibrium for vertical loads as shown, but any lateral loads will cause the frame to collapse.

In following the various rules of formation of plane trusses, already discussed, there is always the possibility of accidentally obtaining a so-called *critical form*, i.e., a
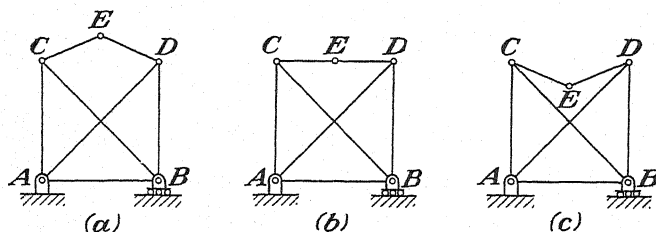
FIG. 135.

certain configuration of the truss that is nonrigid, whereas adjacent configurations are rigid. Sometimes these critical forms are self-evident; sometimes they are not. We consider first the obvious example of a critical form of the simple truss shown in Fig. 135. The configurations (a) and (c) of this truss are completely rigid but between them lies the possibility of the critical form (b). Here the bars CE and DE are collinear, and appreciable movement of the joint E relative to the other joints can result from the most minute changes in the lengths of the bars or from slight play in the hinges. In short, such a truss is not completely rigid. In the same way, the compound truss shown in Fig. 136a has a critical form when the bars 1, 2, and 3 are parallel as shown in Fig. 136b or intersect in one point as shown in Fig. 136c. In each of these latter cases, there is a limited freedom for relative lateral translation between the two shaded portions, and we must regard them as nonrigid forms. Such critical forms in the case of a compound truss are, of course, completely similar to the incompletely rigid systems of support illustrated in Fig. 90.

[1] Various methods of analysis of statically indeterminate trusses will be discussed in Chap. VII.

Another peculiarity of the critical form is that it is always statically indeterminate notwithstanding the fact that the condition $m = 2j$ is satisfied. Consider, for example, the critical form of simple truss shown in Fig. 135b. Loaded as shown in Fig. 137a, this system behaves like the truss in Fig. 134b, and we conclude accordingly
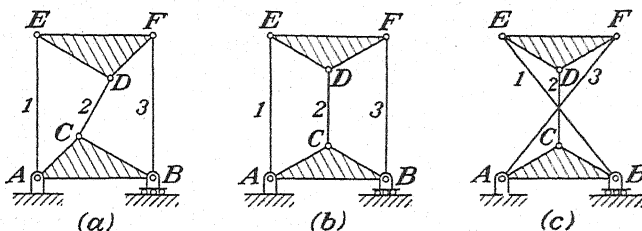
FIG. 136.
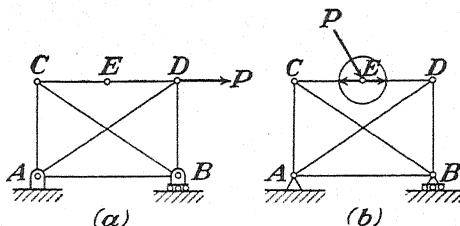
FIG. 137.

that it is statically indeterminate. That is, the portion of the load P that is transmitted to CD (which functions as one bar in this case) depends on the relative elastic deformations of the bars. When loaded as shown in Fig. 137b, we see, by making a free body of the hinge E, that the bars CE and DE must carry infinite tensions in order to balance the vertical component of the external force P; and this, of course, is physically impossible. Actually, upon application of the load P, all bars of the system will deform slightly, allowing the hinge E to assume an appreciably lower position whereby CE and DE become sufficiently inclined to balance the load P with finite tensions. However, these elongations and consequently the final configuration of equilibrium of the system depend on the elastic deformations of the bars, and these deformations must be taken into account in the analysis of the truss. Thus again the truss is statically indeterminate.

(a)

(b)

FIG. 138.

In the more general case of a complex truss, it is not always possible to detect a critical form by inspection. The complex truss in Fig. 138b, for example, has a critical form,[1] while the one in Fig. 138a has not. In such cases a general method of detecting a critical form of truss can be based on a consideration of the *determinant* of the system of $2j$ equations of equilibrium for its j joints. If this determinant is different from zero, the equations yield a unique solution, namely, there is one and only one set of

[1] The student should find it interesting to demonstrate the incomplete rigidity of this truss by direct experiment.
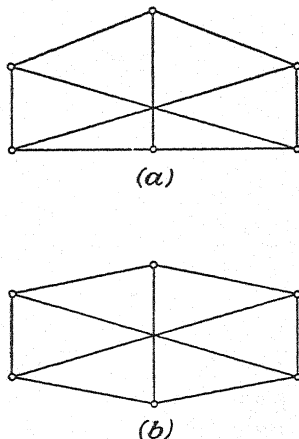
values for the axial forces that can satisfy the conditions of equilibrium at each joint, and the truss is rigid and statically determinate.   On the other hand, if the determinant happens to be zero, the equations of equilibrium fail to yield a unique solution and this will always be an indication that the truss has a critical form.   This suggests, then, a convenient method of testing for critical form, generally known as the *zero-load test*. With no loads on the truss, we see at once that one possible solution satisfying the conditions of equilibrium at each joint will be obtained by assuming all bars to be inactive, *i.e.*, with zero axial force.   Hence, if under the same condition of loading, we can find another set of values different from zero that also satisfy the conditions of equilibrium at each joint, we shall know that the truss has a critical form.

Consider, for example, the truss in Fig. 135*b*.   With no external forces at the joints, we assume a tension S in the bar CE and an equal tension in the bar DE. Then, with the same tension S in each of the bars AC, BD, and AB and with a compression $\sqrt{2}\,S$ in each of the diagonal bars, we can satisfy the conditions of equilibrium at all joints.   Thus, under zero load, we may have forces in the bars different from zero, and this indicates that the truss has a critical form.   Since the determinant mentioned above depends only on the configuration of the truss and not at all upon how it is loaded, we conclude that a truss of critical form will always be statically indeterminate regardless of how it may be loaded.

PROBLEMS

86. The plane truss in Fig. 139 has one redundant member; *i.e.*, $m = 2j - 3 + 1$.
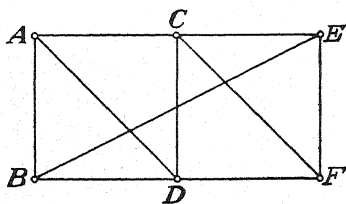
Fig. 139.

If BE is removed, we shall have a simple truss. What kind of truss shall we have if AB is removed; CD, BD, etc., for each bar in turn?

87. Using the zero-load test, prove that the complex truss in Fig. 132*b* is statically determinate.

88. Test each of the compound trusses in Fig. 136 for critical form by the method of zero loads.

89. Apply the zero-load test to each of the complex trusses shown in Fig. 138 and prove that (*b*) has a critical form while (*a*) has not.

90. Demonstrate that any plane truss of the general form shown in Fig. 138 will have a critical form if its six hinges lie on the circumference of an ellipse.

18. Complex Trusses: Henneberg's Method.—In previous articles, we have considered the analysis of simple and compound trusses by the method of joints and the method of sections.   These are very useful methods of analysis for trusses and are applicable in the majority of practical cases.   However, in the case of a complex truss, it usually happens that these elementary methods of analysis are not directly applicable.   In such cases, of course, we can always proceed with the solution of $2j$ simultaneous equations of equilibrium for the j joints of the system, but this will usually prove highly impracticable.   The first workable method of analysis for complex trusses was developed by L. Henneberg[1] and will now be explained.

[1] See L. Henneberg, "Statik der Starren Systeme," Darmstadt, 1886.

As a specific example, let us consider the complex truss supported and loaded as shown in Fig. 140a. We note at once that, the reactions at A and B having been found, no further progress with the analysis can be made by either the method of joints or the method of sections. We observe, however, that, by substituting for the bar AD a bar BE, we obtain a simple truss as shown in Fig. 140b. A complete analysis of this simple truss under any given condition of loading can be made by the method of joints. Let us assume then that this simple truss, corresponding to the given complex truss, has been completely analyzed for two particular conditions of loading, as follows: (1) the same loading as that on the given complex truss (Fig. 140b) and (2) two equal and opposite unit forces acting between A and D (Fig. 140c). Let S_i' denote the axial force in any bar of the simple truss due to the loading of the first case (Fig. 140b) and s_i' the corresponding axial force due to the loading of the second case (Fig. 140c). In the second case, if we have forces of
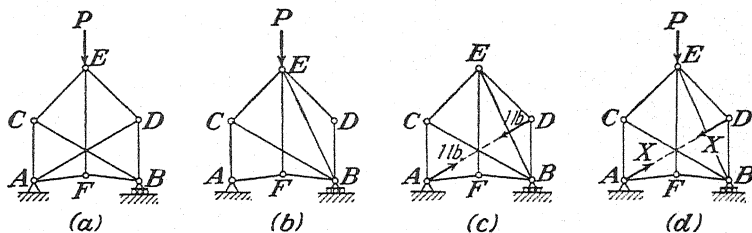
Fig. 140.

magnitude X instead of unit forces, it is obvious that the axial force in any bar will be simply $s_i'X$ instead of s_i'. Finally, then, by superposition of these two cases, we conclude that for the combined loading shown in Fig. 140d the axial force in any bar of the truss will be

$$S_i = S_i' + s_i'X \qquad (a)$$

and that in the particular case of the substituted bar BE, for which we shall use the subscript a, it will be

$$S_a = S_a' + s_a'X. \qquad (b)$$

Now, if we choose X of such magnitude that S_a from Eq. (b) becomes zero, the substituted bar BE becomes inactive and may be removed and the truss in Fig. 140d is then identical with the given truss (Fig. 140a) except that the action of the bar AD on the rest of the system is replaced by the forces X. Hence we conclude that that value of X which makes S_a equal to zero in Eq. (b) represents the true axial force in the bar AD. Proceeding in this manner we write

$$S_a' + s_a'X = 0, \qquad (c)$$

from which

$$X = -\frac{S_a'}{s_a'}.$$
(d)

With the value of X from Eq. (d), the force in any other bar of the given complex truss can be found by using Eq. (a).

A similar procedure may be used in the analysis of a complex truss like that in Fig. 141a, where, to arrive at a simple truss, it is necessary to replace two bars AH and BG by fictitious bars GC and HD, respectively, as shown in Fig. 141b. Considering three conditions of loading
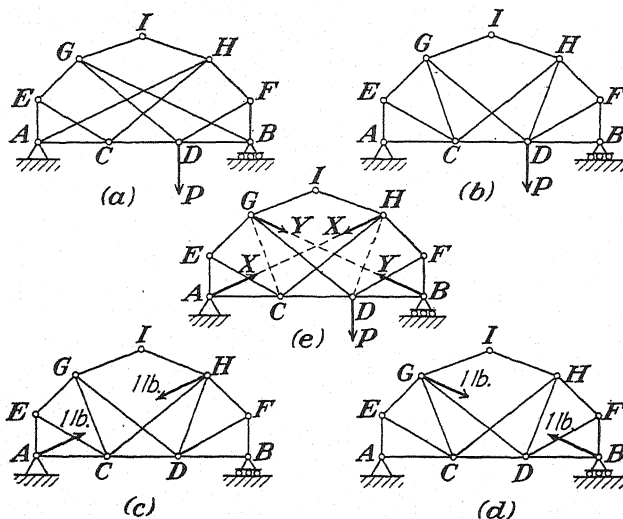
FIG. 141.

of this simple truss as shown in (b), (c), and (d), the corresponding axial forces S_i', s_i', and s_i'' in each bar of the truss can be found without difficulty by the method of joints. Denoting then by X and Y the unknown forces in the bars AH and BG, respectively, of the given complex truss and using the idea of superposition, we find for the axial force in any bar of the fictitious truss loaded as shown in Fig. 141e the following:

$$S_i = S_i' + s_i'X + s_i''Y.$$
(e)

For the fictitious bars GC and HD, denoted, respectively, by the subscripts a and b, we have

$$\begin{aligned} S_a &= S_a' + s_a'X + s_a''Y, \\ S_b &= S_b' + s_b'X + s_b''Y. \end{aligned} \Big\}$$
(f)

Setting these values of S_a and S_b equal to zero, as before, in order to

realize by the superimposed systems the case of the given complex truss, we obtain

$$X = \frac{s_b''S_a' - s_a''S_b'}{s_b's_a'' - s_a's_b''},$$

$$Y = \frac{s_b'S_a' - s_a'S_b'}{s_a's_b'' - s_b's_a''}. \qquad \left.\begin{array}{c}\\[2em]\end{array}\right\} \qquad (g)$$

As soon as the values of X and Y have been found from Eqs. (g), the axial force in any bar of the complex truss is found from Eq. (e).

In the case of a complex truss of critical form we shall find that the denominator of expression (d) or of expressions (g) becomes zero. This, of course, indicates that the system is statically indeterminate.

As a specific application of the Henneberg method, let us consider now a complete analysis of the complex truss in Fig. 142a. Assuming
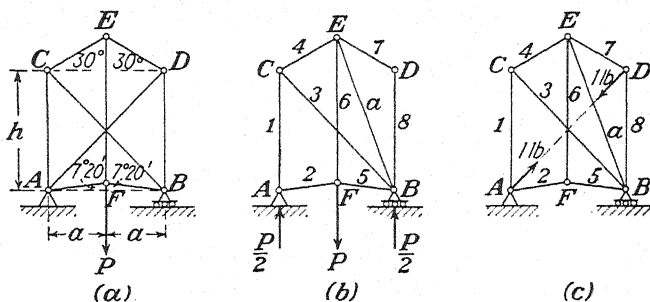
FIG. 142.

$P = 1,000$ lb., $a = 5$ ft., $h = 9$ ft., we begin with the corresponding simple truss and make a complete analysis, (1) for the loading shown in Fig. 142b and (2) for the unit forces acting along the line AD in Fig. 142c. These analyses can readily be made by the method of joints, and the results are recorded in columns (2) and (3), respectively, of Table I.

TABLE I

(1)	(2)	(3)	(4)	(5)
Bar	S_i'	s_i'	$s_i'X$	S_i
1	$-\ 500$	-0.574	$-\ 546$	$-1,046$
2	0	-0.749	$-\ 714$	$-\ 714$
3	$+\ 455$	$+0.522$	$+\ 498$	$+\ 953$
4	$-\ 391$	-0.488	$-\ 427$	$-\ 818$
5	0	-0.749	$-\ 714$	$-\ 714$
6	$+1,000$	-0.191	$-\ 182$	$+\ 818$
7	0	-0.858	$-\ 818$	$-\ 818$
8	0	-1.098	$-1,046$	$-1,046$
a	$-\ 872$	$+0.915$	$+\ 872$	0

Using the values of S_a' and s_a' in Eq. (d), we find

$$X = - \frac{(-872)}{(+0.915)} = +953 \text{ lb.}$$

Having the value of X we may now fill in column (4) of the table, and then from Eq. (a) the axial force for each bar of the given truss may be calculated and recorded in column (5). It will be noted that we obtain zero for the force in the fictitious bar a, which serves as a partial check on the calculations. In this particular case, we obtain a further check by observing that the results in column (5) satisfy the conditions of symmetry in Fig. 141a.

PROBLEMS

91. Determine the axial forces in the bars of the complex truss supported and loaded as shown in Fig. 143. Each inclined bar makes an angle of 30 deg. with the horizontal.
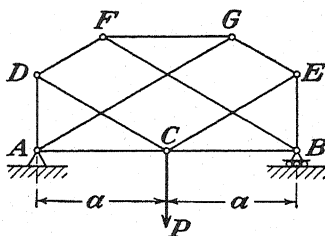
FIG. 143.

92. Using Henneberg's method, make a complete analysis of the complex truss supported and loaded as shown in Fig. 144.
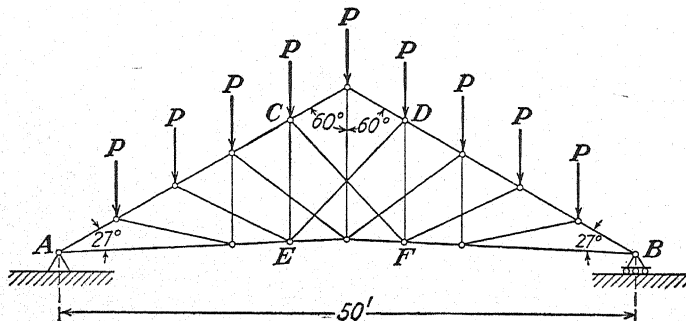
FIG. 144.

HINT: Only the portion $CDEF$ of this truss is of complex form.

93. Using Maxwell diagrams in conjunction with Henneberg's method, make a complete analysis of each of the complex trusses supported and loaded as shown in Fig. 145.
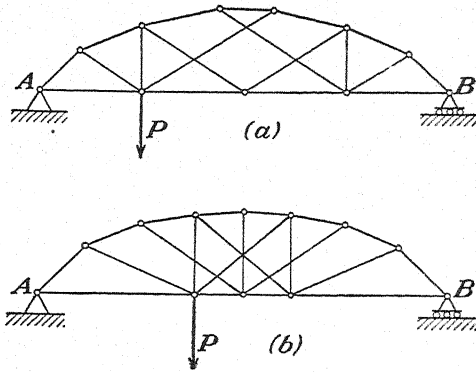
Fig. 145.

94. Make a complete analysis of the complex truss supported and loaded as shown in Fig. 146.   To reduce this system to a simple truss, remove the bar x and substitute a bar a as indicated by the dotted line.
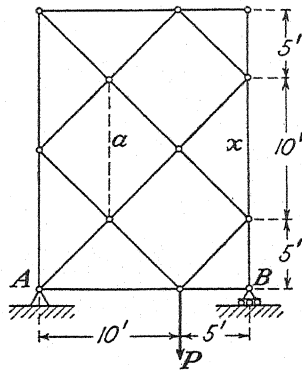
Fig. 146.

95. Make a complete analysis of the lattice truss supported and loaded as shown in Fig. 147.   All diagonals are inclined at 45 deg. with the horizontal, and the small subdivisions are squares.
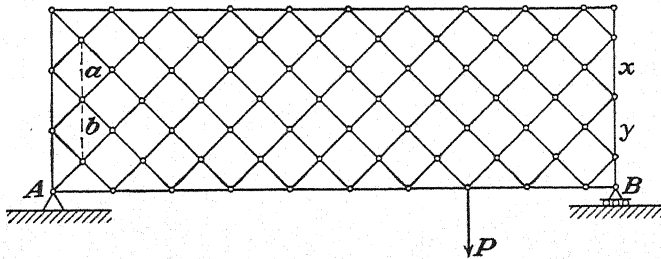
Fig. 147.

Hint: To reduce this truss to a simple truss it is necessary to remove the bars x and y and add the bars a and b.

19. Method of Virtual Displacements.—In many cases, the principle of virtual displacements, as discussed in Arts. 9 and 10, can be used to advantage in the analysis of statically determinate trusses. To find the axial force in a given bar of a truss by this method, we imagine that bar to be removed and its action on the rest of the truss represented by two equal and opposite forces S. In this way, we obtain a nonrigid system with one degree of freedom to which the principle of virtual displacements can be applied.[1]

As a first example, consider the simple truss shown in Fig. 148a, and let it be required to find the axial force in the bar AD. Replacing this bar by collinear forces S at A and D, we obtain a nonrigid system with one degree of freedom as shown in Fig. 148b. A virtual displacement of this system can be defined by an infinitesimal horizontal displacement δ of the upper portion of the truss. We see from the figure that under this
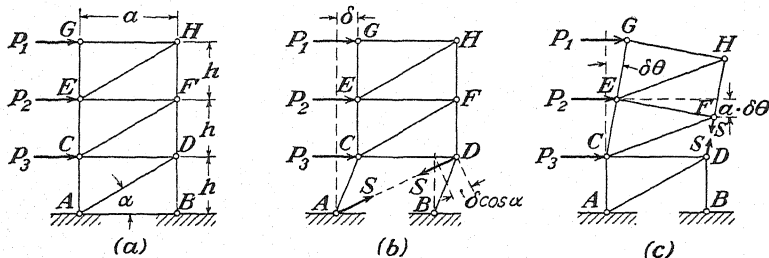
Fig. 148.

displacement, each of the applied loads P_1, P_2, P_3, ... produces a work $P_i \cdot \delta$, while the force S at D produces a work $-S \cdot \delta \cos \alpha$. The force S at A produces no work because its point of application does not move. Thus the equation of virtual work for the system becomes

$$(P_1 + P_2 + P_3) \cdot \delta - S \cdot \delta \cos \alpha = 0, \qquad (a)$$

from which we find $S = (P_1 + P_2 + P_3) \sec \alpha$.

To obtain the force S in the vertical bar FD, we proceed in a similar manner, replace this bar by collinear forces S at D and F, and obtain the nonrigid system shown in Fig. 148c. In this case, a virtual displacement of the system is best defined by the infinitesimal angle of rotation $\delta\theta$ of the upper portion of the truss as shown. The corresponding displacements of points G, E, and F, respectively, are $2h \, \delta\theta$, $h \, \delta\theta$, and $a \, \delta\theta$, and the equation of virtual work becomes

$$P_1 \cdot 2h \, \delta\theta + P_2 \cdot h \, \delta\theta + S \cdot a \, \delta\theta = 0, \qquad (b)$$

from which $S = -(h/a)(2P_1 + P_2)$.

[1] The use of the principle of virtual displacements in the analysis of trusses was introduced by Otto Mohr. See his papers, Beiträge zur Theorie des Fachwerks, *Z. Architekten-Ingenieur-Ver. Hannover*, 1874, p. 509, and 1875, p. 17, also Beitrag zur Theorie des Fachwerks, *Zivilingenieur*, 1885, p. 289.

From the preceding examples, we see that, in general, the determination of the axial force in any one bar of a truss by the method of virtual work necessitates the evaluation of the virtual displacements of the points of application of all active forces. If there are forces at almost every joint of the truss, the amount of calculation required to determine analytically all necessary virtual displacements may be considerable. In such cases, displacement diagrams as discussed in Art. 10 will be found helpful.

While there is usually little advantage in employing the method of virtual work in the analysis of simple or compound trusses, it is often valuable in the case of a complex truss. By way of illustration, let us consider the complex truss shown in Fig. 149a. If we succeed in finding the force in any one bar of this truss by the method of virtual work, the
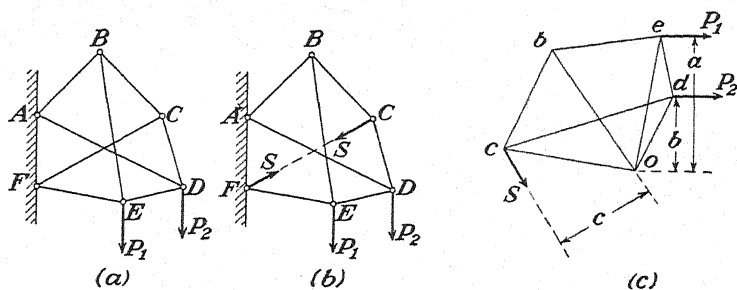
Fig. 149.

remainder of the analysis can be made without difficulty by the method of joints. In this case, we select the bar FC, replace it by collinear forces S at F and C, and obtain the nonrigid system shown in Fig. 149b. A displacement diagram for this system (constructed as explained in Art. 10) is shown in Fig. 149c. Using this diagram as a Joukowski lever hinged at o (see page 42), we may write

$$S \cdot c - P_1 \cdot a - P_2 \cdot b = 0,$$

from which

$$S = \frac{P_1 a + P_2 b}{c}.$$

The displacement diagram must, of course, be constructed to scale and the moment arms a, b, and c measured from it.

Besides displacement diagrams of the kind shown in Fig. 149c, there is another graphical method for determining a set of compatible displacements for the hinges of a truss from which one bar has been removed. To demonstrate this method, we consider first the simple example in Fig. 150. Here we have a rigid triangle ABC supported by two hinged bars so that the system has one degree of freedom. In such a case, a

virtual displacement of the system can be defined by an infinitesimal angular displacement $\delta\theta$ around the instantaneous center O. The corresponding linear displacements $\overline{AA_1}$, $\overline{BB_1}$, and $\overline{CC_1}$ of the hinges A, B, and C are proportional to the radii OA, OB, and OC and perpendicular to them, respectively, as shown. If we rotate each of these displacement
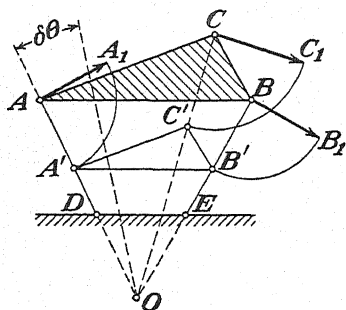
FIG. 150.

vectors clockwise by 90 deg., we obtain the points A', B', and C' on the corresponding radii as shown. The figure $A'B'C'$, so obtained, is geometrically similar to the figure ABC since by virtue of the ratios $AA':BB':CC' = OA:OB:OC$, corresponding sides of the two figures are parallel. This conclusion holds for the virtual displacement of any rigid plane figure with one degree of freedom. Reversing the above procedure, we conclude that a set of compatible virtual displacements for the joints of any rigid plane system having one degree of freedom can be obtained by assuming the magnitude of the displacement of one joint and then constructing the proper similar figure like $A'B'C'$ in Fig. 150.

Take, for example, the simple truss already considered in Fig. 148, and suppose that the vertical bar BD is removed as shown in Fig. 151a.
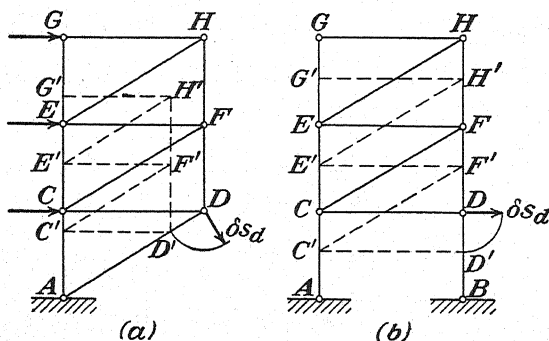
FIG. 151.

In such a case the truss can rotate around the hinge A, and we can define a virtual displacement of the system by any arbitrary linear displacement δs_d of the hinge D normal to AD. Rotating this displacement vector clockwise by 90 deg., we obtain the point D' on the line AD. Corresponding displacements of the other joints are now obtained simply by constructing on AD' the figure $AD'C'F'E'H'G'$ with its sides parallel, respectively, to those of the given truss. Thus, GG' represents in magnitude

the displacement of point G, HH' that of point H, etc.   If the bar AD of the truss is removed (Fig. 151b), the virtual displacement of the system is defined by an arbitrary horizontal displacement δs_d of point D; and, proceeding as before, we obtain the similar figure $ABC'D'E'F'G'H'$ as shown.

The foregoing procedure can be applied also in the case of a complex truss.   For the truss shown in Fig. 149b, for example, we can define a virtual displacement of the system by an arbitrary linear displacement δs_b at right angles to AB as shown in Fig. 152.   Rotating this displacement vector by 90 deg., we obtain the point B' on the line AB. BE being a rigid body, the corresponding displacement of E, as defined by EE', will be obtained by drawing the dotted line $B'E'$ parallel to BE.   Then, having the displacement of E corresponding to the assumed displacement of B, we obtain the corresponding displacement of D, as defined by DD', by drawing $E'D'$ parallel to ED, since ED also is a rigid body.   Finally, the displacement of C, as represented by CC', is found by drawing $B'C'$ and $D'C''$ parallel, respectively, to BC and DC.
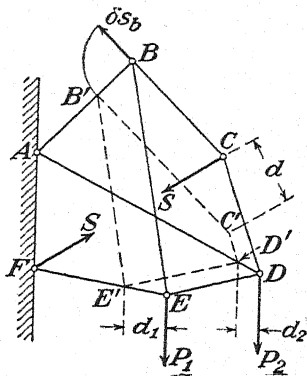
FIG. 152.

Having compatible displacements for all joints of the truss, the unknown force S can now be found by writing the equation of virtual work for the system as before.   In this case, however, it can be noted from the figure that, since the displacements have all been rotated by 90 deg. from their true directions, the corresponding works of the various forces acting on the joints can be obtained by taking their moments with respect to the points E', D', C'.   Thus, for example, the work of the force P_1 on the true displacement of the joint E is identical with the moment of P, with respect to point E', etc.   Upon using this conclusion, the equation for determining S becomes

$$- \Sigma P_i \cdot d_i + S \cdot d = 0, \tag{c}$$

from which

$$S = \frac{\Sigma P_i \cdot d_i}{d}. \tag{d}$$

It should be noted that the value of S as given by Eq. (d) is not changed if all the distances such as BB', EE', . . . are decreased or increased in the same proportion.   Thus any figure $AB'C'D'E'F$ with sides parallel to those of the figure $ABCDEF$ can be used in writing Eq. (c) above.

The graphical constructions illustrated in Fig. 152 are also helpful in detecting a critical form of complex truss (see Art. 17). Referring to Eq. (d), we see that the truss of Fig. 152 can have an indeterminate form only if the distance d is zero, $i.e.$, if the line FC' coincides with the line FC. We can generalize this observation as follows: If, upon removal of one bar of a complex truss, a figure such as $AB'C'D'E'F$ (Fig. 152),

(a)   (b)
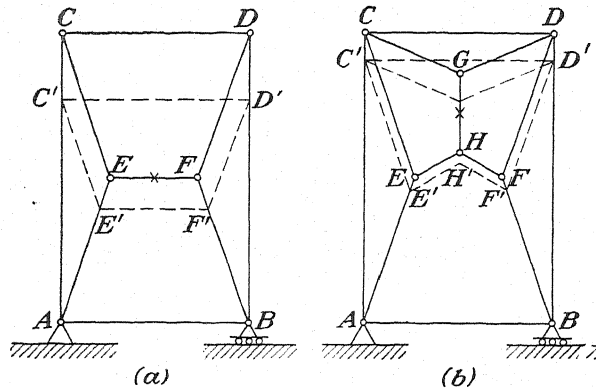
Fig. 153.

defining compatible virtual displacements of the joints of the remaining system, has all its sides (including the one corresponding to the removed bar) parallel to those of the given figure, then the truss has a critical form and is statically indeterminate. Two such examples are shown in Fig. 153.

PROBLEMS

96. Using the method of virtual displacements, find the axial force S_x in the bar x of the complex truss supported and loaded as shown in Fig. 154.
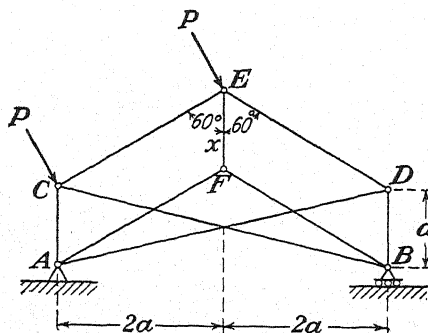
Fig. 154.

97. Using the method of virtual displacements, prove that the complex truss in Fig. 138a is completely rigid, while the one in Fig. 138b is not.

98. Test each of the complex trusses shown in Fig. 155 for rigidity, and identify those which have a critical form.
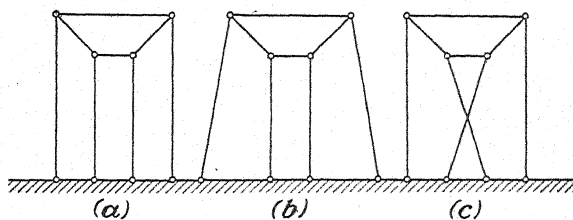
FIG. 155.

99. Study the lattice truss shown in Fig. 156, and prove that it has a critical form as shown but that, if pins are introduced at all intersections, it will become statically determinate.
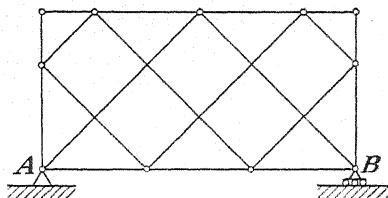
FIG. 156.

100. Prove that the statically determinate complex truss shown in Fig. 138a will become statically indeterminate if a hinge is introduced at the center.

INFLUENCE LINES

20. Moving Loads and Influence Lines.—Engineering structures in general and bridges in particular are frequently submitted to the action of various systems of moving loads such as trucks, trains, automobile traffic, etc. These loads are called *live loads* to distinguish them from *dead loads* such as the weight of a structure itself, etc. Dead loads are always fixed in magnitude and position, whereas live loads, although fixed in magnitude, can have a variety of positions on the structure. One of the most common examples of live load with which we have to deal in the design of railroad bridges is represented by the wheel loads from a pair of 213-ton locomotives, followed by a uniform train of 3 tons per lineal foot, as shown in Fig. 157. This particular system of loads is known as a *standard train* or *Cooper's E-60 loading*. The wheels are numbered consecutively from left to right, and the distances between
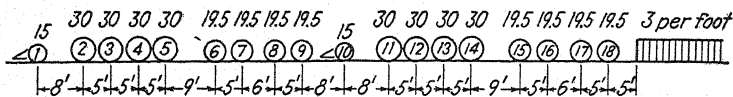
Fig. 157.

them are as shown. It must be understood that these distances between wheels are fixed so that the system can move only as a unit. The numbers directly above the wheels represent the load concentrations in kips per rail or tons per track.

A tabulation of useful numerical data pertaining to the standard train above and known as a *moment table* for Cooper's E-60 loading is shown on page 95. Besides the information given in Fig. 157, the first two horizontal lines of this table give the distance of each wheel from either end of the locomotive system, while the third and fourth lines give successive summations of loads up to and including any chosen wheel from either end of the system. The fifth horizontal line gives the sum of moments, with respect to wheel ①, of all loads back to and including any chosen wheel. Thus, for example, the sum of moments, with respect to wheel ①, of all loads back to and including wheel ⑧, is 4,040 kip-ft. The remaining lines of the table give sums of moments, with respect to each wheel, of all loads between that wheel and any other chosen wheel ahead of it. Thus, for example, the sum of moments of wheels ③ . . . ⑯ with respect to wheel ⑮ is 12,500 kip-ft. To find this figure in the table, we follow vertically downward, under wheel ⑮, to the bottom of the table and then move horizontally to the left and read 12,500 under wheel ③. Examples illustrating the use of the moment table will be discussed later.

MOMENT TABLE
COOPER'S E-60 LOADING

Two 213-ton Engines + 6000 lb. per foot

Moments in foot-kips per rail or foot-tons per track

Loads in kips per rail or tons per track

Scale: 1" = 20'

	∠①15	②30	③30	④30	⑤30	⑥19.5	⑦19.5	⑧19.5	⑨19.5	∠⑩15	⑪30	⑫30	⑬30	⑭30	⑮19.5	⑯19.5	⑰19.5	⑱19.5	3000 lb. per ft.
SPACING	8'	5'	5'	5'	9'	5'	6'	5'	8'	8'	5'	5'	5'	9'	5'	6'	5'	5'	
	0	8	13	18	23	32	37	43	48	56	64	69	74	79	88	93	99	104	
	109	101	96	91	86	77	72	66	61	53	45	40	35	30	21	16	10	5	
	15	45	75	105	135	154.5	174	193.5	213	228	258	288	318	348	367.5	387	406.5	426	
	426	411	381	351	321	291	271.5	252	232.5	213	198	168	138	108	78	58.5	39	19.5	
MOMENTS	0	240	630	1170	1860	2485	3205	4040	4980	5820	5510	4160	2965	1915	1015	605	292.5	97.5	
	24550	22900	19900	17000	14270	11700	10190	8790	7500	6310	4520	3325	2275	1375	624	312	97.5		
	22400	20850	17980	15250	12670	10240	8830	7530	6340	5240	3630	2580	1680	932	332	117			
	20400	18900	16170	13600	11150	8880	7570	6360	5270	4280	2680	1808	1088	518	97.5				
	18050	16650	14120	11720	9470	7370	6180	5090	4110	3230	1980	1260	690	270					
	16220	14900	12500	10250	8150	6200	5110	4120	3240	2460	900	450	150						
	13100	11900	9780	7800	5970	4290	3370	2550	1850	1245	450	150							
	11500	10400	8410	6580	4900	3370	2555	1830	1227	720	150								
	10060	9030	7200	5520	3990	2605	1885	1262	755	345									
	8770	7810	6130	4600	3220	1992	1368	842	432	120									
	6950	6110	4670	3380	2240	1248	780	410	156										
	5240	4520	3325	2275	1375	624	312	97.5											
	4280	3630	2580	1680	932	332	117												
	3230	2680	1808	1088	518	97.5													
	2460	1980	1260	690	270														
	1245	900	450	150															
	720	450	150																
	345	150																	
	120																		

The analysis of structures under the action of live loads presents two major problems not encountered in connection with dead loads. First, the moving loads may have a dynamical effect on the structure, tending to produce vibrations, shock, or other undesirable effects. Second, even the purely statical effect of a system of moving loads is continually changing owing to change in position of the loads, and it becomes necessary to consider the problem of how to place them on the structure in order to realize the most severe stresses. It is only this latter aspect of the problem that we shall consider here.[1]

Sometimes we are able to determine by inspection how to place a given system of loads on a structure so as to realize the most severe

Fig. 158.

stresses. In other cases, it may be necessary to resort to mathematical criteria for maxima and occasionally to trial-and-error procedures. In all cases, however, the problem can be greatly simplified by the use of *influence lines*, which show graphically just how changing the position of a single load on a structure influences various significant quantities such as reactions, bending moments, shearing forces, and deflections. Consider, for example, the cantilever beam shown in Fig. 158a. In the design of this beam, we shall be especially interested in the bending stresses at the built-in end since this is the dangerous section. Thus a diagram showing how the bending moment at A varies with change in position of a load P on the beam will be helpful in deciding the most

critical position of that load. Such a diagram may be constructed as follows: First let the load have any position on the beam as defined by the distance x from the free end. Then the bending moment at the built-in end A is

$$M_a = -P(l - x),$$

and the factor $-(l - x)$ by which the load P is multiplied is called the *influence coefficient* for M_a. Being a linear function of x it can be repre-

[1] For discussions of the dynamical action of live loads on structures, see S. Timoshenko, "Vibration Problems in Engineering," and C. E. Inglis, "A Mathematical Treatise on Vibrations in Railway Bridges," Cambridge University Press, 1934.

sented graphically by the straight line *ab* as shown in Fig. 158*b** and this line is called the *influence line* for bending moment at *A*. Correspondingly, the diagram *abo* is called the *influence diagram*. The influence diagram for bending moment must not be confused with a *bending-moment diagram* for the beam. Whereas the latter shows by each ordinate the bending moment at the corresponding section due to *fixed loads*, the influence diagram shows by each ordinate that factor by which a correspondingly placed load *P* must be multiplied to give the bending moment at a *fixed cross section*. The ordinates of a bending-moment diagram have the dimension of *force × length*; the ordinates of an influence diagram for bending moment, as shown in Fig. 158*b*, have the dimension of *length*. Thus only when multiplied by the load *P* do they give the proper dimension for bending moment. Numerically, however, the ordinates in Fig. 158*b* may be considered as representing the bending moment at *A* due to a correspondingly placed *unit load*, and we shall often use them in this sense.

We see at once from the influence diagram in Fig. 158*b* that for maximum bending moment at *A* the load *P* should be placed in correspondence with the largest ordinate, *i.e.*, at the free end of the beam, and that the corresponding bending moment at *A* is $-Pl$. In this particular case such conclusions, obtained with the aid of the influence diagram, are rather obvious; but, for more complicated systems, we shall find that this diagram can be of more substantial help. For example, if we have a system of concentrated loads as shown in Fig. 158*c* and if y_1, y_2, and y_3 are the ordinates of the influence line corresponding to a certain position of this system of loads on the beam, then it follows from simple statical considerations that the corresponding bending moment at *A* is

$$M_a = -(P_1 y_1 + P_2 y_2 + P_3 y_3). \qquad (a)$$

Since the ordinates y_1, y_2, and y_3 will all be increased by moving the system of loads to the right, we conclude that the most critical condition of loading in this case will be obtained by placing the load P_3 at the free end of the beam. Using the corresponding values of y_1, y_2, and y_3, we obtain the desired maximum bending moment at *A* from Eq. (*a*).

If *R* is the resultant of the loads P_1, P_2, and P_3 and y_c is the corresponding ordinate of the influence line, we have

$$R \cdot y_c = P_1 y_1 + P_2 y_2 + P_3 y_3. \qquad (b)$$

To prove this, we need only recall that the moment of the resultant with respect to any point is equal to the algebraic sum of the corresponding

* We take the ordinates of the influence line down if the influence coefficient is negative.

moments of its components. Equation (*b*) follows directly from this statement together with the fact that the ordinates y_1, y_2, y_3, and y_c are proportional to their distances from the built-in end of the beam. Such replacement of a system of loads by their resultant, as in Eq. (*b*), always holds if the influence line is rectilinear and is very useful in establishing criteria for the most critical position on a structure of a complicated system of loads like the standard train in Fig. 157.
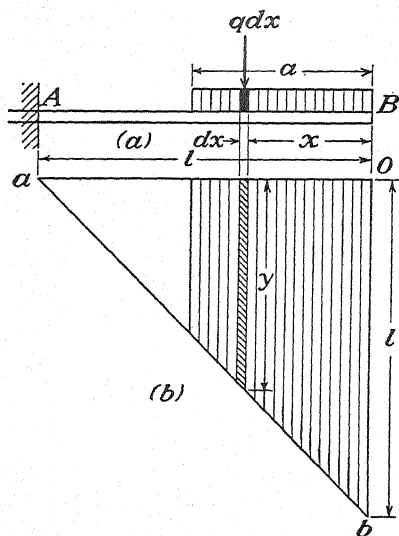
The influence diagram also can be used to advantage in dealing with uniformly distributed live load. Suppose, for example, that we wish to calculate the bending moment at the built-in end of a cantilever beam partly covered by a uniform load of intensity q as shown in Fig. 159*a*. Considering such loading as a series of infinitesimal concentrated loads each of magnitude $q\,dx$ and at the distance x from the free end of the beam, we conclude, by the same reasoning as used above for the case of three loads, that the total bending moment at A is

$$M_a = \int_0^a qy\,dx, \tag{c}$$

Fig. 159.

where y is the ordinate of the influence line corresponding to x. Since

$$\int_0^a qy\,dx = q\int_0^a y\,dx = q[\text{area}]_0^a,$$

we conclude that the bending moment at A due to any partial distribution of uniform load on the beam is obtained simply by taking the area of the corresponding portion of the influence diagram and multiplying it by the intensity of load q. This fact is useful because it enables us to ascertain by inspection of the influence diagram just what portion of the beam should be uniformly loaded to obtain the most severe bending moment at a chosen section. In the case illustrated in Fig. 159, of course, we obtain the greatest negative bending moment at A by loading the entire span.

As mentioned above, we can construct an influence line for any quantity that varies with change in position of load on a structure. Consider, for example, the beam AB supported as shown in Fig. 160*a*.

If a single load P acts on this beam as shown, the tension induced in the tie rod CD will be

$$S = P \cdot \frac{x}{a} \sec \alpha.$$

Here, again, the influence coefficient $(x/a) \sec \alpha$, by which the load P must be multiplied to give the corresponding tensile force S in the tie rod, is a linear function of x, and the corresponding influence line has the form shown in Fig. 160b. We see that as x varies from zero to l, the influence
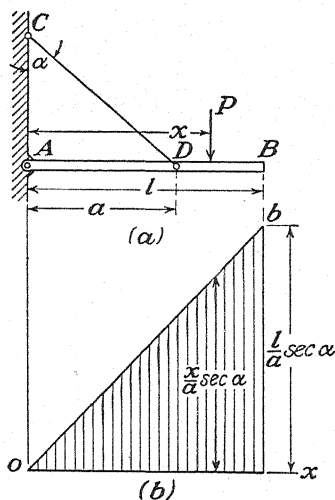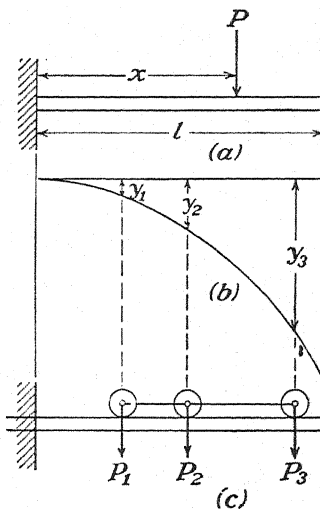
Fig. 160.   Fig. 161.

coefficients, which in this case are pure numbers, vary from zero to $(l/a) \sec \alpha$.

In the two preceding examples, the influence lines happened to be rectilinear, but they may not always be so. Consider, for example, an influence line for deflection δ at the free end of a cantilever beam of uniform flexural rigidity EI (Fig. 161). For a load P at the distance x from the built-in end, this deflection is

$$\delta = P \cdot \left[\frac{x^3}{3EI} + \frac{x^2}{2EI} (l - x) \right],$$

and the influence coefficient obviously is not a linear function of x. Accordingly, the influence line has the curvilinear form shown in Fig. 161b.* It will be noted that the ordinates of this line have the dimension of *length ÷ force*, *e.g.*, inches per pound. Thus when multiplied by the load P they give the proper dimension (*length*) for δ. Since, for small deflections, the effects of several loads on the beam will be independent of each other, we can conclude at once that, for the loading shown in Fig. 161c, the deflection at the free end will be

$$\delta = P_1 y_1 + P_2 y_2 + P_3 y_3, \tag{d}$$

* This influence line for the deflection δ at the free end must not be confused with the elastic line of the bent beam itself.

where y_1, y_2, and y_3 are the ordinates of the influence line corresponding to the positions of the loads P_1, P_2, and P_3, respectively. Equation (b) must not be used in this case because of the nonrectilinear character of the influence line.

21. Influence Lines for Beam Reactions.—Influence lines can often be used to advantage in the determination of simple beam reactions. Consider, for example, the simply supported beam shown in Fig. 162a.
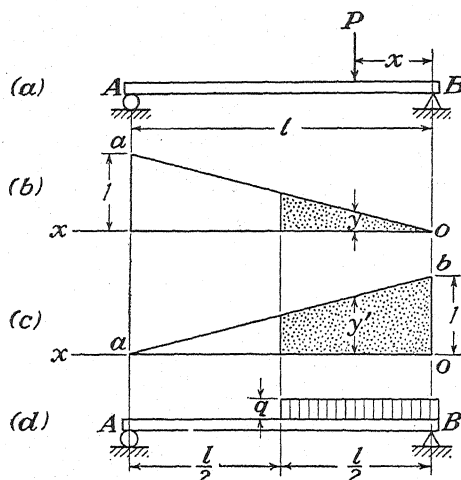
Fig. 162.

If a load P acts on this beam at the distance x from the right support, the vertical reactions at A and B are

$$R_a = P \cdot \frac{x}{l},$$
$$R_b = P \cdot \left(1 - \frac{x}{l}\right), \qquad (a)$$

which we shall consider positive when directed upward. The factors x/l and $(1 - x/l)$, by which P must be multiplied to give the corresponding reactions, are the influence coefficients and can be represented graphically by the influence lines oa and ba as shown in Figs. 162b and 162c.

By using these influence lines and proceeding as explained in the previous article, we can obtain the reactions for any given system of loads on the beam. For example, if there are several loads P_1, P_2, . . . acting on the beam and y_1, y_2, . . . are the corresponding ordinates of the influence line for R_a (Fig. 162b), then we may write

$$R_a = \Sigma(P_i y_i). \qquad (b)$$

In the same way, denoting by y_1', y_2', . . . the corresponding ordinates of the influence line for R_b (Fig. 162c) we have

$$R_b = \Sigma(P_i y_i'). \qquad (b')$$

If a portion of the span carries a uniformly distributed load of intensity q, each reaction will be obtained by multiplying by q the corresponding area of the proper influence diagram. Thus for a uniform load that extends from B to mid-span (Fig. 162d), we obtain

$$R_a = q \cdot \frac{1}{4} \cdot \frac{l}{2} = \frac{1}{8} ql,$$

$$R_b = q \cdot \frac{3}{4} \cdot \frac{l}{2} = \frac{3}{8} ql,$$

where $\frac{1}{4} \, l/2$ and $\frac{3}{4} \, l/2$ are the shaded areas shown in Figs. 162b and 162c, respectively.
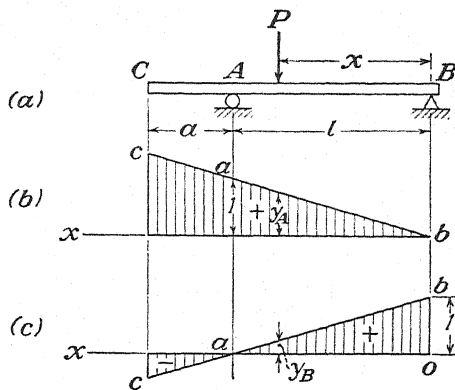
Fig. 163.

In the case of a simply supported beam with overhang (Fig. 163a), expressions (a) for the reactions due to a moving load P still hold. However, since the value of x can now vary from zero to $l + a$, we obtain the influence lines shown in Figs. 163b and 163c. For values of x between l and $l + a$, we see that the influence coefficient for R_a becomes greater than unity, while that for R_b becomes negative. Thus their sum remains constant and equal to unity. The negative ordinates for R_b simply indicate that when the load is on the overhang this reaction is directed downward.

Since the influence coefficients x/l and $(1 - x/l)$ in expressions (a) can be regarded numerically as the reactions that would be produced at A and B by a *unit load* in place of the load P, we can devise a very simple method of construction of influence lines for reactions. As a first example, let us reconsider the influence line for the reaction R_b in Fig. 163c. If we imagine a *unit load* placed at B, the reaction R_b obvi-

ously has the magnitude of unity; when the unit load is at A, it is zero. Thus, having the key points b and a and keeping in mind that the reaction is a linear function of x, we construct the straight line bac through these key points and the diagram is completed.

The procedure above can be used also in more complicated cases where the writing of analytical expressions for the reactions may become involved. Consider, for example, the compound beam ACD supported as shown in Fig. 164a. To construct the influence lines for the vertical reactions at A, B, and D in this case, we proceed as follows: Beginning with the reaction at A, we note that this force must have magnitudes of unity and zero, respectively, as a unit load successively takes positions at A and B. Thus through the key points a and b (Fig. 164b) we can construct the straight line abc. When the load is at D, the reaction R_a is again zero and we complete the influence diagram with the straight line cd. The same procedure is used in the construction of the influence lines for R_b (Fig. 164c) and R_d (Fig. 164d).
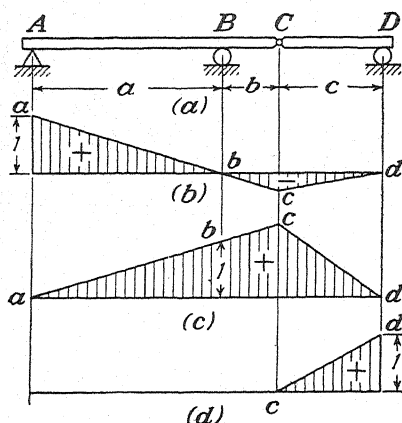
Although influence lines for reactions are hardly necessary for such simple beams as those shown in Figs. 162 and 163, they may prove very helpful in more complicated cases like that shown in Fig. 164. In such a case, we can see clearly from the influence diagrams just how to place given loads on the beam in order to obtain maximum values of the reactions. For example, under uniform load, we see that the most severe uplift on the reaction at A will be obtained when only that portion of the span between B and D is loaded. Again, it is evident at a glance that loads on the beam AC have no effect on the reaction at D. For the maximum reaction at B, we must put as many loads as possible on the entire span, etc.
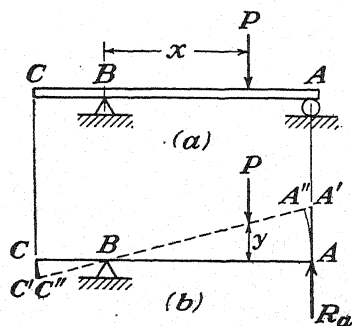
The principle of virtual displacements as discussed in Art. 9 can be used to advantage in the construction of influence lines for reactions. Consider, for example, the simply supported beam ABC with overhang

FIG. 164.

FIG. 165.

loaded as shown in Fig. 165a. To find the reaction at A by the method
of virtual displacements, we remove the constraint at A and replace it
by a vertical force R_a as shown in Fig. 165b. This leaves the rigid bar
AC free to rotate around the fixed hinge B. Defining such a virtual dis-
placement of the system by a linear displacement $\overline{AA'}$* of point A, we
see that all other points on the axis of the beam must have displacements
as shown by the ordinates to the dotted line $A'C'$. Thus the equation
of virtual work becomes

$$R_a \cdot \overline{AA'} - P \cdot y = 0,$$

from which

$$R_a = P \cdot \frac{y}{\overline{AA'}}, \qquad\qquad (c)$$

where y is the displacement of the point of application of the load P.
From expression (c), we conclude that by taking $AA' =$ unity, we can
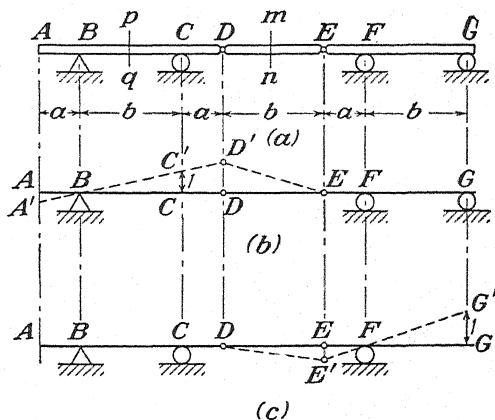
FIG. 166.

consider the dotted line $A'C'$ as the influence line for the reaction R_a.
The negative ordinates to the left of B indicate that this reaction will be
directed downward when the load is on the overhang.

The procedure above can be used also in more complicated cases
like that shown in Fig. 166a, where we have a statically determinate
compound beam AG on four supports. To obtain an influence line for
the vertical reaction at C, we simply remove the constraint at C and make
a positive (upward) displacement $\overline{CC'}$ of this point as shown in Fig. 166b.
By taking CC' equal to unity, the ordinates to the dotted lines defining
the new configuration of the system will represent the corresponding
influence coefficients for R_c. In the same manner, removal of the con-

---

* Actually the displacements are infinitesimal circular arcs that we can consider
as coincident with their own vertical tangents; thus the tangent AA' for the arc AA''
etc.

straint at G and a subsequent positive unit displacement of this point as shown in Fig. 166c leads to the influence line for R_g as shown by dotted lines. Thus we see that to obtain an influence line for any statically determinate reaction, it is necessary only to remove the corresponding constraint and make a positive unit displacement of its point of application. Then the new configuration of the system defines the required influence line. It is left as an exercise for the student to construct influence lines for the reactions at B and F by this procedure.

We have now discussed several methods of constructing influence lines for reactions. Their application in the analysis of beams under various systems of live loads can best be illustrated by an example. For this purpose, we take the simple beam with overhang as shown in Fig. 167a and assume that we wish to evaluate the maximum reaction which can be induced at B by the standard train shown in Fig. 157. With the
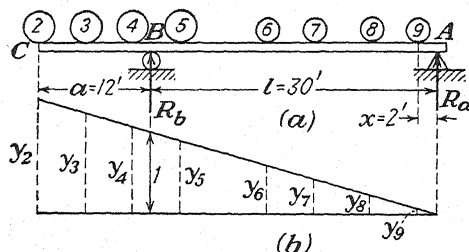
FIG. 167.

aid of the influence line for R_b (Fig. 167b), we see that in this case the most critical position of the train will be obtained by placing wheel ② at C as shown. That is, as the train moves slowly across the bridge from right to left, the reaction R_b will have its largest value after the wheel ① leaves the bridge and just as wheel ② reaches the end. Thus, the question of placement of the loads having been disposed of, we are ready to consider the numerical calculation of R_b for the chosen condition of loading. This calculation can be made in two ways: In one case, we scale the influence coefficients y_2, y_3, y_4, . . . , multiply each by the corresponding wheel load, and use the formula

$$R_b = \Sigma(P_i y_i), \qquad (d)$$

as explained on page 97. An easier and more accurate method, however, will be to discard the influence diagram completely as soon as the critical position of the loads has been selected and to calculate R_b simply by equating to zero the algebraic sum of moments of all forces with respect to point A. Thus, denoting by ΣM_a the sum of moments of all loads on the beam with respect to A, we have

$$R_b = \frac{\Sigma M_a}{l}. \qquad (e)$$

The numerical calculations indicated by Eq. (*e*) can be made in a very simple manner by using the *moment table* for Cooper's *E*-60 loading as shown on page 95. To use this table, we first write expression (*e*) in the equivalent form

$$R_b = \frac{\Sigma M_{\circled9} + (\Sigma P_i) \cdot x}{l},\qquad (e')$$

where $\Sigma M_{\circled9}$ denotes the sum of moments of all loads on the beam with respect to wheel $\circled9$ and ΣP_i denotes the summation of all loads on the beam, x being the distance between A and wheel $\circled9$. Taking the numerical values of $\Sigma M_{\circled9}$ and ΣP_i directly from the moment table and using $l = 30$ ft. and $x = 2$ ft. as shown in Fig. 167a, we have

$$R_b = \frac{4{,}520 + 198 \cdot 2}{30} = 163.5 \text{ kip.}$$

This discussion assumes that the bridge consists of two parallel beams and that there is a single track, *i.e.*, that the load on each girder is the same as that for one rail.

PROBLEMS

101. Construct an influence line for the axial force in the strut CD supporting the horizontal beam AB as shown in Fig. 168.
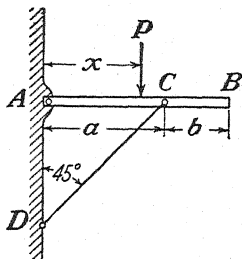
FIG. 168.

102. Construct influence lines for the axial forces developed in the bars AF, BE, and BD, which support the beam ABC as shown in Fig. 169.
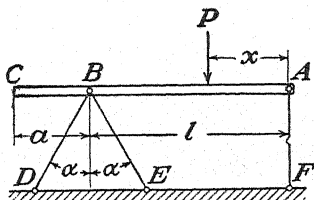
FIG. 169.

103. Construct influence lines for the reactions at A and B of the simply supported beam shown in Fig. 170. Using a standard train (Cooper's E-60), calculate the greatest possible value of R_b if $a = 10$ ft., $l = 30$ ft., and $b = 12$ ft.

$\qquad\qquad\qquad\qquad\qquad\qquad$ *Ans.* Max. $R_b = 322$ kip.
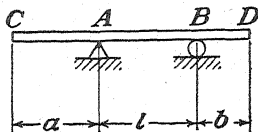
Fig. 170.

104. Construct influence lines for the reactions at A, C, and D of the compound beam shown in Fig. 171. How should a standard train be placed to make R_a a maximum? What is this maximum value of R_a if a, b, and l have the same numerical values as in Prob. 103? $\qquad\qquad\qquad$ *Ans.* Max. $R_a = 189.1$ kip.
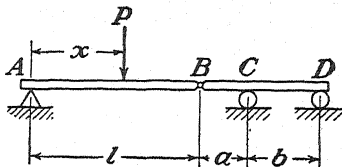
Fig. 171.

105. Construct influence lines for the reactions at A, B, and C of the system shown in Fig. 172.
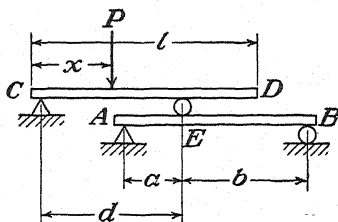
Fig. 172.

22. Influence Lines for Shearing Force.—In the case of a simply supported beam (Fig. 173a), an influence line for shearing force at a given section mn can be obtained as follows: When a load P is to the right of the section mn, we note that the shearing force at the section is positive and numerically equal to the reaction R_a. Likewise, when the load is to the left of the section, the shearing force is negative and numerically equal to the reaction R_b. Hence we obtain the influence diagram for shearing force at mn simply by taking the shaded portions of the two influence diagrams for the reactions R_a and $-R_b$ as shown in Fig. 173b. Any ordinate of this diagram is numerically equal to the shearing force at the fixed section mn when a unit load has that position on the beam corresponding to the chosen ordinate. As this load crosses the section from

right to left, the shearing force changes abruptly from a maximum positive value b/l to a maximum negative value a/l.

From the influence diagram (Fig. 173b), it is evident that under the action of a single load P the maximum shearing force at any chosen section will occur with the load at that section (theoretically, an infinitesimal distance to one side). Likewise, under uniform load, the numerical maximum of shearing force at a given section occurs when the distribution is continuous between that section and the more distant support. The magnitude of such shearing force will be obtained as the product of the intensity of load q and that area of the influence diagram corresponding to the loaded portion of the beam. For example, in the case represented in Fig. 173, the uniform load should extend from the section mn to the support B, and the corresponding shearing force at mn is
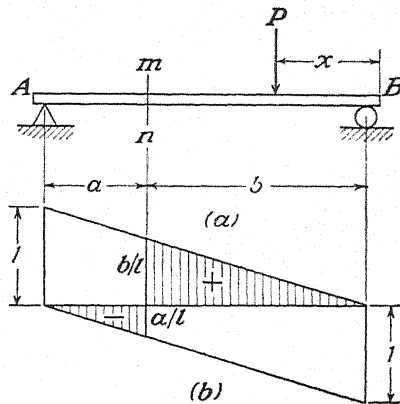
FIG. 173.

$$V_{mn} = q \cdot \frac{b}{l} \cdot \frac{b}{2} = \frac{qb^2}{2l}.$$

The principle of virtual displacements can be used also in the construction of influence lines for shearing forces in beams. To illustrate, we consider the simply supported beam with overhang as shown in Fig. 174a. Assuming that we are interested in the shearing force at the section mn, we imagine the resistance to transverse sliding at this section to be destroyed and replace it by shearing forces V as shown. At the same time, the resistance to bending at the section mn is assumed to remain intact. To realize such conditions, we imagine that at the section mn one element of the beam of length dx is replaced by two links mm' and nn' as shown in Fig. 174b. This preserves the resistance against relative angular displacement between the two portions of the beam and yet allows a small relative transverse displacement as shown in Fig. 174c. Thus we introduce one degree of freedom into the system and can define a corresponding virtual displacement by a small relative displacement δ as shown in Fig. 174d.* Noting that the two portions of the beam have to remain parallel, we conclude that the displaced system must satisfy

* It should be kept in mind that we are discussing displacements of infinitesimal magnitude and that we exaggerate the distortion only for the sake of clarity in the figure.

the condition $om:on = a:b$, and the configuration is completely deter-
mined. Since only the shearing forces V and the applied load P produce
work during the displacement, the equation of virtual work becomes

$$V \cdot \delta - P \cdot y = 0,$$

from which

$$V = \frac{P}{\delta} \cdot y. \tag{a}$$

We see now that the numbers represented by the ratios y/δ are influence
coefficients for shearing force at the section mn. Thus the diagram in
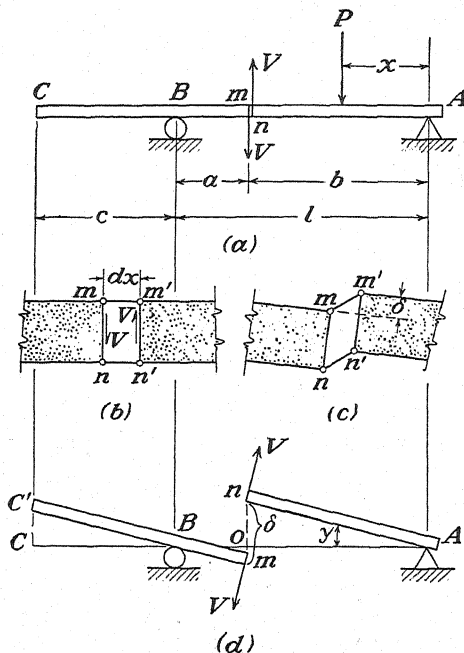
FIG. 174.

Fig. 174d has the shape of an influence diagram, and to use it as such we
need only select a vertical scale that makes $\delta = 1$.

The above procedure is perfectly general and applicable to more
complicated cases. Consider, for example, the compound beam shown
in Fig. 175a, and assume that we require an influence diagram for shearing
force at the section mn. To obtain this by the usual methods of statics
will involve considerable labor because of the necessity of first finding
all reactions. Only the principle of virtual displacements offers a method
of approach by which we can ignore the reactive forces. By this method,
we simply induce a unit transverse sliding displacement at the section mn,
keeping all other constraints (both external and internal) intact. The

corresponding configuration of the system as shown in Fig. 175 defines
an influence diagram for shearing force at the section mn. With the aid
of such a diagram it is easy to see how to place given loads on the beam
in order to obtain maximum shearing force at this section. The dis-
tribution of uniform load illustrated in Fig. 175c, for example, is selected
to give maximum negative shearing force at mn.

In the case of a beam submitted to the action of a series of concen-
trated loads like the standard train in Fig. 157, the condition of loading
for maximum shearing force at a given section is not always self-evident.
However, with the aid of an influence diagram, it is possible to develop
general criteria to determine the most critical position of the loads in
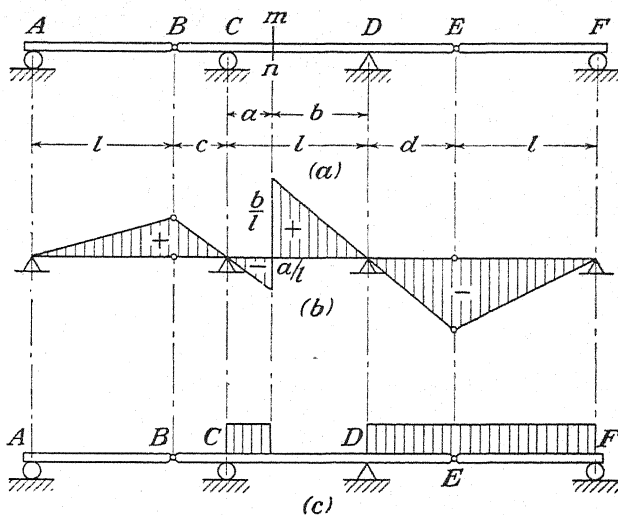
Fig. 175.

any given case. These criteria follow directly from a consideration of
the fluctuations in shearing force at a given section as a series of con-
centrated loads moves across the span. To illustrate, let us suppose
that a standard train moves from right to left across the simply supported
beam shown in Fig. 176a. As it does so, we see from the influence line
that the shearing force at the section mn increases steadily until wheel
① reaches this section, since the influence coefficients under the loads
will be increasing both in number and in magnitude. As wheel ① crosses
the section, there will be an abrupt drop in the shearing force by an
amount equal to the load on this wheel; but, with further movement to
the left (Fig. 176b), the positive shearing force at mn continues its gradual
increase since the positive ordinates of the influence line are increasing
and the negative ordinate under the wheel ① is decreasing. This con-

dition prevails until wheel ② crosses the section, when there is again a corresponding abrupt drop in the shearing force, followed by another gradual rise, etc. These fluctuations in the shearing force at *mn* are represented graphically in Fig. 176c, where, for each position of the leading wheel ①, the corresponding shearing force at *mn* is plotted as an ordinate. The diagram obtained in this manner, of course, extends beyond the end *A* of the beam because, even after wheel ① leaves the span, we continue to have maxima of shearing force at *mn* every time a new wheel comes up to this section. The graphical representation
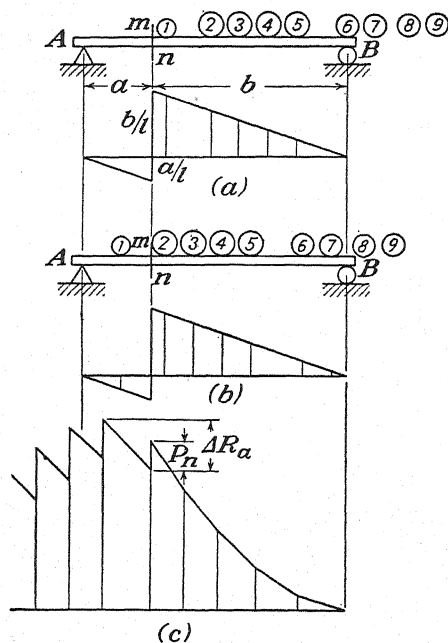
FIG. 176.

shows clearly that there will be as many maxima of shearing force as there are wheels and that each maximum occurs just as some wheel reaches the section. Thus, as a first criterion for maximum shearing force at a chosen cross section, we conclude that the system of loads must be placed so that one of the wheels is at this section.

To determine which load of the series should be placed at the given section in order to obtain a maximum shearing force, we begin with the first wheel at the section and consider the *change in shearing force* as each new wheel is moved up. From Fig. 176c, we note that this change in shearing force between any two successive peaks consists of two parts: (1) a sudden drop equal to the load P_n that crosses the section and (2) a gradual rise equal to the increase ΔR_a in the reaction at *A* as the next

load P_{n+1} comes up to the section.   Denoting the total change in shearing force by ΔV, we have then

$$\Delta V = \Delta R_a - P_n. \tag{5}$$

If expression (5) is positive, this indicates that the shearing force at the section has been increased by advancing the loads.   Hence the procedure is repeated until there is a change in sign of expression (5), which indicates that the greatest peak in Fig. 176c has been passed.   Thus, we may regard a change in sign of expression (5) as the second criterion for maximum shearing force.
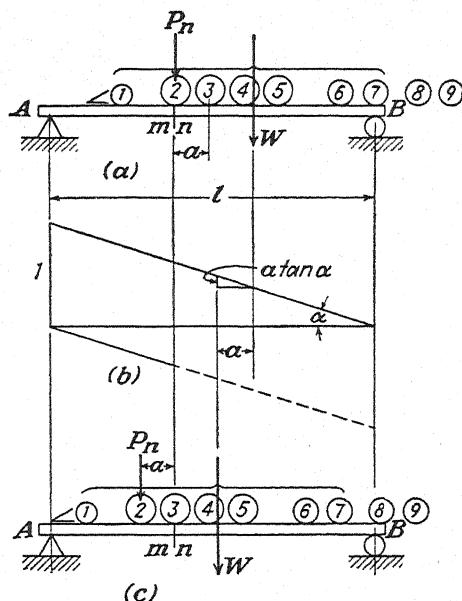
Fig. 177.

If no loads enter or leave the span during one of the advances discussed above, the change ΔR_a may be calculated in a very simple manner. Suppose, for example, that we are advancing the loads from the position shown in Fig. 177a to that shown in Fig. 177c.   From the influence line for R_a (Fig. 177b), we see that, if W is the resultant of all loads on the span and a the distance the loads are advanced, then the change in R_a will be

$$\Delta R_a = Wa \tan \alpha = \frac{Wa}{l},$$

where $\tan \alpha = 1/l$ is the slope of the influence line.   Substituting the expression for ΔR_a in Eq. (b) we obtain

$$\Delta V = \frac{Wa}{l} - P_n. \tag{5a}$$

Loads entering or leaving the span complicate the calculation of ΔR_a. In such case, (Fig. 178), let W be the resultant of all loads on the span before the advance, Q' a load that enters the span a distance b, and P' a load that goes beyond A a distance c. Then, for the change in R_a as the loads are advanced from the position shown in Fig. 178a to that shown in Fig. 178c, we have

$$\Delta R_a = \frac{Wa}{l} - P'\left(1 + \frac{c}{l}\right) + \frac{Q'b}{l}.$$

In this expression, the first term Wa/l represents the increase in R_a, if we assume that there is sufficient overhang at the left to carry the load P' which has gone beyond A, while the second term simply corrects for the fact that there is no such overhang. The third term represents the increase in R_a due to the appearance on the span of the load Q', which was not included in W. Substituting the foregoing expression for ΔR_a in Eq. (5), we obtain
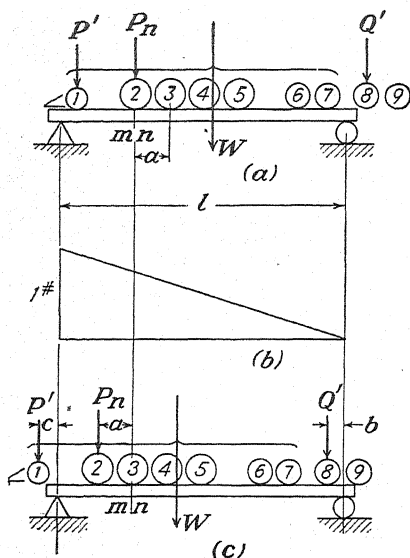
$$\Delta V = \frac{Wa}{l} - (P' + P_n) - \frac{P'c}{l} + \frac{Q'b}{l}.$$

Now, since the ratios c/l and b/l are usually small compared with unity, the last two terms in this expression can be safely neglected and we have

$$\Delta V \approx \frac{Wa}{l} - (P' + P_n). \tag{5b}$$

Thus we see that the effect on ΔV of a load Q' entering the span a small distance b can be completely neglected, while the effect of a load P' leaving the span can be approximately accounted for by adding it to the load P_n, which crosses the section. If no load leaves the span, $P' = 0$ and Eq. (5b) coincides with Eq. (5a). For all cases, then, we may, with good accuracy, consider a change in sign of Eq. (5b) as the criterion for maximum shearing force at a chosen section.

As an application of the above criterion, we shall now determine the maximum shearing force that a Cooper's E-60 loading can induce at the section mn of the simple beam shown in Fig. 179. Beginning with wheel

Fig. 178.

① at the section and moving up wheel ②, we have, by Eq. (5b),

$$\Delta V = \frac{213 \cdot 8}{70} - 15 = +9.34 \text{ kip.}$$

This being positive, the shearing force has been increased, and we start again with wheel ② at the section and move up wheel ③.   Then, by Eq. (5b),

$$\Delta V = \frac{228 \cdot 5}{70} - 30 = -13.7 \text{ kip.}$$

This being negative, the shearing force has been reduced by the second advance, and we put wheel ② at the section for maximum shearing force
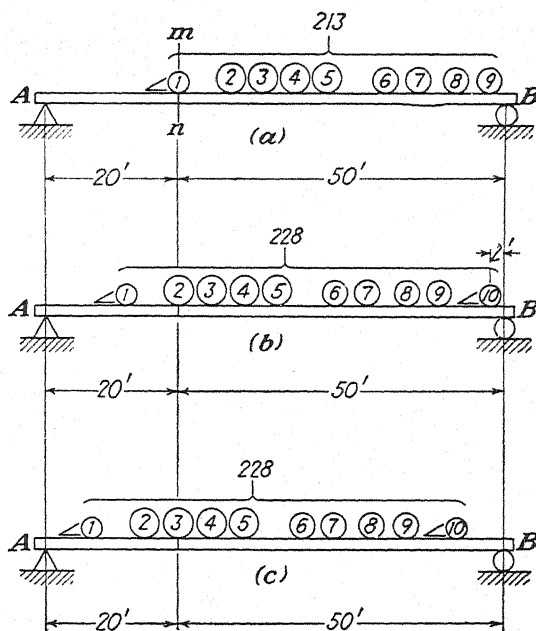
FIG. 179.

there (Fig. 179b).   Now, to calculate this maximum shearing force, we use the formula[1] $V = R_a - 15$.   Calculating R_a with the aid of the moment table (page 95) as explained in the preceding article, this becomes

$$V = \frac{M_{⑩} + 228 \cdot 2}{70} - 15 = \frac{6,950 + 456}{70} - 15 = 90.8 \text{ kip.}$$

It must be emphasized here that the procedure above, *i.e.*, the use of Eq. (5) as a criterion for maximum shearing force, is applicable only to

[1] We assume that wheel ② is just to the right of the section.

the case of a simply supported beam without overhang. In more complicated cases, the influence line should always be drawn and used as a guide in selecting the most critical condition of loading.

PROBLEMS

106. A simply supported girder has a clear span of 20 ft. What maximum shearing force can be induced by a standard train (Cooper's E-60), and at what cross section does such shearing force occur? *Ans.* $V_{max.} = 75$ kip.

107. A simply supported beam has a clear span of 90 ft. Construct the influence line for shearing force at a cross section 20 ft. from the left support. How should Cooper's E-60 loading be placed on the beam to give maximum shearing force at this section, and what is this maximum shearing force? *Ans.* $V_{max.} = 126.9$ kip.

108. A simply supported beam with an over-all length of 44 ft. has a clear span of 32 ft. with a 12-ft. overhang on one end. Construct an influence line for shearing force at a cross section that is 22 ft. from either end of the beam. How should Cooper's E-60 loading be placed on the beam to give maximum shearing force at this section? Evaluate this shearing force. *Ans.* $V_{max.} = 57.1$ kip.

109. Assuming a uniform live load of 6 kip per lineal foot and a uniform dead load of 2 kip per lineal foot, what maximum uplift must be provided for at the support D of the compound beam shown in Fig. 171? Assume $l = 30$ ft., $a = 10$ ft., and $b = 20$ ft.

110. Construct an influence line for shearing force on the pin B of the system shown in Fig. 171. What maximum shearing force can be induced in this pin by a Cooper's E-60 loading? By a uniform live load of 6 kip per lineal foot? Use the same numerical data as in Prob. 109.

23. Influence Lines for Bending Moment.—The question of variation in bending moment at a chosen section of a beam or girder with change
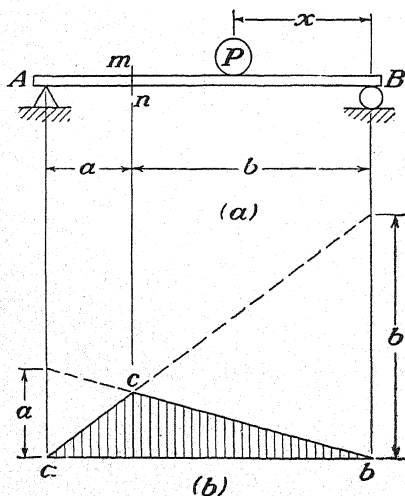
FIG. 180.

in position of a system of moving loads is one of great practical importance. Consider, for example, a simply supported beam AB under the action of a moving load P as shown in Fig. 180a. In such a case, we conclude that, so long as the load is to the right of a given section mn, the bending moment at this section will be $R_a \cdot a$. Likewise, when the load has any position to the left of the section, the bending moment at the section will be $R_b \cdot b$. In both cases, the bending moment is positive. Thus, as in the case of shearing force, we obtain the influence line for bending moment at the given section mn directly from the influence lines for the reactions R_a and R_b. For the portion of the beam to the right of the section, we use the influence line for R_a and simply multiply each ordinate

by the length a.   Similarly, for the portion of the beam to the left of the section, we use the influence line for R_b and multiply each ordinate by the length b.   Thus the complete influence diagram for bending moment at the section mn is represented by the shaded triangle acb shown in Fig. 180b.   We see that the ordinates of an influence line for bending moment always have the dimension of length.   Thus the product between one of these ordinates and the load P has the proper dimension (*force* $\times$ *length*) for bending moment.

From the constructions indicated in Fig. 180b, it can be seen that the maximum ordinate of the diagram occurs under the section mn and has the magnitude ab/l.   Thus, for maximum bending moment due to a
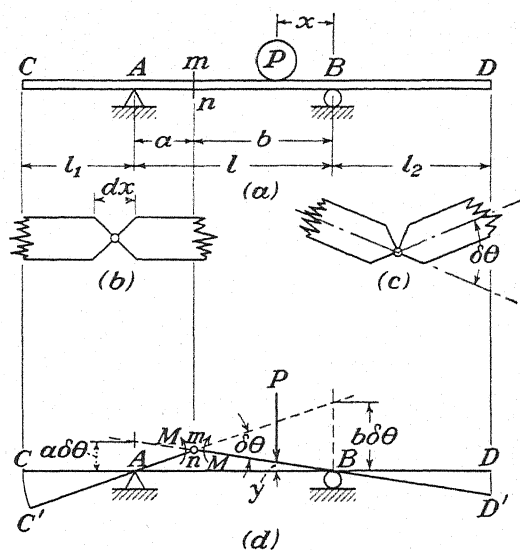
FIG. 181.

single concentrated load P, the load should be placed at the section, and the corresponding bending moment is Pab/l.   For maximum bending moment due to uniformly distributed load, the entire span should be covered.   Since the area of the diagram is $ab/2$, the corresponding magnitude of this maximum bending moment will be $qab/2$, where q is the intensity of load.   If we take $a = b = l/2$, this reduces to the well-known expression $ql^2/8$.

The influence line for bending moment in a beam can also be obtained by using the principle of virtual displacements.   Consider, for example, the simply supported beam with overhangs as shown in Fig. 181a.   To construct an influence line for bending moment at the section mn, we imagine that an element of the beam at this section is replaced by an ideal hinge as shown in Fig. 181b.   This allows relative rotation between

the two portions of the beam as shown in Fig. 181c but at the same time keeps the resistance to shear and direct tension intact. Thus, we obtain a system with one degree of freedom as shown in Fig. 181d. Now to this movable system we apply at any point a load P and at the hinge two equal and opposite couples M as shown. Obviously, the relation between P and M for equilibrium of this fictitious system represents the desired relation between P and the bending moment at the section mn of the original beam in Fig. 181a. This relation is found by assuming a virtual displacement of the system as shown in Fig. 181d and equating to zero the corresponding virtual work. Thus

$$M \cdot \delta\theta - Py = 0,$$

where $\delta\theta$ is the total angular displacement between the two parts of the beam and y is the vertical displacement of the point of application of the load P. From this equation of virtual work, we find

$$M = \frac{Py}{\delta\theta},$$

and we see that the lengths $y/\delta\theta$ are the influence coefficients for bending moment at the section mn. Hence the diagram in Fig. 181d has the shape
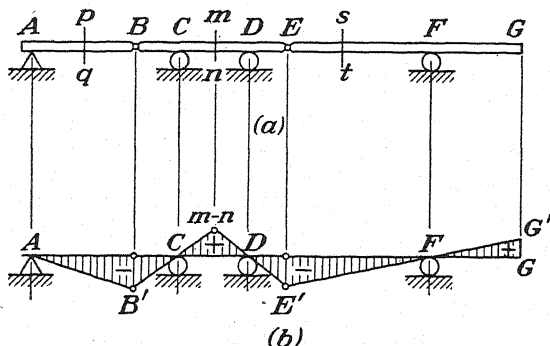
FIG. 182.

of an influence diagram, and to use it as such we need only magnify the vertical scale in the ratio $1:\delta\theta$. Thus, if $\delta\theta = \frac{1}{10}$ radian, we use a magnification factor of 10.

The conclusion above is general and can be used to great advantage in more complicated cases. Consider, for example, the compound beam shown in Fig. 182a, and let it be required to construct an influence line for bending moment at the section mn. To accomplish this, we simply introduce an imaginary hinge at this section (Fig. 182b) and make, between the two portions of the beam BE, a relative angle of rotation in such a direction that positive bending moment at mn will do positive work. The corresponding configuration of the system, compatible with all

remaining constraints, defines the required influence line from which any desired influence coefficient can be scaled directly.

With the aid of the influence line in Fig. 182b, we can see at once how to place given loads on the structure so as to obtain the maximum bending moment at the section *mn*. The maximum negative bending moment under the action of a single load P, for example, occurs with the load at the hinge B. Again, under uniform live load, the worst condition will be realized when the spans AC and DF of the system are loaded, and this condition of loading also induces negative bending moment at the section *mn*.

We shall consider now the question of how to place a series of concentrated loads such as a standard locomotive on a simply supported girder so as to induce the greatest possible bending moment at a given section. We begin with the influence line ACB for bending moment at
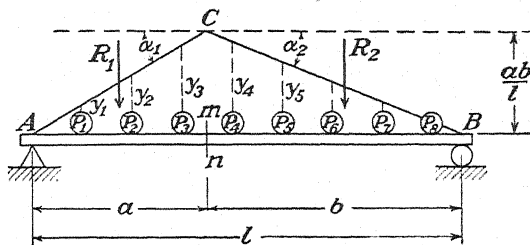
Fig. 183.

a section *mn* as shown in Fig. 183 and allow the system of loads $P_1 \ldots P_n$ to move onto the span from right to left. Then, for any position of the loads as shown in the figure, the bending moment at the section will be obtained simply by taking the sum of moments produced by the individual loads. Thus,

$$M = P_1 y_1 + P_2 y_2 + P_3 y_3 + \cdots P_n y_n, \qquad (a)$$

where $y_1, y_2, \ldots$ are the influence coefficients as shown in the figure. Now imagine that the loads are moved a short distance δx to the left. Then the corresponding change δM in bending moment at the section can be expressed as the algebraic sum of the individual changes in the terms $P_i y_i$ of expression (a). Denoting by R_1 the resultant of all loads to the left of the section and by R_2 the resultant of all loads to the right, we can express the change δM as follows,

$$\delta M = \delta x (R_2 \tan \alpha_2 - R_1 \tan \alpha_1), \qquad (b)$$

where α_1 and α_2 are the slopes of the lines AC and BC, respectively, as shown. Since $\tan \alpha_1 = b/l$ and $\tan \alpha_2 = a/l$, expression (b) can be

written in the form

$$\delta M = \frac{ab}{l} \cdot \delta x \left[\frac{R_2}{b} - \frac{R_1}{a} \right]. \qquad (c)$$

In this expression, the terms R_2/b and R_1/a represent, respectively, the *average loads* on the right and left portions of the span. Thus, we conclude from expression (c) that the bending moment at the section will continue to increase with movement of the loads to the left so long as

$$\frac{R_2}{b} > \frac{R_1}{a}, \qquad (6)$$

i.e., so long as the average load on the right portion of the span is greater than that on the left. As soon as this condition is reversed, the bending moment will begin to decrease.

If, during movement of the loads to the left, a new load enters the span from the right, R_2/b will be increased, while R_1/a will remain unaffected. Hence, to reach a maximum bending moment at mn, further movement to the left is indicated. Likewise, if a load leaves the span on the left, R_1/a will be decreased and R_2/b will be unaffected, so that in this case also further movement to the left is indicated. We conclude, then, that the entrance of a load on the right or the exit of a load on the left cannot invalidate the conclusion of the preceding paragraph and is not significant in determining the position of the loads for greatest
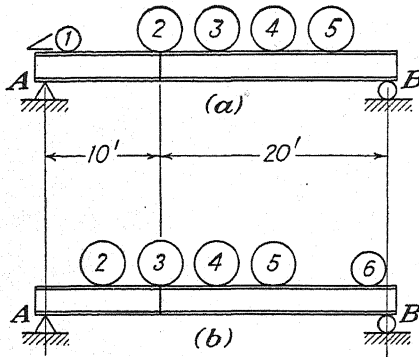
FIG. 184.

bending moment at the section mn. On the other hand, each time a load crosses the section mn there will be a sudden increase in R_1/a and a corresponding decrease in R_2/b, which may reverse condition (6). From this we conclude that the maximum bending moment at mn will occur with some load at the section. The proper load will be that one which, when moved across the section, reverses condition (6).

As a full series of loads moves from right to left across the span, there may be several reversals of condition (6). This simply means that the bending moment at the section passes through several maxima, as we have already seen for shearing force (page 110). In such a case, each maximum (with some load at the section) must be evaluated, and then the one that is numerically greatest will be used as a basis for design. An example will serve to illustrate these remarks.

In Fig. 184, we have a short girder AB for which it is required to determine the maximum bending moment at the third-point under the action of a Cooper's E-60 loading (see Fig. 157, page 94). With wheel ② just to the right of the section (Fig. 184a), expression (6) becomes

$$\frac{120}{20} > \frac{15}{10},$$

while, with the same wheel just to the left of the section, we have

$$\frac{90}{20} = \frac{45}{10}.$$

This condition of equality indicates that the bending moment remains constant as wheel ② crosses the section and up to the time when wheel ① leaves the span. As wheel ③ comes up to the section (Fig. 184b), condition (6) becomes

$$\frac{109.5}{20} > \frac{30}{10},$$

which indicates that the bending moment is still increasing; but as this wheel crosses the section, condition (6) drops to

$$\frac{79.5}{20} < \frac{60}{10},$$

and the bending moment begins to decrease. Hence, for maximum bending moment at the third-point, we place the loads as shown in Fig. 184b. The corresponding bending moment $M = 556.5$ kip-ft. can be found very easily with the help of the moment table (page 95).

PROBLEMS

111. Construct influence lines for bending moment at the sections pq and st of the compound beam shown in Fig. 182a.

112. Construct influence lines for bending moment at the sections mn and pq of the compound beam shown in Fig. 166.

113. A simply supported girder AB has a clear span of 60 ft. Under the action of a standard Cooper's E-60 loading, what is the maximum bending moment that can occur, (a) at the mid-point of the span, (b) at a third-point?
   Ans. (a) 1907.5 kip-ft. (b) 1738.7 kip-ft.

114. A simply supported beam 30 ft. long has a clear span of 24 ft. with a 6-ft. overhang at one end. What maximum bending moment can be produced by a standard train, (a) at the mid-point of the 24-ft. span, (b) at the overhung support?
   Ans. (a) 412.5 kip-ft. (b) −210.0 kip-ft.

115. How should Cooper's E-60 loadings be placed on the compound beam shown in Fig. 175 to produce maximum bending moment at the cross section mn, and what is this maximum bending moment? Assume $l = 30$ ft., $c = 10$ ft., $d = 20$ ft., and $a = 10$ ft.
   Hint: Use two trains, one approaching from each end of the beam.

24. Absolute Maximum Bending Moment.—In the preceding article, we have considered the question of how to place a given system of concentrated loads on a beam in order to realize the maximum bending moment at some chosen section. We shall now consider a method of determining that particular cross section of the beam for which the maximum bending moment is greater than for any other cross section. That is, as a given system of loads moves across the span, what is the maximum bending moment that occurs in the beam and at what cross section does it occur? This particular cross section is called the *dangerous section*, and the maximum bending moment occurring there is called the *absolute maximum bending moment*. It is, of course, for the case of a beam of uniform cross section the bending moment that should be used as a basis for design.

In the case of a single concentrated load P moving across a simply supported beam (Fig. 185a) the question is a simple one. From the bending-moment diagram for this case (Fig. 185b), we see that
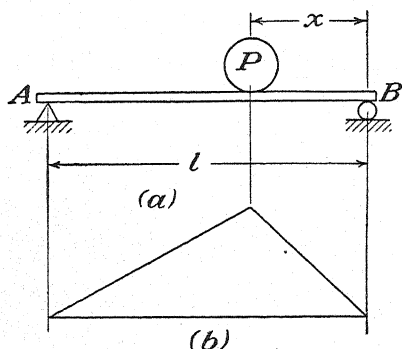
Fig. 185.
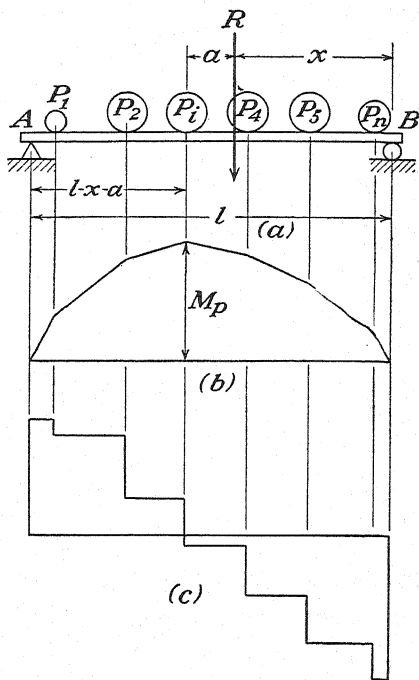
Fig. 186.

for any position of the load as defined by the distance x from the right support the dangerous section is that section under the load; and here the bending moment is

$$M_p = \frac{Px}{l}(l - x).$$ (a)

Considering M_p as a continuous function of x, we find the value of x for which it will be a maximum by setting $dM_p/dx = 0$. This gives

$$\frac{P}{l}(l - 2x) = 0,$$

from which we obtain $x = l/2$. Thus the absolute maximum bending moment occurs at the middle cross section when the load is at that section. The value of this absolute maximum bending moment is $Pl/4$.

Now let us consider the more general case where we have a simple beam carrying a series of concentrated loads as shown in Fig. 186a. Since all loads on the span produce positive bending moment at all sections, we can conclude at once that to obtain an absolute maximum bending moment we should place as many heavy loads on the beam

as possible.   Then, for any assumed position of these loads, we know that the maximum bending moment will occur under that load where the shearing force in the beam changes sign.   Let us assume in Fig. 186 that this load is P_i, and let R denote the resultant of all the loads on the span and x its distance from the support B.   Also, let M denote the sum of moments of all loads to the left of P_i with respect to the point of application of P_i; and, finally, let a denote the distance between R and P_i as shown. With these notations, the bending moment under the load P_i can be expressed as follows:

$$M_p = \frac{Rx}{l}(l - x - a) - M. \tag{b}$$

We assume now that we can vary x slightly without any loads going on or off the span. Then, within these limits, dM_p/dx can be regarded as a continuous function of x and can be treated in the same manner as expression (a).   Setting this derivative equal to zero, we find

$$\frac{R}{l}(l - 2x - a) = 0,$$

from which

$$l - x - a = x. \tag{c}$$

This expression shows that M_p will be an absolute maximum when the load P_i and the resultant of all the loads on the span are equidistant from the ends of the beam.   The foregoing conclusions can be summarized by the following criterion: *The maximum bending moment in a simply supported beam under a series of concentrated loads occurs under that load where the shear changes sign and is an absolute maximum when the loads are so placed that the mid-point of the span bisects the distance a between this load and the resultant R of all the loads on the beam.*

In using the criterion above for absolute maximum bending moment, it must be kept in mind that, as a given series of loads moves across the beam, there may be several absolute maxima of bending moment as different wheels occupy the middle region of the span.   However, experience shows that the section of absolute maximum bending moment, *i.e.*, the dangerous section, is never far removed from the middle cross section.   Thus we can often reduce the amount of labor in calculation by first determining, in accordance with the method of Art. 23, the position of the loads for maximum bending moment at the middle cross section.   This done, the loads can be shifted slightly to satisfy the criterion for absolute maximum bending moment, and then the moment can be evaluated.   For all practical purposes it can be taken for granted, without further investigation, that this will be the greatest possible absolute maximum bending moment.

A graphical method of determining the absolute maximum bending moment in a beam under a given series of concentrated loads is sometimes useful.   This method is based on the fact, as shown in Art. 8, that a funicular polygon can, with a proper closing line, be used as a bending-moment diagram.   Suppose, for example, that we have the series of loads $P_1 \ldots P_9$ as shown in Fig. 187a, for which $abcdefghijk$ (Fig. 187b) is a funicular polygon corresponding to an arbitrarily chosen pole O (Fig. 187c). Then, for a beam of span l to which these loads can be applied, we can study the effect of change in position of load simply by holding the loads stationary and shifting the beam to the left or right under them.   Thus, for example, if the beam has the position A_1B_1 relative to the loads, we obtain the corresponding bending-moment diagram simply by drawing to the funicular polygon the closing side a_1b_1.   Similarly, for the position A_2B_2 of the beam relative to the loads, the bending-moment diagram is

obtained by drawing the closing side a_2b_2, etc. In each case it is easy to locate by inspection the maximum ordinate of the diagram; and, of course, the corresponding bending moment is obtained by multiplying this ordinate by the *pole distance H*.
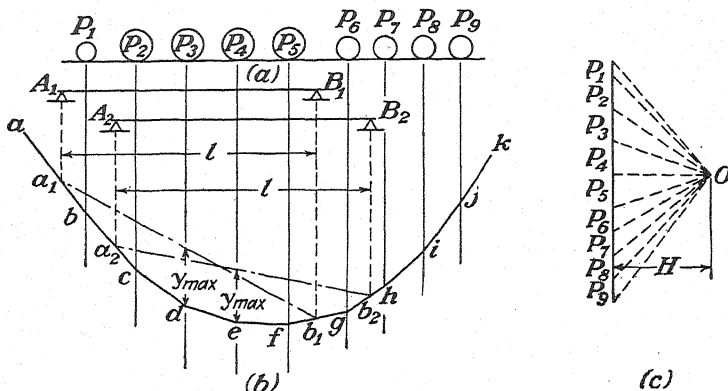
Fig. 187.

With a little practice one can determine the absolute maximum bending moment by this method with sufficient accuracy for all practical purposes.

PROBLEMS

116. Find the absolute maximum bending moment in the simple beam loaded as shown in Fig. 188. How does this compare with the maximum bending moment at the mid-point of the span?
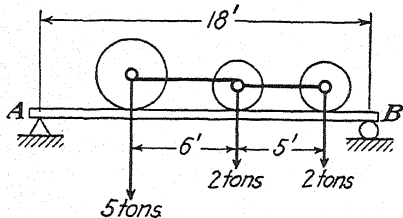
117. (*a*) Determine the absolute maximum bending moment in a simply supported beam having a clear span of 46 ft. if the live load is a standard train (Cooper's E-60).

Fig. 188.

(*b*) Construct a funicular polygon for one locomotive, and use it to check graphically the results of the preceding calculation.

118. Compute the maximum bending moment in a 28-ft. highway bridge span during the passage of a 20-ton motor truck having a 14-ft. wheel base and 80 per cent of its load on the rear wheels.

119. Determine the absolute maximum bending moment induced in the beam *AB* loaded as shown in Fig. 189. The crane *CDE* can roll freely along the beam.
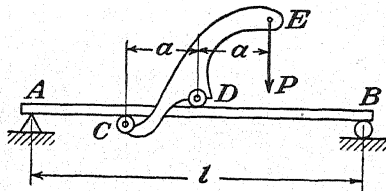
Fig. 189.

120. Determine the absolute maximum bending moment induced in the beam CD of the system shown in Fig. 190.
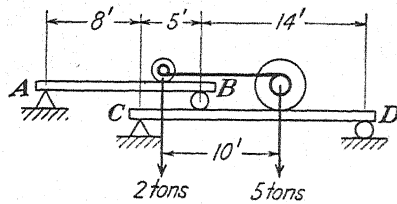
FIG. 190.

25. Girders with Floor Beams.—In those cases where long-span girders are used in bridge construction, the live loads are rarely applied directly to the girder. Instead, as illustrated in Fig. 191a, the main girders AB carry several crossbeams at $a, b, c, \ldots$ which are called *floor beams*, and these in turn carry a series of *stringers* $ab, bc, cd, \ldots$ by which the floor system of the bridge is supported. Those portions of the
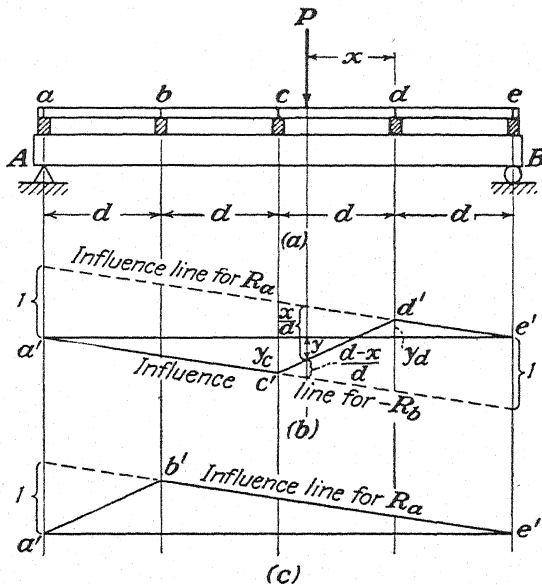
FIG. 191.

main girder between the floor beams are called *panels*, and the points $a, b, c, \ldots$ are called *panel points*. It follows from such construction that a load P applied to any stringer will be transmitted to the main girder only at the two corresponding panel points. Such division of the load between two panel points has no effect upon the reactions at A and B, and the influence lines for these quantities will be the same as for a girder without floor beams. In the construction of influence lines for

shearing force and bending moment, however, it becomes necessary to modify slightly our previous discussions.

We begin with the question of influence lines for shearing force. Since loads can be transmitted to the girders only at panel points, we conclude at once that, for any condition of loading on the stringers, the shearing force in a girder will be constant throughout any one panel. Thus, without ambiguity, we may speak of the *shearing force in a panel* instead of the shearing force at any particular cross section of that panel. With this idea in mind, we shall now consider the construction of an influence line for shearing force in the panel *cd* of the girder shown in Fig. 191*a*. For any position of the load P to the left of panel point c, the shearing force in the panel *cd* is negative and numerically equal to R_b, while, for any position of P to the right of d, it is positive and equal to R_a. Thus, for the portions *de* and *ac* of the span, we use directly the corresponding portions $d'e'$ and $a'c'$ of the influence lines for R_a and R_b, respectively, as shown in Fig. 191*b*.

Now let the load P have any position within the panel *cd* as defined by the distance x. Then, at c and d, the corresponding panel-point loads are, respectively,

$$P_c = P\frac{x}{d} \qquad \text{and} \qquad P_d = P\frac{d-x}{d}, \qquad (a)$$

where d is the panel distance as shown. Using the corresponding influence coefficients y_c and y_d, we find that the shearing force in the panel is

$$V = y_c \cdot P\frac{x}{d} + y_d \cdot P\frac{d-x}{d}. \qquad (b)$$

This expression is a linear function of x and reduces to Py_d when $x = 0$ and to Py_c when $x = d$. Hence, to obtain that portion of the influence line corresponding to positions of the load within the panel *cd*, we need only connect the established points c' and d' by a straight line as shown (Fig. 191*b*). By the same procedure, we obtain the influence diagram for shearing force in the panel *ab* as shown in Fig. 191*c*.

To construct an influence line for bending moment at some given cross section *mn* of a girder with floor beams (Fig. 192*a*) we proceed in a similar manner. Again we note that, for any position of the load P to the right of d, we have at the section *mn* the bending moment $R_a \cdot a$, while, for any position to the left of point c, we have a bending moment $R_b \cdot b$. Hence, as for a girder without floor beams, we obtain the portions $a'c'$ and $e'd'$ of the desired influence diagram (Fig. 192*b*) simply by multiplying by a and b, respectively, the corresponding ordinates of the influence lines for R_a and R_b. Now, let the load have any position within the panel as defined by the distance x. Then, as before, the panel

point loads at c and d are given by expressions (a); and using these, together with the established influence coefficients y_c and y_d, we find for the bending moment at the section mn

$$M_{mn} = y_c \cdot P\frac{x}{d} + y_d \cdot P\frac{d-x}{d} \qquad (c)$$

Like expression (b), this is a linear function of x, reducing to Py_d when $x = 0$ and to Py_c when $x = d$. Accordingly, we conclude that the straight line $c'd'$ in Fig. 192b completes the influence diagram for bending moment at the section mn.
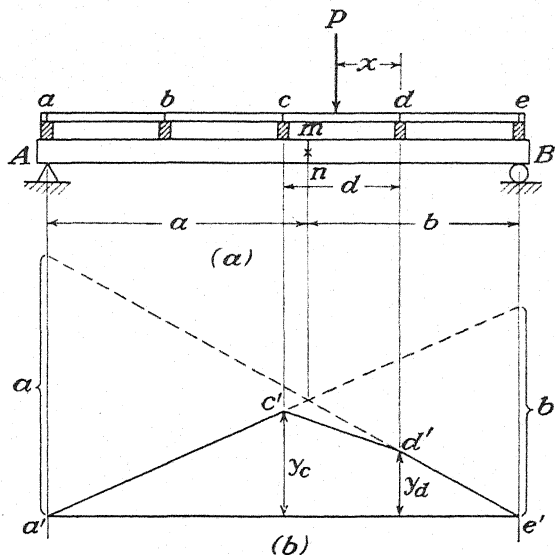
FIG. 192.

In general, we can state that, in the case of a girder with floor beams, any influence line can be obtained directly from the corresponding influence line for a girder without floor beams. It is necessary only to connect by a straight line the points of the latter influence line corresponding to the ends of the panel under consideration. This follows from the fact that if the load is applied at any panel point it is transmitted directly to the girder, while, for any position of the load within a panel, the shearing force and bending moment at a given section vary linearly with change in position of the load.

In the case of a girder with floor beams the development of criteria for the placement of concentrated load systems to produce maximum effects does not require much additional discussion. Since the shearing force in an end panel will always be greater than in any intermediate panel and since the influence line (Fig. 191c) in such a case has the same

form as an influence line for bending moment, we may use the criteria already developed in Art. 23 for maximum bending moment at a given section. Again, in the case of actual bending moment, the maximum will occur at one of the panel points since loads are transmitted to the girder only at such points. Thus, in this case, also, the criteria already developed for maximum bending moment at a given section are applicable, and the question of absolute maximum moment as discussed in Art. 24 need not be considered.

As an example illustrating the numerical calculation of maximum live-load shearing force and maximum live-load bending moment in the case of a girder with floor beams, we assume that Fig. 193a represents a single-track plate-girder railroad bridge having a span of 88 ft. and sub-
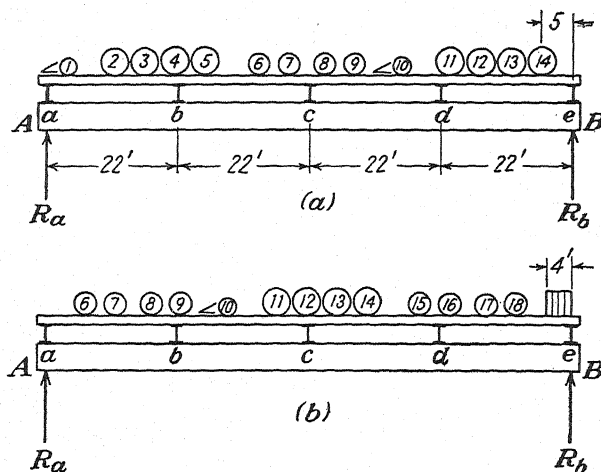
Fig. 193.

divided into four equal panels as shown. We assume also that the live load is a standard Cooper's E-60 loading.

For shearing force in an end panel, we have the influence diagram shown in Fig. 191c and can use, as a criterion of maximum, the reversal of condition (6) as discussed on page 118. With wheel ④ just to the right of panel point b (Fig. 193a), expression (6) becomes

$$\frac{273}{66} > \frac{75}{22},$$

while, with this wheel just to the left of b, we have

$$\frac{243}{66} < \frac{105}{22}.$$

Thus there is a reversal of condition (6) as wheel ④ crosses the section, and we place this wheel at b for maximum shearing force in the end panel

ab. The corresponding value of this shearing force is

$$V_{ab} = R_a - P_a,$$

where R_a is the reaction at A and P_a is the panel-point load at a. Using the moment table for Cooper's E-60 loading (page 95), we find

$$R_a = \frac{13,100 + 348 \cdot 5}{88} = 168.5 \text{ kip,}$$

$$P_a = \frac{720}{22} = 32.7 \text{ kip,}$$

so that

$$V_{ab} = 168.5 - 32.7 = 135.8 \text{ kip.}$$
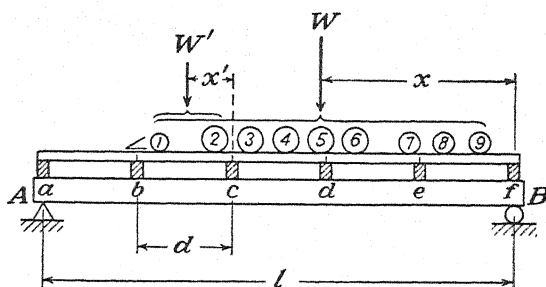
FIG. 194.

For maximum bending moment, which will occur at the panel point c, we put wheel ⑫ at this point (Fig. 193b) because, as this wheel crosses mid-span, condition (6) changes from

$$\frac{180}{44} > \frac{123}{44} \qquad \text{to} \qquad \frac{150}{44} < \frac{153}{44}.$$

The corresponding value of the reaction at A is (see moment table)

$$R_a = \frac{11,700 + 291 \cdot 4 + 12 \cdot 2}{88} = 146.3 \text{ kip,}$$

and the bending moment at c then becomes

$$M_c = 146.3 \cdot 44 - 2,605 = 3,840 \text{ kip-ft.}$$

With the foregoing maxima of shearing force and bending moment, a trial section can be chosen for the girder on the basis of which more detailed investigations of stresses can be made.

Sometimes the maximum live-load shearing force in an intermediate panel of a girder with floor beams will be required. For such cases, a criterion for placing the loads can be developed as follows: Referring to Fig. 194 and assuming that we require the maximum shearing force in the panel bc as a standard train moves from right to left across the span,

we denote by W the resultant of all loads on the girder and by x its distance from B as shown. Likewise, let W' be the resultant of all loads within the panel bc and x' its distance from the panel point c. Then by statics the shearing force in the panel bc is

$$V_{bc} = \frac{Wx}{l} - \frac{W'x'}{d}. \tag{d}$$

If the loads are now advanced a distance Δx to the left, the shearing force becomes

$$V_{bc}' = \frac{W}{l}(x + \Delta x) - \frac{W'}{d}(x' + \Delta x) \tag{e}$$

and we see that the change in shearing force is

$$\Delta V = \left(\frac{W}{l} - \frac{W'}{d}\right)\Delta x \tag{f}$$

As long as this expression is positive, *i.e.*, as long as

$$\frac{W}{l} > \frac{W'}{d}, \tag{7}$$

the shearing force in the panel bc continues to increase as the loads advance from right to left. Thus a maximum value of V_{bc} will be reached only when there is a reversal of condition (7), and from Fig. 194 we see that this will occur just as some wheel enters the panel bc. Consequently, for maximum shearing force in the panel bc, we place at panel point c that wheel which upon entering the panel bc reverses condition (7).

PROBLEMS

121. How should a standard train be placed on the girder in Fig. 193 to produce a maximum shearing force in the panel bc? Evaluate this maximum shearing force.
    Ans. 65.9 kip.

122. Evaluate the maximum bending moment at the panel point b of the girder in Fig. 193 if the loading is a standard Cooper's E-60 train. *Ans.* 2,990 kip-ft.

123. Determine the greatest floor-beam reaction (*i.e.*, panel-point load) produced by the passage of a Cooper's E-60 train across the girder shown in Fig. 193.
    Ans. 105.3 kip.

124. Evaluate the maximum live-load bending moment at the center of the span in Fig. 194 if $l = 50$ ft. and $d = 10$ ft. Assume a Cooper's E-60 loading. Compare this with the maximum bending moment at c or d.

125. Referring to Fig. 195, find the maximum live-load shearing force and bending moment produced in the girder AB as a standard train (Cooper's E-60) crosses the span.
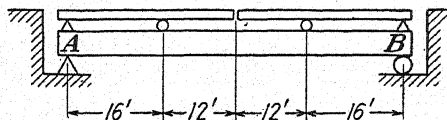
FIG. 195.

26. Influence Lines for Three-hinged Arch Ribs.—In discussing influence lines for three-hinged arches, we begin with the case of a non-symmetrical arch ACB (Fig. 196a) and assume that a moving vertical load P acts directly upon the rib as shown.   This load induces reactions

at the supports A and B, each of which we resolve into two components, one vertical and the other directed along the line AB as shown. Then, by equating to zero the algebraic sum of moments of all forces with respect to the points A and B, we conclude that the vertical components R_a and R_b of the reactions are the same as for a simple beam of span l.   Denoting by H' the components in the direction of AB and projecting all forces onto a horizontal axis, we conclude that these components are equal in magnitude and opposite in direction.   The horizontal projection of H' is called the *horizontal thrust* of the arch, and we denote it by H, that is, $H = H' \cos \alpha$.   To determine the

Fig. 196.

magnitude of H, we consider the portion AC of the arch as a free body and equate to zero the algebraic sum of all forces with respect to the hinge C.   Thus we write

$$R_a \cdot a - H' \cdot f \cos \alpha = 0,$$

where f is the *vertical rise* of the arch as shown in the figure.   From this equation we find

$$H' \cos \alpha = H = R_a \cdot \frac{a}{f} \qquad (a)$$

Observing that $R_a \cdot a$ is the bending moment that would be produced at the distance a from the left end of a simple beam of span l, we conclude that, during motion of the load P along the arch, the horizontal thrust H is always proportional to this simple-beam bending moment.   Hence, to obtain the influence line for H, we simply divide by f the ordinates of the corresponding influence line for bending moment at C in a simple beam, as shown in Fig. 196b.

If a system of vertical loads acts on the arch and it is required to find their position to make H a maximum, we simply use the criterion already developed for maximum bending moment at point C in a simple beam
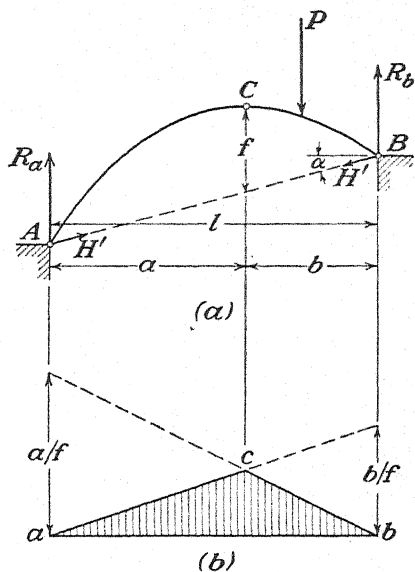
[see Eq. (6) page 118]. To obtain the horizontal thrust H when vertical load is uniformly distributed along the span of the arch, we simply multiply the area acb of the influence diagram by the intensity q of this load. Since the ordinates of the diagram are pure numbers in this case, the area acb has the dimension of length and its product with intensity of load q has then the dimension of force.

Let us consider now the construction of an influence diagram for bending moment at some chosen cross section D of the unsymmetrical
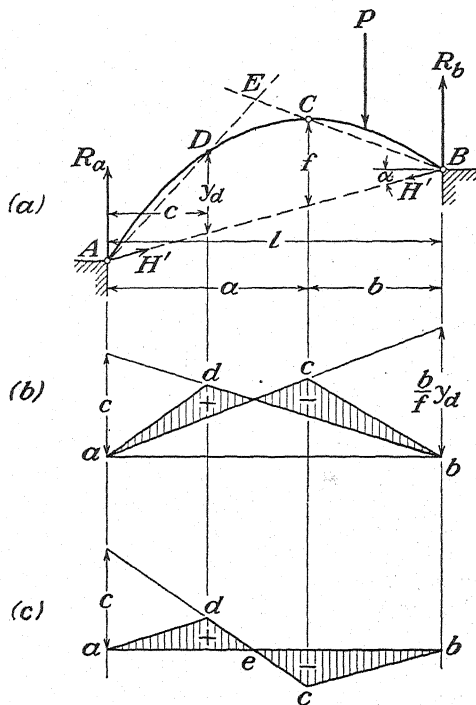
FIG. 197.

arch in Fig. 197a. If the position of this cross section is defined by its distance c from the reaction R_a, the bending moment for the loading shown may be expressed as follows:

$$M_d = R_a c - H y_d. \qquad (b)$$

The first term on the right side of this expression represents the corresponding bending moment in a simple beam of span l, while the second term represents the moment contributed by the horizontal thrust H. Hence the influence diagram for M_d is obtained by subtracting, from the ordinates of the influence line for bending moment in a simple beam, the ordinates of the influence line for H (Fig. 196b) multiplied by y_d. The

result of such subtraction is shown by the shaded areas in Fig. 197b. This influence diagram can be represented in a somewhat simpler form by plotting the ordinates from a horizontal base ab as shown in Fig. 197c. To obtain this simplified diagram, we note that the zero point e must lie on the vertical through E (Fig. 197a) where the lines BC and AD intersect. This follows from the fact that, when the load P passes through point E, the total reaction at A evidently passes through point D and M_d vanishes. Observing further that the points d and c are on verticals through D and C and that at the left end of the diagram the
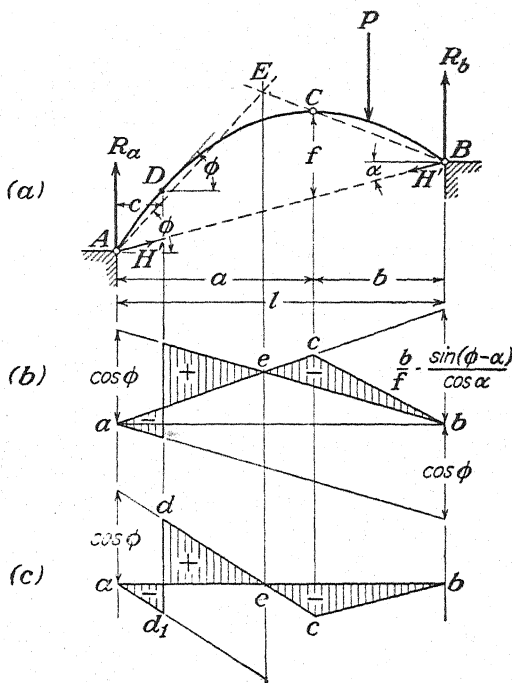
FIG. 198.

ordinate of the straight line ced must be equal to c, we can readily make the simplified constructions shown in Fig. 197c.

The shearing force produced at the cross section D (Fig. 198a) by a vertical load P on the arch is given by the equation

$$V_d = R_a \cos \phi - H' \sin (\phi - \alpha) = R_a \cos \phi - H \frac{\sin (\phi - \alpha)}{\cos \alpha}, \quad (c)$$

where ϕ is the angle that the tangent to the center line at D makes with the horizontal and α is the angle between the horizontal and the line AB as shown. The first term on the right side of expression (c) represents

the corresponding simple-beam shearing force at D multiplied by cos ϕ, while the second term represents the contribution to shearing force made by the horizontal thrust H. Thus the ordinates of the influence diagram for shearing force at D are obtained as differences between corresponding ordinates for shearing force in a simple beam multiplied by cos ϕ and for thrust H multiplied by sin $(\phi - \alpha)/\cos \alpha$. These differences are shown by ordinates of the shaded areas in Fig. 198b. Here, again, the influence diagram can be presented in simpler form by plotting the ordinates from a horizontal base line ab as shown in Fig. 198c. In this case, we obtain the simplified diagram by noting that the zero point e must lie on the vertical through E obtained as the intersection between the line BC and the line through A which makes the angle ϕ with the horizontal. This follows from the fact that the total reaction at A is parallel to the tangent at D when the load P passes through E. Having the zero point e and noting further that the straight line ced has the ordinate $1 \cdot \cos \phi$ at the left end of the span, we can make the constructions in Fig. 198c without difficulty.

Arches are usually so designed that there can be no direct transmission of live load to the rib as assumed throughout the preceding discussion; instead, the loads are applied to a system of floor beams supported by the arch as shown in Fig. 199a. Under such conditions, forces can be transmitted to the arch proper only at the panel points $I, J, K, \ldots$, and in the construction of influence lines we must proceed in the same manner as for a girder with floor beams (see Art. 25). That is, we construct first the influence lines as for an arch without floor beams and then connect by straight lines those points which correspond to the extremities of the panel under consideration. For example, to obtain the influence line for horizontal thrust H of the arch in Fig. 199a, we begin in Fig. 199b with the influence line acb, which assumes direct transmission of the load P (see Fig. 196b), and then join by a straight line the points j and k corresponding to the panel points J and K as shown. Thus the ordinates of the line $ajkb$ represent the required influence coefficients for horizontal thrust H. The correctness of this procedure follows directly from the fact that H, as we already have seen from Eq. (a), is proportional to the simple-beam bending moment at C, and C is contained within the panel JK. If the floor beams are so arranged that the hinge C becomes a panel point, the influence line for H will be the same as for direct transmission of the load P.

The influence diagram for bending moment at the section D of the arch is obtained in a similar manner as shown in Fig. 199c. The portions acb and adb of this diagram are first constructed on the assumption of direct transmission of live load (compare with Fig. 197b) and then the points j, k and i, j_1 corresponding to the panel points I, J, K, are con-

nected by straight lines as shown.   The ordinates of the shaded portions
of the diagram represent the required influence coefficients for bending
moment at D.

The influence diagram for shearing force at the cross section D,
obtained by the same general procedure, is shown in Fig. 199d.   It should
be noted in connection with this latter diagram that, owing to the
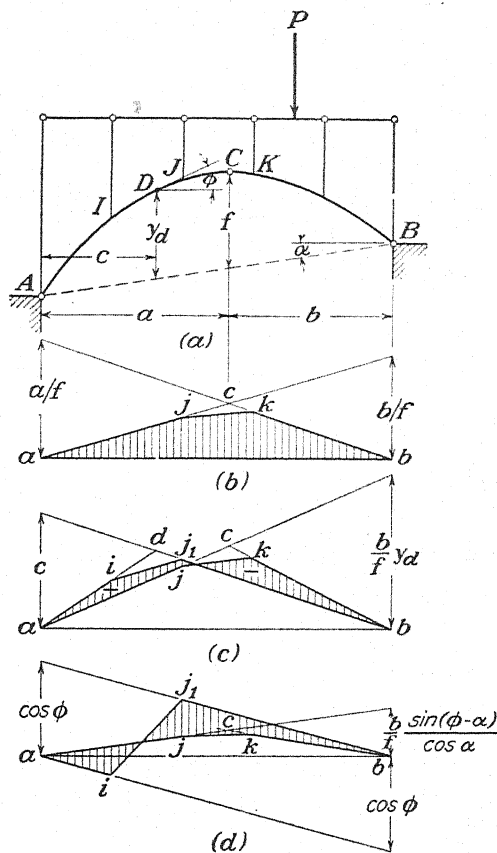
Fig. 199.

curvature of the arch rib, the shearing force is not constant throughout
the panel IJ as in the case of a girder with floor beams.

Expressions (a), (b), and (c), developed for the case of a simple three-
hinged arch, hold also for the arch with overhangs as shown in Fig. 200a.
Accordingly, from Eq. (a) we conclude that the influence line for hori-
zontal thrust H in this arch will be obtained by dividing by f the ordinates
of an influence line for bending moment at C in a corresponding com-
pound beam $D'F'G'E'$, supported as shown in Fig. 200b.   To obtain this

influence line, we use the method of virtual displacements and make at c (corresponding to C) such a relative angular displacement $n \cdot \delta\theta$ as shown in Fig. 200c that $aa' = a/f$ and $bb' = b/f$. The ordinates of the shaded diagram so obtained represent the required influence coefficients for horizontal thrust H of the arch. The influence diagram for bending moment at N is obtained in a similar manner as shown in Fig. 200d.
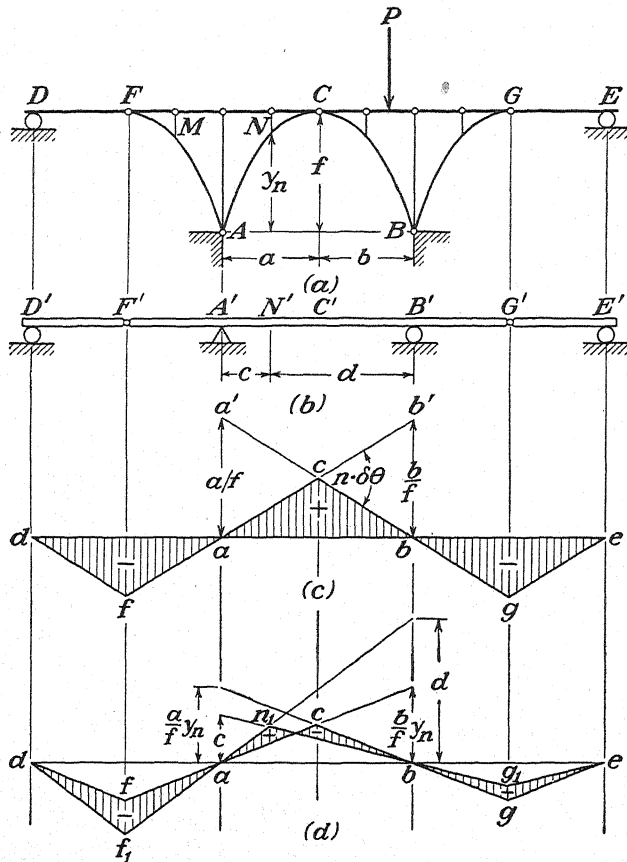
FIG. 200.

Here $df_1n_1g_1e$ represents the influence line for bending moment at N' of the corresponding compound beam (Fig. 200b), while $dfcge$ is simply the foregoing influence line for H with all ordinates multiplied by y_n. In accordance with Eq. (b), the differences in ordinates obtained by superposition of these two diagrams represent the required influence coefficients for bending moment at N in the arch of Fig. 200a. An influence diagram for shearing force at N can be obtained in a similar manner.

PROBLEMS

126. Construct an influence line for horizontal thrust H in a symmetrical three-hinged arch for which $l = 60$ ft. and $f = 8$ ft. (a) Using this line, determine the magnitude of H produced by a uniformly distributed load of intensity $q = 1$ kip per ft. and extending over the entire span. (b) Find the maximum value of H produced by a standard train (Cooper's E-60) assuming that the crown C is a panel point.

<div align="right">

Ans. (a) 56.25 kip. (b) 239.8 kip.
</div>

127. Assuming that the arch in Fig. 197a has the form of a parabola with vertical axis and vertex at C and that $a = b = l/2$, that is, that the arch is symmetrical, find the maximum positive bending moment at D due to a uniform live load of intensity q per unit length of span. Note that only the portion AE of the span should be loaded and that for a symmetrical parabola the length ae (Fig. 197c) is equal to $l^2/(3l - 2c)$, where c defines the position of point D as shown in Fig. 197a.

128. Referring to Fig. 198 and assuming, as in the preceding problem, that the arch is a symmetrical parabola of span $l = 60$ ft. and rise $f = 15$ ft., find the numerical maximum of shearing force at the quarter point D ($c = l/4$) under the action of a uniform live load of intensity $q = 1$ kip per ft. of span. Assume a direct transmission of load to the arch rib.

<div align="center">

Ans. 3.35 kip.
</div>

129. Construct influence diagrams for horizontal thrust H, bending moment M_d, and shearing force V_d in the case of a symmetrical semicircular three-hinged arch of span l as shown in Fig. 201. Assuming direct transmission of a uniformly distributed live load of intensity $q = 1$ kip per ft. of span, find the maximum numerical value of each of the foregoing quantities. Where do these maxima occur, *i.e.*, for what values of ϕ?
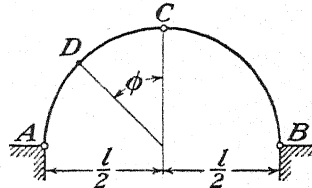
FIG. 201.

130. Construct influence diagrams for shearing force at N and for bending moment at M of the arch shown in Fig. 200.

27. Influence Lines for Simple Trusses.

—In the design of a truss we must find for each member the most unfavorable position of live load and then evaluate the corresponding axial force in that member. For such investigations, we shall see that influence lines can be used to advantage. We begin, for example, with the simple truss shown in Fig. 202a and assume that all loads are transmitted by means of floor beams to the joints $A, C, D, \ldots$ of the lower chord. Then, to construct an influence line for the axial force in an upper chord member such as EF, we assume a vertical load P acting on the truss and make a section mn as shown. Considering that portion of the truss to the left of this section as a free body and writing an equation of moments with respect to joint D, we obtain

$$R_a a + S_1 h_1 = 0,$$

from which

$$S_1 = -\frac{R_a a}{h_1}. \tag{a}$$

From this expression, we see that the compressive force S_1 is proportional to the bending moment $R_a a$ which would occur at the cross section D of a corresponding loaded simple beam of span l. The same observation holds also if the load P is to the left of D. Hence, we conclude that the influence line for S_1 will be obtained by dividing by $-h_1$ the ordinates of an influence line for bending moment at the cross section D of a simple
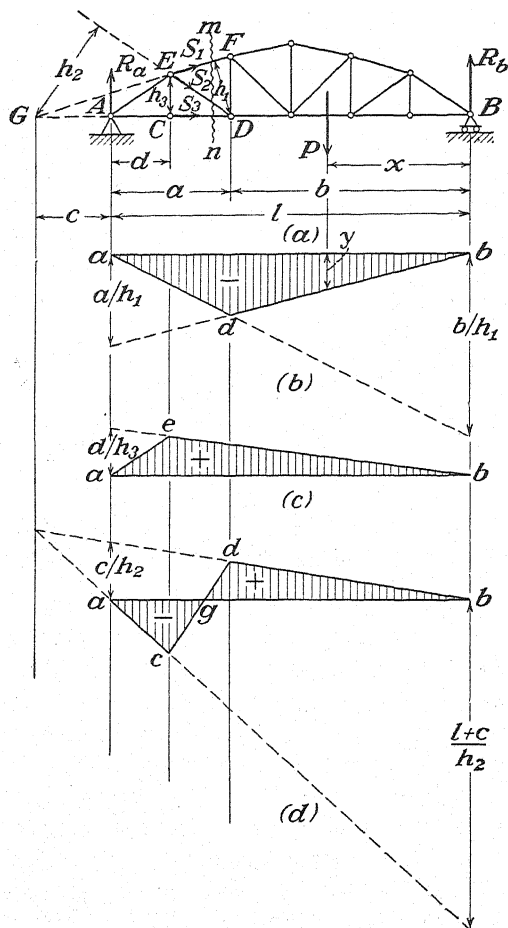
Fig. 202.

beam AB. This construction is shown in Fig. 202b, and adb is the desired influence line for axial force in EF. Multiplying the load P by the ordinate y of this line, which is a pure number, we obtain the corresponding value of S_1. In the same way, if a uniformly distributed load extends over the entire span, the corresponding axial force S_1 is obtained as the product of the intensity q of this load and the area abd

of the influence diagram. To find the maximum value of S_1 that can be induced by a system of loads like the standard train in Fig. 157, we proceed in the same manner as to find the maximum bending moment at D of a simple beam (see page 118).

An influence line for the axial force in a lower chord member such as CD can be obtained in a similar manner. In this case, we use E as a moment center and note that the force S_3 is proportional to the simple-beam bending moment at this point. Hence the desired influence line will be obtained by dividing by h_3 the ordinates of an influence line for bending moment at E of a simple beam of span l. This construction is shown in Fig. 202c, and we note that the influence coefficients are positive, indicating tension in the bar CD.

We shall now consider the construction of an influence line for axial force in the diagonal ED of the truss in Fig. 202a. Assuming first that the load P acts to the right of joint D and equating to zero the algebraic sum of moments of all forces to the left of mn with respect to point G, we obtain

$$S_2 = \frac{R_a c}{h_2}. \tag{b}$$

Thus, so long as P is to the right of D, the ordinates of the influence line for S_2 can be obtained simply by multiplying by c/h_2 the ordinates of the influence line for R_a. In this way we obtain the portion bd of the required influence line as shown in Fig. 202d. When the load P is to the left of joint C, we consider the equilibrium of the right portion of the truss; and an equation of moments with respect to point G then gives

$$S_2 = -\frac{R_b(l + c)}{h_2}. \tag{c}$$

Thus, for positions of the load to the left of C, the ordinates of the influence line for S_2 can be obtained by multiplying by $-(l + c)/h_2$ the ordinates of the influence line for R_b. This construction is shown in Fig. 202d by the straight line ac, having at b the ordinate $-(l + c)/h_2$. Now, when P is between C and D, we follow the same reasoning used in the case of a girder with floor beams (see page 124) and conclude that to complete the diagram we need only connect the established points c and d by a straight line as shown. We see that this influence diagram for a diagonal has a form similar to that for shearing force in an intermediate panel of a girder with floor beams (see Fig. 191b) and that the axial force S_2 may be either tension or compression depending on the placement of the live load. For example, to realize the maximum tensile force in ED due to uniformly distributed live load of intensity q, we must load only the portion gb of the span. Then the corresponding magnitude of S_2 is obtained as the product between q and the area of the triangle gbd.

Similarly, the maximum compressive force in ED occurs when the distributed load extends only over the portion ag of the span. In finding the maximum value of S_2 due to a series of concentrated loads like a standard train, we proceed in a manner similar to that used in finding maximum shearing force in an intermediate panel of a girder with floor beams (see page 128).

The influence lines for vertical members of a truss will usually be constructed in a manner similar to that discussed above for diagonal members.
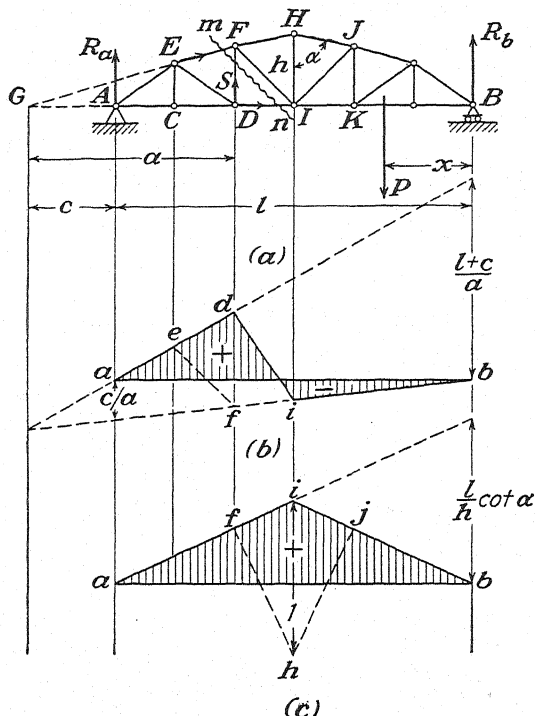
FIG. 203.

For example, if we require an influence line for the axial force S in the vertical bar DF of the truss in Fig. 203a, we make the section mn as shown and then, with G as a moment center, write equations of equilibrium for the left and right portions of the truss as P is successively to the right of I and to the left of D. This gives

$$S = -\frac{R_a c}{a} \qquad \text{and} \qquad S = R_b \frac{l + c}{a},$$

from which we conclude that the required influence line for S will be obtained from the influence lines for R_a and R_b modified as shown in Fig. 203b.

The above procedure is not applicable in the case of the middle vertical HI. To construct the influence line for axial force in this bar, we must consider the equilibrium of the joint H. Denoting by S_1 the force in HI and by S_2 the force in each of the chord members FH and HJ, we see that

$$S_1 = -2S_2 \cos \alpha, \qquad (d)$$

where α is the angle that each chord member makes with the vertical as shown. Thus the required influence line for S_1 is obtained by multiplying by $-2 \cos \alpha$ the ordinates of an influence line for S_2 as shown in Fig. 203c. The influence line for S_2 in an upper chord member is constructed in the manner already shown in Fig. 202b.

Throughout the preceding discussions, we have assumed the live load to be transmitted to the joints of the lower chord of the truss. Let us consider now the case in which loads are transmitted to the joints of the upper chord. Repeating the previous reasoning regarding influence lines for chord members and diagonals, we shall find that such change in the application of live load does not alter the diagrams in Fig. 202. On the other hand, the influence lines for verticals as shown in Fig. 203 will be somewhat changed. Considering first the vertical DF and making the section mn as before, we see that the ordinates of the line bi of the diagram in Fig. 203b can still be used so long as the load P (now applied to the upper chord) is to the right of joint F. Thus this line can be extended to point f. In the same manner, we find that the ordinates of the line ad can be used so long as the load P is to the left of joint E. Hence, the portion ae of this line also can be used. Then connecting the points e and f as shown by the dotted line, we obtain the influence diagram $aefb$ for the vertical DF when the live load is applied to the upper chord of the truss. We note finally that changing the live-load application from the lower to the upper chord results only in replacing the line di by the line ef as shown. In the case of the middle vertical HI, we assume first that the load P acts at H. Then, from the equilibrium of this joint, we find

$$S_1 = -2S_2 \cos \alpha - P. \qquad (e)$$

Comparing this expression with expression (d), we conclude that, in the case of application of live load to the upper chord, we obtain the middle ordinate of the influence diagram for axial force in HI simply by subtracting unity from the corresponding ordinate of the diagram aib in Fig. 203c. In this manner, we obtain the point h as shown. Now if P is to the right of J or to the left of F, the condition of equilibrium of the joint H is represented by expression (d) instead of expression (e). Hence the portions af and bj of the diagram in Fig. 203c are still valid, and to complete the modified diagram we simply connect the points f, h and j, h as shown by dotted lines.

The method of virtual displacements can often be used to advantage in the construction of influence lines for truss members. Consider, for example, the truss shown in Fig. 204a, and assume that live load is transmitted to the joints of the lower chord. Then, to obtain the influence line for a member EF of this truss, we imagine this bar to be removed and its action on the remainder of the truss represented by two equal but opposite forces S_1 as shown. In this way, we obtain a system with one degree of freedom, as represented by the possibility for relative rotation about joint D between the two shaded rigid portions. A virtual dis-
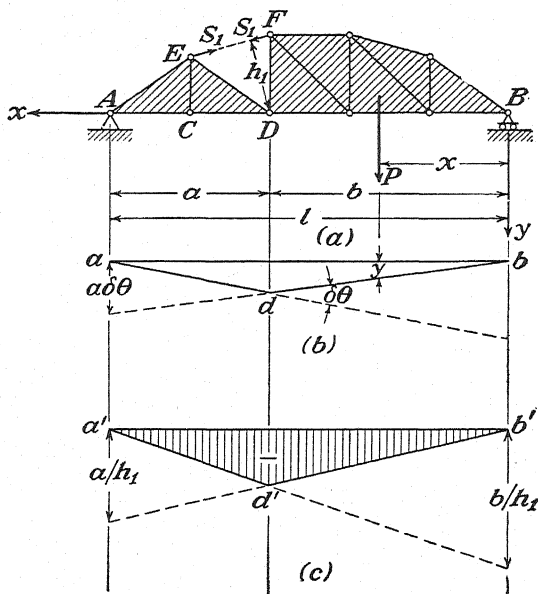
FIG. 204.

placement of this system can be defined by the line adb (Fig. 204b), the ordinates of which represent the vertical deflections of points on the lower chord corresponding to a small relative angular displacement $\delta\theta$ between the two rigid portions. If y denotes the deflection of the point of application of the load P and Δ the shortening of the distance EF during the assumed virtual displacement, the equation of virtual work becomes

$$S_1\Delta + Py = 0,$$

and we obtain

$$S_1 = -\frac{Py}{\Delta}. \qquad (f)$$

We see from this expression that S_1 is proportional to y, and hence the deflection line adb gives us the general shape of the required influence

diagram. To obtain the influence coefficients to scale, we need only
divide the ordinates y of this diagram by $-\Delta$. To do this, we note from
the figure that for the portion bd of the line we can write $y = xa\,\delta\theta/l$
and also that $\Delta = \delta\theta \cdot h_1$. Hence, for positions of the load P to the right
of D, the influence coefficients are

$$-\frac{y}{\Delta} = -\frac{xa}{h_1 l}.$$

In Fig. 204c, then, the corresponding portion $b'd'$ of the true influence
line for S_1 must have the ordinate a/h_1 when $x = l$ as shown.   In the
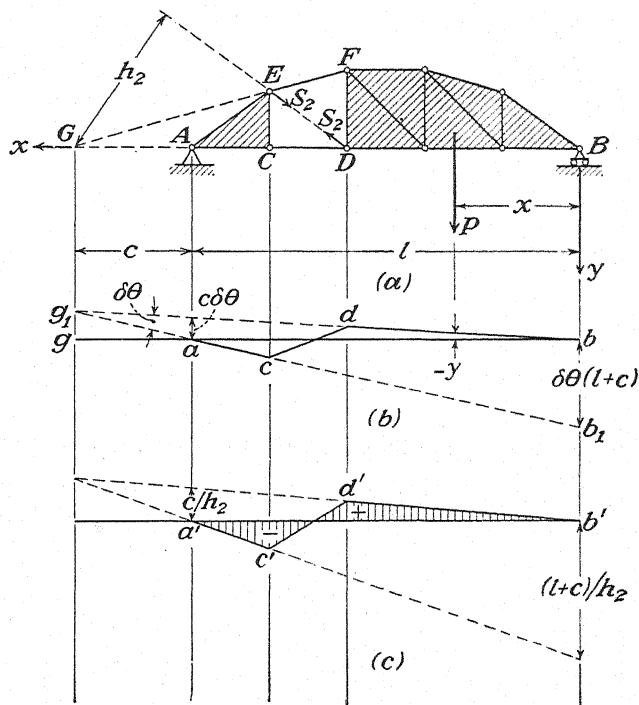
FIG. 205.

same manner, we can show that for the left portion of the truss the line
$a'd'$ must have at b' the ordinate b/h_1.   The same procedure can be used
in constructing the influence line for any lower chord member.

To obtain an influence line for the diagonal ED by the method of
virtual displacements, we first replace this bar by forces S_2 as shown in
Fig. 205a.   Then a virtual displacement of the system can be defined
by a relative angular displacement $\delta\theta$ between the two rigid shaded
portions.   This relative rotation must take place about the instantaneous
center G in such a manner that the supported points A and B of the truss

do not move vertically. To accomplish this, we assume first that the support at B is removed and rotate the entire truss as a rigid body about the hinge A. Small vertical displacements of the lower chord corresponding to this rotation are indicated in Fig. 205b by the straight line ab_1, and we see that, while b goes to b_1, the instantaneous center g goes to g_1. Now, keeping the left portion of the truss stationary, we rotate the right portion about g_1 by such an angle $\delta\theta$ that point B comes back to its original position, *i.e.*, in Fig. 205b, point b_1 comes back to b. The final configuration of the bottom chord then is represented by the line $acdb$ as shown. Denoting by y the vertical displacement of the load P corresponding to the assumed virtual displacement of the system, the equation of virtual work becomes

$$S_2 \cdot \Delta + Py = 0,$$

from which

$$S_2 = -\frac{Py}{\Delta}, \qquad (g)$$

where Δ, as before, is the shortening of the distance ED corresponding to $\delta\theta$. Again, we see that S_2 is proportional to y and conclude that the line $acdb$ gives us the general shape of the required influence line for S_2. To get the influence coefficients $-y/\Delta$ to scale, we note from Fig. 205b that

$$-y = c \cdot \delta\theta \cdot \frac{x}{l} \qquad \text{and} \qquad \Delta = \delta\theta \cdot h_2.$$

Hence, for the right portion of the truss, the influence coefficients are

$$-\frac{y}{\Delta} = \frac{x}{l} \cdot \frac{c}{h_2},$$

and the corresponding portion $b'd'$ of the true influence line has, at $x = l$, the ordinate c/h_2 as shown in Fig. 205c. In the same manner, we conclude that the line $a'c'$ must have at b' the ordinate $-(l + c)/h_2$ as shown. Comparing Fig. 205c with Fig. 202d, we see that the influence line obtained by the method of virtual displacements is identical with that previously obtained by the method of sections.

In the analysis of trusses, we often use influence diagrams only to find the most unfavorable positions of live load and then calculate the corresponding axial forces in the members without further reference to these diagrams. For such purpose, it is evident that we do not need the actual magnitudes of the influence coefficients but only the general shapes of the diagrams, which, as we have just seen, can be obtained very easily by the method of virtual displacements.

PROBLEMS

131. (a) Assuming that live load is transmitted to the joints of the lower chord, construct influence diagrams for the members AE and AC of the truss in Fig. 202a. (b) Find the maximum force that can be induced in the bar CD of this truss, due to a uniformly distributed live load of intensity $q = 1$ kip per ft. (c) Assuming a Cooper's E-60 loading, find the maximum tensile force in the diagonal ED of this truss. Assume $l = 120$ ft., $h_3 = 18$ ft., and $c = 30$ ft.   *Ans.* (b) 66.7 kip. (c) 80.2 kip.

132. Using the method of sections, construct influence diagrams for the axial forces S_1, S_2, and S_3 in the truss shown in Fig. 114. Assume that the live load is transmitted to the joints of the upper chord. How must these diagrams be changed if the live load is applied to the lower chord?

133. Using the method of virtual displacements and assuming the live load applied to the joints of the upper chord of the truss in Fig. 206a, we obtain, for the diagonal
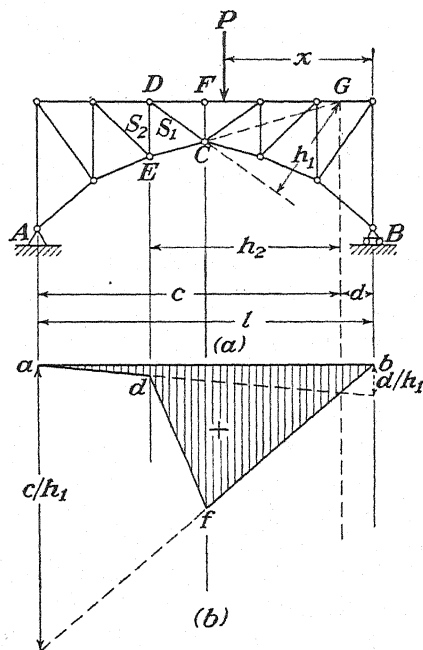
Fig. 206.

CD, the influence diagram $adfb$ shown in Fig. 206b. Following the same procedure, construct the influence diagram for axial force S_2 in the vertical bar DE. What is the maximum tension in CD due to a uniformly distributed live load of intensity q?

134. Assuming that live load is transmitted to the joints of the lower chord, construct an influence diagram for the middle vertical of each of the simple trusses shown in Fig. 118.

135. Construct influence diagrams for S_1, S_2, and S_3 in each of the simple trusses shown in Fig. 207. At those intersections where no joints are indicated, the bars are understood to pass each other freely. How will each of these diagrams be changed if the live load P is transmitted to the joints of the lower chord?
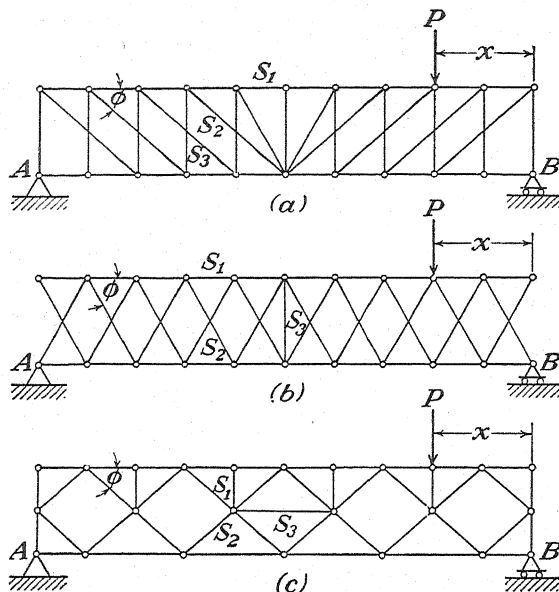
FIG. 207.

28. Influence Lines for Compound Trusses.—A compound truss with subdivided panels like that shown in Fig. 208a may be considered as consisting of a basic simple truss (Fig. 208b) on which are superposed several secondary trusses (Fig. 208c). In the analysis of such a system under dead load, we determine first the axial forces in the bars of the basic truss and then add algebraically the forces in the corresponding bars of the secondary truss (see Art. 16). The same procedure can be used in the construction of influence lines for the compound truss. We begin with the influence lines for the bars of a secondary truss as shown in Fig. 208c. These are shown, respectively, in Fig. 208d for the vertical member, Fig. 208e for the horizontal member, and Fig. 208f for either inclined member. With these secondary diagrams, the influence diagram for any bar of the compound truss can easily be obtained. Consider, for example, the member CD. For the corresponding member of the basic truss (Fig. 208b) the influence diagram is represented by the triangle $a_1c_1b_1$ shown in Fig. 208g. Now on the ordinates of this diagram we must superpose the ordinates of the diagram in Fig. 208e. Since $\frac{1}{2} \tan \phi = \frac{1}{2}d/h$, this is accomplished simply by extending the line a_1c_1 to point e_1 and then connecting points e_1 and d_1 by a straight line as shown. The shaded figure $a_1e_1d_1b_1$ obtained in this way represents the required influence diagram for the member CD of the given compound truss.

To obtain the influence diagram for the lower portion FD of a diagonal of the compound truss, we construct first the influence diagram $a_2c_2d_2b_2$

(Fig. 208h) for the corresponding diagonal of the basic truss. Then, on the ordinates of this diagram, we superpose the ordinates of the secondary diagram in Fig. 208f as shown. In this way, we obtain the shaded diagram $a_2e_2d_2b_2$ (Fig. 208h), the ordinates of which represent the required influence coefficients for the member FD of the given compound truss. The upper portions of the diagonals as well as the verticals
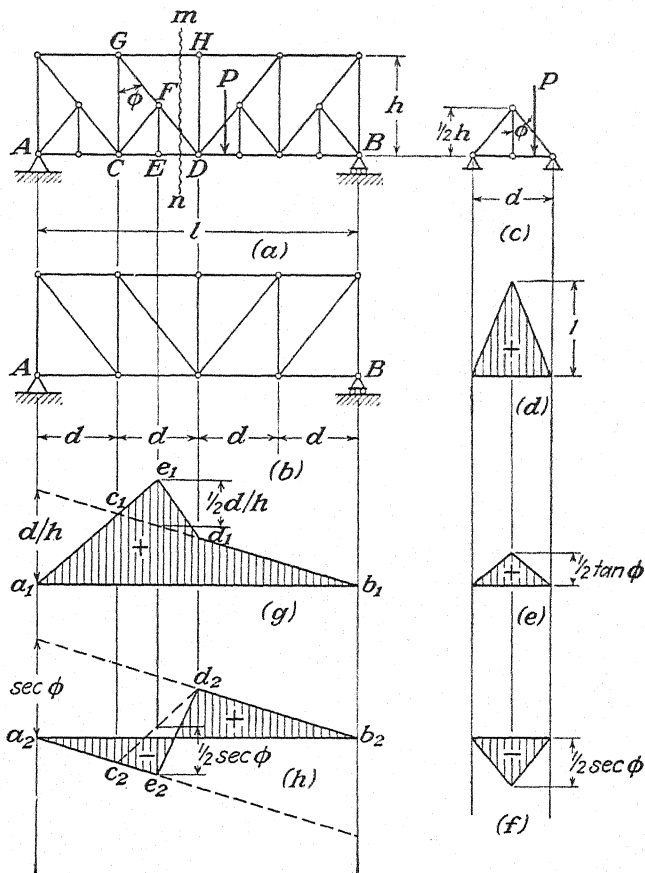
Fig. 208.

and upper chord members of the compound truss will, of course, have the same influence lines as the corresponding members of the basic truss. Thus in Fig. 208h, for example, the line $a_2c_2d_2b_2$ may be used as the influence line for the member GF of the compound truss.

In the case of a compound truss like that in Fig. 208a, the influence diagrams in Figs. 208g and 208h can also be constructed by direct application of the method of sections as in the preceding article. If the load P is to the right of joint D, we consider the equilibrium of that portion of

the truss to the left of the section *mn* (Fig. 208*a*) and find that the lines b_1d_1 and b_2d_2 must be the same as for the basic truss (Fig. 208*b*). Likewise, if the load *P* is to the left of joint *E*, we consider the equilibrium of that portion of the truss to the right of the section *mn* and find the lines a_1e_1 and a_2e_2 as shown. Then, to complete the constructions, it remains
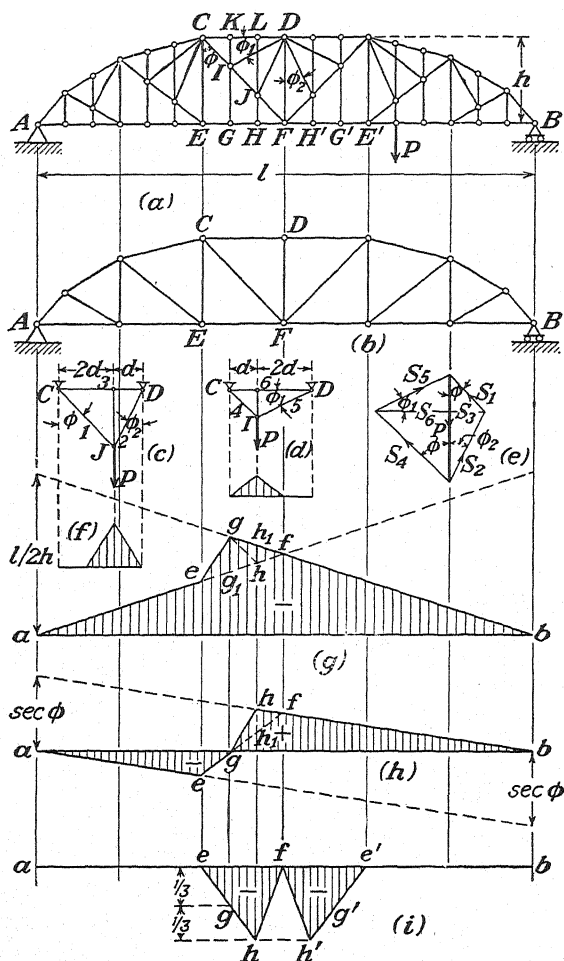
Fig. 209.

only to draw the straight lines e_1d_1 and e_2d_2 corresponding to positions of the load within the panel *ED*.

As a second example of a truss with subdivided panels, let us consider the compound truss shown in Fig. 209*a*, the corresponding basic system for which is shown in Fig. 209*b*. If it is desired to construct influence diagrams for various members within the portion *CDEF* of this truss,

we have to consider first the secondary frames CJD and CID shown in Figs. 209c and 209d, respectively. To obtain influence diagrams for the bars of these secondary frames, we assume that the load P acts on the lower joints J and I as shown. Then the axial forces in all members are given by the force diagram shown in Fig. 209e. From this diagram we find

$$S_1 = +\frac{P}{3} \sec \phi, \qquad S_2 = +\frac{2}{3} P \sec \phi_2, \qquad S_3 = -\frac{P}{3} \tan \phi, \left.\right\}$$
$$S_4 = +\frac{2}{3} P \sec \phi, \qquad S_5 = +\frac{P}{3} \csc \phi_1, \qquad S_6 = -\frac{P}{3} \cot \phi_1. \left.\right\} \quad (a)$$

Noting now that the secondary truss CJD (Fig. 209c) is inactive except when the live load is within the panels GH and HF of the given compound truss, we conclude that the influence diagram for each bar of this secondary truss is a simple isosceles triangle as shown in Fig. 209f and that the maximum ordinate of this triangle, depending on which bar we are interested in, is given by the corresponding influence coefficient from one of expressions (a) above. For example, taking the height of this triangle equal to $\frac{1}{3} \sec \phi$, we obtain the influence diagram for S_1. Again, if the height is taken equal to $-\frac{1}{3} \tan \phi$, we obtain the influence diagram for S_3, etc. In the same manner, we conclude that for each bar of the secondary truss CID (Fig. 209d), which is inactive except when live load is within the panels EG and GH, the influence diagram is also an isosceles triangle as shown and that the maximum ordinate is given by the corresponding influence coefficient from one of expressions (a).

We are now ready to consider the construction of an influence diagram for any member of the portion $CDEF$ of the given compound truss. Let us take, first, the upper chord member CK. For the corresponding member of the basic truss (Fig. 209b), the influence diagram is represented by the triangle afb in Fig. 209g. On the ordinates of this diagram we must now superpose the ordinates of the diagram for S_3 (Fig. 209c) and the ordinates for S_6 (Fig. 209d), since the member CK belongs to both secondary frames. The superposed diagram for S_6 is represented in Fig. 209g by the triangle egh and we note from the figure that its height $gg_1 = 2d/h = \frac{1}{3} \cot \phi_1$, which agrees with the last of Eqs. (a). Likewise, the diagram for S_3 is represented by the triangle ghf, for which the height $hh_1 = d/h = \frac{1}{3} \tan \phi$. Finally, then, the ordinates of the diagram $aegb$ represent the required influence coefficients for the bar CK of the given compound truss.

To construct the influence diagram for the middle portion IJ of the diagonal CF, we begin in Fig. 209h with the diagram $aefb$ for the corresponding member of the basic truss. Then, on the ordinates of this diagram, we must superpose the ordinates of the diagram for S_1 of the secondary truss CJD shown in Fig. 209c. This diagram is the isosceles

triangle in Fig. 209f with the maximum ordinate $\frac{1}{3}$ sec ϕ. Hence, the required superposition is accomplished in Fig. 209h by extending the line bf to h and connecting g and h by a straight line as shown. This follows from the fact that such construction makes $hh_1 = \frac{1}{3}$ sec ϕ, as can easily be seen from a study of the figure. Finally then, for IJ we have the influence diagram $aeghb$.
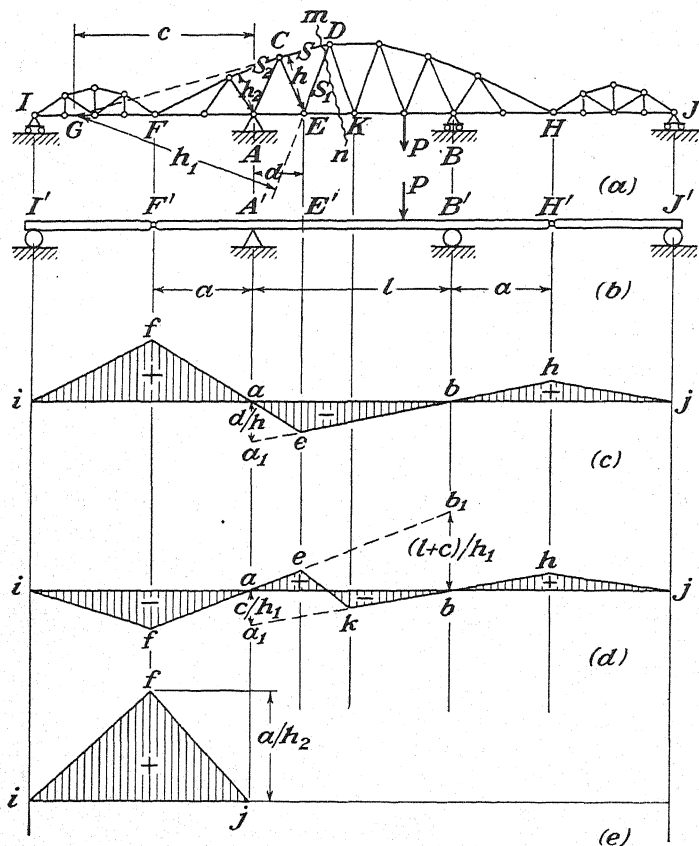
Fig. 210.

The influence diagram for the vertical FD of the given compound truss is shown in Fig. 209i. In this case the corresponding member of the basic truss is completely inactive for live load transmitted to the joints of the lower chord of the truss so that FD serves only as a support for the secondary frames. Thus, putting the load P successively at E, G, H, and F, we conclude that FD carries compressive forces equal to 0, $\frac{1}{3}P$, $\frac{2}{3}P$, and 0, respectively, and that the corresponding influence coefficients are 0, $-\frac{1}{3}$, $-\frac{2}{3}$, and 0 as shown.

Influence diagrams for various members of the cantilever truss shown in Fig. 210a can be readily constructed by considering the compound

beam in Fig. 210b as the corresponding basic system. Let us consider, for example, the influence diagram for the upper chord member CD of this truss.   Making a section mn as shown and writing an equation of moments with respect to the joint E, we conclude that for any position of the load P on the lower chord the axial force S in the bar CD is obtained by dividing by $-h$ the corresponding bending moment at E' of the compound beam shown in Fig. 210b.   Hence, the desired influence diagram for S is obtained by dividing by h the ordinates of an influence diagram for bending moment at E' as shown in Fig. 210c.*   Influence diagrams for members of the lower chord of the cantilever truss can be constructed in a similar manner.

In the case of a diagonal member DE, the axial force S_1 is obtained by using the same section mn and writing an equation of moments with respect to point G (Fig. 210a).   If the load P is to the right of joint K, this equation gives

$$S_1 = -\frac{R_a c}{h_1} \tag{b}$$

and we see that the corresponding portion of the influence diagram for S_1 can be obtained by multiplying by $-c/h_1$ the ordinates of an influence line for the reaction R_a of the compound beam in Fig. 210b.   This construction is represented by the line jhbk in Fig. 210d.   If the load P is to the left of joint E, we consider the equilibrium of the portion of the truss to the right of the section mn and obtain

$$S_1 = R_b \frac{l + c}{h_1}. \tag{c}$$

Thus, in Fig. 210d, we obtain the portion ife of the required diagram by multiplying by $(l + c)/h_1$ the ordinates of an influence line for the reaction R_b of the compound beam in Fig. 210b.   Finally, for positions of the load P within the panel EK, we draw the straight line ek, and the required influence diagram ifekhj for S_1 is completed.

The influence diagram for the axial force S_2 is shown in Fig. 210e. This diagram is obtained by dividing by h_2 the ordinates of an influence line for bending moment at the support A' of the compound beam in Fig. 210b.

As another example of a cantilever truss, let us consider the compound system shown in Fig. 211a.   We see that the middle portion CD of this structure is supported at each end by two bars attached to the overhanging ends of the two cantilever portions.   Such construction is equivalent to having hinged supports at the intersection points A and B. Hence, we conclude that in this case the corresponding basic system can be taken as the compound beam shown in Fig. 211b.   Then, if the

---

* For methods of constructing the influence diagram for bending moment in a compound beam, see Art. 23, p. 116.

influence diagram for axial force S_1 in the bar FH of the upper chord is required, we make a section mn as shown and write an equation of moments with respect to the hinge E. From this equation it can be concluded that the required influence diagram will be obtained by dividing by $-h_1$ the ordinates of an influence diagram for bending moment at E' of the compound beam in Fig. 211b. This construction is shown in
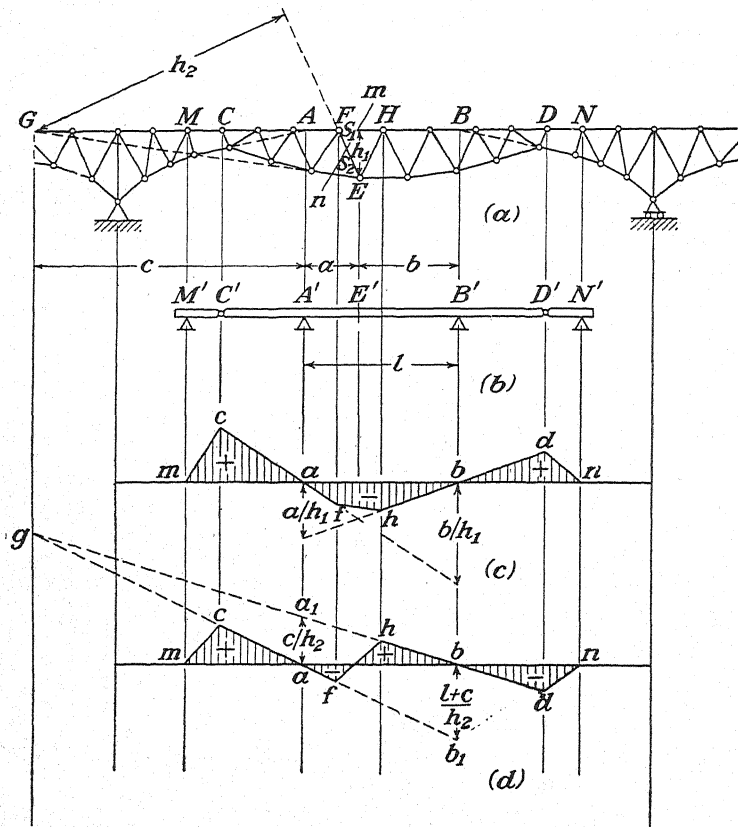
FIG. 211.

Fig. 211c. If the influence diagram for axial force S_2 in the diagonal EF is required, we use the same section mn and write equations of moments with respect to point G (Fig. 211a). When the load P is to the right of H, this equation gives

$$S_2 = \frac{R_a c}{h_2},\tag{d}$$

while, when P is to the left of F, we obtain

$$S_2 = -\frac{R_b(l + c)}{h_2}.\tag{e}$$

Thus, in Fig. 211d, we obtain the portion ndh of the required diagram by multiplying by c/h_2 the ordinates of an influence line for the reaction R_a of the compound beam in Fig. 211b.   Similarly, the portion mcf of this diagram is obtained by multiplying by $-(l + c)/h_2$ the ordinates of an influence line for R_b of the compound beam.   Finally, for positions of the load P within the panel FH, we complete the diagram by joining the established points f and h by a straight line as shown.   It is left as an exercise for the student to show that the lines cf and hd of this diagram intersect at point g corresponding to the moment center G above.

PROBLEMS

136. Construct influence diagrams for the axial forces S_1, S_2, and S_3 in each of the compound trusses shown in Fig. 212.
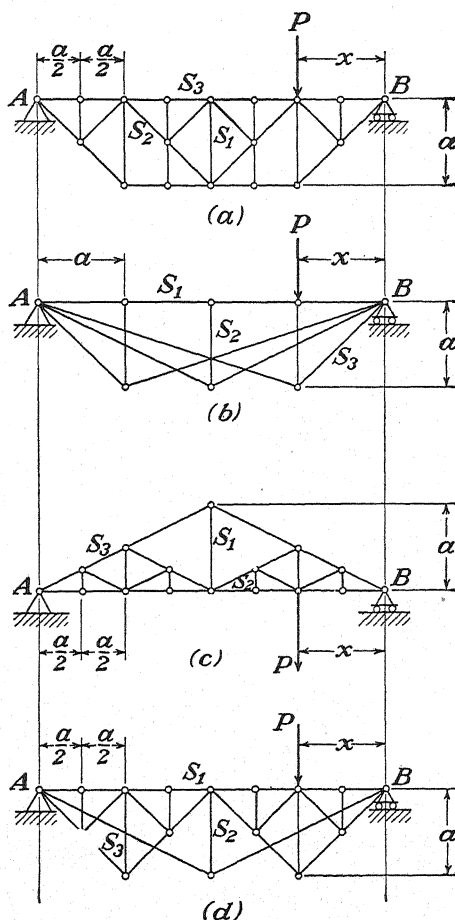
FIG. 212.

137. Construct influence diagrams for S_1, S_2, S_3, and S_4 of the cantilever bridge shown in Fig. 117 (see page 68).

138. Construct influence diagrams for the axial forces S_1, S_2, and S_3 in each of the trusses with subdivided panels as shown in Fig. 213.
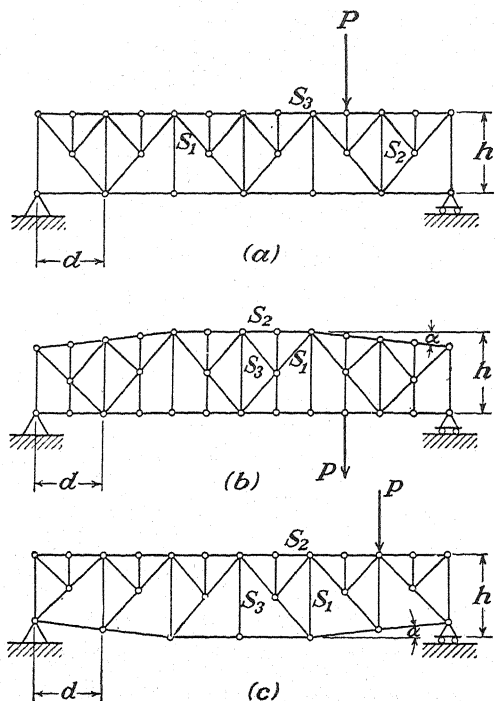
FIG. 213.

139. Assuming live load transmitted to the joints of the lower chord, construct influence diagrams for the vertical members of each of the complex trusses shown in Fig. 145 (see page 87).

140. Construct influence diagrams for the axial forces S_1, S_2, S_3, and S_4 in the cantilever bridge shown in Fig. 214. The panel distance d is uniform throughout the structure as shown.
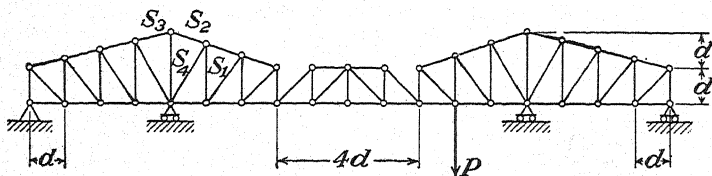
FIG. 214.

29. Influence Lines for Three-hinged Arch Trusses.—In the case of a three-hinged arch under vertical load as shown in Fig. 215a, we note that the reactive forces at A and B differ from those for a simply supported truss AB only by the presence of the horizontal thrust H. Hence,

we conclude that the axial force S_i in any bar of the system can be obtained by superimposing on the axial force $\mathcal{S}_i$, calculated as for a simply
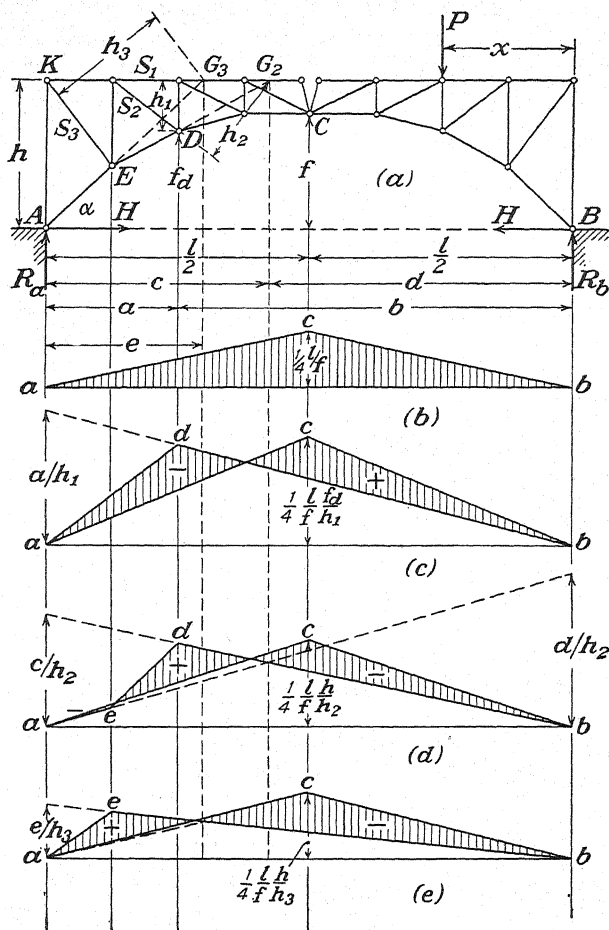
FIG. 215.

supported truss, the additional axial force induced by the thrust action H. Thus, for the system in Fig. 215a,

$$\left. \begin{array}{l} S_1 = \mathcal{S}_1 + H\,\dfrac{f_d}{h_1}, \\[2mm] S_2 = \mathcal{S}_2 - H\,\dfrac{h}{h_2}, \\[2mm] S_3 = \mathcal{S}_3 - H\,\dfrac{h}{h_3}. \end{array} \right\}$$

From these expressions, we see now that to obtain an influence diagram for the axial force S_i in any bar of the three-hinged arch, we need only

to construct the corresponding S_i-influence line, as for a simply supported truss, and then superimpose on it a certain modification of the H-influence line shown in Fig. 215b.* In Fig. 215c, for example, the line adb with negative ordinates is the influence line for the axial force S_1 in a simply supported truss, and acb is the influence line for H with all ordinates multiplied by f_d/h_1. The shaded areas obtained by superposition of these two diagrams represent the desired influence diagram for the axial
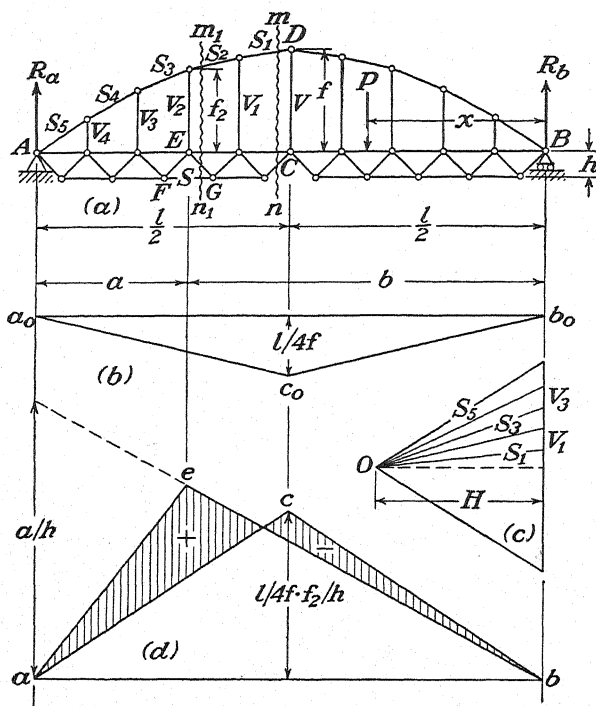
FIG. 216.

force S_1 in the three-hinged arch. The influence diagrams for S_2 and S_3 are obtained in a similar manner as shown in Figs. 215d and 215e, respectively.

As a second example, let us consider the compound truss shown in Fig. 216a. In the construction of influence lines for the various bars of this system, we can proceed in the same manner as for the three-hinged arch in Fig. 215a. We begin with a consideration of the horizontal thrust H in the arch ADB. Making a section mn as shown and writing an equation of moments with respect to point C, we find that for any

---

* See Art. 26 for the construction of the influence line for H and Art. 27 for the construction of influence lines for simply supported trusses.

position of the load P to the right of C the horizontal thrust (numerically equal to the horizontal projection of S_1) is

$$H = \frac{R_a l}{2f}. \tag{a}$$

Likewise, when the load P is to the left of C, we obtain

$$H = \frac{R_b l}{2f}. \tag{b}$$

Thus the influence line for H is obtained from the influence lines for R_a and R_b, modified as shown in Fig. 216b. Knowing H, we can readily find the corresponding forces S_1, S_2, . . . in the bars of the arch and also the forces V_1, V_2, . . . in the vertical hangers. A graphical determination of these forces is shown in Fig. 216c, and we conclude that the corresponding influence lines will be obtained from the H-influence line simply by multiplying its ordinates in each case by a proper factor. In the case of S_3, for example, the proper factor, obtained from Fig. 216c, is $-S_3/H$. The negative sign simply indicates that S_1 is a compressive force. Likewise, for the vertical V_2 the proper factor is $+V_2/H$, etc.

Let us consider now the axial force S in a lower chord member of the simple truss AC. Making a section $m_1 n_1$ as shown and writing equations of moments with respect to the joint E, we find, for positions of the load P to the right of E, that

$$S = R_a \cdot \frac{a}{h} - H \cdot \frac{f_2}{h}, \tag{c}$$

while, for positions of P to the left of E,

$$S = R_b \cdot \frac{b}{h} - H \cdot \frac{f_2}{h}. \tag{d}$$

From these expressions, we conclude that

$$S = \mathcal{S} - H \frac{f_2}{h},$$

where, as before, $\mathcal{S}$ is the axial force as for a simply supported truss AB. Accordingly, in Fig. 216d, we obtain the required influence diagram for S by constructing first the influence line aeb as for a simply supported truss and then superimposing the H-influence line with ordinates multiplied by $-f_2/h$ as shown. Influence diagrams for other members of the system can be obtained in a similar manner.

Influence lines for three-hinged arches can also be constructed by the method of virtual displacements. Consider, for example, the arch in Fig. 217a, and suppose that an influence line for the axial force S_1 in a bar of the upper chord is required. Then, to apply the method of virtual displacements, we remove this bar and represent its action on the rest of the structure by two equal but opposite forces, as shown. In this way, we obtain a movable system consisting of the three rigid shaded portions
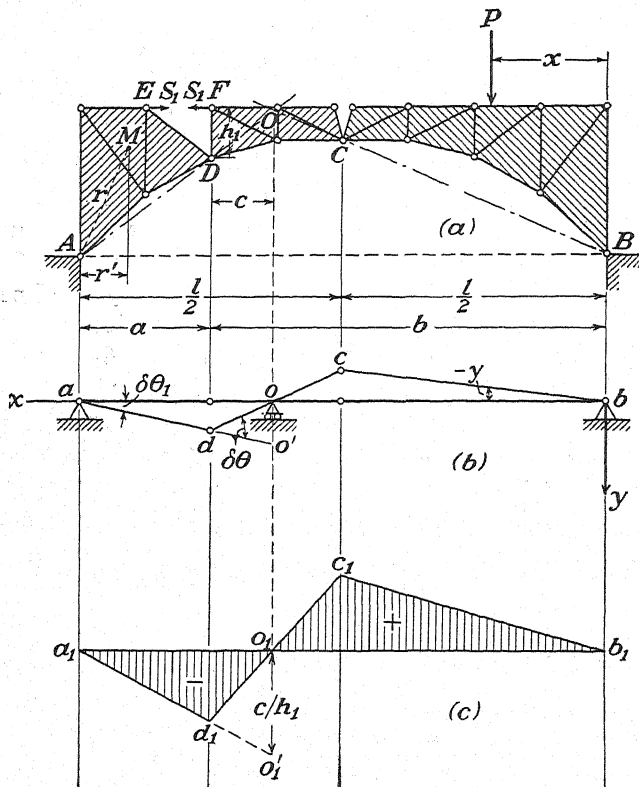
Fig. 217.

hinged together at D and C and to the supports at A and B. Such a system has one degree of freedom, and a virtual displacement can be defined by giving to the portion AD a small angle of rotation $\delta\theta_1$ about the hinge A. Under such rotation, any point M at the distance r from A suffers a linear displacement $r\,\delta\theta_1$ perpendicular to AM, and the vertical component of this displacement is $r'\,\delta\theta_1$. Thus vertical displacements of all points in this portion of the system are proportional to their horizontal distances from A and are represented by the ordinates of the line ad in Fig. 217b. Now, let us consider displacements of points within

the portion DC of the system. During the assumed virtual displacement, as defined by $\delta\theta_1$, this part of the arch rotates about its instantaneous center O obtained as the intersection of the lines AD and BC as shown. Thus the point O remains stationary, and vertical displacements of other points within DC are proportional to their horizontal distances from O as represented by ordinates of the straight line doc in Fig. 217b. Finally, since BC rotates about the fixed hinge B, we obtain vertical displacements of points within this portion of the arch by drawing the straight line cb in Fig. 217b. Ordinates y of this diagram, considered positive downward, now represent vertical displacements of all points of the system corresponding to the assumed virtual displacement. Also, the angle $\delta\theta$, as shown between ad and dc, represents the decrease in the angle EDF, and we see that the corresponding decrease in the distance EF is $h_1\delta\theta$. Thus the equation of virtual work becomes

$$S_1 h_1 \delta\theta + Py = 0,$$

from which

$$S_1 = -\frac{Py}{h_1\delta\theta}. \tag{e}$$

Noting that S_1 is proportional to y, we conclude that the diagram $adcb$ in Fig. 217b gives us the general shape of the required influence diagram for S_1, from which we can always decide the question of most unfavorable position of live load without consideration of vertical scale. If numerical values of the influence coefficients are required, we must divide each ordinate of the diagram in Fig. 217b by the constant factor $-h_1\delta\theta$ [see Eq. (e)]. To do this, we note from Fig. 217b that $oo' = c\,\delta\theta$. Hence the corresponding diagram in Fig. 217c for which

$$o_1 o_1' = -\frac{c\,\delta\theta}{h_1\delta\theta} = -\frac{c}{h_1}$$

gives the influence coefficients to scale. It is left as an exercise for the student to show that the ordinates of this diagram are identical with those of the diagram obtained in Fig. 215c by another method.

Referring to Fig. 218a, we shall now consider the construction of an influence diagram for the axial force S_2 in a diagonal of the three-hinged arch by the method of virtual displacements. Removing this diagonal and representing its action on the remainder of the arch by two equal but opposite forces S_2, we obtain a movable system with one degree of freedom and consisting of three rigid shaded portions interconnected between themselves and the foundation as shown. The connections at A, B, and C are simple hinges, while the bars EF and HD, which connect the rigid portions AE and FC, are equivalent to a hinge at G obtained

as the intersection of their axes.   Hence, in our further discussion, we shall consider point G as a hinge common to both the parts AE and FC of the system.   Thus it follows that the instantaneous center for the middle portion of the system is obtained by extending the lines AG and BC to their intersection O.   Keeping these points in mind, we may now define a virtual displacement of the entire system by giving to the portion
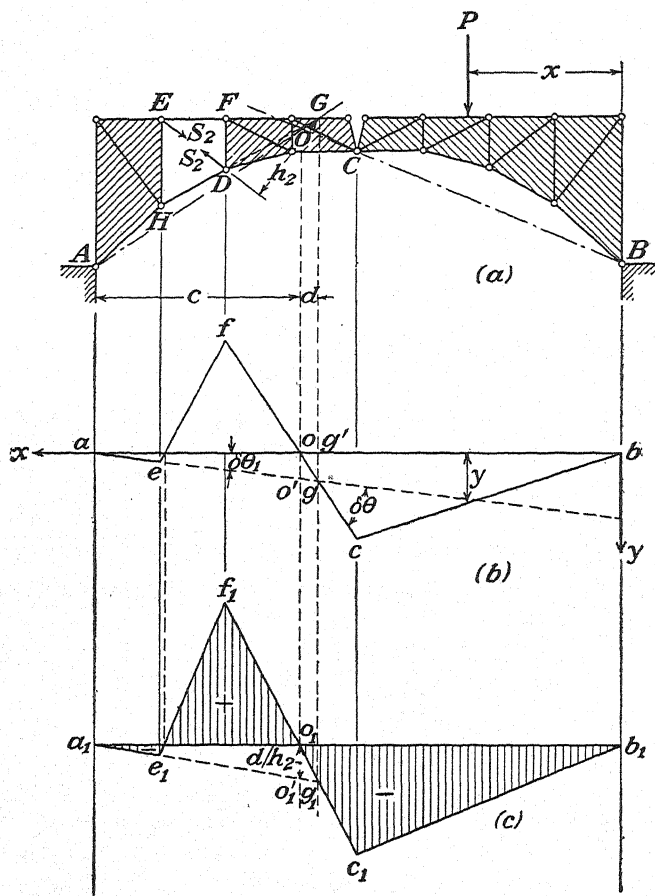
Fig. 218.

AE a small angle of rotation $\delta\theta_1$ about the fixed hinge A.   Corresponding vertical displacements of points within this portion will then be proportional to their horizontal distances from A and can be represented by the ordinates of the line ae in Fig. 218b.   Prolonging this line to point g, we obtain the vertical displacement $g'g$ of the imaginary hinge G.   Since this hinge belongs also to the middle portion FC of the system and since

the point O of this portion remains stationary, the straight line gof in Fig. 218b will give the vertical displacements of points between F and G. Extending this line to point c and then connecting points c and b by a straight line as shown, we obtain vertical displacements for all points between G and B. Finally, connecting the established points e and f, we obtain the complete diagram $aefcb$ defining vertical displacements of all points corresponding to the assumed virtual displacement $\delta\theta_1$. Also, the angle $\delta\theta$ between the lines ag and fc represents the relative rotation between the portions AE and FC of the system. Corresponding to this relative rotation, the distance ED is diminished by the amount $h_2\delta\theta$ so that the equation of virtual work for the system becomes

$$S_2 h_2 \delta\theta + Py = 0,$$

from which

$$S_2 = -\frac{Py}{h_2\delta\theta}. \qquad (f)$$

Again we note that, for any position of the load P on the structure, the axial force S_2 is proportional to the corresponding ordinate y of the diagram $aefcb$ in Fig. 218b. Hence this diagram gives the general shape of the required influence diagram for S_2. To obtain the influence coefficients $-y/h_2\delta\theta$ to scale, we note from the figure that the ordinate $oo' = d\ \delta\theta$. Thus, in Fig. 218c, we make the ordinate $o_1o_1' = -d\ \delta\theta/h_2\delta\theta = -d/h_2$ as shown; and then, magnifying all other ordinates in the same proportion, we obtain the true influence diagram $a_1e_1f_1c_1b_1$ for S_2. By geometrical considerations, it can readily be shown that the ordinates of this diagram are identical with those of the diagram in Fig. 215d.

As a last example, let us consider the complex truss shown in Fig. 219a. This statically determinate system is obtained from a simply supported simple truss AB by removing the bar EF from the truss proper and substituting an additional external constraint as represented by the support at C. As we have already seen in Art. 19, the method of virtual displacements is helpful in the analysis of such a system, since, in the calculation of reactions, the ordinary methods of statics do not apply. The same observation holds in the construction of influence lines for complex systems. Let us begin, then, with an influence line for the reaction at C. Replacing the external constraint here by a vertical force R_c as shown, we obtain a movable system with one degree of freedom. This system consists of the two rigid shaded portions of the truss, which are connected between themselves by a hinge D and to the foundation by a fixed hinge at B and a rolling hinge at A. To this system, the joint C is attached by two bars EC and FC as shown. Defining a virtual displacement of the system by a small angle of relative rotation

$\delta\theta$ between the two rigid units AD and BD, we conclude that points along the upper chord will have vertical displacements as represented by the ordinates y of the line adb in Fig. 219b, the middle ordinate being $l\,\delta\theta$. At the same time, the vertical diagonal DC of the rhombus $DEFC$ diminishes by the amount $(d/2)\delta\theta$, since the sum of its interior angles
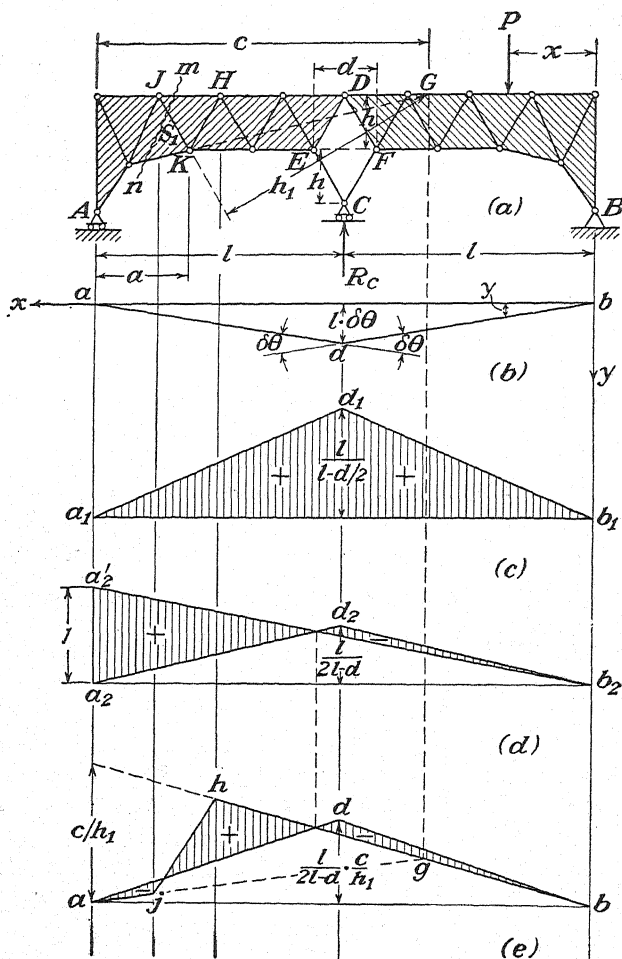
FIG. 219.

must remain unchanged. Thus the net displacement of the joint C in the direction of R_c is $-l\,\delta\theta + (d/2)\delta\theta = -(l - d/2)\delta\theta$, and the equation of virtual work for the system becomes

$$-R_c\left(l - \frac{d}{2}\right)\delta\theta + Py = 0,$$

from which

$$R_c = \frac{Py}{(l - d/2)\delta\theta}.\tag{g}$$

From this expression, we conclude that the influence coefficients for R_c are obtained by dividing the ordinates y of the line adb in Fig. 219b by the constant factor $(l - d/2)\delta\theta$. Thus the middle ordinate of the influence line for R_c must have the magnitude $\dfrac{l\,\delta\theta}{(l - d/2)\delta\theta} = \dfrac{l}{(l - d/2)}$, as shown in Fig. 219$c$.

Knowing the magnitude of R_c, we can readily find, by ordinary methods of statics, the other reactions as well as the axial force S_i in any bar of the system. The reaction at A, for example, is

$$R_a = \frac{Px}{2l} - \frac{1}{2}R_c.\tag{h}$$

Hence, to obtain an influence diagram for R_a (Fig. 219d) we construct first the line b_2a_2' as for a simply supported truss AB. Then from the positive ordinates of this line we must subtract the corresponding ordinates of the R_c-influence line multiplied by the constant factor $\frac{1}{2}$. In this way we obtain the influence diagram for R_a as represented by the shaded areas in Fig. 219d. Likewise, for the axial force S_1 in the bar JK, we begin in Fig. 219e with the influence line $ajhb$ as for a simply supported truss AB and then superimpose the R_c-influence line with all ordinates multiplied by the factor $-c/2h_1$. This follows from the fact that

$$S_1 = \mathcal{S}_1 - \frac{R_c c}{2h_1},\tag{i}$$

where $\mathcal{S}_1$ is the axial force in the member JK of a simply supported truss AB. The same procedure can be used in the construction of influence diagrams for other members of the system. In each case we first construct the $\mathcal{S}_i$-influence line as for a simply supported truss AB and then superpose on it a certain modification of the R_c-influence line in Fig. 219c. Thus the reaction R_c of the complex system in Fig. 219a is analogous to the thrust H in a three-hinged arch (see influence diagrams in Fig. 215).

PROBLEMS

141. Referring to Fig. 215, find the maximum horizontal thrust H that can be produced in the arch by a uniformly distributed live load of intensity $q = 1$ kip per ft. Assume $l = 120$ ft. and $f = 20$ ft. What maximum thrust can occur in the same arch under the action of a standard train?   *Ans.*   90 kip, 344.5 kip.

142. Construct an influence diagram for the vertical AK of the three-hinged arch shown in Fig. 215a. What maximum compressive force can be induced in this member by a uniform live load of intensity $q = 3$ kip per ft.? Assume $l = 120$ ft., $f = 20$ ft., $h = 30$ ft., and $\tan \alpha = \frac{3}{4}$.   *Ans.*   54.7 kip.

143. Construct influence diagrams for the axial forces S_1, S_2, and S_3 in the structure shown in Fig. 220.
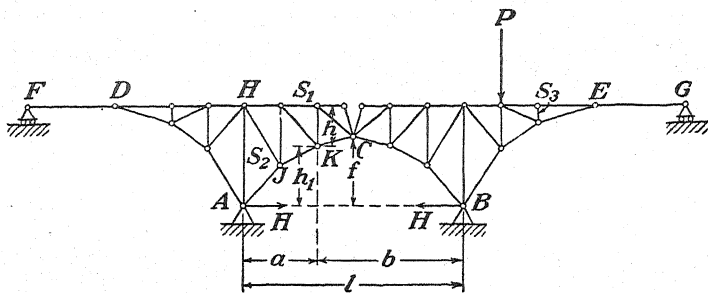
FIG. 220.

HINT: Construct first the influence lines for S_1, S_2, and S_3 as in a cantilever truss (see Art. 28), and then modify for the effect of the horizontal thrust H as was done in Fig. 215c.

144. (a) Construct influence diagrams for axial forces in the bars JH and HK of the complex truss shown in Fig. 219a. Assume that the triangle JHK is equilateral. (b) If $l = 120$ ft. and $d = 15$ ft., what is the maximum uplift that can be produced on the support at A by a standard train (Cooper's E-60)?

145. Construct the influence diagram for axial force in the bar EF of the structure shown in Fig. 216a. Assuming $l = 250$ ft., $f = 50$ ft., and $h = 12.5$ ft., find the maximum compression S in the bar FG of this structure under the action of a uniformly distributed live load of intensity $q = 1$ kip per ft. The vertical hangers are evenly spaced, and the joints of the arch ADB lie on a parabola with vertical axis and vertex at D.

CHAPTER IV

STATICALLY DETERMINATE SPACE STRUCTURES

30. Concurrent Forces in Space.—If several forces in space have the same point of application, they can always be reduced to a single resultant force by using the principle of the parallelogram of forces as discussed in Art. 1. Consider, for example, the three concurrent forces F_1, F_2, and F_3, represented by the vectors $\overline{OA}$, $\overline{OB}$ and $\overline{OD}$ in Fig. 221a. Considering, first, only the vectors $\overline{OA}$ and $\overline{OB}$ and using the principle of the parallelogram of forces, we find their resultant $\overline{OC}$ as shown. Now taking this *partial resultant* together with the remaining force F_3 and again applying the principle of the parallelogram of forces, we find their resultant as represented by the diagonal $\overline{OE}$ of the parallelogram $ODEC$. Obviously, this force $\overline{OE}$, which we denote by R, is the resultant of the three given forces; and we note that it is obtained as the diagonal of the parallelepiped formed on the three given vectors. The same resultant R can also be obtained as the closing side $\overline{O'E'}$ of the *space polygon of forces* $O'A'C'E'$ shown in Fig. 221b. This follows from the fact that the space figure $O'A'C'E'$ is identical with the space figure $OACE$ in Fig. 221a. Since the constructions shown in Fig. 221 can readily be extended to any number of concurrent forces in space, we conclude that the resultant of such a system can

Fig. 221.

always be obtained as the geometric sum of the given forces and that its line of action will always act through the point of concurrence of the given forces.

It may be noted here that if a system of concurrent forces in space (Fig. 221a) and the corresponding space polygon of forces (Fig. 221b) are orthogonally projected onto any plane, we obtain in the plane of projection a polygon of forces the sides of which are equal to the corresponding projections of the given forces. From this fact, we conclude that any projection of the resultant of the given forces is identical with the resultant of the corresponding projections of the forces themselves. In the particular case where the given system of forces in space is in equilibrium, it follows that their orthogonal projections on any plane will represent a coplanar system of forces in equilibrium. As we shall see

163
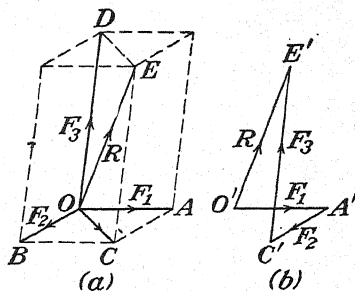
later, this observation can often be used to advantage in dealing with equilibrium of space systems.

From the foregoing discussion, we can conclude at once that the projection on any axis of a resultant of several concurrent forces in space will be equal to the algebraic sum of the projections of the given forces on the same axis. From this it follows that, if the given forces are in equilibrium, the algebraic sums of their projections on mutually orthogonal axes x, y, and z must vanish. Thus we arrive at the well-known *equations of equilibrium*

$$\Sigma X_i = 0, \qquad \Sigma Y_i = 0, \qquad \Sigma Z_i = 0, \tag{8}$$

where X_i, Y_i, and Z_i are the orthogonal projections of any force F_i and the summations are understood to include all forces in the system.

On the basis of Eqs. (8) several general observations can be made that will prove useful in later discussions. (1) Three concurrent forces that do not lie in one plane cannot be in equilibrium unless all three forces are zero. To prove this statement, consider the three forces in Fig. 221a, and equate to zero the algebraic sum of their projections on an axis normal to the plane AOB. Then since F_3 is the only force that has such a projection different from zero, we conclude that $F_3 = 0$. In the same way, by successively projecting the forces onto axes that are normal, respectively, to the planes AOD and BOD, we conclude that $F_2 = 0$ and that $F_1 = 0$. (2) If two of four concurrent forces, that are not all in one plane are collinear, equilibrium can exist only if the other two forces are zero. The two collinear forces, of course, must be equal in magnitude and opposite in direction. This statement may be proved by projecting the system onto a plane normal to the line of action of the two collinear forces. Then in this plane of projection there are only two forces that are not collinear, and two such forces cannot be in equilibrium unless they are both zero. (3) If all but one of any number of concurrent forces in space are coplanar, equilibrium can exist only if this odd force is zero. This is proved by equating to zero the algebraic sum of the projection of all forces on an axis normal to the coplanar forces. (4) If the known lines of action of all but two of any number of concurrent forces in equilibrium are coplanar and the magnitude of one of these two is known, the magnitude of the other can always be found by projecting all forces onto an axis normal to the coplanar forces.

In dealing with space systems, the notion of *moment of a force with respect to an axis* is often useful. To obtain the moment of a force F_i with respect to an axis z (Fig. 222), we first project the force onto a plane MN that is normal to the axis z and then take the moment of this projection F' with respect to the point O where the axis pierces the plane. This moment of the projection F' with respect to the point O is equal to

the doubled area of the triangle $A'OB'$ and is considered positive when directed as shown in the figure. From this definition of moment of a force with respect to an axis, we see that the moment vanishes if the force is parallel to the axis or intersects it. We see also that, if any system of concurrent forces in space is in equilibrium, the algebraic sum of their moments with respect to any axis must be zero, since, by the theorem of moments,[1] the algebraic sum of moments of the given forces is equal to the corresponding moment of their resultant and, when the forces are in equilibrium, the resultant vanishes.
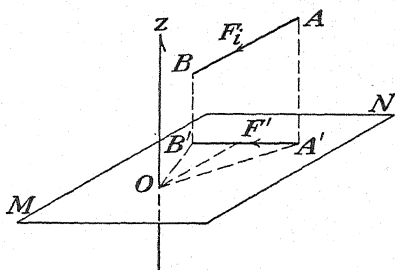
Fig. 222.

Let us now turn our attention for a moment to the purely geometrical question of the complete constraint of a point in space. Referring to Fig. 223a, we see that the attachment of a point O to a rigid foundation by means of two bars OA and OB serves only to establish constraint of the point in the plane AOB of the bars and that there remains the possibility of rotation of this plane about the axis AB. To remove this possibility of rotation, a third bar OC (Fig. 223b) that is not in the plane AOB of the other two is necessary. If all three bars by which the point O is attached to the foundation lie in one plane, complete constraint is not realized. In the case represented in Fig. 223c, for example, the ends A, C, and B of the three bars all lie on one axis, and there is the same unlimited freedom of rotation about this axis as in the case represented in Fig. 223a. Again, in the case shown in Fig. 223d, it is evident that considerable movement of point O in the direction normal to the plane ABC of the bars can take place without appreciable changes in the lengths of the bars. Thus, in this case, also, we have unsatisfactory constraint of the point O in space. From this discussion, we can conclude that complete and satisfactory constraint of a point in space can always be realized by attaching it to a foundation by three bars the axes of which do not lie in one plane.
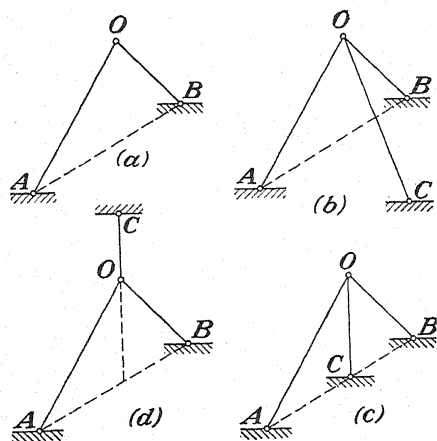
Fig. 223.

[1] See authors' "Engineering Mechanics," 2d ed., p. 168.

Let us assume now that an external load P is applied to the completely constrained point O in Fig. 224. Under the action of this load, axial forces will be induced in the three supporting bars, and accordingly each bar will exert on the joint O a reaction S_i directed along the axis of the bar and representing in magnitude the corresponding axial force. Thus at O we have a system of four concurrent forces that are in equilibrium;
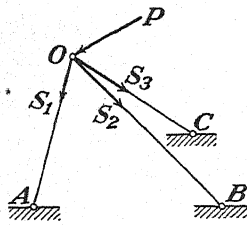
FIG. 224.

and since all lines of action are given, we see that the only unknown elements in the system are the magnitudes S_1, S_2, and S_3. Hence, regardless of the magnitude or direction of the applied load P, the corresponding magnitudes of the three reactions can always be found by using Eqs. (8). For this reason the system is said to be *statically determinate*. If the point O is attached to the foundation by more than three bars, *i.e.*, if there are *redundant supports*, the three necessary and sufficient conditions of equilibrium represented by Eqs. (8) will be insufficient to determine the unknown elements and the system is said to be *statically indeterminate*. If there are fewer than three supporting bars or three bars in one plane, the system is nonrigid and will not remain in equilibrium under the action of an applied load P that does not coincide with the plane of the bars.

Confining our attention to statically determinate systems, we shall now consider various practicable methods of application of the conditions of equilibrium represented by Eqs. (8). As a first example, we take the simple space structure shown in Fig. 225. This system consists of a strut AO hinged at O to a vertical wall MN and supported at A by guy wires AB and AC as shown. Under the action of a vertical load P at A, the analysis of this system can be made without difficulty by direct application of Eqs. (8). We begin with a free-body diagram of point A, which is acted
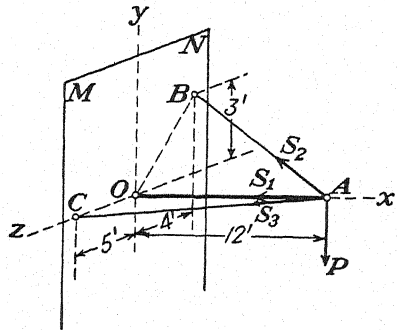
FIG. 225.

upon by the load P, and the three reactions S_1, S_2, and S_3, representing the axial forces in the bars. We intentionally assume each of these unknown reactions to be directed away from the joint so that in our final results plus signs will indicate tension and minus signs compression. Equating to zero the algebraic sum of the projections of all forces at A on each of the orthogonal axes x, y, and z, directed as shown in the figure, Eqs. (8) become, respectively,

$$-S_1 - \tfrac{12}{13}S_2 - \tfrac{12}{13}S_3 = 0,$$
$$-P + \tfrac{3}{13}S_2 = 0, \qquad (a)$$
$$\tfrac{5}{13}S_3 - \tfrac{4}{13}S_2 = 0,$$

from which we find $S_1 = -7.20P$; $S_2 = +4.33P$; $S_3 = +3.47P$. The negative sign for S_1 indicates that the strut is under compression while the guy wires each carry tension.

The same results can be found in another way by using the notion of moment of force with respect to an axis. For example, if we equate to zero the algebraic sum of moments of all forces with respect to the z-axis, we obtain

$$-P \cdot 12 + \tfrac{3}{13}S_2 \cdot 12 = 0,$$

from which, as before, we find $S_2 = +4.33P$.
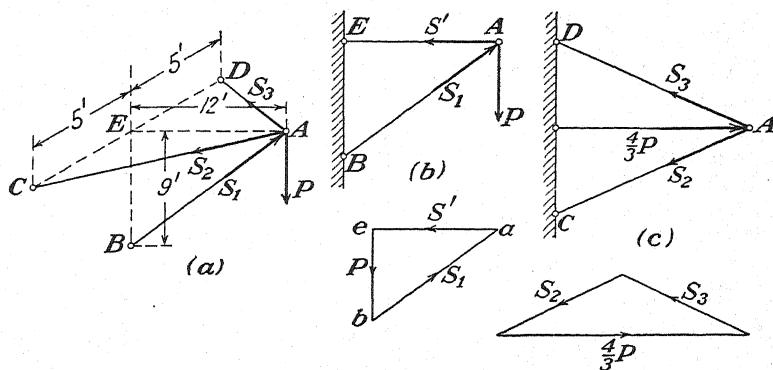
Fig. 226.

Sometimes the analysis of a space structure can be handled to advantage by working with one or more plane projections of the given system. Consider, for example, the simple space system shown in Fig. 226a. We recall that, in general, if a system of concurrent forces in space is in equilibrium, their projections on any plane will also be in equilibrium. This idea can be used to advantage in the present case. Projecting onto the vertical plane AEB, we obtain the coplanar system shown in Fig. 226b, the analysis of which is indicated by the accompanying triangle of forces eba. From this triangle, the compressive force in the strut is seen to be $S_1 = \tfrac{5}{3}P$. In the same way, by projecting the system onto the horizontal plane ACD (Fig. 226c) and using the previously determined value of S_1, the horizontal projection of which is equal but opposite to the force S' in Fig. 226b, we find the tensions in the two guy wires to be $S_2 = S_3 = .722P$.

In dealing with a system of concurrent forces in space, we may often encounter difficulty in determining analytically the projections or moments of the forces with respect to various axes. In such cases, a

semigraphical procedure may be helpful. By way of illustration, let us consider the analysis of the system shown in Fig. 227. This structure consists of three bars OA, OB, and OC, of lengths l_1, l_2, and l_3, respec-
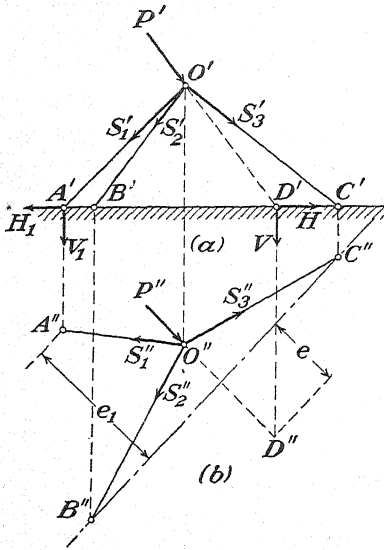
Fig. 227.

tively, that are attached to a horizontal foundation at points A, B, and C and joined together at O. Such a structure will be completely defined by two projections, one on a vertical plane (Fig. 227a) and one on the horizontal plane (Fig. 227b). Likewise, the load P is defined both in magnitude and in direction by its corresponding projections P' and P''. We begin with a determination of the axial force S_1 in the bar OA. At point A, let this force be resolved into horizontal and vertical components H_1 and V_1; and at point D, where the line of action of P pierces the foundation plane, let P be resolved into horizontal and vertical components H and V. Then, equating to zero the algebraic sum of moments of all forces with respect to the axis BC, we obtain

$$V_1 e_1 - Ve = 0. \qquad (b)$$

Now denoting by h the elevation of point O above the foundation plane and by l the distance OD that can be found from its two projections $O'D'$ and $O''D''$, we have

$$V_1 = S_1 \cdot \frac{h}{l_1} \qquad \text{and} \qquad V = P \cdot \frac{h}{l}.$$

Substituting these values in Eq. (b), we obtain $S_1 = P \cdot e/e_1 \cdot l_1/l$. The lengths e and e_1 can be scaled directly from the figure, and the axial force S_1 is determined. By a similar procedure, the forces S_2 and S_3 can be found.

If preferred, any system like that in Fig. 227 can be handled in a completely graphical manner. Suppose, for example, that we desire the axial forces induced in the bars $O1$, $O2$, and $O3$, of the system represented in Fig. 228. Such a problem can be solved graphically by resolving the given load P, defined by its orthogonal projections P' and P'', into three space components coinciding with the axes of the three bars. That

the axial force in each bar will then be that induced by the corresponding component of P follows from the fact that the resultant of the three reactions exerted on the joint O by the bars must be the equilibrant of P. We begin with a determination of the line of intersection of the plane defined by the bar $O1$ and P with the plane defined by the bars $O2$ and $O3$. One point on this line of intersection is obviously point O. Another point on the same line is the point n obtained by using the intersection of the lines $1''4''$ and $2''3''$ in the horizontal projection. With the points O and n, the required line of intersection is completely defined by its projections $O'n'$ and $O''n''$. We next resolve the load P into two components, one along the axis of the bar $O1$ and one along the line On, the projections
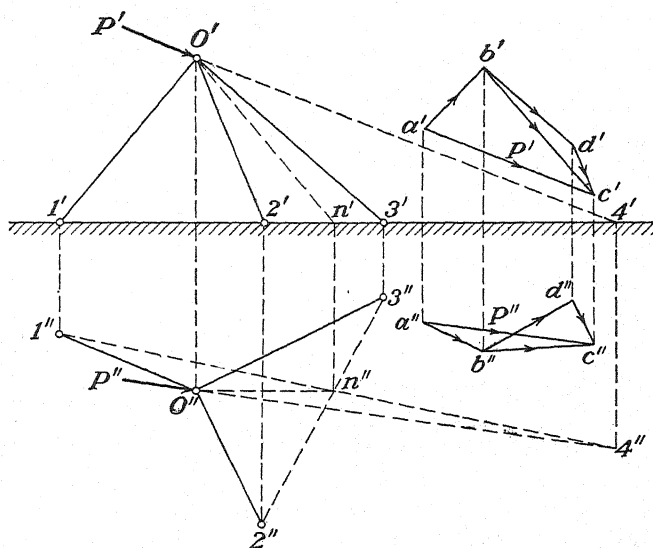
Fig. 228.

of which we have just found. The triangles of forces $a'b'c'$ and $a''b''c''$ represent the vertical and horizontal projections, respectively, of the corresponding triangle of forces abc in space. The side $\overline{ab}$ of this triangle gives the component of P that acts along $O1$ and the side $\overline{bc}$, the component that acts along On. Finally, since the line On is in the plane $O23$, this latter component of P can be resolved into two components $\overline{bd}$ and $\overline{dc}$ that act, respectively, along the axes of the bars $O3$ and $O2$ as shown. With the orthogonal projections $\overline{a'b'}$, $\overline{b'd'}$, $\overline{d'c'}$, and $\overline{a''b''}$, $\overline{b''d''}$, $\overline{d''c''}$ of the three components of P, the components themselves can be obtained without difficulty. As already mentioned, the axial forces in the bars can be found directly from these components. We see that in this case the bar $O1$ will be in tension, while the bars $O2$ and $O3$ are in compression.

PROBLEMS

146. Three bars of equal lengths l are joined together at A and supported at B, C, and D, as shown in Fig. 229.   Find the axial force induced in each bar due to a vertical load P at A, if $OB = OC = OD = l$.

$$Ans. \quad S_1 = -2P/3, \ S_2 = -2P/3, \ S_3 = +P/3.$$
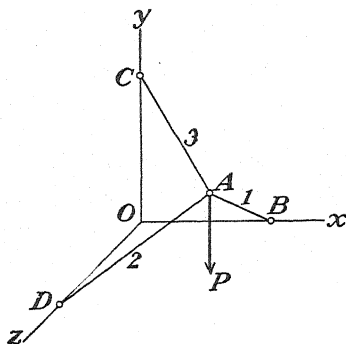
Fig. 229.

147. The legs of a tripod are of equal lengths l and are supported at points A, B, and C, which form an equilateral triangle with sides of length l in a horizontal plane. Find the compressive force S induced in each leg by a vertical load P applied at the apex of the tripod. $\qquad$ *Ans.* $S = -P/\sqrt{6}$.

148. Assuming that the legs of the tripod in Prob. 147 are supported on a frictionless horizontal plane and that they are prevented from spreading by a string ABC, find the tension induced in this string. $\qquad$ *Ans.* $S = +P/3\sqrt{6}$.

149. Determine the axial forces S_1, S_2, and S_3 in the bars of the space system arranged and loaded as shown in Fig. 230.   Note that the distances $O''B''$ and $O''A''$ in the horizontal projection are equal.
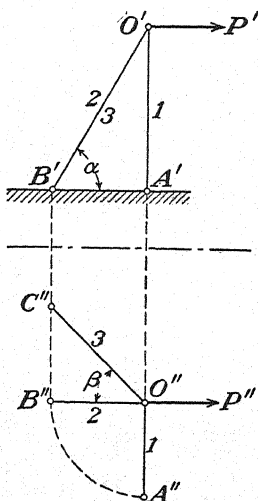
Fig. 230.

150. How will the axial forces S_1, S_2, and S_3 in Fig. 230 be changed if the load P is vertical instead of horizontal as shown?

31. Simple Space Trusses: Method of Joints.—A system of bars in space, joined together at their ends in such a way as to form a rigid space structure is called a *space truss*. Many kinds of engineering structures such as steel-mill buildings, transmission-line towers, and cranes are of such construction. In the fabrication of these structures, it is common practice to make the connections at the joints either by riveting or welding. Of course, the rigidity of this type of connection is bound to interfere to some extent with the free adjustment of the system to applied loads so that some secondary bending of the bars will be induced. However, in most practical cases, the presence of such secondary bending does not materially influence the primary action of the structure, and the axial forces can usually be calculated with good accuracy by ignoring the effect of the rigidity of the joints.[1] Thus we generally assume that the

FIG. 231.

bars are connected at their ends by *ideal spherical hinges* even though such connections can never be realized in practice. In our further discussion here, we shall always assume such hinges.
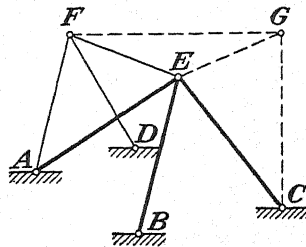
By way of establishing a criterion of rigidity for space trusses with ideal spherical hinges, we recall that the complete constraint of a point in space requires its attachment to a foundation by three bars the axes of which are not in one plane. With this notion of complete constraint of one point in space, we can easily establish a method of assembling a system of bars in space so as to form a rigid structure. Referring to Fig. 231, we begin with three bars AE, BE, and CE by which the joint E is rigidly attached to a foundation $ABCD$. With the joint E completely constrained in space, it follows that by the three bars EF, DF, and AF the joint F is completely constrained in space. E and F now being fixed points like A, B, C, and D, we conclude that the joint G can be rigidly connected to the rest of the structure by the three bars EG, FG, and CG. Since this procedure may be carried on indefinitely, we may state the following rule: *A rigid space truss can always be formed by attaching the first joint to a foundation by means of three bars that do not lie in one plane and establishing each additional joint thereafter by three more bars that do not lie in one plane.* Those three bars by which any joint after the first

---

[1] In some cases, the presence of secondary bending in a space structure may greatly affect its behavior under load and it becomes necessary to consider this effect in detail. Several such examples are discussed by A. Föppl in his book, "Vorlesungen über technische Mechanik," vol. II, p. 276, 1912.

is attached to the existing structure may be joined either to the foundation or to previously established joints. Any space system formed in accordance with this rule is called a *simple space truss*. Several examples of such space trusses are shown in Fig. 232. In each case the joints have been set up in alphabetical order, the first joint being attached to the foundation by three bars not in one plane and succeeding joints being attached to the existing structure in the same manner. It should be noted that in general the rigidity of such structures is not independent of their connection to the foundation. That is, none of the systems shown in Fig. 232 will represent a rigid body if disconnected from the foundation points A', B', C', ...

Suppose now that any one of the space trusses in Fig. 232 is subjected to the action of several applied loads. Under the influence of these
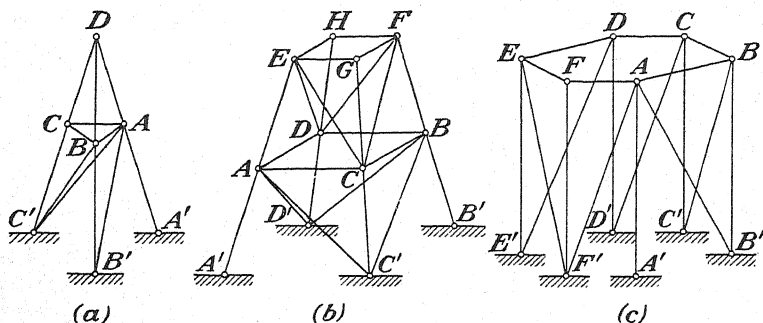
Fig. 232.

external forces, internal forces will be induced in the various bars, and the determination of these internal forces constitutes the analysis of the truss. In dealing with such problems, we make the same idealizing assumptions that we did for plane trusses, namely: (1) the bars themselves are weightless, (2) they are connected at their ends by ideal hinges, and (3) external forces are applied only at the joints. On the basis of these assumptions, it follows that each bar will suffer only simple tension or compression without bending, and thus the equal but opposite reactions that it exerts on the joints at its two ends will be directed along the axis of the bar. We have then at each joint a system of concurrent forces in space, the lines of action of which are known and to which the three conditions of equilibrium represented by Eqs. (8) can be applied directly.

The analysis of space trusses by which we apply successively to each joint the conditions of equilibrium represented by Eqs. (8) is called the *method of joints*. To illustrate, let us consider the analysis of the space system arranged and loaded as shown in Fig. 233. Beginning with the joint D and denoting by S_1, S_2, and S_3, respectively, the axial forces in

the bars 1, 2, and 3, we see that these three forces can be evaluated without difficulty by one of the methods discussed in the preceding article. Assuming then that S_1, S_2, and S_3 have been determined, we find at the joint C only three unknowns, namely, S_4, S_5, and S_6, and these three magnitudes can be found without difficulty.

When this has been done, there will remain only three unknown forces at B, and the equilibrium of this joint can be considered next.   Finally, we may proceed to the joint A, where all forces except S_{10}, S_{11}, and S_{12} will be known, and when these are found the analysis of the truss is completed.

FIG. 233.

In general, we see that to be successful with the method of joints we must, at the beginning, find at least one joint of the truss to which only three bars not in one plane are attached.   Then, when the forces in these three bars have been determined, there must be another joint where only three unknowns will be encountered, etc., until the analysis is completed.   Recalling the method of formation of a simple space truss where each joint is attached to the existing portion of the structure by three bars not in one plane, we see that the method of joints must always be applicable to such trusses.   It is necessary only to begin the analysis with the last joint added to the structure and then consider the joints successively in the reverse order from which they were set up.   By such procedure we encounter only three unknowns at each new joint, and the analysis proceeds without difficulty.

FIG. 234.
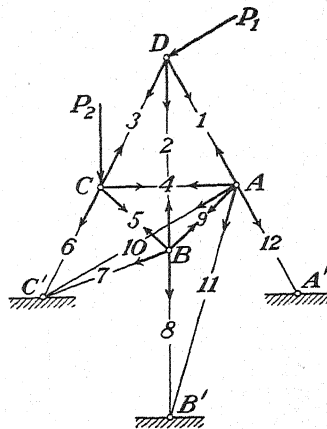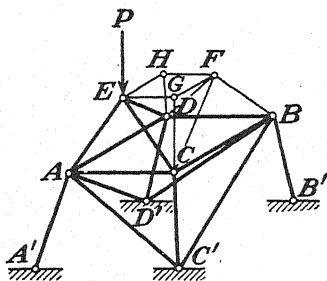
As a preliminary step in the analysis of any space truss, we can often simplify the problem by examining the system for *inactive members*, *i.e.*, bars, which, under a given condition of loading, do not carry either tension or compression.   Consider, for example, the space truss constructed and loaded as shown in Fig. 234.   Beginning with the joint G, we see that there is no external load here, and only three bars not in one plane.   Hence the axial forces in these three bars must all be zero since, as we have already pointed out, three concurrent forces can be in equilibrium only if they are coplanar.   The same reasoning may be applied to the joint H.   Then, since no forces are exerted on the joint F by the bars HF and GF, we conclude that the three remaining

bars DF, BF, and CF must also be inactive since they are three bars not in one plane and since no external force acts at F. Thus the inactive bars (represented in the figure by fine lines) can be removed, leaving, for further analysis, only that portion of the structure represented by heavy lines.

In Fig. 235 we have another example of a simple space truss in which several of the bars are inactive for the particular case of loading shown.

FIG. 235.

In this case we do not begin the analysis at once with a consideration of the joint F to which only three bars are attached. Instead, let us consider the joint B at which there is no external load and four bars, three of which are in one plane. From this fact it follows that the bar AB must be inactive. Similar reasoning with respect to the joints C, D, and E, leads us to conclude that the bars BC, CD, and DE also are inactive. Let us imagine, then, that these inactive bars AB, BC, CD, and DE are removed from the structure. As soon as this is done, we see that at each of the joints B, C, and D there remain only two bars which are not collinear. From this we conclude that the bars BB', BC', CC', CD', DD', and DE' are also inactive since two forces can be in equilibrium only if they are collinear in action. Finally, then, if all inactive bars (represented by fine lines) are removed from the system, we have for further analysis only that portion of the truss represented by heavy lines.

We have already noted that the rigidity of such simple space trusses as those in Fig. 232 is not independent of their attachment to a foundation. Sometimes, as in the case of a dirigible, it is desirable to have a rigid space structure independent of any foundation. To assemble a system of bars in space so as to form a self-contained rigid framework independent of any foundation, we can proceed as follows: Beginning with three bars in the form of a triangle ABC (Fig. 236), we attach to these a fourth joint D by means of the three bars AD, BD, and CD that do not lie in one plane. In this way we obtain a rigid tetrahedron that cannot be distorted by any system of external forces applied to its joints.[1] This tetrahedron represents the simplest form in which a system of bars in
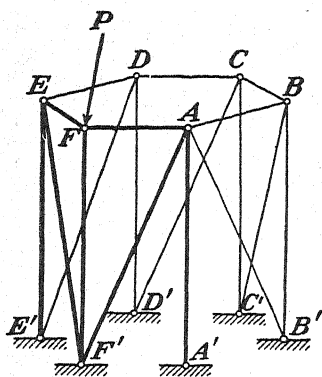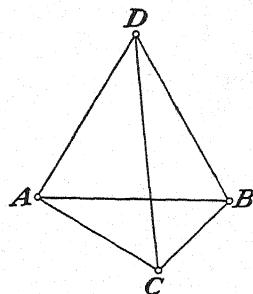
FIG. 236.

[1] We neglect, of course, any slight change in shape that accompanies the small elastic deformations of the bars under axial load.

space can be interconnected to make a self-contained rigid body.   Any such tetrahedron can readily be extended by attaching new joints to the existing system, each by means of three bars the axes of which do not lie in one plane.   Several examples of more extended forms are shown in Fig. 237; such systems also are called *simple space trusses*.   In each case we begin with a triangle ABC and establish succeeding joints in alphabetical order, each by means of three bars not in one plane.

Whenever any self-contained simple space truss like those shown in Fig. 237 is submitted to the action of a balanced system of external forces
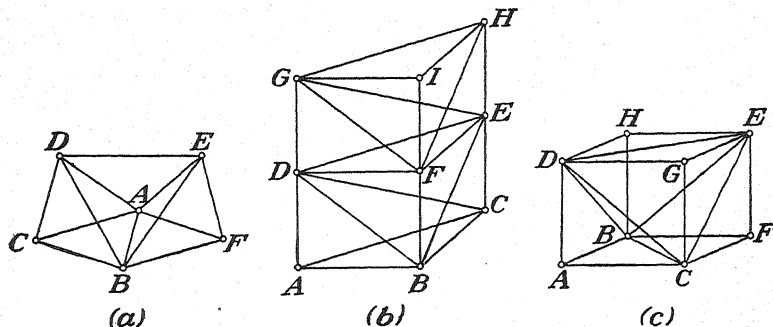
FIG. 237.
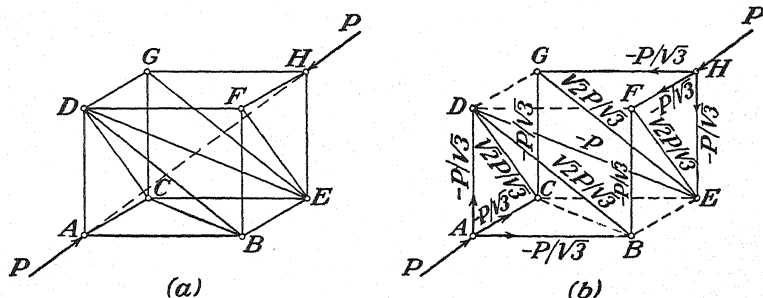
FIG. 238.

applied to its joints, we can always make a complete analysis by the method of joints.   This follows at once from the manner of formation of such trusses; we see that in the process of analysis it is necessary only to consider the joints in the reverse order from which they were set up in the formation of the system.   By way of illustration, let us consider the simple space truss shown in Fig. 238.   This system has the form of a cube at the corners A and H of which are applied two equal and opposite forces P that act along the diagonal AH, as shown.   That the cube as a whole is in equilibrium under the action of two such collinear forces is self-evident, and we may proceed at once with the analysis.   Beginning with the joint H and successively projecting all forces there onto axes

coinciding with HF, HE, and HG, we find that each of these bars carries an axial compression equal to $P/\sqrt{3}$ as shown in Fig. 238b. Conditions at A being identical with those at H, we conclude the same for the bars AB, AC, and AD. Then, at each of the joints G and F, we find four forces in equilibrium, three of which are in one plane. Accordingly, we conclude that GD and FD are inactive bars as shown by dotted lines in Fig. 238b. Also, we find that $GE = FE = +\sqrt{2}\,P/\sqrt{3}$ (tension) and $GC = FB = -P/\sqrt{3}$ (compression). This done, there remain at each of the joints C and B only three bars with unknown axial forces, and we find $CD = DB = +\sqrt{2}\,P/\sqrt{3}$, while $BC = 0$ and $CE = BE = 0$ as shown by dotted lines in Fig. 238b. Finally, from a consideration of the conditions of equilibrium either at D or at E, we conclude that $DE = -P$, and the analysis is completed.

Although the method of joints is always applicable in the analysis of a simple space truss, we need not follow it too rigorously in all cases.
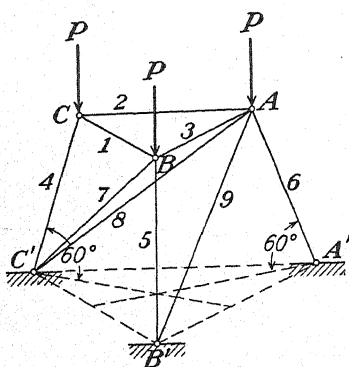
Fig. 239.

That is, it is not always necessary to begin the analysis with the last joint and then systematically proceed through the structure joint by joint until all axial forces have been found. Instead, we can take a somewhat more general view of the problem as follows: Since the joint-by-joint procedure is always applicable and must lead to a definite and unique solution of the problem, we conclude that a simple space truss is always *statically determinate;* i.e., for a given condition of loading there is one and only one set of values for the axial forces that can satisfy the conditions of equilibrium at each and every joint. Hence, if by some indirect procedure, such as guessing, we can succeed in finding a set of values for the axial forces that satisfy the conditions of equilibrium at all joints, we may rest assured that this constitutes the true solution of our problem. Consider, for example, the simple space truss loaded as shown in Fig. 239. In this system, the triangle ABC is equilateral with sides of length a, the triangle $A'B'C'$ is equilateral with sides of length $2a$, and the distance between the horizontal planes ABC and $A'B'C'$ is a. If we remove the bars 7, 8, and 9 from this system, we see that the conditions at the joints A, B, and C will be identical. Accordingly, we conclude, after a consideration of the joint C, that a complete solution, satisfying the conditions of equilibrium of all joints, will be obtained by taking $S_7 = S_8 = S_9 = 0$, $S_4 = S_5 = S_6 = -2P/\sqrt{3}$ (compression), and $S_1 = S_2 = S_3 = -\tfrac{1}{3}P$ (compression).

PROBLEMS

151. Examine the simple space truss shown in plan and elevation in Fig. 240, and identify, by inspection, the bars that are inactive under the action of a single vertical load P applied at A as shown.

152. In Fig. 232b, $EGFH$ and $ACBD$ are two squares with parallel sides of lengths a and $2a$, respectively. The vertical distance between their two horizontal planes is also $2a$. Make a complete analysis of the upper story of this structure if there is a vertical load P at each of the four top joints.

153. Make a complete analysis of the cube shown in Fig. 237c under the action of two equal, opposite, and collinear forces P applied to the joints C and H.

154. Make a complete analysis of the space truss in Fig. 239 if there is a vertical load P at C only.

155. Make a complete analysis of the space truss in Fig. 232b if a tensile force P is introduced in a bar HG (not shown) by means of a turnbuckle. For dimensions of the structure, see Prob. 152.
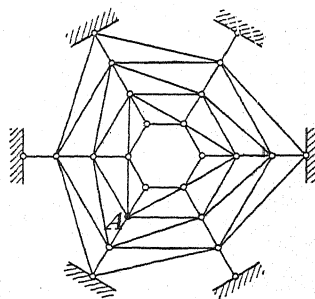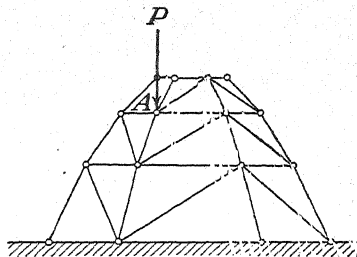
FIG. 240.

32. Statically Determinate Constraint of a Rigid Body in Space.—

In the general case, a system of forces acting on a rigid body may be neither concurrent nor coplanar. Such a system of forces can always be reduced to a *resultant force* and a *resultant couple*. Consider, for example, any single force F_i applied at point A of a body (Fig. 241). This force can be transformed into an equal and parallel force F_i' at the origin O together with a couple formed by the given force F_i at A and an equal and opposite force F_i'' at O. This is done simply by introducing at O the two equal and opposite forces F_i' and F_i'', which, being themselves in equilibrium, do not alter the action of the given force F_i at A. Following the same procedure for each force of the system, we conclude that, in general, any system of forces can be transformed into a system of forces concurrent at O together with a system of couples the moments of which are equal to the corresponding moments of the given forces with respect to point O.
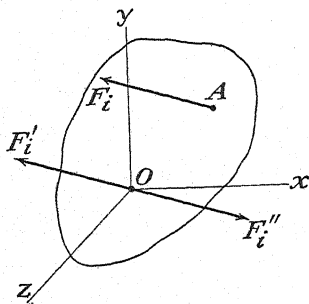
FIG. 241.

We can have equilibrium of two such systems only if the resultant force and the resultant couple are both zero. For the resultant force to

vanish, we must have the algebraic sums of projections of the given forces on the coordinate axes x, y, and z equal to zero; for the resultant couple to vanish, we must have the algebraic sums of moments of the given forces with respect to the three coordinate axes equal to zero. Thus the conditions of equilibrium for a system of forces in space may be expressed as follows:

$$\Sigma X_i = 0, \qquad \Sigma Y_i = 0, \qquad \Sigma Z_i = 0, \\ \Sigma M_x = 0, \qquad \Sigma M_y = 0, \qquad \Sigma M_z = 0. \Big\} \tag{9}$$

These equations will determine any six unknown elements pertaining to a completely general system of forces in equilibrium.

With the foregoing equations of equilibrium in mind, let us now consider the general problem of attaching a rigid body to a foundation in such a way that it will be completely constrained in space. Consider, for example, the rigid body having the form of a rectangular parallepiped
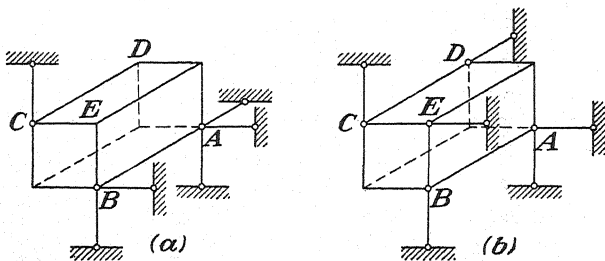
Fig. 242.

as shown in Fig. 242a. As we already know, to fix completely any point A of the body in space, we need *three bars* the axes of which do not lie in one plane as shown. With such attachment to the foundation, it is evident that freedom of motion of the body is limited to rotation about point A. Under such conditions any other point in the body is free to move on the surface of a sphere with center at A and having a radius equal to the distance from A to the point in question. Hence, further constraint of the body can be obtained by completely constraining a second point B in a plane which is tangent to the sphere on which B would otherwise be free to move. This, we know, can be accomplished by *two bars* at B arranged as shown in the figure. Freedom of motion of the body is now limited to rotation about the axis AB, and in this case any point in the body can move only along the arc of a circle the plane of which is normal to the axis AB and the center of which lies on this axis. Thus, at a third point C, *one bar*, the axis of which does not intersect AB, will complete the constraint of the body in space. We conclude then that at least *six bars* are necessary for the complete constraint of a rigid body in space. It is not necessary, however, for them

to be arranged exactly as shown in Fig. 242a. For example, we can replace one of the bars at A by a parallel bar at D and one of the bars at B by a parallel bar at E (Fig. 242b) and still have complete constraint of the body.

It must not be concluded from the discussion above that six bars will always be adequate for the constraint of a rigid body in space. For example, if the bars are all parallel or lie in parallel planes as shown in Fig. 243a, it is evident that there is some freedom for endwise motion without inducing appreciable changes in the lengths of the supporting bars. Hence six bars so arranged cannot be said to furnish complete constraint. In Fig. 243b, we have another case where six bars are not satisfactorily arranged for the complete constraint of a rigid body. In this case four of the bars are attached to one point A, and the other two can be arranged in any manner whatsoever. Under such conditions the axis of the bar at C and the point A define a plane, and the axis of the
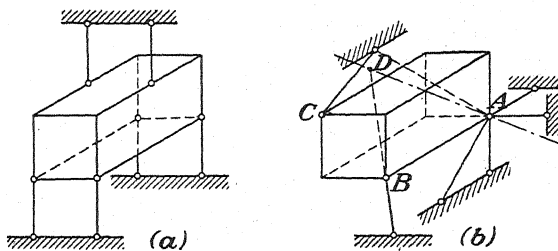
Fig. 243.

bar at B intersects this plane at some point D as shown or is parallel to it. Hence all six bars intersect the axis AD; and if externally applied forces give a moment with respect to this axis, the six supporting bars will be unable to develop a balancing moment and the rigid body will rotate to some other position. Such incomplete constraint of a rigid body in space is analogous to that of a rigid body in a plane where the axes of three bars are parallel or intersect in one point (see page 49).

From the foregoing discussion, we conclude that a system of supports consisting of six bars so arranged that their axes cannot all be intersected by a straight line are always necessary and usually sufficient[1] for the complete constraint of a rigid body in space. Any bars in excess of this number will constitute *redundant constraints*.

Let us assume now that either of the constrained bodies shown in Fig. 242 is subjected to the action of a system of external forces. Under the action of these loads, axial forces will be induced in the supporting bars, and each bar will exert a reaction on the body at the point of

---

[1] In exceptional cases, the determinant of Eqs. (9) may vanish even when all six bars do not intersect one axis; this will always be an indication of incomplete constraint.

attachment and coincident in direction with the axis of the bar.   Considering both active and reactive forces together, we have the general case of a system of forces in equilibrium.   The forces are not concurrent, coplanar, or parallel.   For such a system we have six equations of equilibrium as represented by Eqs. (9), and we see that these six equations will determine the magnitudes of the six reactive forces exerted on the body by the supporting bars.   Thus the six bars that are both necessary and sufficient for the complete constraint of the rigid body also represent a *statically determinate* system of supports.   If there are more than six supporting bars, *i.e.*, if there are redundant constraints, the six equations of statics will be insufficient completely to determine the reactive forces and the system of supports is said to be *statically indeterminate*.   In special cases like those shown in Fig. 243, where there are only six bars but so arranged that their axes can all be intersected by a straight line, the determinant of the six equations of equilibrium will vanish and the system of supports will again prove to be statically indeterminate.

In the analysis of a system of supports of a rigid body in space, we first replace the supporting bars by the reactions that they exert on the body, thus obtaining a free-body diagram.   Since the six reactive forces coincide with the axes of the bars that exert them, their directions are known and, generally speaking, the six unknown magnitudes can always be determined by Eqs. (9).   However, in the solution of practical problems, we shall not always adhere rigorously to the use of this system of equations.   Since the body is in equilibrium, it follows that the algebraic sum of the moments of all the forces with respect to any axis (not necessarily x, y, or z) must be zero and likewise that the algebraic sum of the projections of all forces on any axis must be zero.   Thus, in writing the equations of equilibrium, it is usually possible, by a proper choice of axes, to obtain six equations in each of which only one or two of the unknown forces appear.   In this way we avoid the difficulties connected with the solution of six simultaneous equations with as many unknowns, and our problem is greatly simplified.
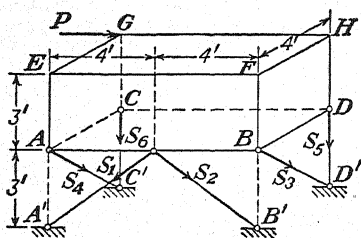
Fig. 244.

To illustrate the application of the foregoing general discussion, let us consider the rectangular parallelepiped $ABCDEFGH$ supported and loaded as shown in Fig. 244.   To make a free-body diagram, we replace the six supporting bars by the reactions which they exert on the body, remembering that each force must act along the axis of the bar which produces it.   We assume all bars to be in tension as shown so that any

negative signs obtained during calculation will simply indicate that the corresponding bars are in compression. Writing first an equation of moments with respect to the vertical axis BF, which is parallel to or intersects all bars except 4, we obtain

$$-\tfrac{4}{5}S_4 \cdot 8 - P \cdot 4 = 0,$$

from which $S_4 = -\tfrac{5}{8}P$. In the same way, by equating to zero the algebraic sum of moments of all forces with respect to the axis AE, we find $S_3 = +\tfrac{5}{8}P$. Since we already know the value of S_4, this latter result may also be obtained directly by equating to zero the algebraic sum of projections of all forces on the axis AC.

Now, taking moments of all forces, first with respect to the axis AB and again with respect to the axis $C'D'$, we conclude, successively, that

$$S_5 = -S_6 \qquad \text{and} \qquad S_1 = -S_2.$$

Then equating to zero the algebraic sum of the projections of all forces on the axis AB, we obtain

$$-\tfrac{4}{5}S_1 + \tfrac{4}{5}S_2 + P = 0,$$

from which $S_1 = -S_2 = \tfrac{5}{8}P$.

Finally, we equate to zero the algebraic sum of moments of all forces with respect to the axis AC and obtain

$$\tfrac{3}{5}S_1 \cdot 4 + \tfrac{3}{5}S_2 \cdot 4 + \tfrac{3}{5}S_3 \cdot 8 + S_5 \cdot 8 + P \cdot 3 = 0,$$

from which, using the previously determined values of S_1, S_2, and S_3, we find $S_5 = -S_6 = -\tfrac{3}{4}P$, and the analysis is completed.

Sometimes a problem involving a general system of forces in space can be simplified by introducing an *equivalent loading*. Consider, for
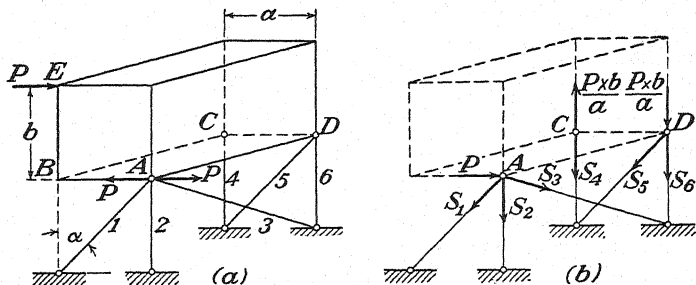
Fig. 245.

example, the rigid body supported by six bars as shown in Fig. 245a and subjected to a horizontal force P in the end plane ABE. We begin by adding to the given system at A the two equal, opposite, and collinear forces P as shown in the figure. Two such forces being in equilibrium do not alter in any way the action of the system, but we may now con-

sider that we have a force P at A together with a couple consisting of the force P at E and the opposite force P at A. This couple, the moment of which in the end plane of the body is Pb, can be transferred to the opposite end of the body and represented by the vertical forces Pb/a at C and D as shown in Fig. 245b. The system of three applied loads shown in Fig. 245b is equivalent in action to the single load P at E in Fig. 245a and will induce in the supporting bars the same axial forces. However, in Fig. 245b we have at A, C, and D three simple systems of con-

current forces that can be analyzed by the most elementary procedures. By inspection, we conclude that $S_3 = S_5 = 0$, while $S_4 = -S_6 = Pb/a$. Considering the remaining forces at A and projecting successively onto horizontal and vertical axes, we find $S_1 = P \csc \alpha$ and $S_2 = -P \cot \alpha$.
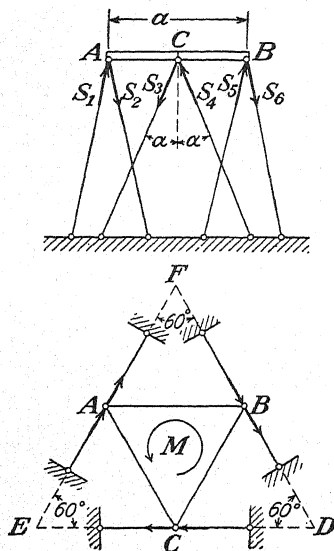
In Fig. 246 we have a plan and elevation of an equilateral triangular slab supported in a horizontal plane by six bars of equal lengths arranged as shown. It is required to find the axial forces induced in these bars by a couple of moment M acting in the plane of the slab as shown. We begin with a free-body diagram of the slab as indicated in the figure. Then, taking AB as an axis of moments, we see that only the reactions S_3 and S_4 have moments different from zero with respect to this axis.

FIG. 246.

Hence we conclude that these forces, which are equally inclined to the vertical, must be equal in magnitude and represent, respectively, tension in one bar and compression in the other as indicated by the arrows in the figure.[1] By similar considerations of moments about the axes AC and BC, we conclude that S_5 and S_6 as well as S_1 and S_2 are equal in magnitude and directed as shown. Now by successively equating to zero the algebraic sums of projections of all forces on the axes AD and BE, we conclude that the six reactive forces must all be equal in magnitude. Finally, then, by balancing moments with respect to a vertical axis through the centroid of the triangle, we obtain

$$6S \sin \alpha \cdot \frac{2}{3} \frac{\sqrt{3}}{2} a = M,$$

from which $S = \sqrt{3}\, M/6a \sin \alpha$, where S is the magnitude of axial force in any one of the bars.

[1] For expediency, we depart here from our usual rule of arbitrarily assuming, to begin with, that all bars are in tension.

PROBLEMS

156. A strut AB is hinged to a vertical wall at B and supported horizontally by two guy wires arranged as shown in Fig. 247.   Find the tension induced in each guy wire by a vertical load P applied at A.
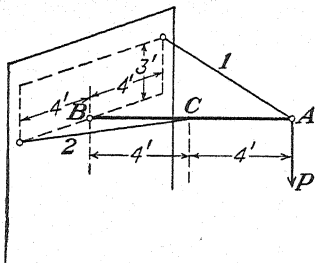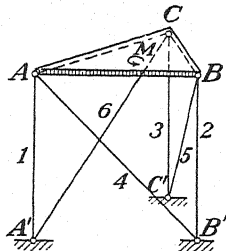
FIG. 247.   FIG. 248.

157. An equilateral triangular slab is supported in a horizontal plane by six bars arranged as shown in Fig. 248.   Each side of the triangle is of length a, and the vertical bars also are of length a.   If the weight of the slab is W, what must be the moment of a couple M, acting in the plane of the slab as shown, for the vertical bars to be inactive? What will be the corresponding compressive forces in the inclined bars?

158. Using the notion of equivalent loading, make an analysis of the system of supports in Fig. 245a if the load P at E is vertical.

Ans. $S_1 = S_3 = S_5 = 0$, $S_2 = S_4 = -S_6 = -P$.

159. Make a complete analysis of each system of supports in Fig. 242 under the action of a vertical load P at D.   Assume in each case that the rectangular parallelepiped has dimensions a, a, and $2a$.

160. Analyze the system of supports in Fig. 244 under the action of a vertical load P at E.   *Ans.* $S_1 = S_2 = -\tfrac{5}{6}P$, $S_3 = S_4 = 0$, $S_5 = -S_6 = \tfrac{1}{2}P$.

33. Compound Space Trusses: Method of Sections.—In the preceding article, we saw how a rigid body can be completely constrained in space by means of six bars so arranged that their axes cannot all be intersected by one straight line.   On this basis, we conclude that any self-contained simple space truss like those shown in Fig. 237 can be rigidly attached to a foundation in the same manner.   Consider, for example, the system shown in Fig. 249, where we have a simple space truss $ABCDEFGH$ attached to the foundation by six bars arranged as shown.   In this way, we obtain a rigid and statically determinate structure capable of holding in equilibrium any system of externally applied loads such as $P_1, P_2, \ldots$.   Such a structure will be called a *compound space truss*.   In the analysis of a compound truss, we shall generally find that the method of joints alone is inadequate.   For example, in this case (Fig. 249) we cannot begin the analysis by the method of joints because there is no joint to which less than four bars are attached.   Consequently, we must first consider the entire portion $ABCDEFGH$ as a free body and, using the six equations of equilibrium of the preceding article [Eqs. (9)], find the axial forces in the six supporting bars.   Such

procedure in the analysis of a space truss is usually called the *method of sections*. As soon as we know completely the balanced system of forces external to the simple truss as a whole, the remainder of the analysis can be made without difficulty by the method of joints.

In Fig. 250, we have an example of a self-contained compound space truss. To obtain this structure, we take two simple space trusses, as represented by the shaded portions of the system, and interconnect them by six bars arranged in accordance with the requirements of complete constraint of a rigid body in space. It must be self-evident, then, that the resulting system is rigid and statically determinate. However, under the action of a balanced system of external forces, we again may be unable to make a complete analysis by the method of joints. To begin the analysis in this case, we make a section cutting the six numbered bars and isolate one of the simple trusses as a free body. Then, with the help of the six available equations of equilibrium, we determine the axial forces in these six interconnecting bars, after which the two simple trusses can be analyzed without difficulty by the method of joints.
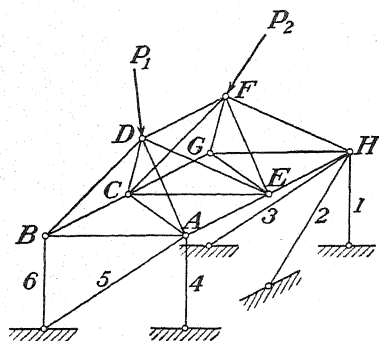
Fig. 249.

If desired, the simple truss *ABCDEFGH* of Fig. 249 can be considered as a compound truss like that in Fig. 250. It is necessary only to regard
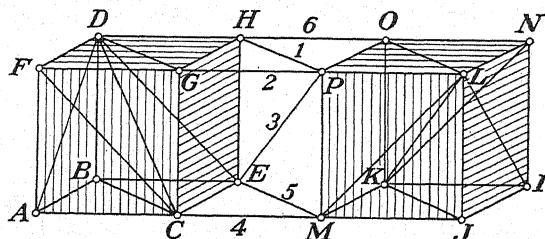
Fig. 250.

it as two simple tetrahedrons *ABCD* and *EFGH* interconnected by the six bars *AE*, *CE*, *DE*, *CF*, *DF*, and *CG*. Accordingly, we conclude that the axial forces in these bars, also, can be found by the method of sections, leaving for analysis by the method of joints only the two tetrahedrons. In the same way, the simple space truss shown in Fig. 232*a* can be considered as a compound space truss consisting of the simple tetrahedron *ABCD* attached to the foundation by six bars arranged in a manner satisfying the conditions of complete constraint of a rigid body in space. On the other hand, no such conclusion can be made for the simple space truss in Fig. 232*b*. In the first place, the portion *ABCDEFGH* of this

structure does not represent a rigid body; and, second, to separate it from the foundation we should have to cut eight bars instead of six. Under such circumstances, the method of sections cannot be used.

The identification of any space structure as a simple or compound truss will always be an indication that it is rigid and statically determinate, *i.e.*, that under any given condition of loading there will be one and only one set of values for the axial forces that can satisfy the conditions of equilibrium at each and every joint. Whether or not we rigorously follow the method of sections or the method of joints in finding this set of values is of no importance. Any procedure by which we succeed in finding a solution that satisfies all conditions of equilibrium is a legitimate procedure.

As an example, let us consider the analysis of the compound space truss shown in Fig. 251. This structure consists of a rigid equilateral
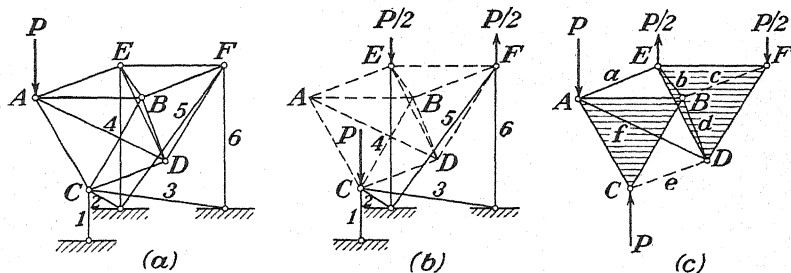
FIG. 251.

prism *ABCDEF*, with edges of length *l*, that is attached to the foundation by six bars arranged as shown and then subjected to the action of a vertical load *P* at *A*. The orthodox procedure in the analysis of this compound space truss would be to find the axial forces in the six supporting bars by the method of sections and then use the method of joints for the simple truss *ABCDEF*. While such a procedure will involve no particular difficulty, it will be somewhat more advantageous in this particular case to find the forces in the supporting bars by using the notion of equivalent loading, which was discussed on page 181. Introducing at *C* two equal and opposite vertical forces *P* that, being in equilibrium, do not affect the system, we see that the given loading can be considered as a vertical load *P* at *C* together with a counterclockwise couple *Pl*/2 in the end plane *ABC* of the structure. Transferring this couple to the end plane *DEF* where we represent it by two vertical forces *P*/2 at *E* and *F*, we obtain the equivalent loading shown in Fig. 251*b*. Regarding this notion of equivalent loading, it must be emphasized here that the loading in Fig. 251*b* is equivalent to that in Fig. 251*a* only insofar as the axial forces induced in the supporting bars are concerned. The forces induced in the other bars of the system will be completely different in the two cases. From Fig. 251*b*, we see by inspection that the supporting

bars 2, 3, and 5 are inactive, while the axial forces in the other three are as follows: $S_1 = -P$, $S_4 = -P/2$, $S_6 = +P/2$. Returning, now, to the true loading and replacing the six supporting bars by the reactions that they exert on the simple truss $ABCDEF$, we obtain, for further analysis,
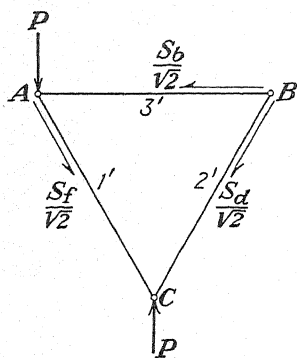
Fig. 252.

the system shown in Fig. 251c. This simple truss, however, can also be considered as a compound truss consisting of the rigid triangles ABC and DEF, which are interconnected by the six bars a, b, c, d, e, and f, as shown. As can be seen by inspection of the joints C and F, the bars e and c of these six are inactive and can be removed from the system. Making a section that cuts the four remaining bars and projecting onto the plane of the triangle ABC all forces that act upon it, we obtain a coplanar system of forces in equilibrium as shown in Fig. 252. Successively equating to zero the algebraic sums of moments of these forces with respect to the points A, B, and C, we find

$$S_d = +\sqrt{\tfrac{2}{3}}\,P, \qquad S_f = -\sqrt{\tfrac{2}{3}}\,P, \qquad \text{and} \qquad S_b = -\sqrt{\tfrac{2}{3}}\,P.$$

To find S_a, we return to Fig. 251c and use the method of joints. Projecting all forces at A onto an axis coinciding with AE, we obtain $S_a = +P/\sqrt{3}$. The two triangles ABC and DEF may now be analyzed as any other plane truss. In Fig. 252, for example, we see that $S_1' = S_2' = -P/\sqrt{3}$, while $S_3' = +P/\sqrt{3}$.

PROBLEMS

161. The compound space truss in Fig. 253 consists of a rigid square pyramid $ABCED$ attached to the foundation by seven bars arranged as shown. Then, by means of a turnbuckle F, a tensile force P is induced in the bar CC'. What axial forces will be induced in the other bars of the system?
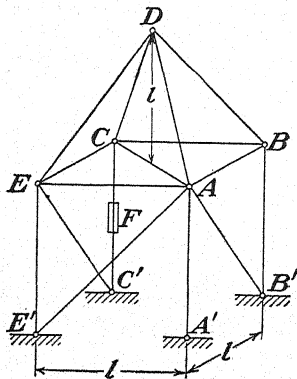
Fig. 253.

162. The rigid cube shown in Fig. 254 is formed by interconnecting the two shaded tetrahedrons by means of six bars DE, DF, BH, CH, BE, and CF the axes of which cannot all be intersected by one straight line. Make a complete analysis of this system under the action of two equal, opposite, and collinear forces P acting along the diagonal AG as shown.
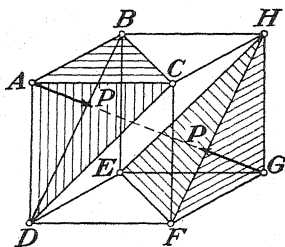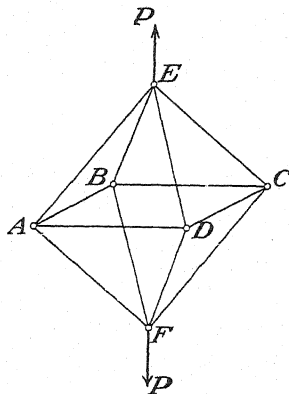
FIG. 254.   FIG. 255.

163. Prove that the system of bars shown in Fig. 255 constitutes a compound space truss and make a complete analysis of the system, (a) under the action of two equal and opposite forces P acting as shown and (b) under the action of two such collinear forces applied at the joints A and C. The system has the form of a regular octahedron.

164. Make a complete analysis of the compound space truss loaded as shown in Fig. 256. Assume that ABC and $A'B'C'$ are equilateral triangles and that $A'B'BA$ is a square.

Ans. $A'C = B'C = +P/\sqrt{2}$, $C'A = C'B = -P/\sqrt{2}$, $A'A = B'B = +P/2$, $CA = CB = -P/2$, $AB = +P/2$.
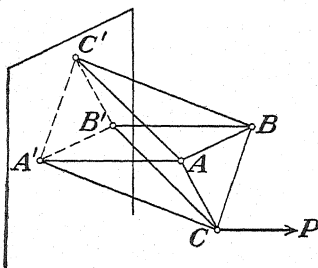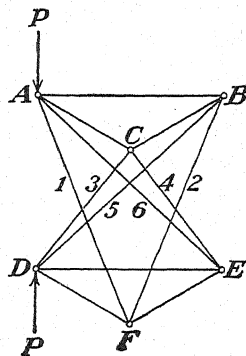
FIG. 256.   FIG. 257.

165. In Fig. 257, the triangles ABC and DEF are equilateral with sides of length a, and the distance between their parallel planes is also a. Find the axial forces in the six bars that interconnect these two triangles if two equal and opposite collinear forces P are applied to the system as shown.

Ans. $S_1 = S_6 = -P/\sqrt{2}$, $S_2 = -S_5 = +P/\sqrt{2}$, $S_4 = -S_3 = +P/\sqrt{2}$.

34. General Theory of Statically Determinate Space Trusses.—In this article, we shall consider the general problem of how to assemble a system of bars in space so as to form a completely rigid space truss. We have already seen in Art. 31 that a *simple space truss* can be formed by beginning with a rigid foundation to which the first joint is attached by means of three bars not in one plane; thereafter, succeeding joints are attached to the foundation or to previously established joints in the same manner. The truss in Fig. 258a has been formed in this way, beginning with joint A and setting up the other joints in alphabetical order. From the rule of formation of a simple space truss, it follows that, between the number of members m and the number of joints j, there must exist the relationship

$$m = 3j, \tag{10a}$$

since we use three bars for each joint.

While the foregoing rule of formation of a space truss is a very simple one, it does not represent the only way in which a system of bars can be
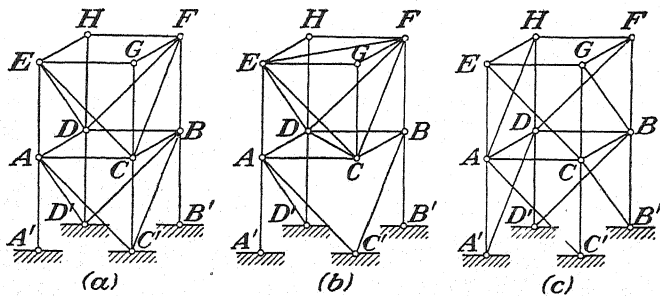
Fig. 258.

assembled to form a rigid space structure. For example, if we remove the bars CC' and BD' of the simple truss in Fig. 258a and introduce instead the bars DC and EF as shown in Fig. 258b, we obtain a *compound space truss* like that shown in Fig. 249. That is, the portion $ABCDEFGH$ of the structure now represents a self-contained simple space truss which is attached to the foundation by six bars the axes of which cannot all be intersected by one straight line. Since, by the above rearrangement of bars, we change neither the number of bars m nor the number of joints j, we conclude that the compound space truss in Fig. 258b also satisfies Eq. (10a). Still another type of rigid space truss can be derived from the simple truss in Fig. 258a simply by changing the directions of the diagonals in the two side panels as shown in Fig. 258c. In this way, we obtain a system that, although it still satisfies the relationship $m = 3j$, can no longer be classed either as a simple truss or as a compound truss. Many of our engineering structures are of this latter form, which is called a *complex space truss*.

From the preceding examples, we may draw the general conclusion that $3j$ bars are always necessary and, when properly arranged, sufficient for the rigid interconnection between themselves and the foundation of j joints in space. This observation holds also for any self-contained space truss that is attached to a foundation by the six bars necessary and sufficient for the complete constraint of a rigid body in space. To demonstrate this, we recall from Art. 31 the rule of formation of a self-contained simple space truss, by which we begin with three bars and three joints in the form of a triangle and attach succeeding joints, each by means of three bars not in one plane. Since, by this rule, we use three bars for each joint except the first three, for which there is only one bar for each joint, we conclude that between the total number of bars m and the total number of joints j of a self-contained simple space truss there must exist the relationship

$$m = 3j - 6. \tag{10b}$$

Then the six additional bars required to complete the constraint of a rigid body in space bring us to $m = 3j - 6 + 6$ or simply $m = 3j$ as before.

In arranging a system of bars to form a rigid space truss, it is often desirable, for purposes of utility, to avoid any obstruction of the inner space. Regarding space structures without internal diagonals, it can be proved that if any self-contained space truss has the form of a closed polyhedron the plane faces of which are triangular or subdivided into triangles, then Eq. (10b) will be satisfied and, generally speaking, the truss will represent a completely rigid body. To prove this statement, we begin with a general theorem of stereometry that is due to Euler. This theorem states the relationship between the number of faces, edges, and apexes of any closed polyhedron and may be established on the basis of the following reasoning: Beginning with one face, represented by any polygon, we see that we have, to start with, an equal number of edges and apexes. Now, when we come to add a second face to the first, there will be one of its edges and two of its apexes already existing. Again, when we come to add a third face to the first and the second, two of its edges and three of its apexes will already exist, etc. Thus, in general, the addition of each face after the first entails the addition of one more new edge than new apexes; and as we proceed, the total number of edges gains on the total number of apexes by exactly the number of faces that up to any moment have been added to the first, or starting, face. Hence we conclude that, at any stage of construction, the number of edges must be equal to the number of apexes plus the number of added faces, *i.e.*, all except the starting face. This relationship holds until we come to the last, or closing, face, the addition of

which entails no new edges and no new apexes; thus we acquire a second extra face. Denoting by m the number of edges, by j the number of apexes, and by f the number of faces, we have, then, for any closed polyhedron the relationship

$$m = j + (f - 2), \tag{a}$$

and this equation expresses the theorem of Euler mentioned above. The foregoing arguments apply to the general case of any closed polyhedron. In the particular case of a closed polyhedron the faces of which are triangular or divided into triangles, we can express a further relationship
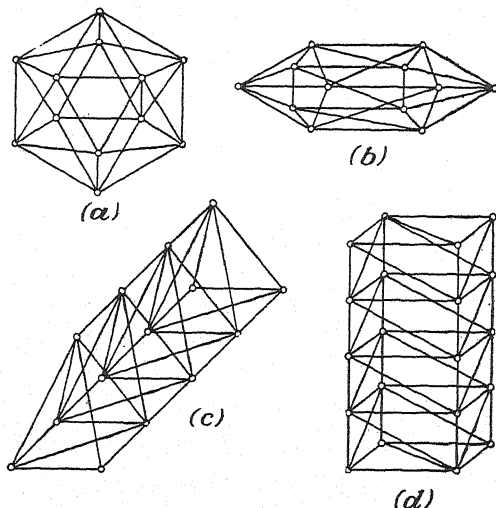
FIG. 259.

between the number of faces and the number of edges, *i.e.*, between f and m. Every edge being common to two faces and all faces being triangles, we see that there must be exactly half as many edges as three times the number of faces. That is,

$$m = \tfrac{3}{2}f. \tag{b}$$

Eliminating f between Eqs. (*a*) and (*b*), we obtain $m = 3j - 6$ as expressed by Eq. (10*b*). Thus we conclude that any self-contained space truss the bars of which represent the edges of a closed polyhedron having triangular faces and being without internal diagonals must satisfy Eq. (10*b*). Several examples of such structures are shown in Fig. 259, and we see that they must be classified as complex trusses. As already stated, these forms have the practical advantage that their inner space is free from obstruction; for this reason, they are commonly employed in all kinds of structural work.

We have seen now that there are three general classes of space trusses, *simple, compound,* and *complex,* and that in each case $m = 3j$ is a general requirement of rigidity and complete constraint.   We shall now discuss another general significance of the relationship $m = 3j$. Consider, for example, any completely constrained space truss comprised of m bars and j joints and submitted to external loads applied only at the joints as shown in Fig. 260.   Under the action of such applied loads, axial forces will, in general, be induced in all the m bars of the system, and the determination of these internal forces constitutes the analysis of the truss.   If we are dealing with a simple or compound truss, we know that the analysis can always be made by the method of joints or by the method of sections; such procedures have already been discussed in detail in Arts. 31 and 33.   In the case of a complex truss, however, these methods of analysis may fail.   In the present case, for example, we see that there are four bars meeting at each joint and so the method of joints cannot be used.   Likewise, there is no possibility of employing the method of sections because no section can be conceived which cuts only six bars that do not all intersect one straight line.   Under such cir-
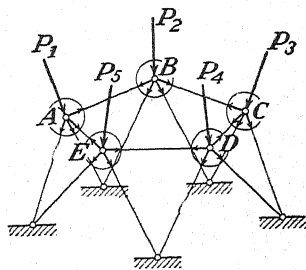
Fig. 260.

cumstances, we must take a more general view of the problem as follows: Replacing each of the m bars by the two equal but opposite reactions that it exerts on the joints at its ends, we obtain j systems of concurrent forces in equilibrium as shown.   Then for each joint we write three equations of statics ($\Sigma X_i = 0$, $\Sigma Y_i = 0$, $\Sigma Z_i = 0$) and obtain $3j$ simultaneous equations involving m unknowns.   We see now that, if $m = 3j$, there are exactly as many unknowns as there are equations and that in all but exceptional cases, where the determinant of these equations vanishes,[1] the system of equations of statics must yield a unique solution to our problem.   For this reason, any completely constrained space truss that satisfies the condition $m = 3j$ is said to be *statically determinate.*   That is, under any condition of loading, the axial forces in all bars can be found from equations of statics alone, and there is no necessity to take account of the elastic deformations of the bars.   The solution of $3j$ simultaneous equations involving as many unknowns is, of course, a problem in itself, but we shall content ourselves for the moment with the knowledge that the axial forces can be found by equations of statics alone if $m = 3j$.[*]

[1] Such exceptional cases will be discussed later.

[*] Practicable methods of analysis of complex space trusses will be discussed in Art. 35.

If $m > 3j$, there will, of course, be more unknown axial forces than there are independent equations of statics and the system of $3j$ equations cannot yield a unique solution. Accordingly, the truss is said to be *statically indeterminate.* Under such conditions, the elastic deformations of the bars must be taken into account to determine the way in which the internal forces adjust themselves to meet the conditions of equilibrium of the joints. On the other hand, if $m < 3j$, the structure is not rigid and will probably collapse under the action of externally applied loads.

Returning to the case where $m = 3j$, let us consider the exceptional trusses for which the determinant of the $3j$ equations of statics vanishes and the equations do not yield a definite solution for the axial forces. This circumstance will always be an indication that the truss is nonrigid and therefore unsuitable for structural purposes. Such exceptions are called *critical forms.* A critical form will be obtained, for example, in the formation of a simple space truss if we forget that those three bars

(a)   (b)
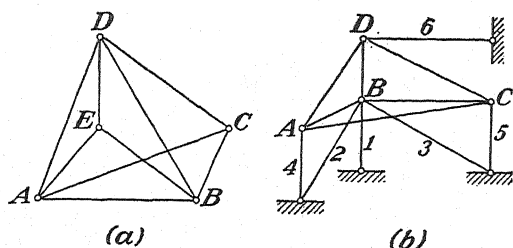
Fig. 261.

by which any joint is attached to the rest of the system must not all lie in one plane. Thus the self-contained simple truss in Fig. 261a has a critical form if the joint E lies in the plane ABD, and we see that under such conditions there is a limited freedom for relative movement of this joint in the direction perpendicular to the plane ABD. Likewise, the compound space truss in Fig. 261b has a critical form because the six bars by which the rigid tetrahedron $ABCD$ is attached to the foundation are so arranged that they all intersect the vertical axis BD or are parallel to it. Thus, again, there is a limited freedom for rotation of the tetrahedron around this axis.

Such critical forms as those shown in Fig. 261 are easily detected by inspection and, in fact, can be avoided by careful observation of the rules of formation of simple and compound space trusses. In the case of a complex truss, however, we may be unable to discover a critical form by inspection, and it is for such trusses that they are most likely to occur. A general method of detection of critical form is based on a consideration of the $3j$ equations of statics for the j joints of the system. If the determinant of these equations is different from zero, we have a

statically determinate system and there is no critical form. If the
determinant is zero, the system is statically indeterminate and we do
have a critical form.

The actual evaluation of the above-mentioned determinant is, of
course, impracticable. However, since it depends only on the configura-
tion of the truss and not at all on how the truss is loaded, it follows that
if for any assumed loading we can find, without ambiguity, the axial
forces in all bars, the determinant evidently is not zero and the truss is
rigid. On the other hand, if under an assumed loading we can discover
some ambiguity regarding the internal forces, the determinant evidently
is zero and the truss has a critical form. In undertaking such an investi-
gation, the simplest procedure is to assume a zero load at each joint.
Then one obvious solution satisfying the conditions of equilibrium at the
joints is obtained by taking all bars with zero axial forces. If no other
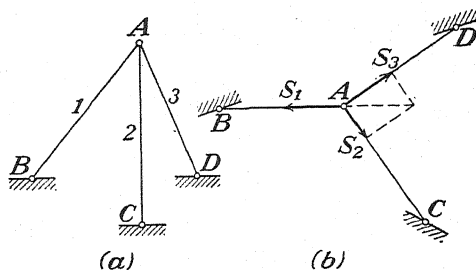
Fig. 262.

set of values different from zero can be found to satisfy the conditions of
equilibrium at the joints, the truss is rigid and statically determinate;
but if, under zero loading, a set of axial forces different from zero can be
found to satisfy the equilibrium of the joints, the solution is ambiguous
and the truss has a critical form. Such analysis of a truss under zero
load for the purpose of detecting a critical form is known as the *zero-load
test*.

As a first example, let us consider the system shown in Fig. 262a,
where the joint A is supported in space by three bars the axes of which
are not in one plane. With zero load at A, we see that equilibrium of
this point can exist only if the axial force in each bar is zero, because three
forces can be in equilibrium only if they are coplanar. Hence the system
does not have a critical form but is rigid and statically determinate.
We repeat that, if the system is determinate for zero load, it will be so
for any other condition of loading. Now consider the system in Fig.
262b, where the joint A is attached to the foundation by three bars the
axes of which do lie in one plane. Again, with zero load at A, we can
have equilibrium if each of the internal forces S_1, S_2, and S_3 is zero.

However, in this case we can also have equilibrium by assuming an arbitrary value for S_1 and then taking S_2 and S_3 such that their resultant is equal, opposite, and collinear with S_1. Thus the solution is ambiguous, and the system has a critical form. Physically this indicates that the joint A can move slightly in the direction normal to the plane BCD without significant changes in the lengths of the bars.

As a second example, we shall consider the complex space truss shown

(a)

in Fig. 263a. This system consists of a square frame $ABCD$ supported in a horizontal plane by eight bars as shown, and we see that the condition $m = 3j$ is satisfied. Now, with a zero load at each joint, we assume an arbitrary tension in AE' and at the same time such compression in AA' that the resultant of these two forces at A is horizontal as shown by the dotted vector through A. This vector is perpendicular to the diagonal AC of the square $ABCD$; and hence, by taking a proper compression in AB and an equal tension in AD, we see that all conditions of equilibrium at the joint A will be satisfied. Similar arguments can be made for the other joints B, C, and D; and we conclude finally that, under zero loads, a set of axial forces different from zero can exist in the bars of the system as shown. Thus the solution is ambiguous, and the truss has a critical form.

(b)
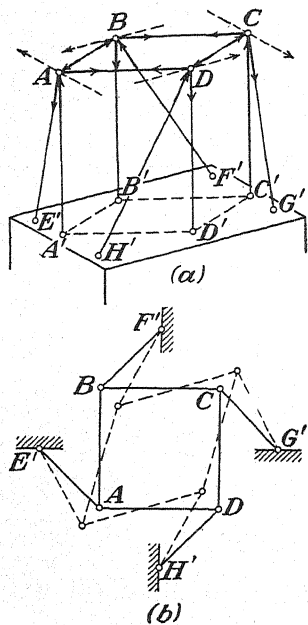
Fig. 263.

The nonrigidity of the system in Fig. 263a can be seen physically by considering a horizontal projection as shown in Fig. 263b. From this figure it is clear that the joints A, B, C, and D can move in or out along the diagonals of the square without changes in the lengths of any of the bars. Thus the truss can take the distorted form indicated by dotted lines, and we have a nonrigid system unsatisfactory for practical use.

PROBLEMS

166. Apply the zero-load test to the complex truss in Fig. 258c, and prove that it is rigid and statically determinate.

167. The complex space truss shown in plan and elevation in Fig. 264 consists of a square $ABCD$ supported in a horizontal plane by eight bars arranged as shown. Using the zero-load test, prove that this system is nonrigid and represents a critical form.

168. Using the zero-load test, prove that the complex space truss shown in plan and elevation in Fig. 265 is rigid and statically determinate notwithstanding its general resemblance to the nonrigid system in Fig. 264.

169. Show in general that a complex space truss like those in Fig. 264 and Fig. 265 will be rigid and statically determinate if the regular polygon $ABCDE$ . . . has an odd number of sides, and nonrigid and statically indeterminate if there is an even number of sides.
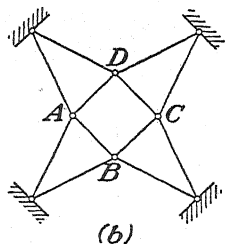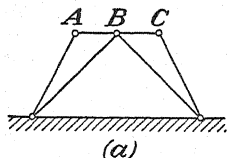
FIG. 264.
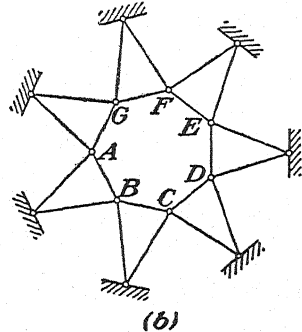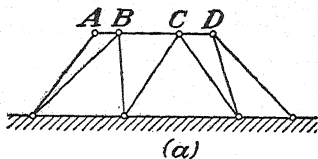
FIG. 265.

170. Using the zero-load test, prove that each of the complex space trusses in Fig. 259 is rigid and statically determinate.

35. Analysis of Complex Space Trusses.

—In the preceding article, we have discussed the general problem of formation of space trusses and a criterion for the detection of critical forms. We shall now turn our attention to the problem of analysis of various complex trusses that have been proved to be rigid and statically determinate.

One of the most useful methods of analysis of space trusses, in general, is the method of joints, which we have already discussed in Art. 31. This method, it will be remembered, is generally applicable only to simple trusses, but there are cases where it can be used successfully in the analysis of a complex truss. The truss in Fig. 266, for example, is of this kind and can be completely analyzed by the method of joints. We begin with

FIG. 266.

joint A and find the axial forces in the bars 1, 2, and 3. Then, replacing these bars by the reactions that they exert on the remainder of the structure at B, C, and D, we find that there are still four unknown
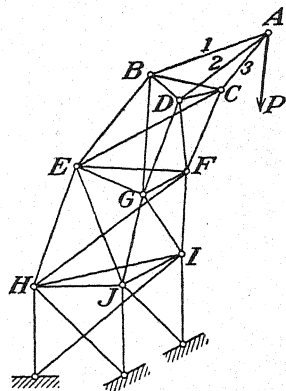
axial forces at each of these joints. However, at D, three of the bars are in one plane, and so the axial force in the fourth bar BD can be found by projecting all forces at D onto an axis normal to the plane DCF. As soon as the force in BD is known, we can proceed to the joint B, where there will now be only three bars (BG, BE, and BC) with unknown axial forces, and these can be found. Then, knowing the action of BC on the joint C, we can consider the equilibrium of this joint and find the forces in CE, CF, and CD. After this, we return to D and find the remaining unknown forces there (DF and DG). Beginning with G, the same procedure may be employed at the joints G, E, and F, and so on, throughout the truss until the analysis is completed. It will be seen that success with this complex truss by the method of joints rests on the fact that, whenever all but one of the unknown forces of a concurrent system lie in one plane, this one force can always be found by projecting onto an axis normal to the plane defined by the lines of action of the other unknown forces, no matter how many (see page 164).

Sometimes the analysis of a complex space truss can be greatly simplified by taking advantage of the symmetry of the system. Consider, for example, the structure shown in Fig. 267, and suppose that there is a vertical load at each joint and that all loads on any one horizontal ring are equal. Under such conditions of symmetry, a complete analysis of the truss can be made in a very simple manner. We begin with the zero-load test for complete rigidity. At each joint of the top ring there are four bars, three of which lie in one plane. Hence, under zero load, the bars of this ring must be inactive and can be removed from the system. This leaves only two bars at each joint that are not collinear, and we conclude accordingly that these bars also are inactive and may be removed. Repeating this reasoning for the joints of succeeding rings, we conclude that no axial forces different from zero can exist in the system under zero load. Hence it is rigid and statically determinate. This indicates that, if, under external loads different from zero, we can find, by any convenient means, a set of axial forces that satisfy the conditions of equilibrium of the joints, we may be sure that we have the true solution.
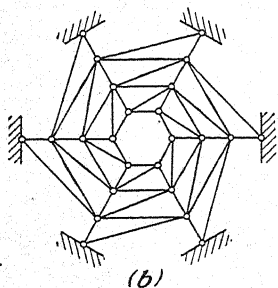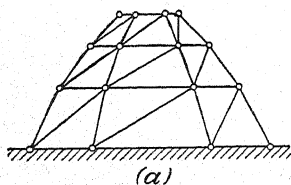
(a)

(b)

Fig. 267.

Keeping the foregoing general remarks in mind, let us consider now any meridian $ABCD$ of the structure as shown in Fig. 268a. Noting that the external loads P_1, P_2, and P_3 lie in the vertical plane of the meridian,

we conclude that this one rib of the structure can be in equilibrium only if at each joint the forces exerted by the bars entering from the two sides have a resultant H which lies in the plane of the meridian. Furthermore, we see that this condition can be realized by assuming that all diagonals are inactive and that all bars comprising any one horizontal ring have equal axial forces. Proceeding on this basis, we isolate the rib $ABCD$ and project all forces onto the plane of the meridian as shown in Fig. 268b. Then, beginning with the joint A, we can construct the polygon of forces for each of the joints A, B, and C, as shown in Fig. 268c.
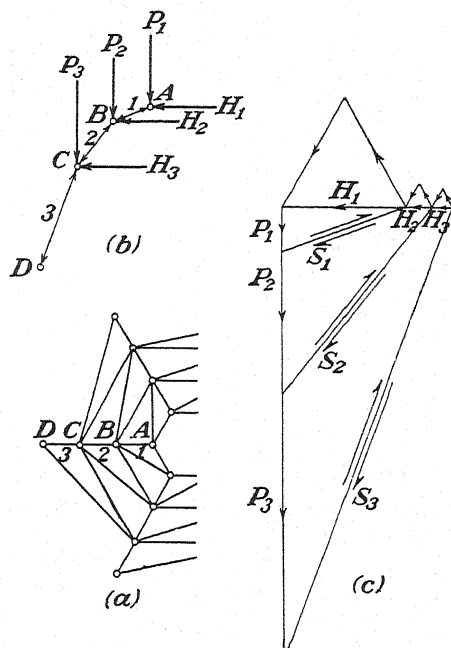
Fig. 268.

By this procedure, we determine the axial forces S_1, S_2, and S_3 in the bars of the rib as well as the resultants H_1, H_2, and H_3 of the two equal horizontal ring-bar forces at each joint. This done, we find the axial forces in the ring bars themselves simply by resolution of H_1, H_2, and H_3 into components parallel to the corresponding bars as indicated by the equilateral triangles in Fig. 268c. Since the conditions along each meridian are identical, the diagram of forces in Fig. 268c constitutes a complete analysis of the truss.

Frequently, the analysis of a complex space truss can be simplified by reducing it to the analysis of several plane trusses. Consider, for example, the space truss shown in Fig. 269a. This complex system is obtained by removing from an otherwise rigid parallelepiped $AA'BB'EE'FF'$ the

bar EF' and introducing instead the extra bar g in the system of supports. In the analysis of this system under the action of a horizontal load P at D, we begin at the joint F, where, by inspection, we see that $S_1 = 0$. Then, proceeding to the joint F' and projecting all forces onto an axis coinciding with FF', we conclude that $S_2 = 0$. We may now consider the joint D, where we find that S_3 is the only unknown force which lies out of the plane $ABFE$. Hence, by projecting all forces at D onto an axis normal to this plane, we find $S_3 = -P$. Now, knowing the action of the bar 3 on the joint D' and projecting all forces at D' onto an axis coinciding with DD', we find $S_4 = +P \sec \alpha$. Continuing in this way and considering the equilibrium of the joints B and B' in succession, we find $S_5 = -P$ and $S_6 = P \sec \beta$. In this way we find the forces in all web members of the top panel.
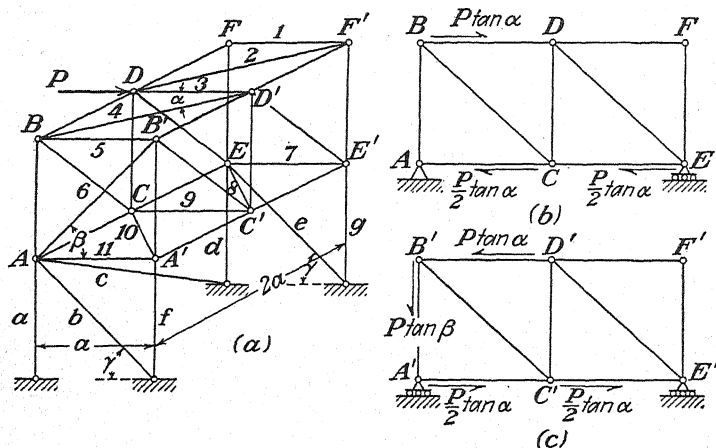
FIG. 269.

To find the axial forces in the web members of the bottom panel, we must first find the force in the bar e of the system of supports. This we accomplish by considering the entire parallelepiped as a free body and equating to zero the algebraic sum of moments of all forces acting on it with respect to an axis coinciding with AB. This gives

$$S_e \cos \gamma \cdot 2a + Pa = 0,$$

from which $S_e = -(P/2) \sec \gamma$. Then starting at E' and considering, in succession, the joints E', E, C', C, and A' of the bottom panel, we find $S_7 = 0$, $S_8 = +(P/2) \sec \alpha$, $S_9 = -P/2$, $S_{10} = +(P/2) \sec \alpha$, and $S_{11} = -P/2$. Finally, replacing the web members of the top and bottom panels by the reactions that we have just found them to exert on the joints of the two side panels, we obtain for further analysis the two plane trusses loaded as shown in Fig. 269b and Fig. 269c. The analysis of these plane systems will be a straightforward procedure and need not be

discussed here. Although we have chosen in the example a very simple case of external loading consisting of a single force P, it should be understood that the same general procedure can be used in case of a more elaborate system of loads.

In general, the resolution of a space truss into several statically determinate plane trusses represents a very practicable method of analysis. As another example, let us consider the complex system loaded as shown in Fig. 270a. This truss satisfies the condition $m = 3j$ and, as can easily be demonstrated by the zero-load test, is rigid and statically determinate. Hence we conclude that under the given loading there is
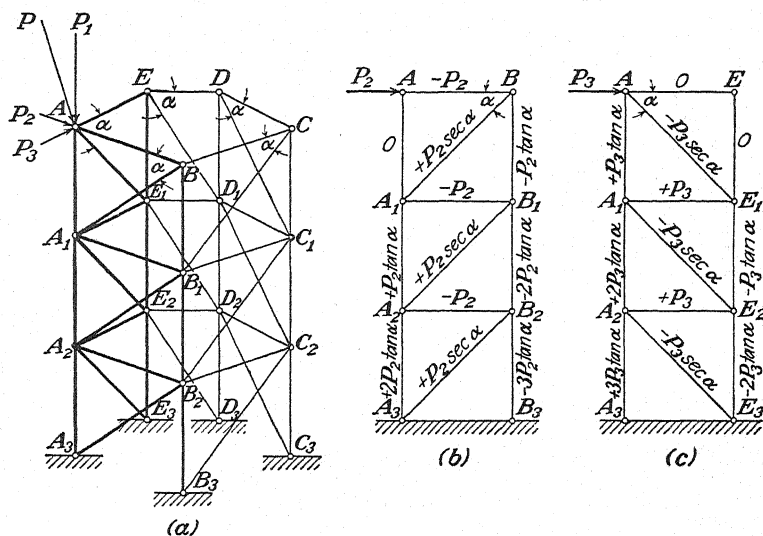
FIG. 270.

one and only one set of values for the axial forces which can satisfy the conditions of equilibrium of the joints and that any procedure by which we can obtain such axial forces will be a legitimate one. We begin by resolving the applied load at A into three components that coincide, respectively, with the lines AA_3, AB, and AE as shown. Then, making a separate analysis of the system for each of these components and superimposing the results, we shall obtain the desired axial forces induced by the given load P.

First, we consider only the component P_1, which coincides with AA_3, and conclude that, under such load, all bars except AA_1, A_1A_2, and A_2A_3 are inactive and that these three bars each carry a compressive force numerically equal to P_1. This done, we consider next the component P_2 which coincides with AB. Again, for this loading it can be seen that only those bars comprising the panel ABA_3B_3 will be active, and our problem

reduces to the analysis of a plane truss loaded as shown in Fig. 270b. We make this analysis and record the results as shown. In the same way, we conclude that, under the action of the force P_3 alone, only the bars of the panel AEA_3E_3 will be active, and we again have a simple problem of analysis of a plane truss as shown in Fig. 270c. Now to obtain the axial force in any bar under the original loading (Fig. 270a) we simply add algebraically the results already obtained. Thus, for example, in the bar AA_1 we have a force $S = -P_1 + P_3 \tan \alpha$; in the bar A_1A_2, we have $S = -P_1 + P_2 \tan \alpha + 2P_3 \tan \alpha$; etc. If there are applied loads at the other joints, they can be handled in the same way.

The method of resolution of a space truss into several plane trusses can be used to advantage in the analysis of the complex system shown in plan and elevation in Fig. 271. This structure is seen to satisfy the condition $m = 3j$; but, as a preliminary to its analysis under load, we must first rule out the possibility of a critical form. Using for this purpose the zero-load test, we begin by isolating the triangle ABG as shown in Fig. 271c. Since all bars that join this triangle at G lie in one plane that intersects the plane of the triangle itself in a horizontal line $A'B'$ through G, it follows that any action exerted on the triangle by such bars must lie along this line of intersection of the two planes. In the same way, all bars that join the triangle at A lie in one plane that intersects the plane of the triangle along AA'; hence the resultant of any action of these bars on the triangle at A must lie along AA'. Likewise, any action on the triangle at B must lie along BB'. Now since three coplanar forces can be in equilibrium only if they are concurrent and since the lines AB, AA', and BB' do not intersect in one point, we conclude that no such forces can exist at A, B, and G. This leaves the statically determinate triangle free from external forces, and hence no internal forces different from zero can exist in the three bars AB, AG, and BG. What is true for the triangle ABG holds for the other triangles like it, and we conclude accordingly that, under zero load, no axial forces different from zero can exist in the system. Thus the system does not have a critical form and will be rigid and statically determinate under any system of applied loads.

FIG. 271.

Now let us consider an analysis of the system under the action of a vertical load P applied at A as shown in Fig. 272. As in the preceding example, we first resolve this force into three components, P_1 coinciding with AA', P_2 coinciding with AB, and P_3 coinciding with AF. Then, making a separate analysis of the system for each of these components and superimposing the results, we shall obtain the required axial forces induced by the given load P.

We begin with the component P_1 acting along AA' as shown in Fig. 273. Since this force does act along AA', our previous reasoning regarding such triangles as ABG (see Fig. 271c) is still valid and we con-
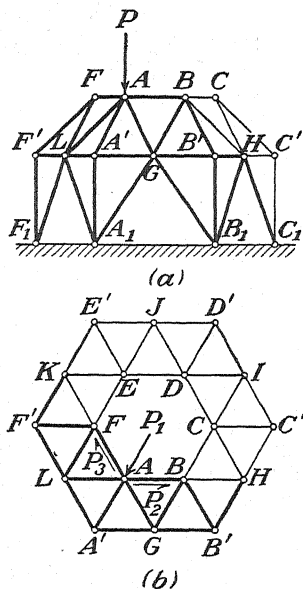
FIG. 272.
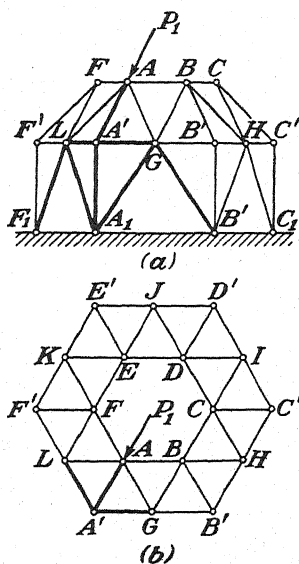
FIG. 273.

clude accordingly that the load P_1 is carried entirely by the bar AA'. Thus, owing to P_1, only the bars shown by heavy lines in Fig. 273 are active, and the axial forces in such bars can be found without difficulty by the method of joints.

Now considering only the component P_2, which, acts along AB (Fig. 274) and proceeding as for the case of zero load, we again conclude that all bars except those shown by heavy lines are inactive. Then, to proceed further, we isolate the triangle ABG again as shown in Fig. 274c and consider its conditions of equilibrium. In this case, we conclude that the resultant of P_2 and the reaction R_a acting along AA' must pass through the point B' where the known lines of action of R_b and R_g intersect. Thus the polygon of forces in Fig. 274d determines the reactions

R_a, R_b, and R_g, and a complete analysis of the triangle ABG can now be made without difficulty by the method of joints. Furthermore, since the adjacent triangles AFL and BCH are inactive, we conclude that the reactions R_a and R_b represent, respectively, the axial forces in AA' and BB'. Knowing these forces and applying the method of joints first to the hinges A' and B' and then to the hinges G, L, and H, we find the forces in the remaining active bars as indicated by heavy lines in Fig. 274. An analysis of the system under the action of the component P_3 that acts along AF can be made in the same manner. Then, adding algebraically the axial forces in any bar due to each of the three components P_1, P_2, and P_3, we shall obtain the required axial forces due to the given
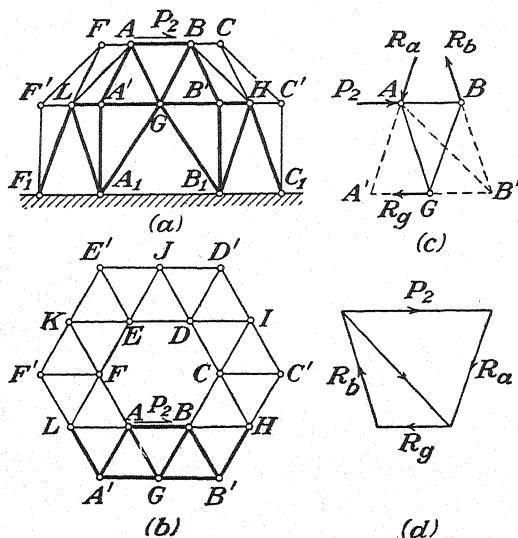
FIG. 274.

load P. If there are loads at the other joints of the structure, the same general procedure may be used.

As a last example, let us consider the complex space truss loaded as shown in Fig. 275. This system, as we have already seen in Art. 34, is rigid and statically determinate, and we may proceed directly with its analysis. As a first step in this direction, we consider the conditions of equilibrium of such joints as B, C, D, and E, at each of which there is no external load and only four bars. Since the two bars that support the ring $ABCDE$ at B, for example, define a plane that intersects the plane of the ring itself in a horizontal line as shown, it follows that the resultant of the reactions exerted at B by the supporting bars must lie along this line. Thus, projecting all forces at B onto a horizontal axis normal to this line, we conclude that $S_1 = -S_2$. Similar arguments can be made with respect to the joints C, D, and E, and we conclude accordingly that

$S_1 = -S_2 = S_3 = -S_4 = S_5$. Now, knowing that $S_1 = S_5$ and projecting all forces at A onto an axis that is normal to the plane $A'AE'$, we may determine S_1 and S_5 without difficulty, after which the remainder of the system can easily be analyzed by the method of joints. If there are external loads at the other joints, we make a separate analysis for each load, as above, and then superimpose the results.

It will be noted that, in each of the last two examples, we have managed the analysis by taking advantage of the fact that whenever a system of concurrent forces in space is such that the forces all lie in two intersecting planes, the resultant of those forces in either plane must lie along the line of intersection of the two planes. This, of course, follows from the fact that, for equilibrium, the resultant of the forces in one plane must be equal, opposite, and collinear with the resultant of the forces in the other plane. In general, this conclusion is very helpful in the analysis of complex space trusses.
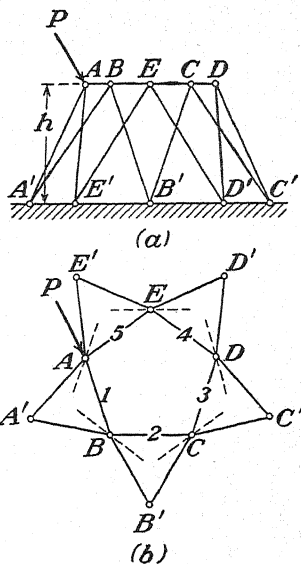
Fig. 275.

PROBLEMS

171. Make a complete analysis of the structure in Fig. 267b under the action of a single vertical load P applied to one joint of the top ring. For simplification, assume that the stories are of equal height, the ribs being straight and inclined by 60 deg. with the horizontal.

172. Make a complete analysis of the system in Fig. 269 under the action of a horizontal force P at each of the joints B, D, and F, instead of only at D as shown. For simplification, assume $\alpha = \beta = \gamma = 45$ deg., *i.e.*, that all panels are subdivided into squares.
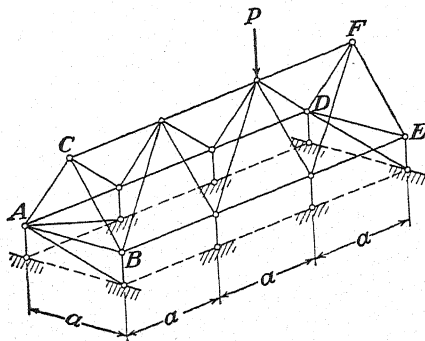
Fig. 276.

173. Make a complete analysis of the structure in Fig. 272 under the action of a single vertical load P at A as shown. Using the results of this analysis, compute the axial force in each bar of the system when there is a vertical load P at each joint of the top ring.

174. Make a complete analysis of the complex system in Fig. 275 if the load P at A is vertical. Assume the following numerical data: $AB = BC = \ldots = 10$ ft. $A'B' = B'C' = \ldots = 15$ ft., and $h = 12.5$ ft. Using the results of this analysis, compute the axial force in each bar of the system when there is a vertical load P at each joint of the ring $ABCDE$.

175. Using the zero-load test, prove that the complex space truss shown in Fig. 276 is rigid and statically determinate. Make a complete analysis of this sytem under the action of a vertical load P applied as shown. Assume that the triangles ABC and DEF are equilateral.

36. Henneberg's Method.—Not infrequently, Henneberg's method of analysis can be used to advantage in working with complex space trusses. This method has already been discussed in Art. 18 for the case
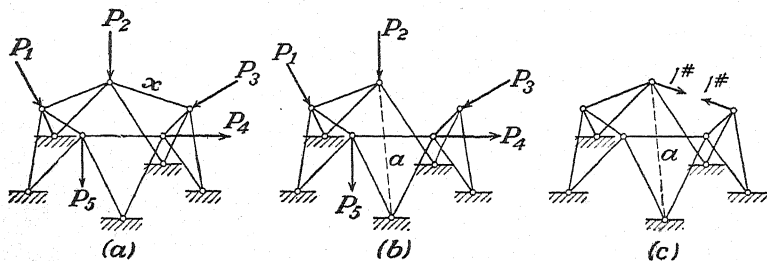
Fig. 277.

of plane trusses, but here we shall review briefly a general outline of the procedure. Suppose, for example, that Fig. 277a represents a complex space truss to which none of the methods of analysis discussed in the preceding article seems to apply but that, by removing the bar x and substituting a bar a as shown in Fig. 277b, we obtain a truss which can be analyzed by elementary methods. This may mean, for example, that the substitution of the bar a for the bar x reduces the system to a simple space truss or to another complex truss which can be more readily analyzed. This fictitious truss we now analyze under each of two separate conditions of loading, (1) the given system of loads $P_1, P_2, \ldots$ as shown in Fig. 277b and (2) two equal and opposite unit forces acting along the axis of the removed bar x as shown in Fig. 277c. Let S_i' be the axial force in any bar due to the P-loading (Fig. 277b) and s_i' the axial force in any bar due to the unit-force loading (Fig. 277c). Now it is obvious that, if we have forces of magnitude X instead of unit forces in Fig. 277c, the axial force in any bar will be simply $s_i'X$ instead of s_i'. Next we superimpose this latter condition of loading on that in Fig. 277b

and conclude that the corresponding axial force in any bar of the fictitious truss under the combined X- and P-loading will be

$$S_i = S_i' + s_i'X. \tag{a}$$

In the particular case of the added bar a, then, we have

$$S_a = S_a' + s_a'X. \tag{b}$$

Now, if we choose X of such magnitude as to make $S_a = 0$, the bar a becomes inactive and can be removed, leaving the fictitious truss identical with the given truss except that the bar x is replaced by forces X. Hence we conclude that the value of X which makes S_a in Eq. (b) equal to zero represents the true axial force in the bar x of the given truss (Fig. 277a). Proceeding in this manner, we write

$$S_a' + s_a'X = 0,$$

from which

$$X = -\frac{S_a'}{s_a'}. \tag{c}$$

Using this value of X in Eq. (a) we may now calculate the axial force S_i in any other bar of the given truss without further difficulty.
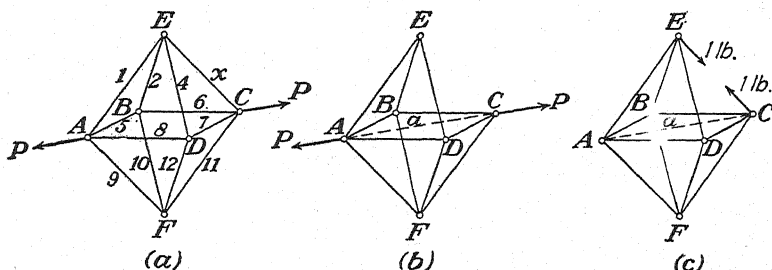
Fig. 278.

If in the procedure above we should find $s_a' = 0$, the value of X defined by Eq. (c) becomes indeterminate or infinite depending on whether S_a' is zero or different from zero and the truss is statically indeterminate. This idea can sometimes be used to advantage in testing a complex truss for critical form.

Let us now consider the application of Henneberg's method to several particular cases. As a first example, we take the octahedron loaded as shown in Fig. 278a. To define the configuration of this system, we assume that $ABCD$ is a square with edges of length 8 ft., while each of the other eight bars has a length of 9 ft. This makes the diagonals of the square $AC = BD = 8\sqrt{2}$ ft. and the vertical diagonal $EF = 14$ ft. The equal and opposite loads P are assumed to act along the diagonal AC of the square so that the system as a whole is in equilibrium.

If we remove the bar EC (marked x) and substitute a bar AC (marked a), we obtain a simple space truss as shown in Fig. 278b. Without difficulty, we can now make a complete analysis of this fictitious truss under the action of the applied loads P (Fig. 278b) and again under the action of two equal and opposite unit forces acting along the axis EC of the removed bar x (Fig. 278c). The results of such analyses are shown in the second and third columns of Table II. Using the values of S_a' and

TABLE II

(1)	(2)	(3)	(4)	(5)
Bar	S_i'	s_i'	$s_i'X$	S_i
1	0	+1.000	+0.397P	+0.397P
2	0	−1.000	−0.397P	−0.397P
x	. .	+1.000	+0.397P	+0.397P
4	0	−1.000	−0.397P	−0.397P
5	0	+0.889	+0.353P	+0.353P
6	0	+0.889	+0.353P	+0.353P
7	0	+0.889	+0.353P	+0.353P
8	0	+0.889	+0.353P	+0.353P
9	0	+1.000	+0.397P	+0.397P
10	0	−1.000	−0.397P	−0.397P
11	0	+1.000	+0.397P	+0.397P
12	0	−1.000	−0.397P	−0.397P
a	+P	−2.515	−1.000P	0

s_a' from this table in Eq. (c) above, we obtain

$$X = -\frac{+P}{-2.515} = +0.397P.$$

Having this value of X, we may now fill in column (4) of the table, and then the values of S_i in column (5) are obtained from Eq. (a).

In using Henneberg's method, the question naturally arises as to which bar of the system to remove and where to place the added bar a. In general, any bar can be taken as x, but the added bar a must then be so placed as to restore the rigidity of the frame, since otherwise the fictitious truss would be statically indeterminate. There is usually more than one possibility for the added bar a, and we try to make a choice that will render the fictitious truss as easy to analyze as possible. For example, by placing the bar a between the joints A and C in the example above, we obtained a very simple case where all bars except a were inactive under the P-loading. A bar a between the joints B and D would have served our general purpose just as well, but then the analysis of the system under the P-loading would have been a little more complicated.

As a second example, let us consider the rectangular parallelepiped supported and loaded as shown in Fig. 279. We have already seen in Fig. 269 (see page 198) that, if the bar EF' of this truss is removed and a bar g introduced between the points E' and H', we obtain a system which can be readily analyzed by resolution into plane trusses. Hence, if we take the truss in Fig. 269 as the fictitious truss, we already have the results of the analysis under the P-loading and can at once fill in column (2) of Table III. This done, we next consider the analysis of the fictitious truss (Fig. 269) under the action of two equal and opposite unit forces applied at E and F' and acting along the line joining these two points. This analysis can be carried out in about the same manner as that already discussed in connection with Fig. 269, and we give simply the final results
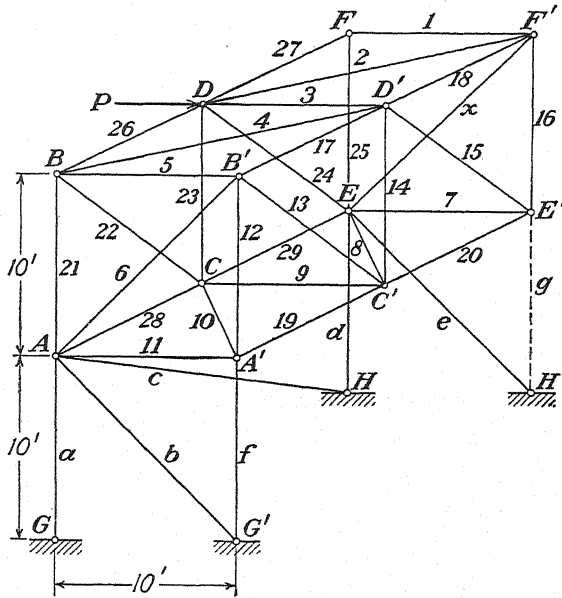
Fig. 279

in column (3) of the table. Using now the values of S_g' and s_g' from the last line of this table in Eq. (c), we find

$$X = +\frac{P}{2\sqrt{2}} = +0.354P.$$

With X, the values of S_i as given in column (5) of the table can now be computed from Eq. (a), and the analysis is completed.

Sometimes, in order to reduce a given complex space truss to a form that can be readily analyzed by elementary methods, it may be necessary to remove several bars $x_1, x_2, \ldots$ and substitute as many others $a_1, a_2, \ldots$. Then, in application of

TABLE III

(1) Bar	(2) S_i'	(3) s_i'	(4) $s_i'X$	(5) S_i
1	0	0	0	0
2	0	-1	$-0.354P$	$-0.354P$
3	$-P$	$+1/\sqrt{2}$	$+0.250P$	$-0.750P$
4	$+\sqrt{2}P$	-1	$-0.354P$	$+1.06P$
5	$-P$	$+1/\sqrt{2}$	$+0.250P$	$-0.750P$
6	$+\sqrt{2}P$	-1	$-0.354P$	$+1.06P$
7	0	0	0	0
8	$+P/\sqrt{2}$	-1	$-0.354P$	$+0.353P$
9	$-P/2$	$+1\sqrt{2}$	$+0.250P$	$-0.250P$
10	$+P/\sqrt{2}$	-1	$-0.354P$	$+0.353P$
11	$-P/2$	$+1/\sqrt{2}$	$+0.250P$	$-0.250P$
12	$-3P/2$	$+\sqrt{2}$	$+0.500P$	$-1.00P$
13	$+P/\sqrt{2}$	-1	$-0.354P$	$+0.353P$
14	$-P/2$	$+1/\sqrt{2}$	$+0.250P$	$-0.250P$
15	$+P/\sqrt{2}$	-1	$-0.354P$	$+0.353P$
16	0	$-1/\sqrt{2}$	$-0.250P$	$-0.250P$
17	$-P/2$	$+1/\sqrt{2}$	$+0.250P$	$-0.250P$
18	0	$+1/\sqrt{2}$	$+0.250P$	$+0.250P$
19	$-P/2$	$+1/\sqrt{2}$	$+0.250P$	$-0.250P$
20	$-P/2$	$+1/\sqrt{2}$	$+0.250P$	$-0.250P$
21	$+P/2$	$-1/\sqrt{2}$	$-0.250P$	$+0.250P$
22	$-P/\sqrt{2}$	$+1$	$+0.354P$	$-0.353P$
23	$+P/2$	$-1/\sqrt{2}$	$-0.250P$	$+0.250P$
24	$-P/\sqrt{2}$	$+1$	$+0.354P$	$-0.353P$
25	0	0	0	0
26	$-P/2$	0	0	$-0.500P$
27	0	0	0	0
28	0	0	0	0
29	0	0	0	0
x	—	$+1$	$+0.354P$	$+0.354P$
g	$+P/2$	$-\sqrt{2}$	$-0.500P$	0

Henneberg's method, we proceed as before and make a complete analysis of the fictitious truss under each of the following conditions of loading: (1) the given P-loading; (2) a pair of unit forces replacing the bar x_1; (3) a pair of unit forces replacing the bar x_2; etc. Then, denoting by S_i' the axial force in any bar due to the P-loading and by s_i', s_i'', . . . the axial forces due to each pair of unit loads, we find by superposition that

$$S_i = S_i' + s_i'X_1 + s_i''X_2 + \cdots , \tag{d}$$

where $X_1, X_2, \ldots$ are so chosen as to satisfy the equations

$$\left. \begin{aligned} S_{a_1} &= S_{a_1}' + s_{a_1}'X_1 + s_{a_1}''X_2 + \cdots = 0, \\ S_{a_2} &= S_{a_2}' + s_{a_2}'X_1 + s_{a_2}''X_2 + \cdots = 0, \\ &\cdots\cdots\cdots\cdots\cdots\cdots\cdots\cdots\cdots\cdots , \\ &\cdots\cdots\cdots\cdots\cdots\cdots\cdots\cdots\cdots\cdots \end{aligned} \right\} \tag{e}$$
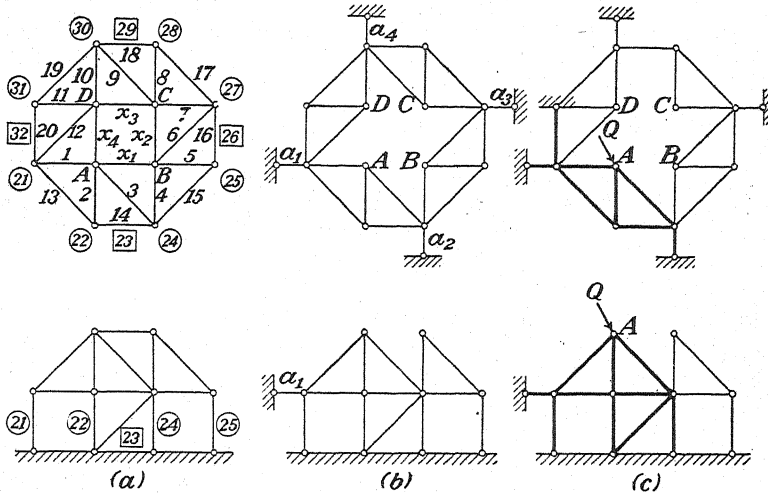
Fig. 280.

As a specific example, let us consider the complex space truss consisting of 12 joints and 36 bars arranged as shown in Fig. 280a. This is a rigid and statically determinate system, but one that does not lend itself to ready analysis by elementary methods. However, if we remove the four bars x_1, x_2, x_3, and x_4 that form the top ring and introduce instead the horizontal constraints a_1, a_2, a_3, and a_4, as shown in Fig. 280b, we obtain a simple space truss that can readily be analyzed by the method of joints. We begin with the observation that, under the action of any applied load Q at the joint A, only the bars indicated in Fig. 280c by heavy lines will be active. Furthermore, owing to the symmetry of the system, we conclude that if we analyze this heavy-line portion under the action of each of three unit-force components as shown in Figs. 281a, b, c, respectively, we can easily obtain from this the axial force in any bar of the system due to any combination of loads applied to the joints A, B, C, D of the top ring. For example, let us assume that the actual loading on the given truss is limited to a single vertical load P at A. Then, by using the results from Fig. 281a, the value of S_i' for each bar of the system will be as shown in column (2) of Table IV. Likewise, if we want the values of s_i' due to two equal and opposite unit forces replacing the bar x_1, we use the results from Figs. 281b and c and obtain the values shown in column (3) of this table. In the same way, the values for s_i'', s_i''', and s_i'''', as shown in columns (4), (5), and (6), are obtained. Now, using the values from the table for the fictitious bars a_1, a_2, a_3, and a_4, in Eqs. (e) above, we may write

$$\left. \begin{aligned} S_{a_1} &= -P - 4X_1 - X_2 - X_4 &= 0, \\ S_{a_2} &= 0 - X_1 - 4X_2 - X_3 &= 0, \\ S_{a_3} &= 0 - X_2 - 4X_3 - X_4 &= 0, \\ S_{a_4} &= -2P - X_1 - X_3 - 4X_4 &= 0, \end{aligned} \right\} \tag{e'}$$

TABLE IV

(1) Bar	(2) S_i'	(3) s_i'	(4) s_i''	(5) s_i'''	(6) s_i''''	(7) $s_i'X_1$	(8) $s_i''X_2$	(9) $s_i'''X_3$	(10) $s_i''''X_4$	(11) S_i
1	−1.414P	0	....	....	....	0	....	....	+0.707P	−0.707P
2	+1.414P	+1.414	....	....	....	−0.177P	....	....	−1.414P	−0.177P
3	−1.732P	+1.732	....	....	....	−0.217P	....	....	−0.866P	−0.650P
4	....	−1.414	....	....	....	+0.177P	....	....	....	+0.177P
5	....	+2.828	....	....	−1.414	−0.354P	....	....	....	−0.354P
6	....	−1.732	0	....	....	+0.217P	....	....	....	+0.217P
7	....	....	+1.414	0	....	....	....	+0.177P	....	0
8	....	....	+1.732	+1.414	....	....	....	+0.177P	....	+0.177P
9	....	....	−1.414	+1.732	....	....	....	−0.217P	....	+0.217P
10	....	....	+2.828	−1.414	0	....	....	−0.177P	0	−0.177P
11	−1.414P	−1.414	....	+2.828	+1.414	....	....	+0.354P	−0.707P	−0.354P
12	−1.000P	−1.000	....	−1.732	+1.732	....	....	−0.217P	+0.866P	+0.650P
13	....	....	−1.414	....	....	....	....	−0.354P	+1.414P	+0.177P
14	....	....	+1.000	....	....	....	....	....	+1.000P	+0.125P
15	....	....	+1.000	....	....	....	....	....	....	+0.354P
16	....	....	....	−1.414	....	+0.250P	....	−0.500P	....	+0.250P
17	....	....	....	+1.000	....	....	....	....	....	−0.177P
18	....	....	−1.000	....	....	....	....	....	....	−0.125P
19	....	....	....	....	−1.414	....	....	−0.354P	−0.707P	−0.354P
20	....	−2.000	....	−1.000	−1.000	−0.250P	....	−0.250P	+0.500P	+0.250P
21	0	+1.000	−1.414	....	−3.000	−0.125P	....	−0.500P	+1.000P	+0.375P
22	+2.828P	+1.000	+1.000	....	....	−0.125P	....	−0.125P	−1.000P	+0.125P
23	−3.000P	+2.828	+1.000	−1.414	....	0	....	−0.354P	−2.121P	+0.707P
24	....	+3.000	....	+1.000	+4.243	+0.250P	....	−0.250P	+2.000P	+0.750P
25	....	....	....	−1.000	−4.000	−0.250P	....	....	....	−0.250P
26	−1.414P	+4.243	+2.828	−1.414	....	−0.530P	....	−0.177P	....	+0.707P
27	....	−4.000	+1.000	+1.000	....	+0.500P	....	+0.125P	....	+0.625P
28	....	....	+2.000	+2.828	....	....	....	+0.125P	+0.707P	+0.125P
29	....	....	....	+3.000	+1.414	....	....	−0.250P	−0.500P	+0.707P
30	....	....	....	....	+1.000	....	....	+0.250P	....	+0.750P
31	....	−1.414	....	....	+2.828	+0.177P	....	+0.530P	....	−0.250P
32	....	....	....	....	−2.828	....	....	....	−0.500P	−0.707P
a₁	−1.000P	−1.000	−1.000	−1.000	−1.000	+0.500P	....	−0.125P	+0.500P	0
a₂	....	−3.000	−3.000	−1.000	−1.000	+0.125P	....	−0.500P	....	0
a₃	−2.000P	−1.000	−1.000	−1.000	−3.000	....	....	−0.125P	+0.500P	0
a₄	....	....	....	....	....	+0.125P	....	−0.125P	+2.000P	0
x₁	....	....	....	....	....	+0.500P	....	−0.125P	+0.500P	−0.125P
x₂	....	....	....	....	....	+0.125P	....	−0.500P	+0.500P	0
x₃	....	....	....	....	....	+0.125P	....	−0.125P	+2.000P	+0.125P
x₄	−2.000P	−1.000	....	....	....	....	....	....	....	+0.500P

FIG. 281.

from which we readily find

$$X_1 = -\frac{P}{8}, \qquad X_2 = 0, \qquad X_3 = +\frac{P}{8}, \qquad X_4 = -\frac{P}{2}.$$

Finally, using these values in Eq. (d), we obtain the desired axial forces S_i as recorded in column (11) of the table. This completes the analysis of the given system under the action of a single vertical load P at A.

PROBLEMS

176. Using Henneberg's method, make a complete analysis of the complex space truss loaded as shown in Fig. 282. To obtain a truss easily analyzed by elementary methods, remove the bar EC and substitute a fictitious bar AB'. $ABCD$ is a square, and each inclined bar makes an angle of 45 deg. with the vertical.
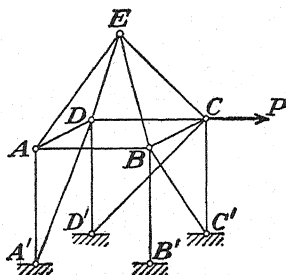
FIG. 282.

177. Repeat the analysis of the system shown in Fig. 282 if there is a vertical load P at E instead of a horizontal load P at C as shown.

178. Using Henneberg's method, make a complete analysis of the complex space truss shown in plan and elevation in Fig. 283, (a) under the action of a single vertical

load P at A as shown; (*b*) under the action of a vertical load P at each of the joints A, B, C, and D.

179. Repeat the analysis of the system in Fig. 283, assuming a horizontal force P applied at E and acting to the right.
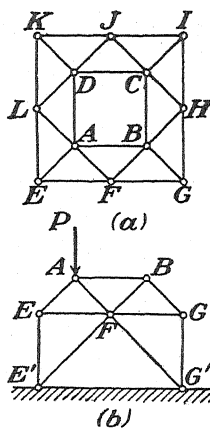
Fig. 283.

180. Make a complete analysis of the complex system shown in Fig. 280*a* if there is a horizontal force P applied at A and acting to the right in the direction coinciding with AB.

CHAPTER V

GENERAL THEOREMS RELATING TO ELASTIC SYSTEMS

37. Strain Energy in Tension, Torsion, and Bending.—It is well known that within certain limits most structural materials can be considered as perfectly elastic. It can be assumed also with good accuracy that they follow Hooke's law. The limiting stress below which these assumptions hold is called the *proportional limit* of the material. Since this stress is usually very small in comparison with the modulus of the material in tension or shear and since the allowable stresses are generally well within the elastic range, the deformations of structures under service conditions will be very small. Thus, in the analysis of statically determinate systems, it is entirely justifiable to use the unloaded configuration of a structure as a basis of calculation of internal forces and completely to ignore the small elastic deformations that take place during loading. In the case of a statically indeterminate system, however, we have seen that such small elastic deformations have a significant effect on the distribution of internal forces and must be taken into account in the analysis of the system. We therefore turn our attention now to various relationships pertaining to the elastic deformations of structures under load.
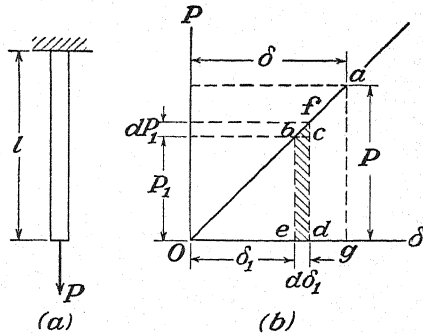
FIG. 284.

When a structure deforms under the action of gradually increasing external forces, these forces produce work that is stored in the elastic structure in the form of *strain energy*. If we neglect any small losses of heat energy due to hysteresis, this strain energy can be recovered during a gradual unloading of the structure. For example, in the case of a prismatic bar submitted to the action of a gradually increasing axial load P. (Fig. 284a), the relation between the load P and the elongation δ that it induces in the bar is represented in Fig. 284b by the straight line Oa. Let us consider the state in which the load has the magnitude P_1 and the elongation the corresponding magnitude δ_1. This state is represented in Fig. 284b by the point b. If at this point an increment dP_1 is added, the elongation of the bar will increase by the amount $d\delta_1$ and

213

the load P_1, which was already attached to the bar, will descend and produce the work $P_1 d\delta_1$. This work is represented in the figure by the area of the shaded rectangle $bcde$.* The total work done by the load during its gradual increase from zero to the final value P is obtained as the sum of all such elemental areas as that shown in Fig. 284b and is equal to the area of the triangle Oag. Thus, denoting by U the strain energy that is stored in the bar during its extension, we have

$$U = \frac{P \cdot \delta}{2}. \qquad (a)$$

Using the known expression

$$\delta = \frac{Pl}{AE} \qquad (b)$$

for the elongation of a prismatic bar of length l, cross-sectional area A, and modulus E, we can represent the strain energy [expression (a)] either

(a)   (b)
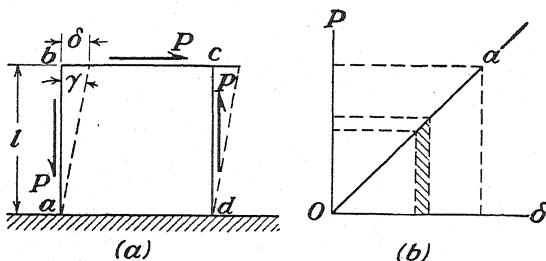
Fig. 285.

as a function of the load P or as a function of the elongation δ. These two forms for the strain energy are

$$U = \frac{P^2 l}{2AE}, \quad (11a) \qquad U = \frac{AE\delta^2}{2l}. \qquad (11b)$$

In practical applications, the strain energy per unit volume is often of importance. Dividing expressions (11) by the volume Al of the bar and denoting strain energy per unit volume by u, we obtain

$$u = \frac{P^2}{2A^2 E} = \frac{\sigma^2}{2E}, \qquad (12a)$$

where $\sigma = P/A$ is the tensile stress in the bar, and

$$u = \frac{E\delta^2}{2l^2} = \frac{E\epsilon^2}{2}, \qquad (12b)$$

where $\epsilon = \delta/l$ is the unit elongation of the bar. Taking, for example, a structural steel with a proportional limit of 30,000 lb. per sq. in. and

---

* The work of the small increment dP_1 of the load on the small displacement $d\delta$, can be neglected as a small quantity of the second order.

with a modulus $E = 30 \cdot 10^6$ lb. per sq. in., we find from Eq. (12a) that the amount of strain energy per cubic inch which can be stored within the elastic range is $u = 15$ lb. per sq. in.

In the case of *pure shear* (Fig. 285a), we have to consider the small sliding displacement δ of the upper cross section bc of the block with respect to the base ad, which is assumed fixed. The relation between P and δ again can be represented by the diagram shown in Fig. 285b; and, by the same reasoning used in the case of axial tension, we conclude that the work done by the force P, equal to the strain energy stored in the material, is

$$U = \frac{P\delta}{2}. \tag{c}$$

Using, for shearing strain γ, the known formula

$$\gamma = \frac{\delta}{l} = \frac{P}{AG}, \tag{d}$$

in which G is the modulus in shear and A is the cross-sectional area, we obtain

$$U = \frac{P^2 l}{2AG} \quad (13a) \qquad \text{or} \qquad U = \frac{AG\delta^2}{2l}. \tag{13b}$$

The corresponding formulas for strain energy per unit volume are

$$u = \frac{P^2}{2A^2 G} = \frac{\tau^2}{2G} \quad (14a) \qquad \text{and} \qquad u = \frac{G\delta^2}{2l^2} = \frac{G\gamma^2}{2}, \tag{14b}$$

where $\tau = P/A$ is the shearing stress.
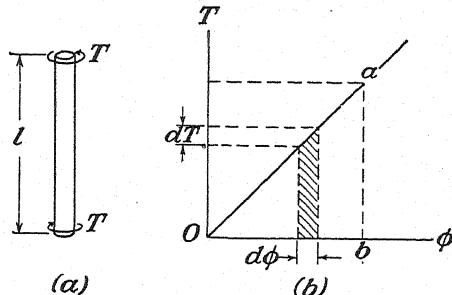
FIG. 286.

The strain energy of torsion of a prismatic shaft (Fig. 286a) can be obtained from the torsion-test diagram shown in Fig. 286b. This diagram shows the relation between the twisting moment, or *torque*, T and the corresponding angle of twist ϕ. We see that, within the elastic range, the angle of twist is proportional to the torque as represented by the straight line Oa. Again, the shaded elemental area in the figure represents the work done by the torque during an infinitesimal increase

$d\phi$ of the angle of twist ϕ and the area of the triangle Oab represents the total work done by the torque as it increases gradually from zero to T. This work is equal to the strain energy stored in the shaft during torsion, and we have

$$U = \frac{T\phi}{2}. \qquad (e)$$

Using, for the angle of twist, the known formula

$$\phi = \frac{Tl}{C}, \qquad (f)$$

in which l is the length of the shaft and C its *torsional rigidity*,[1] we obtain

$$U = \frac{T\phi}{2} = \frac{T^2l}{2C} \quad (15a) \qquad \text{or} \qquad U = \frac{T\phi}{2} = \frac{\phi^2 C}{2l}. \qquad (15b)$$

In the first of these formulas, the strain energy is represented as a function of the torque T and in the second as a function of the angle of twist ϕ.
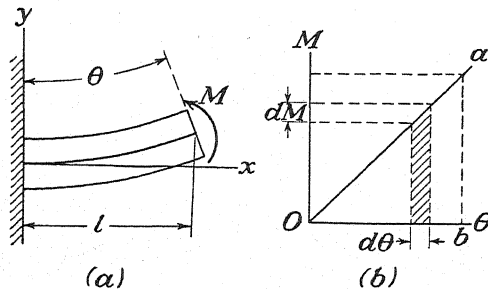
FIG. 287.

In the case of *pure bending* of a prismatic bar in a *principal plane* (Fig. 287a) the angle θ of rotation of one end with respect to the other is proportional to the bending moment M as shown in Fig. 287b. Hence we conclude that the strain energy of bending, equal to the total work produced by the moment M, is

$$U = \frac{M\theta}{2}. \qquad (g)$$

Using for θ the known formula

$$\theta = \frac{Ml}{EI}, \qquad (h)$$

---

[1] In the case of a circular shaft, the torsional rigidity is $C = GJ$, where J denotes the polar moment of inertia of the cross section of the shaft. For further information regarding torsional rigidity, see Timoshenko's "Strength of Materials," 2d ed., vol. II, p. 265, 1941.

in which l is the length of the beam and EI its flexural rigidity, we can represent this strain energy in either of the following two forms:

$$U = \frac{M^2 l}{2EI} \quad (16a) \qquad \text{or} \qquad U = \frac{\theta^2 EI}{2l}. \qquad (16b)$$

Again we see that the strain energy can be represented either as a function of the acting forces, in this case the bending moment M, or as a function of the quantity θ defining the deformation.

In calculating the strain energy for the case of a bar bent by transverse loads (Fig. 288a), we have to consider not only the bending stresses but also the shearing stresses. Those stresses acting on an element cut out of a beam by two adjacent cross sections and by two adjacent planes parallel to the neutral plane are shown in Fig. 288b. Since the distortion produced by the shearing stresses τ does not change the elongation produced by the bending stresses σ_x, the work done by σ_x and the corre-
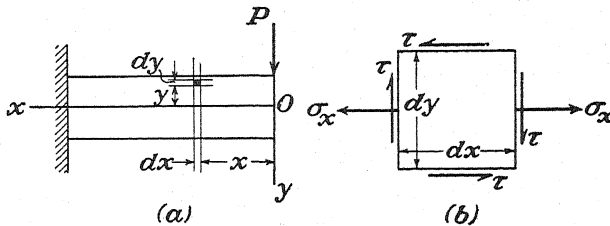
FIG. 288.

sponding strain energy are not affected by a subsequent application of shearing stresses. From this it follows that the total amount of strain energy stored in the element can be obtained by adding to the strain energy produced by σ_x the strain energy produced by the shearing stress τ. Beginning with the bending stresses and considering an element of the beam between two adjacent cross sections, dx apart, we can assume the bending moment constant along the length dx and use the previously derived formulas for pure bending. Substituting dx for l and $d\theta/dx$ for θ/l in formulas (16a) and (16b), respectively, we obtain the following two expressions for the strain energy of bending of one element of the beam:

$$dU = \frac{M^2 dx}{2EI} \quad (i) \qquad \text{or} \qquad dU = \left(\frac{d\theta}{dx}\right)^2 \frac{EI}{2} \, dx. \qquad (j)$$

To obtain the strain energy of bending of the entire beam, we have only to take the sum of expressions (i) and (j) over the length l of the beam. In this way we obtain

$$U = \int_0^l \frac{M^2 dx}{2EI} \quad (17a) \text{ or } U = \int_0^l \frac{EI}{2}\left(\frac{d\theta}{dx}\right)^2 dx \approx \int_0^l \frac{EI}{2}\left(\frac{d^2 y}{dx^2}\right)^2 dx. \quad (17b)$$

Considering, for example, the cantilever beam loaded at the free end (Fig. 288a), we have $M = -Px$. Substituting this in formula (17a), we obtain

$$U = \int_0^l \frac{P^2x^2dx}{2EI} = \frac{P^2l^3}{6EI}. \tag{k}$$

In calculating the strain energy of shear, the distribution of shearing stresses over the cross section of a beam must be considered. In the case of an I-beam, it can be assumed, as an approximation, that the shearing force V is uniformly distributed over the cross-sectional area A_1 of the web. In such a case, the strain energy of shear for an element of the beam cut out by the two adjacent cross sections is obtained from formula (13a) by substituting V, A_1, and dx for P, A, and l, respectively. In this manner we obtain

$$dU = \frac{V^2dx}{2A_1G}. \tag{l}$$
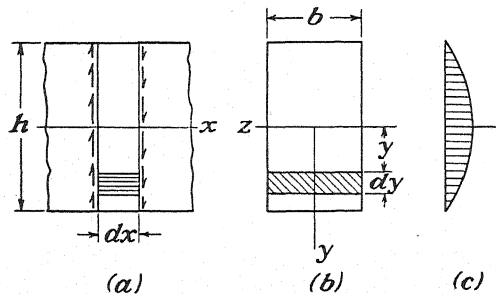
FIG. 289.

The total strain energy of shear is now obtained by summing up the elements (l) along the length of the beam, which gives

$$U = \int_0^l \frac{V^2dx}{2A_1G}. \tag{18}$$

In the case of a beam of rectangular cross section, the shearing stress along the depth of the beam varies according to a parabolic law as shown in Fig. 289c. Thus the shearing stress at a distance y from the neutral axis is

$$\tau = \frac{V}{2I}\left(\frac{h^2}{4} - y^2\right). \tag{m}$$

For the shaded element having the volume $b\,dx\,dy$, the strain energy of shear is obtained by using formula (14a), which gives

$$dU = \frac{V^2}{8GI^2}\left(\frac{h^2}{4} - y^2\right)^2 b\,dx\,dy. \tag{n}$$

The total strain energy of shear for the beam is now obtained by summing up the elements (n) along the depth of the beam, varying y from $-h/2$ to $+h/2$, and then making another summation along the length of the beam by varying x from 0 to l. This gives

$$U = \int_0^l dx \int_{-\frac{h}{2}}^{+\frac{h}{2}} \frac{V^2}{8GI^2}\left(\frac{h^2}{4} - y^2\right)^2 b\,dy = \int_0^l \frac{V^2 h^2}{20GI}\,dx = \int_0^l \frac{6}{10}\frac{V^2 dx}{Gbh}. \quad (19)$$

In the particular case represented in Fig. 288a, the shearing force V is constant along the length of the beam and is numerically equal to the load P. Substituting P for V in Eq. (19) and performing the indicated integration, we obtain

$$U = \frac{lh^2 P^2}{20GI} = \frac{6}{10}\frac{lP^2}{Gbh}. \quad (o)$$

Adding together expressions (k) and (o), we obtain the total strain energy for a cantilever beam having a rectangular cross section and loaded as shown in Fig. 288a. This total strain energy is equal to the work done by the load P during the deflection of the beam. Such work is given by formula (a), provided that δ in that formula denotes the deflection at the end of the cantilever. Thus, for calculating the deflection δ, we obtain the following equation:

$$\frac{P\delta}{2} = \frac{P^2 l^3}{6EI} + \frac{6}{10}\frac{lP^2}{Gbh},$$

from which

$$\delta = \frac{Pl^3}{3EI} + 1.2\frac{lP}{Gbh}. \quad (p)$$

The second term on the right side of this expression represents the effect of shear on the deflection of the cantilever beam.[1]

If, instead of a rectangle, we have any other shape of cross section, it will be necessary only to replace the numerical factor $\frac{6}{10}$ on the right side of Eq. (19) by another numerical value depending on the shape of the cross section. Using the notation $\alpha/2$ for this numerical factor, we obtain, instead of formula (19), the following more general formula for strain energy of shear:

$$U = \int_0^l \frac{\alpha V^2 dx}{2GA}. \quad (20)$$

Correspondingly, the total strain energy for a prismatic beam under transverse loads becomes

$$U = \int_0^l \frac{M^2 dx}{2EI} + \int_0^l \frac{\alpha V^2 dx}{2GA}. \quad (21)$$

[1] For a more complete discussion of this question, see "Theory of Elasticity," p. 95, New York, 1934.

This formula can be used, also, in the case of a beam of variable cross section simply by considering I, A, and α as functions of x.

PROBLEMS

181. Compare the amounts of strain energy in two bars of circular cross section

that are equally loaded as shown in Figs. 290a and b. Assume a uniform distribution of stress over each cross section.
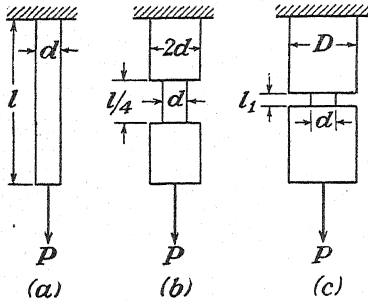
Ans. $U_b : U_a = 7 : 16$.

182. Calculate the amount of strain energy in the grooved bar shown in Fig. 290c if $D = 5d$ and $l_1 = \frac{1}{100}l$.

183. Calculate the amount of strain energy in a vertical steel bar of uniform cross section that is strained by its own weight if the length of the bar is 100 ft., its cross-sectional area 1 sq. in., and the weight of steel 490 lb. per cu. ft. *Ans.* $U = 0.772$ in.-lb.

Fig. 290.

184. Determine the ratio between the elastic limits in tension and shear if the amount of strain energy per cubic inch at the elastic limit is the same in each case.

Ans. $\sigma/\tau = \sqrt{E/G}$.

185. A wooden cantilever beam having a rectangular cross section 8 in. deep and 5 in. wide and a length of 6 ft. carries a uniform load of 200 lb. per ft. Calculate the amount of strain energy in the beam if $E = 1.5 \cdot 10^6$ lb. per sq. in.

Ans. $U = 42$ lb.-in.

186. In what proportion will the amount of strain energy in the beam of the previous problem be diminished if the depth of the cross section is increased from 8 to 10 in.?

187. Two identical beams, one simply supported, the other with built-in ends, are bent by equal concentrated loads applied at the middle. In what ratio are the amounts of strain energy stored? *Ans.* $4 : 1$.

188. Determine from strain-energy considerations the effect of shear on the deflection at the middle of a simply supported beam of rectangular cross section and carrying a concentrated load P at the middle.

189. Solve the previous problem for the case of a uniformly distributed load over the full length of the beam.

190. Compare the strain energy of torsion of a prismatic bar of circular cross section with that of pure bending of the same bar if the applied moments are equal in the two cases, *i.e.*, if $T = M$.

38. Principle of Superposition.

—In the previous article, we considered only the simplest cases of loading in which only one force or one couple was acting. Let us consider now the more general case where there are several forces acting on a structure. Taking, for example, the axial extension of a prismatic bar under the action of several forces P_1, P_2, and P_3 applied as shown in Fig. 291 and using Hooke's law, we find that the total extension of the bar is

$$\delta = \frac{(P_1 + P_2 + P_3)l_1}{AE} + \frac{(P_2 + P_3)(l_2 - l_1)}{AE} + \frac{P_3(l_3 - l_2)}{AE} =$$
$$\frac{P_1 l_1}{AE} + \frac{P_2 l_2}{AE} + \frac{P_3 l_3}{AE}, \quad (a)$$

which is seen to be a linear function of the external forces. The first term on the right side of Eq. (a), for example, is the elongation $P_1 l_1 / AE$ produced by the force P_1 acting alone. The second and third terms, likewise, are the elongations of the bar produced by the forces P_2 and P_3, respectively. Thus, we see that the total elongation is obtained simply by summing up the elongations produced by the individual forces.

As a second example, let us consider bending of a simply supported beam AB under the action of transverse loads P_1, P_2, P_3, as shown in Fig. 292a. In calculating deflections of the beam, we consider in Fig. 292b the *conjugate beam ab* loaded by the bending moment area *acdeb*.
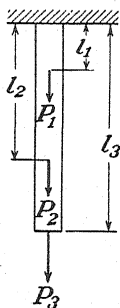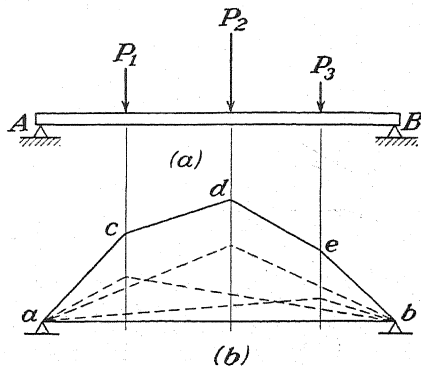
Fig. 291.   Fig. 292.

It is known[1] that the bending moments of this conjugate beam give, to a certain scale, the deflections of the actual beam. Now, from simple statical considerations, it follows that the total moment area *acdeb* can be obtained by summing up the triangular areas indicated in the figure by dotted lines and representing, respectively, the moment areas for the individual loads. Thus the total fictitious load *acdeb* on the conjugate beam is the sum of the fictitious triangular loads corresponding to the individual forces P_1, P_2, and P_3 acting on the beam AB. Repeating the same reasoning in calculating the bending moment at any cross section of the conjugate beam, we conclude that the bending moment produced by the total load *acdeb* is equal to the sum of the bending moments produced by the component triangular loads. Hence the deflection at any cross section of the actual beam AB is equal to the sum of the deflections produced at the same cross section by the individual loads P_1, P_2, and P_3.

[1] See "Strength of Materials," vol. I, p. 153.

Further, since these latter deflections are proportional to the corresponding forces, it can be concluded that the total deflection of any cross section of the beam AB will be a linear function of the forces P_1, P_2, and P_3 and is obtained by summing up the corresponding deflections produced by the individual loads.

In all cases of composite loading where deflections are linear functions of the applied forces, the above conclusion holds, and we obtain the total deflection of any point simply as the sum of the deflections produced by the individual forces. This statement is called the *principle of superposition*.

Under ordinary circumstances, a linear relationship between deflections and applied forces rests solely on the assumption that the material of a structure follows Hooke's law. However, there are certain cases in which this assumption alone will not be sufficient and the deflections will not be linear functions of the applied forces even though the material does follow Hooke's law. One such example we have in the
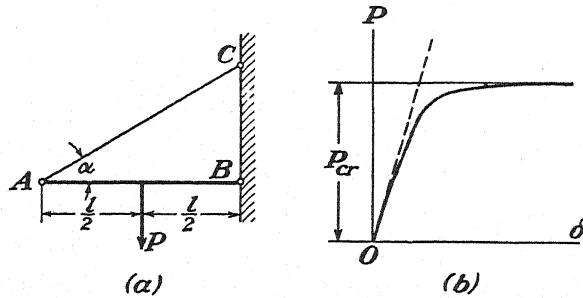
FIG. 293.

case of a bar submitted to the simultaneous action of axial and lateral forces. Considering, for example, the bending of the beam AB loaded as shown in Fig. 293a, we conclude that the deflection under the load P is no longer proportional to the load. Specifically, it can be represented by the formula[1]

$$\delta \approx \frac{Pl^3}{48EI} \cdot \frac{1}{1 - S/S_{cr}},\qquad (b)$$

in which the first factor represents the deflection produced by the lateral load if acting alone and the second factor represents the effect on this deflection of the axial compressive force S. The magnitude of this effect depends on the magnitude of the ratio S/S_{cr} in which $S_{cr} = \pi^2 EI/l^2$ is the critical load for buckling of the beam in the plane of the figure. Since S is proportional to P, expression (b) is no longer a linear function of the load and the relation between δ and P is no longer linear. Representing this relation graphically, we obtain the curve shown in Fig. 293b. It is seen that the deflection is no longer proportional to the load and that it begins to increase very rapidly as the compressive force in the beam approaches the critical value. Thus, if we double the load P, the deflection will always be more than doubled and the principle of superposition does not hold.

[1] See "Strength of Materials," vol. II, p. 49. The elongation of the bar AC is neglected in using this formula.

As another example of a system for which the principle of superposition does not hold, let us consider the system of two identical horizontal bars hinged together, as shown in Fig. 294a.   Under the action of a vertical load P, the bars will undergo some extension and the hinge C will move down by an amount $\overline{CC_1} = \delta$.   Assuming that
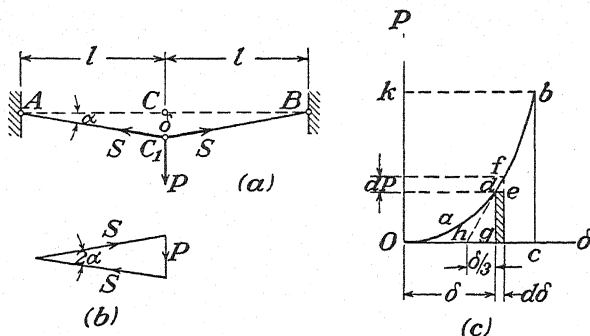
Fig. 294.

this deflection is small, we find for the correspondingly small angle α and for the tensile force S in each bar the following values:

$$\alpha \approx \frac{\delta}{l}, \quad (c) \qquad S \approx \frac{P}{2\alpha}. \tag{d}$$

Considering, now, the unit elongation of each bar, we find

$$\epsilon = \frac{\sqrt{l^2 + \delta^2} - l}{l} \approx \frac{1}{2}\frac{\delta^2}{l^2}.$$

The same elongation, by using Hooke's law, is

$$\epsilon = \frac{S}{AE},$$

and we obtain

$$\frac{1}{2}\frac{\delta^2}{l^2} = \frac{S}{AE} = \frac{P}{2\alpha AE} = \frac{Pl}{2\delta AE}, \tag{e}$$

from which

$$\delta = l\sqrt[3]{\frac{P}{AE}} \quad (f) \qquad \text{and} \qquad P = \frac{\delta^3 AE}{l^3}. \tag{g}$$

Again we see that the deflection δ is not proportional to the load although the material follows Hooke's law.   This case differs from the preceding one in that with increasing deflection the system becomes stiffer and the relation between δ and P is represented by the curve shown in Fig. 294c.   It is typical of the behavior of a system of *critical form* as discussed in Art. 17 (page 80).

Following the same reasoning as for the case of simple tension, it can be shown that the area $OabcO$ in Fig. 294c represents the work done by the load P during the deflection δ and that it is equal to the strain energy stored in the bars AC and CB.   The expression for this energy is obtained by summing up all such elemental areas as the shaded strip shown in the figure.   This gives

$$U = \int_0^\delta P\,d\delta = \frac{AE}{l^3}\int_0^\delta \delta^3\,d\delta = \frac{AE\delta^4}{4l^3} \quad (22a) \qquad \text{or} \qquad U = \frac{lP^{\frac{4}{3}}}{4\sqrt[3]{AE}}. \tag{22b}$$

It is seen that the expressions for strain energy are no longer second-degree functions of the displacement or force such as we had in those examples of the preceding article for which the law of superposition holds.

Considering what is characteristic of the examples represented in Figs. 293 and 294, we see that in each case the action of the external forces is appreciably affected by small deformations which take place in the system. The axial force S in Fig. 293a produces only compression of the beam AB if acting alone. However, when acting in conjunction with the transverse load P it can produce not only compression but also some additional bending. In the case represented in Fig. 294a the tensile force S in the bars depends on the deformation and is inversely proportional to the small deflection δ produced by the load P. Always when we have such conditions that the action of external forces is affected by small deformations produced in the system, stresses and displacements will not be linear functions of the applied forces, and the principle of superposition does not hold. Thus, in conclusion, it can be said that the material must follow Hooke's law if the principle of superposition is to be applicable. But this requirement alone is insufficient, and we have to consider also whether or not the action of the applied forces will be affected by small deformations of the structure. If such an effect is substantial and must be taken into account, in calculating internal forces or stresses, the principle of superposition does not hold.

PROBLEMS
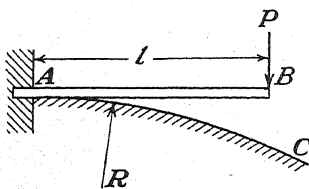
Fig. 295.

191. Referring to Fig. 295, determine the relation between the load P and the deflection δ at the free end of a prismatic beam AB built in at A and so arranged that during bending it gradually comes into contact with a rigid cylindrical surface AC having the constant curvature $1/R$ and a horizontal tangent at A. The flexural rigidity of the beam is EI.

$$Ans. \quad \delta = l^2/2R - \tfrac{1}{6}E^2I^2/R^3P^2.$$

192. Referring to Fig. 296, find the deflection produced at the middle of the bar AB by the load P if, during bending, the bar is always in contact with the supporting cylindrical surfaces of equal radii R.
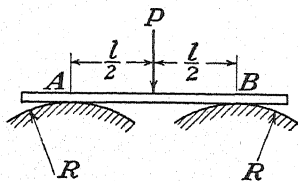
Fig. 296.
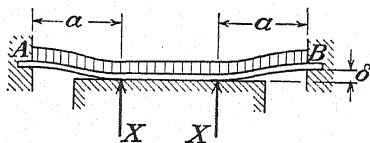
Fig. 297.

193. A uniformly loaded beam with built-in ends is additionally supported along the middle portion by a rigid horizontal foundation as shown in Fig. 297. Find the distances a, assuming $\delta < ql^4/1,152EI$. $Ans. \quad a = \sqrt[4]{72EI\delta/q}, \; X = qa/3.$

39. Strain Energy in General: Generalized Forces.—In Art. 37 we

have seen that the strain energy of an elastic bar in simple tension can be represented as a second-degree function either of the external forces or of the displacements. We shall now show that the same conclusion

holds equally well for any elastic structure provided that the principle of superposition can be applied. Let us consider, for example, an elastic body supported as shown in Fig. 298 and submitted to the action of external forces P_1, P_2, P_3, ... Since the amount of strain energy stored in the body depends not on the order in which the forces are applied but only on their final magnitudes, we can simplify our further discussion by assuming that all the forces are applied simultaneously and then gradually increased in the same proportion. Then, if the principle of superposition holds, the displacements will be linear functions of the forces, and during loading they increase in the same proportion as the forces do. In calculating the work of any force P_n, we shall be interested not in the total displacement of its point of application but only in that component in the direction of the force. Let δ_n denote this component of displacement. Then, during the assumed gradual loading, δ_n increases in the same proportion as P_n, and the relation between these two quantities can be represented by a diagram similar to that shown in Fig. 284b. Hence we conclude that the work produced by the load P_n is $P_n\delta_n/2$. The total work of all external forces, equal to the strain energy stored in the deformed body, is obtained by summing up the works of the individual forces, which gives[1]

FIG. 298.

$$U = \tfrac{1}{2}(P_1\delta_1 + P_2\delta_2 + P_3\delta_3 + \cdot\cdot\cdot).\tag{23}$$

The reactions R_a, R_b, and R_c do not appear in this expression, because, for the conditions of support illustrated in Fig. 298, their work is zero.[2]

Since the displacements δ_1, δ_2, . . . are homogeneous linear functions of the forces P_1, P_2, . . . , it follows that if these functions are substituted in expression (23) we shall find the strain energy to be represented by a homogeneous second-degree function of the external forces P_1, P_2, ... Likewise, if we express the forces as linear functions of the displacements and then substitute these functions in expression (23), we shall find that the strain energy can also be represented as a homogeneous second-degree function of the displacements δ_1, δ_2, ... Both
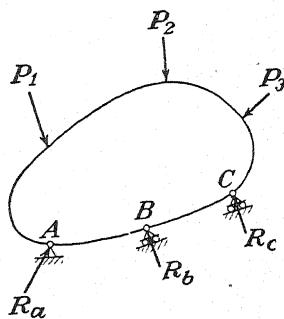
[1] The statement that the strain energy stored in an elastic body is equal to half of the sum of the products of external forces by the corresponding displacements is sometimes called *Clapeyron's theorem*. It is mentioned in Lamé's "Theory of Elasticity," seventh lecture. See also Maxwell's "Scientific Papers," vol. I, p. 598, and Todhunter and Pearson's "History," vol. I, p. 578.

[2] It is assumed that there is no friction in the rollers. If there should be friction, a part of the strain energy would be dissipated and the system would no longer be perfectly elastic as assumed.

forms of representation of the strain energy will be useful in our further discussion.

It should be noted that the foregoing conclusions regarding the degree and homogeneity of the strain-energy function were obtained on the assumption that the principle of superposition holds. If this principle does not hold, the strain energy will no longer be a second-degree function of the forces or of the displacements as can be seen, for example, from Eqs. (22) of the preceding article.

Expression (23) for strain energy can be made more general by using the notion of *generalized forces*.[1] Any group of statically interdependent
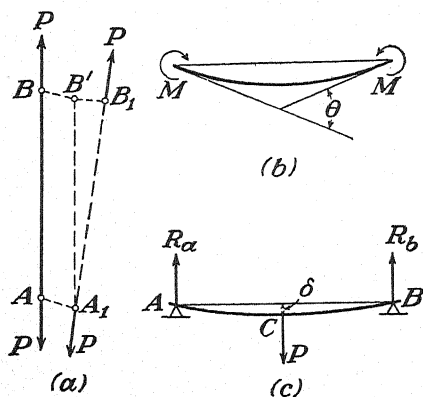
Fig. 299.

forces that can be completely defined by one symbol can be considered as a generalized force. For example, in the case of axial extension of a bar (Fig. 299a), we have two equal and opposite forces acting along the axis of the bar, and one symbol P defines entirely this pair of balanced forces. Again, in the case of pure bending (Fig. 299b), we have two equal and opposite couples that are in equilibrium, and one symbol M completely defines the system. In the case of a transverse load acting on a beam (Fig. 299c), we have a group of three forces that, being in equilibrium, are completely defined by the magnitude P of the applied load. In all such cases where we can define a group of forces by one symbol, we may treat that group as a *generalized force*.

In using the notion of generalized force, we have to generalize also the notion of displacement. In dealing with single forces (Fig. 298), we have already pointed out that not the total displacements of their points of application but only those components in the directions of the forces should be considered, since the work done by the forces depends only on such components. Thus, if δ_n is the component of the displacement of the point of application of the force P_n in the direction of that force, we say that δ_n is the displacement *corresponding* to the force P_n. If a small increment $\Delta\delta_n$ is given to this displacement, the work done by the force P_n is

$$P_n\Delta\delta_n. \tag{a}$$

[1] The notions of *generalized force* and *generalized displacement* were introduced by Lagrange in his famous book "Mécanique analytique," Paris, 1788. In application to the deformations of elastic systems, they were extensively used by Lord Rayleigh. See, for example, his "Scientific Papers," vol. I, p. 225; "Theory of Sound," 2d ed., p. 91.

Now, in using the notion of generalized force, the *corresponding generalized displacement* must be taken in such a way that the product of the generalized force and the increment of the corresponding generalized displacement gives the work. Take, for example, the case of simple tension (Fig. 299a). It is seen that the bar AB can be brought to any new position A_1B_1 by first moving it parallel to itself to the position A_1B' and then rotating it about the point A_1. During such displacement of the bar as a whole, the system of two equal and opposite forces does not produce any work. Work is produced only when the bar elongates by some amount δ. This elongation, then, is the generalized displacement corresponding to the generalized force consisting of two equal and opposite forces P. If an increment $\Delta\delta$ is given to the elongation δ, the generalized force P produces work of the amount $P\,\Delta\delta$, which is similar to expression (a) for the case of a single force. In the case of pure bending (Fig. 299b), the work produced by the couples M is entirely defined by the angle of rotation θ of one end of the bar with respect to the other.
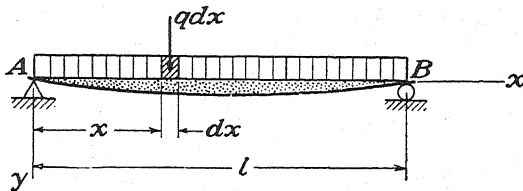
FIG. 300.

Hence this angle must be taken as the generalized displacement corresponding to the generalized force represented by the two equal and opposite couples. If θ obtains an increment $\Delta\theta$, the couples M produce the work $M\,\Delta\theta$ and again we obtain an expression similar to expression (a). In the case of a transverse load acting on a beam (Fig. 299c), the group of forces P, R_a, and R_b does not produce any work when the beam moves as a rigid body. Work is produced only when the beam deflects and point C moves perpendicular to AB. The deflection δ of the point C with respect to the line AB joining the ends of the beam axis is the generalized displacement in this case.

Sometimes the generalized displacement corresponding to a chosen generalized force may not be entirely self-evident. Consider, for example, the simply supported beam under uniform load as shown in Fig. 300. If the intensity q of the load is taken as the generalized force, the corresponding generalized displacement will be the area between the chord AB and the deflection curve as shown in the figure. To prove this, we give to the deflection y of each point on the axis of the beam a small increase Δy. Then the work done on each such additional displacement by the corresponding element of force $q\,dx$ is $q\,dx \cdot \Delta y$ and the entire load will produce the work

$$q \int_0^l \Delta y \cdot dx. \tag{b}$$

Now, observing that the integral $\int_0^l \Delta y \cdot dx$ is an increment of the area between the chord AB and the deflected axis of the beam, we conclude, by definition, that such area is the generalized displacement corresponding to the generalized force q. It is well to note in this case that while the generalized force has the dimension of *force ÷ length*, the corresponding generalized displacement has the dimension of *length squared*, so that their product has the proper dimension for work. Since the work done by a generalized force on an increment of the corresponding generalized displacement has always the same form as expression (a) derived for a single load, we conclude that the total work produced by a generalized force during a gradual loading has the same form as that for single forces and is equal to half the product of the final magnitude of the generalized force
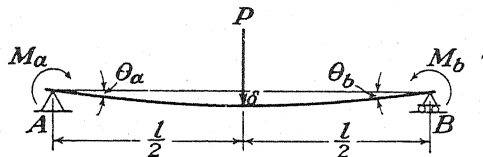
FIG. 301.

and the final value of the corresponding generalized displacement. This means that expression (23) derived for isolated forces can be used also if the forces and the displacements are generalized.

As an example of the application of expression (23), let us calculate the strain energy in a simply supported beam of prismatic form that is loaded by a force P at the middle and by the two couples M_a and M_b applied at the ends as shown in Fig. 301. In such case the system of forces acting on the beam can be represented in terms of three generalized forces, namely, the load P together with its reactions, and each of the couples M_a and M_b together with their reactions. The corresponding generalized displacements will be the deflection δ under the load and the angles of rotation θ_a and θ_b of the ends of the beam. The total strain energy stored in the beam, from expression (23), is

$$U = \tfrac{1}{2}(P\delta + M_a\theta_a + M_b\theta_b). \tag{c}$$

Using now the known expression for the deflection curve,[1] we have

$$\delta = \frac{Pl^3}{48EI} + \frac{M_a l^2}{16EI} + \frac{M_b l^2}{16EI},$$

$$\theta_a = \frac{Pl^2}{16EI} + \frac{M_a l}{3EI} + \frac{M_b l}{6EI}, \tag{d}$$

$$\theta_b = \frac{Pl^2}{16EI} + \frac{M_a l}{6EI} + \frac{M_b l}{3EI}.$$

[1] See "Strength of Materials," vol. I, pp. 142, 158.

Substituting these values of the displacements into expression (c), we obtain

$$U = \frac{l^3}{96EI}\left(P^2 + \frac{6}{l}PM_a + \frac{6}{l}P\,M_b + \frac{16}{l^2}M_a{}^2 + \frac{16}{l^2}M_b{}^2 + \frac{16}{l^2}M_aM_b\right). \quad (e)$$

It is seen that the strain energy is a homogeneous second-degree function of the generalized forces.

Solving Eqs. (d) for P, M_a, and M_b and substituting them in expression (c) we shall obtain the strain energy as a second-degree function of the generalized displacements.

PROBLEMS

194. A simply supported beam AB of uniform flexural rigidity EI and span l carries two equal transverse loads P, one at mid-span and the other at a quarter point. Using expression (23), calculate the strain energy stored.

195. Using expression (23) and the notion of generalized force, compute the strain energy stored in the beam shown in Fig. 300.

196. Make a general expression for the strain energy stored in the beam shown in Fig. 301 if $P = 0$, (a) expressed as a function of the end moments M_a and M_b and (b) expressed as a function of the angles of rotation θ_a and θ_b.

197. A thin steel strip of length l and uniform flexural rigidity EI is bent into a complete circle by end moments. Compute the strain energy U.

198. An elastic body undergoes a uniform compression under a gas pressure p. If this pressure p is taken as the generalized force, what is the corresponding generalized displacement?

40. Principle of Virtual Displacements for Elastic Bodies.—In our previous applications of the principle of virtual displacements (see Art. 9), we assumed absolutely rigid bodies. To extend the principle to elastic bodies, it is necessary to consider the small deformations that occur under the action of externally applied forces. We begin with the simple case of axial tension of a prismatic bar. As a model of an elastic bar, we can take the system shown in Fig. 302a. In this system the hinges represent the molecules of an elastic body and

FIG. 302.

the springs the elastic constraints between them. The tensile stresses are uniformly distributed by the rigid block AB, to which the external force P is applied. Under the action of this force, the model undergoes extension, and elastic forces are induced in the various springs. These internal forces, as shown in Fig. 302b,* can be taken to represent the

* It is assumed in the figure that all springs are in tension, although it can be seen at once that some of them will be compressed so that the axial extension of the model is accompanied by some lateral contraction.

elastic actions existing between the molecules of a bar in tension. Thus, we obtain a complicated system of forces that are in equilibrium with the external force P. Without going into a detailed study of this system, we can apply to it the principle of virtual displacements. Taking, as a virtual displacement of the system, an increment $\Delta\delta$ of the axial extension of the model, we conclude that the work done by all the forces during this displacement must be equal to zero. Upon denoting by ΔT the work of the internal forces, the principle of virtual displacement gives

$$\Delta T + P\,\Delta\delta = 0. \tag{a}$$

Since the quantity $P\,\Delta\delta$ represents the increment of work done by the external forces, which we already know to be equal to the increment ΔU of the strain energy stored in the elastic system, we conclude that Eq. (a) can be put in the form

$$\Delta T = -\Delta U. \tag{b}$$

This equation states that the work done by the internal forces during the virtual displacement $\Delta\delta$ of the system is numerically equal to the increment of strain energy, but of opposite sign. Correspondingly, we conclude that the total work done by the internal elastic forces during a gradual extension δ of a bar is equal to the total strain energy of the bar taken with negative sign. Using expression $(11b)$ for the strain energy and observing that

$$\Delta U = \frac{dU}{d\delta}\,\Delta\delta = \frac{AE\delta}{l}\,\Delta\delta,$$

we obtain, from Eq. (a),

$$-\frac{AE\delta}{l}\,\Delta\delta + P\,\Delta\delta = 0,$$

from which we find the relation

$$P = \frac{AE\delta}{l},$$

representing Hooke's law in the case of simple tension.

A similar consideration can be made also in the case of the block shown in Fig. 303, which undergoes extension in three perpendicular directions. Taking as virtual displacements the increments $\Delta\delta_x$, $\Delta\delta_y$, and $\Delta\delta_z$ of the elongations in the x-, y-, and z-directions, we conclude that the work done by internal forces during the assumed displacements is numerically equal to the increment of strain energy stored in the block, but of opposite sign.

In a general case of deformation of an elastic body we can imagine the body subdivided into infinitely small elements each of which will be in a condition similar to that of the block in Fig. 303. Hence we can

state generally that the work done by the internal forces on any virtual displacement of an elastic body is equal to the corresponding increment of the strain energy taken with negative sign. With this conclusion, and assuming that there are several forces P_1, P_2, . . . acting on a constrained elastic body and that δ_1, δ_2, . . . are the corresponding elastic displacements, the principle of virtual displacements gives

$$\Sigma P_n \Delta \delta_n + (-\Delta U) = 0, \qquad (c)$$

in which the first term on the left side represents the work done by the external forces on a virtual displacement of the system and the second term is the work done by the internal forces. Equation (c) then states that the total work, in the case of a displacement from the configuration of equilibrium, must be equal to zero. To calculate the increment ΔU of the strain energy, it must be represented first as a function of the displacements δ_1, δ_2, ... Then, in the usual way, the increment of U due to the increments $\Delta \delta_1$, $\Delta \delta_2$, . . . of the displacements is

Fig. 303.

$$\Delta U = \frac{\partial U}{\partial \delta_1} \Delta \delta_1 + \frac{\partial U}{\partial \delta_2} \Delta \delta_2 + \frac{\partial U}{\partial \delta_3} \Delta \delta_3 + \cdots \qquad (d)$$

In applying the principle of virtual displacements to an elastic body, we select in any particular case a displacement that is the most suitable for solution of a given problem. For example, we can imagine a virtual displacement that affects only the displacement δ_n, corresponding to the load P_n, and the displacements δ_1, δ_2, . . . remain unchanged. Under such conditions $\Delta \delta_1$, $\Delta \delta_2$, . . . vanish, and the foregoing expression for the increment of U reduces to

$$\Delta U = \frac{\partial U}{\partial \delta_n} \Delta \delta_n. \qquad (e)$$

Using this expression in Eq. (c) we obtain

$$P_n \Delta \delta_n - \frac{\partial U}{\partial \delta_n} \Delta \delta_n = 0, \qquad (24)$$

which may also be expressed in the form

$$\frac{\partial U}{\partial \delta_n} = P_n. \qquad (25)$$

This latter equation states that if the strain energy of a deformed elastic body is represented as a function of the displacements δ_1, δ_2, . . . a
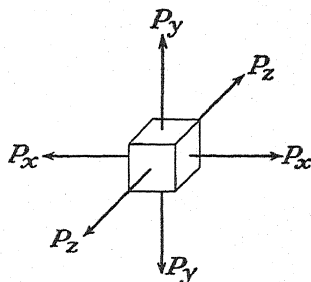
partial derivative of that function with respect to any specific displacement gives the corresponding force.

The foregoing statement can be extended also to the case when P_n is a generalized force and δ_n the corresponding generalized displacement. Take, for example, a simply supported beam AB with couples M_a and M_b applied at the ends.[1] Considering these couples and the corresponding reactions as two generalized forces, the corresponding generalized displacements are the angles θ_a and θ_b, by which the ends A and B of the beam rotate in the directions of the couples. The strain energy of the beam then is

$$U = \frac{2EI}{l}\,(\theta_a{}^2 - \theta_a\theta_b + \theta_b{}^2).$$

Taking the partial derivative of this expression with respect to θ_a, we obtain

$$\frac{\partial U}{\partial \theta_a} = \frac{2EI}{l}\,(2\theta_a - \theta_b),$$

which is the known expression for the moment M_a expressed as a function of the angles θ_a and θ_b. We obtain a similar conclusion by taking the partial derivative of U with respect to θ_b.
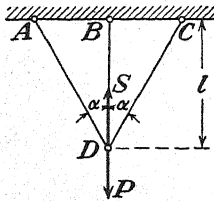
As another application of Eq. (25), let us consider a symmetrical system of three bars hinged together as shown in Fig. 304. If δ is the vertical displacement of the hinge D, the elongation of each inclined bar is $\delta \cos \alpha$, while for the vertical bar it is δ. Assuming that the cross-sectional areas and the moduli of all three bars are equal, the strain energy of the system is

Fig. 304.

$$U = \frac{AE}{2l}\,(\delta^2 + 2\delta^2 \cos^3 \alpha).$$

Now, using Eq. (25), we obtain

$$\frac{AE\delta}{l}\,(1 + 2\cos^3 \alpha) = P,$$

from which we find the force in the vertical bar to be

$$S = \frac{AE\delta}{l} = \frac{P}{1 + 2\cos^3 \alpha}.$$

The principle of virtual displacements can be applied also to the bending of beams. Consider, for example, the simply supported beam,

---

[1] M_a and M_b are taken positive when they produce deflection convex downward.

carrying a transverse load P as shown in Fig. 305a. In such a case the deflection curve can be represented by the trigonometric series[1]

$$y = a_1 \sin \frac{\pi x}{l} + a_2 \sin \frac{2\pi x}{l} + a_3 \sin \frac{3\pi x}{l} + \cdots = \sum_{n=1}^{\infty} a_n \sin \frac{n\pi x}{l}, \quad (f)$$

which means that by a proper selection of the coefficients $a_1, a_2, a_3, \ldots$ the deflection curve can be obtained by superposition of simple sine curves like those shown in Figs. 305b, c, and d. Thus, as soon as the coefficients $a_1, a_2, a_3, \ldots$ are known, the deflection at any cross section of the beam can be calculated from expression (f). In calculating these coefficients, Eq. (24) will be used. First the expression for strain energy is obtained by using formula (17b), into which the series (f) has been substituted for y. Then,
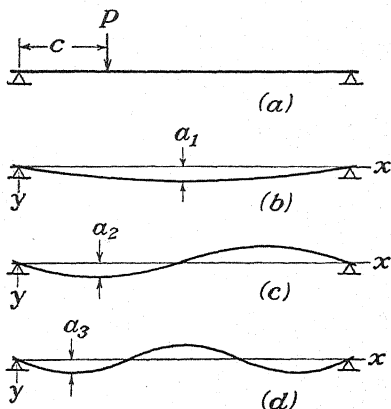
FIG. 305.

$$U = \frac{EI}{2} \int_0^l \left(a_1 \frac{\pi^2}{l^2} \sin \frac{\pi x}{l} + a_2 \frac{4\pi^2}{l^2} \sin \frac{2\pi x}{l} + a_3 \frac{9\pi^2}{l^2} \sin \frac{3\pi x}{l} + \cdots \right)^2 dx. \quad (g)$$

In calculating the square of the series under the integral sign, we obtain only two kinds of terms: those of the form

$$a_n^2 \frac{n^4 \pi^4}{l^4} \sin^2 \frac{n\pi x}{l}, \quad (h)$$

representing the squares of the terms of the series, and those of the form

$$2 a_n a_m \frac{n^2 m^2 \pi^4}{l^4} \sin \frac{n\pi x}{l} \sin \frac{m\pi x}{l}, \quad (i)$$

which are the double products of the terms of the same series. Observing that

$$\int_0^l \sin^2 \frac{n\pi x}{l} \, dx = \frac{l}{2}, \qquad \int_0^l \sin \frac{n\pi x}{l} \sin \frac{m\pi x}{l} \, dx = 0,$$

we conclude that, in performing the indicated integration in Eq. (g), all terms of the type (i) vanish and only terms of the type (h) remain. Hence, we obtain

$$U = \frac{EI}{2} \cdot \frac{l}{2} \left(a_1^2 \frac{1^4 \pi^4}{l^4} + a_2^2 \frac{2^4 \pi^4}{l^4} + a_3^2 \frac{3^4 \pi^4}{l^4} + \cdots \right) = \frac{EI \pi^4}{4 l^3} \sum_{n=1}^{\infty} a_n^2 n^4. \quad (j)$$

---

[1] See "Strength of Materials," vol. II, p. 44.

Now, to apply Eq. (24), we give to one of the coefficients of the series (f), say to the coefficient a_n, an increment Δa_n, which means that on the actual deflection curve, represented by the series (f), a virtual displacement

$$\Delta a_n \sin \frac{n\pi x}{l} \qquad (k)$$

represented by a sine curve having n half waves of infinitesimal amplitude Δa_n is superposed. The deflection of the point of application of the load P (Fig. 305a), corresponding to this virtual displacement, is

$$\Delta \delta = \Delta a_n \sin \frac{n\pi c}{l},$$

and the work done by the load P on the virtual displacement is

$$P \Delta \delta = P \Delta a_n \sin \frac{n\pi c}{l}. \qquad (l)$$

The increment of strain energy corresponding to the virtual displacement (k), obtained from expression (j), is

$$\Delta U = \frac{\partial U}{\partial a_n} \Delta a_n = \frac{EI\pi^4}{2l^3} a_n n^4 \Delta a_n. \qquad (m)$$

Substituting (l) and (m) into Eq. (24), we obtain

$$P \Delta a_n \sin \frac{n\pi c}{l} - \frac{EI\pi^4}{2l^3} a_n n^4 \Delta a_n = 0,$$

from which

$$a_n = \frac{2Pl^3 \sin n\pi c/l}{EI\pi^4 n^4}. \qquad (n)$$

From this formula the coefficients of the series (f) are calculated, and we obtain finally

$$y = \frac{2Pl^3}{EI\pi^4} \left(\sin \frac{\pi c}{l} \sin \frac{\pi x}{l} + \frac{1}{2^4} \sin \frac{2\pi c}{l} \sin \frac{2\pi x}{l} + \frac{1}{3^4} \sin \frac{3\pi c}{l} \sin \frac{3\pi x}{l} + \cdots \right). \qquad (o)$$

In the particular case where the load is at the middle, we calculate the corresponding deflection by substituting $c = x = l/2$ into the series (o), thus obtaining

$$(y)_{x=c=\frac{l}{2}} = \frac{2Pl^3}{EI\pi^4} \left(1 + \frac{1}{3^4} + \frac{1}{5^4} + \cdots \right).$$

This series converges rapidly, and we see that by using only the first term we obtain the deflection with a good accuracy. The representation of the deflection curve in the form of a trigonometric series is especially useful when we have a combined lateral and axial loading of the beam.[1]

[1] Several applications of this kind are shown in "Strength of Materials," vol. II, p. 44.

In the derivation of Eqs. (24) and (25), we did not use the principle of superposition; hence these equations can be applied also in those cases where the principle of superposition does not hold. Take, for example, the case shown in Fig. 294a. The strain energy of the system is given by formula (22a), and we obtain $dU/d\delta = AE\delta^3/l^3$, which is equal to the force P as can be seen from formula (g) (page 223).

PROBLEMS

199. Find the tensile force S in the vertical bar of the statically indeterminate system in Fig. 304 if its cross-sectional area is A while that of each inclined bar is $A/2$.

200. Given a simply supported beam AB of uniform flexural rigidity EI and span l transversely loaded by a force Q applied at mid-span. Using the formula (17b) together with Eq. (25), calculate the magnitude of Q to produce a deflection δ of its point of application. Assume that the elastic line is a half wave of a sine curve, that is, $y = \delta \sin (\pi x/l)$. *Ans.* $Q = \pi^4 EI\delta/2l^3$.

201. Calculate the transverse force Q required to produce a deflection δ in the preceding problem if the beam is under uniform axial compression P.

Solution: When the beam is deflected to the sine curve $y = \delta \sin (\pi x/l)$, its ends come together by the amount

$$\lambda = \frac{1}{2} \int_0^l \left(\frac{dy}{dx}\right)^2 dx = \frac{\pi^2\delta^2}{4l}.$$

Now, giving to the deflection δ an increment $\Delta\delta$, we obtain

$$\frac{dU}{d\delta} \cdot \Delta\delta = Q \cdot \Delta\delta + P \cdot \frac{d\lambda}{d\delta} \cdot \Delta\delta$$

or

$$EI \frac{\pi^4\delta}{2l^3} = Q + P \frac{\pi^2\delta}{2l}$$

from which

$$\delta = \frac{2Ql^3}{\pi^4 EI} \left(\frac{1}{1 - \frac{Pl^2}{\pi^2 EI}}\right).$$

41. Castigliano's Theorem.—In the previous article, we used the expression for strain energy as a function of the displacements and found that a partial derivative of this function with respect to any displacement is equal to the corresponding force. Now let us consider the expression for strain energy as a function of external forces and assume that the principle of superposition holds. *Under such conditions, a partial derivative of the strain energy with respect to one of the external forces gives the displacement corresponding to that force.* Castigliano was the first to make this observation, and the statement is usually called *Castigliano's theorem.*[1] To prove the theorem, let us consider the general case of an

---

[1] ALBERTO CASTIGLIANO, *Trans. Acad. Sci. Turin*, vol. 11, pp. 127–286, 1876. See also his treatise, "Théorème de l'équilibre des systèmes élastiques et ses applications," Paris, 1879. The English translation of this book was made by E. S. Andrews, London, 1919.

elastic body carrying the loads P_1, P_2, P_3, . . . as shown in Fig. 298. During the application of these loads, deformations are produced, and a certain amount of strain energy U is stored within the body. If, subsequently, one of the forces, say P_1, receives an increment ΔP_1, some additional deformation of the body will ensue and the strain energy U will obtain an increment

$$\Delta U = \frac{\partial U}{\partial P_1} \Delta P_1$$

so that the total strain energy becomes

$$U + \frac{\partial U}{\partial P_1} \Delta P_1. \tag{a}$$

Now suppose that, instead of introducing the increment ΔP_1 after the application of the loads P_1, P_2, P_3, . . . , we reverse the procedure and apply first the infinitely small increment ΔP_1 and afterward the loads P_1, P_2, P_3, ... Since the infinitesimal load ΔP_1 produces an infinitesimal displacement, the corresponding work is a small quantity of the second order and can be neglected. Further, during the subsequent application of the loads P_1, P_2, P_3, . . . , we observe, by virtue of the principle of superposition, that the work of these forces will not be affected by the presence of the load ΔP_1 and will be equal to its previous value U. At the same time the acting load ΔP_1 rides through the displacement δ_1 resulting from the application of the loads P_1, P_2, P_3, . . . and produces the work $\Delta P_1 \delta_1$. Thus, in this case, the total work, equal to the total strain energy stored in the body, is

$$U + \Delta P_1 \delta_1. \tag{b}$$

Since the total amount of strain energy stored in the body does not depend on the order in which the loads are applied, we conclude that expressions (a) and (b) must be equal. Thus,

$$U + \frac{\partial U}{\partial P_1} \Delta P_1 = U + \Delta P_1 \delta_1,$$

from which

$$\frac{\partial U}{\partial P_1} = \delta_1, \tag{26}$$

and the theorem is proved.

The same conclusion can be obtained in a somewhat different way, as follows. Considering again the elastic body in Fig. 298, we can state that the displacements δ_1, δ_2, δ_3, . . . are entirely defined by the magnitudes of the forces P_1, P_2, P_3, ... Thus if we give to one of these forces, say P_1, a small increment ΔP_1, the displacements will be slightly

changed, and these changes can be represented in the usual manner as follows:

$$\Delta\delta_1 = \frac{\partial\delta_1}{\partial P_1}\Delta P_1, \qquad \Delta\delta_2 = \frac{\partial\delta_2}{\partial P_1}\Delta P_1, \qquad \Delta\delta_3 = \frac{\partial\delta_3}{\partial P_1}\Delta P_1, \cdots$$

During these changes in displacement, the forces $P_1, P_2, P_3, \ldots$ produce work representing the increment of strain energy corresponding to the increment ΔP_1 of the force P_1. Hence

$$\frac{\partial U}{\partial P_1}\Delta P_1 = P_1\Delta\delta_1 + P_2\Delta\delta_2 + P_3\Delta\delta_3 + \cdots$$

$$= P_1\frac{\partial\delta_1}{\partial P_1}\Delta P_1 + P_2\frac{\partial\delta_2}{\partial P_1}\Delta P_1 + P_3\frac{\partial\delta_3}{\partial P_1}\Delta P_1 + \cdots,$$

from which

$$\frac{\partial U}{\partial P_1} = P_1\frac{\partial\delta_1}{\partial P_1} + P_2\frac{\partial\delta_2}{\partial P_1} + P_3\frac{\partial\delta_3}{\partial P_1} + \cdots. \qquad (c)$$

Using now the general expression for strain energy

$$U = \frac{P_1\delta_1}{2} + \frac{P_2\delta_2}{2} + \frac{P_3\delta_3}{2} + \cdots,$$

and differentiating with respect to P_1, we obtain

$$2\frac{\partial U}{\partial P_1} = \delta_1 + P_1\frac{\partial\delta_1}{\partial P_1} + P_2\frac{\partial\delta_2}{\partial P_1} + P_3\frac{\partial\delta_3}{\partial P_1} + \cdots. \qquad (d)$$

Subtracting Eq. (c) from Eq. (d) we obtain

$$\frac{\partial U}{\partial P_1} = \delta_1$$

as before.

In Fig. 298, $P_1, P_2, P_3, \ldots$ denote single forces; but our derivation holds also if they are generalized forces, and $\delta_1, \delta_2, \delta_3, \ldots$ are the corresponding generalized displacements. Thus we can state that the partial derivative of the strain energy with respect to any generalized force gives the corresponding generalized displacement.

In both derivations of Castigliano's theorem we assumed that it is possible to give an arbitrary increment to one of the forces without changing the other forces. Thus we consider these forces as independent. Such forces as statically determinate reactions do not satisfy this condition since their magnitudes are not independent of $P_1, P_2, P_3, \ldots$ and can be found from equations of statics. From this consideration it follows that the strain energy U in
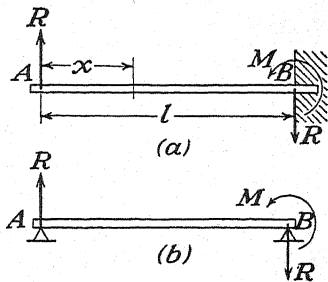
FIG. 306.

Eq. (26) must be represented as a function of *statically independent* external forces. Take, for example, the two beams shown in Fig. 306. The same forces R and M are acting in both cases, and from statics we conclude that $M = Rl$. Thus the strain energy can be represented in either of the following two forms:[1]

$$U = \frac{R^2 l^3}{6EI} \quad (e) \qquad \text{or} \qquad U = \frac{M^2 l}{6EI}. \quad (f)$$

If we use expression (e), we consider R as an independent external force and M as the reaction, as in the case of a cantilever beam (Fig. 306a). In such a case the derivative of expression (e) with respect to R gives

$$\frac{\partial U}{\partial R} = \frac{Rl^3}{3EI},$$

which is the deflection of the end A of the cantilever beam built in at B.
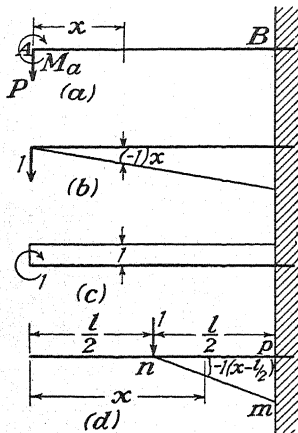
Fig. 307.

If expression (f) is used, we assume that M is the independent external force and R is the reaction as in the case of a simply supported beam (Fig. 306b). Then, taking the derivative of expression (f), with respect to M we obtain

$$\frac{\partial U}{\partial M} = \frac{Ml}{3EI},$$

which is the angle of rotation of the end B of the simply supported beam. This example illustrates the significance of the requirement of representing the strain energy as a function of statically independent forces.

Castigliano's theorem is very useful in calculating deflections of beams. Take, for example, the cantilever beam bent by a force and a couple applied at the end (Fig. 307a). The bending moment at any cross section is

$$M = M_a - Px, \quad (g)$$

and the strain energy stored in the beam, as obtained from formula (17a), is

$$U = \int_0^l \frac{M^2 dx}{2EI}. \quad (h)$$

The derivative of this expression with respect to P gives the displacement corresponding to P, that is, the deflection δ of the end A of the cantilever.

---

[1] Both formulas are readily obtained from the general expression (17a) of the strain energy.

Thus we obtain

$$\delta = \frac{\partial U}{\partial P} = \int_0^l \frac{M}{EI}\frac{\partial M}{\partial P}\,dx = \frac{1}{EI}\int_0^l (M_a - Px)(-x)dx = \frac{Pl^3}{3EI} - \frac{M_a l^2}{2EI}. \quad (i)$$

The derivative of expression (h) with respect to the generalized force M_a gives the corresponding displacement, i.e., the angle of rotation θ_a of the end A of the cantilever, and we obtain

$$\theta_a = \frac{\partial U}{\partial M_a} = \int_0^l \frac{M}{EI}\frac{\partial M}{\partial M_a}\,dx = \frac{1}{EI}\int_0^l (M_a - Px)(1)dx = \frac{M_a l}{EI} - \frac{Pl^2}{2EI}. \quad (j)$$

In this application of Castigliano's theorem we did not calculate the final expression for strain energy as a function of external forces but used it in its general form (h), substituting the value of M only after differentiation under the integral signs in Eqs. (i) and (j). In this way a considerable simplification of calculation is accomplished, especially if there are several external forces.

It can be noted that the partial derivatives $\partial M/\partial P$ and $\partial M/\partial M_a$, which enter in the above calculations, have very simple meanings. The first of these derivatives represents the rate of change of bending moment in the beam with change of the load P. As shown in Fig. 307b, it can be visualized as the bending-moment diagram for a unit load at the end of the beam. The second derivative, representing the rate of change of the bending moment M with change of M_a, is shown in Fig. 307c. Using for these derivatives the notations M_p' and M_m', we can write the expressions for the displacements in the following simplified forms:

(a)

(b)

Fig. 308.

$$\delta = \frac{1}{EI}\int_0^l MM_p'dx, \quad (k)$$

$$\theta_a = \frac{1}{EI}\int_0^l MM_m'dx. \quad (l)$$

We see that in each case we have to integrate along the length of the beam the product of the actual bending moment with the corresponding unit-load bending moment. This conclusion can be extended and applied to beams with any kind of lateral loading. If we have, for example (Fig. 308a), a simply supported beam carrying a uniform load q and a concentrated load P at the middle, the derivative $\partial M/\partial P$ is shown in Fig. 308b and the deflection at the middle is

$$\delta = \frac{1}{EI}\int_0^l MM_p'dx = \frac{2}{EI}\int_0^{\frac{l}{2}}\left(\frac{P}{2}x + \frac{ql}{2}x - \frac{qx^2}{2}\right)\frac{x}{2}dx = \frac{Pl^3}{48EI} + \frac{5}{384}\frac{ql^4}{EI}.$$
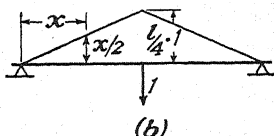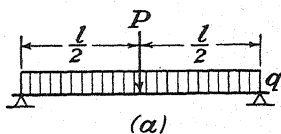
It is seen that by applying Castigliano's theorem we obtain the displacement corresponding to any of the forces acting on the elastic system, but there are cases where we need to find such displacements to which there are no corresponding forces acting. In such cases we add to the actual forces fictitious forces of infinitesimal magnitudes such that they do not change the actual displacement. We then obtain the required displacements by differentiation of the strain energy with respect to these added forces. Take, for example, the cantilever beam in Fig. 307a, and assume that it is required to calculate the deflection at the middle of the beam. Since there is no corresponding force, we assume an infinitesimal fictitious load Q applied at the middle. Then the required deflection is

$$\delta_1 = \frac{\partial U}{\partial Q} = \frac{1}{EI} \int_0^l M \frac{\partial M}{\partial Q} dx. \qquad (m)$$

Since the added load Q is infinitesimal, we use for M the previous expression (g). The derivative $\partial M / \partial Q$, representing the rate of change of the bending moment M with change of the load Q, can be visualized by the unit-load bending-moment diagram mnp shown in Fig. 307d. Substituting these values into expression (m), we obtain

$$\delta_1 = -\frac{1}{EI} \int_{\frac{l}{2}}^l (M_a - Px)\left(x - \frac{l}{2}\right) dx = \frac{5Pl^3}{48EI} - \frac{M_a l^2}{8EI}.$$

In conclusion we note that the derivation of Castigliano's theorem was based on the principle of superposition. Hence the expression for strain energy U must be a homogeneous second-degree function of the acting forces. If the principle of superposition does not hold and U is not a second-degree function of the acting forces, Castigliano's theorem is not applicable. To illustrate this point, let us consider the example shown in Fig. 294. The strain energy in this case is represented by formula $(22b)$, which is not a quadratic function in P. If we take the derivative of that function with respect to P, we obtain

$$\frac{\partial U}{\partial P} = \frac{1}{3} \frac{l \sqrt[3]{P}}{\sqrt[3]{AE}}. \qquad (n)$$

This result represents only one-third of the deflection δ of the point of application of the load P as given by formula (f) (page 223).

To explain why in such cases the derivative with respect to a force does not give the corresponding displacement, let us compare the diagrams in Fig. 284b and Fig. 294c. In Fig. 284b the relation between P and δ is represented by the straight line Oa. The shaded area represents the increment dU of the strain energy due to the increment $d\delta_1$ of the deflection, and we have

$$dU = P_1 d\delta_1. \qquad (o)$$

Considering now the infinitely small triangle bcf, geometrically similar to the triangle Obe, we find

$$\frac{dP_1}{d\delta_1} = \frac{P_1}{\delta_1}, \qquad d\delta_1 = \frac{\delta_1 dP_1}{P_1}.$$

Substituting this value of $d\delta_1$ in Eq. (o), we obtain

$$\frac{dU}{dP_1} = \delta_1$$

as required by Castigliano's theorem.

Now let us repeat the same reasoning with the diagram in Fig. 294c. The shaded elemental area again represents the increment of strain energy, and we obtain

$$dU = P\, d\delta. \tag{p}$$

Considering now the infinitely small triangle def and comparing it with the triangle dgh we find

$$\frac{dP}{d\delta} = \frac{P}{\overline{gh}},$$

from which

$$d\delta = \frac{dP \cdot \overline{gh}}{P}.$$

Substituting this value in Eq. (p), we obtain

$$\frac{dU}{dP} = \overline{gh}.$$

For the cubic parabola Oab the distance $\overline{gh}$ is equal to one-third of $\overline{Og} = \delta$. Hence we again arrive at the incorrect conclusion given by Eq. (n).

To obtain the true deflection by differentiation in this case we have to take instead of the strain energy U, given by the area $Oabc$ in Fig. 294c, the *complementary energy* U_1, given in Fig. 294c by the area $Oabk$. This energy is

$$U_1 = \int_0^P \delta\, dP.$$

Substituting for δ its expression (f) (page 223), we obtain

$$U_1 = \frac{l}{\sqrt[3]{AE}} \int_0^P P^{\frac{1}{3}} dP = \frac{3l}{4\sqrt[3]{AE}} P^{\frac{4}{3}}.$$

The derivative of this expression with respect to P gives the true value of the deflection δ.[*]

Another example in which the principle of superposition does not hold is shown in Fig. 293a. The strain energy is not a function of the second degree; but if the axial force is small in comparison with P_{cr}, we can disregard this fact and use Castigliano's theorem. The error in deflection obtained in this way is a small quantity of the same order of smallness as the ratio P/P_{cr}.

---

[*] The idea of using complementary energy was introduced by F. Engesser, *Z. Architekten-Ingenieur-Ver.*, vol. 35, p. 733, 1889. Several applications of complementary energy are shown in a paper by H. M. Westergaard, *Proc. A.S.C.E.*, February, 1941.

PROBLEMS

202. Find, by using Castigliano's theorem, the angles of rotation of the ends of a simply supported beam under uniform load.

203. Determine the vertical and horizontal displacements of the points A and B of the structure shown in Fig. 309. Consider in this calculation only strain energy of bending, and neglect the effect of the axial force on bending of the vertical portion AC of the structure. Assume the cross section constant along the length CAB.
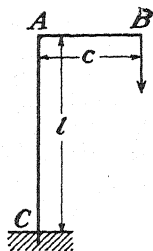
Fig. 309.
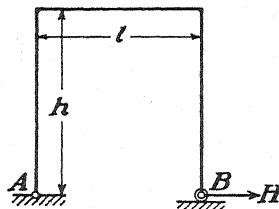
Fig. 310.

204. Taking the same assumptions as in the previous problem, find for the frame in Fig. 310 the horizontal displacement δ_b of the support B produced by the horizontal load H.

205. Determine the horizontal and vertical displacements δ_h and δ_v respectively, of the end A of a circular curved bar built in at B (Fig. 311). Assume that the cross-sectional dimensions of the bar are small in comparison with the radius r, so that the straight-beam formula (17a) can be used in calculating the strain energy of bending. Neglect completely the strain energy due to direct and shearing stresses.
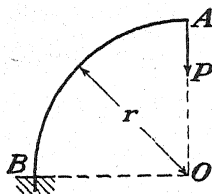
Fig. 311.
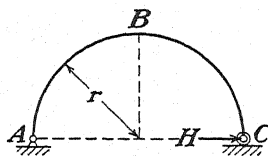
Fig. 312.

206. Using the same assumptions as in the previous problem, find the horizontal displacement of the support C and the vertical displacement of the crown B of the semicircular arch ABC shown in Fig. 312.

42. Method of Least Work.—In the preceding article we have considered applications of Castigliano's theorem to statically determinate systems and found that the displacement of any point is obtained as the derivative of the strain energy of the system with respect to the corresponding force. Applying the theorem in the same way to a statically indeterminate system, we conclude that the derivative of the strain energy with respect to any redundant reaction or internal constraint must be zero since it is the function of such a reactive force to prevent any displacement at its point of application. Hence the magnitudes of

redundant reactions in statically indeterminate systems will be such as to make the strain energy of the system a maximum or a minimum. By calculating the second derivatives and proving that they are always positive, it can be shown that we have the case of a minimum. Thus we obtain a method of calculation of redundant forces that is known as the *method of least work*. We derive the expression for the strain energy of the given system as a function of the redundant forces and then select these forces so as to make this strain energy a minimum.

We shall now illustrate the method of least work by several examples. As a first example, we take a uniformly loaded beam built in at B and having a hinged movable support at A (Fig. 313a). For determining the two vertical reactions and the reactive couple M_b, we have in this case
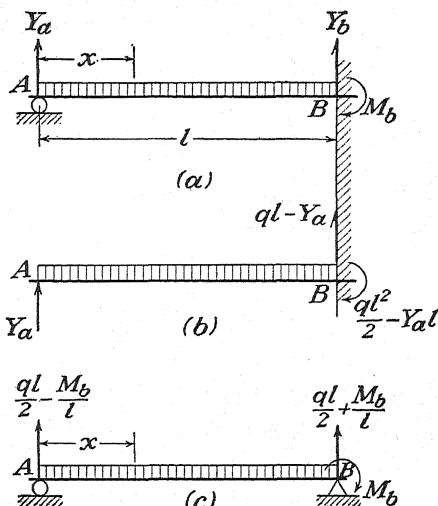
Fig. 313.

only two equations of statics. Hence one of the reactions, say the reaction Y_a at the left support, is statically indeterminate. If this quantity can be found in some way, then the other reactions Y_b and M_b can be found from the two equations of statics,

$$\Sigma Y = 0, \qquad \Sigma M = 0. \qquad (a)$$

To find Y_a, we remove the support at the left end and replace it by the force Y_a (Fig. 313b). It is evident that the true value of this reaction is that value at which the deflection of the cantilever shown in Fig. 313b becomes equal to zero, as is required by the condition of constraint of the actual beam in Fig. 313a. Applying to this cantilever beam Castigliano's theorem and observing that the deflection at A is zero, we obtain

$$\frac{\partial U}{\partial Y_a} = \frac{\partial}{\partial Y_a} \int_0^l \frac{M^2 dx}{2EI} = \frac{1}{EI} \int_0^l M \frac{\partial M}{\partial Y_a} \, dx = 0. \qquad (b)$$

Substituting in this equation

$$M = Y_a x - \frac{qx^2}{2}, \qquad \frac{\partial M}{\partial Y_a} = x,$$

we find

$$\int_0^l \left(Y_a x - \frac{qx^2}{2} \right) x \, dx = \frac{Y_a l^3}{3} - \frac{ql^4}{8} = 0, \qquad (c)$$

which gives

$$Y_a = \tfrac{3}{8} q l.$$

It is seen that, by using Castigliano's theorem, we obtain the additional equation (b) from which the statically indeterminate quantity Y_a has been found. Equation (b) is the equation of least work referred to above and states that the true value of the reaction Y_a is that value which makes the strain energy U of the beam a maximum or minimum. By calculating the second derivative $\partial^2 U / \partial Y_a{}^2$, we can show that it is a minimum.

The method of least work as illustrated in the foregoing example can be applied also to structures having several redundant reactions X, Y, Z, ... Observing that the supports either are immovable or move perpendicularly to the reactions, we conclude, from Castigliano's theorem, that

$$\frac{\partial U}{\partial X} = 0, \qquad \frac{\partial U}{\partial Y} = 0, \qquad \frac{\partial U}{\partial Z} = 0. \qquad (27)$$

Thus we obtain as many additional equations as there are redundant reactions, and these equations state that the redundant reactions X, Y, Z must have such magnitudes as to make the strain energy stored in the structure a minimum. The foregoing conclusion holds also in cases where the redundant reactions are represented by generalized forces. Consider again the beam shown in Fig. 313a, and let us now take the couple M_b as the redundant reaction and consider the simply supported beam shown in Fig. 313c. Again the true value of M_b for this beam is that value for which the tangent at the end B does not rotate. Hence the necessary equation for determining M_b is

$$\frac{\partial U}{\partial M_b} = \frac{\partial}{\partial M_b} \int_0^l \frac{M^2 dx}{2EI} = \frac{1}{EI} \int_0^l M \frac{\partial M}{\partial M_b} \, dx = 0. \qquad (d)$$

The bending moment at any cross section, represented as a function of M_b, is

$$M = \left(\frac{ql}{2} - \frac{M_b}{l} \right) x - \frac{qx^2}{2},$$

from which

$$\frac{\partial M}{\partial M_b} = -\frac{x}{l}.$$

Substituting these values in Eq. (d), we obtain

$$\int_0^l \left[\left(\frac{ql}{2} - \frac{M_b}{l} \right) x - \frac{qx^2}{2} \right] \frac{x}{l} \, dx = 0,$$

which gives

$$M_b = \frac{ql^2}{8}.$$

Sometimes the internal forces acting between two adjacent portions of a structure will be chosen as the statically indeterminate quantities, rather than the reactions at the supports. In such cases the principle of least work still holds and can be used to advantage. Consider, for example, the symmetrical rectangular frame shown in Fig. 314a. Taking a section through the horizontal plane of symmetry *mn* and considering the equilibrium of the upper part of the frame (Fig. 314b) we can repre-
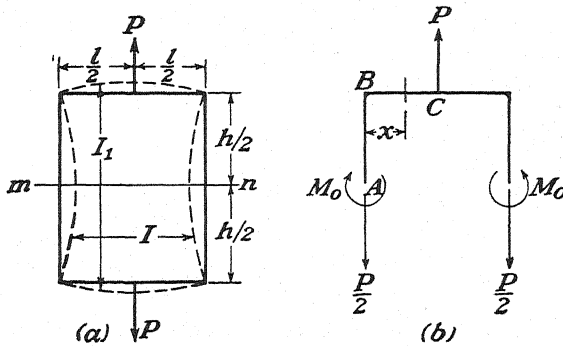
Fig. 314.

sent the action of the lower part on it by the vertical forces[1] $P/2$ and by the couples M_0, the magnitude of which cannot be determined from statics. From the symmetry of the deformation shown in Fig. 314a, we conclude that the cross sections on which the couples M_0 are acting in Fig. 314b do not rotate. Hence the derivative, with respect to M_0, of the strain energy stored in the upper part of the frame must vanish, and we can state, as before, that the magnitude of the statically indeterminate quantity M_0 is such as to make the strain energy a minimum. In calculating this strain energy we neglect the strain energy due to direct stress and assume that the effect of axial forces on bending can be neglected. Thus the bending moment for the portion AB of the frame is M_0, while for the portion BC it is $M_0 - Px/2$. The strain energy of the upper half of the frame then is

$$U = \frac{M_0^2 h}{2EI} + \frac{1}{EI_1} \int_0^{\frac{l}{2}} \left(M_0 - \frac{Px}{2} \right)^2 dx.$$

[1] From symmetry it can be concluded that there will be no shearing forces in the plane *mn*.

Applying the principle of least work, we now obtain

$$\frac{\partial U}{\partial M_0} = \frac{M_0 h}{EI} + \frac{2}{EI_1} \int_0^{\frac{l}{2}} \left(M_0 - \frac{Px}{2} \right) dx = 0,$$

which gives

$$M_0 = \frac{Pl}{8\left(1 + \frac{h}{l}\frac{I_1}{I}\right)}.$$

It is seen that when the cross-sectional moment of inertia I_1 of the horizontal bars of the frame is large in comparison with the corresponding quantity I for the vertical bars, the moment M_0 becomes small and the condition of bending of the horizontal bars approaches that of simply supported beams. On the other hand, if I_1 is small in comparison with I, the moment M_0 approaches the value $Pl/8$ as for a beam with built-in ends.
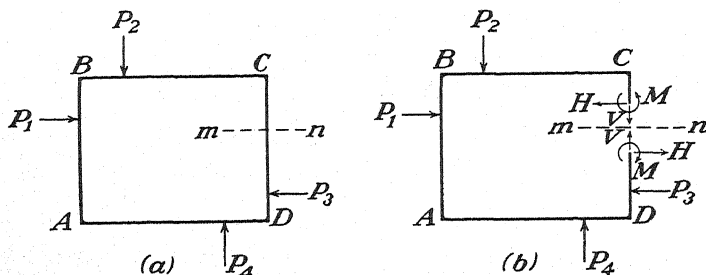
FIG. 315

In the more general case of a nonsymmetrically loaded frame, as shown in Fig. 315, we cut the frame on the section mn and represent the internal action between adjacent portions by forces H and V and moments M as shown in Fig. 315b. If we can find these three quantities in some way, the bending moment, shearing force, and axial force at any other cross section can be readily obtained from equations of statics. Thus we have in this case three statically indeterminate quantities for the determination of which we can use the method of least work. Since, in the actual frame (Fig. 315a), there is no movement of the cross section above the plane mn with respect to the adjacent cross section below the plane mn, we conclude that the displacements corresponding to the generalized forces H, V, and M are zero. Hence the equations of least work become

$$\frac{\partial U}{\partial H} = 0, \qquad \frac{\partial U}{\partial V} = 0, \qquad \frac{\partial U}{\partial M} = 0. \qquad (e)$$

As another example let us consider the circular ring shown in Fig. 316a and determine the moments M_0 and the increase in the vertical

diameter of the ring under the action of forces P applied as shown. Proceeding as in the case of a rectangular frame (Fig. 314) and considering the equilibrium of the upper half of the ring, we conclude that

$$\frac{\partial U}{\partial M_0} = \frac{1}{EI} \frac{\partial}{\partial M_0} \int_0^{\frac{\pi r}{2}} M^2 ds = 0. \tag{f}$$

Substituting in this equation

$$M = M_0 - \frac{Pr}{2}(1 - \cos \phi), \qquad \frac{\partial M}{\partial M_0} = 1,$$

we obtain

$$\int_0^{\frac{\pi}{2}} \left[M_0 - \frac{Pr}{2}(1 - \cos \phi) \right] d\phi = 0,$$

from which

$$M_0 = \frac{Pr}{2}\left(1 - \frac{2}{\pi}\right) = 0.182 Pr. \tag{g}$$
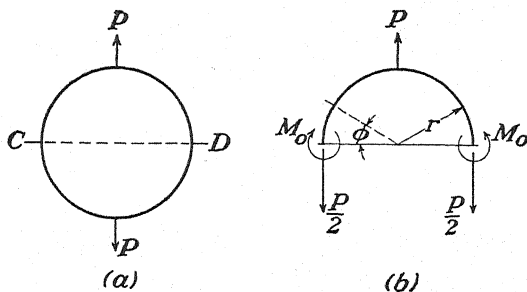
FIG. 316.

To find the increase of the vertical diameter of the ring, we observe that the forces P in Fig. 316a represent the generalized force corresponding to the increase δ of the diameter. Hence this increase[1] is

$$\delta = \frac{\partial U}{\partial P} = \frac{2}{EI} \frac{\partial}{\partial P} \int_0^{\frac{\pi}{2}} M^2 r \, d\phi =$$

$$-\frac{4r}{EI} \int_0^{\frac{\pi}{2}} \left[M_0 - \frac{Pr}{2}(1 - \cos \phi) \right] \frac{r}{2}(1 - \cos \phi) d\phi.$$

Using the value of M_0 from Eq. (g) above, this becomes

$$\delta = -\frac{Pr^3}{EI} \int_0^{\frac{\pi}{2}} \left(\cos \phi - \frac{2}{\pi}\right)(1 - \cos \phi) d\phi = \frac{Pr^3}{EI}\left(\frac{\pi}{4} - \frac{2}{\pi}\right) = 0.149 \frac{Pr^3}{EI}.$$

[1] In this calculation we assume that the strain energy due to direct and shearing stresses can be neglected in comparison with strain energy of bending. This is justifiable only in the case of a thin ring.

As another application of the method of least work, let us calculate the thrust H in the two-hinged arch under vertical load as shown in Fig. 317. The vertical reactions V_a and V_b can be obtained in the usual way from equations of statics; but the horizontal thrust H is a statically indeterminate quantity, and to find it we must use the principle of least work, which requires that

$$\frac{\partial U}{\partial H} = 0. \tag{h}$$

In the case of a flat arch, the strain energy due to direct stress is an important factor and cannot be neglected in comparison with the strain energy of bending. Thus we take

$$U = \int_0^s \frac{M^2 ds}{2EI} + \int_0^s \frac{N^2 ds}{2AE}, \tag{i}$$
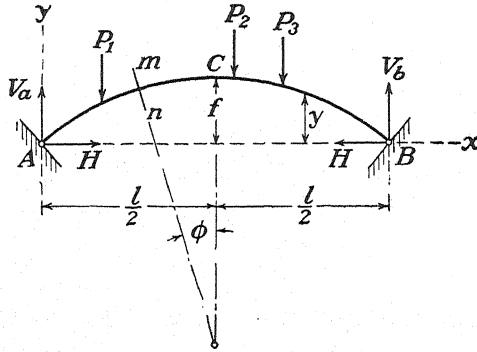
FIG. 317.

where M is the bending moment and N is the axial force at any cross section. The length of the axis of the arch is denoted by s. The bending moment at any cross section can be considered as consisting of two parts; one representing the moment M_0, calculated as for a simple beam ($H = 0$), and the other representing the moment due to the thrust H. Hence

$$M = M_0 - Hy, \tag{j}$$

where y denotes the ordinates of the axis of the arch as shown in the figure. For a flat arch, the axial force N can be assumed, with good accuracy, as equal to the thrust H. Then

$$U \approx \int_0^s \frac{(M_0 - Hy)^2 ds}{2EI} + \int_0^s \frac{H^2 ds}{2AE}.$$

Substituting this expression in Eq. (h), we obtain

$$-\int_0^s \frac{(M_0 - Hy)y\, ds}{EI} + \int_0^s \frac{H\, ds}{AE} = 0,$$

from which

$$H = \frac{\displaystyle\int_0^s \frac{M_0 y \, ds}{EI}}{\displaystyle\int_0^s \frac{y^2 ds}{EI} + \int_0^s \frac{ds}{AE}}. \tag{k}$$

This is a general formula from which H can be calculated if the loading and the dimensions of the arch are given.

In the case of an arch of homogeneous material and uniform cross section, E, I, and A are constants and can be taken from under the integral signs. Then

$$H = \frac{\displaystyle\int_0^s M_0 y \, ds}{\displaystyle\int_0^s y^2 ds + i^2 \int_0^s ds}, \tag{l}$$

where i denotes the radius of gyration of the cross section with respect to its centroidal axis. The second term in the denominator represents the influence of the direct stress on the magnitude of H. If this influence is neglected, we obtain

$$H = \frac{\displaystyle\int_0^s M_0 y \, ds}{\displaystyle\int_0^s y^2 ds}. \tag{m}$$

An especially simple expression for H is obtained in the case of a parabolic arch under the action of a load uniformly distributed along the horizontal span. In such a case

$$y = \frac{4fx}{l^2}(l - x),$$

$$M_0 = \frac{qx}{2}(l - x).$$

Then, substituting into Eq. (m), we obtain

$$H = \frac{ql^2}{8f},$$

where f is the vertical rise as shown in the figure.

PROBLEMS

207. Find, by using the principle of least work, the bending moments M_a and M_b at the ends of a uniformly loaded beam with built-in ends and of uniform flexural rigidity EI. *Ans.* $M_a = M_b = -\, ql^2/12$.

208. Solve the preceding problem if the intensity of load along the length of the beam varies according to the linear law $q = q_0 x/l$.
Ans. $M_a = -q_0 l^2/30$, $M_b = -q_0 l^2/20$.

209. Referring to Fig. 313a, calculate the reactive moment M_b if, instead of the uniform loading shown, the beam carries an isolated load P at the distance c from A.

210. If, instead of the uniform loading shown in Fig. 313a, the beam AB is subjected to an active moment M_a at the end A, show by the method of least work that the corresponding moment induced at B will be $M_b = -M_a/2$.

211. Considering only strain energy of bending, calculate the horizontal thrust H in the case of a two-hinged semicircular arch rib of span l that carries a vertical load P at the crown. Assume a uniform flexural rigidity EI of the rib. *Ans.* $H = P/\pi$.

43. The Reciprocal Theorem.—Let us begin with a simple example, the bending of a cantilever beam, and consider two loading conditions,
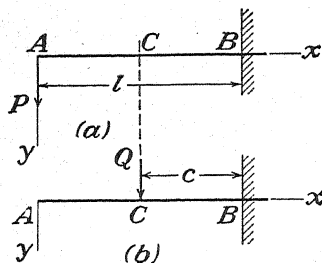
Fig. 318.

(1) a load P at the free end (Fig. 318a) and (2) a load Q at any point C (Fig. 318b). In the first case, the deflection curve is represented by the equation[1]

$$\delta_c = \frac{Pc^2}{6EI}(3l - c). \qquad (a)$$

In the second case the deflection at C is calculated as for a cantilever of length c and is equal to $Qc^3/3EI$. The part AC of the beam remains straight and is tangent to the deflection curve at C so that it has the slope $Qc^2/2EI$. Thus the total deflection at point A in this case is

$$\delta_a = \frac{Qc^3}{3EI} + \frac{Qc^2}{2EI}(l - c) = \frac{Qc^2}{6EI}(3l - c). \qquad (b)$$

Comparing expressions (a) and (b), we see that when $P = Q$ these two deflections are equal, *i.e.*, a load P, placed at point A, produces at point C the same deflection as the load P, placed at C, produces at point A.* In a more general case when P and Q are not equal, the deflections (a) and (b) are no longer equal, but the work done by the force P on the corresponding displacement (b) is equal to the work done by the force Q on the corresponding displacement (a), *i.e.*,

$$P\delta_a = Q\delta_c.$$

Let us consider now a general case of an elastic body subjected to two different conditions of loading. In the first case there act forces P_1 and P_2 (Fig. 319a), and in the second case the forces P_3 and P_4 (Fig. 319b). We shall designate the displacements of the points 1, 2, 3, and 4 in the directions of the forces for the first condition of loading by δ_1', δ_2', δ_3', and δ_4' and for the second condition of loading by δ_1'', δ_2'', δ_3'', and δ_4''. Assume, now, that all four forces are acting on the body

---

[1] See "Strength of Materials," vol. I, p. 148.

* This conclusion was obtained by J. C. Maxwell in considering deformation of trusses; see his "Scientific Papers," vol. I, p. 602.

simultaneously and that the principle of superposition holds. Then the displacements of points 1, 2, . . . corresponding to the forces $P_1, P_2, \ldots$ are obtained by superposition and are equal to $\delta_1' + \delta_1''$, $\delta_2' + \delta_2''$, ... The total strain energy stored in the body is

$$U = \tfrac{1}{2}[(\delta_1' + \delta_1'')P_1 + (\delta_2' + \delta_2'')P_2 + (\delta_3' + \delta_3'')P_3$$
$$+ (\delta_4' + \delta_4'')P_4]. \quad (c)$$

This amount of strain energy does not depend on the order in which the loads are applied. Let us assume, for example, that the loads P_1
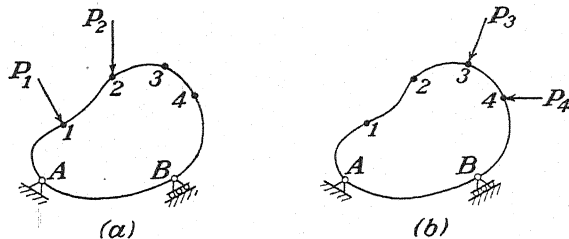
Fig. 319.

and P_2 are applied first. Then the corresponding amount of strain energy is

$$\tfrac{1}{2}(P_1\delta_1' + P_2\delta_2'). \quad (d)$$

Let us apply, now, the loads P_3 and P_4. Since the principle of superposition holds, the displacements produced during the application of P_3 and P_4 will not be affected by the presence of the previously applied loads P_1 and P_2 and will be equal to δ_1'', δ_2'', δ_3'', and δ_4'' as before. The work done by P_3 and P_4 during their gradual application will be

$$\tfrac{1}{2}(P_3\delta_3'' + P_4\delta_4''). \quad (e)$$

At the same time, the previously applied loads P_1 and P_2 will produce work, on the displacements δ_1'' and δ_2'', equal to

$$P_1\delta_1'' + P_2\delta_2''. \quad (f)$$

(a)

(b)

Fig. 320.

Upon summing up expressions (d), (e), and (f), the total amount of strain energy is obtained. Equating this energy to expression (c), we obtain

$$P_1\delta_1'' + P_2\delta_2'' = P_3\delta_3' + P_4\delta_4'. \quad (28)$$

This equation states that the work done by the forces of the first state of loading (Fig. 319a) on the corresponding displacements of the second state (Fig. 319b) is equal to the work done by the forces of the second
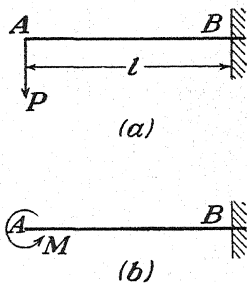
state on the corresponding displacements of the first. This represents the so-called *reciprocal theorem*.[1]

The foregoing derivation of the reciprocal theorem holds also in the case of generalized forces. As an example, let us consider the two conditions of loading of the cantilever beam shown in Fig. 320. In the case of the load P applied at the end, the rotation of the end A is

$$\theta_a = \frac{Pl^2}{2EI}.$$

Likewise, the deflection at A under the action of the couple M is

$$\delta_a = \frac{Ml^2}{2EI}.$$
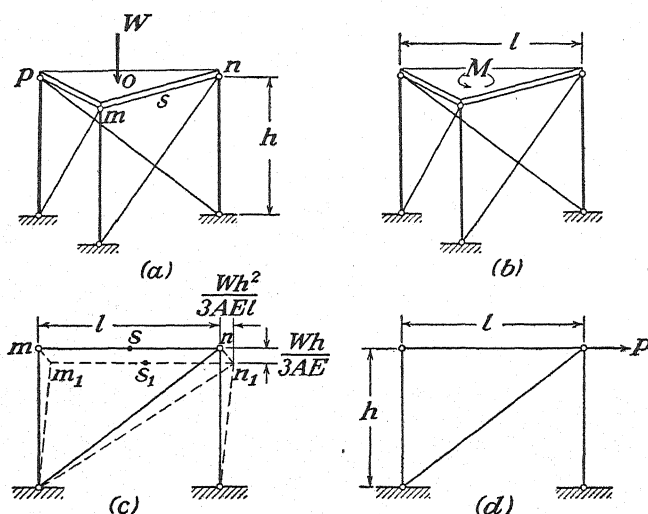
FIG. 321.

It is seen that these values of θ_a and δ_a satisfy the reciprocal theorem, *i.e.*,

$$M\theta_a = P\delta_a.$$

As another example, let us consider the case of a rigid slab having the form of an equilateral triangle supported by three vertical and three inclined bars of equal cross-sectional areas A and hinged at the ends (Fig. 321). In one case, the slab is loaded by W at the center (Fig. 321a), and in another case it is loaded by a couple M acting in the plane of the slab (Fig. 321b). Owing to the action of the load W, the vertical bars will be compressed by the amount $Wh/3AE$; and since the lengths of the diagonals remain unchanged, the compression of the vertical bars

---

[1] In its general form the reciprocal theorem has been proved by E. Betti, *Nuovo cimento*, ser. 2, vols. 7 and 8, 1872. See also Lord Rayleigh's paper in *Proc. London Math. Soc.*, vol. 4, pp. 357–368, 1873.

will be accompanied by lateral distortions in the side planes of the structure as shown in Fig. 321c. Consequently there will be rotation of the slab. In calculating the angle of rotation θ, we observe that the middle point s_1 between the hinges m_1 and n_1 moves along $m_1 n_1$ by the amount $Wh^2/3AEl$, and the angle of rotation of the slab is obtained by dividing this displacement by the distance $l/2\sqrt{3}$ of the point s from the center O of the slab (Fig. 321a). This gives

$$\theta = \frac{Wh^2}{3AEl} \cdot \frac{2\sqrt{3}}{l} = \frac{2Wh^2}{AE\sqrt{3}l^2}. \tag{g}$$

As a result of the loading shown in Fig. 321b, we shall obtain not only rotation of the slab but also some vertical movement. To proceed with this case, we first replace the torque M by a statically equivalent system of three equal forces P coinciding with the three edges of the triangular slab. Then, since

$$3P \cdot \frac{l}{2\sqrt{3}} = M,$$

we have

$$P = \frac{2M}{l\sqrt{3}}.$$

Now each of these three forces P produces a compressive force Ph/l in the corresponding vertical bar as shown in Fig. 321d. Hence the vertical displacement δ of the slab will be

$$\delta = \frac{Ph^2}{lAE} = \frac{2Mh^2}{l^2AE\sqrt{3}}. \tag{g'}$$

Considering the rotation (g) in the first case of loading and the vertical displacement (g') in the second case, we see that the reciprocal theorem is satisfied, *i.e.*,

$$M\theta = W\delta.$$

The reciprocal theorem is especially useful in the construction of influence lines for redundant reactions. Let us consider, for example, a beam on three supports as shown in Fig. 322a and investigate the change in the redundant reaction Y_c at the intermediate support with change of the distance x defining the position of a moving load P. In applying the reciprocal theorem, we have always to compare two conditions of loading of the given structure. As the first state, we take the actual loading, shown in Fig. 322a; as a second state, we select the fictitious loading shown in Fig. 322b, where the load P is removed and in place of the reaction Y_c a unit force acts. This second state is statically determinate, and we

can find the deflection curve ACB. For the left portion of the beam the deflection is[1]

$$y = \frac{1 \cdot l_2 \cdot x}{6(l_1 + l_2)EI} [(l_1 + l_2)^2 - l_2^2 - x^2]. \tag{h}$$

A similar expression can be established for the right portion. The deflection under the unit load is obtained by substituting $x = l_1$ in Eq. (h), which gives

$$\delta_c = \frac{1 \cdot l_1{}^2 \cdot l_2{}^2}{3(l_1 + l_2)EI}. \tag{i}$$

Applying now the reciprocal theorem, we calculate first the work done by the forces of Fig. 322a on the corresponding displacements of Fig. 322b. Such work evidently is

$$Y_c\delta_c - Py.$$
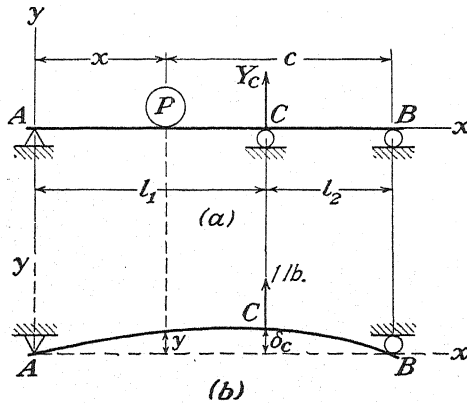
Fig. 322.

Considering now the work of the forces of Fig. 322b on the corresponding displacements of Fig. 322a, we find that this work is zero since, for the unit load in Fig. 322b, the corresponding deflection in Fig. 322a is zero. Hence the reciprocal theorem gives

$$Y_c\delta_c - Py = 0,$$

from which

$$Y_c = \frac{Py}{\delta_c} = \frac{3P(l_1 + l_2)EI}{l_1{}^2l_2{}^2} y. \tag{j}$$

It is seen that when the load P is moving along the beam AB the reaction at C varies in the same proportion as the ordinates y of the deflection curve ACB calculated for a unit load at C. Thus this deflection curve can be taken as the *influence line* for the reaction Y_c. Having such an

[1] See "Strength of Materials," vol. I, p. 142.

influence line, the reaction Y_c for any system of vertical loads P_1, P_2, P_3, . . . can be found in the usual way from the equation

$$Y_c = \frac{1}{\delta_c} (P_1 y_1 + P_2 y_2 + P_3 y_3 + \cdot \cdot \cdot)$$

where y_1, y_2, . . . are the ordinates of the influence line ACB corresponding to the forces P_1, P_2, ...

If we desire an influence line for bending moment M_c at the intermediate support C of the beam in Fig. 322a, we first cut the beam at this section and introduce the equal and opposite couples M_c as shown in
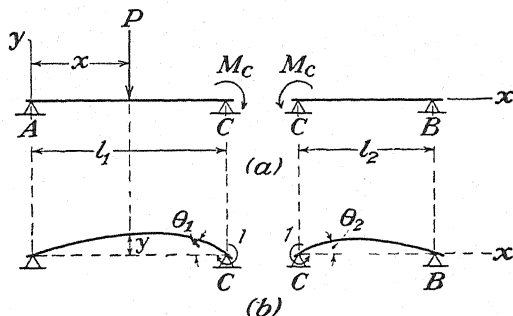
FIG. 323.

Fig. 323a. The corresponding fictitious loading is shown in Fig. 323b. Now, using the reciprocal theorem, we find

$$M_c(\theta_1 + \theta_2) - Py = 0,$$

from which

$$M_c = P \frac{y}{\theta_1 + \theta_2}.$$

Upon substituting the known expressions for y, θ_1, and θ_2, the influence coefficient for the left span becomes

$$\frac{x(l_1{}^2 - x^2)}{2l_1(l_1 + l_2)}. \tag{k}$$

The same expression can be used for the right span if we interchange the subscripts of l_1 and l_2 and measure x from B.

If the derivation of an analytical expression for the influence line is not practicable as in the preceding examples, the line can always be obtained experimentally by making a test with a model of the actual structure. Suppose, for example, that we desire an influence line for the thrust H of the two-hinged arch shown in Fig. 324a. In the fictitious state of loading (Fig. 324b), we make the support B movable and apply to the arch two equal and opposite unit forces as shown. Let δ be the horizontal displacement of the support B produced in this fictitious case and y the vertical deflection of point C. Then the application of the reciprocal theorem gives

$$H\delta - Py = 0,$$

from which

$$H = \frac{Py}{\delta}. \tag{l}$$

This result is similar to that in Eq. (j) obtained for the previous problem. Hence we can state that the ratios y/δ for the case shown in Fig. 324b represent the influence coefficients for the thrust H. It is evident that, by making a model of the arch and loading it as shown in Fig. 324b, the influence coefficients can be obtained from the measured deflections y and δ.

FIG. 324.

The experimental determination of influence lines may be of practical interest in those cases where we have many redundant indeterminate quantities. Take, for example, the rectangular frame built-in at the supports as shown in Fig. 325a. This is a structure with three redundant constraints. Removing the support at the right end and replacing it by reactive forces, we obtain the three statically indeterminate quantities H, V and M_b as shown. To obtain for each of these quantities an influence line by experiment, we use a model of the frame and give in each case to the end B of the model a displacement *corresponding* to the force that we are planning to determine. If we are interested, for example, in the reaction H, we give to the end B of the model a horizontal displacement δ and at the same time by proper constraints we prevent the cross section from both vertical and angular displacement. In this manner we obtain the deformation shown in Fig. 325b. Let H', V' and M_b' be the forces which we apply
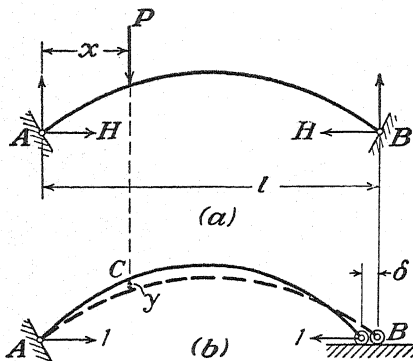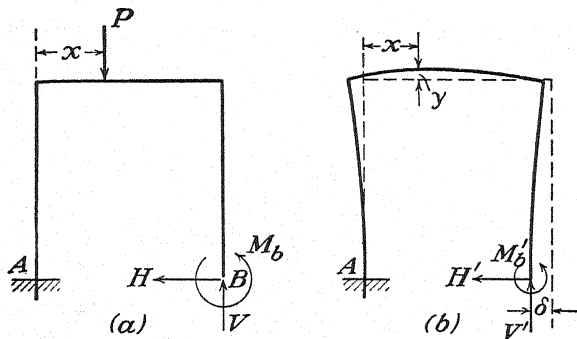
FIG. 325.

to the model at B to realize the above-described displacement. Now, applying the reciprocal theorem to the loading conditions shown in Figs. 325a and 325b and observing that only those displacements in the fictitious state (Fig. 325b) corresponding to the actual forces P and H are different from zero and that the displacements in Fig. 325a corresponding to the forces H', V' and M_b' all are zero, we obtain

$$H\delta - Py = 0,$$

from which

$$H = \frac{Py}{\delta}.$$

Again the influence coefficients for H are obtained by dividing the deflections y by the displacement δ, and all these quantities can be measured in making the experiment with the model. Influence lines for V and M_b can be obtained in a similar manner. To get the influence line for V, we have to give to the end B of the model a vertical displacement and at the same time prevent any horizontal or rotational displacement. In the case of M_b we must give to the end B a rotation and at the same time prevent any horizontal or vertical motion. The measurements of deflections in these two cases give the information required for calculating the ordinates of the required influence lines.[1]

PROBLEMS

212. Derive the equation of the influence line for the reaction at B of the continuous beam in Fig. 322a, and find, by using this influence line, the maximum and minimum magnitudes of R_b.

213. Referring again to the beam in Fig. 322a and using expression (k), find the maximum bending moment M_c at the intermediate support if $l_1 = 40$ ft., $l_2 = 20$ ft., $P = 1,000$ lb. *Ans.* $(M_c)_{max.} = 5,125$ ft.-lb.

214. Construct an influence line for the axial force in the strut CD of the trussed beam shown in Fig. 326. Neglect the effect of changes in length of the bars, and consider only bending of the beam ACB.
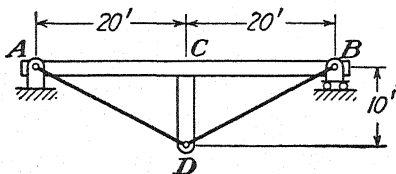
FIG. 326.
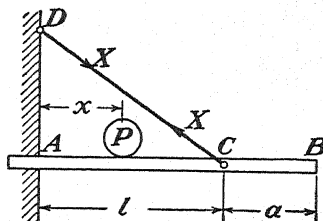
FIG. 327.

215. Construct the influence line for the tension X in the tie rod DC of the statically indeterminate system shown in Fig. 327. As in the preceding problem, neglect the deformations due to axial forces, and consider only bending.

216. Using the reciprocal theorem, derive an expression for the influence coefficient for the end moment M_a in the case of a beam AB with built-in ends. Where should a load P be placed on such a beam to produce the maximum end moment?

$$Ans. \quad -\frac{l^2x - 2lx^2 + x^3}{l^2}, \; x = \frac{l}{3} \text{ for maximum } M_a.$$

[1] Special apparatus, known as *Begg's deformator gauges*, are available for controlling the deformations of models. For a description of these instruments, see *J. Franklin Inst.*, 1927.

CHAPTER VI

DEFLECTION OF PIN-JOINTED TRUSSES

44. Applications of Castigliano's Theorem.—Castigliano's theorem, discussed in Art. 41, can be used to advantage in studying the deflections of trusses, especially if the displacements of only a few joints are required.

(a)

(b)

FIG. 328.

Consider, for example, the simple truss shown in Fig. 328a to which the vertical loads P, Q, and R are applied, and assume that it is required to determine the vertical deflection of the middle joint B of the lower chord. For this purpose, we must derive an expression for the strain energy of the truss as a function of the given loads P, Q, R and then calculate the partial derivative of this expression with respect to the force Q acting at joint B. The expression for strain energy in the case of a statically determinate pin-jointed truss is a very simple one. Let S_i be the force in any bar i due to the actual loading (Fig. 328a). Then the strain energy stored in this bar is

$$\frac{S_i^2 l_i}{2A_i E}, \tag{a}$$

where l_i is the length and A_i the cross-sectional area of the bar. Summing up expressions (a) for all bars of the truss, we obtain[1]

$$U = \sum \frac{S_i^2 l_i}{2A_i E}. \tag{29}$$

In calculating the partial derivative with respect to the load Q, we observe that in expression (29) only the quantities S_i depend upon Q. Hence ordinary differentiation gives the required deflection in the following form:

$$\delta = \frac{\partial U}{\partial Q} = \sum \frac{S_i l_i}{A_i E} \cdot \frac{\partial S_i}{\partial Q}. \tag{b}$$

[1] It is assumed that the material of all bars is the same and that the modulus E is constant.

258

Observing that the derivative $\partial S_i/\partial Q$ in this expression is the rate of change of the force S_i in any member i with respect to the load Q, we can determine the magnitude of this derivative in a very simple manner by considering the action on the truss of the unit load shown in Fig. 328b. Denoting by s_i' the force produced in any bar i by this unit load, the magnitude of the derivative $\partial S_i/\partial Q$ is evidently equal to the ratio $s_i':1$, and expression (b) for the deflection δ can be written in the following form,

$$\delta = \sum \frac{S_i l_i}{A_i E} \cdot s_i', \tag{30}$$

in which the factor $S_i l_i/A_i E$ in each term represents the elongation of the bar i under the *actual loading* and s_i' is an abbreviation for the ratio $s_i':1$, obtained for each bar from the fictitious loading shown in Fig. 328b.[1] Since, in this case, the truss is statically determinate, the calculations of the quantities S_i and s_i' can be made without difficulty and the deflection δ can then be calculated from Eq. (30) provided that the dimensions of the bars and the modulus E are given.

TABLE V

(1)	(2)	(3)	(4)	(5)	(6)	(7)	(8)
i	l_i, in.	A_i, in.²	S_i, lb.	s_i'	$\dfrac{S_i s_i' l_i}{A_i 10^3}$	$s_i'' l_6$	$\dfrac{S_i l_i}{A_i} \cdot s_i''$
1	250	6	$-27{,}500$	-0.625	716.0	0.625	$-2{,}387$
2	150	3	$16{,}500$	0.375	309.4	-0.375	$-1{,}031$
3	200	2	$16{,}000$	0	0	0	0
4	150	3	$16{,}500$	0.375	309.4	-0.375	$-1{,}031$
5	250	2	$7{,}500$	0.625	585.9	0.625	$1{,}953$
6	300	4	$-21{,}000$	-0.750	118.1	0	0
7	250	2	$12{,}500$	0.625	976.6	-0.625	$-3{,}255$
8	150	3	$13{,}500$	0.375	253.1	0.375	844
9	200	2	$8{,}000$	0	0	0	0
10	250	6	$-22{,}500$	-0.625	585.9	-0.625	$1{,}953$
11	150	3	$13{,}500$	0.375	253.1	0.375	844

Assuming, for example, $P = Q = 16{,}000$ lb., $R = 8{,}000$ lb., and taking the lengths of the bars from column (2) of Table V, we obtain for S_i and s_i' the values shown in columns (4) and (5), respectively, of the table. Using now the cross-sectional areas, given in column (3), the figures in column (6) are obtained. The sum of this last column, multiplied by 10^3 and divided by the modulus E, gives the required deflection

---

[1] In our further discussion, we shall always denote the ratio $s_i':1$ simply as s_i', but it should be kept in mind that when so used it must be considered as a pure number, which will be called the *influence number* for the bar i.

δ as shown by Eq. (30). Assuming that the truss is of structural steel and taking $E = 30 \cdot 10^6$ lb. per sq. in., we obtain

$$\delta = \frac{4{,}108 \cdot 10^3}{30 \cdot 10^6} = 0.1369 \text{ in.}$$

The calculations in Table V are made with four significant figures; but calculations with three significant figures, as given by an ordinary slide rule, will have sufficient accuracy for practical purposes.

If the horizontal displacement of the joint B is required, we proceed as explained in Art. 41 and add to the actual loads P, Q, R an infinitesimal force T acting in the direction corresponding to the required displacement (Fig. 329a). Then the derivative $\partial U/\partial T$ gives the required horizontal displacement as follows:

(a)

(b)

Fig. 329.

$$\delta = \sum \frac{S_i l_i}{A_i E} \frac{\partial S_i}{\partial T}. \qquad (c)$$

Since T is an infinitesimal force, the values of S_i are the same as those already recorded in column (4) of Table V. The values of the derivatives $\partial S_i/\partial T$, representing the rates of change of the forces S_i with respect to the force T, are obtained from the loading condition shown in Fig. 329b. For this latter condition of loading, only the bars 2 and 4 are active. Hence in expression (c) only two terms are different from zero, and we obtain for the required horizontal displacement
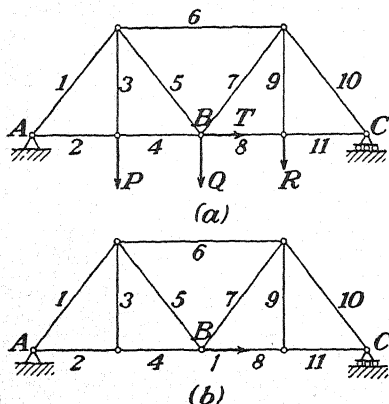
$$\delta = \frac{S_2 l_2}{A_2 E} + \frac{S_4 l_4}{A_4 E} = 2 \cdot \frac{16{,}500 \cdot 150}{3 \cdot 30 \cdot 10^6} = 0.055 \text{ in.,}$$

which is evidently equal to the sum of the elongations of the bars 2 and 4.

Sometimes we have to find the angles of rotation of certain members of a truss during deflection. These angles can also be calculated by using Castigliano's theorem. To illustrate the procedure of such calculation, let us consider again the truss shown in Fig. 328a and find the angle of rotation of the bar 6 produced by the loads P, Q, and R. The generalized force corresponding to this rotation is the couple M applied as shown in Fig. 330a. This follows from the fact that such a group of forces produces work only during rotation of the bar 6 in the plane of the figure. If this bar moves parallel to itself or elongates, keeping its direction unchanged, the work of two such equal and opposite forces perpendicular

to the axis of the bar vanishes.   Since the generalized force M corresponds to rotation of the bar 6, we obtain the angle of rotation by calculating the partial derivative $\partial U/\partial M$.   Upon substituting for U its expression (29), the angle of rotation becomes

$$\theta = \frac{\partial U}{\partial M} = \sum \frac{S_i l_i}{A_i E} \cdot \frac{\partial S_i}{\partial M}. \qquad (d)$$

Assuming that the couple M is infinitesimal, the forces S_i will have the same values as before and are given in column (4) of Table V.   The derivatives $\partial S_i/\partial M$, representing the rates of change of the forces S_i with respect to the couple M, are obtained by applying to the truss the couple equal to unity as shown in Fig. 330b and then calculating the forces s_i'' produced in the members of the truss by this couple.   Thus

$$\frac{\partial S_i}{\partial M} = \frac{s_i''}{1}.$$

FIG. 330.

Since the right side of this equation has the dimension of force divided by moment of force, the partial derivatives $\partial S_i/\partial M$ have the dimension of *length*$^{-1}$, and the angle θ as obtained from expression (d) is a pure number.

Instead of the loads $1/l_6$ as shown in Fig. 330b, it is simpler to use unit loads, as before, and then divide corresponding axial forces $s_i'' \cdot l_6$ by the length l_6 to obtain the numerical values of the derivatives $\partial S_i/\partial M$. For the numerical data already assumed, the values of $s_i'' l_6$ calculated for unit loads instead of $1/l_6$ as shown in Fig. 330b are given in column (7) of Table V.   By using this column together with columns (2), (3), and (4), the numbers in column (8) are calculated.   Summing up these numbers and dividing by E, we obtain, from Eq. (d), the required value of the angle of rotation θ.   For structural steel this value is

$$\theta = \frac{1}{E} \sum \frac{S_i l_i}{A_i} s_i'' = -\frac{2,110}{30 \cdot 10^6} = -70.3 \cdot 10^{-6} \text{ radian} \qquad (e)$$

The minus sign indicates that the bar 6 rotated in the direction opposite to the direction of the unit couple in Fig. 330b.

In the foregoing calculation of the angle of rotation, the notion of generalized force was used.   The same result can be obtained by calculating the vertical deflections of the ends of the bar 6 and dividing their

algebraic sum by the length l_6. If this latter method is used, we have to add to the given loads P, Q, and R the infinitesimal forces N and T as shown in Fig. 331a. Then the required angle of rotation is

$$\theta = \frac{1}{l_6}\left(\frac{\partial U}{\partial N} + \frac{\partial U}{\partial T}\right) = \frac{1}{l_6}\sum \frac{S_i l_i}{A_i E}\left(\frac{\partial S_i}{\partial N} + \frac{\partial S_i}{\partial T}\right). \qquad (f)$$

Observing that the derivatives on the right side of expression (f) are obtained by using the loadings shown in Fig. 331b and Fig. 331c and that the superposition of these two loadings divided by l_6 gives the loading shown in Fig. 330b, we conclude that the parenthesis on the right side of Eq. (f) divided by l_6 is equal to s_i''. Hence expression (f) is identical with expression (e).

Castigliano's theorem can be used also to calculate the change in dis-
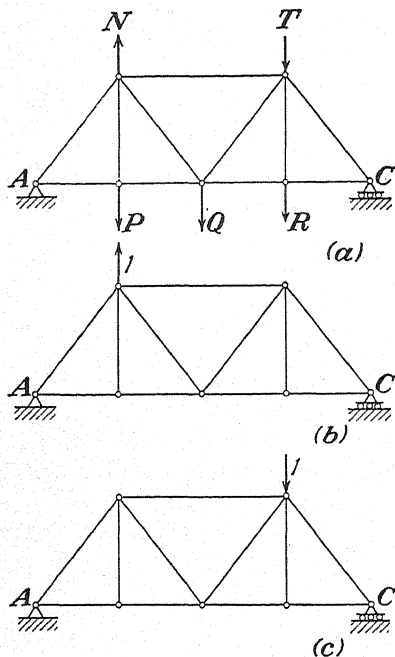
FIG. 331.
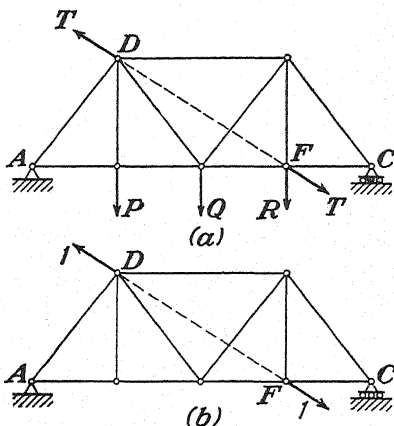
FIG. 332.

tance between two joints of a truss during deflection. Assume, for example, that it is required to find the change in distance between the joints D and F (Fig. 332a) produced by the action of loads P, Q, and R. The generalized force corresponding to this change in distance is evidently a group of two equal and opposite forces T applied at D and F and acting along the line DF as shown. Castigliano's theorem then gives

$$\delta = \frac{\partial U}{\partial T} = \sum \frac{S_i l_i}{A_i E}\cdot\frac{\partial S_i}{\partial T}. \qquad (g)$$

Assuming again that T is an infinitesimal force, the forces S_i are those produced by the actual loads P, Q, and R. The values of the derivatives

$\partial S_i/\partial T$ are obtained by calculating the forces produced in the truss members by unit forces acting as shown in Fig. 332*b*.

If it is required to find the change θ of the angle between the bars 6 and 10 produced by the loads P, Q, and R, we note that the generalized force corresponding to this angular displacement consists of two equal and opposite couples M acting as shown in Fig. 333*a*. It is evident that this group of forces produces work only if the angle DEC changes. The required change in the angle is now obtained by application of Castigliano's theorem, which gives

$$\theta = \frac{\partial U}{\partial M} = \sum \frac{S_i l_i}{A_i E}\frac{\partial S_i}{\partial M}. \quad (h)$$

The forces S_i in this expression are those produced by the actual loads P, Q, and R. The partial derivatives $\partial S_i/\partial M$ are numerically equal to the axial forces induced in the

Fig. 333.

members by the two equal and opposite unit couples acting as shown in Fig. 333*b*.
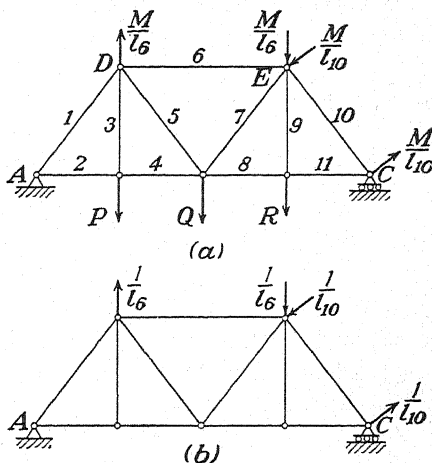
PROBLEMS

217. Using Castigliano's theorem, determine the vertical and horizontal displacements of the joint A of the simple truss shown in Fig. 334. Assume, in calculation, that all bars have the same cross-sectional area $A_i = 1$ sq. in. and the same modulus $E = 30(10)^6$ lb. per sq. in. $P = 1,000$ lb., and $a = 8$ ft.
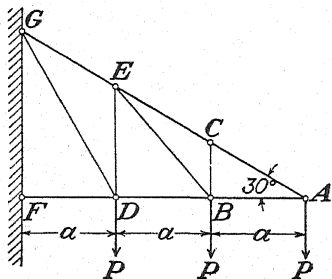
Fig. 334.
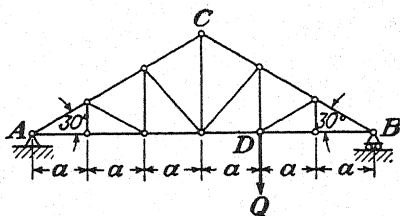
Fig. 335.

218. Referring to Fig. 335 and assuming $Q = 1,000$ lb., find the vertical deflection δ_d of the joint D if $E = 30(10)^6$ lb. per sq. in., $A_i = 2$ sq. in. for each bar, and $a = 10$ ft.

219. Using the same numerical data as in the preceding problem, calculate the change in the 30-deg. angle at A, due to the action of the load $Q = 1,000$ lb.

220. Calculate the vertical deflection δ_l of the joint L of the simple truss shown in Fig. 336, if $P = 1,000$ lb., $A_i = 1$ sq. in. for each bar, and $E = 10(10)^6$ lb. per sq. in. The squares $IJLK$, etc., have sides of length $a = 4$ ft.

Fig. 336.

221. Using the same numerical data as in the preceding problem, calculate the change in length of the diagonal IF of the middle square, due to the action of the load P. In the same manner, find the change in length of the distance BL.

222. Using again the numerical data given in Prob. 220, evaluate the change $\delta\theta$ in the right angle IKL, due to the applied load P.

45. Maxwell-Mohr Method of Calculating Deflections.[1]—To explain this method, let us consider the truss shown in Fig. 337a and calculate the vertical deflection δ of a joint C produced by the given loads P and Q. This deflection can be obtained as the sum of the small deflections due to deformations of single bars of the truss. To find the deflection at C due to the elongation of one single bar,[2] say bar CD, let us consider the
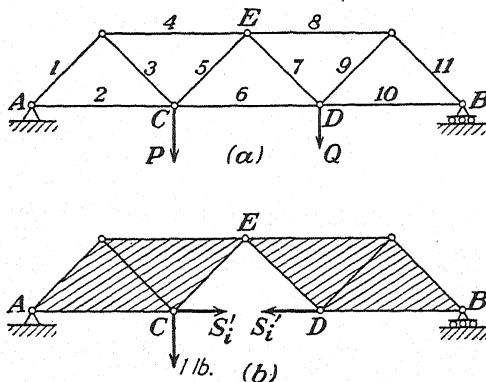
Fig. 337.

system shown in Fig. 337b. The bar CD is removed, and instead of the actual loads only a unit load is acting at joint C. In this way we obtain a movable system consisting of the two rigid portions, shaded in the figure, which can rotate with respect to each other. To ensure the equilibrium of this system the forces s_i' must be added. These forces

---

[1] The method was developed by Maxwell in a paper published in *Phil. Mag.*, vol. 27, 1864. This paper did not come to the attention of engineers, and 10 years later in a paper published in *Z. Architekten-Ingenieur-Ver.*, 1874, p. 223, O. Mohr developed the same method by using another way of reasoning. Since Mohr's work was done independently of Maxwell's and since the method was accepted by engineers only after numerous applications shown by Mohr, it is customary to call it the *Maxwell-Mohr method*.

[2] The other bars are considered as rigid and their lengths unchanged.

are replacing the action of the removed bar CD on the shaded portions of the truss and evidently are equal to the force produced in that bar by the unit load at joint C. We now have a simple geometrical problem, to find the deflection $\Delta\delta$ of the joint C resulting from the movement of the system by which the distance between the joints C and D increases by a small amount δ_i'. To solve this problem, we use the principle of virtual displacements. Since the unit force at C and the forces s_i' together with the reactions at the supports represent a system of forces in equilibrium, their work on the foregoing assumed small displacements must vanish; hence,

$$1 \cdot \Delta\delta - s_i'\delta_i' = 0. \qquad (a)$$

The reactions at the supports do not enter in this equation. They do not produce work since the support A does not move and the support B moves perpendicularly to the reaction at B. From Eq. (a), we obtain

$$\Delta\delta = \delta_i' \cdot \frac{s_i'}{1}. \qquad (b)$$

Thus we see that the deflection of the joint C is obtained by multiplying the change of distance δ_i' between the joints C and D by the ratio $s_i'/1$. Having this relation, we proceed now with the actual case of loading shown in Fig. 337a. Our previous notations being used, the elongation of a bar number i, which is the bar CD in our case, is S_il_i/A_iE. From the relation (b), we now conclude that the deflection of joint C due to the elongation of the bar i is

$$\frac{S_il_i}{A_iE} \cdot \frac{s_i'}{1}. \qquad (c)$$

Proceeding in the same way with all other bars and summing up the corresponding small deflections,[1] we obtain the actual deflection of the joint C in the following form:

$$\delta = \sum \frac{S_il_i}{A_iE} \cdot s_i' = \sum \Delta l_i \cdot s_i'. \qquad (d)$$

It is seen that, for the determination of the deflection of any joint of a truss, we need to find the elongations Δl_i of all members of the truss under the actual load (Fig. 337a) and the forces s_i' produced in the same members by a unit load applied at the joint the deflection of which we have to find (Fig. 337b). Both these calculations can be easily performed in the case of a statically determinate truss and can be presented in tabular form as was done in the previous article (see Table V, page 259).

[1] It is assumed that the principle of superposition holds for the small deformations produced in actual trusses.

Comparing expression (*d*) with expression (30), we see that the Maxwell-Mohr method gives the deflections in the form already obtained by applying Castigliano's theorem. This second derivation is given here because it makes it easier to grasp the purely geometrical character of the problem. It is evident that expression (*d*) holds independently of what causes the changes Δl_i in the lengths of the bars. Sometimes we have to consider the elongations of bars due to a rise in temperature from some specified temperature. If α_i is the coefficient of thermal expansion and t_i is the temperature increase, the corresponding elongation of the bar is $\alpha_i t_i l_i$. Sometimes the length of a bar can be changed by using some mechanical device such as a turnbuckle. The effect of such a change on the deflection of a truss can also be calculated from Eq. (*d*), provided that the change in length Δ_i is known. Superposing deflections produced in a truss by various causes, we can write expression (*d*) in a more general form,

$$\delta = \sum \left(\frac{S_i l_i}{A_i E} + \alpha_i t_i l_i + \Delta_i \right) s_i', \tag{31}$$

in which not only elastic elongations of the bars but also elongations due to temperature changes and elongations produced by some special devices are considered.

Sometimes it is required to find not only deflections due to changes in the lengths of the bars of a truss but also deflections produced by some small movements of the supports. These additional deflections can be readily found from Eq. (31). We assume only that the hinges at the supports are attached to an immovable foundation by some fictitious bars, the changes in length of which are chosen in correspondence with the known displacements of the supports. Including these fictitious bars in the summation shown by expression (31), we automatically take into account the effect on the deflections of the known movements of the supports. For example, let us consider an unsymmetrical arch with three hinges (Fig. 338*a*) and calculate the horizontal displacement of the upper hinge *C* produced by the loads $P_1 \ldots P_4$, a uniform increase in temperature *t*, and the small movements of the supports the components ξ_1, η_1 and ξ_2, η_2 of which are shown to an enlarged scale in the figure. Assuming that each of the hinges *A* and *B* is attached to an immovable foundation by two fictitious bars, one vertical and one horizontal, we can consider that ξ_1, η_1 and ξ_2, η_2 represent the small shortening of these bars. Now, considering the same arch again, we assume that a horizontal unit load is applied at the upper hinge *C* (Fig. 338*b*) and calculate the reactions V_1, H_1, V_2, H_2 and the forces s_i' in the bars produced by this load. Applying, now, expression (31), we obtain the following value of the horizontal displacement of the hinge *C*:

$$\delta = \sum \left(\frac{S_i l_i}{A_i E} + \alpha t l_i \right) s_i{}' + \xi_1 H_1 + \eta_1 V_1 - \xi_2 H_2 - \eta_2 V_2.$$

The summation in this expression includes all actual bars of the arch, and the last four terms correspond to the four fictitious bars. Since these bars are placed in such a manner that the displacements ξ_1, η_1, ξ_2, η_2 represent shortenings of the bars, we take all these displacements with negative signs. We take also with negative signs the reactions H_1 and
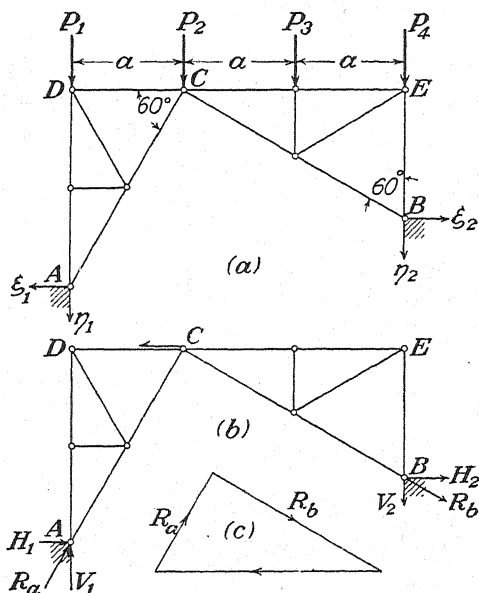
FIG. 338.

V_1 since, from the directions of these reactions in Figs. 338b and 338c, we conclude that they represent compressive forces in the fictitious bars.

PROBLEMS

223. Referring to the truss in Fig. 114 (page 67), calculate the vertical deflection of the hinge C if the load $P = 1,000$ lb. and $a = 5$ ft. Assume $E = 10(10)^6$ lb. per sq. in. and $A_i = 1$ sq. in. for each bar. How will this deflection be changed if the support at B settles 0.1 in.?

224. Referring to the truss in Fig. 118a (page 69) and assuming a span of 60 ft., calculate the vertical deflection δ of the middle joint of the bottom chord. Assume $P = 1,000$ lb. and steel bars each having a cross-sectional area $A_i = 1$ sq. in. In the vertical bar there is a turnbuckle with a thread pitch $h = \frac{1}{8}$ in. How many turns must be given to this turnbuckle to bring the middle joint of the bottom chord back up to the level of the supports?

225. Calculate the vertical movement of the hinge C of the three-hinged arch in Fig. 338a produced by a uniform rise in temperature of 70°F. Assume that all bars are of steel for which $\alpha = 0.0000065$ in. per in. per °F. and that $a = 10$ ft.

46. Graphical Determination of Truss Deflections.—From the discussion of the two preceding articles, we see that the analytical calculation of truss deflections requires consideration of a special loading of the truss for each joint whose deflection is required. If the deflections of many joints are required, the foregoing calculations become tedious and a graphical determination of the displacements can be used to advantage.[1] We begin with a very simple example consisting of a joint A attached to joints B and C by two bars 1 and 2, as shown in Fig. 339a. The displacements BB' and CC' of the joints B and C and the changes in length of the bars 1 and 2 are given; it is required to find the corresponding displacement of joint A. We first assume that the bars are disjointed at A and translate them to the positions $A'B'$ and $A''C'$
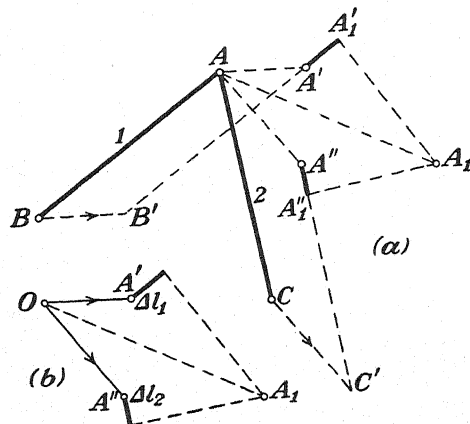
FIG. 339.

parallel to their initial positions and such that BB' and CC' represent the given displacements of the joints B and C. In these new positions, we keep the joints B' and C' fixed and give to the opposite ends of the bars the displacements $A'A_1'$ and $A''A_1''$ as shown by heavy lines. These latter displacements are equal to the given changes in the lengths of the bars, that is, $A'A_1'$ is the known elongation of the bar 1 and $A''A_1''$ is the known compression of the bar 2. Now, to finish the construction, we have to bring the points A_1' and A_1'' together by rotating the bar $B'A_1'$ with respect to the center B' and the bar $C'A_1''$ with respect to the center C'. Since we are dealing with small deformations and small angles of rotation, the arcs of the circles along which the points A_1' and A_1'' travel during such rotations of the bars can be replaced by perpendiculars $A_1'A_1$ and $A_1''A_1$ the intersection of which gives the new

[1] Such graphical constructions for the deflections of trusses are called *Williot diagrams*. See WILLIOT, "Notation pratiques sur la statique graphique," *Publications scientifiques industrielles*, 1877.

position A_1 of the joint A.   Thus the vector AA_1 represents the required displacement of the joint A.

Since the elongations of the bars and the displacements of the joints are very small in comparison with the lengths of the bars, it is necessary to represent these quantities to a large scale and to make all constructions in a separate diagram as shown in Fig. 339b.   We take a pole O and lay out to the chosen scale the given displacements OA' and OA'' of the joints B and C.   Then from the points A' and A'' we draw the vectors Δl_1 and Δl_2, shown by heavy lines and representing the known changes in length of the bars 1 and 2.   Due attention must be paid to the sign of these elongations.   The bar 1 is increasing in length; hence Δl_1 is put in the direction from B to A.   The bar 2 is decreasing in length; hence Δl_2 is put in the direction from A to C.   Finally, perpendiculars constructed at the ends of the vectors Δl_1 and Δl_2 intersect at point A_1, defining the required displacement OA_1 of joint A.   It will be noted that the displacement diagram in Fig. 339b is identical with the portion $AA'A_1'A_1A_1''A''$ of Fig. 339a, except that it can be constructed to a much larger scale if desired.   Figure 339b represents the Williot diagram for the simple structure BAC of Fig. 339a.

The same procedure can be used in the construction of displacement diagrams for all simple trusses that are formed by starting with one bar and attaching each new joint by two bars (see page 45).   We take, as an example, the truss shown in Fig. 340a and begin the determination of the displacements with a calculation of the elongations $\Delta l_1 \ldots \Delta l_7$ of all bars produced by the given load P.   These calculations can be made without difficulty since the system is statically determinate and all dimensions are known.   Starting now with joint A, which is fixed, we assume, for the beginning, that the bar AE retains its horizontal position during deformation.   Hence joint E has only a horizontal displacement equal to the elongation Δl_2 of the bar 2.   Knowing the displacements of the joints A and E, we can now find the displacement of the joint B, which is attached to these joints by the bars 1 and 4.   Proceeding as in Fig. 339b, we start with an arbitrarily chosen pole O (Fig. 340b) and mark points a' and e', which correspond to the joints A and E.   Since joint A is fixed, a' coincides with the pole O.   The vector Oe', equal to the elongation Δl_2* of the bar 2, is taken in the direction from A to E, indicating extension of the bar.   From points a' and e' we draw in the proper directions the vectors Δl_1 and Δl_4, representing the shortening of bar 1 and the elongation of bar 4, respectively.   Making the perpendiculars at the ends of these vectors, we obtain the intersection point b', which determines the displacement Ob' of the hinge B.   Having now points e' and b' on the diagram, we can determine the position of the point c'

---

* To simplify notations we use in the diagram $\Delta_1, \Delta_2, \ldots$ instead of $\Delta l_1, \Delta l_2, \ldots$.

and the displacement Oc' of the joint C, which is attached to joints B and E by the bars 3 and 5. For this purpose we draw from points b' and e' the vectors Δl_3 and Δl_5, representing, respectively, the shortening of bar 3 and the elongation of bar 5. The intersection of the perpendiculars drawn at the ends of these vectors determines the position of point c'. Proceeding further in the same way, we finally obtain the last point d' of the diagram. Vectors drawn from the pole O to the points e', b', c', and d' represent both in magnitude and direction the required displacements of the corresponding hinges of the truss. By using them to some reduced scale, we can construct the distorted shape of the truss as indicated by dotted lines in Fig. 340a.

Since we started with an arbitrary assumption that the bar AE remains horizontal, the deformed shape $AB'C'D'E'$ of the truss does not satisfy the condition at the support D. This support can move only
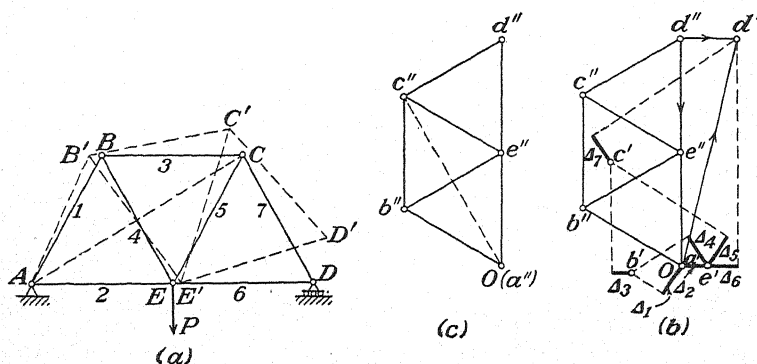
Fig. 340.

horizontally, while the displacement DD', obtained from the diagram in Fig. 340b, is not horizontal. To satisfy the condition at the support, we must rotate the deformed truss, indicated by dotted lines in Fig. 340a, with respect to the hinge A by such an amount that the point D' will reach the horizontal line AD. In this way the conditions at both supports will be satisfied and the true displacements of the hinges will be obtained by geometrically adding to the displacements found in Fig. 340b the displacements produced during such rotation. These latter displacements can be found as follows: Since the distorted shape $AB'C'D'E'$ of the truss (Fig. 340a) is actually very close to its initial shape, it can be assumed with good accuracy that, during rotation about the hinge A, the hinge D' moves perpendicularly to AD, hinge C' moves perpendicularly to AC, etc. Furthermore, the magnitudes of these displacements will be proportional to the radii AD, AC, etc. The required rotatory displacement of the point D' is evidently equal to the vertical component of the displacement DD' represented by the vector

Od' in Fig. 340b. This rotatory displacement of D' having been obtained, the corresponding displacements of the other hinges are readily obtained from Fig. 340c, in which Od'' is taken equal to the vertical component of Od' in Fig. 340b and the other points are obtained by making the figure $Ob''c''d''e''$ geometrically similar to the figure $ABCDE$ of the truss but rotated by 90 deg. with respect to that figure. The vectors $b''O$, $c''O$, $d''O$, and $e''O$ will then represent the rotatory displacements of all hinges of the truss. This follows from the geometric similarity that makes the vectors perpendicular to the corresponding radii and proportional to the lengths of these radii. Thus vector $b''O$ in Fig. 340c is perpendicular to the radius AB in Fig. 340a, and $b''O : AB = d''O : AD$; vector $c''O$ is perpendicular to the radius AC, and $c''O : AC = d''O : AD$; etc. To simplify the geometric addition of the rotatory displacements to the displacements given by the diagram in Fig. 340b, we superimpose Fig. 340c on Fig. 340b so that the poles O coincide. Then the total displacements of the hinges B, C, D, E will be represented by the vectors $b''b'$, $c''c'$, $d''d'$, and $e''e'$. To see this, let us take, for example, the hinge B. Its displacement, corresponding to the dotted-line shape of the truss in Fig. 340a, is given in Fig. 340b by the vector Ob'. The rotatory displacement of the same hinge is given by the vector $b''O$; hence the geometric sum of these two displacements, giving the true displacement of the hinge B, is the vector $b''b'$. Similar reasoning holds for the other hinges.[1]

In the case of a truss with many bars, it may be anticipated that, if we start the construction of the displacement diagram from the support, as we did in Fig. 340, the constructions will extend farther and farther away from the pole O and the diagram may become unwieldy. In such cases, a more compact diagram can be obtained and the unavoidable inaccuracies of drawing can be reduced by starting the construction from the middle of the truss. Considering, for example, the truss in Fig. 341a, we begin with the bar AB. Assuming that the hinge A is immovable and that the hinge B moves only vertically, we find from the displacement diagram (Fig. 341b) that point a' coincides with the pole O and that point b' is vertically above O at a distance Ob' equal to the elongation Δl_1 of the bar 1. Having the points a' and b', we obtain the points corresponding to the other hinges in exactly the same manner as in Fig. 340. Considering the portion of the truss to the right of the bar AB, we obtain in the diagram in Fig. 341b the points c', d', and e'. For the left portion of the truss we obtain the points f', g', and h'. Vectors drawn from the pole O to these points give the displacements of the hinges of the truss during deformation if the middle bar AB is kept fixed. The

---

[1] The foregoing method of correcting the Williot diagram to satisfy the conditions at the supports is due to Otto Mohr. See *Zivil-ingenieur*, vol. 33, p. 639, 1887. The corrected diagram should be called a Williot-Mohr diagram.

corresponding distorted shape of the truss is indicated in Fig. 341a by dotted lines. Since our assumption regarding the bar AB was entirely arbitrary, the displacements obtained do not satisfy the conditions at the supports, which require that the hinge H be immovable and that the hinge E move only horizontally. To satisfy these two conditions, we have to perform two additional movements; first we have to move the distorted truss parallel to itself by the amount $H'H$, so that the condition at the
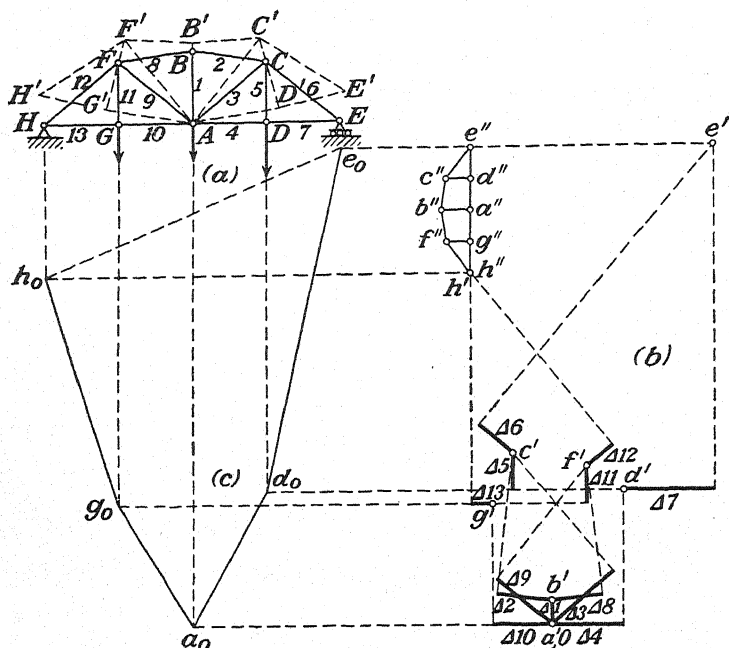
Fig. 341.

left support H will be satisfied. Then, subsequently, we rotate the truss with respect to hinge H by such an amount that the point E' reaches the horizontal line HE in Fig. 341a. When the truss moves parallel to itself, all hinges suffer the same displacement given in Fig. 341b by the vector $h'o$, and this must be geometrically added to the previously obtained displacements. This is readily accomplished by taking point h', instead of o, as the pole in Fig. 341b. Thus, for example, to obtain the result of superimposing the parallel motion, represented by the vector $h'o$ on the previously obtained displacement oe' of the joint E, we have only to take the geometric sum of these two vectors, which is given by the vector $h'e'$. Similar conclusions will be obtained for the other hinges. Hence, by taking point h', instead of o, as a pole, we accomplish the required geometric addition of the translatory displacement $h'o$. After this operation, the displacement of the hinge E is represented by the vector

$h'e'$. Now, to satisfy the condition at the support E, we must rotate the truss with respect to the hinge H by such an amount that the rotatory displacement $e''h'$ of the hinge E, when added geometrically to $h'e'$, makes the resultant displacement $e''e'$ of the hinge E horizontal (Fig. 341b). The corresponding rotatory displacements of the remaining hinges of the truss are then obtained by constructing the diagram $e'h''f''b''c''$ geometrically similar to the shape of the truss. The vectors $a''a'$, $b''b'$, $c''c'$, . . . will then give the true displacements of the hinges of the truss.

Having the total displacements of the hinges, we can readily obtain, by projection, the vertical components of the displacements of the lower chord joints as shown by the polygon $h_o g_o a_o d_o e_o$ in Fig. 341c. Such a polygon is called the *deflection polygon* for the truss.

From the preceding examples it will be appreciated that in the case of simple trusses there is no difficulty in constructing the displacement diagram corresponding to known changes in the lengths of all bars. In proceeding with this construction, it is necessary only to repeat with each new hinge the construction illustrated in Fig. 339b. In the case of statically determinate trusses that are compound or complex in form some additional considerations are required, which we shall now illustrate by examples. As a first example, we take the compound roof truss shown in Fig. 342a. To construct the displacement diagram for this truss, we first disregard the web members on the right side and consider HIQ as one triangle. Accordingly we consider HI, IQ, and HQ as simple bars, the changes in length of which will be obtained by summing up the elongations of the component bars. Thus the elongation of the bar IQ is obtained by adding together the elongations of the bars $6'$ and $5'$. In this manner a simple truss is obtained, and the displacement diagram can readily be constructed. Such a diagram, constructed on the assumption that the hinge A is immovable and that the bar AB retains its original direction, is shown in Fig. 342b. Point a' coincides with the pole o, and point b' is obtained by making ob' parallel to the bar AB and equal to the compression of that bar. Proceeding in this way with the construction of the diagram, we finally obtain points e' and q' defining the displacements oe' and oq' of the points of support. To satisfy, now, the actual conditions at the supports, we displace the truss parallel to itself by the amount $e'o$ so that the hinge E coincides with the fixed support and then rotate the truss about this support by such an amount that the hinge Q coincides with the horizontal line EQ in Fig. 342a. As already explained, the geometric addition of this translatory displacement is readily obtained by taking point e', instead of o, as the pole. The rotatory displacement of the hinge Q is vertical and of such magnitude $q''e'$ that, when geometrically added to the displacement $e'q'$, it makes

the resultant displacement $q''q'$ of the support Q horizontal. The corresponding rotatory displacements of the remaining hinges are then obtained, as before, by making the figure $e'h''q''i''a''$ geometrically similar to the simple truss that we are considering. The vectors measured on the diagram (Fig. 342b) from the points with two primes to the cor-
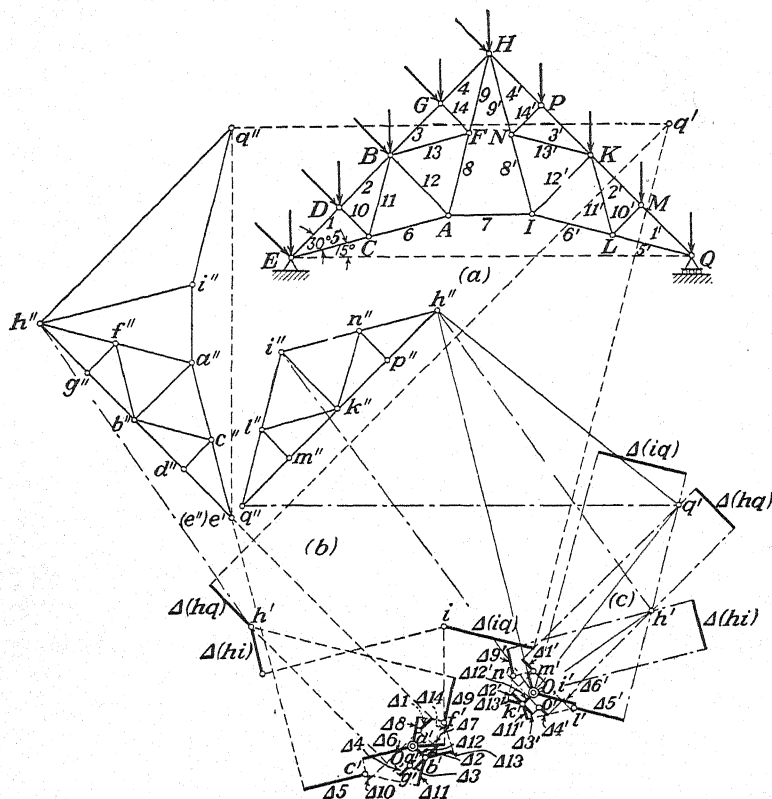
Fig. 342.

responding points with one prime give, then, the true displacements of the hinges of the truss.

To finish the problem, we have to consider the displacements of the hinges K, L, M, N, P, which were disregarded in our previous constructions. For this purpose, we make, in the usual way, the displacement diagram for the right half of the truss, assuming that the hinge I is immovable and that the bar IK retains its direction. Such a diagram is shown in Fig. 342c. From this diagram, we find the displacements oh' and oq' of the hinges H and Q. Since this latter diagram was constructed with an arbitrary assumption regarding the displacements of hinges I and K, the displacements oh' and oq' differ from the true displacements

$h''h'$ and $q''q'$, which were determined from the diagram shown in Fig. 342b. To remove this discrepancy and obtain in Fig. 342c the true displacements, we superimpose on the displacements there a proper translation and rotation. For the translation, we take such a displacement $h''o$ that the geometric sum of $h''o$ and oh' gives the true displacement $h''h'$ of the hinge h, taken from Fig. 342b. In this way we bring the hinge H of the right half of the truss into coincidence with the hinge H of the left half. Now we have to perform rotation of the right portion of the truss with respect to the hinge H and of such an amount that the hinge Q will finally obtain its true displacement. Thus in Fig. 342c we begin with the displacement oq' and add to it the translatory displacement $h''o$, thus obtaining, as the geometric sum, the displacement $h''q'$. To this displacement the rotatory displacement must still be added. The direction of this displacement is evidently perpendicular to the chord HQ in Fig. 342a, and its magnitude $q''h''$ must be such that the geometric sum of $q''h''$ and $h''q'$ gives the true displacement $q''q'$ as obtained before in Fig. 342b. Having points h'' and q'', we obtain the remaining points with two primes by constructing the figure $q''l''h''k''$ geometrically similar to the right half of the truss in Fig. 342a. The vectors measured from the points with two primes to the points with one prime in Fig. 342c give the required displacements of the remaining hinges.

In Fig. 343, the displacement diagram for a three-hinged arch is constructed. We start with separate diagrams for each half of the arch, assuming that the hinges A and C are fixed and that the bars AD and CE retain their vertical directions. In this way the diagrams in Fig. 343b, and Fig. 343c are obtained. Since these constructions are made on the arbitrary assumption that the bars AD and CE do not rotate, we obtain for the displacement of the upper hinge B two different values ob' in the two diagrams. To remove this discrepancy and obtain in both diagrams the same displacement for B, we rotate the left half of the arch with respect to the hinge A and the right half with respect to the hinge C. Considering the hinge B as belonging to the left part of the arch, we conclude that its rotatory displacement must be perpendicular to the line AB in Fig. 343a and that the point b'' in Fig. 343b defining the magnitude $b''o$ of this displacement must lie on the line mn perpendicular to AB. By the same reasoning, we conclude that the point b'' in Fig. 343c must lie on the line $m'n'$ perpendicular to BC. Constructing the lines mn and $m'n'$, we have now only to select such positions for the two points b'' that the geometric additions of the rotatory displacements $b''o$ and the previously found displacements ob' give, in both diagrams, the same resultant displacement $b''b'$. It is seen from the drawing that this requirement is satisfied if we select the positions of points b'' on the

lines mn and $m'n'$ in such a way that $b''b''$ becomes equal and parallel to $b'b'$. After determining the rotatory displacement of the hinge B, the corresponding rotatory displacements of the other hinges are obtained, as before, by constructing the figures $od''b''f''$ and $ob''e''g''$ geometrically similar to the portions $ADBF$ and $BECG$, respectively, of the arch (Fig.
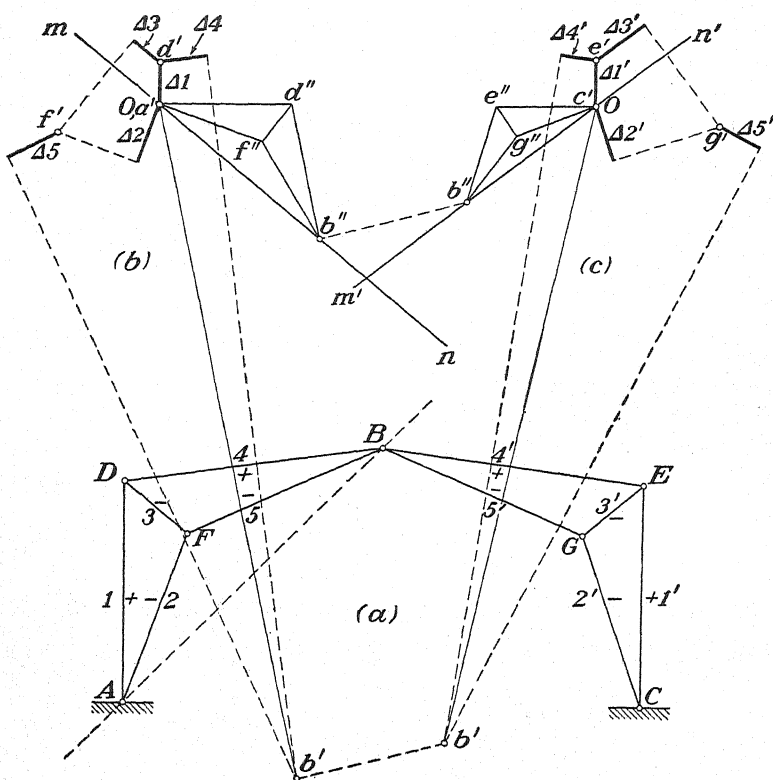
Fig. 343.

343a). The final displacements are obtained by measuring the vectors from the points with two primes to the corresponding points with one prime in Figs. 343b and 343c. With this we conclude our discussion of the Williot-Mohr diagram.[1]

PROBLEMS

226. Find the displacement of the hinge A in Fig. 344 if the hinge B performs a given horizontal displacement BB' and the hinge C a given vertical displacement CC'. The lengths of the bars AB and AC remain unchanged.

[1] The construction of displacement diagrams for several more complicated cases can be found in H. Müller-Breslau's book "Die graphische Statik der Baukonstruktionen," 4th ed., vol. II, pp. 59–87, 1907.

227. Find the displacements of the hinges of the truss in Fig. 345a by using the
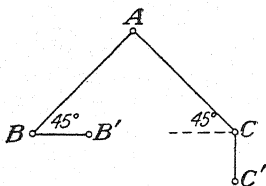
Fig. 344.

Williot-Mohr diagram shown in Fig. 345b. This diagram was started on the assumption that the hinge D is immovable and that the bar DB does not rotate.

228. Construct a Williot-Mohr diagram for the simple truss shown in Fig. 92a (page 51), assuming that each bar suffers a unit strain of 1/1,000. Be sure to distinguish between tension and compression members.

229. Construct a Williot-Mohr diagram for the truss shown in Fig. 103 (page 60). Assume that all bars are of steel with cross-sectional areas $A = 1$ sq. in. and lengths $l = 8$ ft. and that $P = 10,000$ lb.

230. Construct a Williott-Mohr diagram for the truss in Fig. 336. Use the numerical data given in Prob. 220.
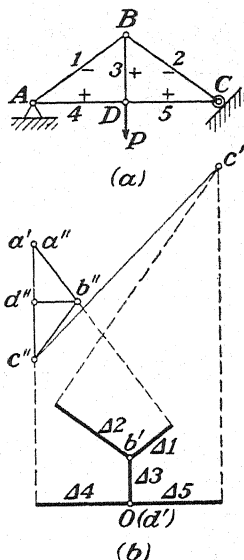
Fig. 345.

47. Method of Fictitious Loads.—The graphical method of finding displacements described in the preceding article tends to become inaccurate in the case of a truss containing many bars. The unavoidable errors of construction increase rapidly with the number of graphical operations, especially if it is necessary to determine the intersections of lines that are too nearly parallel. In practical applications we often need to know only the vertical deflections of the chord joints of a truss. This limited problem can be solved by using a method of fictitious loads[1] similar to that applied in calculating deflections of beams. Take, for example, the truss in Fig. 346a, and assume that the elongations of all bars produced by the given loads P_1, P_2, . . . are known. Then, to calculate the vertical deflections of the joints resulting from an elongation Δl_i of one bar, say bar CD, we use the method explained in Art. 45. Accordingly, the deflection δ_m of any joint m (Fig. 346b) is obtained from the equation

$$\delta_m = \Delta l_i \cdot \frac{s_i'}{1}, \qquad (a)$$

in which s_i' is the axial force in the bar CD due to a unit load at m. Since all bars, except CD, are considered rigid, the two portions of the

[1] The application of fictitious loads in calculating deflections of trusses was introduced by O. Mohr, Beitrag zur Theorie des Fachwerks, *Z. Architekten-Ingenieur-Ver. Hannover*, 1875, p. 17. See also his book, "Abhandlungen aus dem Gebiete der Technischen Mechanik," p. 377, 1906.

truss, shaded in Fig. 346b, move as rigid bodies, rotating with respect to each other about the hinge m, and the vertical deflections of all joints are evidently given by the corresponding ordinates of the diagram amb in Fig. 346c. Observing that the axial force s_i' produced in the bar CD by the unit load at m is equal to the bending moment at m divided by the distance h, we conclude, from Eq. (a), that the deflection diagram in Fig. 346c can be considered as the bending-moment diagram for a fictitious beam AB acted upon by a fictitious load

$$\frac{\Delta l_i}{h} \tag{b}$$

as shown in Fig. 346d. In a similar manner the deflections resulting from a change in length Δl_i of any other chord member of the given truss can be found. Using, now, the method of superposition, we conclude that the deflection of the truss resulting from changes in length of all chord members can be calculated for each joint as the bending moment
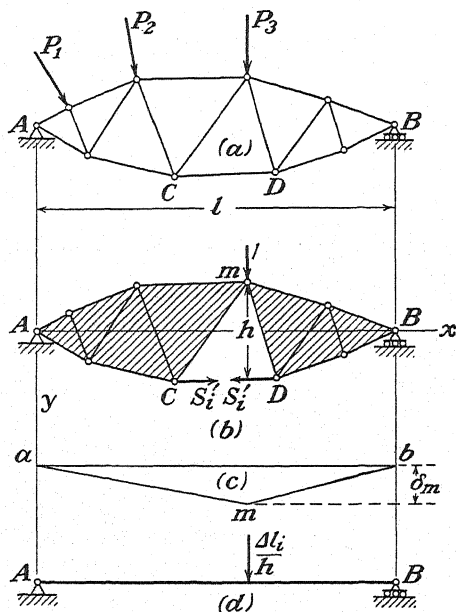
Fig. 346.

at the corresponding cross section of a simple beam subjected to fictitious loads defined for each joint by Eq. (b).* Regarding the sign of the fictitious loads, we observe that compression of any upper chord member or elongation of any lower chord member results in a downward deflection

---

* These loads, as we see, are pure numbers, and the corresponding bending moments have the dimension of length as it should be.

of the truss.   This indicates that shortening of the upper chord or elongation of the lower chord implies a downward or positive fictitious load.

Let us consider, now, the effect of changes in length of web members on the deflection of a truss.   If only one bar, say the bar DE of the truss in Fig. 347a, changes in length by the amount Δl_i, the deflection of a
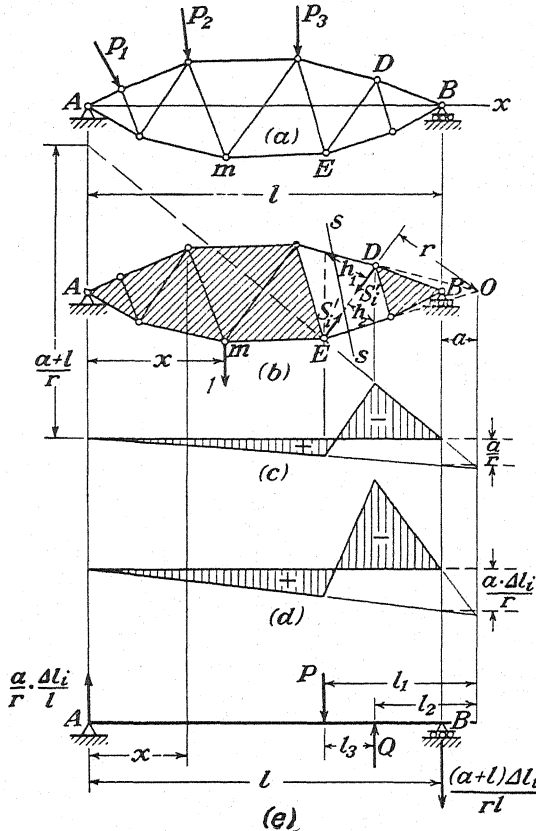
Fig. 347.

joint m (Fig. 347b) is again obtained from Eq. (a).   Applying this equation to all joints in succession, we conclude that their deflections are obtained by multiplying by Δl_i the corresponding ordinates of the influence diagram for the bar DE as shown in Fig. 347c.   To construct this influence diagram, we note that, for any position of the unit load to the left of joint E, the force s_i' (Fig. 347b) is obtained from the equation

$$s_i' = 1 \cdot \frac{x}{l} \cdot \frac{a}{r}, \tag{c}$$

in which the distances a and r are as shown in the figure. If the unit load is to the right of joint D, the force s_i' is given by the equation

$$s_i' = \frac{l + a}{r}\left(\frac{x}{l} - 1\right). \tag{d}$$

Thus the influence diagram for s_i' has the form shown in Fig. 347c. Upon multiplying the ordinates of this diagram by Δl_i, the deflections of the truss produced by the change in length Δl_i of the bar DE are obtained (Fig. 347d). In all cases where the influence diagram has the shape shown in Fig. 347c, the shaded area in Fig. 347d can be considered as the bending-moment diagram for a simply supported beam loaded as shown in Fig. 347e. This loading consists of two fictitious loads P and Q the magnitudes of which are obtained from the conditions that the reactions at the ends of the beam are

$$R_a = \frac{a\,\Delta l_i}{rl} \qquad \text{and} \qquad R_b = -\frac{(a + l)\Delta l_i}{rl}.$$

This gives

$$P = \frac{\Delta l_i}{r}\frac{l_2}{l_3} \qquad \text{and} \qquad Q = \frac{\Delta l_i}{r}\frac{l_1}{l_3}, \tag{e}$$

where l_1, l_2, and l_3 are the distances indicated in Fig. 347e. As a check, we calculate the bending moment for a point of the beam to the left of the load P and at a distance x from the support A (Fig. 347e). This moment

$$M = \frac{a}{r}\frac{x}{l}\,\Delta l_i$$

is seen to agree with expression (c) multiplied by Δl_i. In a similar manner, the bending moment for the portion of the beam to the right of the load Q is represented by expression (d) multiplied by Δl_i. This indicates that the bending-moment diagram for the beam in Fig. 347e is identical with the deflection diagram in Fig. 347d. We conclude, then, that by introducing for each web member the two fictitious loads, defined by expressions (e) and using the method of superposition, the deflections of the truss due to changes in length of all web members are obtained by calculating the bending moments in the corresponding simple beam carrying the above-mentioned fictitious loads.

Expressions (e) for the fictitious loads P and Q can be somewhat simplified as follows: Drawing verticals through the ends of the web member DE (Fig. 347b), we see from geometric similarity that $h_1/r = l_3/l_2$ and $h_2/r = l_3/l_1$. Substituting these values in (e) we obtain

$$P = \frac{\Delta l_i}{h_1} \qquad \text{and} \qquad Q = \frac{\Delta l_i}{h_2}. \tag{f}$$

The directions of these fictitious loads in each particular case are readily obtained from the signs of the ordinates of the influence diagram.   We can use, also, the rule stating that the fictitious load at either end of a web member acts downward if, at this end, the chord member and the web member cut by a section such as section ss in Fig. 347b have axial forces of the same sign.   The load acts upward if the axial forces are of opposite sign.

To illustrate the method, let us consider the truss shown in Fig. 348a. The lengths and cross-sectional areas for the bars of this truss are given in Table VI.   There are given also in this table the axial forces in the bars and the elongations[1] produced by a 24,000-lb. load applied at the joint q.   To find the deflections due to the corresponding changes in length of the chord members, we calculate the fictitious loads by using Eq. (b).   Since the chords are parallel, all values of h are equal to 60 in. in this case.   The values of these fictitious loads, multiplied by $E/1,000$, are shown in Fig. 348b and are given also in the table.   Assuming that

<div align="center">TABLE VI</div>

i	l, in.	A, in.^{2}	S	$\dfrac{\Delta l \cdot E}{1,000}$	Fictitious loads at joints multiplied by $E/1,000$				
					m	n	p	q	s
1	84.8	3.66	−11,310	−262	6.18				
2	120	3.66	8,000	262	4.37				
3	84.8	3.66	11,310	262	−6.18	6.18			
4	120	4.98	−16,000	−385	......	6.42			
5	84.8	2.48	−11,310	−385	......	−9.08	9.08		
6	120	3.66	24,000	785	......	......	13.08		
7	84.8	2.48	11,310	385	......	......	−9.08	9.08	
8	120	4.98	−32,000	−771	......	......	......	12.85	
9	84.8	3.66	22,620	524	......	......	......	12.36	−12.36
10	120	3.66	16,000	524	......	......	......	.....	8.73
11	84.8	3.66	−22,620	−524	......	......	......	.....	12.36

these loads are acting on a simple beam AB (Fig. 348c), the bending moments at their points of application, divided by $E/1,000$, give the deflections of the corresponding joints of the truss.   Considering, for example, the joint p, the corresponding bending moment for the simple beam is

$$M = 20.19 \times 180 - 4.37 \times 120 - 6.42 \times 60 = 2,725.$$

Hence the deflection of the joint p due to elastic deformation of the chord

---

[1] The elongations are multiplied by E and divided by 1,000 in the table.

members is

$$\delta = \frac{M \cdot 1,000}{E} = \frac{2,725 \cdot 1,000}{30 \cdot 10^6} = 0.0908 \text{ in.}$$

To calculate the deflections due to the elastic deformations of the web members, we apply to the ends of each web member the fictitious loads found from Eqs. (f), in which, for this case, the distances h_1 and h_2 are equal to $60/\sqrt{2} = 42.4$ in. The magnitudes of all these loads are given with the proper signs in Table VI. After summation, we obtain the
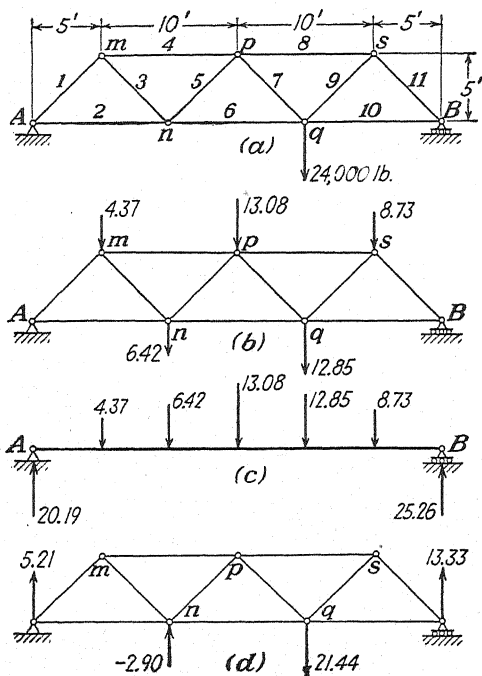
Fig. 348.

fictitious loading of the truss shown in Fig. 348d. The bending moment produced by these loads at the cross section of a fictitious beam, corresponding to joint p, is

$$M = 13.33 \times 180 - 21.44 \times 60 = 1,113,$$

and the corresponding deflection of the joint p of the truss is

$$\delta_1 = \frac{1,113 \cdot 1,000}{30 \cdot 10^6} = 0.0371 \text{ in.}$$

The total deflection of the joint p is obtained by adding δ_1 to the previously found deflection δ.

In the foregoing discussion of the effect of web members on deflection, we considered a case in which these members were not vertical. To extend the method to the case of vertical web members, we take the truss shown in Fig. 349a and consider the vertical member CD. To apply our previous reasoning, we assume, at the beginning, that the member CD is slightly inclined to the vertical as indicated in the figure by the dotted line. Then our previous reasoning is applicable, and the ficti-
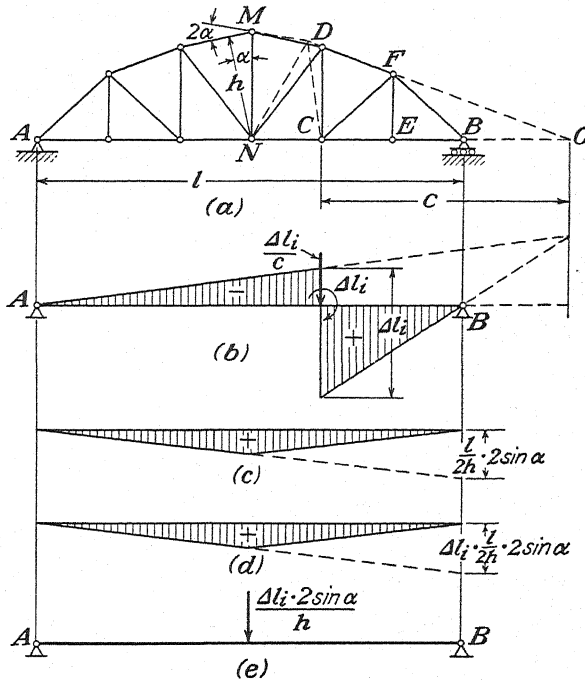
FIG. 349.

tious loads at the ends of the member are given by Eqs. (e). Assuming, now, that the angle of inclination indefinitely diminishes and approaches zero, the distances r, l_2, and l_1 in Eqs. (e) become equal to the distance c in Fig. 349a, while l_3 approaches zero. Thus, both fictitious loads increase indefinitely; but their difference, equal to $\Delta l_i/r$, approaches the value $\Delta l_i/c$, and their moment with respect to joint C approaches the magnitude $(\Delta l_i/l_3) \cdot l_3 = \Delta l_i$. The corresponding bending-moment diagram for the fictitious beam is shown in Fig. 349b. The discontinuity in this diagram at the point of application of the fictitious couple Δl_i indicates that the deflection of the joint C of the lower chord is larger than the deflection of the joint D of the upper chord by the amount equal to the elongation Δl_i of the vertical member CD.

Considering, now, the vertical member EF (Fig. 349a), we readily see that change in length of this bar has no general influence on the deflection of the truss. The deflection of joint F is obtained by completely disregarding the presence of the bar EF, and to obtain the deflection of joint E we have only to add the elongation of the bar EF to the deflection of joint F.

To obtain the deflections produced by a change in length of the middle vertical MN, we consider the influence diagram for this member as shown in Fig. 349c.* Multiplying the ordinates of this diagram by Δl_i, we obtain, in accordance with Eq. (a), the deflection line of the lower chord of the truss as shown in Fig. 349d. This line can be considered as the bending-moment diagram for the fictitious beam AB loaded as shown in Fig. 349e. From this discussion, we see that the deflection of a truss due to changes in length of vertical web members can also be obtained as the bending moment produced by certain fictitious loads, which can be readily obtained in each particular case.

As a specific example dealing with vertical web members, let us consider the truss shown in Fig. 350a and assume that the load is symmetrically distributed with respect to the vertical axis of symmetry of the truss. Tension and compression members are indicated in the figure by plus and minus signs, respectively, on the left side of the truss, and the magnitudes of the stresses are so assumed that the unit elongation or contraction of each active member is equal to 1/2,000. Considering first the deflections due to chord members and using expression (b) for fictitious loads, we find that the loading on the fictitious beam is that shown in Fig. 350b. For the diagonals we use expressions (f) and find

$$P = Q = \frac{1}{1,000}.$$

These fictitious loads act down at the lower ends of the diagonals and up at the upper ends. After summation, we obtain the loading shown in Fig. 350c.

Coming now to the verticals and using the reasoning illustrated in Fig. 349b, we find that the corresponding loading on the fictitious beam consists of the fictitious couples shown in Fig. 349d. At the point of application of each couple we have an abrupt change in the bending moment by the amount 0.036 in. equal to the shortening of the verticals. By calculating the bending moments just to the left of the points of application of the fictitious couples, we obtain the deflections of the joints of the lower chord of the truss. The bending moments just to the right of the same points give the deflections for the joints of the upper chord.

---

* It is assumed that the unit load moves along the lower chord of the truss. Hence we shall obtain the deflections of that chord.

Considering the deflections of the lower chord, we see that, instead of fictitious couples, we can take the fictitious load shown in Fig. 350e. This load produces reactions at the ends equal to 1/2,000, and the bending moments at the points corresponding to the joints of the lower chord are the same as those produced by the fictitious couples of Fig. 350d. Finally, to get the total deflection of any joint of the lower chord of the truss in Fig. 350a, we have to combine the fictitious loadings shown in
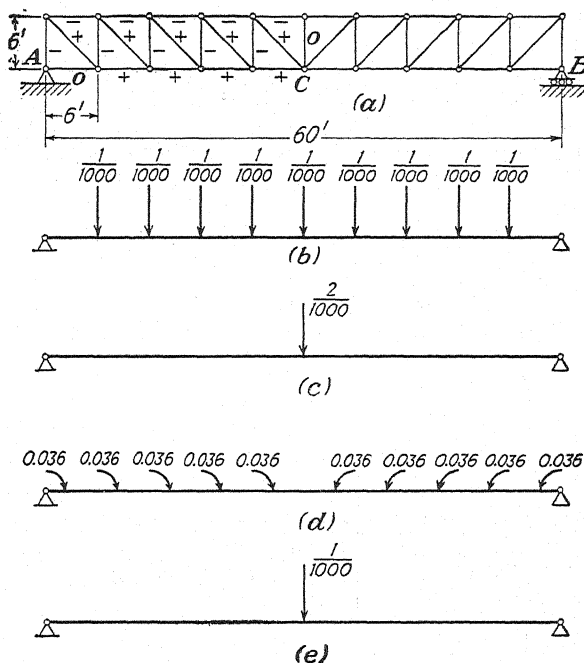
FIG. 350.

Figs. 350b, c, and e.   The deflection at the middle, obtained in this way, is

$$\delta = \frac{4.5}{1,000} \cdot 360 - \frac{4}{1,000} \cdot 180 + \frac{1}{1,000} \cdot 360 + \frac{1}{2,000} \cdot 360$$
$$= 0.9 + 0.36 + 0.18 = 1.44 \text{ in.}$$

It consists of three parts, a deflection of 0.9 in. due to chord members, a deflection of 0.36 in. due to diagonals, and a deflection of 0.18 in. due to verticals.

PROBLEMS

231. Using the method of fictitious loads, find the deflection of each joint of the upper chord of the truss shown in Fig. 114 (page 67) if $a = 5$ ft.   Assume, for calculation, that each bar suffers a unit elongation or contraction of 1/2,000.

232. Using the method of fictitious loads, find the deflection of each joint of the lower chord of the truss shown in Fig. 116 (page 68) if $a = 4$ ft. and $\alpha = 20$ deg. As in the preceding problem, assume that the unit elongation or contraction of each active bar is $1/2,000$.

233. Referring to Fig. 348a, calculate the deflection of the joint p if the 24,000-lb. load acts at this joint instead of at q. Use the numerical data given in Table VI (page 281).

234. Referring to Fig. 350a, calculate the deflections of the lower chord joints due to a single load $P = 10,000$ lb. applied at C. Assume that each bar has a cross-sectional area $A_i = 1$ sq. in. and $E = 30(10)^6$ lb. per sq. in.

235. Calculate the deflections of the joints of the lower chord of the truss shown in Fig. 118a (page 69). Assume that the span $l = 60$ ft. and that each active bar suffers a unit elongation or contraction of $1/2,000$.

48. Alternate Method of Fictitious Loads.—The problem of finding the deflections of the joints of one chord of a truss can be solved by considering only the members of that chord. This solution is especially simple if the chord is a horizontal straight line. Take, for example, the
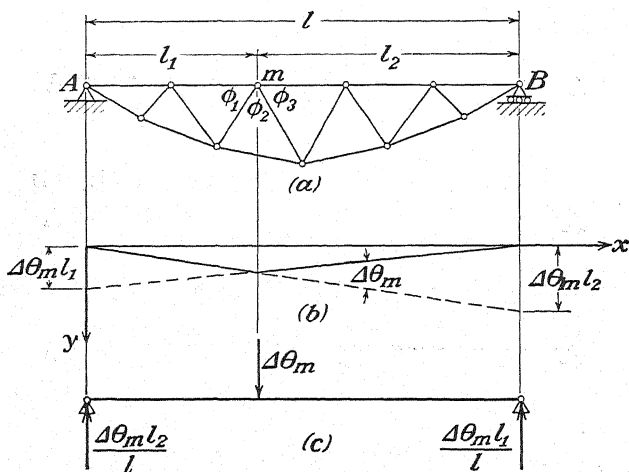
Fig. 351.

truss shown in Fig. 351a, and let it be required to find the vertical deflections of the upper chord joints. It is evident that such displacements will be completely defined if we know the changes in the lengths of the bars of the upper chord together with their angles of rotation during deflection of the truss. Since the chord is a horizontal straight line, changes in the lengths of its bars result only in horizontal displacements of the upper chord joints. Thus, vertical displacements of these joints depend only on rotations of the upper chord members. In calculating these rotations, we assume that the changes in the lengths of all bars of the truss are known. Then the corresponding changes in the angles of each triangle

can be calculated without difficulty, as will be shown later.   Assuming for the moment that such changes in the angles ϕ_1, ϕ_2, and ϕ_3 at an upper joint (Fig. 351a) have been found, we obtain by their sum a small angle $\Delta\theta_m$ representing the angle between the two chord members at the joint m after deflection.   The corresponding deflection of the upper chord, assuming that $\Delta\theta_m$ is positive, is shown in Fig. 351b.   The deflection for any point of the chord to the left of joint m is equal to $\Delta\theta_m l_2 x/l$, while, for any point to the right of m, it is $\Delta\theta_m l_1(l - x)/l$.   We see now that these expressions for deflections are identical with those for bending moments produced in a simply supported beam by the fictitious load $\Delta\theta_m$ acting as shown in Fig. 351c.   Thus we conclude that, by calculating the values of $\Delta\theta_i$ for each joint i of the upper chord and using the method of superposition, the required deflections will be obtained as the bending moments for a simply supported beam subjected to fictitious loads $\Delta\theta_i$.[*]

We shall now show the method of calculating the changes in the angles of a triangle if the changes in the lengths of its three sides are known.   Since we are dealing with very small elongations, the Williot diagram discussed in Art. 46 is very useful for this purpose.   Consider, for example, a triangle ABC (Fig. 352a) with sides of lengths l_1, l_2, and l_3 and altitude h, and let it be required to find the changes in the angles due to known elongations Δl_1, Δl_2, and Δl_3 of the sides of the triangle.   To accomplish this, we assume that the joint A is fixed and that the bar AB retains its horizontal direction.   Then, to find the displacement $\overline{CC'}$ of the vertex C, due to the known elongations Δl_1, Δl_2, and Δl_3 of the sides of the triangle, we construct the usual Williot diagram as shown in Fig. 352b.   If ρ_1 and ρ_2 denote the lengths of the perpendiculars $\overline{C_1 C'}$ and $\overline{C_2 C'}$ in Fig. 352b, the corresponding changes in the angles α_1 and α_2 at B and A in Fig. 352a are[1]

$$\Delta\alpha_1 = \frac{\rho_2}{l_2} = \frac{\rho_2 \sin \alpha_1}{h} \qquad \text{and} \qquad \Delta\alpha_2 = \frac{\rho_1}{l_1} = \frac{\rho_1 \sin \alpha_2}{h}.$$

Remembering, now, that the sum of the angles of a triangle must always be 180 deg., we conclude that the required change in the angle α_3 at C is

$$\Delta\alpha_3 = -(\Delta\alpha_1 + \Delta\alpha_2) = -\frac{\rho_2 \sin \alpha_1 + \rho_1 \sin \alpha_2}{h}. \qquad (a)$$

The numerator on the right side of this expression represents the sum b of the horizontal projections of the perpendiculars ρ_1 and ρ_2 in Fig. 352b.

---

[*] This method of calculating deflections of trusses was introduced by H. Müller-Breslau, *Z. Architekten-Ingenieur-Ver. Hannover*, 1888, p. 605. See also his book "Die graphische Statik der Baukonstructionen," vol. II, p. 1, p. 96, 1904.

[1] The small changes Δl_1 and Δl_2 in the lengths l_1 and l_2 are neglected in these expressions.

Measuring this sum and dividing it by the height h, we obtain the decrease in the angle α_3.

Expression (a) can be represented in a simple analytical form very useful for numerical calculations. We note that the length b is equal to the sum of the horizontal projections of the lengths $\overline{C_2C_3}$ and $\overline{C_1C_3}$
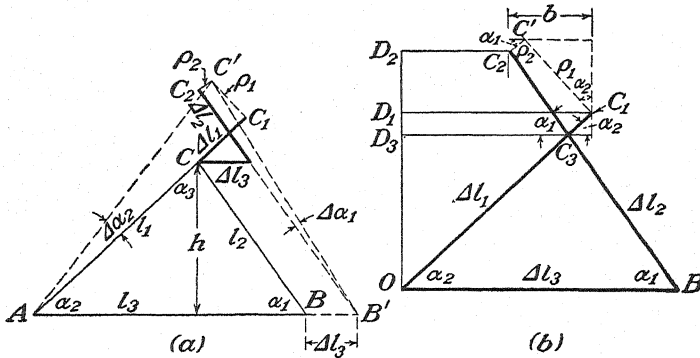
Fig. 352.

in Fig. 352b. The vertical projections of the same lengths are $\overline{D_2D_3}$ and $\overline{D_1D_3}$. Hence

$$b = \overline{D_2D_3} \cot \alpha_1 + \overline{D_1D_3} \cot \alpha_2. \qquad (b)$$

Observing that the triangle OC_3B in Fig. 352b is similar to the triangle ACB in Fig. 352a, we conclude that $OD_3 = h\,\Delta l_3/l_3$. Then,

$$\overline{D_2D_3} = \overline{OD_2} - \overline{OD_3} = \Delta l_2 \sin \alpha_1 - \frac{h\,\Delta l_3}{l_3} = h\left(\frac{\Delta l_2}{l_2} - \frac{\Delta l_3}{l_3}\right),$$

$$\overline{D_1D_3} = \overline{OD_1} - \overline{OD_3} = \Delta l_1 \sin \alpha_2 - \frac{h\,\Delta l_3}{l_3} = h\left(\frac{\Delta l_1}{l_1} - \frac{\Delta l_3}{l_3}\right).$$

Substituting these values in expression (b), we obtain

$$b = h\left(\frac{\Delta l_2}{l_2} - \frac{\Delta l_3}{l_3}\right) \cot \alpha_1 + h\left(\frac{\Delta l_1}{l_1} - \frac{\Delta l_3}{l_3}\right) \cot \alpha_2,$$

and Eq. (a) becomes

$$\Delta\alpha_3 = -\frac{b}{h} = \left(\frac{\Delta l_3}{l_3} - \frac{\Delta l_2}{l_2}\right) \cot \alpha_1 + \left(\frac{\Delta l_3}{l_3} - \frac{\Delta l_1}{l_1}\right) \cot \alpha_2. \qquad (c)$$

Upon introducing, for the stresses in the bars, the notations

$$\sigma_1 = E\,\frac{\Delta l_1}{l_1}, \qquad \sigma_2 = E\,\frac{\Delta l_2}{l_2}, \qquad \sigma_3 = E\,\frac{\Delta l_3}{l_3},$$

Eq. (*c*) can be finally represented in the following simple form:

$$E \, \Delta\alpha_3 = (\sigma_3 - \sigma_2) \cot \alpha_1 + (\sigma_3 - \sigma_1) \cot \alpha_2. \qquad (d)$$

Obviously this expression for the change in α_3 may be used also for the changes in α_1 and α_2 by a proper change of subscripts. Hence, for further reference, we write

$$\left. \begin{aligned} E \, \Delta\alpha_1 &= (\sigma_1 - \sigma_2) \cot \alpha_3 + (\sigma_1 - \sigma_3) \cot \alpha_2, \\ E \, \Delta\alpha_2 &= (\sigma_2 - \sigma_1) \cot \alpha_3 + (\sigma_2 - \sigma_3) \cot \alpha_1, \\ E \, \Delta\alpha_3 &= (\sigma_3 - \sigma_2) \cot \alpha_1 + (\sigma_3 - \sigma_1) \cot \alpha_2. \end{aligned} \right\} \qquad (32)$$

These three equations furnish a simple way of calculating the changes in the angles of all triangles of a truss if the stresses in the bars are known. In using them we have only to remember that σ_1, σ_2, and σ_3 denote the stresses in the bars opposite to the angles α_1, α_2, and α_3, respectively.
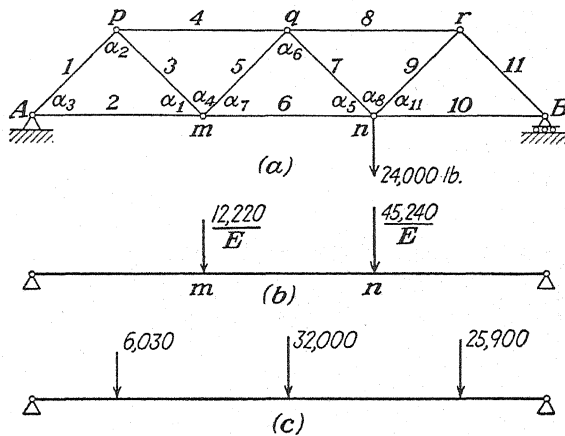
Fig. 353.

To illustrate the application of Eqs. (32), we take the example shown in Fig. 353*a* and assume that all dimensions and stresses are the same as those given in Table VI (page 281). Then, using the first of Eqs. (32) and observing that $\cot \alpha_2 = 0$ and $\cot \alpha_3 = 1$, we obtain

$$E \, \Delta\alpha_1 = - \frac{11,310}{3.66} - \frac{8,000}{3.66} = -5,276.$$

In a similar manner, we find $E \, \Delta\alpha_4 = -4,956$, $E \, \Delta\alpha_7 = -1,985$, $E \, \Delta\alpha_5 = -11,110$, $E \, \Delta\alpha_8 = -23,590$, $E \, \Delta\alpha_{11} = -10,540$. Since all these changes are negative, the angles decrease and we obtain deflection downward. The corresponding fictitious loads are shown in Fig. 353*b*. To obtain the deflection of joint *n*, we calculate the bending moment

at the cross section n of the fictitious beam and obtain

$$\delta_n = \frac{1}{E}\left(\frac{1}{3}\cdot 12{,}220 + \frac{2}{3}\cdot 45{,}240\right)120 = \frac{34{,}230\cdot 120}{E}.$$

The same result is obtained by using the fictitious loads in Figs. 348c and d.

If the chord whose deflection is required is of polygonal form as, for example, the lower chord of the truss in Fig. 351a, we have to consider the deflections of the *bar chain* shown in Fig. 354a. The deflections due to changes in the angles between the bars of this chain can be calculated in exactly the same manner as in the case of a straight chord. To show this, let us assume that the angle between the two chain members at a joint m diminishes by the amount $\Delta\theta_m$ while the other angles remain unchanged. To find the corresponding deflections, we assume first that the part Am of the chain remains immovable, while the part mB rotates with respect to the hinge m and the end B describes a small arc $r\,\Delta\theta_m$, the vertical projection of which is equal to $l_2\Delta\theta_m$. After this rotation, the vertical deflections of the joints to the left of m are zero, while the joints to the right of m have upward deflections,

$$y = -l_2\Delta\theta_m\cdot\frac{x - l_1}{l_2}. \tag{e}$$

To satisfy the condition of zero deflection at the right support B, we now rotate the bar chain as a rigid body with respect to joint A by such an amount that the joint B makes a vertical displacement equal to $l_2\Delta\theta_m$. The corresponding vertical displacements of other joints are then obtained from the equation

$$y = l_2\Delta\theta_m\cdot\frac{x}{l}. \tag{f}$$

Superposing these deflections on the deflections previously found, we conclude that expression (f) gives the total vertical deflections for the part Am of the bar chain, while for the part mB the final deflections are

$$y = -l_2\Delta\theta_m\frac{x - l_1}{l_2} + l_2\Delta\theta_m\frac{x}{l} = \Delta\theta_m l_1\frac{l - x}{l} \tag{g}$$

Expressions (f) and (g) coincide with those previously found for straight line chords (see page 287). Hence the vertical deflections of the joints of a bar chain, due to changes in the angles between the bars, can be found, as before, by calculating the bending moments produced in a simply supported beam by fictitious loads $\Delta\theta_i$.

In addition to the deflections produced by the changes $\Delta\theta_i$ in the angles there will be also deflections due to changes in the lengths of the

bars.   Referring to Fig. 354a, let us consider the bar i and assume that it makes an angle ϕ_i with the horizontal and has an elongation Δl_i.   Then, if we consider the left portion of the bar chain as immovable, the right portion, due to the elongation Δl_i, obtains a vertical displacement equal to

$$y = -\Delta l_i \sin \phi_i. \tag{h}$$

To bring the joint B back to the level AB, we now rotate the chain as a rigid body with respect to the joint A by an angle $\Delta l_i \sin \phi_i/l$.   Then
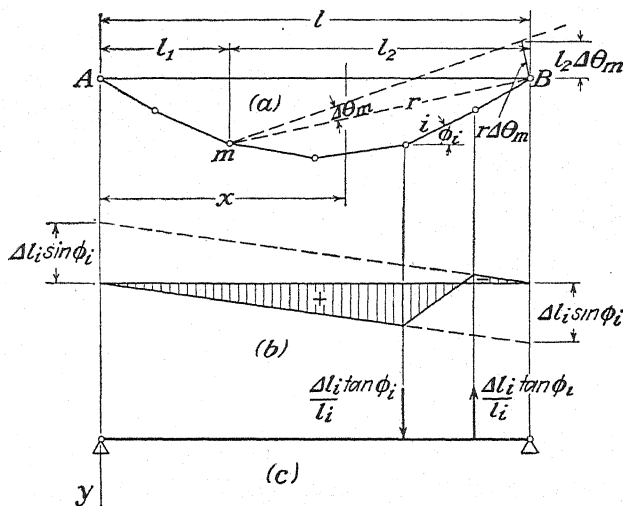
Fig. 354.

the final deflection for the left portion of the chain, due to the elongation Δl_i, is

$$y = \Delta l_i \sin \phi_i \cdot \frac{x}{l}. \tag{i}$$

For the right portion, combining the displacement (h) with the displacement (i), we find

$$y = \Delta l_i \sin \phi_i \frac{x}{l} - \Delta l_i \sin \phi_i = -\Delta l_i \sin \phi_i \cdot \frac{l-x}{l}.$$

These deflections are shown in Fig. 354b.   The shaded area in this figure is identical with the bending-moment diagram for the fictitious loads shown in Fig. 354c.   Hence the additional deflections, due to elongations of the chain bars, can be obtained by calculating the bending moments produced in a simply supported beam by the fictitious vertical loads

$$\frac{\Delta l_i \tan \phi_i}{l_i} \qquad \text{and} \qquad -\frac{\Delta l_i \tan \phi_i}{l_i} \tag{j}$$

applied at the ends of each bar. In this derivation Δl_i is taken positive when it represents an elongation, and ϕ_i is positive if the bar i is rotated in a counterclockwise direction with respect to the axis AB as we pass along the bar chain from A to B.

To show an application of the above formulas, let us calculate the deflections of the upper joints of the truss in Fig. 353a. We have to consider here the inclined bars 1 and 11, which, together with the two horizontal bars 4 and 8, form the bar chain attached to the supports A and B. Using the numerical data in Table VI and Eqs. (32), we calculate the changes in the angles between the chord members. These calculations give the fictitious loads

$$E \, \Delta\theta_p = 3{,}017, \qquad E \, \Delta\theta_q = 32{,}000, \qquad E \, \Delta\theta_r = 19{,}710. \qquad (k)$$

To take care of the changes in the lengths of the chain bars, we use expressions (j), which give for the joints p and r the additional fictitious loads in the downward direction equal to[1]

$$\frac{E \, \Delta l_1}{l_1} = 3{,}010 \qquad \text{and} \qquad E \, \frac{\Delta l_{11}}{l_{11}} = 6{,}200. \qquad (l)$$

The total fictitious loading is shown in Fig. 353c, and for the deflection of the middle joint we obtain

$$\delta_q = \frac{1}{E} \, (32{,}000 \cdot 90 + 25{,}900 \cdot 30 + 6{,}030 \cdot 30) = \frac{3{,}838 \cdot 10^3}{E}.$$

This result coincides with that previously obtained by using the Maxwell-Mohr method (see page 282).

[1] The bending moment produced by these loads must be divided by E to obtain the deflections.

CHAPTER VII

STATICALLY INDETERMINATE PIN-JOINTED TRUSSES

49. General Considerations.—In Chap. II we have already seen that any pin-jointed truss in one plane is generally rigid and *statically determinate* if its j joints are interconnected between themselves and the foundation by $m = 2j$ bars. · If the bars exceed this number, the available $2j$ simultaneous equations of statics are insufficient to determine the internal forces and the truss is said to be *statically indeterminate*. Those
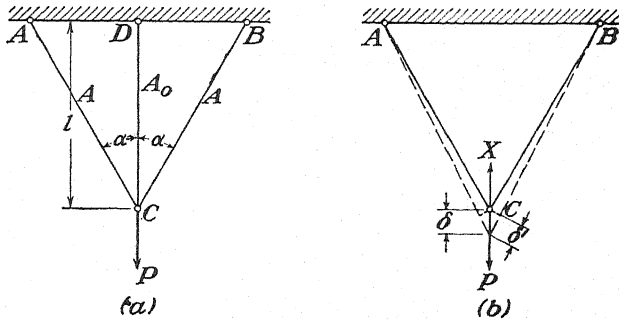
Fig. 355.

bars in excess of the $2j$ which are both necessary and sufficient for the rigidity of a truss are usually called *redundant members*. A simple example of a truss with one redundant member is shown in Fig. 355a. Here we have a single joint C attached to a foundation by three bars arranged in one plane as shown. For simplicity, we assume the two inclined bars to be identical so that the system is symmetrical with respect to the vertical axis CD. If a vertical load P is applied at C as shown, some axial force will be induced in each of the three bars; but since, for the joint C, we have only two equations of equilibrium

$$\Sigma X = 0 \quad \text{and} \quad \Sigma Y = 0, \tag{a}$$

there is evidently one redundant element and the system is statically indeterminate. That is, so long as we consider the bars to be absolutely rigid, we can assume any value X for the tension in the vertical bar (Fig. 355b); and then, using Eqs. (a), we shall find that each inclined bar carries a tensile force

$$S = \tfrac{1}{2}(P - X) \sec \alpha. \tag{b}$$

293

To find the true value of X, we must now consider the elastic deformations of the bars. Denoting by δ the elongation of the middle bar, we see from Fig. 355b that the corresponding elongation of each inclined bar must be[1]

$$\delta' = \delta \cos \alpha. \qquad (c)$$

Now, by using expression (b) for the axial force in an inclined bar and denoting by A and A_0 the cross-sectional areas of the bars as shown in the figure, condition (c) may be written in the following form,

$$\frac{(P - X)l}{2 \cos^3 \alpha A E} = \frac{Xl}{A_0 E},$$

from which

$$X = \frac{P}{1 + 2(A/A_0) \cos^3 \alpha}.$$

Using this value of X in Eq. (b), we can now find the corresponding value of S for each inclined bar, and the analysis is completed.

Reviewing the foregoing procedure, we see that, to solve the given statically indeterminate problem, we first removed the redundant bar CD and replaced it by the force X which it exerted on the remaining statically determinate system. Then this system (Fig. 355b) was analyzed by the ordinary equations of statics and all axial forces expressed in terms of the unknown quantity X. Finally, to find the true value of X, we established an additional equation (c) by taking account of the elastic deformations of the bars.

The same procedure can be applied in more complicated cases. We begin with a proper selection of the members that will be considered as redundants. Removing these bars, we obtain a statically determinate system, called the *primary system*. This primary system can then be analyzed by the methods already discussed in preceding chapters, and we can readily find the forces in all bars and also the displacements of all joints. We shall be especially interested in the changes in distance between those joints corresponding to the removed redundant members; for evidently these changes must be equal to the changes in length of the corresponding redundant bars in the actual truss. In this way we obtain as many equations, similar to Eq. (c), as there are redundant bars; and, from these equations, the forces in the redundant bars are obtained. The forces in the remaining bars are then found from statics.

From the discussion we see that the redundant bars must be so selected that after their removal we obtain a rigid statically determinate truss. Take, for example, the statically indeterminate system shown in Fig.

---

[1] This relation assumes that the elastic elongations of the bars are small compared with the over-all dimensions of the structure.

356. The truss proper has 14 bars, and in addition to this we have to consider a vertical supporting bar replacing the movable support at the right end of the truss and two bars replacing the immovable support at the left end. All together, then, we have 17 unknown forces, while the doubled number of joints is 16. Thus we have a truss with one redundant member. As a redundant member we can select, for example, one of the diagonals in the middle panel of the truss. But we cannot take the diagonal in one of the other panels as a redundant bar, for after removing such a diagonal we obtain a nonrigid system.
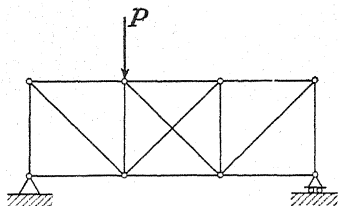
Fig. 356.
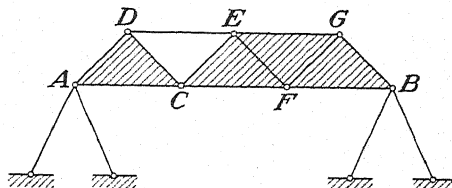
Fig. 357.

In Fig. 357 we have another example of a truss with one redundant member. As the redundant member in this case, we can take any one of the supporting bars; but such a bar as DE cannot be selected, for after its removal we obtain a system having a critical form. That is, we have the two rigid shaded portions supported at A and B and joined together by a hinge C like a three-hinged arch; but since the hinge C lies on the straight line AB, it can have considerable vertical movement without appreciable changes in length of any of the bars. There are, however, other possibilities besides the removal of one of the supporting bars. For example, if we remove the bar CF, we obtain, as our primary system, an ordinary three-hinged arch

Fig. 358.

in which the hinge E does not lie on the straight line AB. Hence there is no critical form in such case, and the bar CF can be chosen as the redundant bar, if desired.
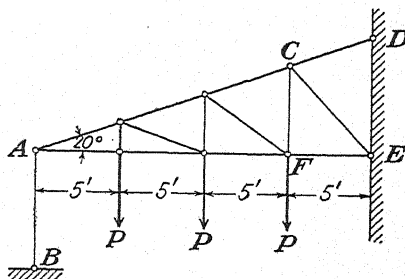
Figure 358 represents another system with one redundant bar. As the redundant in this case, we can take the bar AB or the bar CD; but we cannot select the bar CE, for after its removal we obtain a rigid frame ACF attached to the foundation by three bars AB, CD, and EF that intersect in one point. Such a system, as we already know (see page 49), is not rigid.

The truss represented in Fig. 359 is statically indeterminate and has one redundant member. Without counting the number of bars, it may be seen that by removal of only one bar AB we transform the given
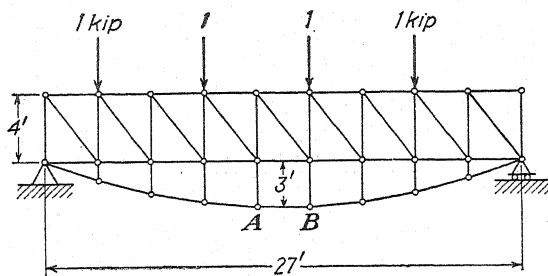
Fig. 359.

truss into a statically determinate simple truss. Thus it is advisable to select the bar AB as the redundant member in this truss.

Sometimes a system may prove to be nonrigid even though it has redundant members. Take, for example, the truss in Fig. 360. It has two redundant members, but at the same time it is not a rigid system and may suffer considerable distortion, if not complete collapse, under load. In our further discussion of statically indeterminate systems, we shall rule out all such *critical forms*.

50. Trusses with One Redundant Member.—As a first example of a system with one redundant member, let us consider the truss on three supports as shown in Fig. 361a. As a redundant member, we take the intermediate sup-
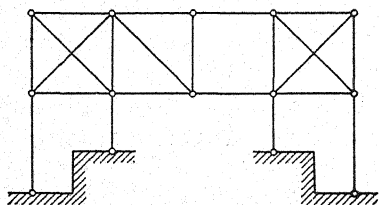
Fig. 360.
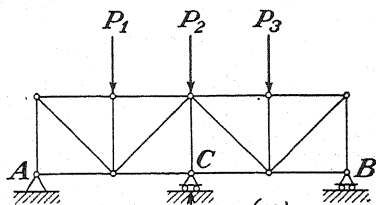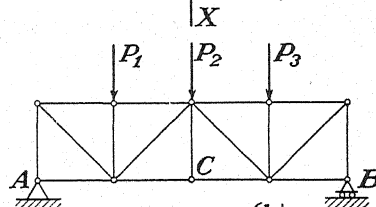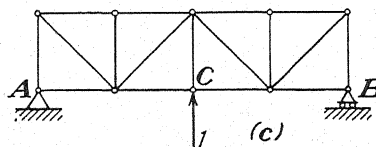
Fig. 361.

port C. Removing this support, we obtain a statically determinate simple truss (Fig. 361b) that can be readily analyzed. The redundant reaction X at the intermediate support is now determined from the condition that the deflection of joint C produced by the combined action of the

loads P_1, P_2, P_3 and the reaction X must vanish. Using expression (31) for this deflection we obtain

$$\Sigma\, \Delta l_i s_i' = 0, \tag{a}$$

in which $\Delta l_i = S_i l_i / A_i E$ denotes the change in length of any bar i due to the loads P_1, P_2, P_3 and the redundant reaction X, and s_i' is obtained by using the unit loading[1] shown in Fig. 361c and represents the ratio of the force in any bar i to the unit load at C that produces it. In calculating the values Δl_i, in expression (a), we note that the force S_i in a bar i is given by the equation

$$S_i = S_i' + s_i' X, \tag{b}$$

in which S_i' is the force in any bar i produced by the known external loads P_1, P_2, P_3, acting on the simple truss shown in Fig. 361b, and $s_i' X$ is the force produced in the same bar by the reaction X. Then the required elongation of any bar i is

$$\Delta l_i = \frac{(S_i' + s_i' X) l_i}{A_i E} = (S_i' + s_i' X)\rho_i, \tag{c}$$

where

$$\rho_i = \frac{l_i}{A_i E}. \tag{d}$$

Substituting expression (c) into Eq. (a), we obtain

$$\Sigma (S_i' + s_i' X)\rho_i s_i' = 0, \tag{e}$$

from which

$$X = -\frac{\Sigma S_i' s_i' \rho_i}{\Sigma (s_i')^2 \rho_i}. \tag{33}$$

With the value of the redundant reaction X, the forces in the bars of the given statically indeterminate truss (Fig. 361a) are obtained from Eq. (b), and the analysis is completed. It is seen that our statically indeterminate problem (Fig. 361a) is reduced to the two statically determinate problems shown in Fig. 361b and Fig. 361c. The values S_i', s_i', and ρ_i for all members of the truss can be put in tabular form as was done in Table V, p. 259. Then, with the aid of such a table, the values of the sums entering in Eq. (33) can be readily calculated.

As a second example, let us consider the statically indeterminate truss shown in Fig. 362a. The reactions in this case can be readily calculated from equations of statics, but the forces in the bars cannot be determined by statics alone because the truss contains one redundant member. Let us take the vertical bar BC as the redundant bar. Then, after removal

---

[1] The unit load at C is taken in the upward direction so that we may consider the redundant reaction X as positive in this direction.

of this bar, we obtain a statically determinate simple truss (Fig. 362b) on which, in addition to the known loads P_1, P_2, P_3, there will act the two equal and opposite forces X replacing the removed bar as shown. The magnitude of X is found from the condition that the change in the distance between the joints B and C of the statically determinate truss (Fig. 362b) must be equal to the change in length of the vertical bar BC of the actual truss (Fig. 362a). This change in the distance BC is

$\Sigma \Delta l_i s_i'$, in which the summation includes all bars of the statically determinate truss (Fig. 362b) and the values of Δl_i are given by the equation

$$\Delta l_i = (S_i' + s_i' X)\rho_i, \qquad (f)$$

in which S_i' denotes the force produced in any bar i by the given loads P_1, P_2, P_3 and s_i' is found, as before, by using the unit loading shown in Fig. 362c.

The equation for calculating X then becomes

$$\Sigma(S_i' + s_i' X)\rho_i s_i' = -X\rho_0, \qquad (g)$$

where

$$\rho_0 = \frac{l_0}{A_0 E} \qquad (h)$$

FIG. 362.

is the quantity defining the extensibility of the redundant bar BC. The minus sign in the right-hand side of Eq. (g) follows from the directions of the unit loads in Fig. 362c. With these directions, shortening of the distance BC becomes positive, which corresponds to compression of the vertical bar BC. Solving Eq. (g) for X, we obtain
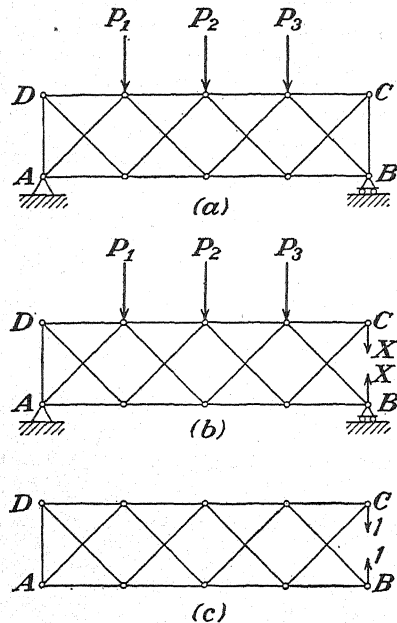
$$X = -\frac{\Sigma S_i' s_i' \rho_i}{\Sigma (s_i')^2 \rho_i + \rho_0}. \qquad (34)$$

In this example we see again that calculation of the redundant force X is reduced to two statically determinate problems, (1) the calculation of the forces S_i' and (2) the calculation of the forces s_i'. When all these forces are found and the quantities ρ_i and ρ_0 are determined from the given dimensions of the truss, the sums entering into Eq. (34) can be readily evaluated.

In each of the foregoing examples, we used expression (31) as a basis of evaluation of displacements. However, we can come to the same

results by using the principle of least work as discussed in Art. 42. On this basis, for example, the value X for the redundant reaction at C in Fig. 361 must be such as to make the total strain energy of the statically indeterminate system a minimum. Using expression (b) for the forces in the bars, the total strain energy of the truss becomes

$$U = \sum \frac{(S_i' + s_i'X)^2 l_i}{2A_i E}.$$

Equating to zero the derivative of this expression with respect to X and using the notation in expression (d), we obtain

$$\Sigma(S_i' + s_i'X)\rho_i s_i' = 0,$$

which coincides with our previous expression (e) and leads to Eq. (33).
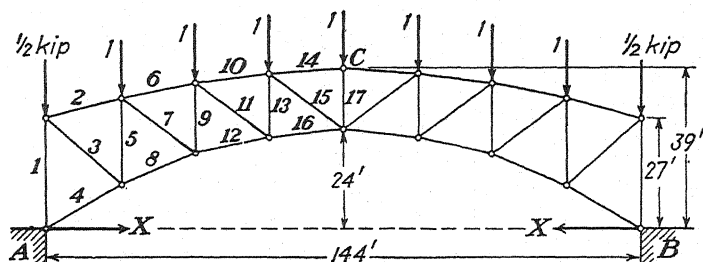
FIG. 363.

In the same way the total strain energy of the statically indeterminate truss in Fig. 362 becomes

$$U = \sum \frac{(S_i' + s_i'X)^2 l_i}{2A_i E} + \frac{X^2 l_0}{2A_0 E},$$

where the summation includes all bars of the primary system (Fig. 362b). Equating to zero the derivative of this expression with respect to X and using the notations in expressions (d) and (h), we obtain our previous expression (g), leading to Eq. (34).

As a specific example with numerical data and all calculations, let us consider the two-hinged arch loaded as shown in Fig. 363 and calculate the magnitude X of the horizontal thrust. The over-all dimensions of the structure are shown in the figure, and the lengths of the individual bars are given in column (2) of Table VII. Here also are given, for each bar, the cross-sectional area A_i, the quantity ρ_i, assuming $E = 30(10)^6$ lb. per sq. in., and the axial forces S_i' and s_i'.* Using the data from the

* These axial forces can be found without difficulty by constructing Maxwell diagrams for the statically determinate primary system obtained by removing the horizontal constraint at B.

table and forming the sums appearing in Eq. (33), we find

$$X = -\frac{-117,109}{29.171} = 4,015 \text{ lb.}$$

TABLE VII

(1)	(2)	(3)	(4)	(5)	(6)	(7)	(8)	(9)
i	l_i, in.	A_i, in.²	$\rho_i \cdot (10)^6$, in. /lb.	S_i', lb.	s_i'	$(s_i')^2$	$S_i's_i'\rho_i(10)^6$	$(s_i')^2\rho_i(10)^6$
1	324	11.5	0.940	−4,000	+0.59	0.35	− 2,220	0.329
2	227	11.8	0.641	−3,000	+0.50	0.25	− 962	0.160
3	292	9.0	1.081	+3,900	−0.65	0.42	− 2,740	0.454
4	259	11.5	0.750	0	−1.16	1.35	− 0	1.012
5	263	9.0	0.974	−3,800	+0.47	0.22	− 1,740	0.214
6	220	11.8	0.621	−6,200	+1.00	1.00	− 3,850	0.621
7	277	9.0	1.026	+3,950	−0.64	0.41	− 2,600	0.421
8	234	11.5	0.678	+3,150	−1.60	2.56	− 3,420	1.735
9	216	9.0	0.800	−2,750	+0.30	0.09	− 660	0.072
10	216	11.8	0.610	−8,600	+1.43	2.04	− 7,500	1.244
11	270	9.0	1.000	+3,200	−0.55	0.30	− 1,760	0.300
12	223	11.5	0.646	+6,200	−2.05	4.20	− 8,210	2.712
13	192	9.0	0.711	−1,150	+0.03	0.00	− 24	0
14	216	11.8	0.610	−9,700	+1.60	2.56	− 9,470	1.560
15	277	9.0	1.026	+1,400	−0.23	0.05	− 330	0.051
16	216	11.5	0.626	+8,600	−2.43	5.90	− 13,080	3.694
							−117,132	29.158
17	180	9.0	0.667	− 250	−0.14	0.02	+ 23	0.013
Σ.							−117,109	+29.171

PROBLEMS

236. Find the horizontal thrust X for the statically indeterminate truss shown in Fig. 364a. All dimensions are given in the figure, and the cross-sectional areas of the bars are as follows: $A_1 = A_4 = 5$ sq. in., $A_2 = A_5 = 3$ sq. in., and $A_3 = 2$ sq. in.

Ans. $X = (540.9/616.5)P$.

237. Determine the axial force in the redundant horizontal bar AB of the truss shown in Fig. 364b if the cross-sectional area of this bar is A_6. Assume that the other bars have the same dimensions as in the preceding problem.

Ans. $X = \dfrac{540.9P}{300/A_6 + 616.5}$.

238. Determine the axial forces in all bars of the statically indeterminate system shown in Fig. 365a, assuming that the cross-sectional areas of all bars are equal.

HINT: Take the axial force X in the diagonal bar 6 as the redundant element.

Ans. $X = [(3 + 2\sqrt{2})/(4 + 2\sqrt{2})]P$.

239. Calculate the axial forces in all bars of the statically indeterminate system

shown in Fig. 358. Take the bar AB as the redundant member, and assume that all bars are 1 sq. in. in cross section. $P = 1,000$ lb.
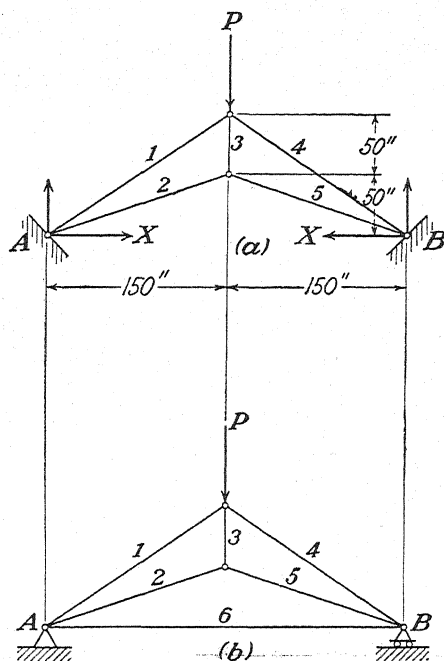
FIG. 364.
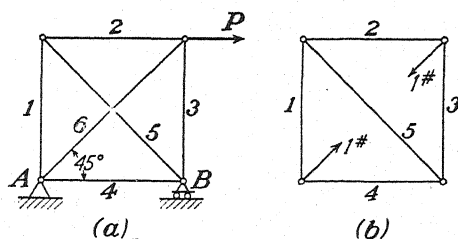
FIG. 365.

240. Make a complete analysis of the statically indeterminate truss shown in Fig. 359. Assume, in calculation, that each bar has a cross-sectional area $A_i = 1$ sq. in. and that the lower chord is of parabolic form.

51. Trusses with Several Redundant Members.—The method used in the preceding article for the analysis of statically indeterminate trusses with one redundant member can be readily extended to trusses with two or more redundant members. As a first example let us consider the simple truss with two redundant supports as shown in Fig. 366a. Removing these supports and replacing them by the reactive forces X and Y as

shown in the figure, we obtain a statically determinate system on which, in addition to the given loads P_1, P_2, P_3, the two redundant reactions X and Y are acting. The magnitudes of these reactions will now be found from the conditions that the deflections of the joints C and D must vanish. For these deflections, we use expression (31), which gives in this case the following equations,

$$\left. \begin{array}{l} \Sigma \, \Delta l_i s_i' = 0, \\ \Sigma \, \Delta l_i s_i'' = 0, \end{array} \right\} \tag{a}$$

in which the quantities s_i' and s_i'' are obtained by using the unit loadings shown in Figs. 366b and 366c, respectively. The quantities Δl_i are the actual elongations of the bars of the system (Fig. 366a) produced by the
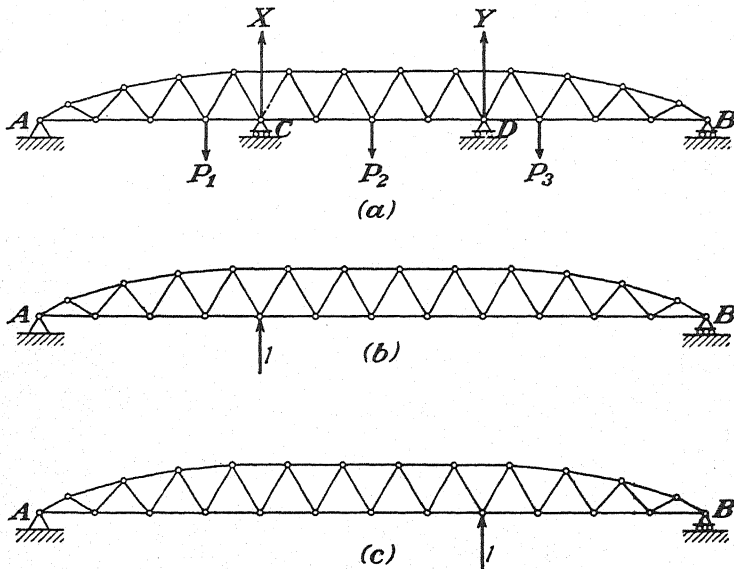
FIG. 366.

given loads P_1, P_2, P_3 and the unknown reactions X and Y. The force in any bar i of the primary system (Fig. 366b) due to the given loads P_1, P_2, P_3 is denoted, as before, by S_i'. The forces produced in the same bars by the redundant reactions X and Y are obtained by using the unit loads shown in Figs. 366b and 366c and are equal to $s_i'X$ and $s_i''Y$, respectively. Hence the total force in any bar i is

$$S_i = S_i' + s_i'X + s_i''Y, \tag{b}$$

and the corresponding elongation is

$$\Delta l_i = (S_i' + s_i'X + s_i''Y)\rho_i.$$

Substituting into Eqs. (*a*), we obtain the following two equations for calculating X and Y:

$$\Sigma(S_i' + s_i'X + s_i''Y)\rho_i s_i' = 0, \\ \Sigma(S_i' + s_i'X + s_i''Y)\rho_i s_i'' = 0, \Bigg\} \qquad (c)$$

or

$$X\Sigma(s_i')^2\rho_i + Y\Sigma s_i' s_i''\rho_i = -\Sigma S_i' s_i'\rho_i, \\ X\Sigma s_i' s_i''\rho_i + Y\Sigma(s_i'')^2\rho_i = -\Sigma S_i' s_i''\rho_i. \Bigg\} \qquad (d)$$

Having the values of S_i', s_i', s_i'', and ρ_i tabulated, we can readily evaluate the sums that appear in Eqs. (*d*) and solve the equations for X and Y. Then upon substituting these values in Eq. (*b*), we can calculate the forces in all bars of the truss. It is seen from this discussion that the analysis of a system with two redundant supports reduces to the analysis of three statically determinate problems, *i.e.*, to the evaluation of the forces S_i', s_i', and s_i''.

Equations (*c*) for calculating the redundant reactions can be obtained also by using the principle of least work. The total strain energy of the system shown in Fig. 366*a* is

$$U = \tfrac{1}{2}\Sigma(S_i' + s_i'X + s_i''Y)^2\rho_i.$$

Equating to zero the derivatives of this expression with respect to X and Y we obtain Eqs. (*c*).

As a second example let us consider the statically indeterminate truss shown in Fig. 367*a*. This truss has 83 bars. Adding to this number six elements of constraint for the system of supports, we have all together 89 unknown forces; twice the number of joints is 86. Hence there are three redundant members. As these redundants we select the two horizontal bars *ab* and *cd* and the horizontal constraint at the support *D*. Removing these three redundant elements and replacing their actions by forces X, Y, and Z, we obtain a statically determinate system consisting of the three simple trusses shown in Fig. 367*b*. The forces produced in the members of this statically determinate system by the given loads P_1, P_2, P_3 we denote by S_i'. The forces produced in the members of the same system by the redundant forces X, Y, and Z are found, as before, by using the unit loadings shown in Figs. 367*c*, 367*d*, and 367*e*. The corresponding axial forces in any bar i we denote, respectively, by s_i', s_i'', and s_i'''. Then the total force in a bar i of the given system (Fig. 367*a*) is

$$S_i = S_i' + s_i'X + s_i''Y + s_i'''Z. \qquad (e)$$

The values of the three redundant forces X, Y and Z are obtained, now, from the conditions that the changes in distance between the joints *a* and *b* and the joints *c* and *d* (Fig. 367*b*) must be equal to the changes in length of the bars *ab* and *cd* (Fig. 367*a*), while the horizontal displace-

ment of the support at D must vanish. Denoting by ρ_x and ρ_y the extensibility factors for the redundant bars ab and cd and using expression
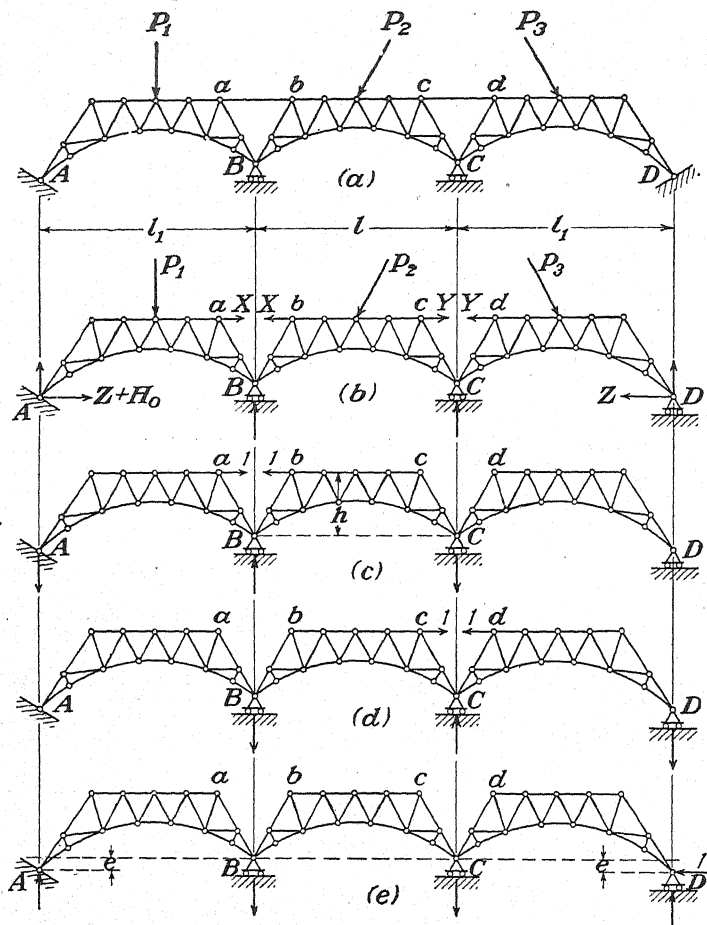
FIG. 367.

(31) for displacements, we can represent the foregoing conditions in the form of equations as follows:

$$\left.\begin{array}{l}
\Sigma(S_i' + s_i'X + s_i''Y + s_i'''Z)\rho_i s_i' = -X\rho_x, \\
\Sigma(S_i' + s_i'X + s_i''Y + s_i'''Z)\rho_i s_i'' = -Y\rho_y, \\
\Sigma(S_i' + s_i'X + s_i''Y + s_i'''Z)\rho_i s_i''' = 0.
\end{array}\right\} \qquad (f)$$

The minus signs in the first two equations result from the fact that, for the directions of the unit loads in Figs. 367c and 367d, positive displacements correspond to shortening of the distances ab and cd and hence to compressive forces in the redundant bars ab and cd. If the values $\rho_i, s_i', s_i'', s_i'''$ for all bars of the primary system (Fig. 367b) are tabulated,

the sums appearing in Eqs. (f) can be evaluated and we obtain three linear equations, with numerical coefficients, that can be solved for the unknown redundant forces X, Y, and Z.

From the foregoing discussion it may be seen that, as the number of redundant forces increases, the number of equations required for their determination increases also and the problem of analysis becomes more and more involved. Sometimes we find cases where each equation contains only a few of the redundant forces; such equations can be solved without much difficulty even though the total number of unknowns may be large. As an example of this kind, let us consider the truss with five redundant bars as shown in Fig. 368a. Selecting one diagonal from each panel as a redundant bar and representing the actions of these bars on the remainder of the truss by redundant forces X, Y, Z, . . . , we obtain as our primary system a statically determinate simple truss loaded as shown in Fig. 368b. This sytem can be readily analyzed, and the force in any bar i will be

$$S_i = S_i' + s_i'X + s_i''Y + s_i'''Z + \cdots$$

The quantity S_i' in this expression denotes the force produced in any bar i of the primary system (Fig. 368b) by the given loads P_1, P_2, P_3, while the quantities s_i', s_i'', s_i''', . . . are obtained, as before, by using such unit loadings as those shown in Figs. 368c and 368d. Considering these loadings, we see that in each case the applied unit loads produce axial forces only in those bars which comprise the corresponding panel. Thus, in Fig. 368c we conclude that the axial forces s_i' are different from zero only for the bars of the first panel as shown by heavy lines. Likewise, in Fig. 368d, the forces s_i'' vanish for all members except those indicated by heavy lines, etc. With the foregoing observations in mind, let us now consider the equations for determining the redundant

Fig. 368.

forces. The first of these equations will be written on the basis of the fact that the change in the distance between joints A and B of the simple truss (Fig. 368b) is equal to the change in length of the redundant diagonal AB in the actual truss (Fig. 368a). This change in the distance AB obviously depends only on the deformations of the bars within the first panel of the truss, and the forces in these bars depend only on the given loads P_1, P_2, P_3 and the redundant forces X and Y. The remaining redundant forces do not affect the bars of the first panel and need not be considered. Hence the first equation becomes

$$\sum_{i=1}^{i=5} (S_i' + s_i'X + s_i''Y)\rho_i s_i' = -X\rho_x. \tag{g}$$
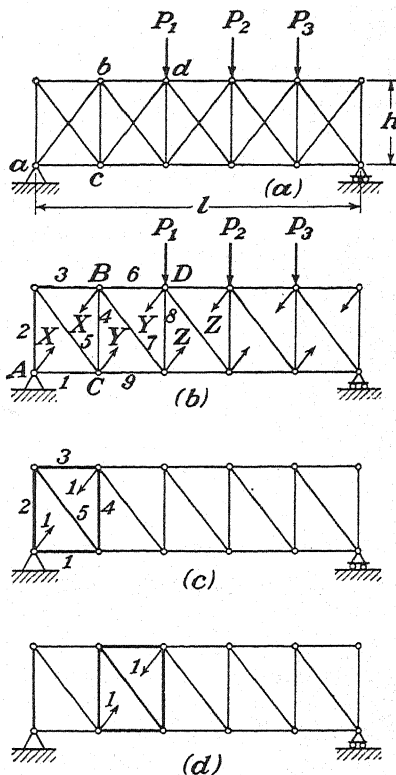
This equation contains only two unknowns, X and Y, and the summation includes only the five bars of the first panel. For the remaining bars, as already mentioned, s_i' vanishes.

The second equation is obtained by equating the change in the distance between joints C and D (Fig. 368b) to the change in length of the diagonal CD in the redundant truss (Fig. 368a). This change in the distance CD depends only on the deformations of the bars within the second panel of the truss (Fig. 368b), and these deformations in turn depend only on the lateral loads P_1, P_2, P_3 and on the redundant force Y in the second panel, together with the redundant forces X and Z in the adjacent panels. Hence the second equation becomes

$$\Sigma(S_i' + s_i'X + s_i''Y + s_i'''Z)\rho_i s_i'' = -Y\rho_y, \tag{h}$$

where the summation includes all bars of the second panel. This equation contains three unknowns, X, Y, and Z.

Similar equations can be written for the third and fourth panels. The fifth equation will again have only two unknowns like Eq. (g). Thus we obtain a system of five equations, two of which have two unknowns each, while the remaining three have three unknowns each. Such a system of equations can be readily solved. They are similar to *three-moment equations* as used in the analysis of continuous beams, and the same methods of solution can be applied.

A method of successive approximations is sometimes useful in the analysis of a statically indeterminate system with many redundant elements. For example, to obtain a first approximation X_1, Y_1, Z_1, . . . for the unknown forces X, Y, Z, . . . in the system above, we assume that the shear in each panel is equally divided between the two diagonals of that panel. Then, coming to Eqs. (g), (h), . . . and noting that the most important terms are those having for coefficients the summations of squares like $\Sigma(s_i')^2$, $\Sigma(s_i'')^2$, . . . , we replace the unknowns X, Y, Z, . . . in the remaining terms by their first approximations X_1, Y_1, Z_1, . . . and obtain in this way the equations

$$\Sigma S_i' s_i'\rho_i + [\Sigma(s_i')^2\rho_i + \rho_x]X + \Sigma s_i' s_i''\rho_i Y_1 = 0,$$
$$\Sigma S_i' s_i''\rho_i + \Sigma s_i' s_i''\rho_i X_1 + [\Sigma(s_i'')^2\rho_i + \rho_y]Y + \Sigma s_i'' s_i'''\rho_i Z_1 = 0, \tag{i}$$
. . . .

Each of these equations contains only one unknown and can be easily solved. In this manner, we obtain a second approximation X_2, Y_2, Z_2, . . . for the unknown forces. Then, upon putting these new values, instead of X_1, Y_1, Z_1, . . . , in Eqs. (i) and solving again for X, Y, Z, . . . , a further approximation for the unknowns can be calculated. Usually this process converges fairly rapidly so that the third approximation will be satisfactory for all practical purposes.

PROBLEMS

241. Evaluate the redundant reactions at the intermediate supports C and D of the truss shown in Fig. 369 if the load $P = 20,000$ lb. All bars of the truss are identical.
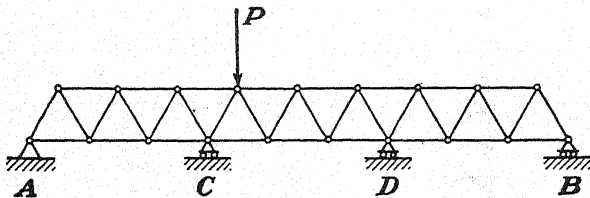
FIG. 369.

242. Solve the preceding problem if the rollers at C and D are replaced by vertical bars like those comprising the truss itself.

243. Make a complete analysis of the statically indeterminate truss shown in Fig. 368, if $P_1 = P_2 = P_3 = 20,000$ lb., $l = 45$ ft., and $h = 12$ ft. Assume that each chord member has a cross-sectional area of 3 sq. in., each diagonal of 2 sq. in., and each vertical of 1 sq. in.

52. Assembly and Thermal Stresses in Statically Indeterminate Trusses.

—From the preliminary discussion of statically indeterminate trusses given in Art. 49, it is evident that the lengths of redundant bars must satisfy certain geometrical requirements. The shape of a truss and the mutual distances of all its joints are entirely defined by the lengths of the members of the *primary system.* Hence a redundant member can be freely placed between two joints only if its length is exactly equal to the distance between these joints. Otherwise the bar will not fit its proper place and can be forced into the primary system only by applying some initial extension or compression. Under such conditions, it is evident that some axial forces, usually called *assembly forces,* will be induced in the bars during the formation of the truss. These internal forces exist even in the absence of external loads and must be superimposed on the axial forces produced by external loading in order to get the total force in each bar.

Take, as a simple example, the statically indeterminate system shown in Fig. 355a, and assume that in consequence of small errors in the lengths of the inclined bars the distance between the hinges C and D, measured after assembly of the inclined bars, is larger by an amount Δ than the length of the vertical bar. Then, to put this latter bar in place, we must somewhat extend it. Thus after assembly it will pull up on the joint C and induce compression in the inclined bars while remaining under some tension itself. If X is the magnitude of the tensile force in the vertical bar, after assembly, the compressive forces in the inclined bars will be equal to $X/2 \cos \alpha$ and the corresponding upward displacement of the joint C will be $Xl/2AE \cos^3 \alpha$. The magnitude of the force X is now found from the condition that the vertical displacement of the joint C together with the elongation of the vertical bar must be equal to the initial discrepancy Δ in length. Hence,

$$\frac{Xl}{2AE \cos^3 \alpha} + \frac{Xl}{A_0 E} = \Delta,$$

where A_0 is the cross-sectional area of the vertical bar and A the cross-sectional area of an inclined bar. From this equation, we find

$$X = \frac{\Delta A E}{l(\frac{1}{2} \sec^3 \alpha + A/A_0)}.$$

Similar reasoning can be applied in more complicated cases of statically indeterminate trusses. Let us consider, for example, the truss in Fig. 362a and find the assembly forces that will result from inaccuracies in the lengths of the bars. Let Δ_i be the error in length of any bar i, considered positive if the bar is too long, and Δ_0 the error in length of the redundant bar BC. The effect of the errors Δ_i on the distance between the joints B and C of the primary system (Fig. 362b) is found by using Eq. (31), from which it follows that the above-mentioned distance is shorter than that theoretically designed for by an amount

$$\Sigma \, \Delta_i s_i'. \tag{a}$$

To take care of this error and also of the error Δ_0 in the length of the redundant bar BC, we have to produce some compression in this latter bar before placing it between the joints B and C. After assembly, then, the redundant bar will be pushing on the joints B and C, and assembly forces will be induced throughout the truss. If X denotes the assembly force in the redundant member,[1] the corresponding elongations of the members of the principal system are $s_i'X\rho_i$ and the diminishing of the distance BC, due to these elongations, is $\Sigma(s_i')^2 X\rho_i$. This change in distance, together with the elongation $X\rho_0$ of the redundant bar, must be numerically equal to the initial discrepancy between the distance BC in the primary system and the length of the redundant bar BC. Hence we obtain

$$\Sigma(s_i')^2 X\rho_i + X\rho_0 = -[\Sigma \, \Delta_i s_i' + \Delta_0]. \tag{b}$$

The minus sign on the right follows from the fact that we like to consider positive X as tension, while the expression in the brackets indicates how much the distance BC (Fig. 362b) is shorter than the length of the redundant bar. Solving the equation for X, we obtain

$$X = - \frac{\Sigma \, \Delta_i s_i' + \Delta_0}{\Sigma(s_i')^2 \rho_i + \rho_0}. \tag{35}$$

Upon adding this force to that produced by lateral loading of the truss [see Eq. (34)], the total force in the redundant bar becomes

$$X = - \frac{\Sigma(S_i'\rho_i + \Delta_i)s_i' + \Delta_0}{\Sigma(s_i')^2 \rho_i + \rho_0}. \tag{36}$$

Assembly forces can be calculated in the same way if the redundant force is an external reaction. Take, for example, the truss shown in Fig. 361a, and assume that the middle support is too high by an amount Δ_0. Denote also, as before, by Δ_i the error in length of any bar i. Owing to these errors the joint C of the primary system (Fig. 361b) is displaced

---

[1] Tension considered positive.

upward by an amount equal to $\Sigma \, \Delta_i s_i'$, where the values of s_i' are obtained from the unit loading shown in Fig. 361c. The required reaction will be found from the condition that the upward deflection of the primary system produced by X is equal to $\Delta_0 - \Sigma \, \Delta_i s_i'$. Hence,

$$\Sigma X(s_i')^2 \rho_i = \Delta_0 - \Sigma \, \Delta_i s_i',$$

and we obtain

$$X = \frac{-\Sigma \, \Delta_i s_i' + \Delta_0}{\Sigma (s_i')^2 \rho_i}. \tag{37}$$

Adding this to the previously found reaction produced by lateral loading of the truss [see Eq. (33)], we obtain for the total reaction at the intermediate support

$$X = -\frac{\Sigma (S_i' \rho_i + \Delta_i) s_i' - \Delta_0}{\Sigma (s_i')^2 \rho_i}. \tag{38}$$

If the middle support settles by an amount Δ_0, we simply take this quantity with negative sign in Eqs. (37) and (38).

The equations derived for calculating assembly forces can be used also in calculating forces produced in a statically indeterminate truss by a temperature change. If the temperature of a bar i is increased by an amount t_i above a certain specified uniform temperature of the truss, the length of the bar increases by the amount $\alpha_i t_i l_i$, where α_i is the coefficient of linear thermal expansion for the bar. Treating these thermal elongations of the bars in the same way as the errors in length Δ_i in our preceding discussion, the thermal stresses in statically indeterminate trusses can be readily calculated. Taking, for example, the truss in Fig. 362a and using Eq. (35), we find that the force produced in the redundant bar BC by the temperature change is

$$X = -\frac{\Sigma \alpha_i t_i l_i s_i' + \alpha_0 t_0 l_0}{\Sigma (s_i')^2 \rho_i + \rho_0}. \tag{39}$$

The method of calculating assembly and thermal stresses applied to trusses with one redundant member can be extended to more complicated cases of two or more redundant members. Let us take, for example, the truss on four supports, as shown in Fig. 366a, and determine the intermediate reactions X and Y, considering not only the lateral loads P_1, P_2, P_3, but also a change in temperature and some settlement of the supports.[1] Using for thermal expansions of the bars the values $\alpha_i t_i l_i$ and denoting by δ_c and δ_d the settlements of the supports C and D, the equations for calculating the reactions X and Y [see Eqs. (c), page 303] become

[1] Settlement of the supports may have considerable influence on the stresses in a statically indeterminate truss, and a preliminary study of this factor is of great practical importance. We usually do not know the probable settlements, but in a preliminary analysis we assume certain values for these settlements and then find the corresponding stresses. If such calculations show that the system is very sensitive to settlement of the supports, it can be recommended only in the case of reliable foundations.

$$\Sigma[(S_i' + s_i'X + s_i''Y)\rho_i + \alpha_i t_i l_i]s_i' = -\delta_c, \left.\vphantom{\begin{array}{c}1\\1\end{array}}\right\}$$
$$\Sigma[(S_i' + s_i'X + s_i''Y)\rho_i + \alpha_i t_i l_i]s_i'' = -\delta_d, \left.\vphantom{\begin{array}{c}1\\1\end{array}}\right\} \tag{c}$$

or

$$X\Sigma(s_i')^2\rho_i + Y\Sigma s_i's_i''\rho_i = -\delta_c - \Sigma S_i's_i'\rho_i - \Sigma\alpha_i t_i l_i s_i',$$
$$X\Sigma s_i's_i''\rho_i + Y\Sigma(s_i'')^2\rho_i = -\delta_d - \Sigma S_i's_i''\rho_i - \Sigma\alpha_i t_i l_i s_i''.$$

The first terms on the right side of these equations represent the effect of settlement of the supports; the third terms represent the effect of thermal expansions.

PROBLEMS

244. Study the effect of settlement of the intermediate supports on the axial forces in the bars of the truss shown in Fig. 369. Assume that the maximum probable settlement of either support will be 1/1,000 of the span.

245. What vertical displacement will the crown C of the two-hinged arch in Fig. 363 suffer if there is a change in temperature of the arch of 100°F.? See Table VII for numerical data.

53. Influence Lines for Trusses with One Redundant Member.—In preceding articles, we have discussed the analysis of statically indeterminate trusses under the action of stationary loads. If, as in the case of bridges, we are dealing with moving loads and must consider various positions of these loads, influence lines can be used to great advantage. In general, the construction of influence lines for statically indeterminate trusses can be greatly simplified by using the reciprocal theorem, discussed in Art. 43, together with deflection curves for trusses (see Chap. VI). The general statement of the reciprocal theorem is represented by Eq. (28) (see page 251), and its application in the construction of influence lines will now be illustrated by several examples.

As a first example, let us consider the truss in Fig. 370a having one redundant support, assuming that the moving loads are transmitted to the joints of the lower chord. Taking the reaction X at the intermediate support as the redundant force, we construct the influence line for this force by applying the reciprocal theorem to the two loading conditions shown in Figs. 370a and 370b. In the first case a unit load acts at the joint m of the given truss and produces a reaction X at the intermediate support C. In the second case the intermediate support is removed, and a unit load is applied at the joint C. This second case is statically determinate, and we can readily calculate the axial forces and elongations of all bars. Having such elongations, we calculate the deflections of the lower chord joints by using the method of fictitious loads discussed in Art. 47. Let δ_m and δ_c be the deflections of the joints m and C obtained in this manner. Then, observing that the forces of Fig. 370a produce on the displacements calculated for Fig. 370b the work equal to $1 \cdot \delta_m - X\delta_c$, and that the work of the forces of Fig. 370b on the corresponding displacements of Fig. 370a vanishes, we find that Eq. (28) becomes

$$1 \cdot \delta_m - X\delta_c = 0,$$

and we obtain

$$X = 1 \cdot \frac{\delta_m}{\delta_c}. \tag{a}$$

Hence, for any position of the moving unit load in Fig. 370a, the intermediate reaction X is proportional to the deflection of the corresponding joint of the truss in Fig. 370b. Upon dividing these deflections by the
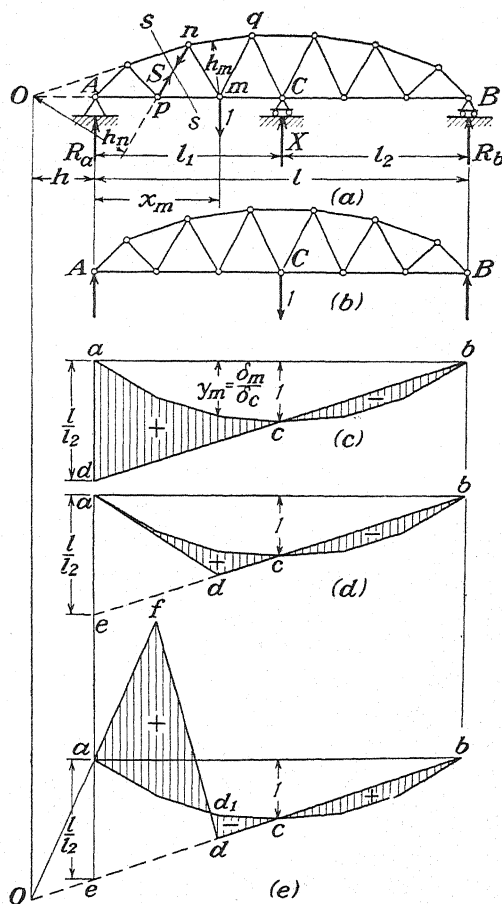
Fig. 370.

deflection δ_c, the ordinates of the influence line acb for the reaction X are obtained as shown in Fig. 370c. By use of this influence line, the redundant reaction X for any system of moving loads $P_1, P_2, P_3, \ldots$ can now be obtained from the equation

$$X = \Sigma y_m P_m.$$

With the influence line for the redundant force X, the influence diagrams for other quantities are readily obtained by using the methods developed in Chap. III for statically determinate trusses. Take, for example, the influence diagram for the reaction R_a. For any position of the unit load, this reaction is obtained from the statics equation,

$$R_a = 1 \cdot \frac{l - x_m}{l} - X \frac{l_2}{l}. \tag{b}$$

The first term on the right side of this equation represents the reaction for a simple beam supported at A and B, while the second term takes care of the intermediate reaction X. Thus the ordinates of the required influence diagram will be obtained by subtracting the ordinates of the influence line acb, diminished in the ratio l_2/l, from the ordinates of the influence line constructed as for a simply supported beam AB. This will be accomplished by drawing the straight line bcd as shown in Fig. 370c and then reducing in the ratio l_2/l the ordinates of the shaded portions of the diagram.

The bending moment for a cross section through the joint m is evidently obtained by subtracting the moment Xl_2x_m/l, due to the intermediate reaction, from the moment calculated for a simple beam supported at A and B. Thus, to obtain the influence diagram for bending moment at m, we begin with the influence line acb for X, on which we superimpose the triangle adb as shown in Fig. 370d. This triangle represents the influence line for simple-beam bending moment at m except that the straight line bde has the ordinate l/l_2 at a instead of the ordinate x_m as it should have. Hence, to obtain the influence coefficients for simple-beam bending moment at m, the ordinates of the triangle adb must be multiplied by $x_m l_2/l$. This, however, is·the same factor by which the ordinates of the X-influence line must be multiplied to obtain the bending moment due to X. Hence the ordinates of the shaded area in Fig. 370d, when multiplied by $x_m l_2/l$, represent the required influence coefficients for bending moment at m.

The same diagram can be used also as the influence diagram for axial force in the bar nq of the upper chord of the truss opposite the hinge m. To obtain the force in this bar, we have only to divide the bending moment at m by the distance h_m and change the sign. Hence the influence diagram for the above-mentioned bar is obtained by multiplying the ordinates of the shaded area in Fig. 370d by the numerical factor $-x_m l_2/h_m l$. In a similar manner, influence diagrams for the bars of the lower chord can be constructed.

Let us consider now a web member np (Fig. 370a). If the unit load is to the right of joint m, we consider the equilibrium of the left portion of the truss. Taking the moments of all forces acting on this portion

with respect to point O, we find that the force in the web member np is

$$S = -R_a \frac{h}{h_n}. \tag{c}$$

Hence, for positions of the load to the right of joint m, the influence diagram for S is obtained by using the same shaded areas already used for R_a in Fig. 370c, except that in this case the ordinates must be multiplied by $-l_2h/lh_n$. When the unit load is to the left of panel pm and at the distance x from the support A, we obtain for S, instead of Eq. (c), the following equation:

$$S = -R_a \frac{h}{h_n} + 1 \frac{h+x}{h_n}. \tag{d}$$

All necessary constructions for the required influence diagram are indicated in Fig. 370e. For the portion of the span to the right of joint m we use, as already mentioned, the same areas as in Fig. 370c, while for the portion to the left of panel pm the second term on the right side of Eq. (d) must be taken into account. We shall accomplish this by drawing the line oaf as previously explained in Chap. III (see page 137). The ordinates included between the straight lines oaf and ocb, after multiplication by the factor l_2h/lh_n, give us the second term on the right side of Eq. (d). Hence the ordinates of the shaded areas in Fig. 370e, after multiplication by this factor l_2h/lh_n, give the required influence coefficients for axial force in the bar np. The proper signs of these ordinates are readily determined from Eqs. (c) and (d) and are indicated in Fig. 370e.

For a second example, we consider the two-hinged arch shown in Fig. 371a and take the horizontal thrust H as the redundant force. Then, to construct the influence line for H, we apply the reciprocal theorem to the two loading conditions shown in Figs. 371a and 371b. In the first case, a unit load, moving along the upper chord, acts at the joint k. In the second case, the redundant constraint is removed, and two equal but opposite unit forces are applied as shown. This second case is statically determinate, and we can calculate the elongations of all bars. With these elongations, the increase δ_h in the distance AB can be found by using Eq. (30), and the deflections of the upper chord joints can be found by applying the method of fictitious loads discussed in Art. 47. The deflection curve obtained in this manner is shown in Fig. 371c. Applying, now, the reciprocal theorem, we obtain

$$-H\delta_h + 1 \cdot \delta_k = 0.$$

Hence,

$$H = 1 \cdot \frac{\delta_k}{\delta_h}.$$

We see that the ordinates of the required influence line for H are obtained by dividing by δ_h the deflections of the upper chord joints. This line is given by the polygon acb in Fig. 371d. The influence line for the redundant force H having been obtained, the influence diagram for any other quantity can be readily constructed by using the methods developed
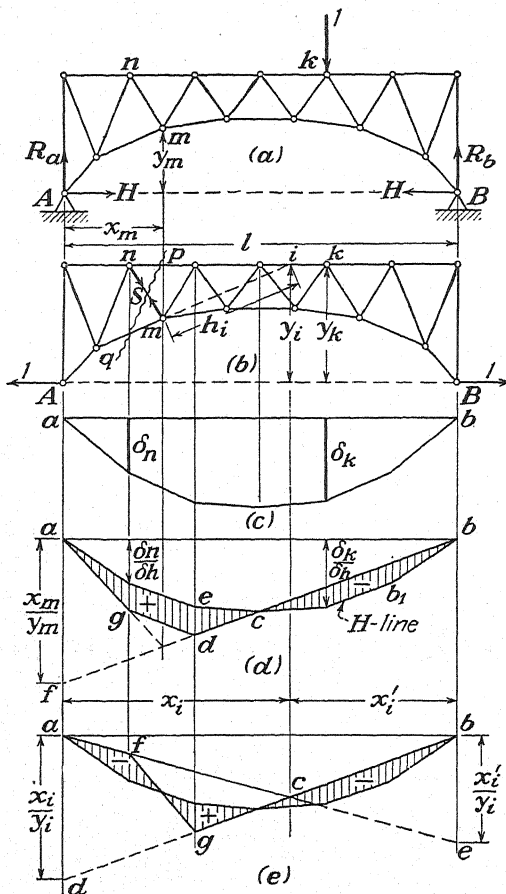
FIG. 371.

in Chap. III. In Fig. 371d, for example, the influence diagram for bending moment with respect to the joint m is shown. With such influence diagrams for bending moment, the corresponding influence diagrams for axial forces in the chord members can also be obtained without difficulty.

Let us consider now the influence line for the axial force S in a web member mn (Fig. 371a). Making a section pq through that member as shown and considering the equilibrium of the left portion of the truss, we obtain

$$S = S_0 - H \cdot \frac{y_i}{h_i} = \frac{y_i}{h_i}\left(S_0 \frac{h_i}{y_i} - H\right), \tag{e}$$

where S_0 is the force in the member mn when $H = 0$, and the distances y_i and h_i are as indicated in Fig. 371b. Upon drawing the lines ae and bd as shown in Fig. 371e, the influence line $afgb$ for the quantity $S_0 h_i/y_i$ is obtained. Subtracting from this the ordinates of the influence line for H, we obtain the shaded areas, shown in Fig. 371e. The ordinates of these areas multiplied by y_i/h_i give us the required influence coefficients for S. Influence diagrams for other web members can be constructed in a similar manner.

As a third example, let us consider an arch with a stiffening truss as shown in Fig. 372a. In this case the reactions R_a and R_b are statically determinate, but the truss proper contains one redundant member. Let this be the horizontal bar CD, the compressive force in which we denote by X, as shown. Removing this bar and applying two unit forces, we obtain the statically determined system shown in Fig. 372b. Assuming that the moving loads act on the upper chord joints of the stiffening truss, we obtain the influence line for X by applying the reciprocal theorem to the two loading conditions shown in Figs. 372a and 372b. In the first case, we have the redundant forces X and the unit load acting on the truss. In the second case we have only the two equal and opposite unit forces at C and D. This second case is statically determinate. Considering the bars of the arch as the sides of a funicular polygon, drawing rays parallel to these bars, and taking a pole distance equal to unity, we can easily obtain the forces in the bars of the arch and in the verticals. After this the forces in all bars of the stiffening truss can be calculated. With these forces, the shortening δ of the distance between the joints C and D can be calculated by using Eq. (31), and the deflections of the upper joints of the stiffening truss can be found by applying the method of fictitious loads discussed in Art. 47. If δ_m is the deflection of joint m, the reciprocal theorem gives the equation

$$1 \cdot \delta_m - X\delta = X\rho_0 \cdot 1, \tag{f}$$

in which $\rho_0 = l_0/EA_0$ determines the extensibility of the redundant bar. The right side of the equation is now different from zero because the displacement in Fig. 372a corresponding to the unit forces shown in Fig. 372b does not vanish but is equal to the compression of the redundant bar. Solving Eq. (f), we obtain

$$X = 1 \cdot \frac{\delta_m}{\delta + 1 \cdot \rho_0}.$$

It is seen that the influence line for the compressive force X is obtained

by dividing by $(\delta + 1 \cdot \rho_0)$ the deflections of the upper chord joints of the stiffening truss. Let the polygon acb in Fig. 372c represent this influence line. The influence diagrams for other quantities can then be constructed as for a statically determinate system.
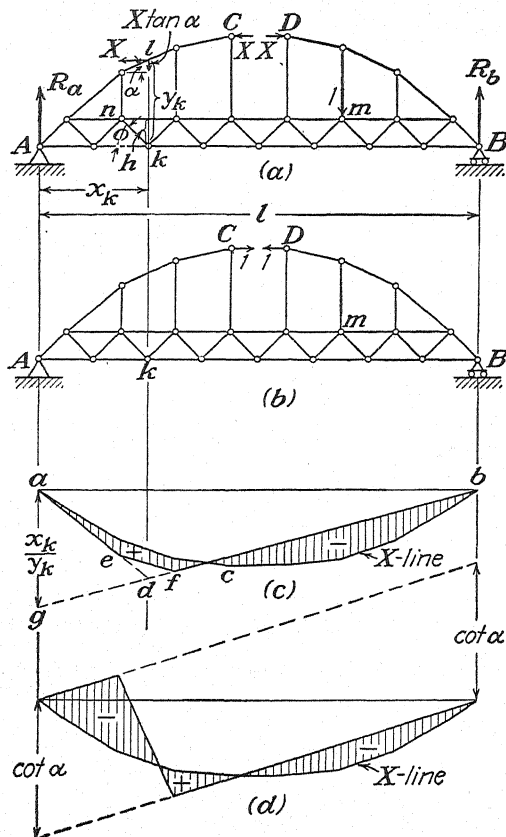
Fig. 372.

Considering, for example, the bending moment with respect to joint k and taking the vertical cross section kl (Fig. 372a), we see that the moment with respect to k of all forces acting on the left portion of the truss is

$$M_k = R_a x_k - X y_k. \tag{g}$$

The first term on the right side represents the moment for a simple beam AB. The second term represents the action of the arch. In Fig. 372c the polygon $aefb$ is constructed as the influence line for simple-beam bending moment except that all ordinates are divided by the length y_k shown in Fig. 372a. From the ordinates of this line the ordinates of the

X-line are subtracted, and in this way the shaded areas are obtained. Upon multiplying by y_k the ordinates of these areas, the required influence coefficients for M_k are obtained [see Eq. (g)]. The same areas can be used in calculating the influence coefficients for the axial force S in the upper chord member opposite the joint k. This force is obtained from the equation

$$S = -\frac{M_k}{h}.$$

Hence the required influence coefficients are obtained by multiplying by $-y_k/h$ the ordinates of the shaded area in Fig. 372c.

In Fig. 372d the influence diagram for axial force in the web member kn is shown. The force in this bar is obtained from the equation of equilibrium of the left portion of the truss (Fig. 372a), which gives

$$S = \frac{1}{\sin \phi} (R_a - X \tan \alpha) =$$

$$\frac{\tan \alpha}{\sin \phi} (R_a \cot \alpha - X). \quad (h)$$

It is seen that the shaded area in Fig. 372d represents the expression in the parentheses on the right side of this equation. Hence the required influence coefficients are obtained by multiplying the ordinates of these areas by $\tan \alpha / \sin \phi$.

As a last example, let us consider the statically indeterminate truss shown in Fig. 373 and con-

Fig. 373.

struct the influence diagram for axial force in the bar mn. Assuming that the moving loads are applied to the joints of the lower chord and applying the reciprocal theorem to the two loading conditions shown in Figs. 373a and 373b, we obtain

$$X \cdot \delta + 1 \cdot \delta_k = -1 \cdot X \rho_0,$$

where δ denotes the decrease in the distance mn produced by the unit loads (Fig. 373b), δ_k is the deflection of the hinge k under the same load, and ρ_0 is the extensibility factor for the redundant bar mn. Thus the redundant force is

$$X = -1 \cdot \frac{\delta_k}{\delta + 1 \cdot \rho_0}.$$
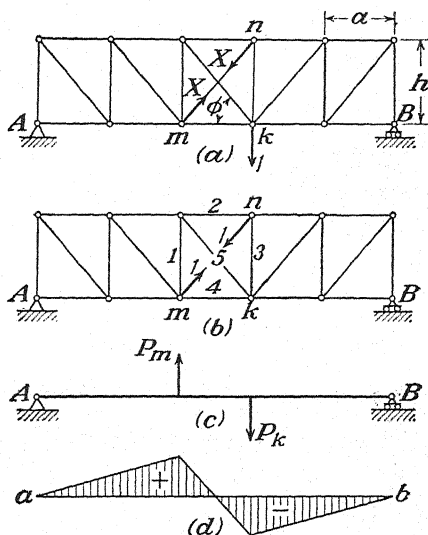
The value of δ is obtained by using Eq. (31), and δ_k is found from the deflection line of the lower chord of the truss. This deflection line is obtained as the bending-moment diagram (Fig. 373d) for the fictitious loads shown in Fig. 373c. The magnitudes of the fictitious loads are found by using the changes in length $\Delta_1 \ldots \Delta_5$ of the bars in the stressed panel of Fig. 373b, together with the equations of Art. 47. In this way we obtain

$$P_m = -\frac{1}{h}\left(\frac{\Delta_5}{\cos\phi} - \Delta_4 - \Delta_1\frac{h}{a}\right),$$

$$P_k = \frac{1}{h}\left(\frac{\Delta_5}{\cos\phi} - \Delta_2 - \Delta_1\frac{h}{a}\right).$$

PROBLEMS

246. Construct an influence diagram for the intermediate reaction X of the statically indeterminate truss shown in Fig. 370a if the middle support C is placed on a pontoon.

HINT: If A is the water-line area of the pontoon and w is the specific weight of water, the deflection of the pontoon under the action of the force X is X/Aw. Thus, instead of Eq. (a) (page 311), we have

$$X = 1 \cdot \frac{\delta_m}{\delta_c + 1/Aw}.$$

247. Construct an influence diagram for the axial force S in a diagonal of the truss shown in Fig. 374.
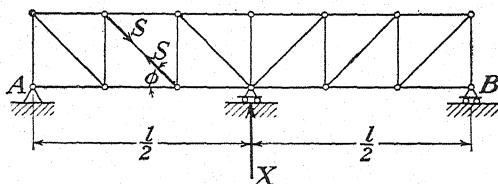
FIG. 374.

248. Construct an influence diagram for axial force in the vertical member CD of the statically indeterminate truss shown in Fig. 375.
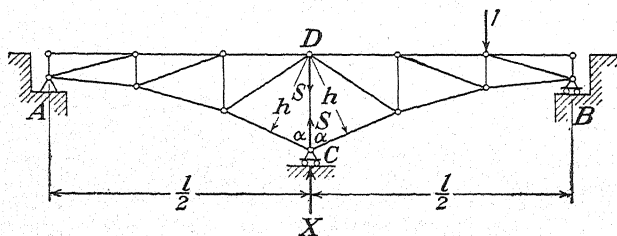
FIG. 375.

249. Construct an influence diagram for axial force in the horizontal bar AB of the statically indeterminate truss shown in Fig. 376.
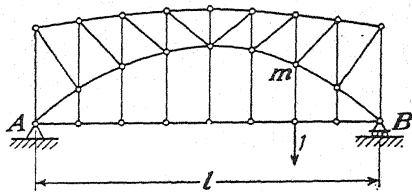
Fig. 376.

250. Construct an influence diagram for axial force in the vertical bar CD of the statically indeterminate truss shown in Fig. 377.
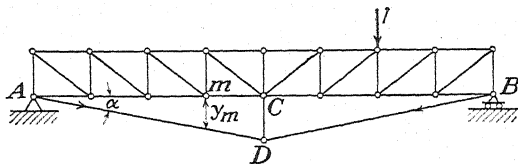
Fig. 377.

54. Influence Lines for Trusses with Two or More Redundant Members.—As an example of a system with two redundant elements, let us consider the truss on four supports as shown in Fig. 378a. It is assumed that the moving loads are transmitted to the joints of the lower chord. For the redundant forces, we select the reactions X and Y at the intermediate supports. In addition to the actual loading condition shown in Fig. 378a, we consider the two cases shown in Figs. 378b and 378c in which the intermediate supports are removed and a unit load is applied at joint C and at joint D, respectively. The latter two cases are statically determinate, and we can calculate the deflections of the lower chord for each of these cases by using the method of fictitious loads. Let δ_{cc}, δ_{cd}, and δ_{cm} denote the deflections at C, D, and m, respectively, when the unit load is acting at C, while δ_{dc}, δ_{dd}, and δ_{dm} denote the deflections produced at the same joints by the unit load at D. Assuming that the supports C and D do not displace vertically under the action of the unit load in Fig. 378a and applying the reciprocal theorem to Figs. 378a and 378b, we obtain

$$-X\delta_{cc} - Y\delta_{cd} + 1 \cdot \delta_{cm} = 0. \tag{a}$$

Similarly, considering Figs. 378a and 378c, we obtain

$$-X\delta_{dc} - Y\delta_{dd} + 1 \cdot \delta_{dm} = 0. \tag{b}$$

Solving Eqs. (a) and (b) for X and Y and observing that $\delta_{cd} = \delta_{dc}$, from the reciprocal theorem, we find the following expressions for the redundant reactions:

$$X = \frac{\delta_{dd}}{\delta_{cc}\delta_{dd} - \delta_{cd}{}^2}\,\delta_{cm} - \frac{\delta_{cd}}{\delta_{cc}\delta_{dd} - \delta_{cd}{}^2}\,\delta_{dm}, \qquad (c)$$

$$Y = \frac{\delta_{cc}}{\delta_{cc}\delta_{dd} - \delta_{cd}{}^2}\,\delta_{dm} - \frac{\delta_{cd}}{\delta_{cc}\delta_{dd} - \delta_{cd}{}^2}\,\delta_{cm}. \qquad (d)$$

It is seen that when the unit load changes position along the truss (Fig. 378a) only the quantities δ_{cm} and δ_{dm} in expressions (c) and (d) change in
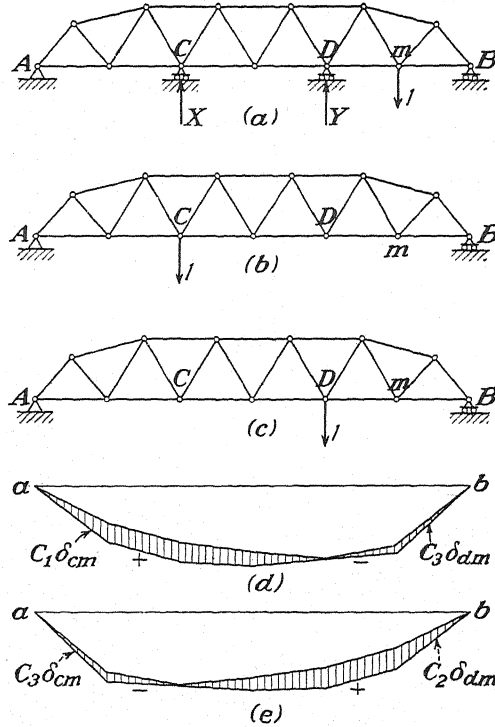
FIG. 378.

magnitude; the other quantities remain constant. Introducing the notations

$$\frac{\delta_{dd}}{\delta_{cc}\delta_{dd} - \delta_{cd}{}^2} = C_1, \qquad \frac{\delta_{cc}}{\delta_{cc}\delta_{dd} - \delta_{cd}{}^2} = C_2, \qquad \frac{\delta_{cd}}{\delta_{cc}\delta_{dd} - \delta_{cd}{}^2} = C_3, \quad (e)$$

we obtain

$$\left.\begin{array}{l} X = C_1\delta_{cm} - C_3\delta_{dm}, \\ Y = C_2\delta_{dm} - C_3\delta_{cm}. \end{array}\right\} \qquad (f)$$

The constants C_1, C_2, and C_3 are readily calculated from Eqs. (e) provided that the deflection curves for the loadings in Figs. 378b and 378c have been constructed. The expressions on the right sides of Eqs. (f) are

plotted in Figs. 378d and 378e, and the required influence coefficients for the redundant reactions X and Y are given by the ordinates of the shaded areas. With these constructions, the influence diagram for axial force in any bar of the truss (Fig. 378a) can be easily obtained. For this purpose, we observe that the force S_i in any member can be represented in the following form,

$$S_i = S_i' - s_i'X - s_i''Y, \qquad (g)$$

where S_i' is the force in that member when the redundant supports are removed and s_i' and s_i'' are the *influence numbers*[1] for the same member calculated for the unit loads shown in Figs. 378b and 378c, respectively. Thus we see that the required influence diagram for axial force in any bar can be obtained by combining the ordinates of the influence diagram, constructed as for a simply supported truss, with those of the $s_i'X$-diagram and the $s_i''Y$-diagram. These latter diagrams are obtained simply by multiplying the ordinates of the shaded areas in Figs. 378d and 378e by the influence numbers s_i' and s_i''.

The foregoing method of obtaining influence diagrams for trusses with two redundant forces can be applied also in the case of three or more redundant forces. Since the number of equations similar to Eqs. (a) and (b) will always be equal to the number of redundant forces, the complications involved in their solution increase rapidly with the number of unknowns. The problem can be greatly simplified by a proper selection of the redundant forces, such that each equation will contain only one unknown. In such a case, each equation can be solved independently of the others, and the corresponding influence diagram will be obtained directly, as in the case of trusses with one redundant element. The proper selection of the unknown[2] we shall explain first by an example with only two redundant forces. Considering Eqs. (a) and (b), we see that each of them contains both unknowns. This occurs because the force X produces deflection, not only of the joint C where it is applied, but also of the joint D, where the force Y acts (Fig. 378a). A similar conclusion applies to the force Y. To simplify the problem and obtain equations each of which contains only one unknown, we must select the redundant forces in such a manner that each force does not produce a displacement corresponding to the other. This can be achieved easily

[1] These influence numbers s_i', s_i'', as defined on p. 259 should not be confused with influence coefficients as defined on p. 96.

[2] The importance of the proper selection of the redundant forces was discussed first and was illustrated by various examples by R. Krohn, *Z. Baukunde*, vol. 3, p. 219, 1880, and by O. Mohr, *Z. Architekten-Ingenieur-Ver. Hannover*, vol. 27, p. 243, 1881. Several examples are discussed also in "Die graphische Statik der Baukonstruktionen" by H. Müller-Breslau, vol. II, pt. 1, p. 296, 1907.

if both forces are applied at the same joint.   Let us consider, for example, the two-span arch shown in Fig. 379a.   This structure has two redundant elements.   As such let us take two components of the reaction at A.   If we choose the directions of these components arbitrarily, application of the reciprocal theorem will give, for their determination, two equations similar to Eqs. (a) and (b) each of which contains both unknowns.   However, by a proper selection of the directions of the two components, the problem can be simplified and we can obtain two equations each of which contains only one of the unknowns.   To accomplish this, we
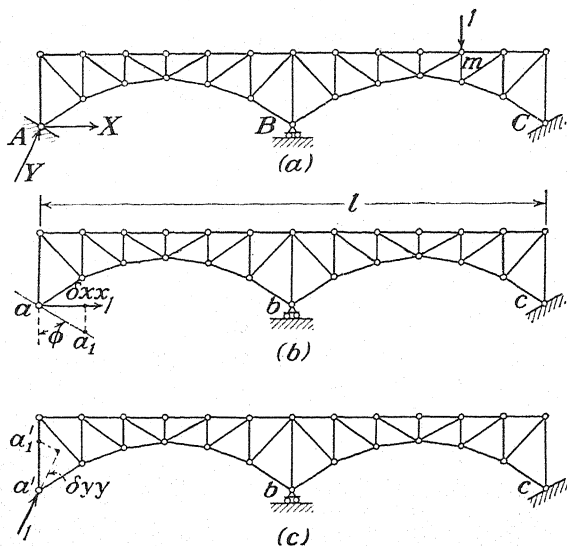
Fig. 379.

take the direction of one component arbitrarily; say we assume the component X horizontal.   Then to determine the proper direction for the other component Y, we remove the support A and consider the unit loading shown in Fig. 379b.   This case is statically determinate, and we can obtain, by one of the established methods, say by the construction of a Williot diagram, the displacements of all joints of the truss.   Let aa_1 be the direction in which the joint A moves under the action of this horizontal unit load (Fig. 379b).   Then, if we select the direction of the component Y perpendicular to the direction aa_1, the horizontal force X does not produce a displacement corresponding to the force Y and, by the reciprocal theorem, we conclude that the force Y will not produce a displacement corresponding to the force X; i.e., the displacement of joint A, produced by the force Y, will be vertical.   After establishing the directions of the component reactions X and Y, we determine the corresponding influence lines by using the loading conditions shown in Figs.

379*b* and 379*c* together with the reciprocal theorem. We assume that moving loads are transmitted to the joints of the upper chord and denote by δ_{mx} the vertical displacement[1] of any joint m under the action of the unit load in the X-direction (Fig. 379*b*) and by δ_{xx} the horizontal com-
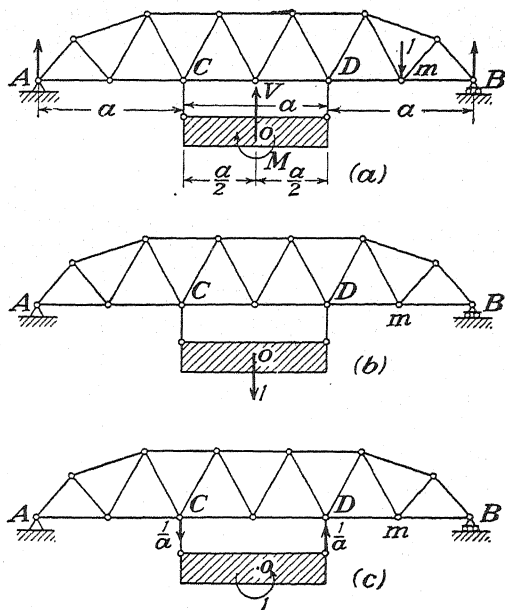
FIG. 380.

ponent of the displacement aa_1 of the hinge A. Then the reciprocal theorem applied to Figs. 379*a* and 379*b* gives

$$X\delta_{xx} + 1 \cdot \delta_{mx} = 0. \tag{h}$$

The force Y does not appear in this equation since the corresponding displacement in Fig. 379*b* vanishes. In a similar manner we apply the reciprocal theorem to Figs. 379*a* and 379*c* and obtain

$$Y\delta_{yy} + 1 \cdot \delta_{my} = 0. \tag{i}$$

From Eqs. (*h*) and (*i*), we find

$$X = -1 \cdot \frac{\delta_{mx}}{\delta_{xx}}, \qquad Y = -1 \cdot \frac{\delta_{my}}{\delta_{yy}}. \tag{j}$$

Hence the upper chord deflection curves constructed for the loadings of Figs. 379*b* and 379*c* give us directly the influence lines for the redundant reactions X and Y.

To achieve the same simplification in the case of the system shown in

---

[1] Downward displacements considered positive.

Fig. 378, we replace the reactions X and Y by a statically equivalent system consisting of a vertical force V and a moment M as indicated in Fig. 380a* and defined by the equations

$$X = \frac{V}{2} + \frac{M}{a}, \qquad Y = \frac{V}{2} - \frac{M}{a}. \tag{k}$$

To obtain the influence line for the force V, we apply the reciprocal theorem to the loadings shown in Figs. 380a and 380b. Assuming that the truss is symmetrical with respect to the vertical axis through the middle, we conclude that, for the case in Fig. 380b, the shaded block moves parallel to itself. Hence the displacement corresponding to the couple M in Fig. 380a vanishes, and the reciprocal theorem gives

$$-V\delta + 1 \cdot \delta_{vm} = 0,$$

where δ is the vertical displacement of the shaded block and δ_{vm} is the deflection at joint m in Fig. 380b. From this equation we conclude that the lower chord deflection curve for the loading of Fig. 380b gives the influence line for the force V. To obtain the influence line for M, we consider Figs. 380a and 380c. From symmetry it can be concluded that in the case of Fig. 380c the shaded block does not move vertically but only rotates with respect to its center O by an angle α, which can be readily calculated if the vertical deflections of the joints C and D are determined. Hence the reciprocal theorem gives

$$-M\alpha + 1 \cdot \delta_{Mm} = 0,$$

where δ_{Mm} is the deflection of joint m in Fig. 380c. Thus we conclude that the deflection curve for the loading of Fig. 380c gives the influence line for M. The influence lines for V and M having been obtained, the values of the reactions X and Y for any loading are readily found by using Eqs. (k).

In the case of the arch shown in Fig. 381a, we have a system with three redundant elements. If we take the forces S_1, S_2, and S_3 acting at the hinges A and B and in the directions of the bars 1, 2, and 3, respectively, and proceed as in the case of two unknowns (Fig. 378a), we shall obtain three equations, similar to Eq. (a), each of which will contain all three unknowns S_1, S_2, and S_3. To simplify the problem and obtain three equations each of which contains only one unknown, we replace the system of forces S_1, S_2, and S_3 by a statically equivalent system of three forces so selected that each of them, if acting alone, does not produce displacements corresponding to the other two. To accomplish this,

---

* The shaded block transmitting the force V and the couple M to the hinges C and D is considered as absolutely rigid. It is attached to C and D by two vertical absolutely rigid bars.

we assume that the hinges A and B are attached to an absolutely rigid block AOB as shown in Fig. 381b. Then to this block we apply the properly selected forces X, Y, and M as shown. To find the point O at which the forces X and Y must be applied, we investigate the deflections of the arch produced by a unit couple acting on the block AOB. In this case $X = Y = 0$ and $M = 1$. We can readily find the corresponding forces in all bars of the arch and, by constructing a Williot diagram, the displacements of all joints and also the displacement of the block AOB attached to the joints A and B. In general, we know that any displacement of this block in the plane of the truss can be accomplished by rotation with respect to a certain center. Let point O be this center for the displacements just found. Then this point must be taken as the
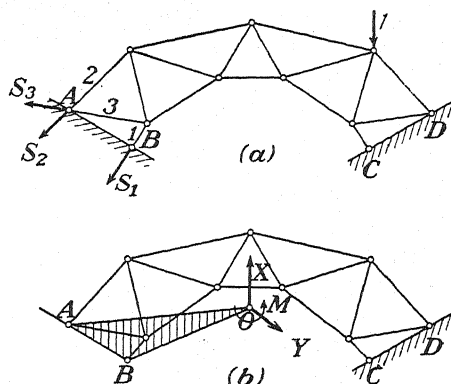
FIG. 381.

point of application of the forces X and Y. Since point O does not move under the action of the unit couple $M = 1$, we conclude, from the reciprocal theorem, that a force applied at O will not produce any rotation of the block. Applying the forces X and Y at point O, we do not produce a displacement corresponding to the couple M, and as a result of this the reciprocal theorem will give an equation containing only one unknown M. To obtain separate equations for the other two unknowns X and Y, we proceed as in the case shown in Fig. 379, take the direction of X arbitrarily, and find the direction of the corresponding displacement of the center O. Then, the direction of Y must be taken perpendicular to this displacement. With such selection of the point O and the directions of the forces X and Y, we meet the requirement that each redundant force shall not produce any displacements corresponding to the other two forces, and therefore we shall obtain three equations containing only one unknown each. We shall use this method[1] later in discussing stresses in frames and solid arches.

[1] Extension of the method to systems with any number of redundant forces has

55. Statically Indeterminate Space Structures.—If a structure in space has n joints and more than $3n$ bars, including supporting bars or their equivalent, the number of equations that can be obtained from statics will be insufficient to determine the unknown axial forces in all members and the system is statically indeterminate. In analyzing such systems, the elastic deformations of the bars must be considered. This can be accomplished by using the methods already developed for plane
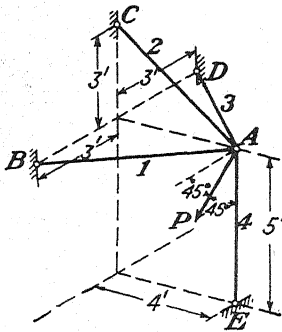
Fig. 382.

trusses. To illustrate the application of these methods to space systems, let us consider the simple system consisting of a single joint A attached to the foundation by four bars as shown in Fig. 382. Such a system has one redundant bar. To define the configuration, we assume that all bars are identical and have the length $l = 5$ ft., that the bars 1 and 3 are in a horizontal plane ABD and that the bars 2 and 4 are in a vertical plane ACE bisecting the angle BAD. The force P applied at A acts in a vertical plane parallel to the plane BCD and makes an angle of 45 deg. with the vertical bar AE. We select the bar AE as the redundant bar and denote by X the axial force in it. Then the forces in the other bars will be found from the equation

$$S_i = S_i' + s_i'X, \qquad (a)$$

in which S_i' is the force produced by the load P in any bar i of the primary system, *i.e.*, of the system that remains after removal of the redundant bar AE, and s_i' is the influence number for any bar i. These influence numbers are obtained by applying at joint A of the primary system a vertical unit load and calculating the corresponding axial forces in the bars. To obtain the redundant force X by the principle of least work, we make the expression for strain energy

$$U = \sum \frac{S_i^2 l_i}{2A_i E} + \frac{X^2 l_0}{2A_0 E} = \frac{1}{2}\left(\sum S_i^2 \rho_i + X^2 \rho_0\right), \qquad (b)$$

where the summations are understood to include all bars of the primary system. Setting the derivative of this expression with respect to X equal to zero, we obtain

$$\frac{\partial U}{\partial X} = \sum S_i s_i' \rho_i + X \rho_0 = 0. \qquad (c)$$

been discussed by S. Müller, *Zentr. bl. Bauverw.*, 1907, pp. 23, 253 and by M. Grüning, "Der Eisenbau," p. 305, 1921.

Observing that in this case ρ_i is the same for all members and substituting expression (a) for S_i, we obtain

$$X = -\frac{\Sigma S_i' s_i'}{\Sigma (s_i')^2 + 1}. \qquad (d)$$

The values of S_i' and s_i' together with all calculations necessary to determine X are shown in Table VIII. The load P is taken equal to 1 ton, and Eq. (d) then gives

$$X = -\frac{2.95}{5.165} = -0.570 \text{ ton.}$$

Finally, using Eq. (a) we obtain the values of S_i as recorded in the last column of the table.

TABLE VIII

i	S_i', ton	s_i'	$S_i' s_i'$, ton	$(s_i')^2$	S_i, ton
1	$-5\sqrt{2}/6$	$-\frac{5}{6}$	0.983	0.694	-0.705
2	$5\sqrt{2}/6$	$\frac{5}{3}$	1.967	2.777	0.230
3	0	$-\frac{5}{6}$	0	0.694	0.475
4	....	....	.....	.....	-0.570
Σ..........................			2.95	4.165	

Equation (c) for calculating X can also be obtained by applying the principle of virtual displacements as discussed in Art. 45. In this case the principle states that the work done on the actual displacements by the forces corresponding to the unit load must vanish. If it is desired to consider a change in temperature and possible errors Δ_i in the lengths of the bars, we have only to substitute in Eq. (c) the expression $S_i\rho_i + \alpha t_i l_i + \Delta_i$ instead of $S_i\rho_i$ and $X\rho_0 + \alpha t_0 l_0 + \Delta_0$ instead of $X\rho_0$. In this way we obtain the equation

$$\Sigma(S_i\rho_i + \alpha t_i l_i + \Delta_i)s_i' + X\rho_0 + \alpha t_0 l_0 + \Delta_0 = 0$$

from which

$$X = -\frac{\Sigma(S_i'\rho_i + \alpha t_i l_i + \Delta_i)s_i' + \alpha t_0 l_0 + \Delta_0}{\Sigma (s_i')^2\rho_i + \rho_0}. \qquad (40)$$

This equation can be used to calculate the redundant force in any pin-connected space structure with one redundant member. It is necessary only to extend the summations to include all members of the primary system.

As a more complicated example, let us consider the space structure shown in Fig. 383 to which a horizontal force $P = 1$ ton is applied. This structure has 12 joints and 39 bars. Hence there are three redundant

bars. For these redundants, we choose the three horizontal diagonals and denote their axial forces by X, Y, and Z, as shown. After removal of these bars, we obtain the statically determinate primary system shown in Fig. 384. The forces S_i' produced in the bars of this system by the load $P = 1$ ton are given in the second column of Table IX on page 330. We consider now the unit loads acting on the primary system as shown in Figs. 384a, 384b, 384c and calculate the corresponding influence numbers s_i', s_i'', s_i''', given in columns (3), (4), and (5) of the table. The force
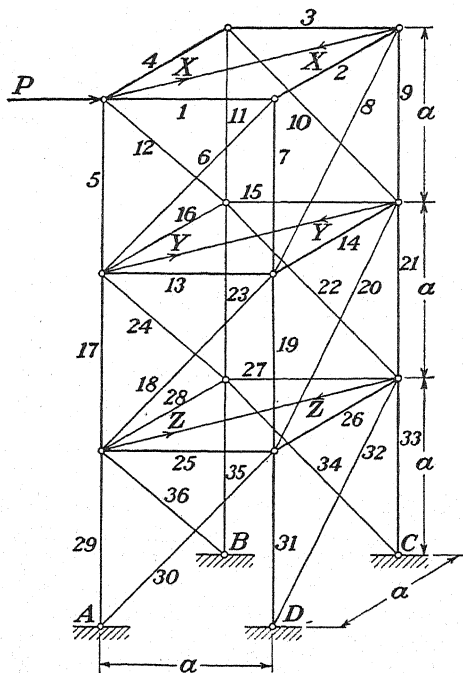
Fig. 383.

in any bar i of the given structure (Fig. 383) will now be represented by the expression

$$S_i = S_i' + s_i'X + s_i''Y + s_i'''Z,$$

and the principle of least work gives the following three equations for calculating the redundant forces:

$$\left.\begin{array}{l} \Sigma s_i'(S_i' + s_i'X + s_i''Y + s_i'''Z)\rho_i + X\rho_x = 0, \\ \Sigma s_i''(S_i' + s_i'X + s_i''Y + s_i'''Z)\rho_i + Y\rho_y = 0, \\ \Sigma s_i'''(S_i' + s_i'X + s_i''Y + s_i'''Z)\rho_i + Z\rho_z = 0. \end{array}\right\} \qquad (e)$$

In these equations, ρ_x, ρ_y, and ρ_z denote the extensibility factors for the three redundant diagonals. The magnitudes of the redundant forces

will, of course, depend on the cross-sectional dimensions of the bars. Assuming, for example, that the extensibilities of all bars are equal, the quantities ρ cancel in Eqs. (e), and the numerical values of all coefficients
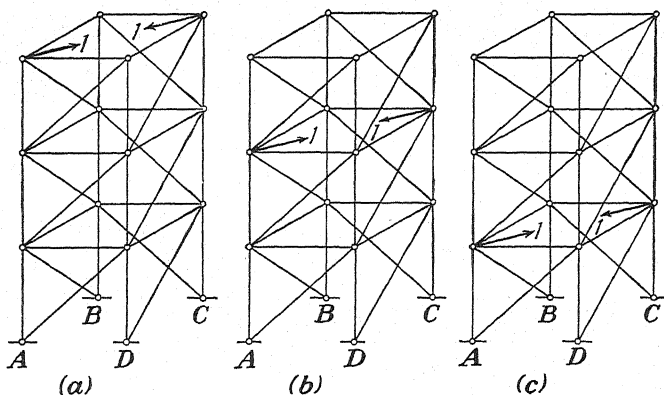
FIG. 384.

in these equations are obtained by making summations of columns (6) to (14) of the table. In this way, Eqs. (e) finally become

$$
\left.
\begin{array}{l}
88X + 47Y + 15Z = -22\sqrt{2}, \\
47X + 32Y + 11Z = -12\sqrt{2}, \\
15X + 11Y + 8Z = -4\sqrt{2},
\end{array}
\right\}
\qquad (f)
$$

from which we find

$$ X = -0.2327\sqrt{2}\ \text{ton}, \quad Y = -0.0215\sqrt{2}\ \text{ton}, \quad Z = -0.0341\sqrt{2}\ \text{ton}. $$

It is seen that the upper diagonal is the most stressed of the three redundant bars. Owing to its action, the forces acting on the upper joints of the structure will be as shown in Fig. 385a. From this we can conclude that the true forces in the bars of
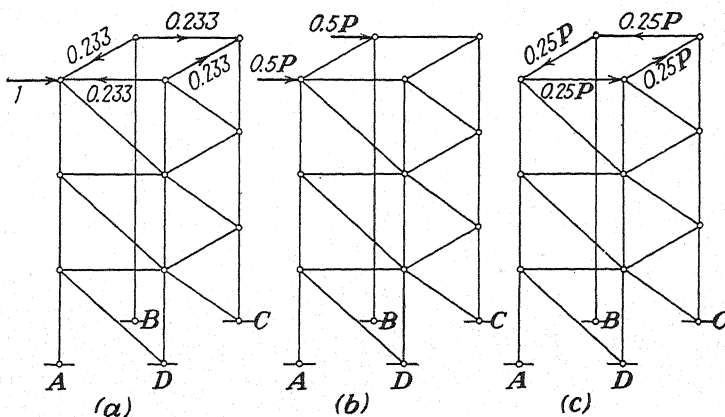
FIG. 385.

TABLE IX

(1)	(2)	(3)	(4)	(5)	(6)	(7)	(8)	(9)	(10)	(11)	(12)	(13)	(14)
i	S_i'	s_i'	s_i''	s_i'''	$(s_i')^2$	$(s_i'')^2$	$(s_i''')^2$	$S_i's_i'$	$S_i's_i''$	$S_i's_i'''$	$s_i's_i''$	$s_i's_i'''$	$s_i''s_i'''$
1	-1	$-1/\sqrt{2}$	0	0	$\frac{1}{2}$	0	0	$1/\sqrt{2}$	0	0	0	0	0
2	0	0	0	0	0	0	0	0	0	0	0	0	0
3	0	$-1/\sqrt{2}$	0	0	$\frac{1}{2}$	0	0	0	0	0	0	0	0
4	0	0	0	0	0	0	0	0	0	0	0	0	0
5	0	$1/\sqrt{2}$	0	0	$\frac{1}{2}$	0	0	0	0	0	0	0	0
6	$\sqrt{2}$	1	0	0	1	0	0	$\sqrt{2}$	0	0	0	0	0
7	-1	$-1/\sqrt{2}$	0	0	$\frac{1}{2}$	0	0	$1/\sqrt{2}$	0	0	0	0	0
8	0	-1	0	0	1	0	0	0	0	0	0	0	0
9	0	$1/\sqrt{2}$	0	0	$\frac{1}{2}$	0	0	0	0	0	0	0	0
10	0	1	0	0	1	0	0	0	0	0	0	0	0
11	0	$-1/\sqrt{2}$	0	0	$\frac{1}{2}$	0	0	0	0	0	0	0	0
12	0	-1	0	0	1	0	0	0	0	0	0	0	0
13	-1	$-1/\sqrt{2}$	$-1/\sqrt{2}$	0	$\frac{1}{2}$	$\frac{1}{2}$	0	$1/\sqrt{2}$	$1/\sqrt{2}$	0	$\frac{1}{2}$	0	0
14	0	$1/\sqrt{2}$	0	0	$\frac{1}{2}$	0	0	0	0	0	0	0	0
15	0	$-1/\sqrt{2}$	$-1/\sqrt{2}$	0	$\frac{1}{2}$	$\frac{1}{2}$	0	0	0	0	$\frac{1}{2}$	0	0
16	0	$1/\sqrt{2}$	0	0	$\frac{1}{2}$	0	0	0	0	0	0	0	0
17	1	$3/\sqrt{2}$	$1/\sqrt{2}$	0	$\frac{9}{2}$	$\frac{1}{2}$	0	$3/\sqrt{2}$	$1/\sqrt{2}$	0	$\frac{3}{2}$	0	0
18	$\sqrt{2}$	1	1	0	1	1	0	$\sqrt{2}$	$\sqrt{2}$	0	1	0	0
19	-2	$-3/\sqrt{2}$	$-1/\sqrt{2}$	0	$\frac{9}{2}$	$\frac{1}{2}$	0	$3\sqrt{2}$	$\sqrt{2}$	0	$\frac{3}{2}$	0	0
20	0	-1	-1	0	1	1	0	0	0	0	1	0	0
21	0	$3/\sqrt{2}$	$1/\sqrt{2}$	0	$\frac{9}{2}$	$\frac{1}{2}$	0	0	0	0	$\frac{3}{2}$	0	0
22	0	1	1	0	1	1	0	0	0	0	1	0	0
23	0	$-3/\sqrt{2}$	$-1/\sqrt{2}$	0	$\frac{9}{2}$	$\frac{1}{2}$	0	0	0	0	$\frac{3}{2}$	0	0
24	0	-1	-1	0	1	1	0	0	0	0	1	0	0
25	-1	$-1/\sqrt{2}$	$-1/\sqrt{2}$	$-1/\sqrt{2}$	$\frac{1}{2}$	$\frac{1}{2}$	$\frac{1}{2}$	$1/\sqrt{2}$	$1/\sqrt{2}$	$1/\sqrt{2}$	$\frac{1}{2}$	$\frac{1}{2}$	$\frac{1}{2}$
26	0	$1/\sqrt{2}$	$-1/\sqrt{2}$	0	$\frac{1}{2}$	$\frac{1}{2}$	0	0	0	0	$\frac{1}{2}$	0	0
27	0	$-1/\sqrt{2}$	$-1/\sqrt{2}$	$-1/\sqrt{2}$	$\frac{1}{2}$	$\frac{1}{2}$	$\frac{1}{2}$	0	0	0	$\frac{1}{2}$	$\frac{1}{2}$	$\frac{1}{2}$
28	0	$1/\sqrt{2}$	$1/\sqrt{2}$	0	$\frac{1}{2}$	$\frac{1}{2}$	0	0	0	0	$\frac{1}{2}$	0	0
29	2	$5/\sqrt{2}$	$3/\sqrt{2}$	$1/\sqrt{2}$	$\frac{25}{2}$	$\frac{9}{2}$	$\frac{1}{2}$	$5\sqrt{2}$	$3\sqrt{2}$	$\sqrt{2}$	$\frac{15}{2}$	$\frac{5}{2}$	$\frac{3}{2}$
30	$\sqrt{2}$	1	1	1	1	1	1	$\sqrt{2}$	$\sqrt{2}$	$\sqrt{2}$	1	1	1
31	-3	$-5/\sqrt{2}$	$-3/\sqrt{2}$	$-1/\sqrt{2}$	$\frac{25}{2}$	$\frac{9}{2}$	$\frac{1}{2}$	$15/\sqrt{2}$	$9/\sqrt{2}$	$3/\sqrt{2}$	$\frac{15}{2}$	$\frac{5}{2}$	$\frac{3}{2}$
32	0	-1	-1	-1	1	1	1	0	0	0	1	1	1
33	0	$5/\sqrt{2}$	$3/\sqrt{2}$	$1/\sqrt{2}$	$\frac{25}{2}$	$\frac{9}{2}$	$\frac{1}{2}$	0	0	0	$\frac{15}{2}$	$\frac{5}{2}$	$\frac{3}{2}$
34	0	1	1	1	1	1	1	0	0	0	1	1	1
35	0	$-5/\sqrt{2}$	$-3/\sqrt{2}$	$-1/\sqrt{2}$	$\frac{25}{2}$	$\frac{9}{2}$	$\frac{1}{2}$	0	0	0	$\frac{15}{2}$	$\frac{5}{2}$	$\frac{3}{2}$
36	0	-1	-1	-1	1	1	1	0	0	0	1	1	1
Σ					87	31	7	$22\sqrt{2}$	$12\sqrt{2}$	$4\sqrt{2}$	47	15	11

the primary system will be obtained with good accuracy if we replace the force P by two forces $P/2$ applied as shown in Fig. 385b and by a torque $\frac{1}{2}Pa$ applied as shown in Fig. 385c and then superimpose the axial forces in the bars obtained for these two statically determinate cases. In this manner we take into account the most stressed redundant diagonal and neglect the actions of the other two.

If the cross-sectional dimensions of the redundant diagonals are diminished, they may become insufficiently rigid to redistribute the force P as shown in Fig. 385; then the larger part of P will be carried by the front panel. Assuming that the extensibilities of the redundant diagonals are ten times larger than the extensibilities of the other bars, we obtain, instead of Eqs. (f), the following equations:

$$\left.\begin{array}{l} 97X + 47Y + 15Z = -22\sqrt{2}, \\ 47X + 41Y + 11Z = -12\sqrt{2}, \\ 15X + 11Y + 17Z = -4\sqrt{2}, \end{array}\right\} \qquad (g)$$

from which

$$X = -0.1900\sqrt{2}\ \text{ton}, \qquad Y = -0.0687\sqrt{2}\ \text{ton}, \qquad Z = -0.0233\sqrt{2}\ \text{ton}.$$

If we take the extensibilities of the redundant diagonals 100 times larger than the extensibilities of the other bars, we shall find

$$X = -0.1030\sqrt{2}\ \text{ton}, \qquad Y = -0.0532\sqrt{2}\ \text{ton}, \qquad Z = -0.0175\sqrt{2}\ \text{ton}.$$

Proceeding as shown in Fig. 385a, we shall find that that part of the load carried by the front panel increases with the flexibilities of the redundant members.

CHAPTER VIII

BEAMS AND FRAMES

56. Slope-deflection Equations.—Frame structures like that shown in Fig. 386a usually consist of straight prismatic members which can be treated as beams elastically constrained at the ends. Such a member as *ab*, for example, can be isolated as shown in Fig. 386b and the elastic constraints at the ends replaced by reactive couples M_a and M_b. In this way, we reduce the problem to that of a simply supported beam acted
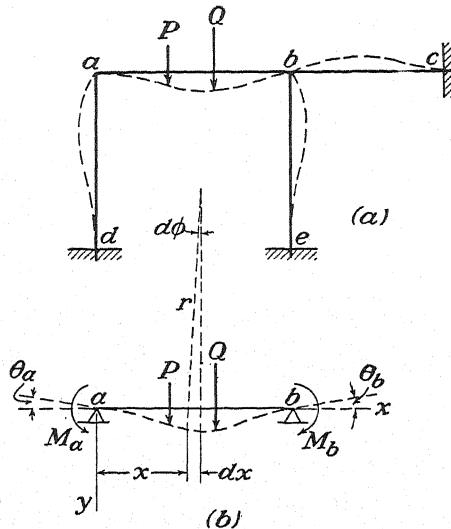
FIG. 386.

upon by lateral loads together with end moments. Under such loading, the beam deflects and the end tangents rotate by small angles θ_a and θ_b as shown. For our further discussion, it will be helpful to establish analytical relationships between these angles, the end moments, and the lateral loading. Such relationships are generally known as *slope-deflection equations*, and we shall now consider their derivation.

Assuming that the beam is bent in a principal plane, the curvature of the *elastic line* at any cross section is given by the well-known equation

$$\frac{1}{r} = \frac{M}{EI},$$

(41)

in which M is the bending moment and EI the flexural rigidity at the cross section under consideration. In using this equation, we shall take the longitudinal axis of the beam as the x-axis and shall consider the y-axis positive downward as shown. We shall also assume that deflections of the beam are small so that the length of an element of the elastic line can be taken equal to the length dx of its projection on the x-axis. In such a case, the small angle $d\phi$ between two adjacent cross sections after bending is

$$d\phi = \frac{dx}{r} = \frac{M\,dx}{EI}. \qquad (a)$$

With this expression, the rotations of the end tangents can be calculated by the method of fictitious loads that we have already used in the analysis of trusses (see page 277). In Fig. 387a, for example, let the curve def be the bending-moment diagram for a transversely loaded simple beam
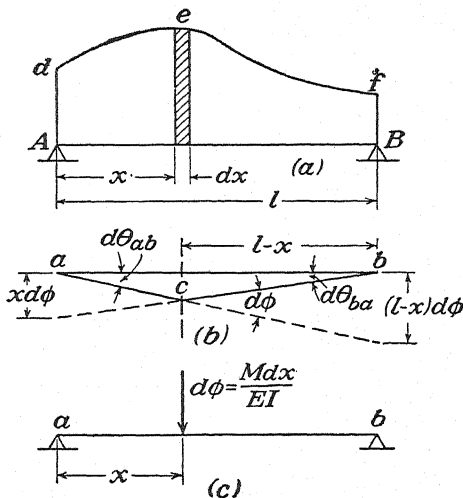
FIG. 387.

AB. If we assume that only one infinitesimal element dx of this beam is elastic, while the rest of it remains absolutely rigid, the elastic line acb will be as shown in Fig. 387b. This line consists simply of two straight portions ac and cb having between them the angle $d\phi$ as defined by Eq. (a). Owing to such deflection, the left end of the beam, as we see from the figure, rotates by an infinitesimal angle of the magnitude

$$d\theta_{ab} = \frac{l-x}{l}\,d\phi. \qquad (b)$$

Considering clockwise rotations as positive, we take expression (b) with positive sign. The end b of the beam rotates counterclockwise, and the

corresponding angle of rotation is

$$d\theta_{ba} = -\frac{x}{l}\,d\phi. \tag{c}$$

Expressions (b) and (c) permit a very simple interpretation. Imagine a simply supported beam on which a fictitious load $d\phi = M\,dx/EI$ is acting as shown in Fig. 387c. Then expressions (b) and (c) represent the shearing forces at the ends of this beam due to such a fictitious load.

Having the angles of rotation of the ends resulting from bending of one element of the beam, we shall obtain the total angles of rotation by summing up expressions (b) and (c) over the entire length of the beam. This gives

$$\left.\begin{aligned}
\theta_{ab} &= \int_0^l \frac{l-x}{l}\,d\phi = \int_0^l \frac{l-x}{l}\cdot\frac{M\,dx}{EI},\\
\theta_{ba} &= -\int_0^l \frac{x}{l}\,d\phi = -\int_0^l \frac{x}{l}\,\frac{M\,dx}{EI}.
\end{aligned}\right\} \tag{42}$$

Observing that $M\,dx$ is the area of an elemental strip of the bending-moment diagram in Fig. 387a and that EI is constant for beams of uniform cross section,[1] we conclude that, to obtain the angles of rotation of
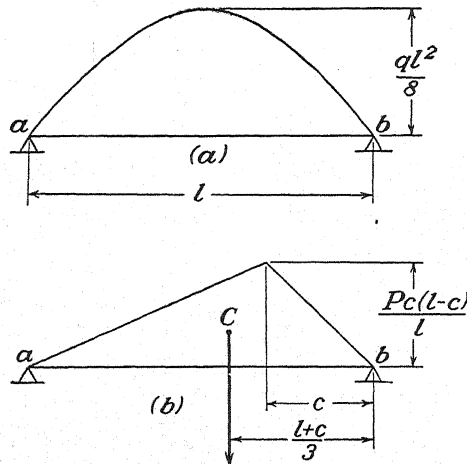
Fig. 388.

the ends of such beams, we need only consider the bending moment area $AdefB$ as a fictitious load and then divide by EI the shearing forces produced at the ends of the beam by this load.

Taking, for example, a uniformly loaded beam, the bending-moment area is a parabolic segment (Fig. 388a) having the area

$$A = \frac{2}{3}\,l\cdot\frac{ql^2}{8} = \frac{ql^3}{12}.$$

[1] For beams of variable cross section see Art. 70.

If we treat this area as a fictitious load, the corresponding reactions at the supports are $ql^3/24$ and we obtain

$$\theta_{ab} = \frac{ql^3}{24EI}, \qquad \theta_{ba} = -\frac{ql^3}{24EI}.$$

In the case of a concentrated load P applied at a distance c from the right support, the bending-moment area is represented by the triangle in Fig. 388b. Treating the area of this triangle as a fictitious load, we obtain for the reactions at the supports

$$R_{ab} = \frac{Pc(l^2 - c^2)}{6l} \qquad \text{and} \qquad R_{ba} = \frac{Pc(l - c)(2l - c)}{6l}.$$

Hence,

$$\theta_{ab} = \frac{Pc(l^2 - c^2)}{6lEI}, \qquad \theta_{ba} = -\frac{Pc(l - c)(2l - c)}{6lEI}.$$

Let us consider now the specific case of bending of a simply supported beam AB by couples applied as shown in Fig. 389a. In our further
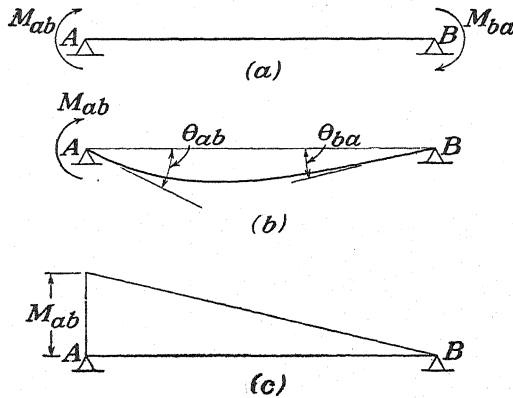
FIG. 389.

discussion these couples will be called *end moments*, and we shall denote them by the symbols M_{ab} and M_{ba}, the two subscripts indicating the ends of the beam as shown in Fig. 389a. Clockwise end moments will be considered as positive. This means that, with the conventional rule for sign of bending moment, the end moment M_{ab} is identical with the bending moment at A, while the end moment M_{ba} is equal but opposite in sign to the bending moment at B. Beginning with the case where only the moment M_{ab} is acting (Fig. 389b) and observing that the corresponding bending-moment diagram is a triangle (Fig. 389c), we obtain

$$\theta_{ab} = \frac{M_{ab}l}{3EI}, \qquad \theta_{ba} = -\frac{M_{ab}l}{6EI}.$$

We obtain similar formulas for the case where the moment M_{ba} is acting alone.   Combining the actions of the two end moments (Fig. 389a), we obtain

$$\theta_{ab} = \frac{M_{ab}l}{3EI} - \frac{M_{ba}l}{6EI}, \qquad \theta_{ba} = \frac{M_{ba}l}{3EI} - \frac{M_{ab}l}{6EI}. \tag{43}$$

Solving these two equations for M_{ab} and M_{ba}, we obtain

$$M_{ab} = \frac{2EI}{l}\,(2\theta_{ab} + \theta_{ba}), \qquad M_{ba} = \frac{2EI}{l}\,(2\theta_{ba} + \theta_{ab}). \tag{44}$$

From these two equations the end moments can be calculated if the rotations θ_{ab} and θ_{ba} of the end tangents are known.
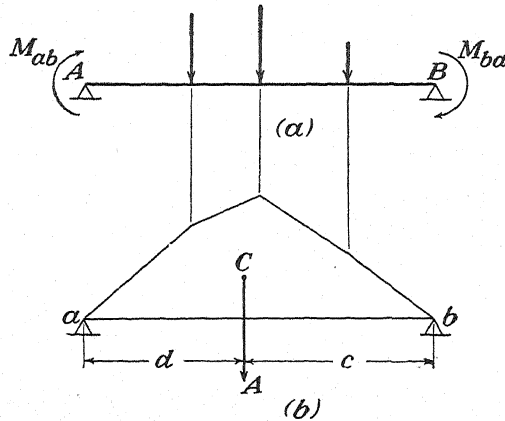
FIG. 390.

Let us consider now a more general case in which there are both end moments and lateral load acting as shown in Fig. 390a.   The angles of rotation produced by the end moments alone are given by expressions (43).   To obtain the angles of rotation produced by the lateral load, we consider the corresponding bending-moment diagram as shown in Fig. 390b.   Upon denoting by c and d the distances from the ends of the beam to the vertical through the centroid C of this bending-moment area and by A the magnitude of the area, the reactions at the ends produced by such fictitious loading are

$$R_{ab} = \frac{Ac}{l}, \qquad R_{ba} = \frac{Ad}{l},$$

and the corresponding angles of rotation are

$$\theta_{ab} = \frac{Ac}{EIl}, \qquad \theta_{ba} = -\frac{Ad}{EIl}.$$

Combining these angles with those produced by the end moments

[Eqs. (43)], we obtain the following total angles:

$$\left.\begin{aligned}
\theta_{ab} &= \frac{M_{ab}l}{3EI} - \frac{M_{ba}l}{6EI} + \frac{Ac}{EIl}, \\
\theta_{ba} &= \frac{M_{ba}l}{3EI} - \frac{M_{ab}l}{6EI} - \frac{Ad}{EIl}.
\end{aligned}\right\} \tag{45}$$

Solving these equations for M_{ab} and M_{ba}, we obtain

$$\left.\begin{aligned}
M_{ab} &= \frac{2EI}{l}(2\theta_{ab} + \theta_{ba}) - \frac{2A}{l^2}(2c - d), \\
M_{ba} &= \frac{2EI}{l}(2\theta_{ba} + \theta_{ab}) + \frac{2A}{l^2}(2d - c).
\end{aligned}\right\} \tag{46}$$

From these equations the end moments can be readily calculated if the rotations of the ends and the bending-moment diagram for the lateral load are known.
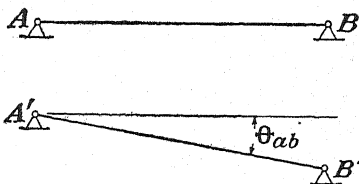
Sometimes, as a result of displacements of the supports, a beam moves from a position AB to a position $A'B'$ (Fig. 391). In such case it has rotation as a rigid body and we denote the angle of this rotation by Θ_{ab}, considered positive if the rotation is clockwise.

FIG. 391.

The total angles of rotation of the ends will then be

$$\left.\begin{aligned}
\theta_{ab} &= \frac{M_{ab}l}{3EI} - \frac{M_{ba}l}{6EI} + \frac{Ac}{EIl} + \Theta_{ab}, \\
\theta_{ba} &= \frac{M_{ba}l}{3EI} - \frac{M_{ab}l}{6EI} - \frac{Ad}{EIl} + \Theta_{ab}.
\end{aligned}\right\} \tag{47}$$

Solving these equations for the end moments, we obtain

$$\left.\begin{aligned}
M_{ab} &= \frac{2EI}{l}(2\theta_{ab} + \theta_{ba}) - \frac{2A}{l^2}(2c - d) - \frac{6\Theta_{ab}EI}{l}, \\
M_{ba} &= \frac{2EI}{l}(2\theta_{ba} + \theta_{ab}) + \frac{2A}{l^2}(2d - c) - \frac{6\Theta_{ab}EI}{l}.
\end{aligned}\right\} \tag{48}$$

Equations (43) to (48) represent the required slope-deflection equations so widely used in the analysis of frame structures.

We shall now discuss briefly the effect of shearing forces on the angles of rotation of the ends of a beam, beginning with the case of a single concentrated load P acting as shown in Fig. 392a. The deflection due to shear in such a case will be as shown in exaggerated form in the figure, and the sum of the shearing strains on the two sides of the load is given by the small angle ϕ, the magnitude of which is

$$\phi = \frac{\alpha P}{AG}. \tag{d}$$

Here A is the cross-sectional area of the beam, G the modulus of elasticity in shear, and α a numerical factor, larger than unity, the magnitude of which depends on the shape of the cross section.[1] For a rectangular cross section, we usually take $\alpha = 1.2$; for an I-beam, α = ratio of the total cross-sectional area to the cross-sectional area of
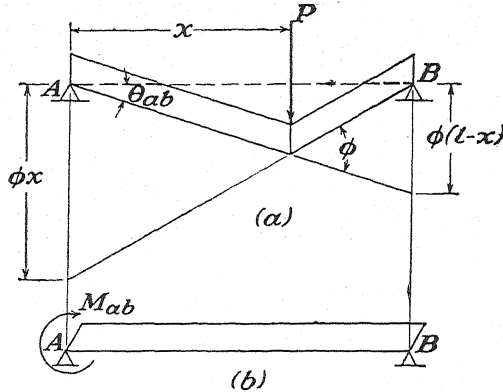
FIG. 392.

the web. With the value of ϕ from Eq. (d), the angles of rotation of the ends are readily obtained from Fig. 392a, which gives

$$\theta_{ab} = \phi \, \frac{l - x}{l} = \frac{\alpha P}{AG} \cdot \frac{l - x}{l}, \qquad \theta_{ba} = -\phi \frac{x}{l} = -\frac{\alpha P}{AG} \cdot \frac{x}{l}. \tag{49}$$

In the case of a continuously distributed load of intensity q, the rotations of the ends produced by an elemental load $q \, dx$ is obtained by substituting $q \, dx$ for P in Eqs. (49). The total angles of rotation will then be

$$\theta_{ab} = \int_0^l \frac{\alpha q}{AG} \cdot \frac{l - x}{l} \, dx, \qquad \theta_{ba} = - \int_0^l \frac{\alpha q}{AG} \cdot \frac{x}{l} \, dx. \tag{50}$$

We obtain some idea of the magnitude of the angles produced by shear by taking the case of a beam loaded at the middle. The rotation of the left end of the beam due to bending is $Pl^2/16EI$. The rotation of the same end, due to shear, from the first of Eqs. (49), is $\alpha P/2AG$. Hence the total angle of rotation is

$$\theta_{ab} = \frac{Pl^2}{16EI} + \frac{\alpha P}{2AG} = \frac{Pl^2}{16EI} \left(1 + 8\alpha \, \frac{E}{G} \cdot \frac{i^2}{l^2} \right), \tag{e}$$

where i is the centroidal radius of gyration of the cross section. Taking, for example, a rectangular beam of depth h, we have $\alpha = 1.2$, $i^2 = h^2/12$, and the second term in the parentheses of expression (e) becomes

$$8 \cdot 1.2 \, \frac{E}{G} \cdot \frac{h^2}{12l^2} = 0.8 \cdot \frac{E}{G} \cdot \frac{h^2}{l^2}.$$

If the depth of the beam is one-tenth of the span, this quantity is about 0.02 and the rotation produced by shear is only about 2 per cent of the rotation produced by bending.

[1] For a discussion of the effect of shearing force on deflection of beams, see "Strength of Materials," 2d ed. vol. I, p. 170, 1940.

If a beam is uniformly loaded, we use Eqs. (50) and obtain for the angle of rotation

$$\theta_{ab} = \frac{ql^3}{24EI} \left(1 + 12\alpha \frac{E}{G} \cdot \frac{i^2}{l^2} \right).$$

In this case, the effect of shear on the angle of rotation for the rectangular beam with $h/l = 0.1$ will be about 3 per cent of the rotation produced by bending.

For a beam bent by one end moment, the shearing force is constant along the span, and the distortion due to shear has the form shown in Fig. 392b. It is seen that in this case there is no additional rotation of the end tangents and no additional deflection due to shear. In practical calculations, the effect of shear on the angles of rotation of the end tangents is usually neglected, which is justifiable if the depth of the beam is small in comparison with its length, say if $h/l < \frac{1}{5}$ in the case of a rectangular cross section.

57. Beams with Fixed Ends.—Using the slope-deflection equations developed in the preceding article, various cases of statically indeter-
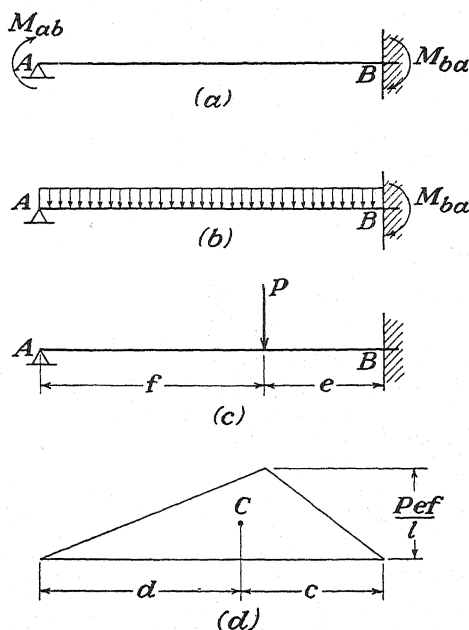
FIG. 393.

minate beams can be readily analyzed. We shall discuss here only a few particular cases that are of especial interest in connection with the analysis of frames. We begin with a beam built-in at one end and simply supported at the other, as shown in Fig. 393a. Assuming that the magnitude of the active end moment M_{ab} is given, let it be required to find the corresponding magnitude of the reactive end moment M_{ba} produced at the fixed end B and also the relation between the active moment M_{ab} and the angle of rotation θ_{ab}. Observing that the end B

of the beam does not rotate and substituting $\theta_{ba} = 0$ in the second of Eqs. (43), we find

$$M_{ba} = \tfrac{1}{2} M_{ab}.$$

This shows that, if an active moment M_{ab} is applied at the end A, a reactive moment M_{ba}, equal to $\tfrac{1}{2} M_{ab}$, is produced at the fixed end B. This latter moment is of particular interest in rigid-frame analysis and will be called the *carry-over moment*.

Substituting $\theta_{ba} = 0$ in the first of Eqs. (44), we obtain

$$M_{ab} = \frac{4EI}{l}\, \theta_{ab}. \tag{51}$$

From this equation, the moment M_{ab} is readily calculated if the angle of rotation θ_{ab} is known.

It is interesting to note that if both ends of the beam are simply supported the relation between the end moment M_{ab} and the angle θ_{ab} is

$$M_{ab} = \frac{3EI}{l}\, \theta_{ab}.$$

This shows that, in calculating M_{ab} by using the angle θ_{ab}, the placing of a hinge at B is equivalent to reduc ng the flexural rigidity EI of the beam to the value $3EI/4$.

In the case of a uniformly loaded beam (Fig. 393b), the reactive end moment M_{ba} is found from the second of Eqs. (45). Substituting into this equation

$$M_{ab} = 0, \qquad \theta_{ba} = 0, \qquad A = \frac{ql^3}{12}, \qquad d = \frac{l}{2},$$

we obtain

$$M_{ba} = \frac{ql^2}{8}.$$

We note that this end moment has the same value as the bending moment at the middle of a simply supported beam.

If a concentrated force P acts on the beam (Fig. 393c), the corresponding bending-moment diagram is represented by the triangle shown in Fig. 393d and we obtain

$$A = \frac{Pef}{2}, \qquad d = \frac{l+f}{3}.$$

The second of Eqs. (45), with $\theta_{ba} = 0$ and $M_{ab} = 0$, then gives

$$M_{ba} = \frac{3Ad}{l^2} = \frac{Pf(l^2 - f^2)}{2l^2}.$$

If the built-in end B of the beam suffers a vertical downward displacement Δ without rotation, the end moment M_{ba} produced by such

displacement is obtained by using Eqs. (48). Substituting in the first of these equations $M_{ab} = 0$, $\theta_{ba} = 0$, $A = 0$, and $\Theta_{ab} = \Delta/l$, we obtain

$$\theta_{ab} = \frac{3}{2}\frac{\Delta}{l}.$$

Substituting this value in the second of Eqs. (48), we find

$$M_{ba} = -\frac{3EI}{l} \cdot \frac{\Delta}{l}. \tag{52}$$

Applications of Eqs. (51) and (52) will be shown later in the analysis of frames.

In the case of a beam with both ends built-in (Fig. 394a) and carrying any lateral load, we use Eqs. (46) to calculate the statically indeterminate end moments. Substituting $\theta_{ab} = \theta_{ba} = 0$ into these equations, we obtain

$$M_{ab} = -\frac{2A}{l^2}(2c - d), \qquad M_{ba} = \frac{2A}{l^2}(2d - c). \tag{53}$$

For any given lateral load, the corresponding bending-moment diagram, such as that shown in Fig. 394b, can be constructed, and its area A together with the centroidal distances c and d can be calculated. Substituting these quantities into Eqs. (53), we obtain the required end moments. These moments are called the *fixed-end moments* and will be denoted in our further discussion by the symbols $\mathfrak{M}_{ab}$ and $\mathfrak{M}_{ba}$. Observing that they are taken positive when they act clockwise, we conclude that $\mathfrak{M}_{ab}$ is identical with the bending moment at the end A of the beam, while $\mathfrak{M}_{ba}$ is numerically equal but opposite in sign to the bending moment at the end B.

(a)

(b)
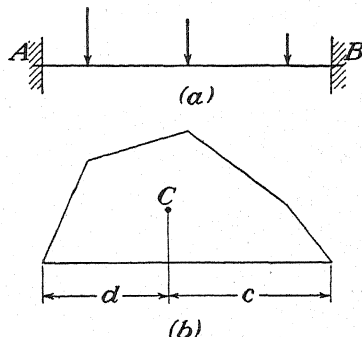
Fig. 394.

In the case of a load uniformly distributed along the entire length of the beam, $A = ql^3/12$, $c = d = l/2$, and Eqs. (53) become

$$\mathfrak{M}_{ab} = -\frac{ql^2}{12}, \qquad \mathfrak{M}_{ba} = \frac{ql^2}{12}. \tag{54}$$

In the case of a concentrated load P applied at the distance f from the support A, the bending-moment diagram is a triangle (Fig. 393d) and we obtain $A = Pfe/2$, $c = (l + e)/3$, $d = (l + f)/3$. Substituting these

values into Eqs. (53), we find

$$\mathfrak{M}_{ab} = -\frac{Pe^2f}{l^2}, \qquad \mathfrak{M}_{ba} = \frac{Pef^2}{l^2}. \tag{55}$$

For any value of the distance f, the values of the fixed-end moments can be readily calculated.

Let us consider now the bending of a fixed-end beam produced by nonequal settlements of the supports. Assume, for example, that the support B settles by an amount Δ, while the support A remains stationary. Assume, also, that no rotations of the ends of the beam occur during such displacement. Then in calculating the end moments produced by such settlement, we use Eqs. (48). Substituting $\theta_{ab} = \theta_{ba} = 0$ and $A = 0$ in these equations and observing that $\Theta_{ab} = \Delta/l$, we obtain

$$\mathfrak{M}_{ab} = \mathfrak{M}_{ba} = -\frac{6\,\Delta EI}{l^2} = -\frac{6EI}{l}\,\Theta_{ab}. \tag{56}$$

Equations (51) to (56) developed in this article for a single beam will find a wide application in the analysis of frames, which will be discussed later.

58. Continuous Beams.—Equations (45), derived in Art. 56, can be used to advantage in the analysis of continuous beams. Starting from the left end of the beam, we denote by 0, 1, 2, . . . the consecutive supports, by l_1, l_2, . . . the lengths of the spans, and by I_1, I_2, . . . the cross-sectional moments of inertia, assumed constant along each span. This done, we consider any two adjacent spans l_n and l_{n+1} as shown in Fig. 395a and construct the corresponding bending-moment diagrams for the lateral loading as shown in Fig. 395b. The areas of these diagrams are denoted by A_n and A_{n+1} and the positions of their centroids C_n and C_{n+1} by the distances c_n, d_n and c_{n+1}, d_{n+1}, respectively. Considering bending of each span, we must take into account not only the lateral load acting on the span but also the end moments representing the action of the adjacent spans on the span under consideration. The magnitudes of these moments we denote for the span l_n by $M_{n-1,n}$ and $M_{n,n-1}$ and for the span l_{n+1} by $M_{n,n+1}$ and $M_{n+1,n}$, as shown in Fig. 395c. The equations for calculating these moments can be written on the basis of the continuity of the elastic line. From this continuity it follows that the angle of rotation $\theta_{n,n-1}$ of the right end of the span l_n must be equal to the angle of rotation $\theta_{n,n+1}$ of the left end of the span l_{n+1}. These angles of rotation will be found from Eqs. (45), which give

$$\left. \begin{aligned} \theta_{n,n-1} &= \frac{M_{n,n-1}l_n}{3EI_n} - \frac{M_{n-1,n}l_n}{6EI_n} - \frac{A_n d_n}{l_n EI_n}, \\ \theta_{n,n+1} &= \frac{M_{n,n+1}l_{n+1}}{3EI_{n+1}} - \frac{M_{n+1,n}l_{n+1}}{6EI_{n+1}} + \frac{A_{n+1}c_{n+1}}{l_{n+1}EI_{n+1}}. \end{aligned} \right\} \tag{a}$$

Let us introduce now the conventional bending moments M_{n-1}, M_n, M_{n+1} at the supports, instead of the end moments. From the assumed
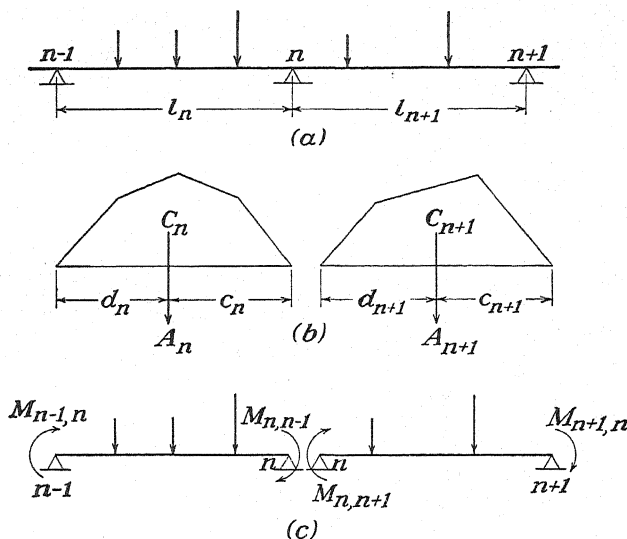
FIG. 395.

positive directions of the end moments (see page 335) and the conventional rule for sign of bending moment it follows that

$$M_{n-1,n} = M_{n-1}, \qquad M_{n+1,n} = -M_{n+1},$$
$$M_{n,n+1} = -M_{n,n-1} = M_n,$$

and expressions (a) become

$$\theta_{n,n-1} = -\frac{M_n l_n}{3EI_n} - \frac{M_{n-1}l_n}{6EI_n} - \frac{A_n d_n}{l_n EI_n},$$

$$\theta_{n,n+1} = \frac{M_n l_{n+1}}{3EI_{n+1}} + \frac{M_{n+1}l_{n+1}}{6EI_{n+1}} + \frac{A_{n+1}c_{n+1}}{l_{n+1}EI_{n+1}}.$$

Equating these two angles, we obtain

$$M_{n-1}\frac{l_n}{I_n} + 2M_n\left(\frac{l_n}{I_n} + \frac{l_{n+1}}{I_{n+1}}\right) + M_{n+1}\frac{l_{n+1}}{I_{n+1}} = -\frac{6A_n d_n}{l_n I_n} - \frac{6A_{n+1}c_{n+1}}{l_{n+1}I_{n+1}},$$

$$(57)$$

which is the well-known *equation of three moments*. Such an equation can be written for each intermediate support of a continuous beam; and if the ends of the beam are simply supported, the number of the equations is equal to the number of statically indeterminate moments at the supports. Hence all unknowns can be found from these equations.

If the left end of the beam is built-in at the support 0, we have an

additional condition stating that the left end of the beam does not rotate. In our previous notations, this means that $\theta_{0,1}$ vanishes. Using the first of Eqs. (45), we find that this condition becomes

$$\frac{M_{0,1}l_1}{3EI_1} - \frac{M_{1,0}l_1}{6EI_1} + \frac{A_1c_1}{l_1EI_1} = 0.$$

Introducing bending moments again, instead of end moments, we obtain

$$2M_0 + M_1 = -\frac{6A_1c_1}{l_1^2}. \tag{58}$$

It is seen that a built-in end introduces an additional unknown moment M_0, but at the same time we have an additional equation (58). Hence the number of unknowns is again equal to the number of equations. An equation similar to Eq. (58) can also be written for the right end of the beam if that end is built-in.

As a first application of the three-moment equation (57), let us consider the case of a beam carrying a uniformly distributed load on each span. If q_n is the intensity of load on the span l_n, we have $A_n = q_n l_n^3/12$ and $c_n = d_n = l_n/2$. We obtain similar expressions for the span l_{n+1}. Equation (57) then becomes

$$M_{n-1}\frac{l_n}{I_n} + 2M_n\left(\frac{l_n}{I_n} + \frac{l_{n+1}}{I_{n+1}}\right) + M_{n+1}\frac{l_{n+1}}{I_{n+1}} = -\frac{q_n l_n^3}{4I_n} - \frac{q_{n+1}l^3_{n+1}}{4I_{n+1}}. \tag{59}$$

Take, for example, a beam of uniform cross section on five supports and with simply supported ends. In this case $M_0 = M_4 = 0$ and the moments M_1, M_2, M_3 at the intermediate supports will be calculated from Eqs. (59), which are

$$2M_1(l_1 + l_2) + M_2l_2 = -\frac{q_1l_1^3}{4} - \frac{q_2l_2^3}{4},$$

$$M_1l_2 + 2M_2(l_2 + l_3) + M_3l_3 = -\frac{q_2l_2^3}{4} - \frac{q_3l_3^3}{4},$$

$$M_2l_3 + 2M_3(l_3 + l_4) = -\frac{q_3l_3^3}{4} - \frac{q_4l_4^3}{4},$$

If all spans are equal, $l_1 = l_2 = l_3 = l_4 = l$, and the equations give

$$\left.\begin{aligned}
M_1 &= -\frac{l^2}{224}(15q_1 + 11q_2 - 3q_3 + q_4), \\
M_2 &= -\frac{l^2}{224}(-4q_1 + 12q_2 + 12q_3 - 4q_4), \\
M_3 &= -\frac{l^2}{224}(q_1 - 3q_2 + 11q_3 + 15q_4).
\end{aligned}\right\} \tag{60}$$

Taking, for example, $q_2 = q_3 = q_4 = 0$ and only q_1 different from zero, we obtain the case shown in Fig. 396a. The moments at the intermediate supports, from Eqs. (60), are $M_1 = -\frac{15}{224}q_1l^2$, $M_2 = +\frac{1}{56}q_1l^2$,
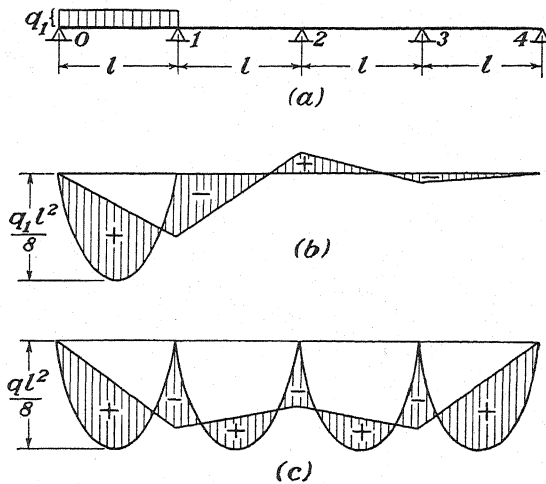
FIG. 396.

$M_3 = -\frac{1}{224}q_1l^2$. The corresponding bending-moment diagram is shown in Fig. 396b.

If a load of constant intensity covers the entire length of the beam, $q_1 = q_2 = q_3 = q_4 = q$, and Eqs. (60) give

$$M_1 = -\frac{3}{28}ql^2, \qquad M_2 = -\frac{1}{14}ql^2, \qquad M_3 = -\frac{3}{28}ql^2.$$

The corresponding bending-moment diagram is shown in Fig. 396c.

If a concentrated load P_n acts in a span l_n (Fig. 397a), the area A_n is represented by the triangle shown in Fig. 397b and we obtain

$$A_n = \frac{P_n e_n f_n}{2}, \qquad c_n = \frac{1}{3}(l_n + e_n),$$

$$d_n = \frac{1}{3}(l_n + f_n). \qquad (b)$$
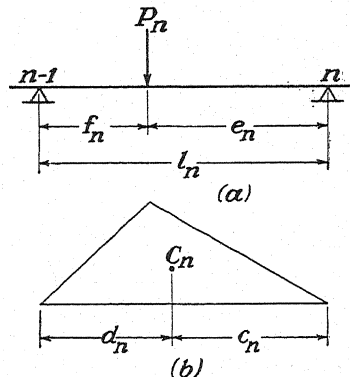
Such expressions for each concentrated force acting on the beam must be used in calculating the right side of Eq. (57).

As an example involving concentrated forces, let us consider a beam of uniform

FIG. 397.

cross section on five supports and loaded as shown in Fig. 398a. From symmetry we conclude that $M_1 = M_3$, and we have to write only two

equations. For the loads and distances indicated in the figure, we find $A_1 = \frac{405}{2}$ ton-ft.^{2}, $c_1 = d_1 = 9$ ft., $A_2 = 360$ ton-ft.^{2}, $c_2 = d_2 = \frac{21}{2}$ ft. Substituting in Eqs. (57), we obtain

$$2M_1 \cdot 39 + M_2 \cdot 21 = -\frac{6 \cdot 405}{4} - \frac{6 \cdot 360}{2},$$

$$M_1 \cdot 21 + 2M_2 \cdot 42 + M_1 \cdot 21 = -6 \cdot 360,$$

which give

$$M_1 = -17.0 \text{ ton-ft.}, \qquad M_2 = -17.2 \text{ ton-ft.}$$

Using these moments, the bending-moment diagram shown in Fig. 398b can be constructed.
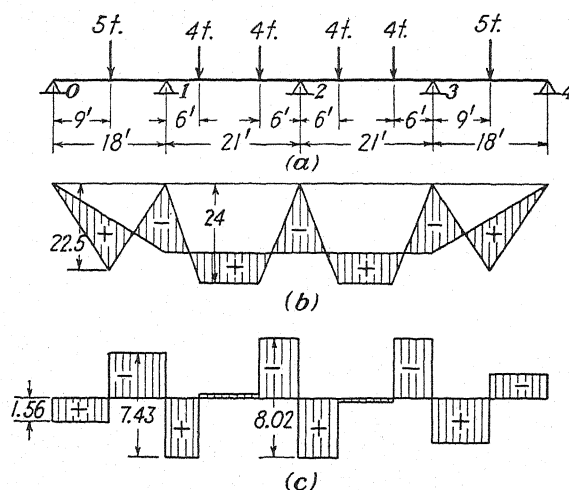
Fig. 398.
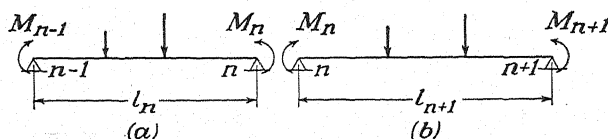
Fig. 399.

When the bending moments at the intermediate supports have been calculated, the reactions at the supports can be found from equations of statics. Considering the support n (Fig. 399), we calculate separately the reaction R_n produced by bending of the span l_n and of the span l_{n+1} and then take the sum of these two reactions. Thus, from Fig. 399a, we conclude that the first part of the reaction R_n is

$$R_n' + \frac{M_{n-1} - M_n}{l_n}, \tag{c}$$

where R_n' represents the reaction produced by lateral loads.   Considering Fig. 399b in the same manner, we conclude that the second part of the reaction at the support n is

$$R_n'' + \frac{M_{n+1} - M_n}{l_{n+1}}. \tag{d}$$

Taking the sum of expressions (c) and (d), we find for the total reaction at the support n

$$R_n = R_n' + R_n'' + \frac{M_{n-1} - M_n}{l_n} + \frac{M_{n+1} - M_n}{l_{n+1}}, \tag{61}$$

where $R_n' + R_n''$ is the magnitude of the reaction at the support n that would be obtained if the continuous beam were cut at all intermediate supports and thus transformed into a system of simply supported beams. It should be noted that if loads are applied over the supports they will be transmitted directly to the supports and reactions equal to these loads must then be added to those calculated from Eq. (61).

Using Eq. (61) in the case shown in Fig. 398, we obtain the following values of the reactions:

$$R_0 = R_4 = 1.56 \text{ ton}, \qquad R_1 = R_3 = 7.43 \text{ ton}, \qquad R_2 = 8.02 \text{ ton}.$$

The corresponding shearing-force diagram is shown in Fig. 398c.

In all previous examples, we have assumed a continuous beam of uniform cross section.   In such a case, the moments of inertia appearing in Eq. (57) cancel, and the magnitudes of moments at the supports do not depend on the cross-sectional dimensions of the beam.   If the cross-sectional dimensions of the beam in different spans are different, we multiply Eq. (57) by an arbitrary constant moment of inertia I_0* and introduce the notations

$$l_n \frac{I_0}{I_n} = l_n', \qquad l_{n+1} \frac{I_0}{I_{n+1}} = l_{n+1}', \qquad A_n \frac{I_0}{I_n} = A_n', \qquad \frac{A_{n+1}I_0}{I_{n+1}} = A_{n+1}'. \tag{e}$$

With these notations, Eq. (57) becomes

$$M_{n-1}l_n' + 2M_n(l_n' + l_{n+1}') + M_{n+1}l_{n+1}' = - \frac{6A_n'd_n}{l_n} - \frac{6A_{n+1}'c_{n+1}}{l_{n+1}}. \tag{62}$$

This equation does not contain moments of inertia, explicitly, and the problem is reduced to that of a beam of uniform cross section for which the modified lengths of spans l_1', l_2', . . . and the modified moment areas A_1', A_2', . . . are calculated from Eqs. (e).

Let us consider now the effect of settlement of supports on bending of a continuous beam.   Assuming that the vertical displacements of three consecutive supports $n - 1$, n, and $n + 1$ are Δ_{n-1}, Δ_n, and Δ_{n+1}

---

* Usually we take for I_0 the cross-sectional moment of inertia in one of the spans.

and considering the two consecutive spans shown in Fig. 395c as simply supported beams, we conclude that the angle of rotat on of the span l_n due to settlement of the supports is $(\Delta_n - \Delta_{n-1})/l_n$. In the same manner for the span l_{n+1}, we obtain $(\Delta_{n+1} - \Delta_n)/l_{n+1}$. Using these angles together with Eqs. (47) (see page 337), we obtain, instead of Eqs. (a), (page 342), the following equations:

$$\left.\begin{array}{l} \theta_{n,n-1} = \dfrac{M_{n,n-1}l_n}{3EI_n} - \dfrac{M_{n-1,n}l_n}{6EI_n} - \dfrac{A_n d_n}{l_n EI_n} + \dfrac{\Delta_n - \Delta_{n-1}}{l_n}, \\[3mm] \theta_{n,n+1} = \dfrac{M_{n,n+1}l_{n+1}}{3EI_{n+1}} - \dfrac{M_{n+1,n}l_{n+1}}{6EI_{n+1}} + \dfrac{A_{n+1}c_{n+1}}{l_{n+1}EI_{n+1}} + \dfrac{\Delta_{n+1} - \Delta_n}{l_{n+1}}. \end{array}\right\} \quad (f)$$

Again, introducing bending moments, instead of end moments, and equating the angles $\theta_{n,n-1}$ and $\theta_{n,n+1}$, we obtain

$$M_{n-1}\frac{l_n}{I_n} + 2M_n\left(\frac{l_n}{I_n} + \frac{l_{n+1}}{I_{n+1}}\right) + M_{n+1}\frac{l_{n+1}}{I_{n+1}} = -\frac{6A_n d_n}{l_n I_n} - \frac{6A_{n+1}c_{n+1}}{l_{n+1}I_{n+1}}$$
$$+ 6E\left(\frac{\Delta_n - \Delta_{n-1}}{l_n} - \frac{\Delta_{n+1} - \Delta_n}{l_{n+1}}\right). \quad (g)$$

If the beam has a constant cross section with moment of inertia I along the entire length, we multiply Eq. (g) by I and obtain

$$M_{n-1}l_n + 2M_n(l_n + l_{n+1}) + M_{n+1}l_{n+1} = -\frac{6A_n d_n}{l_n} - \frac{6A_{n+1}c_{n+1}}{l_{n+1}}$$
$$+ 6EI\left(\frac{\Delta_n - \Delta_{n-1}}{l_n} - \frac{\Delta_{n+1} - \Delta_n}{l_{n+1}}\right). \quad (63)$$

If the moments of inertia in different spans are different, we multiply Eq. (g) by an assumed constant moment of inertia I_0. Then, using notations (e), we represent the three-moment equation in the following form:

$$M_{n-1}l_n' + 2M_n(l_n' + l_{n+1}') + M_{n+1}l_{n+1}' = -\frac{6A_n' d_n}{l_n} - \frac{6A_{n+1}'c_{n+1}}{l_{n+1}}$$
$$+ 6EI_0\left(\frac{\Delta_n - \Delta_{n-1}}{l_n} - \frac{\Delta_{n+1} - \Delta_n}{l_{n+1}}\right). \quad (64)$$

It is seen that in this case the three-moment equation has the same form as before. Hence the moments at the supports can be readily calculated if the magnitudes of settlement Δ_{n-1}, Δ_n, and Δ_{n+1} are known.

PROBLEMS

251. Find the bending moment M_1 at the intermediate support of the two-span continuous beam of uniform cross section shown in Fig. 400a if a uniformly distributed load acts on the first span and the ratio $l_2:l_1$ is equal to α.
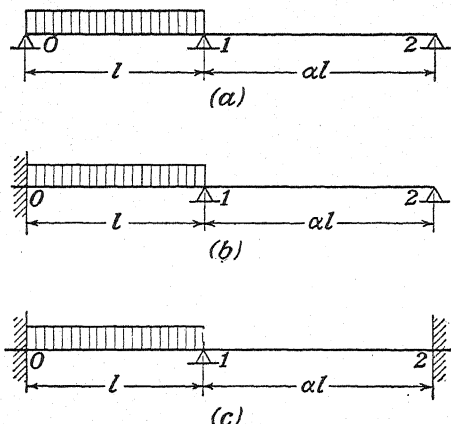
$$Ans. \quad M_1 = -\frac{ql^2}{8} \cdot \frac{1}{1 + \alpha}.$$

Fig. 400.

252. Solve the previous problem if the ratio $I_2:I_1$ is equal to γ.

$$Ans. \quad M_1 = -\frac{ql^2}{8} \cdot \frac{\gamma}{\alpha + \gamma}.$$

253. Find M_0 and M_1 for the continuous beam shown in Fig. 400b. Assume that the cross section is uniform along the entire length and that the intensity of load is q.

$$Ans. \quad M_0 = -\frac{ql^2}{8} \cdot \frac{2 + 4\alpha}{3 + 4\alpha}, \quad M_1 = -\frac{ql^2}{8} \cdot \frac{2}{3 + 4\alpha}.$$

254. Solve the previous problem if both ends of the beam are built-in (Fig. 400c) and the cross section is uniform along the entire length.

$$Ans. \quad M_0 = -\frac{ql^2}{8} \cdot \frac{2 + 3\alpha}{3(1 + \alpha)}, \quad M_1 = -\frac{ql^2}{8} \cdot \frac{2}{3(1 + \alpha)}, \quad M_2 = +\frac{ql^2}{8} \cdot \frac{1}{3(1 + \alpha)}.$$

255. A beam of uniform cross section rests on four supports and is loaded as shown in Fig. 401a. Find the bending moments at the supports if the intensity of load is q.

$$Ans. \quad M_1 = -\frac{ql^2}{8} \cdot \frac{4(\alpha + \beta)}{4(1 + \alpha)(\alpha + \beta) - \alpha^2}, \quad M_2 = +\frac{ql^2}{8} \cdot \frac{2\alpha}{4(1 + \alpha)(\alpha + \beta) - \alpha^2}.$$

(a)

(b)
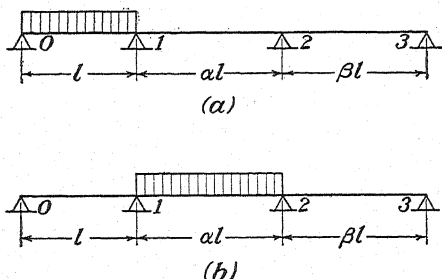
Fig. 401.

256. Solve the previous problem if the middle span is loaded as shown in Fig. 401b.

$$Ans. \quad M_1 = -\frac{ql^2}{8} \cdot \frac{2\alpha^3(\alpha + 2\beta)}{4(1 + \alpha)(\alpha + \beta) - \alpha^2}, \quad M_2 = -\frac{ql^2}{8} \cdot \frac{2\alpha^3(2 + \alpha)}{4(1 + \alpha)(\alpha + \beta) - \alpha^2}.$$

257. Solve the preceding problem if both ends of the beam are built-in and $\beta = 1$.

$$Ans. \quad M_0 = M_3 = \frac{ql^2}{8} \cdot \frac{2\alpha^3}{3(1 + 2\alpha)}, \quad M_1 = M_2 = -\frac{ql^2}{8} \cdot \frac{4\alpha^3}{3(1 + 2\alpha)}.$$

59. Influence Lines for Continuous Beams.—In the preceding article, we considered the analysis of continuous beams under the action of stationary loads only. In the case of moving loads, we must begin the problem with a selection of the most unfavorable load distribution, *i.e.*, the one that produces maximum stresses. This can be accomplished with the help of influence lines, the construction of which requires an analysis of continuous beams loaded in only one span. Some special features of this problem will be considered first.
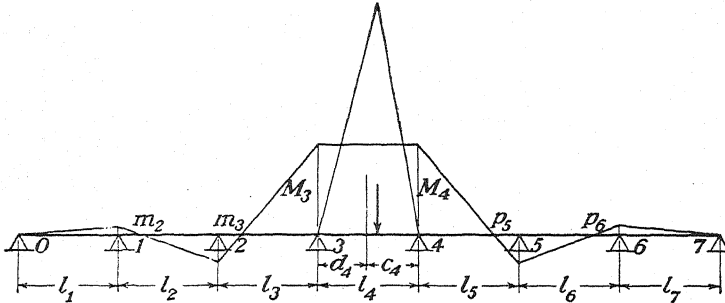
FIG. 402.

Referring to Fig. 402, assume that a beam with seven spans is loaded in only one span as shown and that the cross section is uniform along the entire length[1] of the beam. In such a case, the three-moment equation has the form

$$M_{n-1}l_n + 2M_n(l_n + l_{n+1}) + M_{n+1}l_{n+1} = -\frac{6A_n d_n}{l_n} - \frac{6A_{n+1}c_{n+1}}{l_{n+1}}. \tag{a}$$

Applying this equation to the first two spans of the beam and observing that there is no load on these spans and that $M_0 = 0$, we obtain

$$2M_1(l_1 + l_2) + M_2 l_2 = 0. \tag{b}$$

From this equation, we find

$$\frac{M_2}{M_1} = -\frac{2(l_1 + l_2)}{l_2} = -k_2, \tag{c}$$

where k_2 is a number depending on the ratio of the span lengths l_1 and l_2. Since there is no load in the second span and the moments M_1 and M_2 are of opposite sign, the bending-moment diagram for this span is an inclined straight line intersecting the axis of the beam at a point m_2. The position of this point is completely defined by the ratio $M_2:M_1$ and, as can be seen from Eq. (c), is entirely independent of the kind of load acting to the right of support 2. For any loading of that portion of the beam, the bending moment at m_2 vanishes, that is, m_2 will be an inflection point. Such a point m_2 is called a *fixed point*[2] for the span l_2. Proceeding now to the third span and

---

[1] It has already been shown that in the case of different values of the cross-sectional moment of inertia in different spans the problem can readily be brought to that of a beam of uniform cross section (see p. 347).

[2] The notion of fixed points was introduced in the theory of continuous beams by C. Culman; see his "Anwendungen der Graphischen Statik" prepared for publication by W. Ritter, vol. III, Zürich, 1900. There is given in that book a graphical method of treating continuous beams.

again using Eq. (*a*), we obtain

$$M_1 l_2 + 2M_2(l_2 + l_3) + M_3 l_3 = 0. \tag{d}$$

Eliminating M_1 from this equation, by using Eq. (*b*), we obtain

$$\frac{M_3}{M_2} = -\frac{2(l_2 + l_3)}{l_3} + \frac{l_2}{l_3}\frac{l_2}{2(l_1 + l_2)} = -k_3, \tag{e}$$

from which

$$k_3 = 2 + \frac{l_2}{l_3}\left(2 - \frac{1}{k_2}\right). \tag{f}$$

It is seen that the moments M_2 and M_3 are again of opposite sign and that the bending-moment diagram for the span l_3 is a straight line intersecting the axis of the beam at the fixed point m_3, the position of which is entirely defined by the constant k_3 and is independent of the load acting to the right of the third span. In general, if there are no loads acting on the first n spans, we can proceed as above and will find that the position of the fixed point m_n in the span l_n is defined by the quantity

$$k_n = 2 + \frac{l_{n-1}}{l_n}\left(2 - \frac{1}{k_{n-1}}\right). \tag{65}$$

Applying this equation to the case of equal spans ($l_1 = l_2 = l_3 = \cdots = l$), we obtain

$$k_2 = 4, \qquad k_3 = 3.75, \qquad k_4 = k_5 = \cdots \approx 3.73.$$

In determining the fixed points $m_2, m_3, \ldots m_n$, we started from the left end of the beam and assumed that the load is applied somewhere to the right of the span under consideration. In a similar manner we can start from the right end of the beam and determine the fixed points $p_6, p_5, \ldots$, as shown in Fig. 402, assuming that the load is applied somewhere to the left of the span under consideration. Denoting by k_n' the ratio $-M_{n-1}:M_n$ defining the position of the fixed point p_n in the span l_n and proceeding as before, we obtain the following expression for this ratio:

$$k_n' = 2 + \frac{l_{n+1}}{l_n}\left(2 - \frac{1}{k_{n+1}'}\right). \tag{66}$$

Using Eqs. (65) and (66), we can, in each particular case, determine the two series of fixed points m_n and p_n. One series gives the inflection point in each span when the load is applied anywhere to the right of that span. The second series gives the inflection point in each span when the load is applied anywhere to the left of that span. In the first span, the moment at the left end of the beam vanishes, $k_1 = \infty$, and one of the fixed points coincides with the end of the beam. The second fixed point is found from Eq. (66). For the last span, one of the fixed points coincides with the right end of the beam, and the other is found by using Eq. (65).

With these two series of fixed points, the construction of the bending-moment diagram for the case in which only one span is loaded is reduced to the calculation of bending moments at the ends of that span. If we know, for example, the moments M_3 and M_4 in Fig. 402, we finish the construction of the bending-moment diagram by drawing the system of straight lines through the fixed points m_3, m_2 on one side of the loaded span and through the points p_5, p_6 on the other side.

To find the moments M_3 and M_4, we apply Eq. (*a*) first to the spans 3 and 4 and afterward to the spans 4 and 5. In this manner, we obtain

$$M_2 l_3 + 2M_3(l_3 + l_4) + M_4 l_4 = -\frac{6A_4 c_4}{l_4}.$$

$$M_3 l_4 + 2M_4(l_4 + l_5) + M_5 l_5 = -\frac{6A_4 d_4}{l_4}.$$

These equations can be represented in the following form:

$$\left.\begin{array}{l} M_4 l_4 + M_3 l_4 \left[2 + \dfrac{l_3}{l_4} \left(2 + \dfrac{M_2}{M_3} \right) \right] = -\dfrac{6A_4 c_4}{l_4}, \\[2mm] M_3 l_4 + M_4 l_4 \left[2 + \dfrac{l_5}{l_4} \left(2 + \dfrac{M_5}{M_4} \right) \right] = -\dfrac{6A_4 d_4}{l_4}. \end{array}\right\} \qquad (g)$$

Observing that

$$\frac{M_2}{M_3} = -\frac{1}{k_3} \qquad \text{and} \qquad \frac{M_5}{M_4} = -\frac{1}{k_5'}$$

and using Eqs. (65) and (66), we write Eqs. (g) in the simplified form

$$M_4 l_4 + M_3 l_4 k_4 = -\frac{6A_4 c_4}{l_4},$$

$$M_3 l_4 + M_4 l_4 k_4' = -\frac{6A_4 d_4}{l_4},$$

from which

$$M_3 = \frac{6A_4(c_4 k_4' - d_4)}{l_4^2(1 - k_4 k_4')}, \qquad M_4 = \frac{6A_4(d_4 k_4 - c_4)}{l_4^2(1 - k_4 k_4')}. \qquad (h)$$

In the general case, when the nth span is loaded we shall obtain

$$M_{n-1} = \frac{6A_n(c_n k_n' - d_n)}{l_n^2(1 - k_n k_n')}, \qquad M_n = \frac{6A_n(d_n k_n - c_n)}{l_n^2(1 - k_n k_n')}. \qquad (67)$$

By using these equations together with Eqs. (65) and (66) defining the fixed points, a beam with any number of spans and loaded in one span can be readily analyzed. Assume, for example, that all spans in Fig. 402 are equal and that the middle span carries a uniform load. Then $k_2 = k_6' = 4$, $k_3 = k_5' = 3.75$, $k_4 = k_4' = 3.73$, $A_4 = ql^3/12$, $c_4 = d_4 = l/2$, and Eqs. (h) give

$$M_3 = M_4 = -\frac{ql^2}{18.9}.$$

From the positions of the fixed points, we then obtain

$$M_2 = M_5 = -\frac{M_3}{k_3} = -\frac{M_3}{3.75},$$

$$M_1 = M_6 = -\frac{M_2}{k_2} = \frac{M_3}{4 \cdot 3.75} = \frac{M_3}{15}.$$

It is seen that the moments at the supports away from the loaded span diminish rapidly from one support to the next and remote spans have only a negligible effect on the magnitude of the moments at the ends of the loaded span. If we take, for example, only five spans in the preceding numerical example, removing the first and last spans, we obtain $M_3 = M_4 = -\frac{1}{19}ql^2$, which differs from the previously obtained value only by about one-half of 1 per cent.

Having the solution of the problem in which only one span is loaded, we can readily answer the question regarding the most unfavorable distribution of uniform live load on a continuous beam. For example, to produce maximum positive bending moment at the middle of the span l_n (Fig. 403a), we must load that and alternate spans as shown. The same load distribution must also be used to produce maximum negative bending moment at the middle of the span l_{n-1}. To produce maximum negative bending moment at the support $n - 1$, the load must be put on the two spans adjacent to this support, and the loaded and unloaded spans must alternate as

shown in Fig. 403*b*. The load distribution shown in Fig. 403*c* is selected to produce maximum positive bending moment at the support $n - 1$.
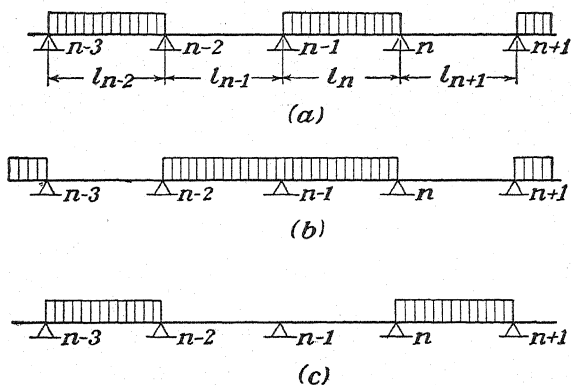
FIG. 403.
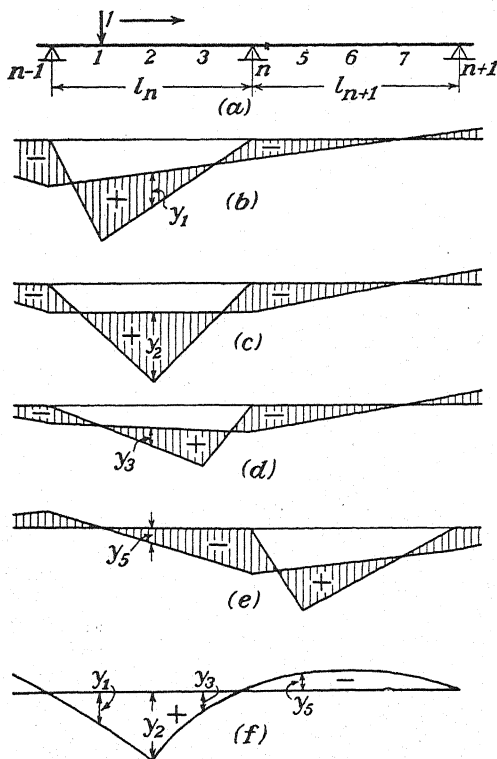
FIG. 404.

In the case of concentrated moving loads, the most unfavorable position of load is usually determined with the help of influence lines. To construct an influence line, we divide each span of the continuous beam into several equal parts and assume

that a unit load is successively placed at each division point. Then for each position of this load we calculate the required quantity, bending moment, or shearing force at a certain cross section, for which we wish to construct the influence line. This quantity gives the corresponding influence coefficient. Figure 404, for example, shows the construction of the influence line for bending moment at the middle of the span l_n. Putting the unit load at the division points 1, 2, . . . in succession, we construct the corresponding bending-moment diagrams as already shown in Fig. 402. Several such diagrams are shown in Figs. 404b to 404e. Taking from these diagrams
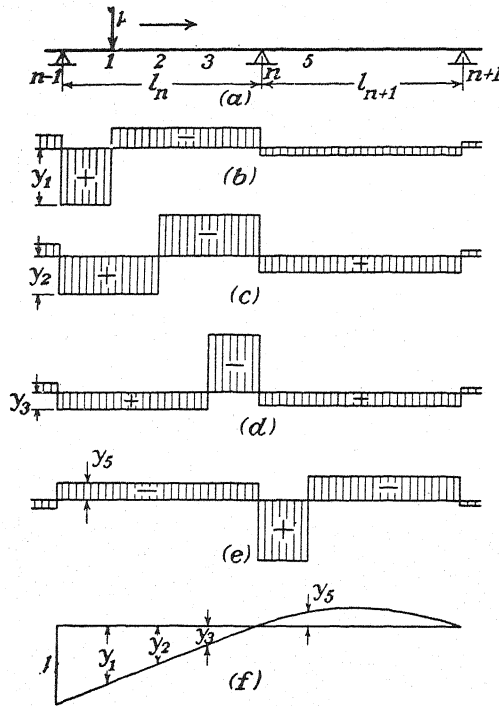
Fig. 405.

the values of the bending moment at the middle of the span l_n, we obtain the ordinates y_1, y_2, . . . of the required influence line, shown in Fig. 404f.

All details of the construction of an influence line for shearing force at the left end of the span l_n are shown in Fig. 405. Having, from the previous analysis, the bending moments at the supports for each position of the unit load (Fig. 404), we can calculate the reactions at the supports from equations of statics [see Eqs. (61), page 347] and can construct shearing-force diagrams for each position of the load as shown in Figs. 405b to 405e. From these diagrams the ordinates y_1, y_2, . . . of the required influence line, shown in Fig. 405f, are obtained. With influence lines for bending moments and shearing forces, the most unfavorable position of a moving load in each particular case can be readily determined.

The reciprocal theorem can also be used for the construction of influence lines. It becomes especially simple in the case of an influence line for bending moment at one of the supports of a continuous beam. As the first state of loading, we consider

the case in which a unit load acts on the beam as shown in Fig. 406a. Then, to obtain the influence line for bending moment M_n, we take as the second state of loading the case shown in Fig. 406b. The continuous beam is cut at the support n, and two equal and opposite unit couples are applied to the two portions of the beam as shown. By using fixed points, the bending-moment diagram and the deflection curve for the second state of loading can be readily obtained.[1] Thus we have no
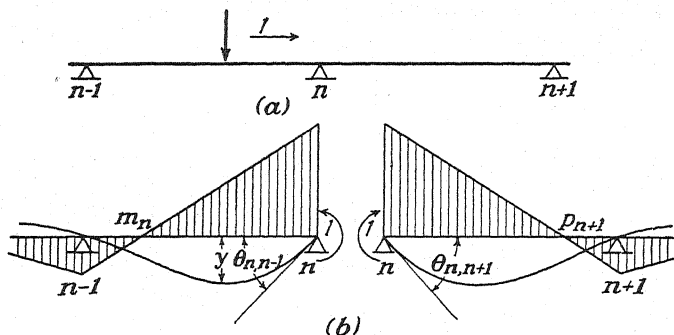
FIG. 406.

difficulty in calculating the deflection y and the angles of rotation $\theta_{n,n-1}$ and $\theta_{n,n+1}$. Applying now the reciprocal theorem to these two states of loading, we obtain

$$1 \cdot y + M_n(\theta_{n,n+1} - \theta_{n,n-1}) = 0.$$

Hence,

$$M_n = -\frac{1 \cdot y}{\theta_{n,n+1} - \theta_{n,n-1}}, \qquad (i)$$

from which we see that the deflection curves shown in Fig. 406b give the shape of the required influence line for M_n. To establish the scale for this line, we have only to divide the deflections y by the quantity $(\theta_{n,n+1} - \theta_{n,n-1})$.

Having the moments at the supports, we can calculate the bending moment and shearing force at any cross section of the beam which indicates that all necessary influence lines can be obtained from the influence lines for bending moments at the supports discussed above.

PROBLEMS

258. Construct the influence line for bending moment at the middle support of a continuous beam with two equal spans (Fig. 407).
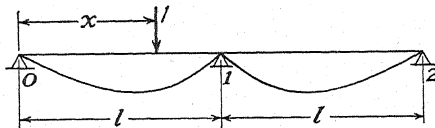
FIG. 407.

Solution: Since the required influence line will be symmetrical about the middle support, we need to consider only one span. For the load in the first span,

[1] Each span represents a beam bent by couples applied at the ends. For this case there are ready equations for the deflection curve and for the angles of rotation of the ends; see "Strength of Materials," vol. I, p. 159.

$$M_1 = -1 \cdot \frac{x(l^2 - x^2)}{4l^2}.$$

Hence the required influence line will be the curve shown in Fig. 407. The numerical maximum of the moment M_1 is obtained when $x = l/\sqrt{3}$.

259. Construct the influence line for bending moment at the cross section *mn* of a continuous beam with two equal spans (Fig. 408).

Solution: When the unit load is to the left of the cross section *mn* and at a distance x from the support, the bending moment at *mn* is

$$M = 1 \cdot \frac{x(l - a)}{l} - 1 \cdot \frac{x(l^2 - x^2)}{4l^2} \cdot \frac{a}{l}.$$

When the load is to the right of the cross section *mn* in the first span of the beam, the bending moment at *mn* is

$$M = 1 \cdot \frac{(l - x)a}{l} - 1 \cdot \frac{x(l^2 - x^2)}{4l^2} \cdot \frac{a}{l}.$$

When the load is in the second span, the moment at *mn* is

$$M = \frac{M_1 a}{l}.$$

The three corresponding branches of the influence line are shown in Fig. 408.
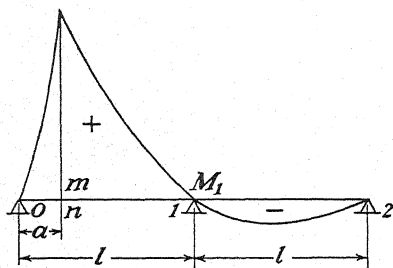
FIG. 408.
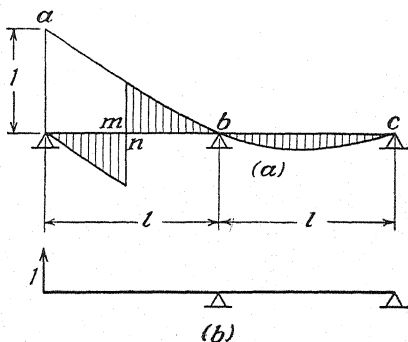
FIG. 409.

260. Construct the influence line for the reaction at the left end and for the shearing force at a cross section *mn* of a continuous beam with two equal spans (Fig. 409a).

Ans. The influence line *abc* for the reaction is obtained as the deflection curve of the beam loaded as shown in Fig. 409b. For the shearing force at *mn*, the ordinates of the shaded areas must be used.

261. Referring to Fig. 410, calculate $M_{max.}$ and $M_{min.}$ produced at the middle of the first span of the two-span beam by the 24-ton carriage shown in the figure.

Ans. The influence line for bending moment at *mn*, calculated as in Prob. 259, is shown in Fig. 410b. To obtain $M_{max.}$, one of the wheels must be at the cross section *mn*, and we measure the ordinates indicated in the first span. Thus

$$M_{max.} = 12(2.40 + 3.72) = 73.44 \text{ ton-ft.}$$

To obtain $M_{min.}$ the carriage is put on the second span as indicated, and we obtain
$M_{min.} = -12(1.11 + 1.11) = -26.64 \text{ ton-ft.}$
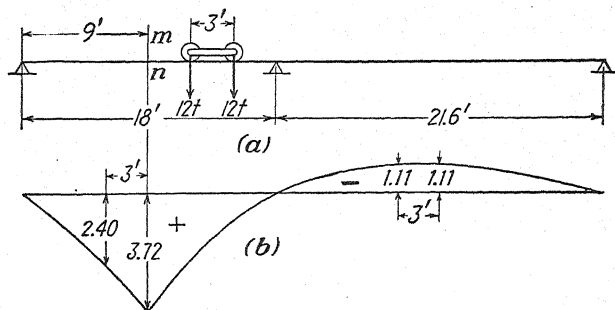
FIG. 410.

60. Simple Bents and Frames.—In the analysis of simple bents and frames like those shown in Fig. 411, the slope-deflection equations, derived in Art. 56, can be used to advantage. Beginning with the case shown in
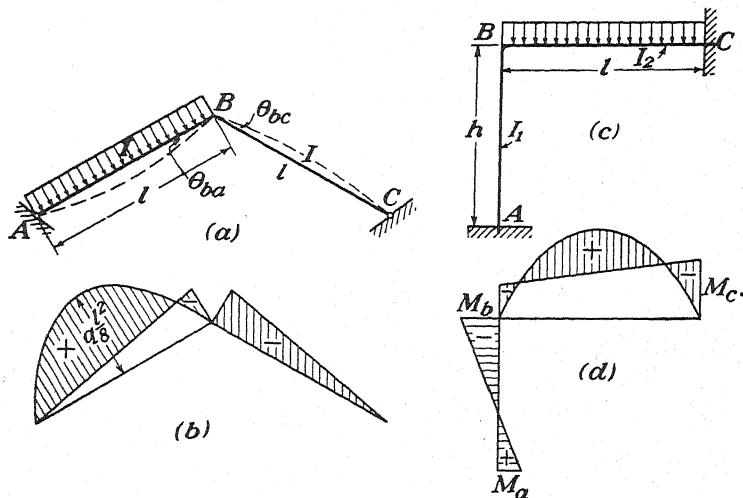
FIG. 411.

Fig. 411a, we see that lateral load acting on the bar AB produces not only bending, as indicated by dotted lines, but also axial compression of the bars. When the bars are sufficiently rigid so that the compressive axial forces are small in comparison with Euler's critical load, the influence of axial forces on bending can be neglected. We can also neglect the corresponding small shortening of the bars and assume as a first approximation that the rigid joint B does not move laterally but only rotates by a certain angle due to bending of the bars. With these assumptions, the bending moment M_b at the joint B will be found from the condition that the angles θ_{ba} and θ_{bc}, indicated in the figure, must be equal in the case of a rigid joint at B. Using Eqs. (45) and assuming that the two bars

are identical, we obtain

$$\theta_{ba} = \frac{M_{ba}l}{3EI} - \frac{ql^3}{24EI},$$

$$\theta_{bc} = \frac{M_{bc}l}{3EI}.$$

Equating these angles and observing, from the equilibrium of joint B, that $M_{ba} = -M_{bc}$, we obtain

$$\frac{2}{3}\frac{M_{bc}l}{EI} = -\frac{ql^3}{24EI}.$$

Since the end moment M_{bc} is identical with the bending moment M_b (see page 335), we find

$$M_b = -\frac{ql^2}{16}.$$

The corresponding bending-moment diagram is shown in Fig. 411b. It should be noted that the equality condition $\theta_{ba} = \theta_{bc}$ is the same as was used in the derivation of the three-moment equation, which suggests the use of this equation in the analysis of frames.   Treating the frame ABC as a two-span continuous beam and using the three-moment equation [Eq. (59)], we obtain directly

$$4M_bl = -\frac{ql^3}{4},$$

which gives the same value for M_b as that calculated above.

Having the magnitude of the bending moment M_b, we can find from statics the axial compressive forces in the bars AB and BC and the corresponding small displacement of the rigid joint B, which was neglected in the first step of our analysis.   Upon introducing the additional angles of rotation of the two bars, due to this displacement, a correction to the previously calculated value of M_b can be found by using Eqs. (47). This correction is usually small and can be disregarded in most practical calculations.

As another example, let us consider the bent shown in Fig. 411c. Again neglecting the axial deformations of the bars, we conclude that the bending-moment diagram will be the same as for a two-span continuous beam with built-in ends.   Using the three-moment equation (57) together with Eq. (58) for the two built-in ends, we obtain

$$2M_a + M_b = 0,$$

$$M_a\frac{h}{I_1} + 2M_b\left(\frac{h}{I_1} + \frac{l}{I_2}\right) + M_c\frac{l}{I_2} = -\frac{ql^3}{4I_2},$$

$$M_b + 2M_c = -\frac{ql^2}{4}.$$

From these equations we find

$$M_b = -\frac{ql^2}{12}\frac{1}{\alpha\gamma+1}, \qquad M_a = -\frac{1}{2}M_b, \qquad M_c = -\frac{1}{2}M_b - \frac{ql^2}{8}, \quad (a)$$

where

$$\alpha = \frac{h}{l}, \qquad \gamma = \frac{I_2}{I_1}.$$

When I_1 is very large in comparison with I_2, the quantity γ becomes very small and the moments M_b and M_c approach the value $-ql^2/12$ as for a beam with fixed ends. For any given values of the ratios α and γ, the values of the moments M_a, M_b, and M_c are readily calculated from expressions (a). The corresponding bending-moment diagram is shown in Fig. 411d.
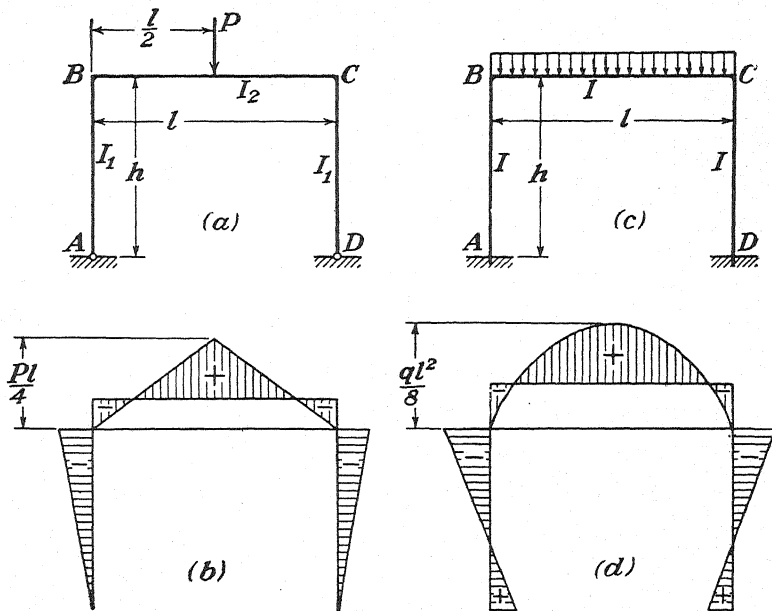
Fig. 412.

In the case of a symmetrical frame loaded as shown in Fig. 412a, there will be no lateral sway, and the three-moment equation can be applied in calculating the bending moments at the rigid joints B and C. Using Eq. (57) and observing from symmetry that $M_b = M_c$, we obtain

$$2M_b\left(\frac{hI_2}{I_1}+l\right) + M_bl = -\frac{3Pl^2}{8}.$$

Using the notations

$$\alpha = \frac{h}{l}, \qquad \frac{I_2}{I_1} = \gamma,$$

we find

$$M_b = M_c = -\frac{3}{8} Pl \cdot \frac{1}{2\alpha\gamma + 3}. \tag{b}$$

The corresponding bending-moment diagram is shown in Fig. 412b.

If the columns are built-in and the load is applied as shown in Fig. 412c, the bending-moment diagram is the same as for a three-span continuous beam with built-in ends and loaded along the middle span. Assuming that the cross section is uniform along the entire length of the frame, the bending moments will be the same as for the continuous beam discussed in Prob. 257 (see page 349). Hence,

$$M_b = M_c = -\frac{ql^2}{8} \cdot \frac{4\alpha^3}{3(1 + 2\alpha)}, \qquad M_a = M_d = -\frac{1}{2} M_b,$$

where $\alpha = l/h$. The corresponding bending-moment diagram is shown in Fig. 412d.

If there is no symmetry, the top of the loaded frame will move laterally and this motion must be considered in calculating the bending moments at the rigid joints. Take, as an example, the case shown in Fig. 413a, where a load P is applied nonsymmetrically. To solve the problem by using the three-moment equation, we assume first that there is a horizontal force H applied as shown and of such magnitude that the lateral sway of the frame is prevented. Then, proceeding as before, the bending moments M_b' and M_c' at the rigid joints B and C are obtained from the following three-moment equations:

$$\left.\begin{array}{l} 2M_b'\left(\dfrac{h}{I_1} + \dfrac{l}{I_2}\right) + M_c'\dfrac{l}{I_2} = -\dfrac{Pe(l^2 - e^2)}{lI_2}, \\[2ex] M_b'\dfrac{l}{I_2} + 2M_c'\left(\dfrac{l}{I_2} + \dfrac{h}{I_1}\right) = -\dfrac{Pe(l - e)(2l - e)}{lI_2}. \end{array}\right\} \tag{c}$$

When the bending moments M_b' and M_c' have been found, the axial forces acting on the horizontal girder BC can be calculated from equations of statics. These forces, assuming positive bending moments M_b' and M_c', are indicated in Fig. 413b. The condition of equilibrium then gives

$$H - \frac{M_b'}{h} + \frac{M_c'}{h} = 0,$$

and the force required to restrain the frame against lateral sway is

$$H = -\frac{M_c' - M_b'}{h}. \tag{d}$$

To find the values M_b and M_c of the bending moments when there is no horizontal restraining force H, we consider the auxiliary problem shown

in Fig. 413c. The required moments will evidently be obtained by super-
posing the solutions for this case and that shown in Fig. 413a. Denoting
by M_b'' and M_c'' the bending moments at B and C for the case in Fig.
413c, we obtain

$$\left. \begin{array}{l} M_b = M_b' + M_b'', \\ M_c = M_c' + M_c''. \end{array} \right\} \tag{e}$$

The bending of the frame in this case is of a very simple nature since,
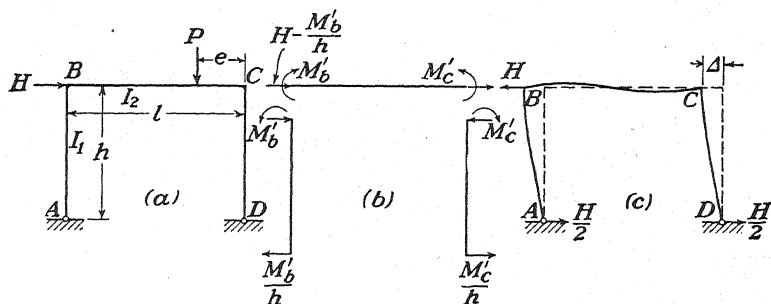
FIG. 413.

from symmetry of the frame, the horizontal reactions of the hinges A
and D must each be equal to $H/2$. Hence,

$$M_b'' = -M_c'' = -\frac{hH}{2}.$$

Substituting for H its value (d), we obtain

$$M_b'' = -M_c'' = \frac{M_c' - M_d'}{2}, \tag{f}$$

and Eqs. (e) give

$$M_b = M_c = \frac{M_b' + M_c'}{2}. \tag{g}$$

The sum of the moments M_b' and M_c' is obtained by adding together
Eqs. (c), which gives

$$M_b' + M_c' = -\frac{3Pe(l - e)}{l\left(3 + 2\dfrac{h}{l}\dfrac{I_2}{I_1}\right)}.$$

Hence the required solution is

$$M_b = M_c = -\frac{3Pe(l - e)}{2l\left(3 + 2\dfrac{h}{l}\dfrac{I_2}{I_1}\right)}. \tag{h}$$

In the foregoing example, we obtained the required solution by super-
posing the solutions of two separate problems as shown in Figs. 413a

and 413c. In the first of these problems the lateral sway was restrained, and in the second only the effect of lateral sway was considered. This same method of analysis will often be used in our further discussions of more complicated frame structures.

PROBLEMS

262. Find the bending moment M_b for the bent shown in Fig. 411c if, in addition to the uniform load, there is a vertical concentrated force P acting on the girder BC at a distance e from the support C.

$$Ans. \quad M_b = \frac{1}{\alpha\gamma + 1}\left[-\frac{ql^2}{12} - \frac{Pe^2(l - e)}{l^2}\right], \text{ where } \alpha = h/l, \ \gamma = I_2/I_1.$$
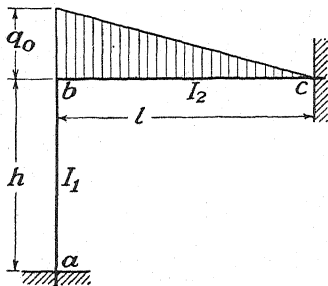
263. Find the bending moment M_b for the bent loaded as shown in Fig. 414.

$$Ans. \quad M_b = -\frac{q_0 l^2}{20(1 + \alpha\gamma)}, \text{where } \alpha = h/l, \gamma = I_2/I_1.$$

264. Find the bending moments M_b and M_c for the frame shown in Fig. 413a if the girder BC is uniformly loaded along the right half of the span and the frame is free to sway.

$$Ans. \quad M_b = M_c = -\frac{ql^2}{8(3 + 2\alpha\gamma)}, \text{ where } \alpha = h/l, \ \gamma = I_2/I_1.$$

FIG. 414.

265. Find the bending moments at A, B, C, and D for the frame shown in Fig. 413a if lateral sway is restrained and the columns are built-in at A and D. *Ans.* With $\alpha = h/l$ and $\gamma = I_2/I_1$, we find

$$M_b = -\frac{2Pe(l - e)[\alpha\gamma(l + e) + 2e]}{l^2(\alpha\gamma + 2)(3\alpha\gamma + 2)},$$

$$M_c = -\frac{2Pe(l - e)[\alpha\gamma(2l - e) + 2(l - e)]}{l^2(\alpha\gamma + 2)(3\alpha\gamma + 2)},$$

$$M_a = -\frac{M_b}{2}, \qquad M_d = -\frac{M_c}{2}.$$

266. Solve the preceding problem if the load is uniformly distributed along the right half of the girder.

HINT: Substitute qde, instead of P, in the answers of the preceding problem, and integrate with respect to e from 0 to $l/2$.

61. Frame Structures with Lateral Restraint.—Such structures as continuous frames, office buildings, and trusses with rigid joints represent highly statically indeterminate systems with many redundant elements. The previously discussed methods of analysis of statically indeterminate systems (see Chap. V) become impractical in such cases since their application results in a system of many linear algebraic equations, the solution of which represents a cumbersome problem. A more satisfactory method of analysis of frame structures can be developed by using the slope-deflection equations (46) and (48) derived in Art. 56.*

* This method was developed by Axel Bendixen; see his book, "Die Methode der Alpha-Gleichungen zur Berechnung von Rahmenkonstruktionen," Berlin, 1914. See

In general, we consider two kinds of frame structures, those which remain rigid if hinges are placed at all joints (see Fig. 411) and those the rigidity of which depends entirely on the rigidity of the joints as in the case shown in Fig. 412. In the first case there can occur only very small displacements of the joints due to changes in the lengths of the members produced by axial forces. In frames of the second kind, displacements of the joints result from bending of the members and can be of considerable magnitudes. Analyzing frame structures, we proceed as in the previous article and, as a first approximation, neglect the changes in length of members produced by axial forces. We assume also that, in the case of frames of the second kind, displacements of the joints are prevented by some special constraints. In this manner we obtain frame structures without lateral sway, the deformation of which is entirely defined by the angles of rotation of the rigid joints. The analysis of such structures will be discussed in this article. The additional stresses that occur in frames of the second kind when we remove the special constraints, mentioned above, will be discussed in Art. 63. The effect of changes in length of members on the magnitude of end moments will be considered in Arts. 67 and 68.

To simplify our writing in using the slope-deflection equations, we introduce the notation

$$\frac{EI_{mn}}{l_{mn}} = k_{mn} \tag{68}$$

and call the quantity k_{mn} the *stiffness factor* of member mn. We also observe that the terms in Eqs. (46), which contain the bending-moment area A as a factor, are the *fixed-end moments* and for them we use the notation introduced in Art. 57. With these notations for any member mn, Eqs. (46) become

$$\left. \begin{array}{l} M_{mn} = 2k_{mn}(2\theta_{mn} + \theta_{nm}) + \mathfrak{M}_{mn}, \\ M_{nm} = 2k_{mn}(2\theta_{nm} + \theta_{mn}) + \mathfrak{M}_{nm}. \end{array} \right\} \tag{69}$$

From these equations the end moments can be calculated if the angles of rotation of the ends and the fixed-end moments are known.

In the particular case where the end n of the member mn is built-in, we have $\theta_{nm} = 0$ and Eqs. (69) become

$$\left. \begin{array}{l} M_{mn} = 4k_{mn}\theta_{mn} + \mathfrak{M}_{mn}, \\ M_{nm} = 2k_{mn}\theta_{mn} + \mathfrak{M}_{nm}. \end{array} \right\} \tag{70}$$

If the end n of the member mn is hinged and no moment is acting on that

---

also the paper by Wilson and Maney in *Univ. Ill. Eng. Expt. Sta.*, *Bull.* 80, 1915. A further development of the method is due to A. Ostenfeld; see his book, "Die Deformationsmethode," Berlin, 1926.

end, we have $M_{nm} = 0$ and the second of Eqs. (69) gives

$$\theta_{nm} = -\frac{1}{2}\theta_{mn} - \frac{1}{4k_{mn}}\mathfrak{M}_{nm}. \tag{71}$$

Substituting this value of θ_{nm} in the first of Eqs. (69), we obtain

$$M_{mn} = 3k_{mn}\theta_{mn} + \mathfrak{M}_{mn} - \tfrac{1}{2}\mathfrak{M}_{nm}. \tag{72}$$

This equation, instead of the first of Eqs. (69), must be used if the end n of the member mn is free to rotate.

By putting $\theta_{mn} = 0$ in Eq. (72), we obtain a member fixed at m and hinged at n. The last two terms together in Eq. (72) therefore represent the end moment at the fixed end m of such a member.
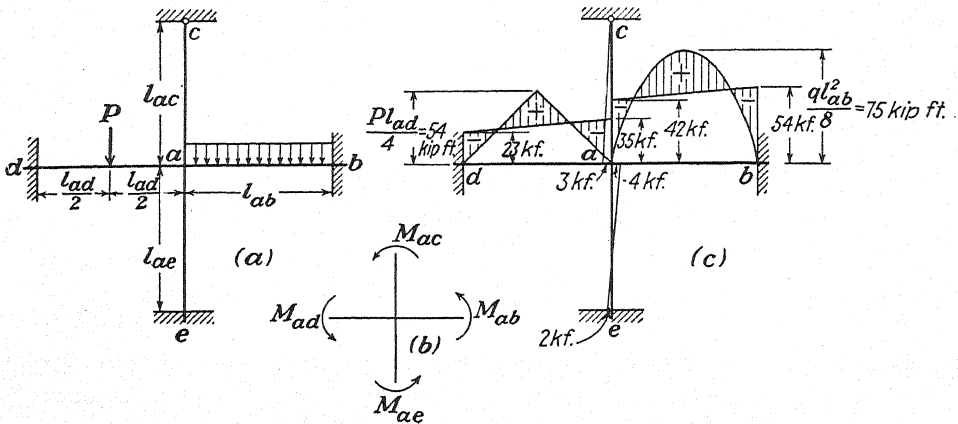
Fig. 415.

The application of the derived equations will now be explained on the example shown in Fig. 415a. Observing that at each built-in end we have three unknown reactive elements (two components of reactive force and an end moment) and that at a hinged end, like the support c, we have two unknowns, we can conclude that the structure in Fig. 415a has eight redundant elements. If we disregard the axial forces in the members of the structure, the number of statically indeterminate quantities reduces to six. We can take, for example, the end moments acting on the members ad, ab, and ae as redundant quantities and use for their determination one of the methods discussed in Chap. V, for example, the principle of least work. But the solution of the problem can be greatly simplified by the use of Eqs. (70) and (72).

Observing that the angles of rotation at the fixed ends b, e, and d vanish and that rotation at c is entirely free, we conclude that the end moments of all members of the structure can be readily calculated from

Eqs. (70) and (72) if only we know the angle of rotation θ_a of the rigid joint a.   To determine this quantity, we need only one equation, and this equation can be derived from the condition of equilibrium of the joint a. Considering the actions of the members of the structure on the joint a, we obtain the system of moments shown in Fig. 415b.*   All these moments are evidently equal and opposite to the corresponding end moments of the bent members of the structure; and, from equilibrium of the joint a, we obtain

$$M_{ab} + M_{ac} + M_{ad} + M_{ae} = 0. \tag{a}$$

Now applying the first of Eqs. (70) and using for the fixed-end moments the known values[1]

$$\mathfrak{M}_{ab} = -\frac{ql_{ab}^2}{12}, \qquad \mathfrak{M}_{ad} = \frac{Pl_{ad}}{8}, \qquad \mathfrak{M}_{ac} = \mathfrak{M}_{ae} = 0, \tag{b}$$

we obtain

$$\left.\begin{aligned}
M_{ab} &= 4k_{ab}\theta_a - \frac{ql_{ab}^2}{12}, \\
M_{ad} &= 4k_{ad}\theta_a + \frac{Pl_{ad}}{8}, \\
M_{ae} &= 4k_{ae}\theta_a,
\end{aligned}\right\} \tag{c}$$

and, from Eq. (72),

$$M_{ac} = 3k_{ac}\theta_a. \tag{d}$$

Substituting the end moments (c) and (d) in the equation of equilibrium (a), we obtain

$$\theta_a(4k_{ab} + 4k_{ad} + 4k_{ae} + 3k_{ac}) = \frac{ql_{ab}^2}{12} - \frac{Pl_{ad}}{8},$$

from which

$$\theta_a = \frac{(ql_{ab}^2/12) - (Pl_{ad}/8)}{4(k_{ab} + k_{ad} + k_{ae}) + 3k_{ac}}. \tag{e}$$

Substituting this value of θ_a in Eqs. (c) and (d), we obtain

$$\left.\begin{aligned}
M_{ab} &= -\frac{ql_{ab}^2}{12} + r_{ab}\left(\frac{ql_{ab}^2}{12} - \frac{Pl_{ad}}{8}\right), \\
M_{ad} &= \frac{Pl_{ad}}{8} + r_{ad}\left(\frac{ql_{ab}^2}{12} - \frac{Pl_{ad}}{8}\right), \\
M_{ae} &= r_{ae}\left(\frac{ql_{ab}^2}{12} - \frac{Pl_{ad}}{8}\right), \\
M_{ac} &= r_{ac}\left(\frac{ql_{ab}^2}{12} - \frac{Pl_{ad}}{8}\right),
\end{aligned}\right\} \tag{f}$$

* There are also shearing forces transmitted to the joint a.   These forces will be in equilibrium with the axial forces of the members and will not enter into the equation for calculating θ_a.

[1] Observe that end moments and angles of rotation are taken positive if they are clockwise in direction (see p. 335).

where

$$r_{ab} = \frac{k_{ab}}{k_{ab} + k_{ad} + k_{ae} + \frac{3}{4}k_{ac}}, \qquad r_{ad} = \frac{k_{ad}}{k_{ab} + k_{ad} + k_{ae} + \frac{3}{4}k_{ac}},$$
$$r_{ae} = \frac{k_{ae}}{k_{ab} + k_{ad} + k_{ae} + \frac{3}{4}k_{ac}}, \qquad r_{ac} = \frac{\frac{3}{4}k_{ac}}{k_{ab} + k_{ad} + k_{ae} + \frac{3}{4}k_{ac}}. \tag{73}$$

The expression in parentheses on the right side of Eqs. (*f*) is the algebraic sum of moments acting on the joint *a*, calculated on the assumption that this joint does not rotate. This sum, equal to the sum of the fixed end moments of all members meeting at *a*, but with opposite sign, is called the *unbalanced moment* at joint *a* and will be denoted by $\mathbf{M}_a$. It is seen from Eqs. (*f*) that, owing to rotation of joint *a*, the unbalanced moment *distributes* between the members in proportion to their stiffness factors. In the case of a member the far end of which is hinged, only three-quarters of the stiffness factor must be used. The factors (73) by which the unbalanced moment is multiplied in Eqs. (*f*) are called *distribution factors*. We see that their magnitudes are independent of the loading and can be readily calculated if the dimensions of the members are known. It is also seen that in this calculation only the ratios of the stiffness factors *k* enter. Hence we can use, instead of the actual values of these factors, some numbers proportional to them.

With the introduced notions of *unbalanced moment* and *distribution factors* we can recapitulate the solution of the problem in Fig. 415, in a more condensed form, and give it a physical interpretation that will be useful in our further discussion. We start the problem with the assumption that joint *a* does not rotate, *i.e.*, is *locked* by some constraint, and calculate all fixed-end moments. The sum of these moments at joint *a* is the moment with which the constraint is acting on the joint to prevent its rotation. *Unlocking* the joint is equivalent to the application of the *unbalanced moment*, which is equal and opposite to the moment of the constraint. This unbalanced moment is distributed among the members meeting at joint *a* in proportion to their *distribution factors*. The final end moments at joint *a* are then obtained by superimposing the *distributed moments* on the previously calculated *fixed-end moments*, as shown by Eqs. (*f*).

Returning to our example in Fig. 415, let us assume that $k_{ab} = k_{ad}$ and $k_{ac} = k_{ae} = \frac{1}{2}k_{ab}$; we assume also that

$$\frac{ql_{ab}^2}{12} = 50 \text{ kip-ft.}, \qquad \frac{Pl_{ad}}{8} = 27 \text{ kip-ft.}$$

Then the unbalanced moment at joint *a* is

$$\mathbf{M}_a = \frac{ql_{ab}^2}{12} - \frac{Pl_{ad}}{8} = 50 \text{ kip-ft.} - 27 \text{ kip-ft.} = 23 \text{ kip-ft.}$$

The distribution factors are obtained from Eqs. (73), which give

$$r_{ab} = r_{ad} = \tfrac{8}{23}, \qquad r_{ac} = \tfrac{3}{23}, \qquad r_{ae} = \tfrac{4}{23}.$$

The distributed moments then are

$$r_{ab}\mathbf{M}_a = 8 \text{ kip-ft.}, \qquad r_{ad}\mathbf{M}_a = 8 \text{ kip-ft.},$$
$$r_{ac}\mathbf{M}_a = 3 \text{ kip-ft.}, \qquad r_{ae}\mathbf{M}_a = 4 \text{ kip-ft.}$$

Superposing these moments on the fixed-end moments, we obtain the final values of end moments at joint a as follows:

$$M_{ab} = -50 + 8 = -42 \text{ kip-ft.}, \qquad M_{ad} = 27 + 8 = 35 \text{ kip-ft.},$$
$$M_{ac} = 3 \text{ kip-ft.}, \qquad M_{ae} = 4 \text{ kip-ft.}$$

For the end moments at the far ends of the members meeting at a, we use the second of Eqs. (70), which states that the end moments there are obtained by superposing on the fixed-end moments the *carry-over moments* (see page 340) each equal to half the corresponding distributed moment. In this way we obtain

$$M_{ba} = 50 + 4 = 54 \text{ kip-ft.}, \qquad M_{da} = -27 + 4 = -23 \text{ kip-ft.},$$
$$M_{ea} = 2 \text{ kip-ft.}$$

The corresponding bending-moment diagrams are shown in Fig. 415c.

Let us consider, now, a more general case and assume that joint a, the angle of rotation of which we are calculating, is attached by several bars to other portions of an elastic structure as shown in Fig. 416. We begin the solution with a calculation of the end moments at joint a. With notations θ_a, θ_b, θ_c, . . . for the angles of rotation of joints a, b, c, . . . , respectively, Eqs. (69)* give
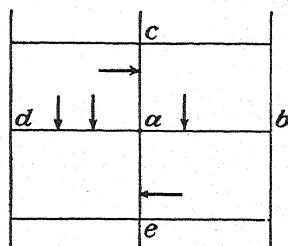
FIG. 416.

$$\left. \begin{aligned} M_{ab} &= +2k_{ab}(2\theta_a + \theta_b) + \mathfrak{M}_{ab}, \\ M_{ac} &= +2k_{ac}(2\theta_a + \theta_c) + \mathfrak{M}_{ac}, \\ M_{ad} &= +2k_{ad}(2\theta_a + \theta_d) + \mathfrak{M}_{ad}, \\ M_{ae} &= +2k_{ae}(2\theta_a + \theta_e) + \mathfrak{M}_{ae}. \end{aligned} \right\} \qquad (g)$$

Adding these equations together and observing that the sum of all end moments at joint a must vanish, we obtain

$$4(k_{ab} + k_{ac} + k_{ad} + k_{ae})\theta_a + 2k_{ab}\theta_b + 2k_{ac}\theta_c + 2k_{ad}\theta_d + 2k_{ae}\theta_e = \mathbf{M}_a$$

$$(74)$$

where $\mathbf{M}_a = -(\mathfrak{M}_{ab} + \mathfrak{M}_{ac} + \mathfrak{M}_{ad} + \mathfrak{M}_{ae})$ is the unbalanced moment

* It is assumed as before that any lateral sway of the structure is prevented by certain constraints.

at joint a.   A similar equation can be written for each joint of a structure, and we shall obtain as many equations as there are unknown angles of rotation.   Upon solving them for these angles and using the angles in Eqs. (69), all end moments can be calculated and bending-moment diagrams drawn.

If one of the bars jointed at a, say the bar ab, is built-in at the other end, we have only to substitute $\theta_b = 0$ in Eq. (74).   If a bar, say the bar ae, is hinged at the end e, we use Eq. (71), which gives

$$\theta_e = -\frac{\theta_a}{2} - \frac{1}{4k_{ae}}\,\mathfrak{M}_{ea}. \qquad (h)$$

This value of θ_e must be substituted into Eq. (74) if the bar ae is hinged at e.   In this manner we obtain

$$4(k_{ab} + k_{ac} + k_{ad} + \tfrac{3}{4}k_{ae})\theta_a + 2k_{ab}\theta_b + 2k_{ac}\theta_c + 2k_{ad}\theta_d = \mathbf{M}_a, \qquad (75)$$

where

$$\mathbf{M}_a = -(\mathfrak{M}_{ab} + \mathfrak{M}_{ac} + \mathfrak{M}_{ad} + \mathfrak{M}_{ae} - \tfrac{1}{2}\mathfrak{M}_{ea}).$$

The last two terms in parentheses on the right side of this equation represent, as we see from Eq. (72), the end moment at the end a of the bar ae assumed fixed at a and hinged at e. $\mathbf{M}_a$ is then again, following our terminology, the unbalanced moment, and Eq. (75) differs from Eq. (74) only in that $\tfrac{3}{4}k_{ae}$, instead of k_{ae}, is used on the left side.

If there is an external moment applied at joint a, this moment must be added with proper sign[1] to the unbalanced moment at joint a.
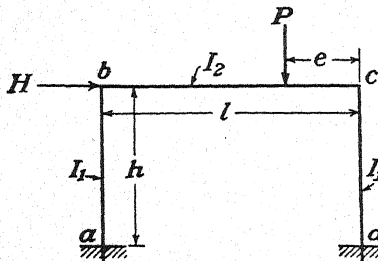
Equations (74) and (75) were derived on the assumption that there are four members jointed at a, but evidently it can be readily extended to any number of bars.

As a first application of the derived equation, let us find the end moments for the members of the frame in Fig.

Fig. 417.

417 if lateral movement is prevented by a horizontal force H.   Applying Eqs. (74) to joints b and c of the frame and observing that only the member bc is laterally loaded, we obtain

$$4(k_{ab} + k_{bc})\theta_b + 2k_{bc}\theta_c = -\mathfrak{M}_{bc},$$
$$4(k_{bc} + k_{cd})\theta_c + 2k_{bc}\theta_b = -\mathfrak{M}_{cb}.$$

From these equations, we find

[1] It is taken positive if acting clockwise.

$$\left.\begin{aligned}
\theta_b &= \frac{-2(k_{bc} + k_{cd})\mathfrak{M}_{bc} + k_{bc}\mathfrak{M}_{cb}}{8(k_{ab} + k_{bc})(k_{bc} + k_{cd}) - 2k_{bc}{}^2}, \\
\theta_c &= \frac{-2(k_{ab} + k_{bc})\mathfrak{M}_{cb} + k_{bc}\mathfrak{M}_{bc}}{8(k_{ab} + k_{bc})(k_{bc} + k_{cd}) - 2k_{bc}{}^2}.
\end{aligned}\right\} \tag{i}$$

In the case of a single concentrated load P (Fig. 417) we have (see page 342).

$$\mathfrak{M}_{bc} = -\frac{Pe^2(l - e)}{l^2}, \qquad \mathfrak{M}_{cb} = \frac{Pe(l - e)^2}{l^2}.$$

Using the notation

$$\frac{k_{bc}}{k_{ab}} = \frac{k_{bc}}{k_{cd}} = \frac{h}{l}\frac{I_2}{I_1} = \alpha\gamma,$$

expressions (i), substituted into Eqs. (70), give

$$M_{ba} = 4k_{ab}\theta_b = \frac{2Pe(l - e)[\alpha\gamma(l + e) + 2e]}{l^2(\alpha\gamma + 2)(3\alpha\gamma + 2)},$$

$$M_{cd} = 4k_{ab}\theta_c = -\frac{2Pe(l - e)[\alpha\gamma(2l - e) + 2(l - e)]}{l^2(\alpha\gamma + 2)(3\alpha\gamma + 2)},$$

$$M_{ab} = \tfrac{1}{2}M_{ba}, \qquad M_{dc} = \tfrac{1}{2}M_{cd}.$$

From these expressions we obtain the values of the bending moments already given in problem 265.
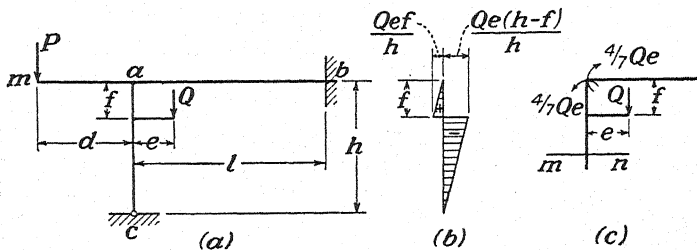
FIG. 418.

As a second example, let us consider the frame shown in Fig. 418a. The action of the load P on the overhang we replace by the axial force P acting on the column and by the external moment $-Pd$ applied at the joint. a. Then, using Eq. (75), we obtain

$$4\theta_a(k_{ab} + \tfrac{3}{4}k_{ac}) = -\mathfrak{M}_{ac} + \tfrac{1}{2}\mathfrak{M}_{ca} - Pd, \tag{j}$$

$$\theta_a = \frac{-\mathfrak{M}_{ac} + \tfrac{1}{2}\mathfrak{M}_{ca} - Pd}{4k_{ab} + 3k_{ac}}.$$

The required end moments, from Eqs. (70) and (72), are

$$M_{ab} = \frac{4k_{ab}}{4k_{ab} + 3k_{ac}} \cdot \left(-\mathfrak{M}_{ac} + \frac{1}{2}\mathfrak{M}_{ca} - Pd\right), \tag{k}$$

$$M_{ba} = \tfrac{1}{2}M_{ab},$$

$$M_{ac} = \mathfrak{M}_{ac} - \frac{1}{2}\,\mathfrak{M}_{ca} + \frac{3k_{ac}}{4k_{ab} + 3k_{ac}}\left(-\mathfrak{M}_{ac} + \frac{1}{2}\,\mathfrak{M}_{ca} - Pd\right). \qquad (l)$$

We have now to calculate and to substitute into expressions (k) and (l) the fixed-end moments $\mathfrak{M}_{ac}$ and $\mathfrak{M}_{ca}$. Considering the column ac as a simply supported beam, the bending-moment diagram is as shown in Fig. 418b.[*] Applying Eqs. (53) to each of the two triangles forming the bending-moment area, we obtain[1]

$$\mathfrak{M}_{ca} = \frac{Qef(2h - 3f)}{h^2}, \qquad \mathfrak{M}_{ac} = \frac{Qe(h - f)(3f - h)}{h^2}.$$

Upon substituting these values of the fixed-end moments into Eqs. (k) and (l), the required end moments can be readily calculated for any value of the ratio f/h. Assume, for example, that $h = l = 16$ ft., $f = 6$ ft. and that the cross sections of the column and of the girder are identical. In such a case $f/h = \frac{3}{8}$, $k_{ab} = k_{ac}$, and we obtain

$$\mathfrak{M}_{ca} = \tfrac{21}{64}Qe, \qquad \mathfrak{M}_{ac} = \tfrac{5}{64}Qe,$$
$$M_{ab} = \tfrac{4}{7}(\tfrac{11}{128}Qe - Pd), \qquad M_{ac} = -\tfrac{11}{128}Qe + \tfrac{3}{7}(\tfrac{11}{128}Qe - Pd).$$

In the particular case in which f becomes infinitesimal the same calculations as above give

$$\mathfrak{M}_{ca} = 0, \qquad \mathfrak{M}_{ac} = -Qe,$$
$$M_{ab} = \tfrac{4}{7}(Qe - Pd), \qquad M_{ac} = -Qe + \tfrac{3}{7}(Qe - Pd). \qquad (m)$$

It is seen that the external moment $-Pd$ is divided in such a manner that $\frac{4}{7}$ of it is transmitted to the girder and $\frac{3}{7}$ to the column, while the moment Qe, which also is acting on the joint a, since $f = 0$, is distributed in a different way. To explain the cause of this discrepancy, we assume that f is not zero but very small. Then the bending moment at joint a produced by the moment Qe is $4Qe/7$ (Fig. 418c), and the end moment M_{ac} is equal to $-4Qe/7$, as given by Eq. (m). When we are considering the moment Qe as an external moment applied at joint a, we must take a cross section mn very close to joint a but below the cross section in which the moment Qe is applied. The moment acting on the cross section mn is equal to $-4Qe/7 + Qe = 3Qe/7$ as it should be in the case of an external moment Qe.

PROBLEMS

267. Make bending-moment diagrams for the girder and column in Fig. 418a if $P = Q = 6{,}000$ lb., $d = 4$ ft., $e = 2$ ft., $l = h = 16$ ft., $f = 6$ ft.

268. Draw a bending-moment diagram for the frame in Fig. 418a if a uniform load q is distributed along the beam mab.

269. Draw a bending-moment diagram for the uniformly loaded continuous beam bac, with built-in ends and rigidly connected at a to the column ad (Fig. 419a). Assume $q = 1{,}000$ lb. per ft., $k_{ac} = k_{ad} = 0.8k_{ab}$.

        Ans. The bending moments in kip-feet are shown in Fig. 419b.

---

[*] In determining the signs in this diagram we assumed that bar ac is made horizontal by rotating clockwise and then used the conventional rule.

[1] Notations shown in Fig. 418 are used in these formulas.
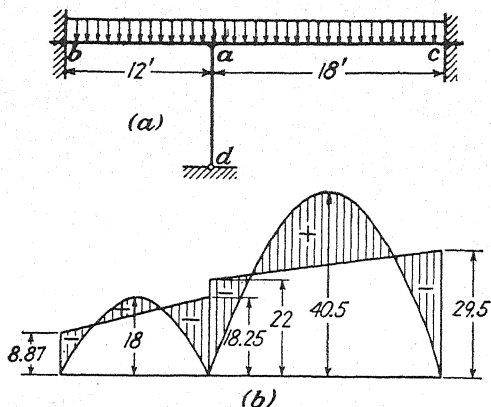
FIG. 419.

62. Calculation of Axial Forces in Members of a Frame.—In the discussion of the previous article, we assumed that the lateral movements of frames are restrained. We also neglected the changes in length of members of a frame due to axial forces. With these assumptions the deformation of a frame is completely defined by the angles of rotation of its rigid joints. These angles can be calculated in each particular case by using Eqs. (74) or (75), and after this all end moments can be found
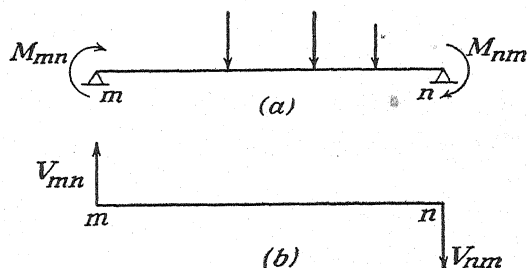
FIG. 420.

from Eqs. (69). The axial forces in the members of a frame and the forces of constraint preventing lateral movements do not enter in these calculations. For their determination, shearing forces acting at the ends of the members of a frame must be considered. Let a bar with simply supported ends (Fig. 420a) be acted upon by lateral loads and end moments. Considering shearing forces positive when they have the directions shown in Fig. 420b, and using equations of statics, we obtain

$$\left. \begin{aligned} V_{mn} &= V_{mn}' - \frac{M_{mn} + M_{nm}}{l_{mn}}, \\ V_{nm} &= V_{nm}' - \frac{M_{mn} + M_{nm}}{l_{mn}}. \end{aligned} \right\} \qquad (76)$$

The symbols V_{mn}' and V_{nm}' in these equations denote the shearing forces at the ends produced by lateral loading. Equations (76) can be applied to each member of a frame. Assuming that the end moments are already calculated, as explained before, the shearing forces at the ends of each member will be found from these equations. The forces equal and opposite to these shearing forces represent the shear actions of the bent members of a frame on its joints. Considering these actions as external forces applied at the joints, we can calculate the axial forces in all members and also the forces restraining lateral movements of a frame.

Let us consider, as an example, the frame in Fig. 421a. In this case,

$$k_{ab} = k_{cd} = \frac{EI_1}{h}, \qquad k_{bc} = \frac{EI_2}{l}.$$

Assuming that

$$\frac{k_{bc}}{k_{ab}} = m,$$

we obtain for the end moments the following values (see page 369):

$$M_{ba} = \frac{2Pe(l - e)[m(l + e) + 2e]}{l^2(m + 2)(3m + 2)},$$

$$M_{cd} = -\frac{2Pe(l - e)[m(2l - e) + 2(l - e)]}{l^2(m + 2)(3m + 2)},$$

$$M_{ab} = \tfrac{1}{2}M_{ba}, \qquad M_{dc} = \tfrac{1}{2}M_{cd}.$$

Substituting these values of the end moments into Eqs. (76), we obtain shearing forces in all members for any values of m and e. Assume, for example, that $I_1 = I_2$, $h = l$, $e = 0.3l$. Then,

$$M_{ba} = -M_{bc} = 0.0532Pl, \qquad M_{cd} = -M_{cb} = -0.0868Pl,$$
$$M_{ab} = 0.0266Pl, \qquad M_{dc} = -0.0434Pl.$$

Substituting these values into Eqs. (76), we obtain

$$V_{ab} = V_{ba} = -0.0798P, \qquad V_{bc} = 0.3P - 0.0336P,$$
$$V_{cb} = -0.7P - 0.0336P, \qquad V_{cd} = V_{dc} = 0.1302P.$$
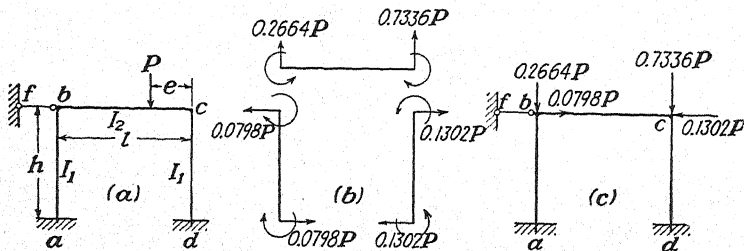
Fig. 421.

The actual directions of the end moments and of the shearing forces are shown in Fig. 421b. To obtain the shear actions on the joints b and c

we have to reverse the directions of the forces shown in Fig. 421*b*. In this manner we obtain the forces shown in Fig. 421*c*. From this figure we conclude that all bars are under compression. The compressive force in the girder *bc* is 0.1302*P*. The compressive forces in the columns *ab* and *cd* are 0.2664*P* and 0.7336*P*, respectively. Finally, the compressive force in the bar *bf*, preventing any lateral movement of the frame, is 0.0504*P*.

In the case shown in Fig. 415, assuming the length of all bars equal to 24 ft. and using the values of the end moments given in the preceding article, we find that on joint *a* there acts a vertical force of 17 kip and a horizontal force of $\frac{1}{8}$ kip as shown in Fig. 422. It is seen that the calculation of axial forces in this case represents a statically indeterminate problem. The magnitudes of these forces depend on the ratios of the cross-sectional areas. Assuming, for example, the cross sections of the vertical bars equal, we conclude that the vertical force of 17 kip will be equally divided between the two vertical bars and we shall have a tensile force of $\frac{17}{2}$ kip in the bar *ac* and a compressive force of $\frac{17}{2}$ kip in the bar *ae*. The horizontal bars *ad* and *ab* can be treated

FIG. 422.

similarly. From the two examples considered, it is seen that the axial forces in the bars can be calculated without any difficulty provided that the end moments are known.
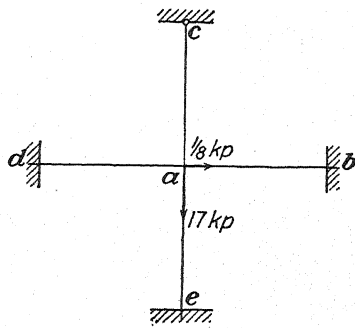
63. Frames without Lateral Restraint.—In the discussion of the two preceding articles, it was assumed that any lateral movement of a frame under consideration was restrained. If there is no such restraint, some lateral movement of the frame will usually occur under the action of external forces and must be considered in the calculation of end moments and axial forces. In discussing such cases, it is advantageous to divide the analysis into two steps. First, we calculate the end moments and shear actions on the joints, assuming lateral constraints. Then we remove the lateral constraints and consider the effect of lateral movements alone. The true values of the lateral movements are found from the condition that the shear actions on the joints due to these movements must balance the previously calculated shear actions produced by external loads in conjunction with lateral restraint.

In calculating end moments produced by lateral movements alone, we use Eqs. (48), which in the absence of lateral loads and with notation (68) become

$$\left. \begin{aligned} M_{mn} &= 2k_{mn}(2\theta_{mn} + \theta_{nm}) - 6k_{mn}\Theta_{mn}, \\ M_{nm} &= 2k_{mn}(2\theta_{nm} + \theta_{mn}) - 6k_{mn}\Theta_{mn}. \end{aligned} \right\} \tag{77}$$

It is seen that the end moments M_{mn} and M_{nm} can be readily calculated if the angles of rotation of the ends θ_{mn}, θ_{nm} and also the angle Θ_{mn}, determined by the amount of lateral movement, are known. Equations (77) have the same form as Eqs. (69), which were previously used, and we can state that the end moments produced by lateral movements alone can be calculated in the same manner as in the case of frames with lateral constraints. It is necessary only to replace the fixed-end moments $\mathfrak{M}_{mn}$, $\mathfrak{M}_{nm}$ by the quantity $-6k_{mn}\Theta_{mn}$.

In a particular case where the end n of a member mn is hinged, we have $M_{nm} = 0$, and the second of Eqs. (77) gives

$$\theta_{nm} = -\frac{\theta_{mn}}{2} + \frac{3}{2}\Theta_{mn}. \tag{78}$$

Substituting this in the first of Eqs. (77), we obtain

$$M_{mn} = 3k_{mn}\theta_{mn} - 3k_{mn}\Theta_{mn}. \tag{79}$$

We shall now apply the derived equations to the case shown in Fig. 423. The end moments and the shear forces in this frame, when it is laterally restrained, have already been calculated in the preceding article (Fig. 421), and we consider now only the moments and forces produced by the lateral movement Δ as shown in Fig. 423a. From symmetry of the frame we conclude that $\theta_b = \theta_c$. We also have $\theta_a = \theta_d = 0$, $\Theta_{ab} = -\Delta/h$. Hence, there is only one unknown, the angle of rotation θ_b, and for its determination we need one equation, which is the equation of equilibrium of joint b,

$$M_{bc} + M_{ba} = 0. \tag{a}$$

Substituting for the end moments their expressions through the angles of rotation [Eqs. (77)],

$$4\theta_b(k_{ab} + k_{bc}) + 2k_{bc}\theta_b = 6k_{ab}\Theta_{ab}. \tag{b}$$

From this equation the angle θ_b for any magnitude of the lateral displacement Δ can be calculated. Taking the numerical example of the preceding article (Fig. 421) and putting $h = l$, $I_1 = I_2$, we have $k_{bc} = k_{ab}$, and Eq. (b) gives

$$\theta_b = \tfrac{3}{5}\Theta_{ab}.$$

The corresponding end moments are now calculated from Eqs. (77), which give

$$\left.\begin{aligned}
M_{ab} = M_{dc} &= 2k_{ab}\theta_b - 6k_{ab}\Theta_{ab} = -\tfrac{24}{5}k_{ab}\Theta_{ab}, \\
M_{ba} = M_{cd} &= 4k_{ab}\theta_b - 6k_{ab}\Theta_{ab} = -\tfrac{18}{5}k_{ab}\Theta_{ab}, \\
M_{bc} = M_{cb} &= 6k_{ab}\theta_b = \tfrac{18}{5}k_{ab}\Theta_{ab}.
\end{aligned}\right\} \tag{c}$$

The shearing forces at the ends of the members of the frame are now

obtained from Eqs. (76), which give

$$V_{ab} = V_{ba} = \frac{42}{5} \frac{k_{ab}\Theta_{ab}}{l},$$

$$V_{bc} = V_{cb} = -\frac{36}{5} \frac{k_{ab}\Theta_{ab}}{l}.$$

Noting the rule of signs for shearing forces (Fig. 420) we conclude that for positive Θ_{ab}, that is, for clockwise rotation, the horizontal shear action at b is as shown in Fig. 423b.   For the negative value of Θ_{ab}, assumed in Fig. 423a, the shearing force V_{ba}, equal to V_{cd}, is negative, and the corresponding horizontal shear action on the girder bc will be as shown in
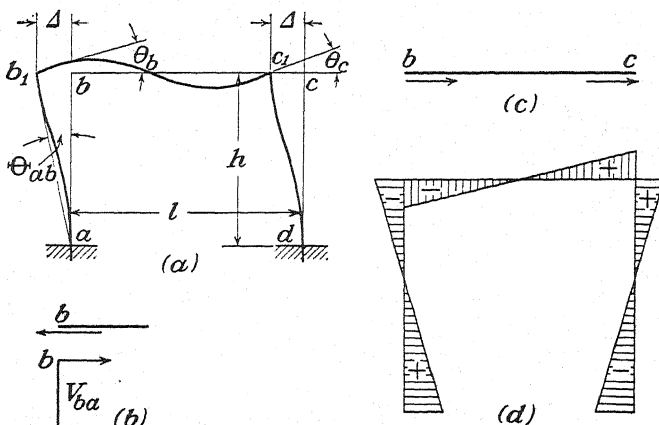
FIG. 423.

Fig. 423c.   The magnitude of the lateral movement of the frame will now be found from the condition that the horizontal forces indicated in Fig. 423c must balance the horizontal forces shown in Fig. 421c.   In our previous discussion these forces were balanced by the force in the restraining bar bf (Fig. 421c).   In the present case there is no such bar, and the frame moves laterally (Fig. 423a) far enough for the corresponding shear actions to become sufficient to establish the required equilibrium.   The equation of equilibrium then is

$$2 \cdot \frac{42}{5} \cdot \frac{k_{ab}\Theta_{ab}}{l} + 0.1302P - 0.0798P = 0,$$

and we obtain

$$\Theta_{ab} = -\frac{5}{84} \frac{l}{k_{ab}} \cdot 0.0504P.$$

The corresponding end moments, from Eqs. (c), are

$$M_{ab} = M_{dc} = \tfrac{2}{7}l \cdot 0.0504P,$$
$$M_{ba} = M_{cd} = \tfrac{3}{14}l \cdot 0.0504P.$$

Having these moments, we can construct the bending-moment diagram shown in Fig. 423d. These moments must be superimposed on the moments found for the laterally restrained frame in Fig. 421a. The result of this superposition gives the bending moments for the frame without lateral restraint.

In the previous discussion, the symbol Θ_{ab} was used to define the rotation due to lateral movement. In a numerical calculation of the lateral movement of a given frame it is often advantageous to assume at the beginning a certain numerical value for this movement, say 1 in., and calculate the corresponding values of the end moments and shear actions on the joints. Naturally, these shear actions will not balance the shear actions calculated for the laterally restrained frame. But, since the shear actions on the joints are proportional to the assumed value of the lateral displacement, it is easy to find in each particular case a numerical factor x by which the assumed lateral displacement must be multiplied in order to ascertain the required equilibrium of the frame.

To show this method of calculation, let us consider the nonsymmetrical frame shown in Fig. 424a and calculate the end moments, assuming that the frame is free to move laterally. The problem will be solved again in two steps. First we calculate the end moments and shear forces for each member of the frame assuming that no lateral movement is allowed. Then we separately investigate the moments and the shear forces produced by an assumed lateral movement alone. The true magnitude of the lateral movement will be finally adjusted so as to satisfy the equilibrium requirement.

Considering the frame with lateral restraint and using Eqs. (74) and (75), we obtain for joints b and c the following two equations:

$$\left.\begin{array}{l} 4(k_{ab} + k_{bc})\theta_b + 2k_{bc}\theta_c = -\mathfrak{M}_{ba} - \mathfrak{M}_{bc}, \\ 4(k_{bc} + \tfrac{3}{4}k_{cd})\theta_c + 2k_{bc}\theta_b = -\mathfrak{M}_{cb} - \mathfrak{M}_{cd} + \tfrac{1}{2}\mathfrak{M}_{dc}. \end{array}\right\} \quad (d)$$

Let us assume that the cross sections of all three members of the frame are identical and that their lengths and lateral loads are as shown in the figure. Then

$$k_{bc} = k_{ab}, \qquad k_{cd} = 2k_{ab}, \qquad \mathfrak{M}_{ab} = -192 \cdot 10^2 \text{ ft.-lb.,}$$
$$\mathfrak{M}_{ba} = 288 \cdot 10^2 \text{ ft.-lb.,} \qquad \mathfrak{M}_{bc} = -576 \cdot 10^2 \text{ ft.-lb.,}$$
$$\mathfrak{M}_{cb} = 384 \cdot 10^2 \text{ ft.-lb.,} \qquad \mathfrak{M}_{cd} = \mathfrak{M}_{dc} = 0.$$

Thus, Eqs. (d) give

$$\left.\begin{array}{l} 4\theta_b + \theta_c = \dfrac{288 \cdot 10^2}{2k_{ab}}, \\[2mm] \theta_b + 5\theta_c = -\dfrac{384 \cdot 10^2}{2k_{ab}}, \end{array}\right\} \quad (e)$$

and we obtain

$$\theta_b = -\theta_c = \frac{96 \cdot 10^2}{2k_{ab}}.$$

Denoting by M_{ab}', M_{ba}', ... the end moments if there is no lateral movement and using Eqs. (69), we obtain

$$\left.\begin{aligned}
M_{ab}' &= \mathfrak{M}_{ab} + 2k_{ab}\theta_b = -96 \cdot 10^2 \text{ ft.-lb.,} \\
M_{ba}' &= -M_{bc}' = \mathfrak{M}_{ba} + 4k_{ab}\theta_b = 480 \cdot 10^2 \text{ ft.-lb.,} \\
M_{cb}' &= -M_{cd}' = \mathfrak{M}_{cb} - 2k_{ab}\theta_b = 288 \cdot 10^2 \text{ ft.-lb.}
\end{aligned}\right\} \qquad (f)$$

Using these values of the end moments, we calculate from Eqs. (76) the shear forces in the columns and the horizontal shear actions on the joints b and c as shown in Fig. 424b.

$P = 20 \times 10^3$ lb.

$Q = 10 \times 10^3$ lb.

(a)

7920 lb. b c 2880 lb.

(b)

b c
$\dfrac{0.0458}{l_{ab}} k_{ab}$ (c) $\dfrac{0.0269}{l_{cd}} k_{ab}$
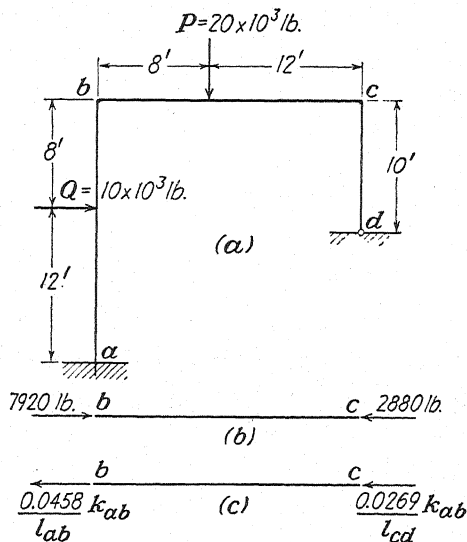
Fig. 424.

Now remove the lateral restraint and assume that the girder bc moves to the right by an amount $\Delta = 0.1$ ft. Then

$$\Theta_{ab} = \tfrac{1}{200}, \qquad \Theta_{bc} = 0, \qquad \Theta_{cd} = \tfrac{1}{100}. \qquad (g)$$

Equations for calculating the corresponding values of θ_b and θ_c are obtained from Eqs. (d) by substituting $-6k_{ab}\Theta_{ab}$ for $\mathfrak{M}_{ba}$, $-6k_{cd}\Theta_{cd}$ for $\mathfrak{M}_{cd}$ and $\mathfrak{M}_{dc}$, and zero for $\mathfrak{M}_{bc}$ and $\mathfrak{M}_{cb}$, which gives

$$\begin{aligned}
4(k_{ab} + k_{bc})\theta_b + 2k_{bc}\theta_c &= 6k_{ab}\Theta_{ab}, \\
(4k_{bc} + 3k_{cd})\theta_c + 2k_{bc}\theta_b &= 3k_{cd}\Theta_{cd}.
\end{aligned}$$

Observing that in this case $k_{bc} = k_{ab}$ and $k_{cd} = 2k_{ab}$ and using the numeri-

cal values (g), we obtain the equations

$$4\theta_b + \theta_c = 0.015,$$
$$\theta_b + 5\theta_c = 0.030,$$

from which

$$\theta_b = 0.00237, \qquad \theta_c = 0.00552.$$

The end moments due to lateral sway, from Eqs. (77), and (79), are

$$\left.\begin{array}{l} M_{ab}'' = 2k_{ab}\theta_b - 6k_{ab}\Theta_{ab} = -0.0253k_{ab}, \\ M_{ba}'' = -M_{bc}'' = 4k_{ab}\theta_b - 6k_{ab}\Theta_{ab} = -0.0205k_{ab}, \\ M_{cd}'' = -M_{cb}'' = 3k_{dc}\theta_c - 3k_{dc}\Theta_{dc} = -0.0269k_{ab}. \end{array}\right\} \qquad (h)$$

The shear actions on the joints b and c, due to these moments, are shown in Fig. 424c. Since the magnitude of the lateral displacement was taken arbitrarily, these forces usually will not balance the forces shown in Fig. 424b. To obtain equilibrium, we multiply the assumed displacement by a factor x. The shear actions shown in Fig. 424c must then be also multiplied by x, and the equilibrium equation is

$$\left(\frac{0.0458k_{ab}}{l_{ab}} + \frac{0.0269k_{ab}}{l_{cd}}\right)x = 7{,}920 - 2{,}880 = 5{,}040.$$

Observing that $l_{ab} = 20$ ft., $l_{cd} = 10$ ft., we obtain

$$x = \frac{5{,}040 \cdot 20}{0.0996k_{ab}}.$$

Multiplying the moments (h) by this factor, we obtain the true moments produced by the lateral displacement of the frame.

$$M_{ab}''' = x \cdot M_{ab}'' = -\frac{5{,}040 \cdot 20}{0.0996} \cdot 0.0253 = -25{,}600 \text{ ft.-lb.},$$

$$M_{ba}''' = -M_{bc}''' = x \cdot M_{ba}'' = -\frac{5{,}040 \cdot 20}{0.0996} \cdot 0.0205 = -20{,}750 \text{ ft.-lb.},$$

$$M_{cd}''' = -M_{cb}''' = x \cdot M_{cd}'' = -\frac{5{,}040 \cdot 20}{0.0996} \cdot 0.0269 = -27{,}200 \text{ ft.-lb.}$$

Adding these moments to the moments (f), we obtain the required total end moments.

$$M_{ab} = M_{ab}' + M_{ab}''' = -35{,}200 \text{ ft.-lb.}$$
$$M_{ba} = -M_{bc} = M_{ba}' + M_{ba}''' = 27{,}250 \text{ ft.-lb.}$$
$$M_{cd} = -M_{cb} = M_{cd}' + M_{cd}''' = -56{,}000 \text{ ft.-lb.}$$

With these moments, the bending-moment diagram can be readily constructed. Several more complicated cases of calculating end moments due to lateral sway will be discussed later.

64. Continuous Frames.—Very often, especially in reinforced-concrete structures, we have to analyze continuous frames like those shown in Fig. 425. Application of the general Eqs. (74) and (75) gives us a simple solution of this problem. If the ends of the girder are built-in at a and e (Fig. 425a), there will be no lateral movement and the deformation of the frame is completely defined by the angles of rotation θ_b, θ_c, and θ_d. Equations (74) for the determination of these angles are

$$\left.\begin{aligned}
4(k_{ab} + k_{bc} + k_{bf})\theta_b + 2k_{bc}\theta_c &= -(\mathfrak{M}_{ba} + \mathfrak{M}_{bc} + \mathfrak{M}_{bf}) = \mathbf{M}_b, \\
4(k_{bc} + k_{cd} + k_{cg})\theta_c + 2k_{bc}\theta_b + 2k_{cd}\theta_d &= -(\mathfrak{M}_{cb} + \mathfrak{M}_{cd} + \mathfrak{M}_{cg}) = \mathbf{M}_c, \\
4(k_{cd} + k_{de} + k_{dh})\theta_d + 2k_{cd}\theta_c &= -(\mathfrak{M}_{dc} + \mathfrak{M}_{de} + \mathfrak{M}_{dh}) = \mathbf{M}_d.
\end{aligned}\right\} \tag{a}$$

If the dimensions and lateral loads are given, all values of k and of fixed-end moments can be readily calculated and we obtain, from Eqs. (a), three linear numerical equations of the same kind as we had in the case of continuous beams. The solution of these equations in each particular case does not present any difficulty. Take, for example,

$$l_1 = l_4 = l, \qquad l_2 = l_3 = 2l, \qquad I_1 = I_2 = I_3 = I_4 = I, \qquad h = l,$$
$$I_5 = I_6 = I_7 = 0.5I. \tag{b}$$

Then,

$$k_{ab} = k_{de}, \qquad k_{bc} = k_{cd} = 0.5k_{ab}, \qquad k_{bf} = k_{cg} = k_{dh} = 0.5k_{ab}. \tag{c}$$

Assume also that a uniform load of constant intensity q covers the entire length of the girder ae. Then,

$$\mathfrak{M}_{ab} = \mathfrak{M}_{de} = -\mathfrak{M}_{ba} = -\mathfrak{M}_{ed} = -\frac{ql}{12},$$

$$\mathfrak{M}_{bc} = \mathfrak{M}_{cd} = -\mathfrak{M}_{cb} = -\mathfrak{M}_{dc} = -\frac{ql^2}{3},$$

and the fixed-end moments for the columns vanish. Equations (a) then become

$$8k_{ab}\theta_b + k_{ab}\theta_c = \frac{ql^2}{4},$$

$$k_{ab}\theta_b + 6k_{ab}\theta_c + k_{ab}\theta_d = 0,$$

$$k_{ab}\theta_c + 8k_{ab}\theta_d = -\frac{ql^2}{4},$$

and we obtain

$$\theta_b = -\theta_d = \frac{ql^2}{32k_{ab}}, \qquad \theta_c = 0.$$

The end moments are now calculated from Eqs. (69), which give

$$M_{ab} = -M_{ed} = -\frac{ql^2}{12} + \frac{ql^2}{16} = -\frac{ql^2}{48},$$

$$M_{ba} = -M_{de} = \frac{ql^2}{12} + \frac{ql^2}{8} = \frac{5}{24} ql^2,$$

$$M_{bc} = -M_{dc} = -\frac{ql^2}{3} + \frac{ql^2}{16} = -\frac{13}{48} ql^2,$$

$$M_{cb} = -M_{cd} = \frac{ql^2}{3} + \frac{ql^2}{32} = \frac{35}{96} ql^2,$$

$$M_{bf} = -M_{dh} = \frac{ql^2}{16}.$$

If, instead of built-in ends, there are hinges at a and e (Fig. 425b) and lateral motion is restrained, we use Eq. (75) for joints b and d. In this manner,

$$\left.\begin{array}{l} (3k_{ab} + 4k_{bc} + 4k_{bf}) \theta_b + 2k_{bc}\theta_c = -\mathfrak{M}_{ba} - \mathfrak{M}_{bc} + \tfrac{1}{2}\mathfrak{M}_{ab} - \mathfrak{M}_{bf} = \mathbf{M}_b, \\ 4(k_{bc} + k_{cd} + k_{cg}) \theta_c + 2k_{bc}\theta_b + 2k_{cd}\theta_d = -(\mathfrak{M}_{cb} + \mathfrak{M}_{cd} + \mathfrak{M}_{cg}) = \mathbf{M}_c, \\ (4k_{cd} + 3k_{de} + 4k_{dh}) \theta_d + 2k_{cd}\theta_c = -\mathfrak{M}_{dc} - \mathfrak{M}_{de} + \tfrac{1}{2}\mathfrak{M}_{ed} - \mathfrak{M}_{dh} = \mathbf{M}_d. \end{array}\right\} \quad (d)$$

These equations are of the same form as Eqs. (*a*) and can be readily solved for any particular kind of loading.
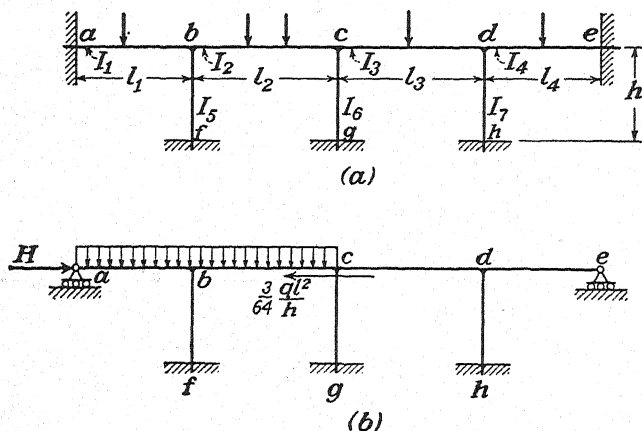
FIG. 425.

Let us now consider the case where the frame is free to move laterally. If the frame and the load are both symmetrical with respect to the vertical cg (Fig. 425b), there will be no lateral motion and Eqs. (*d*) give us the final values of the angles θ_b, θ_c, θ_d. If there is no symmetry, the continuous frame in Fig. 425b will have a lateral movement and the

effect of this movement on the end moments must be investigated separately, as was shown in the preceding article.

As an example let us consider the case in which a uniform load covers only half of the girder, as shown in Fig. 425b. The problem will be solved in two steps as before. Assuming first that there is a lateral constraint and using Eqs. (d) together with assumptions (b), we obtain

$$\left.\begin{array}{c} 7k_{ab}\theta_b + k_{ab}\theta_c = \frac{5}{24}ql^2, \\ k_{ab}\theta_b + 6k_{ab}\theta_c + k_{ab}\theta_d = -\frac{ql^2}{3}, \\ k_{ab}\theta_c + 7k_{ab}\theta_d = 0. \end{array}\right\} \qquad (e)$$

Solving these equations, we obtain

$$\theta_b = 0.0388 \frac{ql^2}{k_{ab}}, \qquad \theta_c = -0.0635 \frac{ql^2}{k_{ab}}, \qquad \theta_d = 0.00908 \frac{ql^2}{k_{ab}}.$$

With these values of the angles of rotation we calculate all end moments by using Eqs. (69) and (72). Assuming, for example, $q = 1$ kip per ft. and $l = 12$ ft., we obtain

$$\left.\begin{array}{lll} M_{ba} = 34.8 \text{ kip-ft.}, & M_{bc} = -46.0 \text{ kip-ft.}, & M_{cb} = 35.3 \text{ kip-ft.}, \\ M_{cd} = -17.00 \text{ kip-ft.}, & M_{dc} = -6.57 \text{ kip-ft.}, & M_{de} = 3.92 \text{ kip-ft.} \end{array}\right\} \quad (f)$$

In our further discussion we shall need the end moments in the columns, which are

$$M_{bf} = 2M_{fb} = 2k_{ab}\theta_b, \qquad M_{cg} = 2M_{gc} = 2k_{ab}\theta_c, \qquad M_{dh} = 2M_{hd} = 2k_{ab}\theta_d.$$

The corresponding shearing forces at the upper ends of the columns, from Eqs. (76), are

$$V_{bf} = -\frac{3k_{ab}\theta_b}{h}, \qquad V_{cg} = -\frac{3k_{ab}\theta_c}{h}, \qquad V_{dh} = -\frac{3k_{ab}\theta_d}{h}.$$

Using the rule of sign for shearing forces, given in Fig. 420b, we conclude that a positive shearing force at the upper end of a column has the direction from left to right. The corresponding shear action on the girder has the opposite direction. Hence the total horizontal force transmitted from the columns to the girder in the direction from right to left is

$$V_{bf} + V_{cg} + V_{dh} = -\frac{3k_{ab}}{h}(\theta_b + \theta_c + \theta_d). \qquad (g)$$

The sum of the angles in parentheses is obtained by adding Eqs. (e), which gives

$$\theta_b + \theta_c + \theta_d = - \frac{ql^2}{64k_{ab}}.$$

Then,

$$V_{bf} + V_{cg} + V_{dh} = \frac{3}{64} \frac{ql^2}{h}. \tag{h}$$

It is seen that the total horizontal shear action on the girder is positive, *i.e.*, it acts from right to left as shown in Fig. 425*b*. To prevent any lateral motion, the horizontal force H must be applied as shown in the figure.

Let us consider now the effect of a lateral movement of the frame. Assuming that the girder *ae* moves to the left by an amount Δ, we have

$$\Theta_{bf} = \Theta_{cg} = \Theta_{dh} = \Theta_0 = - \frac{\Delta}{h},$$

$$\Theta_{ab} = \Theta_{bc} = \Theta_{cd} = \Theta_{de} = 0,$$

and equations for calculating the angles of rotation of the joints b, c, and d are obtained from Eqs. (*d*) by substituting $-6k_{bf}\Theta_0$, $-6k_{cg}\Theta_0$, $-6k_{dh}\Theta_0$ for $\mathfrak{M}_{bf}$, $\mathfrak{M}_{cg}$, and $\mathfrak{M}_{dh}$, respectively, and making the rest of the fixed-end moments vanish. Hence,

$$\left.\begin{aligned}
(3k_{ab} + 4k_{bc} + 4k_{bf})\theta_b + 2k_{bc}\theta_c &= 6k_{bf}\Theta_0, \\
(4k_{bc} + 4k_{cd} + 4k_{cg})\theta_c + 2k_{bc}\theta_b + 2k_{cd}\theta_d &= 6k_{cg}\Theta_0, \\
(4k_{cd} + 4k_{dh} + 3k_{de})\theta_d + 2k_{cd}\theta_c &= 6k_{dh}\Theta_0.
\end{aligned}\right\} \tag{i}$$

Using assumptions (*b*), we obtain

$$\left.\begin{aligned}
7\theta_b + \theta_c &= 3\Theta_0, \\
\theta_b + 6\theta_c + \theta_d &= 3\Theta_0, \\
\theta_c + 7\theta_d &= 3\Theta_0.
\end{aligned}\right\} \tag{j}$$

From these equations, the angles θ_b, θ_c, θ_d for any assumed value of Θ_0 can be readily obtained. The corresponding end moments will then be calculated by using Eqs. (77). For the columns these end moments are

$$\begin{aligned}
M_{bf} &= 2k_{ab}\theta_b - 3k_{ab}\Theta_0, & M_{fb} &= k_{ab}\theta_b - 3k_{ab}\Theta_0, \\
M_{cg} &= 2k_{ab}\theta_c - 3k_{ab}\Theta_0, & M_{gc} &= k_{ab}\theta_c - 3k_{ab}\Theta_0, \\
M_{dh} &= 2k_{ab}\theta_d - 3k_{ab}\Theta_0, & M_{hd} &= k_{ab}\theta_d - 3k_{ab}\Theta_0.
\end{aligned}$$

The corresponding shear forces at the tops of the columns are

$$V_{bf} = - \frac{3k_{ab}(\theta_b - 2\Theta_0)}{h}, \qquad V_{cg} = - \frac{3k_{ab}(\theta_c - 2\Theta_0)}{h},$$

$$V_{dh} = - \frac{3k_{ab}(\theta_d - 2\Theta_0)}{h}.$$

The total shear action on the girder from right to left is

$$V_{bf} + V_{cg} + V_{dh} = -\frac{3k_{ab}}{h}(\theta_b + \theta_c + \theta_d - 6\Theta_0). \qquad (k)$$

By adding Eqs. (j), we obtain

$$\theta_b + \theta_c + \theta_d = \tfrac{9}{8}\Theta_0.$$

Substituting this in Eq. (k), we find that the total shear action induced on the girder by the lateral movement Δ is

$$V_{bf} + V_{cg} + V_{dh} = \frac{3k_{ab}}{h} \cdot \frac{39}{8}\Theta_0. \qquad (l)$$

The true value of the lateral displacement is now found from the condition of equilibrium of the forces (l) and (h), which gives

$$\frac{3}{64}\frac{ql^2}{h} + \frac{3k_{ab}}{h} \cdot \frac{39}{8}\Theta_0 = 0$$

and

$$\Theta_0 = -\frac{\Delta}{h} = -\frac{ql^2}{8 \cdot 39k_{ab}}. \qquad (m)$$

From this equation the actual value of the lateral displacement can be calculated in each particular case if the magnitude of the load and the dimensions of the frame are given. Substituting this value in Eqs. (j), we shall then find that the angles of rotation of the joints produced by the lateral motion are

$$\theta_b = \theta_c = \theta_d = -\frac{ql^2}{8 \cdot 8 \cdot 13 \cdot k_{ab}}.$$

The corresponding end moments, for $q = 1$ kip per ft. and $l = 12$ ft., are

$$M_{ba} = M_{bc} = M_{cb} = M_{cd} = M_{dc} = M_{de} = -\frac{3 \cdot ql^2}{8 \cdot 8 \cdot 13} = -0.519 \text{ kip.-ft.}$$

These moments must be added to the previously calculated moments (f) to take care of the lateral movement of the system. It is seen that in our numerical example the numerically largest moment will be only slightly changed by the lateral movement.

65. Calculation of End Moments by Successive Approximations.— We have seen in preceding articles that the calculation of end moments for the members of a frame structure with rigid joints requires the solution of a system of linear equations like Eq. (74). In many cases these equations have the same form as three-moment equations previously used in the analysis of continuous beams. Such equations can be readily solved in each particular case. But sometimes we have more complicated systems of equations, and their solution becomes cumbersome. We encounter examples of such systems in studying secondary stresses in

trusses (see Art. 68) and in the analysis of complicated building frames. In the solution of such equations, the application of the method of successive approximations is very useful.[1] To explain this method let us consider again the frame in Fig. 425b. With the assumption of lateral constraint we have already obtained the following system of equations (see page 380):

$$4(\tfrac{3}{4}k_{ba} + k_{bc} + k_{bf})\theta_b + 2k_{bc}\theta_c = \mathbf{M}_b, \\ 2k_{cb}\theta_b + 4(k_{cb} + k_{cd} + k_{cg})\theta_c + 2k_{cd}\theta_d = \mathbf{M}_c, \\ 2k_{dc}\theta_c + 4(k_{dc} + \tfrac{3}{4}k_{de} + k_{dh})\theta_d = \mathbf{M}_d. \tag{a}$$

In each of these equations one of the coefficients is considerably larger than the others, and this fact is utilized in the calculation of successive approximations.[2] We begin the calculation with the second equation, corresponding to the joint c, in which the unbalanced moment, produced by the load shown in Fig. 425b, is numerically the largest. The first approximation θ_c' for the angle θ_c is obtained by neglecting the terms containing θ_b and θ_d, which gives

$$\theta_c' = \frac{\mathbf{M}_c}{4(k_{cb} + k_{cd} + k_{cg})}. \tag{b}$$

Substituting this first approximation for θ_c in the first and the third of Eqs. (a), we obtain the first approximations for the angles θ_b and θ_d.

$$\theta_b' = \frac{1}{4(\tfrac{3}{4}k_{ba} + k_{bc} + k_{bf})}\left(\mathbf{M}_b - \frac{1}{2}\frac{k_{bc}}{k_{cb} + k_{cd} + k_{cg}}\mathbf{M}_c\right), \\ \theta_d' = \frac{1}{4(k_{dc} + \tfrac{3}{4}k_{de} + k_{dh})}\left(\mathbf{M}_d - \frac{1}{2}\frac{k_{dc}}{k_{cb} + k_{cd} + k_{cg}}\mathbf{M}_c\right). \tag{c}$$

To calculate the second approximations for the angles, we again use Eqs. (a). Substituting the first approximations (c) for θ_b and θ_d in the

---

[1] This method was developed in connection with calculation of secondary stresses in trusses and is described in the book by O. Mohr, "Abhandlungen aus dem Gebiete der Technischen Mechanik," p. 429, 1906. In this country the method was first used by S. Hardesty and is fully explained in the book by J. A. L. Waddell, "Bridge Engineering," 1916. The extension of the method to the analysis of highly statically indeterminate frame structures is due to K. A. Čališev, who used it in analysis of building frames with and without lateral constraints. See *Tech. List.*, 1923, No. 17–21, Zagreb. A German translation of this paper appeared in *Pub. Intern. Assoc. Bridge Structural Eng.*, vol. 4, pp. 199–215, 1936. The final form of the method of successive approximations was obtained in the paper by H. Cross; see *Trans. A.S.C.E.*, vol. 96, 1932. Solutions of many engineering problems by using the methods of successive approximations are discussed in the book by R. V. Southwell, "Relaxation Methods in Engineering Science," Oxford, 1940.

[2] Various methods of solving systems of linear equations, such as are obtained in the analysis of highly statically indeterminate systems, are discussed in the paper by R. Mises and H. Pollaczek-Geiringer, *Z. angew. Math. Mech.*, vol. 9, pp. 58, 152, 1929.

second of Eqs. (a), we shall obtain the second approximation for the angle θ_c. Instead of calculating this second approximation it is preferable to calculate the correction that must be added to the previously found value θ_c' to obtain the second approximation for the angle. Denoting this correction by θ_c'', we shall write the second of Eqs. (a) in the following form:

$$2k_{cb}\theta_b' + 4(k_{cb} + k_{cd} + k_{cg})(\theta_c' + \theta_c'') + 2k_{cd}\theta_d' = \mathbf{M}_c.$$

Substituting for θ_c' its value (b), we obtain

$$4(k_{cb} + k_{cd} + k_{cg})\theta_c'' = -2k_{cb}\theta_b' - 2k_{cd}\theta_d' \qquad (d)$$

and

$$\theta_c'' = \frac{-2k_{cb}\theta_b' - 2k_{cd}\theta_d'}{4(k_{cb} + k_{cd} + k_{cg})}. \qquad (e)$$

In the same manner we calculate the corrections θ_b'' and θ_d'' from the first and third of Eqs. (a). Substituting $\theta_c' + \theta_c''$ for θ_c in those equations and using Eqs. (c), we find

$$\left.\begin{array}{l} 4(\tfrac{3}{4}k_{ba} + k_{bc} + k_{bf})\theta_b'' = -2k_{bc}\theta_c'', \\ 4(k_{dc} + \tfrac{3}{4}k_{dc} + k_{dh})\theta_d'' = -2k_{dc}\theta_c''. \end{array}\right\} \qquad (f)$$

Continuing the calculation of consecutive corrections, we shall always obtain equations of the same form as Eqs. (d) and (f). To get, for example, the second correction θ_c''' to the angle θ_c, we have only to substitute θ_b'' and θ_d'' for θ_b' and θ_d', and θ_c''' for θ_c'' in Eq. (d). Substituting θ_c''' for θ_c'' in Eqs. (f), we shall find the second corrections θ_b''' and θ_d''' for the angles θ_b and θ_d, etc. Such calculations of consecutive corrections must be continued until the calculated corrections become very small. Then the expressions

$$\theta_c = \theta_c' + \theta_c'' + \theta_c''' + \cdots, \qquad \theta_b = \theta_b' + \theta_b'' + \theta_b''' + \cdots,$$
$$\theta_d = \theta_d' + \theta_d'' + \theta_d'' + \cdots$$

give the angles of rotation with sufficient accuracy. Upon substituting these angles in Eqs. (69), the end moments for all members of the structure can be calculated and bending-moment diagrams constructed.

Instead of calculating the angles of rotation first and the end moments afterward, we can work directly with the end moments. In our previous discussion we started with the second of Eqs. (a) and calculated θ_c', assuming that θ_b and θ_d vanish. This operation is equivalent to the assumption that joints b and d are locked and the joint c is allowed to rotate freely under the action of the unbalanced moment $\mathbf{M}_c$. This case is similar to that discussed in Art. 61 (see Fig. 415). We know that the unbalanced moment $\mathbf{M}_c$ will be distributed between the members cb, cd, and cg in proportion to their stiffness factors, and the distributed

moments will be

$$M_{cb}' = r_{cb}\mathbf{M}_c, \qquad M_{cd}' = r_{cd}\mathbf{M}_c, \qquad M_{cg}' = r_{cg}\mathbf{M}_c, \qquad (80)$$

where

$$r_{cb} = \frac{k_{cb}}{k_{cb} + k_{cd} + k_{cg}}, \qquad r_{cd} = \frac{k_{cd}}{k_{cb} + k_{cd} + k_{cg}}, \qquad r_{cg} = \frac{k_{cg}}{k_{cb} + k_{cd} + k_{cg}}, \qquad (g)$$

are the distribution factors for the members meeting at joint c. The first approximations for the end moments at joint c are obtained by adding the distributed moments (80) to the initially calculated fixed-end moments $\mathfrak{M}_{cb}$, $\mathfrak{M}_{cd}$, $\mathfrak{M}_{cg}$.

When we are unlocking the joint c, the joints b, d, and g are considered as fixed. Hence the moments equal to $\frac{1}{2}M_{cb}'$, $\frac{1}{2}M_{cd}'$, and $\frac{1}{2}M_{cg}'$ will be carried over to the far ends of the members cb, cd, and cg, respectively, where they must be algebraically added to the fixed-end moments at those ends. Taking, now, joint b, we have to distribute not only the initially calculated unbalanced moment $\mathbf{M}_b$ but also the carry-over moment $-\frac{1}{2}M_{cb}'$ produced during unlocking of the joint c. The distributed moments at joint b then are

$$\left. \begin{array}{l} M_{ba}' = r_{ba}(\mathbf{M}_b - \tfrac{1}{2}M_{cb}'), \\ M_{bc}' = r_{bc}(\mathbf{M}_b - \tfrac{1}{2}M_{cb}'), \\ M_{bf}' = r_{bf}(\mathbf{M}_b - \tfrac{1}{2}M_{cb}'), \end{array} \right\} \qquad (h)$$

where

$$r_{ba} = \frac{\frac{3}{4}k_{ba}}{\frac{3}{4}k_{ba} + k_{bc} + k_{bf}}, \qquad r_{bc} = \frac{k_{bc}}{\frac{3}{4}k_{ba} + k_{bc} + k_{bf}}, \qquad r_{bf} = \frac{k_{bf}}{\frac{3}{4}k_{ba} + k_{bc} + k_{bf}}.$$

The factor $\frac{3}{4}k_{ba}$ instead of k_{ba} appears in these formulas since the joint a is hinged, while joints c and f are assumed fixed during unlocking of joint b. Equations similar to Eqs. (h) can be written also for the distributed moments at joint d. Adding the distributed moments, calculated in this manner, to the previously calculated fixed-end moments at the joints b and d, we obtain the first approximations of the end moments at these joints.

In the calculation of consecutive corrections, we start again with joint c. During unlocking of the joints b and d, the moments $\frac{1}{2}M_{bc}'$ and $\frac{1}{2}M_{dc}'$ were carried over to the joint c, and an unbalanced moment of the magnitude $-\frac{1}{2}(M_{bc}' + M_{dc}')$ was created at this joint. Distributing this moment, we obtain the first corrections to the end moments at joint c. Now we can calculate corrections to the end moments at joints b and d, distributing the unbalanced moments created at these joints during the unlocking of joint c. To calculate the second corrections, we again start with joint c and proceed as before. The calculation of consecutive corrections must go as far as to make these corrections negligibly small.

The end moments will then be obtained with sufficient accuracy by adding to the first approximations all the calculated consecutive corrections. Whether we work with angles or with end moments, we obtain the same consecutive corrections to the end moments, since in both cases we unlock only one joint each time.

Recapitulating the described method of successive approximations, we see that the process of calculation consists in repetition of very simple operations of distribution of unbalanced moments and carrying over moments to the adjacent joints. In each particular case, we assume first that all joints, except hinged ends, are locked and calculate on this assumption the fixed-end moments for all members of the structure. The sums of these moments for each joint, taken with reversed signs,

|←———12'———→|←———12'———→|←——8'——→|←——8'——→|

$q = 2000\ lb/ft.$ $16{,}000\ lb.$

a $r_{ba}=0.5\ \triangle\ r_{bc}=0.5\ b$ $r_{cb}=0.6\ \triangle\ r_{cd}=0.4\ c$ d

a	b (ba)	b (bc)	c (cb)	c (cd)
−24.00	+24.00	−24.00	+24.00	−48.00
		+ 7.20	+14.40	+ 9.60
−1.80	− 3.60	− 3.60	−1.80	
		+ .54	+1.08	+ .72
−.14	− .27	− .27	−.14	
		+ .04	+ .08	+ .05
−.01	− .02	− .02		
−25.95	+20.11	−20.11	+37.62	−37.62
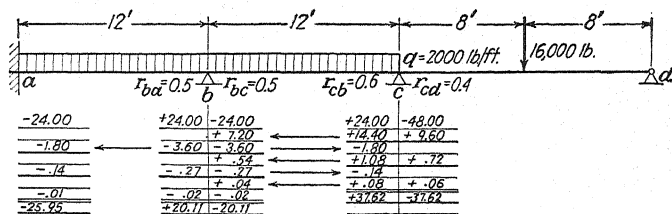
Fig. 426.

give us the unbalanced moments. We calculate also for each joint the distribution factors for the members meeting at that joint. After this preliminary work, we begin preferably with the joint in which the largest unbalanced moment is found. We unlock this joint and distribute the moment between the members meeting at the joint. In our previous example it was joint c, and the distribution of the moment $\mathbf{M}_c$ was accomplished by using Eqs. (80). Now we carry over moments to the adjacent joints and add to the unbalanced moments at these joints the moments equal to the carry-over moments, but with opposite sign. The obtained sums we again distribute, using equations similar to Eqs. (80). When the distribution of moments is accomplished at all joints, we obtain the first approximations for all end moments by adding the distributed moments to the previously found fixed-end moments. To get the first corrections, we repeat the moment-distribution process, but this time we distribute only the carry-over moments remaining after the first cycle of calculation, etc.

Since we always repeat the same simple operations, it is not necessary to write equations, which were used in our previous discussion. Instead, all calculations can be put in proper order on a sketch of the structure. Take, for example, the continuous beam shown in Fig. 426. Assuming that, at the supports a, b, and c, the cross sections of the beam cannot

rotate and that at the support d the rotation is free, we obtain the fixed-end moments in kip-ft. as shown in the first line of the table attached to the figure. In calculating the distribution factors, we assume that $k_{ab} = k_{bc} = \frac{3}{8}k_{cd}$. Then,

$$r_{ba} = r_{bc} = \frac{k_{ab}}{k_{ab} + k_{bc}} = 0.5,$$

$$r_{cb} = \frac{k_{cb}}{k_{cb} + \frac{3}{4}k_{cd}} = 0.6, \qquad r_{cd} = \frac{\frac{3}{4}k_{cd}}{k_{cb} + \frac{3}{4}k_{cd}} = 0.4.$$

In this calculation we observe that the end d of the member cd is free to rotate and introduce $\frac{3}{4}k_{cd}$, instead of k_{cd}, in our formulas. The calculated values of the distribution factors are shown in the figure. We now begin with joint c. The unbalanced moment at this joint is

$$-(24.0 - 48.0) = +24 \text{ kip-ft.}$$

Distributing this moment between the members cd and cb in proportion to their distribution factors r_{cd} and r_{cb}, we obtain the distributed moments at c, equal to $+9.6$ kip-ft. and $+14.4$ kip-ft. Taking now joint b, we find that the fixed-end moments at this joint balance each other, and we have to consider only the moment -7.2 kip-ft., equal and opposite to the carried-over moment 7.2 kip-ft. produced during unlocking of the joint c. This moment will be equally distributed between the members bc and ba, and we obtain the distributed moments at b each equal to -3.6 kip-ft. Considering now joint a and observing that the end a is built-in, we conclude that the correction moment -3.6 kip-ft. acting at b produces the carry-over moment -1.8 kip-ft. at the fixed end. All distributed moments are shown in the second and third lines of the table in Fig. 426, and the heavy horizontal lines below these corrections indicate that the first cycle of calculation is concluded. The second cycle we again begin with joint c. Considering the carry-over moment -1.8 kip-ft. created during unlocking joint b, we have an unbalanced moment $+1.8$ kip-ft. at joint c. Distributing this moment between the members cd and cb, we obtain the corrections $+0.72$ kip-ft. and $+1.08$ kip-ft. Taking now joint b, we have to distribute the moment -0.54, equal and opposite to the carry-over moment $+0.54$, which gives the corrections -0.27 and -0.27; and finally we obtain the correction -0.14 at the built-in end. We see that the corrections are already small, and we can limit ourself to two cycles of calculations. The third cycle of calculation is also indicated in the figure, and under the double horizontal lines there are given the final values of the end moments equal to the algebraic sums of the initially calculated fixed-end moments and all the corrections.

As a second example, let us consider the continuous frame shown in Fig. 425b and assume that lateral movement is restrained. The solution

of the corresponding system of Eqs. (a) by successive approximations has already been discussed, and we give in Fig. 427 only the numerical calculations, assuming that $l = 12$ ft., $q = 1$ kip per ft. and that the other dimensions are as given by Eqs. (b) of the preceding article (see page 379). With these numerical data the distribution factors are calculated as shown in the figure. We start with a calculation of the fixed-end moments, assuming that joints b, c, and d are locked and that there are hinges at the ends a and e. The calculated values of these moments in kip-ft. are given in the first horizontal line of the table above Fig. 427. The distribution of the unbalanced moments we begin from
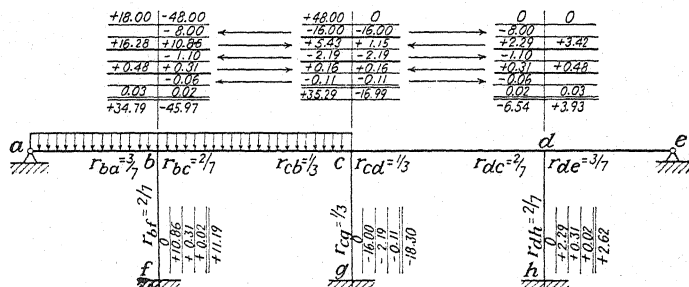
Fig. 427.

joint c, at which the unbalanced moment has the largest numerical value. The results of this distribution are given in the second horizontal line above joint c and in the second vertical line to the right of column cg. Considering, now, joints b and d, we distribute the moments there as shown in the third horizontal line above joints b and d and in the vertical lines to the right of columns bf and dh. This finishes the first cycle of calculation, the results of which are underlined in Fig. 427. The second cycle we again begin with joint c, at which we have the unbalanced moment $-(5.43 + 1.15)$. The results of the second distribution at this joint and also at the joints b and d are again underlined in the figure. There is given in the figure also the third cycle of calculation, which gives only very small corrections of end moments; thus we conclude the calculations with this cycle and put under the double lines the sums of the initially calculated fixed-end moments and of all corrections that give us the required end moments. The same numerical values were obtained [see Eqs. (f), page 381] by the direct solution of the corresponding system of Eqs. (d) (see page 380).

The method of successive approximations can be used also in case the continuous frame is free to move laterally. Let us take again the example shown in Fig. 427. The calculated end moments in the columns produce on the girder ae the horizontal shear action in the direction

from right to left equal to

$$-\frac{3}{2}\frac{M_{bf} + M_{cg} + M_{dh}}{h} = \frac{3}{2} \cdot \frac{-11.19 + 18.30 - 2.62}{12} = 561 \text{ lb.} \quad (i)$$

To prevent a lateral movement, a horizontal external force of the same magnitude but acting from left to right must be applied. If there is no such force and the frame is free to move laterally, it will move to the left by such an amount as to produce shearing forces at the top of the columns sufficient to balance the above-calculated force (i). In discussing the end moments and shearing forces produced by lateral movement alone, we assume first that the joints b, c, and d do not rotate during
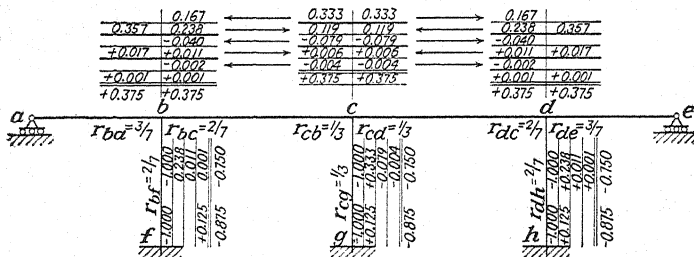
Fig. 428.

this movement. Then the end moments equal to $-6k_{bf}\Theta_{bf}$, $-6k_{cg}\Theta_{cg}$, $-6k_{dh}\Theta_{dh}$ will be produced at the ends of the columns bf, cg, and dh [see Eqs. (77)]. In our case all these end moments are equal since the stiffness factors and the angles of rotation are the same for all columns. Since we do not know in advance the magnitude of the displacement, we start the calculation by assuming that it is of such magnitude that

$$6k_{bf}\Theta_{bf} = 6k_{cg}\Theta_{cg} = 6k_{dh}\Theta_{dh} = +1.000 \text{ kip-ft.}$$

The corresponding end moments are indicated in the first vertical lines to the right of the columns in Fig. 428. It is seen that there are unbalanced moments equal to 1.000 kip-ft. in joints b, c, and d. Distributing them in the usual way, we finally obtain the values of the end moments written under the double lines. Having these moments, we calculate the shearing forces in the columns by using Eqs. (76), and we find that the total horizontal force acting on the girder ae in the direction from right to left is

$$3\frac{(0.875 + 0.750) \text{ kip-ft.}}{12} = 406 \text{ lb.}$$

It is seen that to balance the horizontal force given in Eq. (i) we have to take

$$6k_{bf}\Theta_{bf} = 6k_{cg}\Theta_{cg} = 6k_{dh}\Theta_{dh} = -1.000 \cdot \tfrac{561}{406} \text{ kip-ft.} = -1.38 \text{ kip-ft.,}$$

instead of the previously assumed value 1.000 kip-ft. Hence the end moments due to lateral movement will be obtained by multiplying by -1.38 the values given in Fig. 428. In this manner we find

$$M_{ba} = M_{bc} = M_{cb} = M_{cd} = M_{dc} = M_{de} = -0.375 \cdot 1.38 = -0.518$$
$$\text{kip-ft.}$$

These moments were obtained before by solving the system of equations of equilibrium in the preceding article (see page 383).

66. Analysis of Building Frames.—In the design of building frames we have to analyze complicated structures of the kind shown in Fig. 429. The solution of the problem is usually divided into two parts, (1) a calculation of end moments produced by vertical loads, assuming that there are no lateral movements; (2) a calculation of end moments produced by lateral movements, the latter being produced, not only by lateral, but also by vertical loads.

If there are no lateral movements, we apply the method of successive approximations described in the preceding article. Using the known dimensions of the structural elements, we calculate the distribution factors for the members meeting at each joint. We calculate also the fixed-end moments produced by actual loads. When this preliminary work is finished, we start with distribution of unbalanced moments and proceed in exactly the same manner as already described in the preceding article.

FIG. 429.

If the load is applied in one span only, the end moments produced by it diminish rapidly as we consider joints farther and farther away from the loaded span. Using this fact, we can simplify the calculations by considering, instead of the entire struc-
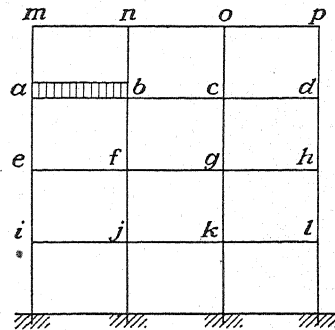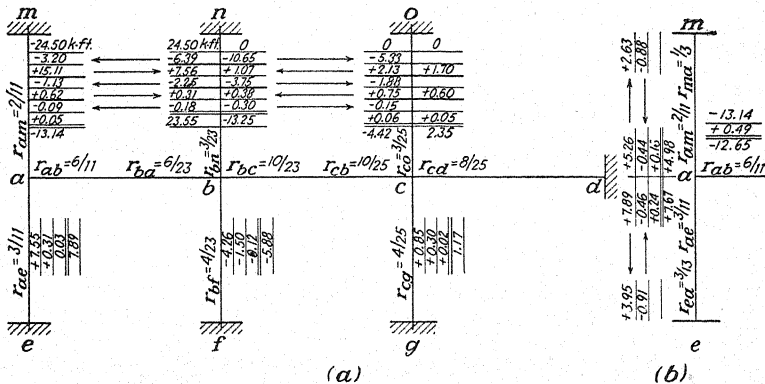

(a)   *(b)*

FIG. 430.

ture, only a portion of the structure adjacent to the loaded member. Assume, for example, that, for the case shown in Fig. 429, the load covers only one span ab. Then

an approximate solution is obtained if we consider only the portion of the structure shown in Fig. 430a and assume that the upper joints m, n, o, the lower joints e, f, g, and joint d are fixed. Assuming that the fixed-end moments and the distribution factors have the numerical values indicated in the figure, the results of the first cycle of calculation will be as underlined by the heavy lines in the second and third lines in the figure. There are shown in the figure, also, the calculations of the second and third cycles, and under the double lines the final values of the end moments are given.

If more accurate values of the end moments at the joints a and b are required, the effect of rotations of the joints m, n, e, and f on these moments can be readily taken

FIG. 431.

into account. This calculation is shown in Fig. 430b. We start by writing in the end moments M_{ab} = -13.14, M_{ae} = $+7.89$, and M_{am} = $+5.26$, obtained from our previous calculation. The carry-over moments at joints m and e are then $+2.63$ and $+3.95$, respectively, as shown in the first vertical line in the figure. Hence at joints m and e there are the unbalanced moments -2.63 and -3.95. Unlocking these joints and assuming that $r_{ma} = \frac{1}{3}$ and $r_{ea} = \frac{3}{13}$, we distribute the moments and find the carry-over moments -0.44 and -0.46 at joint a as shown in the second vertical line. Distributing, now, the corresponding unbalanced moment $+(0.46 + 0.44)$ at a, we finally obtain under the double lines the required corrected values of the end moments at joint a. In a similar manner the corrected values of the end moments at joint b can be calculated. When all calculations, made on the assumption that there are no lateral movements of the structure, are finished and the numerical values of all end moments for columns are obtained, we calculate, by using Eqs. (76), the horizontal forces acting on each floor of the building.
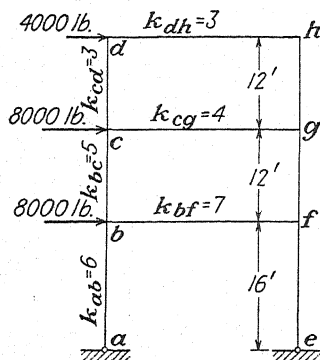
The calculation of the end moments produced by horizontal forces will now be explained by a simple example of a symmetrical three-story frame loaded as shown in Fig. 431.* We begin with a discussion of the three auxiliary problems shown in Fig. 432, in each of which we assume a relative horizontal displacement in one story only. In the case shown in Fig. 432a, we assume first that the upper part of the frame is displaced horizontally without any bending. To produce such a displacement, a proper horizontal force is applied at b, and also couples are applied at joints b and f of such magnitude as to prevent any rotation of these joints. If Δ_1 is the magnitude of the displacement, the end moments at the tops of the columns of the first story will be

$$M_{ba} = M_{fe} = -3k_{ab}\frac{\Delta_1}{h_1}.$$

For our further calculation let us assume some numerical value for these moments, say $M_{ba} = M_{fe} = -9$ kip-ft. Now we assume that any further lateral movements of the joints of the frame are prevented by special constraints, and we unlock the joints b and f. In calculating the end moments resulting from rotations of the joints, we observe from symmetry that there will be inflexion points at the middles of the girders. We can assume hinges in these points and consider only one-half of the frame

* This example is discussed in the mimeographed course of lectures on frame structures given at the University of Michigan by L. C. Maugh.

as shown in Fig. 433a. The numbers proportional to the stiffness factors of the girders, indicated in Fig. 431, must now be multiplied by 2, and three-quarters of these values must be used in calculating the distribution factors. The values of these factors are indicated in Fig. 433a. Starting calculations with joint b, in which we assumed an unbalanced moment of 9 kip-ft., we obtain as usual the values of all end moments. They are written under double lines in Fig. 433a. Upon substituting these moments in Eqs. (76), the shearing forces in all columns and the horizontal forces acting on the girders are obtained. These latter forces in kips are as indicated
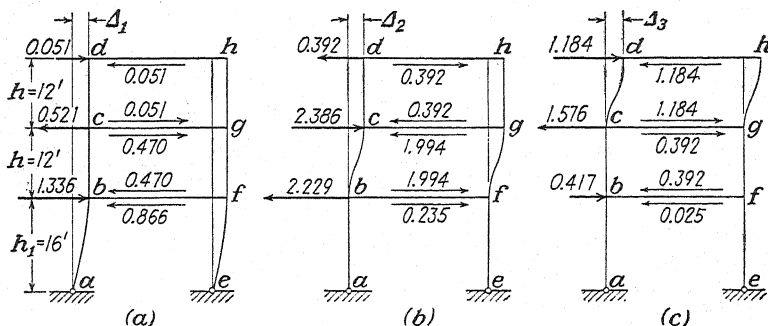
FIG. 432.

in Fig. 432a. Combining them, we obtain the horizontal forces that must be applied at joints b, c, and d to keep the frame in the assumed displaced position with all joints unlocked. These forces are also indicated in Fig. 432a.

Considering the problem in Fig. 432b, we assume that, by a proper application of horizontal forces and couples at the joints b, c, g, and f, the upper story of the frame is displaced with respect to the lower story so that only the columns bc and fg are bent. If Δ_2 denotes the amount of horizontal displacement, the end moments for these columns are

$$M_{bc} = M_{cb} = M_{fg} = M_{gf} = -6k_{bc}\frac{\Delta_2}{h}.$$

Taking for these moments an arbitrary value, say −10 kip-ft., and assuming that there is no lateral movement of the frame from its displaced position, we unlock the joints and calculate as usual the resulting end moments and horizontal shear forces. These moments are given in Fig. 433b, and the shear forces and horizontal forces required to produce the assumed lateral displacement Δ_2 are shown in Fig. 432b. The case shown in Fig. 432c can be treated in a similar manner. Assuming for the end moments in columns cd and gh the value −6 kip-ft., we obtain the values of the end moments and horizontal shear forces as shown in Fig. 433c and Fig. 432c, respectively.

After solving the three auxiliary problems in Fig. 432, we can, by a proper combination of these solutions, obtain the required solution for the horizontal forces shown in Fig. 431. It is evident that, if the displacements Δ_1, Δ_2, and Δ_3, which were assumed in the auxiliary problems, are changed in a certain proportion, the corresponding horizontal forces will change in the same proportion. Assume, now, that the displacements are $\Delta_1 x$, $\Delta_2 y$, $\Delta_3 z$, and select the values of x, y, and z in such a way that the superposition of the horizontal forces corresponding to these displacements will give us the actual horizontal forces. To accomplish this, we have only to multiply the horizontal forces given in Figs. 432a, 432b, and 432c by x, y, and z, respectively,

and after superposing them put the obtained resultant forces equal to the actual horizontal loads in Fig. 431. In this manner we obtain the equations

$$\left.\begin{array}{r} 0.051x - 0.392y + 1.184z = 4, \\ -0.521x + 2.386y - 1.576z = 8, \\ 1.336x - 2.229y + 0.417z = 8, \end{array}\right\} \qquad (a)$$

which give

$$x = 26.61, \qquad y = 13.63, \qquad z = 6.75.$$

To calculate the actual end moments for the members of the frame in Fig. 431, we have to multiply the moments given in Figs. 433a, 433b, and 433c, respectively, by x, y, and z and then superpose the obtained results. In this manner we obtain

$$M_{ba} = -6.928 \cdot 26.61 + 1.882 \cdot 13.63 - 0.202 \cdot 6.75 = -160.1 \text{ kip-ft.} \qquad (b)$$

To check this result, we observe that in our case the total horizontal load $4 + 8 + 8 = 20$ kip-ft. is equally divided between the two supports a and e. Hence the true value of M_{ba} is $-10 \cdot 16 = -160$ kip-ft. For the remaining end moments in the columns, we obtain, by using equations similar to Eq. (b), the following values: $M_{bc} = -25.3$ kip-ft., $M_{cb} = -46.7$ kip-ft., $M_{cd} = -7.8$ kip-ft., $M_{dc} = -16.1$ kip-ft.
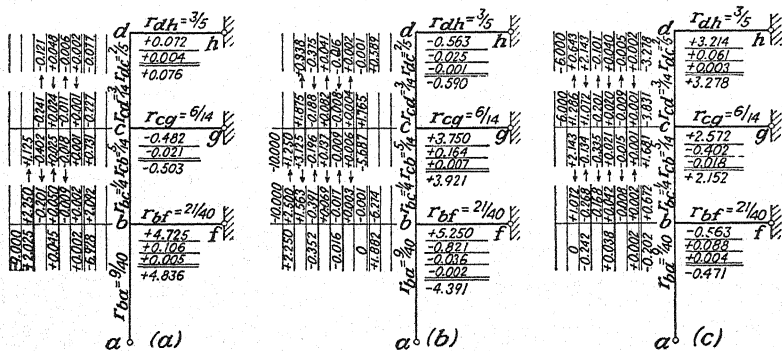
Fig. 433.

We have considered here a frame with three stories (Fig. 431), but the same method can be used for any number of stories. As the number of stories increases, the number of equations of equilibrium similar to Eqs. (a) naturally increases and the amount of arithmetical work required may become very great. However, to obtain a satisfactory approximate solution, we do not need to consider all stories of the frame simultaneously. The effect on the end moments of the lateral distortion assumed in one story dies out rapidly as we go farther and farther from the distorted story. Hence we can get a satisfactory approximation by considering each time only three consecutive stories. In analyzing lateral deflections of a building frame like that shown in Fig. 429, we start from the top of the building and consider the three upper stories. Assuming that there are hinges at the mid-points of the columns in the third story from the top, we obtain a problem similar to that in Fig. 431, and we can calculate all end moments after solving a system of three equilibrium equations similar to Eqs. (a). The results obtained in this way will not be exact, but they will be accurate enough for the top floor. We can then remove the upper story, replace its action on the remaining portion of the frame by the forces and the moments that

have already been calculated, and consider again only three consecutive stories by assuming hinges at the mid-points of the columns of the fourth story from the top, etc.

67. Effect of Temperature Change on Bending of Frames.—Let us begin with a uniform change in temperature of a structure. If the supports are arranged in such a manner that the structure is free to expand, as shown in Fig. 434, no additional stresses will be produced by a uniform temperature change. Often, however, especially in reinforced-concrete structures, the members are rigidly attached to the foundation, and any temperature change produces bending, which must be considered. Take, for example, a symmetrical frame *abcd* (Fig. 435*a*). Any uniform temperature increase of this frame increases the length of its members, which produces bending of the members as indicated in the figure by dotted lines. It is seen that equal elongations of the two columns can occur freely and that the girder *bc* moves in this case ver-
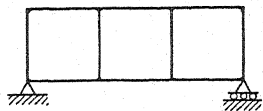
FIG. 434.
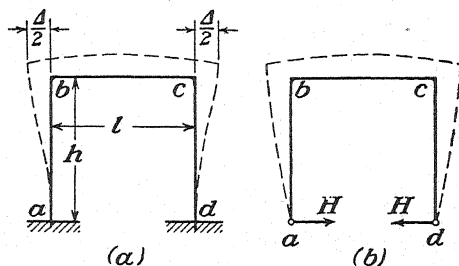
FIG. 435.

tically without bending. On the other hand, an expansion of the girder produces bending in all members of the frame. Let Δ denote the thermal expansion of the girder. Then, from symmetry, we conclude that the deflections of the upper ends of the columns are equal to $\Delta/2$, and we obtain

$$\Theta_{cd} = -\Theta_{ab} = \frac{\Delta}{2h}. \tag{a}$$

Assuming first that the joints *b* and *c* are locked, we find the fixed-end moments from Eqs. (77) (page 373), which give

$$\mathfrak{M}_{ba} = -\mathfrak{M}_{cd} = 6k_{ab} \cdot \frac{\Delta}{2h}. \tag{b}$$

Now unlocking the joints and observing that from symmetry $\theta_c = -\theta_b$, we find the angle of rotation of joint *c* from the equilibrium equation (74), which gives

$$(4k_{ab} + 2k_{bc})\theta_c = 6k_{ab}\frac{\Delta}{2h}, \tag{c}$$

and

$$\theta_c = \frac{3k_{ab}}{4k_{ab} + 2k_{bc}} \cdot \frac{\Delta}{h}.$$

The end moments at joint c, then, are

$$M_{cb} = -M_{cd} = 2k_{bc}\theta_c = \frac{3k_{ab}k_{bc}}{2k_{ab} + k_{bc}} \cdot \frac{\Delta}{h}. \qquad (d)$$

Furthermore, from symmetry we conclude that

$$M_{bc} = -M_{cb}, \qquad M_{ba} = -M_{cd}.$$

If the lower ends of the columns are hinged, as shown in Fig. 435b, we obtain, instead of Eq. (b),

$$\mathfrak{M}_{ba} = -\mathfrak{M}_{cd} = 3k_{ab}\frac{\Delta}{2h}$$

and, instead of Eq. (c),

$$(3k_{ab} + 2k_{bc})\theta_c = 3k_{ab}\frac{\Delta}{2h}.$$

Then,

$$M_{cb} = -M_{cd} = \frac{3k_{ab}k_{bc}}{3k_{ab} + 2k_{bc}} \cdot \frac{\Delta}{h}.$$

In the case of a nonsymmetrical frame (Fig. 436) we divide the calculation of moments, produced by a uniform temperature change, into two steps. First we assume that any lateral displacement of joint b is prevented by some constraint and calculate the angles Θ_{bc} and Θ_{cd}, shown in Fig. 436, by using the known thermal elongations Δ_1, Δ_2, Δ_3 of the members. The corresponding fixed-end moments then are

Fig. 436.

$$\mathfrak{M}_{cd} = -6k_{cd}\Theta_{cd}, \qquad \mathfrak{M}_{cb} = \mathfrak{M}_{bc} = -6k_{bc}\Theta_{bc}.$$

With these fixed-end moments we calculate, in the usual manner, the end moments in all members of the frame and also the horizontal shear forces acting on the girder bc. In the second step of our calculation, we assume some lateral movement of the girder; and, proceeding as before (see page 377), we finally adjust this movement in such a way as to balance the previously calculated horizontal shear forces acting on the girder by the shear forces due to lateral movement. More complicated frames can be analyzed in the same manner.
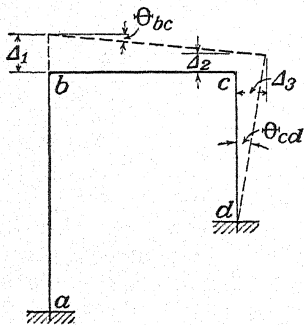
The described method of analysis can be applied also to investigate the effect that the elongations of the members of a frame due to axial

forces may have on the bending of a frame. The analysis of frames in Art. 61 was based on the assumption that axial deformations of structural members can be neglected. If we wish to take these deformations into consideration, we treat our previous results as an approximation and apply them to calculate the axial forces and axial deformations in all members of the structure. The changes in length, obtained in this way, can then be used in exactly the same manner as we just used the thermal changes in length, and we can calculate the additional moments at joints

produced by axial deformations. These moments are usually negligible in frame structures, but they may become important in trusses with rigid joints. This latter question will be discussed in the next article.

Let us consider now a particular case of nonuniform temperature distribution in a member of a frame and assume that the temperature at the neutral plane of the member remains unchanged, while in other planes it varies in proportion to the distance from the neutral plane. In such a case the length of the member remains unchanged, but the

FIG. 437.

member becomes curved. Let t denote the difference in temperatures of the two most remote fibers of the member, α the coefficient of thermal expansion, and d the depth of the cross section. Then the curvature of the member produced by such nonuniform heating is found from the equation (see Fig. 437a)
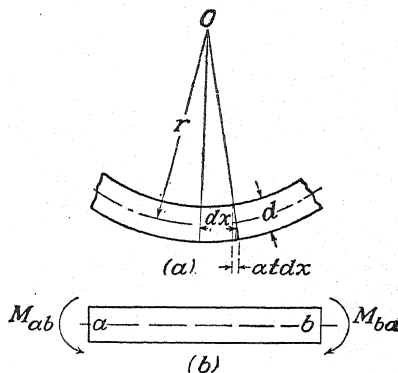
$$\frac{d}{r} = \frac{\alpha t \, dx}{dx},$$

which gives

$$\frac{1}{r} = \frac{\alpha t}{d}. \tag{e}$$

We can prevent the member from bending and keep its axis straight by applying end moments (Fig. 437b) of the magnitude[1]

$$M_{ba} = -M_{ab} = \frac{EI}{r} = \frac{EI\alpha t}{d}. \tag{f}$$

Having these moments for each nonuniformly heated member of a frame and considering them as fixed-end moments, we can calculate the end moments for all members by the same procedure we should use if the fixed-end moments were produced by lateral loads.

Take, for example, the frame in Fig. 435a. If the horizontal girder bc is nonuniformly heated, as assumed in Fig. 437, there will be fixed-end moments

$$\mathfrak{M}_{cb} = -\mathfrak{M}_{bc} = k_{bc}\alpha t \cdot \frac{l}{d}.$$

[1] In the derivation it was assumed that for an observer moving from a to b the temperature is higher to the right of axis ab.

Unlocking the joints, we obtain the angle of rotation θ_c from Eq. (74), with $\theta_b = -\theta_c$, which gives

$$(4k_{cd} + 2k_{cb})\theta_c = -k_{bc}\alpha t \frac{l}{d},$$

from which

$$\theta_c = -\frac{\kappa_{bc}}{4k_{cd} + 2k_{cb}} \alpha t \frac{l}{d}.$$

The thermal end moments then are

$$M_{cd} = -M_{cb} = -\frac{4k_{bc}k_{cd}}{4k_{cd} + 2k_{cb}} \alpha t \frac{l}{d}.$$

The same method is applicable if there are several nonuniformly heated members in the frame.

68. Secondary Stresses in Trusses.—In our previous analysis of trusses, it was always assumed that the truss members are joined by ideal hinges and that the loads are applied only at the joints. Thus the members of a truss are subjected to axial forces only, and these can be determined by the methods discussed in Chaps. II and VII. In actual cases the joints are usually riveted or welded; and because of this fact the members undergo, not only axial forces, but also bending. This bending can be analyzed as explained in the preceding article. In the case of building frames, in which the members carry lateral loads, the influence of such secondary bending on maximum stresses is usually negligible. But in bridge trusses, where the loads are applied only at the joints, all fixed-end moments vanish, and the only bending we have to consider is that due to changes in the lengths of the truss members. Naturally, under such circumstances, it must be considered in more detail.

Stresses produced by axial forces are usually called *primary stresses*, while those due to bending are called *secondary stresses*. In discussing secondary stresses we shall consider only trusses in one plane and assume that this plane represents the plane of symmetry for all members and that external loads are acting in the same plane. Then secondary bending of the members of a truss will occur in the plane of symmetry and there will be no twisting of members.[1]

Let us begin with a discussion of the symmetrical structure *abc*, shown in Fig. 438*a*, which consists of three members rigidly connected at the joints. Under the action of a vertical load P the inclined bars *ab* and *bc* undergo compression, while the horizontal bar *ac* undergoes extension. Owing to the rigidity of the joints, the ends of the members cannot rotate with respect to each other during deformation, and some bending ensues. In this case the bending is easy to visualize since joint *b* must move down to b_1 and joints *a* and *c* are moving apart to positions a_1 and c_1. At the same time the angles between the tangents to the elastic lines at the ends of the bars must remain unchanged. Hence, bending must be as shown with some exaggeration in the figure. The rigid joint *b*, from symmetry, does not rotate during this deformation, while joint *a* rotates clockwise and joint *c* counterclockwise by the same amount. On the bar *ab* there will act, not only the axial forces S (Fig. 438*b*), but also the end moments M_{ba}, M_{ab} and the shearing forces V_{ab} and V_{ba}. Considering, now, the forces acting on joint *b* (Fig. 438*c*), we see that the load P is balanced, not only by the axial forces S in the bars, but also by the shearing forces V. This indicates that the axial forces calculated on the assumption of ideal hinges at the joints are not the exact values of these forces in the case of a truss with rigid joints. However, this dis-

---

[1] For a discussion of twist see "Strength of Materials," vol. II, p. 265.

crepancy is small and usually can be neglected. Some idea regarding the magnitudes of the shearing forces V in our example (Fig. 438) can be obtained from the following considerations: Let us assume that $M_{ba} = M_{ab}$* and introduce the notations

σ_p = primary stress,

σ_s = maximum secondary stress,

l = length of the bar,

d = depth of the bar in the plane of bending,

A = cross-sectional area of the bar,

$Z = Ai^2/c$, the section modulus of the cross section of the bar.

Then,

$$S = A\sigma_p, \tag{a}$$

$$V = \frac{2M_{ba}}{l} = \frac{2\sigma_s Ai^2}{lc}. \tag{b}$$
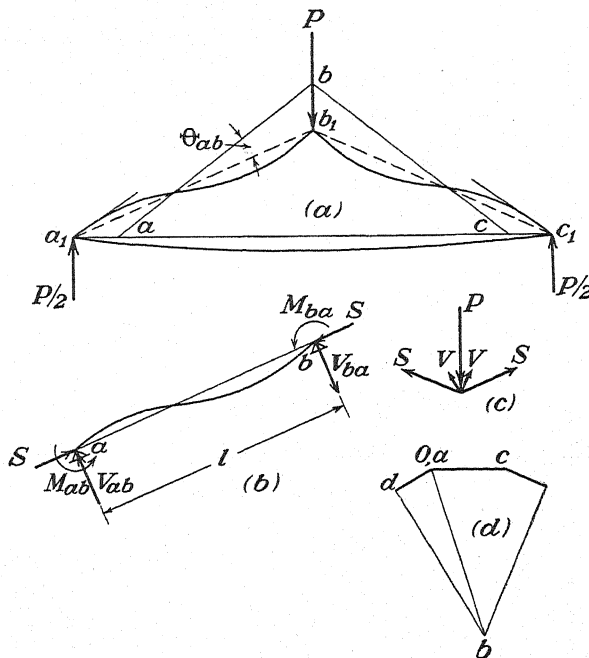
FIG. 438.

Assuming $d = 0.1l$, $i = 0.4d$, $c = 0.5d$, we find, by comparing expressions (a) and (b) that

$$V = 0.064S\frac{\sigma_s}{\sigma_p}.$$

This shows that, when σ_s is as large as 50 per cent of σ_p, the shearing force is only about 3 per cent of the axial force. In our further discussion it will be assumed that the shearing forces are negligible and that the axial forces calculated on the assumption

* This is the case if the horizontal member ac is absolutely rigid. Owing to flexibility of this member, M_{ab} is smaller than M_{ba}, and the discussion gives for V an exaggerated value.

of ideal hinges represent with sufficient accuracy the true axial forces in the members of a truss with rigid joints.[1]

We assume also that the changes in distance between joints depend entirely on the extensions or contractions of the members and that the changes of length due to curvature of the members can be neglected. This assumption is also accurate enough if we are dealing with stocky members such as compression members of heavy riveted bridges, where the calculation of secondary stresses becomes of practical importance.

The foregoing assumptions greatly simplify the analysis of secondary stresses since they allow us to divide the problem into two steps. First, assuming ideal hinges, we calculate all axial forces and the corresponding displacements of the joints. For this latter part of the calculation, we can use the methods discussed in Chap. VI. Using, for example, the Williot diagram, we obtain graphically the displacements of all joints. Then, taking a specific member, we determine from this diagram the components of the displacements of its ends in the direction perpendicular to the axis of the member. With these components, the angles of rotation such as the angle Θ_{ab} in our example (Fig. 438a) can be calculated readily. This finishes the first step in the analysis of secondary stresses.

In the second step, we introduce one more simplification, namely: we neglect the effect of axial forces on bending of the truss members. This does not cause substantial errors in the case of stocky compression members, for which secondary stresses are of practical importance, and represents common practice in bridge engineering.[2] With this final simplification, the problem of secondary stresses becomes similar to that of calculating end moments in frame structures. We write for each joint of the truss an equation of equilibrium [see Eq. (74) and Eq. (77)],

$$4\theta_a \Sigma k_{ai} + 2\Sigma k_{ai}\theta_i = 6\Sigma k_{ai}\Theta_{ai}, \tag{c}$$

in which the summation includes all members meeting at the joint under consideration. The right sides of these equations can be readily calculated since the angles Θ_{ai} are already determined from the Williot diagram. The solution of Eqs. (c) can then be made by successive approximations as explained in Art. 65. We have only to consider, instead of fixed-end moments, produced by lateral loads, the fixed-end moments, such as $-6k_{ai}\Theta_{ai}$, due to angular displacements Θ_{ai} of a bar ai.

For the example in Fig. 438, the Williot diagram is shown in Fig. 438d. Upon taking joint a as immovable and observing that joint c has a horizontal displacement $\overline{Oc}$, the displacement of joint b is represented by the vector $\overline{Ob}$, and the component of this displacement perpendicular to the member ab is $\overline{db}$. Dividing the length db by the length of the bar ab, we obtain the angle Θ_{ab}. Assume, for example, that the numerical value of the angle obtained in this manner is 0.001. Assume also that

$$k_{ab} = k_{bc} = k_{ac} = 2 \cdot 10^6 \text{ ft.-lb.}$$

---

[1] The effect of shearing forces can be taken into account later, as explained on p. 401.

[2] The first complete analysis of secondary stresses is due to H. Manderla, *Jahresber. Tech. Hochschule München*, 1878–1879, p. 18, and *Allgemeine Bauzeitung*, 1880. It considers the effect of axial forces on bending of members, which naturally complicates the calculations. Omitting this effect of axial forces, O. Mohr considerably simplified the secondary-stress analysis and gave it a form that has found wide practical application; see his work in *Zivilingenieur*, 1892, p. 577, and 1893, p. 67. A review of methods of secondary-stress analysis in bridges is given in the book by C. R. Grimm, "Secondary Stresses in Bridge Trusses," 1908. A more recent review is given by Cecil Von Abo in *Trans. A.S.C.E.*, vol. 89.

Then the fixed-end moments are

$$\mathfrak{M}_{ab} = \mathfrak{M}_{ba} = -\mathfrak{M}_{bc} = -\mathfrak{M}_{cb} = -6k_{ab}\Theta_{ab} = -12{,}000 \text{ ft.-lb.} \qquad (d)$$

Unlocking the joints and observing from symmetry that $\theta_b = 0$ while $\theta_c = -\theta_a$, we obtain for joint a, from Eq. (c),

$$(4k_{ab} + 2k_{ac})\theta_a = 6k_{ab}\Theta_{ab}.$$

Hence,

$$\theta_a = \Theta_{ab} = 0.001.$$

The distributed moments then are

$$M_{ab}{}' = 4k_{ab}\theta_a = 8{,}000 \text{ ft.-lb.,}$$
$$M_{ac}{}' = 2k_{ac}\theta_a = 4{,}000 \text{ ft.-lb.}$$

The total end moments are obtained by superposing the distributed moments on the fixed-end moments (d), which gives

$$M_{ab} = -12{,}000 + 8{,}000 = -4{,}000 \text{ ft.-lb.,}$$
$$M_{ac} = -M_{ca} = 4{,}000 \text{ ft.-lb.}$$

Considering also the carry-over moments, we obtain

$$M_{ba} = -M_{bc} = -12{,}000 + 4{,}000 = -8{,}000 \text{ ft.-lb.}$$

The largest moments are at joint b. They must be considered in calculating maximum secondary stress.

Having the foregoing values of end moments, we can improve our solution by calculating the shearing forces V and evaluating that part of the load P which is balanced by these forces. Only the remaining part of P is balanced by the axial forces S, and we can obtain a better approximation for these forces and for the axial deformations of the members. With these new values of the axial deformations, a better approximation for the angle Θ_{ab} and for the end moments can be obtained. In practical applications, however, such refinement in calculation is usually not justified.

With the approximate values of axial forces and end moments, we can investigate also the deflection of members and find the magnitude of errors that result from omitting the influence of axial forces on bending, and the effect of curvature on lengths of members.[1]

As a second example, let us consider the truss shown in Fig. 439, loaded at the middle.[2] All necessary dimensions are given in Table X.* By using the figures in the last column of this table, the axial deformations of all bars can be calculated, and the Williot diagram can be constructed. The angles Θ for all bars can be obtained from this diagram. Multiplying these angles by the corresponding values of $-6EI/l$, we obtain the fixed-end moments given in the sixth column of the table. All these moments are negative since each Θ is positive for the left-hand part of the truss. The

---

[1] These effects may become important in the case of slender members as in airplane structures. See papers by B. W. James, *N.A.C.A. Tech. Note* 534, 1935, and by N. J. Hoff, *J. Aeronautical Sci.*, vol. 8, p. 319, 1941.

[2] This example is discussed by using somewhat different methods in the book by Johnson, Bryan, and Turneaure, "Modern Framed Structures," pt. 2, p. 441, and also in the book by J. I. Parcel and G. A. Maney, "Statically Indeterminate Stresses," p. 323.

* The truss is symmetrical, and all calculations are made for the left half. Joints 6 and 7, from symmetry, do not rotate.

calculations required in using the method of successive approximations are given in Fig. 440. Starting the distribution of moments with joint 5, in which the unbalanced moment is the largest, and proceeding in the usual way, we finally obtain the end moments written under the double lines in Fig. 440. Using these moments and the
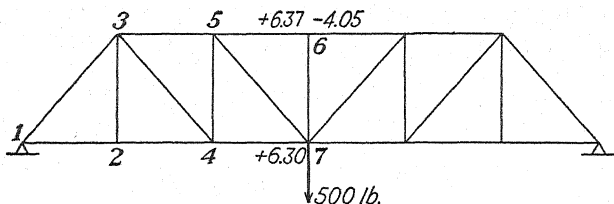
Fig. 439.

figures in columns (4) and (5) of the table,[1] we can calculate the secondary stress at each end of each member. The largest secondary stresses in this case occur in the horizontal bars at joints 7 and 6. These stresses are shown in Fig. 439. For the bar 4-7, the secondary stress is about 66 per cent of the primary stress given in column (7) of the table.

TABLE X

(1)	(2)	(3)	(4)	(5)	(6)	(7)
Member	Area, in.^{2}	Length, in.	I, in.^{4}	c, in.	$-\dfrac{6EI}{l}\Theta$, lb.in.	σ_p, lb./in.^{2}
1-2	29.44	320	1,218	9.12	−1,145	+ 7.30
1-3	58.49	490.7	4,490	$\begin{cases} 9.54 \\ 14.08 \end{cases}$	−2,384	− 5.63
2-3	16.00	372	94.8	5.4	− 49	0
2-4	29.44	320	1,218	9.12	−1,107	+ 7.30
3-4	29.42	490.7	805	7.5	− 350	+11.35
3-5	52.35	320	3,978	$\begin{cases} 9.19 \\ 14.43 \end{cases}$	−4,440	− 8.20
4-5	26.48	372	750	7.5	− 226	− 9.42
4-7	45.48	320	1,907	9.12	−1,932	+ 9.45
5-6	52.35	320	3,978	$\begin{cases} 9.19 \\ 14.43 \end{cases}$	−3,220	−12.3
5-7	20.58	490.7	358	6.0	− 107	+16.0
6-7	14.70	372	288	6.0	0	0

The foregoing example shows that, by using the method of successive approximations, the secondary stresses may be obtained without much difficulty. Such stresses are especially important in the design of compression members.

In the analysis above it was assumed that the axes of all members meeting at a joint intersect in one point. If some members are attached to a joint with certain eccentricities, the corresponding moments must be treated as external moments and must be algebraically added to the previously considered unbalanced moments produced by rotations of the members.

[1] For bars 1-3, 3-5, and 5-6, unsymmetrical with respect to their gravity axes, two values of c are given in column 5.

The lengths of members in the preceding analysis were taken as the theoretical lengths, *i.e.*, the distances between the centers of joints. Actually, the ends of each member are reinforced by plates at the joints; and, to take this fact into consideration,
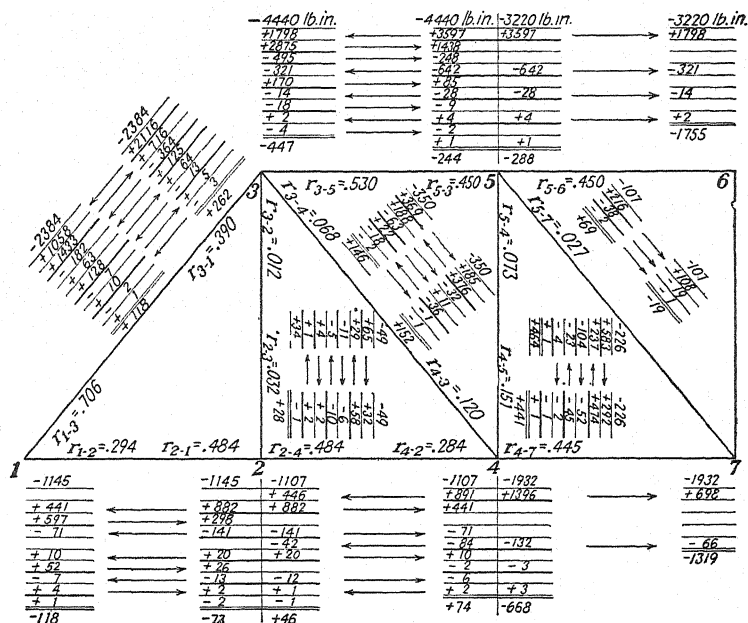
FIG. 440.

Eqs. (c) must be replaced by those developed for members of variable cross section.[1] Calculations of this kind indicate that reinforcements at the joints may have a considerable influence on the magnitude of secondary stresses.[2]

69. Simply Supported Beams of Variable Cross Section.—Often, especially in reinforced-concrete structures, beams are deepened near their supports as shown in Figs. 441a and 441b in order to avoid the sharp re-entrant corner that otherwise occurs at the junction of a beam with a column. In such a case there arises the question of how the haunches affect the angles of rotation of the ends of the beam. To calculate these angles, we use Eqs. (42) of Art. 56. Multiplying and dividing these equations by the constant moment of inertia I_0 of the uniform portion of the beam, we obtain

$$\left.\begin{aligned}
\theta_{ab} &= \int_0^l \frac{l-x}{l} \cdot \frac{M}{EI_0} \cdot \frac{I_0}{I}\, dx, \\
\theta_{ba} &= -\int_0^l \frac{x}{l} \cdot \frac{M}{EI_0} \cdot \frac{I_0}{I}\, dx.
\end{aligned}\right\} \tag{81}$$

[1] See Art. 70.

[2] See paper by K. A. ČALIŠEV previously mentioned (p. 384).

In this manner the problem is reduced to that of a beam of uniform flexural rigidity EI_0. To take care of the cross-sectional variation, we have only to use MI_0/I, instead of M. This means that the fictitious load is given in this case by the modified bending-moment diagram, obtained by multiplying the bending moment at each cross section by the
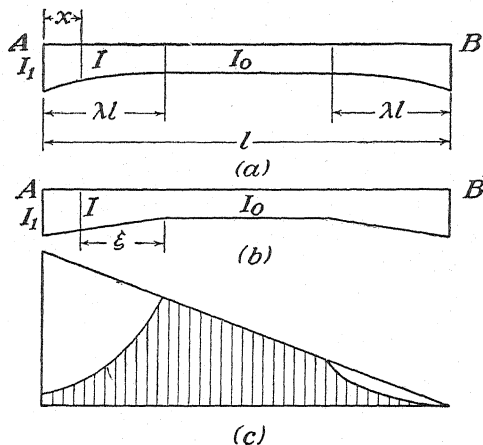
Fig. 441.
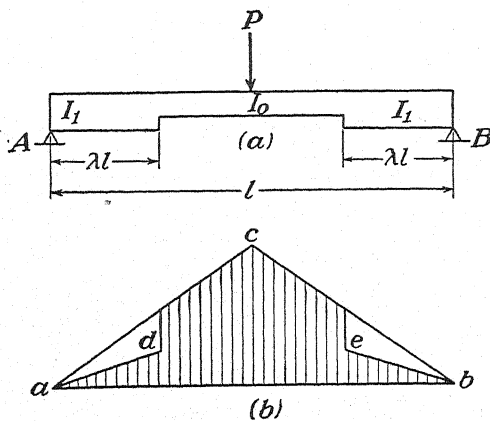
Fig. 442.

ratio I_0/I. Take, for example, the case shown in Fig. 442a. A beam with reinforced ends is bent by a load P applied at the middle. The modified bending-moment diagram is shown by the shaded area in Fig. 442b. Along the reinforced portions of the beam, of length λl, the ordinates of the bending-moment diagram acb are reduced in a constant ratio $I_0:I_1$. The angles of rotation of the ends of the beam are now obtained if we divide by EI_0 the shearing forces produced at the ends of the beam by the fictitious load represented by the shaded area in Fig.

442*b*.   It is seen that owing to the reinforcement of the ends of the beam these angles of rotation will be diminished in the same ratio as the fictitious load is diminished when we replace the bending-moment area *acb* by the modified bending-moment area. Assume, for example, that $\lambda = \frac{1}{4}$ and $I_0/I_1 = \frac{1}{2}$. Then the fictitious load is reduced in the ratio 7:8, and the angles of rotation will be diminished by one-eighth of the values obtained for a beam having uniform flexural rigidity EI_0.

In such cases as shown in Fig. 441, the ratio I_0/I varies along the length of the haunches, and instead of the straight lines *ad* and *eb* shown in Fig. 442*b* we shall obtain certain curves. We always can trace these curves with sufficient accuracy by dividing the length λl of a haunch into several parts and calculating the ratio I_0/I for each division part. Naturally the shape of the modified bending-moment diagram will depend on the form of the haunches. Assume, for example, that the beam with straight haunches (Fig. 441*b*) is bent by a couple M_{ab} applied at the end *A*. Then the bending-moment diagram is the triangle shown in Fig. 441*c*. Since the depth of the beam increases linearly with the distance ξ from the uniform portion of the beam and since I is proportional to the cube of the depth, we obtain

$$I = I_0 \left[1 + \left(\sqrt[3]{\frac{I_1}{I_0}} - 1 \right) \frac{\xi}{\lambda l} \right]^3,$$

where I_1 is the moment of inertia at the support. Taking, for example, $I_1/I_0 = 10$, $\lambda = 0.3$, we find

$\xi/\lambda l =$	0	$\frac{1}{4}$	$\frac{1}{2}$	$\frac{3}{4}$	1
$I_0/I =$	1	0.467	0.255	0.154	0.100

The corresponding modified bending-moment area is shaded in Fig. 441*c*. Treating this area as a fictitious load and calculating the corresponding shearing forces at the ends of the beam, we obtain the angles of rotation

$$\theta_{ab} = 0.526 \, \frac{M_{ab}l}{3EI_0}, \qquad \theta_{ba} = -0.760 \, \frac{M_{ab}l}{6EI_0}.$$

In a similar manner the angles of rotation of the ends can be calculated for other shapes of haunches and for various kinds of loading.

For the shapes of haunches that are most often encountered in practical applications, there are tables calculated from Eqs. (81). Using such tables, the problems of bending of beams of variable cross section can be easily solved.[1]   For illustration we shall consider the sym-

---

[1] Such tables were calculated by A. Strassner; see his book, "Neure Methoden zur

metrical beams of rectangular cross section shown in Fig. 441. The first of these beams has parabolic haunches, and the second has straight haunches. If an end moment M_{ab} acts on such a beam, the angles of rotation can be calculated from Eqs. (81) and represented by the following equations,

$$\theta_{ab} = \frac{M_{ab}l}{3EI_0}\,\varphi_{ab}, \qquad \theta_{ba} = -\frac{M_{ab}l}{6EI_0}\,\varphi_{ba}, \tag{82}$$

where φ_{ab} and φ_{ba} are numerical factors, smaller than unity, representing the effect of haunches on the angles of rotation. These constants depend on the ratio λ of the length of a haunch to the length l of the beam and also on the ratio $n = I_0/I_1$. The values of these factors for parabolic and straight haunches are given in Tables XI and XII, respectively.

TABLE XI.—CONSTANTS φ_{ab} AND φ_{ba} FOR PARABOLIC HAUNCHES (FIG. 441a)

λ	$n =$	0.60	0.30	0.20	0.15	0.12	0.10	0.08	0.06	0.05	0.04	0.03	0.02
0.50	$\varphi_{ab} =$	0.820	0.640	0.559	0.510	0.476	0.451	0.422	0.389	0.370	0.348	0.323	0.292
	$\varphi_{ba} =$	0.904	0.790	0.731	0.693	0.665	0.642	0.616	0.585	0.566	0.543	0.515	0.479
0.40	$\varphi_{ab} =$	0.850	0.699	0.631	0.589	0.560	0.539	0.515	0.486	0.470	0.452	0.430	0.403
	$\varphi_{ba} =$	0.935	0.858	0.818	0.792	0.773	0.757	0.739	0.718	0.704	0.689	0.670	0.644
0.35	$\varphi_{ab} =$	0.866	0.730	0.669	0.631	0.605	0.586	0.564	0.538	0.524	0.507	0.487	0.462
	$\varphi_{ba} =$	0.949	0.889	0.857	0.837	0.821	0.809	0.795	0.777	0.767	0.754	0.739	0.719
0.30	$\varphi_{ab} =$	0.883	0.763	0.709	0.676	0.653	0.635	0.616	0.593	0.580	0.565	0.547	0.525
	$\varphi_{ba} =$	0.962	0.916	0.892	0.876	0.865	0.856	0.845	0.832	0.824	0.814	0.803	0.787
0.25	$\varphi_{ab} =$	0.899	0.797	0.751	0.722	0.702	0.687	0.671	0.651	0.639	0.626	0.611	0.592
	$\varphi_{ba} =$	0.973	0.940	0.923	0.913	0.904	0.897	0.889	0.880	0.874	0.867	0.859	0.848
0.20	$\varphi_{ab} =$	0.918	0.834	0.795	0.771	0.755	0.743	0.729	0.712	0.703	0.692	0.679	0.663
	$\varphi_{ba} =$	0.982	0.961	0.950	0.942	0.937	0.932	0.927	0.921	0.917	0.913	0.907	0.900
0.15	$\varphi_{ab} =$	0.937	0.872	0.842	0.823	0.811	0.801	0.790	0.777	0.770	0.761	0.751	0.738
	$\varphi_{ba} =$	0.990	0.977	0.971	0.967	0.964	0.961	0.958	0.954	0.952	0.950	0.946	0.942

If a uniformly distributed load acts on a beam of the form shown in Fig. 441, the angles of rotation of the ends are numerically equal and are represented by the equation[1]

Statik der Rahmentragwerke," 4th ed., vol. I, Berlin, 1937. Following the work of Strassner, W. Ruppel prepared an extensive set of tables for haunched beams; see *Trans. A.S.C.E.*, vol. 90, p. 152, 1927. A useful series of charts for calculating beams of variable cross section are given also in the book by R. Guldan, "Rahmentragwerke und Durchlaufträger," Vienna, 1940. The curves used in our further discussion of beams of variable cross section are taken from the latter book.

[1] This can be proved by using Eqs. (81). See the above-mentioned book by A. Strassner, p. 83.

$$\theta_{ab} = -\theta_{ba} = \frac{ql^3}{24EI}\, \varphi_{ba}, \tag{83}$$

where φ_{ba} is the constant which we already have had in the second of Eqs. (82) and the values of which can be taken from Tables XI and XII.

TABLE XII.—CONSTANTS φ_{ab} AND φ_{ba} FOR STRAIGHT HAUNCHES (FIG. 441b)

λ	$n =$	0.60	0.30	0.20	0.15	0.12	0.10	0.08	0.06	0.05	0.04	0.03	0.02
0.50	$\varphi_{ab} =$	0.753	0.519	0.421	0.364	0.326	0.298	0.267	0.233	0.214	0.193	0.169	0.141
	$\varphi_{ba} =$	0.845	0.637	0.548	0.492	0.453	0.424	0.390	0.351	0.328	0.302	0.272	0.235
0.40	$\varphi_{ab} =$	0.792	0.595	0.512	0.463	0.431	0.407	0.381	0.351	0.335	0.317	0.297	0.273
	$\varphi_{ba} =$	0.881	0.751	0.689	0.650	0.623	0.602	0.578	0.551	0.535	0.517	0.495	0.468
0.35	$\varphi_{ab} =$	0.813	0.635	0.560	0.516	0.486	0.465	0.441	0.414	0.400	0.383	0.365	0.343
	$\varphi_{ba} =$	0.906	0.803	0.753	0.723	0.701	0.684	0.665	0.643	0.630	0.616	0.598	0.577
0.30	$\varphi_{ab} =$	0.835	0.678	0.611	0.572	0.545	0.526	0.505	0.481	0.468	0.453	0.436	0.417
	$\varphi_{ba} =$	0.928	0.850	0.813	0.789	0.773	0.760	0.745	0.728	0.719	0.707	0.694	0.677
0.25	$\varphi_{ab} =$	0.858	0.723	0.665	0.631	0.608	0.591	0.573	0.552	0.540	0.527	0.513	0.496
	$\varphi_{ba} =$	0.949	0.893	0.866	0.849	0.836	0.828	0.817	0.805	0.798	0.789	0.780	0.768
0.20	$\varphi_{ab} =$	0.883	0.771	0.722	0.694	0.675	0.661	0.645	0.628	0.618	0.607	0.595	0.580
	$\varphi_{ba} =$	0.966	0.929	0.911	0.900	0.892	0.886	0.879	0.871	0.866	0.861	0.854	0.846
0.15	$\varphi_{ab} =$	0.909	0.822	0.784	0.762	0.747	0.736	0.724	0.710	0.702	0.694	0.684	0.672
	$\varphi_{ba} =$	0.980	0.959	0.949	0.942	0.937	0.934	0.930	0.925	0.922	0.919	0.915	0.911

If end moments together with a uniform load act on a symmetrical beam of variable cross section, we use Eqs. (82) and (83) together, and by superposition we obtain for the angles of rotation of the ends the following expressions:

$$\left.\begin{aligned}
\theta_{ab} &= \frac{M_{ab}l}{3EI_0}\, \varphi_{ab} - \frac{M_{ba}l}{6EI_0}\, \varphi_{ba} + \frac{ql^3}{24EI_0}\, \varphi_{ba}, \\
\theta_{ba} &= \frac{M_{ba}l}{3EI_0}\, \varphi_{ab} - \frac{M_{ab}l}{6EI_0}\, \varphi_{ba} - \frac{ql^3}{24EI_0}\, \varphi_{ba}.
\end{aligned}\right\} \tag{84}$$

Using Tables XI and XII for the factors φ_{ab} and φ_{ba}, we can readily calculate these angles for any given values of end moments and uniform load. When the beam has a uniform cross section, $\varphi_{ab} = \varphi_{ba} = 1$ and Eqs. (84) coincide with Eqs. (45) for prismatical bars.

If there is a rotation Θ_{ab} of a beam as a rigid body (Fig. 391), the angles of rotation of the ends are

$$\left.\begin{aligned}
\theta_{ab} &= \frac{M_{ab}l}{3EI_0}\, \varphi_{ab} - \frac{M_{ba}l}{6EI_0}\, \varphi_{ba} + \frac{ql^3}{24EI_0}\, \varphi_{ba} + \Theta_{ab}, \\
\theta_{ba} &= \frac{M_{ba}l}{3EI_0}\, \varphi_{ab} - \frac{M_{ab}l}{6EI_0}\, \varphi_{ba} - \frac{ql^3}{24EI_0}\, \varphi_{ba} + \Theta_{ab}.
\end{aligned}\right\} \tag{85}$$

Solving these equations for M_{ab} and M_{ba}, we obtain

$$M_{ab} = \frac{EI_0}{l} (\alpha\theta_{ab} + \beta\theta_{ba}) - \gamma \frac{EI_0}{l} \Theta_{ab} - \delta \frac{ql^2}{12},$$
$$M_{ba} = \frac{EI_0}{l} (\alpha\theta_{ba} + \beta\theta_{ab}) - \gamma \frac{EI_0}{l} \Theta_{ab} + \delta \frac{ql^2}{12},$$

$$(86)$$

where α, β, γ, and δ are *beam constants* having the following values:

$$\alpha = \frac{12\varphi_{ab}}{4\varphi_{ab}^2 - \varphi_{ba}^2}, \qquad \beta = \frac{6\varphi_{ba}}{4\varphi_{ab}^2 - \varphi_{ba}^2},$$
$$\gamma = \frac{6}{2\varphi_{ab} - \varphi_{ba}} = \alpha + \beta, \qquad \delta = \frac{3\varphi_{ba}}{2\varphi_{ab} + \varphi_{ba}}.$$

$$(87)$$

Equations (86) are the slope-deflection equations for uniformly loaded symmetrical beams of variable cross section.
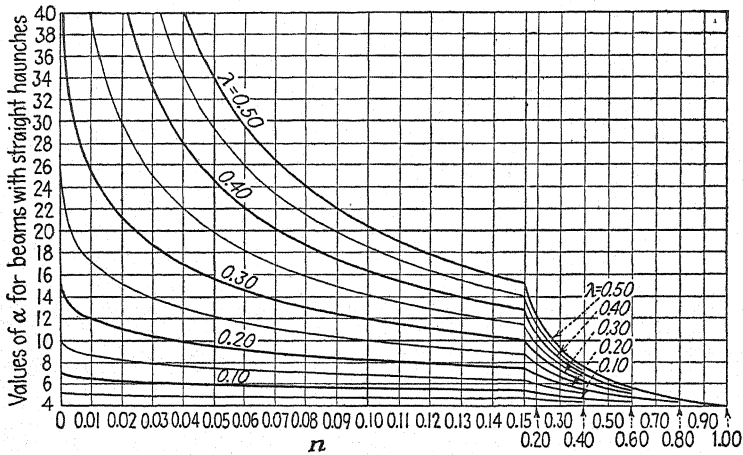
FIG. 443.

When $n = I_0/I_1 = 1$, we have $\varphi_{ab} = \varphi_{ba} = 1$, $\alpha = 4$, $\beta = 2$, $\gamma = 6$, $\delta = 1$ and Eqs. (86) coincide with Eqs. (48). To simplify the use of Eqs. (86), charts for the coefficients α, β, and δ have been constructed for various shapes of beams. Figures 443, 444, and 445 represent such charts of α, β, and δ, respectively, for beams with straight haunches as shown in Fig. 441b. Some applications of these curves will be shown later.

In the case of a concentrated load P (Fig. 446) the slope-deflection equations are

$$M_{ab} = \frac{EI_0}{l} (\alpha\theta_{ab} + \beta\theta_{ba}) - \gamma \frac{EI_0}{l} \Theta_{ab} - \eta_{ab}Pl,$$
$$M_{ba} = \frac{EI_0}{l} (\alpha\theta_{ba} + \beta\theta_{ab}) - \gamma \frac{EI_0}{l} \Theta_{ab} + \eta_{ba}Pl.$$

$$(88)$$
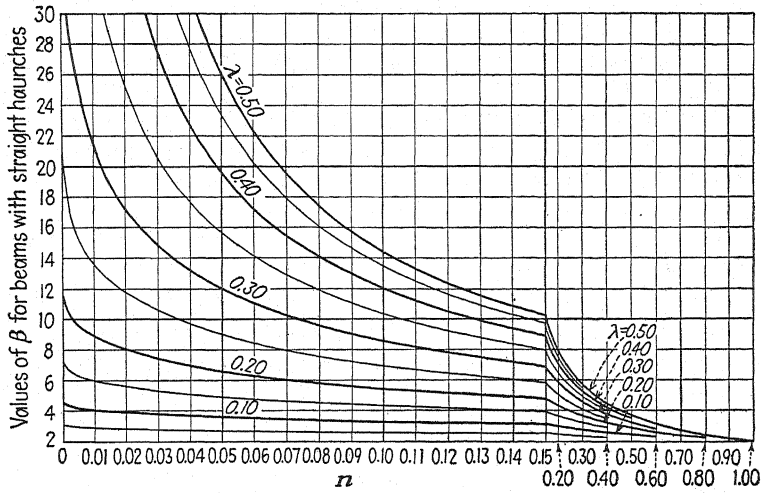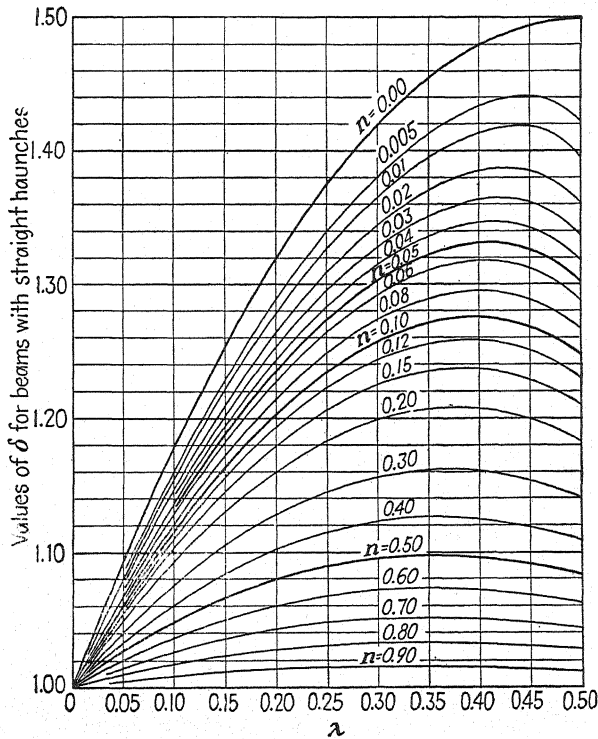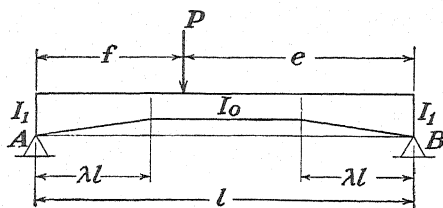
Fig. 444.

Fig. 445.

Fig. 446.
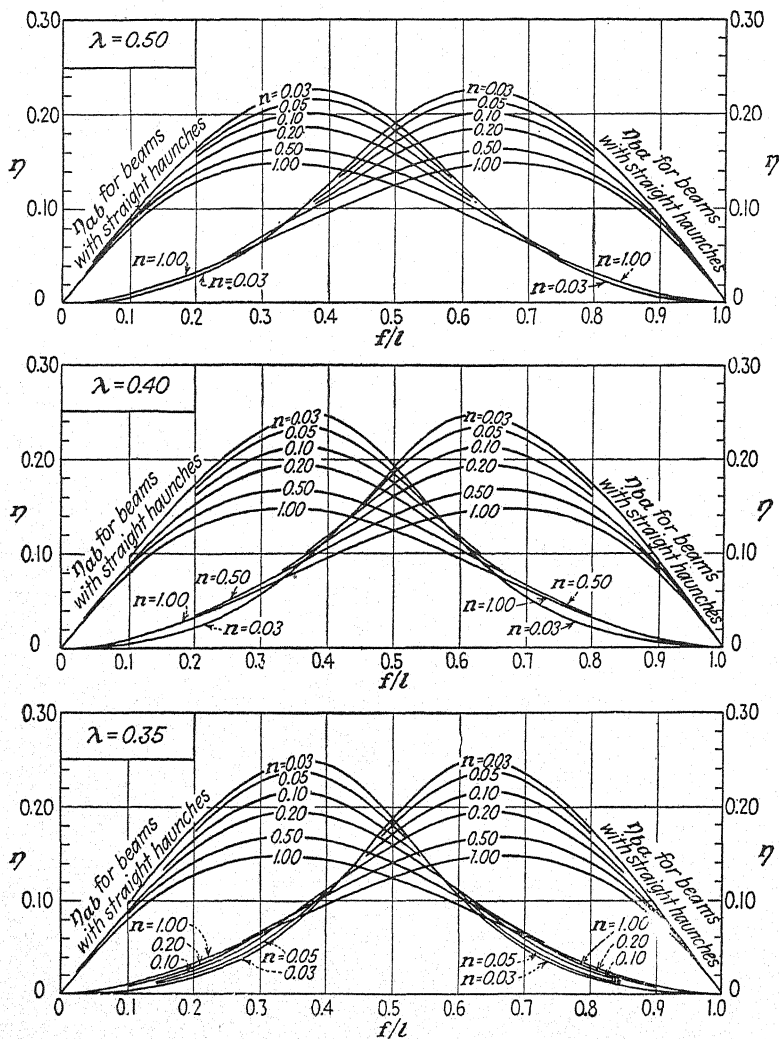
Fig. 447.

These equations differ from Eqs. (86) only in the last terms, depending on the kind of lateral load. The values of the constants η_{ab} and η_{ba} calculated for beams with straight haunches and for various positions of the load P are given by the curves in Figs. 447 and 448.*
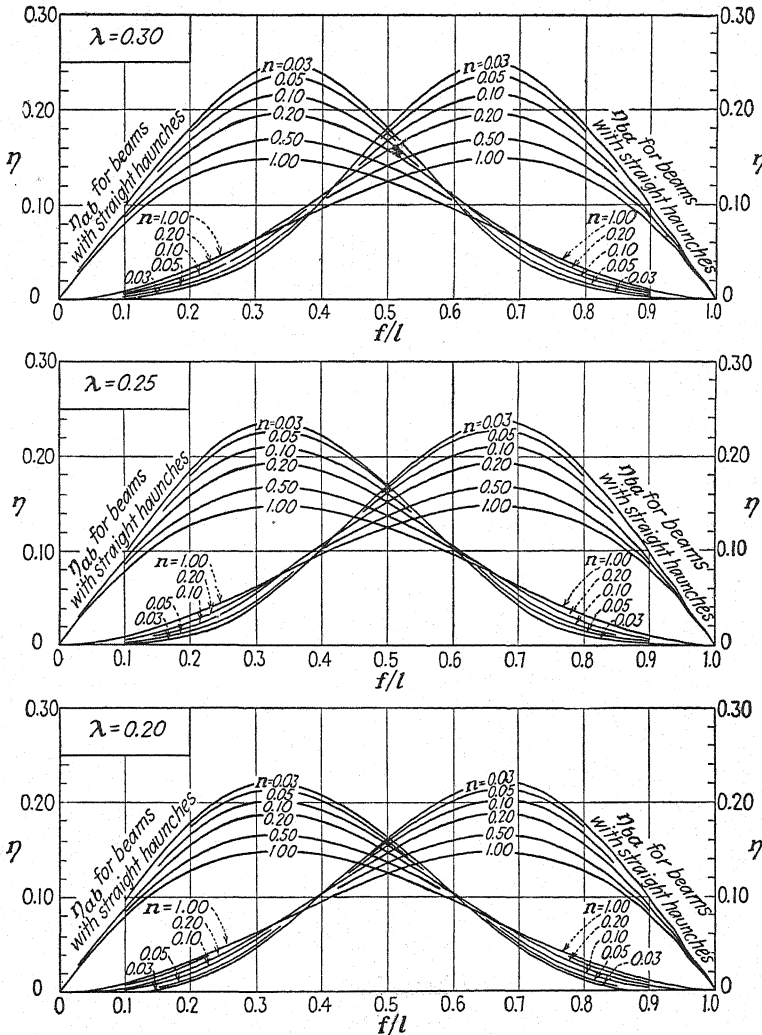
FIG. 448.

70. Statically Indeterminate Beams of Variable Cross Section.— By using the slope deflection equations of the preceding article, various statically indeterminate problems for beams of variable cross section

* In the previously mentioned book by R. Guldan there are given charts also for symmetrical beams with parabolic haunches and for some unsymmetrical beams.

can be readily solved. Let us begin with a beam one end of which is hinged and the other built-in (Fig. 393). If a known end moment M_{ab} acts, as shown, the magnitude of the end moment M_{ba} produced at the fixed end B is found from the second of Eqs. (84). Substituting $\theta_{ba} = 0$ and $q = 0$ in this equation, we obtain

$$M_{ba} = \frac{\varphi_{ba}}{2\varphi_{ab}} M_{ab}. \tag{89}$$

If the form of the beam is such as is shown in Fig. 441a or Fig. 441b, the values of the constants φ_{ba} and φ_{ab} can be taken from Table XI or XII and the magnitude of the moment M_{ba}, carried over to the fixed end B, can be readily calculated. Since φ_{ba} is larger than φ_{ab} the *carry-over factor* $\varphi_{ba}/2\varphi_{ab}$ is larger than $\frac{1}{2}$ as for uniform beams (see page 340).

To establish the relation between M_{ab} and θ_{ab}, we use the first of Eqs. (86). Substituting $\theta_{ba} = 0$, $\Theta_{ab} = 0$, $q = 0$ in this equation, we obtain

$$M_{ab} = \alpha \frac{EI_0}{l} \theta_{ab}. \tag{90}$$

In the case of a symmetrical beam with straight haunches the value of α can be taken from the curves in Fig. 443. In the case of parabolic haunches, α can be calculated from the first of Eqs. (87) by using Table XI.

If a uniform load acts on a symmetrical beam with one end built-in (Fig. 393b), the redundant end moment M_{ba} is obtained from the second of Eqs. (84). Substituting $M_{ab} = 0$, $\theta_{ba} = 0$ in this equation, we obtain

$$M_{ba} = \frac{\varphi_{ba}}{\varphi_{ab}} \frac{ql^2}{8}. \tag{91}$$

This moment can be readily calculated by using Table XI or XII.

In the case of a concentrated force acting on the beam, we use Eqs. (88). Substituting $M_{ab} = 0$, $\theta_{ba} = 0$, $\Theta_{ab} = 0$ in these equations, we obtain

$$M_{ba} = \left(\frac{\beta}{\alpha} \eta_{ab} + \eta_{ba} \right) Pl. \tag{92}$$

To calculate this moment, we have in each particular case to substitute for the beam constants α, β, η_{ab}, and η_{ba} the values taken from Figs. 443, 444, 447 and 448.

Let us consider now the case of symmetrical beams (Fig. 441) with both ends built-in and find the fixed-end moments. If the beam is uniformly loaded along the entire span, we use Eqs. (86). Substituting $\theta_{ab} = \theta_{ba} = \Theta_{ab} = 0$ in these equations, we find for the required fixed-end moments the following expressions:

$$\mathfrak{M}_{ab} = -\delta \frac{ql^2}{12}, \qquad \mathfrak{M}_{ba} = \delta \frac{ql^2}{12}. \tag{93}$$

The values of δ for straight haunches are given by the curves in Fig. 445. These curves show clearly how the end moments are affected by reinforcement of the ends. Take, for example, $\lambda = 0.3$ and $n = I_0/I_1 = 0.3$. Then, from the corresponding curve in Fig. 445, we find $\delta = 1.155$, and the required moments are

$$\mathfrak{M}_{ab} = -\mathfrak{M}_{ba} = -1.155 \cdot \frac{ql^2}{12}.$$

We see that, owing to haunches, the fixed-end moments in this case become larger by about 16 per cent than for a uniform beam. We see also from the curves in Fig. 445 that for smaller values of n and larger values of λ the fixed-end moments may become still larger and that they approach the value $1.5 ql^2/12$ as n approaches zero and λ approaches the value 0.5. It should be noted that, although the end moments are increased owing to the haunches, the section modulus at the ends of the beam is increased in a greater proportion. Thus any reinforcement of the ends of the beam results in some decrease of bending stresses at the supports.

In the case of parabolic haunches the values of the coefficient δ in Eqs. (93) can be readily calculated by using the last of Eqs. (87) together with Table XI on page 406.

If a beam with built-in ends is loaded by a concentrated force P, we use Eqs. (88). Substituting $\theta_{ab} = \theta_{ba} = \Theta_{ab} = 0$ in these equations, we obtain

$$\mathfrak{M}_{ab} = -\eta_{ab} Pl, \qquad \mathfrak{M}_{ba} = \eta_{ba} Pl. \tag{94}$$

The values of the factors η_{ab} and η_{ba} for symmetrical beams with straight haunches are given by the curves in Figs. 447 and 448. We can see from these curves how haunches affect the values of the fixed-end moments if we observe that the curves marked $n = 1$ give us fixed-end moments for beams of uniform cross section.

If bending of a symmetrical beam of variable cross section is produced by displacement of support B by an amount Δ with respect to support A and no rotations of the ends are allowed to occur during that displacement, we obtain the end moments from Eqs. (88) by substituting

$$\theta_{ab} = \theta_{ba} = P = 0.$$

This gives

$$\left. \begin{aligned} M_{ab} &= -\gamma \frac{EI_0}{l} \Theta_{ab} = -\gamma \frac{EI_0}{l} \cdot \frac{\Delta}{l}, \\ M_{ba} &= -\gamma \frac{EI_0}{l} \Theta_{ab} = -\gamma \frac{EI_0}{l} \cdot \frac{\Delta}{l}. \end{aligned} \right\} \tag{95}$$

In the case of straight haunches, the factor $\gamma = \alpha + \beta$ in these equations can be determined by using the curves in Figs. 443 and 444. In the case of parabolic haunches, we use Eqs. (87) together with Table XI to calculate γ.

Now let us consider a continuous beam of variable cross section. Assuming that all spans have symmetrical form as in Fig. 441 and considering two adjacent spans as shown in Fig. 395, we obtain, for a uniformly distributed load, from Eqs. (84),

$$\theta_{n,n-1} = \frac{M_{n,n-1}l_n}{3E(I_0)_n}\,\varphi_{n,n-1} - \frac{M_{n-1,n}l_n}{6E(I_0)_n}\,\varphi_{n-1,n} - \frac{q_n l_n{}^3}{24E(I_0)_n}\,\varphi_{n-1,n},$$

$$\theta_{n,n+1} = \frac{M_{n,n+1}l_{n+1}}{3E(I_0)_{n+1}}\,\varphi_{n,n+1} - \frac{M_{n+1}l_{n+1}}{6E(I_0)_{n+1}}\,\varphi_{n+1,n} + \frac{q_{n+1}l_{n+1}{}^3}{24E(I_0)_{n+1}}\,\varphi_{n+1,n}.$$

In the particular case where all spans have the same constants and the same cross sections within the uniform portions of the spans, we obtain

$$(I_0)_n = (I_0)_{n+1} = I_0, \qquad \varphi_{n,n-1} = \varphi_{n,n+1} = \varphi_{ab}, \qquad \varphi_{n-1,n} = \varphi_{n+1,n} = \varphi_{ba}.$$

Equating the angles $\theta_{n,n-1}$ and $\theta_{n,n+1}$ and introducing bending moments at the supports instead of end moments, we obtain the following three-moment equation:

$$M_{n-1}l_n\varphi_{ba} + 2M_n\varphi_{ab}(l_n + l_{n+1}) + M_{n+1}l_{n+1}\varphi_{ba}$$
$$= -\frac{\varphi_{ba}}{4}\,(q_n l_n{}^3 + q_{n+1}l_{n+1}{}^3). \quad (96)$$

In the case of a beam of uniform cross section, we have

$$\varphi_{ab} = \varphi_{ba} = 1,$$

and Eq. (96) coincides with that for a continuous beam of uniform cross section.

Take, for example, a uniformly loaded beam with four equal spans, and assume that within each span the form of the beam is as shown in Fig. 449a. Assume also that $n = I_0/I_1 = 0.12$ and $\lambda = 0.25$. Then from Table XII on page 407 we obtain $\varphi_{ab} = 0.608$, $\varphi_{ba} = 0.836$. Writing Eq. (96) for spans 1 and 2 and then for spans 2 and 3 and observing that, from symmetry, $M_1 = M_3$, we obtain the following equations:

$$4M_1 l \cdot 0.608 + M_2 l \cdot 0.836 = -\frac{ql^3}{2} \cdot 0.836,$$

$$2M_1 l \cdot 0.836 + 4M_2 l \cdot 0.608 = -\frac{ql^3}{2} \cdot 0.836.$$

From these equations, we find

$$M_1 = -0.148ql^2, \qquad M_2 = -0.0703ql^2.$$

The corresponding bending-moment diagram is shown in Fig. 449b.

For comparison there is shown also, by a dotted line, the bending-moment diagram for the case of a beam of uniform cross section. It is seen that owing to the effect of haunches the bending moments at the supports 1 and 3 are increased by about 38 per cent, while at the middle of the spans the bending moments are decreased.
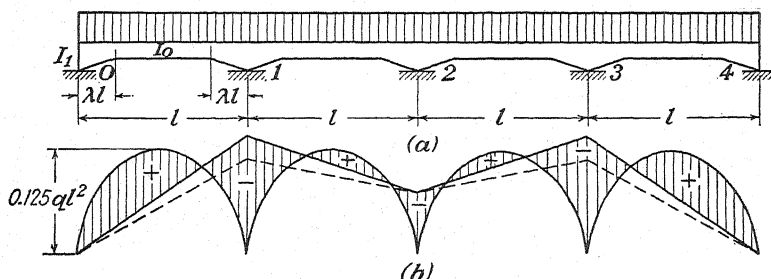

FIG. 449.

71. Frames with Nonprismatic Members.—In our previous analysis of frames, we always assumed that the members are of uniform cross section. However, the same methods of analysis can be extended to cases where the members are of variable cross section. In the analysis of a frame by the method of successive approximations, we have to perform three kinds of operations in which the variation in cross section must be considered, namely: (1) calculation of fixed-end moments, (2) calculation of distribution factors, and (3) calculation of carry-over factors. The fixed-end moments for symmetrical members are obtained from Eqs. (93) or (94). In the case of straight haunches, the beam constants δ and η appearing in these equations can be taken from the curves in Figs. 445, 447, 448. Otherwise, it will be necessary to determine the beam constants by using the general method described in Art. 69.

In calculating distribution factors, we have to use Eq. (90) (page 412), which determines the moment required to rotate the simply supported end of a member through a given angle when the other end is fixed. Using the notation k with proper subscripts for the quantities EI_0/l, we obtain from Eq. (90)

$$M_{ab} = \alpha_{ab} k_{ab} \theta_{ab}, \tag{a}$$

where α_{ab} is a beam constant that, in the case of straight haunches, can be taken from the curves in Fig. 443. If there are several members meeting at joint a with their far ends fixed and an unbalanced moment $\mathbf{M}_a$ acts on the joint, the angle of rotation θ_a of the joint is obtained from the equation of equilibrium

$$\theta_a \Sigma \alpha_{ai} k_{ai} = \mathbf{M}_a,$$

where the summation includes all members meeting at joint a. The portion of the unbalanced moment that is transmitted to a member ab is

$$M_{ab} = \alpha_{ab} k_{ab} \theta_a = \frac{\alpha_{ab} k_{ab}}{\Sigma \alpha_{ai} k_{ai}} \cdot \mathbf{M}_a.$$

Hence the distribution factor in this case is

$$r_{ab} = \frac{\alpha_{ab} k_{ab}}{\Sigma \alpha_{ai} k_{ai}}. \tag{97}$$

Having calculated these factors for all members at each joint, we can accomplish the distribution of unbalanced moments in the same manner as in the case of prismatic members.

If one of the members meeting at joint a, say the member ab, is hinged at the far end, we use the first of Eqs. (82) (page 406) and, instead of Eq. (a), we obtain

$$M_{ab} = \frac{3k_{ab}}{\varphi_{ab}} \theta_{ab}. \qquad (b)$$

In the case of symmetrical beams with straight or parabolic haunches, φ_{ab} can be taken from Tables XI and XII. In calculating the distribution factor r_{ab}, we have then to substitute $3/\varphi_{ab}$, instead of α_{ab}, into Eq. (97).

In calculating carry-over moments, we use Eq. (89) (page 412), which states that the ratio of the moment induced at a fixed end B to the moment producing rotation at the other end A is

$$c_{ab} = \frac{\varphi_{ba}}{2\varphi_{ab}}. \qquad (98)$$

The beam constants φ_{ba} and φ_{ab} for symmetrical beams with straight and parabolic haunches are given in Tables XI and XII. It is seen that, in the analysis of frames
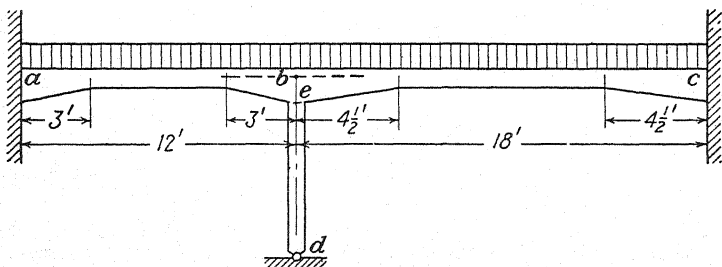

Fig. 450.

with nonprismatic members, the fixed-end moments, the distribution factors, and the carry-over factors depend on the shapes of the members. All these quantities can be readily calculated if the necessary beam constants are given by curves or tables. In such cases frames with nonprismatic members can be analyzed by the same methods as already shown for frames with prismatic members.

Take, for example, the frame in Fig. 450, the girder abc of which carries a uniform load $q = 1,000$ lb. per ft. The bending-moment diagram, calculated on the assumption that the members are prismatic, is shown in Fig. 419. In Fig. 450 the beams ab and bc have symmetrical straight haunches. Owing to this reinforcement of the ends, the fixed-end moments will be larger than previously calculated. Assuming that for both beams $\lambda = 0.25$ and $n = I_0/I_1 = 0.10$,* we find, from the curves in Fig. 445, the beam constants $\delta_{ab} = \delta_{bc} = 1.235$ and we obtain from Eqs. (93)

$$\mathfrak{M}_{ba} = -\mathfrak{M}_{ab} = 1.235 \cdot 12 \cdot 10^3 = 14,820 \text{ lb.-ft.},$$
$$\mathfrak{M}_{bc} = -\mathfrak{M}_{cb} = 1.235 \cdot 27 \cdot 10^3 = -33,350 \text{ lb.-ft.}$$

The unbalanced moment at joint b is

$$\mathbf{M}_a = -(14,820 - 33,350) = 18,530 \text{ lb.-ft.}$$

* In calculating λ and n at b we assume that the straight-line haunches are prolonged up to the axis ed of the column, as shown by dotted lines.

In calculating the distribution factors, let us assume that the prismatical portions of the members ab, bc, and bd are of such dimensions that

$$k_{bc} = k_{bd} = 0.8 k_{ab}.$$

Furthermore, from the curves in Fig. 443, we obtain, for $\lambda = 0.25$, $n = 0.10$,

$$\alpha_{ba} = \alpha_{bc} = 10.$$

In considering the column bd, hinged at the bottom, we have to calculate the beam constant φ_{bd}, corresponding to φ_{ab} in Eq. (b). A satisfactory approximation is obtained on the assumption that the column is absolutely rigid along the portion be of its length. Assuming that this portion represents one-tenth of the length of the column and using the method illustrated in Fig. 441c, we obtain

$$\theta_{bd} = \frac{M_{bd}l^2}{3EI_0} (0.9)^3.$$

Hence,

$$\varphi_{bd} = 0.9^3 = 0.729 \qquad \text{and} \qquad \frac{3}{\varphi_{bd}} = 4.12.$$

With the calculated beam constants we obtain, from Eq. (97), the following values of the distribution factors,

$$r_{ba} = \frac{10k_{ab}}{10k_{ab} + 8k_{ab} + 4.12 \cdot 0.8k_{ab}} = 0.470, \qquad r_{bc} = 0.375, \qquad r_{bd} = 0.155,$$

and the distributed moments are

$$M_{ba}' = 0.470 \cdot 18{,}530 = 8{,}710 \text{ ft.-lb.}, \qquad M_{bc}' = 6{,}950 \text{ ft.-lb.}, \quad M_{bd}' = 2{,}870 \text{ ft.-lb.}$$

The carry-over moments are calculated by using Eq. (98). For our case we find from Table XII, for $\lambda = 0.25$, $n = 0.10$,

$$\varphi_{ab} = 0.591, \qquad \varphi_{ba} = 0.828.$$

Hence,

$$c_{ba} = c_{bc} = \frac{0.828}{2 \cdot 0.591} = 0.701,$$

and the carry-over moments are

$$M_{cb}' = 0.701 M_{bc}' = 4{,}870 \text{ ft.-lb.}, \qquad M_{ab}' = 6{,}110 \text{ ft.-lb.}$$

The moments that result because of unlocking joint b must be superposed on the previously calculated fixed-end moments, and we finally obtain

$$\begin{aligned} M_{ab} &= -8{,}710 \text{ ft.-lb.}, & M_{ba} &= 23{,}530 \text{ ft.-lb.}, \\ M_{bc} &= -26{,}400 \text{ ft.-lb.}, & M_{cb} &= 38{,}220 \text{ ft.-lb.}, \\ & & M_{bd} &= 2{,}870 \text{ ft.-lb.} \end{aligned}$$

Comparing these moments with those calculated for prismatical members as shown in Fig. 419, we see that, owing to haunches, a considerable increase of moments at the supports occurs, while the bending moments at the middle of the spans decrease.

In our example any lateral movement of the frame is prevented by the fixity of the ends of the girder. In the case of a frame that is free to move laterally such motion must be considered. The procedure in calculating the lateral motion is the same as in the case of a frame with prismatical members. We assume first that, by an additional constraint, any lateral movement is eliminated, and we calculate all

end moments as explained in the previous example. Knowing these moments, we calculate the shearing forces acting on the girder by using Eq. (76). In the second step, we assume a certain lateral movement Δ while the joints do not rotate and calculate the angles of rotation Θ of the columns and the corresponding end moments. In the case of a column mn symmetrical with respect to the middle, these moments are [see Eqs. (88), page 408]

$$M_{mn} = M_{nm} = -\gamma_{mn}k_{mn}\Theta_{mn}. \tag{c}$$

The values of γ_{mn} for the cases of parabolic and straight haunches can be readily calculated by using the third of Eqs. (87), together with Tables XI and XII.

Having the end moments from Eqs. (c) and using the same procedure as in the case of frames with prismatical members (see page 376), we find the shearing forces corresponding to the assumed value of Δ and then adjust the value of Δ so as to balance the shear forces previously calculated on the assumption of no lateral movement.

CHAPTER IX

ARCHES

72. Stresses in Curved Bars.[1]—In discussing stresses in an arch rib, it is common practice to assume that the cross-sectional dimensions of the rib are small in comparison with the radius of curvature and to use in the calculation of stresses the formulas derived for a straight bar.   Before
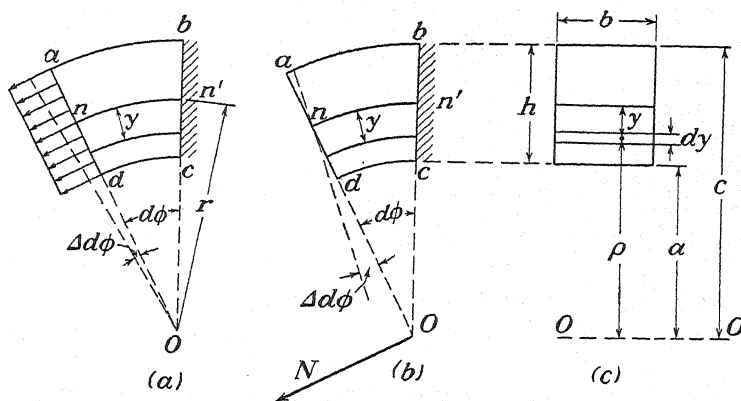

FIG. 451.

going into such a simplification of the problem, we shall consider here the arch rib as a curved bar and shall investigate under what conditions it is permissible to neglect the effect of curvature and use the straight-bar formulas without substantial errors.   Let *abcd* (Fig. 451*a*) represent an element of an arch between two adjacent cross sections normal to the center line *nn'*, of the arch.   To simplify our discussion, we assume that

---

[1] The theory of curved bars and its application to analysis of arches were developed by Bresse, "Recherches analytiques sur la fléxion et la résistance des pièces courbes," Paris, 1854, and by E. Winkler, Formänderung und Festigkeit gekrümmter Körper, ins besondere der Ringe, *Civilingenieur* vol. 4, p. 232, 1858, and *Mitt. Arch. Ing. Ver. Böhmen*, 1868, p. 6.   A further development of the theory of arches in connection with the design of arch bridges and voussoir arches will be found in the following publications: W. Ritter, "Anwendungen der graphischen Statik," vol. IV, Zürich, 1906; H. Müller-Breslau, "Die graphische Statik der Baukonstructionnen," vol. II, pt. 2, Leipzig, 1908; J. Melan and Th. Gesteschi, "Bogenbrücken, Handbuch für Eisenbetonbau," vol. XI, 1931; E. Mörsch, "Der Eisenbetonbau," vol. II, pt. 3, Stuttgart, 1935.   In the last two publications many applications of the theory of arches to analysis of modern important structures can be found.

419

cross sections of the arch have an axis of symmetry in the plane of the center line and that all external forces are acting in this plane. In such a case, we have to consider deformation of the arch in one plane only, namely, the plane of symmetry. The radius of curvature of the center line we denote by r, the distances of the fibers from the cylindrical surface nn' passing through the center line and perpendicular to the plane of that line we denote by y, and the angle between two adjacent cross sections we denote by $d\phi$. Then, the length of the element nn' is

$$ds = r\, d\phi,$$

and that of an element of a fiber at distance y

$$(r - y)d\phi.$$

The distance y is taken positive if it is measured from nn' toward the center of curvature O.

The calculation of stresses in an arch will be based on the assumption that cross sections of the arch during bending remain plane.[1] On this assumption, let us consider first the case of tensile stresses σ uniformly distributed over the cross sections ad and bc (Fig. 451a) of an infinitely short element between two adjacent cross sections of the arch. Owing to these stresses a fiber at a distance y from the cylindrical surface nn' will elongate by an amount[2]

$$\frac{\sigma(r - y)d\phi}{E}. \tag{a}$$

This elongation is proportional to the distance $r - y$ from the center of curvature O of the center line. Hence, a uniformly distributed tensile stress produces, not only elongation of the center line nn' by an amount $\Delta(ds) = \sigma r\, d\phi/E$, but also rotation of the cross section ad with respect to the cross section bc by an angle (Fig. 451a) equal to

$$\Delta(d\phi) = \frac{\Delta(ds)}{r} = \frac{\sigma\, d\phi}{E} = \frac{N\, d\phi}{AE}, \tag{99}$$

where N is the total axial force and A the cross-sectional area of the arch.

As a second simple case of deformation of the element of the arch let us consider the case in which the cross section ad rotates with respect to the axis through n and perpendicular to the plane of the figure as shown

---

[1] A rigorous solution of the problem of bending of curved bars of rectangular cross section indicates that the hypothesis of plane cross sections assumed above gives, for stresses, very accurate results. See "Theory of Elasticity," p. 61, 1934.

[2] A rigorous solution of the problem indicates that radial stresses acting on the lateral surface of a fiber are negligible, and we can assume that the fiber is in the state of simple tension.

by the dotted line in Fig. 451b. Denoting the angle of rotation by $\Delta(d\phi)$, we conclude that the elongation of a fiber at a distance y from the surface nn' is $y\,\Delta(d\phi)$ and the corresponding stress is

$$\sigma = \frac{y\,\Delta(d\phi)}{(r-y)d\phi}\cdot E. \tag{b}$$

Summing up the elemental forces corresponding to stresses (b) and their moments with respect to the axis of rotation through n, we obtain the axial force N and the bending moment M that must be applied to the cross section ad to produce the assumed deformation of the arch element. These quantities are

$$N = \int_A \frac{y\,\Delta(d\phi)}{(r-y)d\phi}\cdot E\,dA = \frac{E\,\Delta(d\phi)}{d\phi}\int_A \frac{y\,dA}{r-y}, \tag{c}$$

$$M = \int_A \frac{y^2\Delta(d\phi)}{(r-y)d\phi}\,E\,dA = \frac{E\,\Delta(d\phi)}{d\phi}\int_A \frac{y^2 dA}{r-y}. \tag{d}$$

Observing that

$$\frac{y^2}{r-y} = \frac{ry}{r-y} - y \qquad \text{and} \qquad \int_A y\,dA = 0^* \quad \bullet$$

we can represent the bending moment M in a simpler form, namely:

$$M = \frac{E\,\Delta(d\phi)}{d\phi}\int_A \frac{y^2 dA}{r-y} = \frac{E\,\Delta(d\phi)}{d\phi}\left(r\int_A \frac{y\,dA}{r-y} - \int_A y\,dA\right) = rN. \tag{e}$$

It is seen that in the assumed case, the resultant of the forces acting on the cross section ad passes through the center of curvature O of the center line nn'. This conclusion could be reached at once by applying the reciprocity theorem to the two loading conditions shown in Fig. 451a and Fig. 451b. In the first of these figures, the resultant force N is applied at the centroid n of the cross section ad, and the displacement of the cross section is such that point O on the radius ad remains fixed. In the second figure, point n remains immovable; hence the resultant force N must pass through point O.

For the calculation of stresses, we apply Eqs. (d) and (b). Using the notation

$$\int_A \frac{y^2 dA}{1-y/r} = I', \tag{100}$$

we obtain from the first of these equations

$$\frac{\Delta(d\phi)}{r\,d\phi} = \frac{\Delta(d\phi)}{ds} = \frac{M}{EI'}. \tag{101}$$

---

* Since nn' is the center line of the arch, y is measured from the axis through the centroid of the cross section.

Substituting this in Eq. (b), we obtain

$$\sigma = \frac{My}{I'} \cdot \frac{1}{1 - y/r} = \frac{My}{I'} \cdot \frac{r}{\rho}, \tag{102}$$

where ρ denotes the distance of a fiber from the axis through the center of curvature O. It is seen that the stress can be readily calculated if we know the quantity I'. If the depth of the cross section is very small in comparison with the radius of curvature r, the quantity y/r in Eq. (100) can be neglected in comparison with unity and we find as a first approximation that I' can be taken equal to the moment of inertia of the cross section. To obtain a more accurate value for I' we substitute in Eq. (100)

$$\frac{1}{1 - y/r} = 1 + \frac{y}{r} + \frac{y^2}{r^2} + \cdots. \tag{f}$$

Then

$$I' = \int_A y^2 \left(1 + \frac{y}{r} + \frac{y^2}{r^2} + \cdots \right) dA. \tag{g}$$

Since y is small in comparison with r, the series for I' is rapidly converging and the sum of the first few terms gives a sufficiently accurate value for I'. Take, for example, a rectangular cross section (Fig. 451c). In this case $dA = b\, dy$, and Eq. (g) gives

$$I' = b \int_{-\frac{h}{2}}^{+\frac{h}{2}} y^2 \left(1 + \frac{y}{r} + \frac{y^2}{r^2} + \cdots \right) dy$$

$$= \frac{bh^3}{12} \left[1 + \frac{3}{5} \left(\frac{h}{2r} \right)^2 + \frac{3}{7} \left(\frac{h}{2r} \right)^4 + \cdots \right]. \tag{103}$$

Taking only the first two terms in the parentheses of expression (103) we obtain

$$I' = \frac{bh^3}{12} \left[1 + \frac{3}{5} \left(\frac{h}{2r} \right)^2 \right].$$

It is seen that when h is small in comparison with r the value of I' is very close to $bh^3/12$, which is the value of the moment of inertia of the cross section.

A similar method of calculating I' can be applied also in the cases of other shapes of cross sections.

Equations (101) and (102) give us the rate of change of the angle and the normal stresses for the case shown in Fig. 451b, in which the internal forces distributed over the cross section ad can be reduced to a force N applied at the center of curvature O. Combining this case with the action of an axial compressive force $N = M/r$, we readily derive formulas for pure bending of an element (Fig. 452). Using Eqs.

(101) and (99) and observing that the rotation of the cross section ad is clockwise in Fig. 451b and counterclockwise in Fig. 451a, we find that for pure bending the change in the angle is

$$\Delta(d\phi) = \frac{M}{EI'}\, r\, d\phi + \frac{M}{AEr}\, d\phi = \frac{M\, ds}{EI'}\left(1 + \frac{I'}{Ar^2}\right). \qquad (104)$$

Taking, for example, a rectangular cross section and using for I' the first two terms in the series (103), we obtain

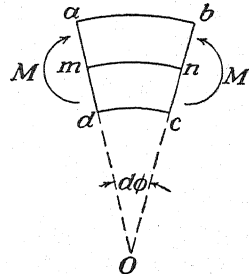$$\Delta\, d\phi = \frac{M\, ds}{EI} \cdot \frac{1}{1 + \frac{4}{15}\, (h/2r)^2} \qquad (105)$$

The second factor on the right-hand side of this equation represents the effect of curvature of the center line on the change in the angle. It is seen that this effect is very small if h is small in comparison with r.

FIG. 452.

To obtain stresses in the case of pure bending of a curved bar, we have only to superpose on the stresses given by Eq. (102) the uniformly distributed compressive stress produced by the axial force $N = M/r$. Hence

$$\sigma = \frac{My}{I'}\, \frac{1}{1 - y/r} - \frac{M}{rA}. \qquad (106)$$

Taking, for example, a rectangular cross section (Fig. 451c) and substituting $y = \pm h/2$, we obtain

$$\left.\begin{aligned}
\sigma_{\max} &= \frac{Mhr}{2I'a} - \frac{M}{rbh} = \frac{Mh}{2I}\left(\frac{I}{I'}\,\frac{r}{a} - \frac{h}{6r}\right),\\[2mm]
\sigma_{\min} &= -\frac{Mhr}{2I'c} - \frac{M}{rbh} = -\frac{Mh}{2I}\left(\frac{I}{I'}\,\frac{r}{c} + \frac{h}{6r}\right),
\end{aligned}\right\} \qquad (107)$$

where a and c denote the radii of the intrados and extrados, respectively. When h is small in comparison with r, the expression in parentheses approaches unity and the maximum stress approaches that calculated by the straight-bar formula.

Substituting $y = 0$ in Eq. (106) we see that a positive bending moment, shown in Fig. 452, produces some compression of the center line nn'. Owing to this action the initial length ds of the center line is diminished by an amount

$$\Delta(ds) = \frac{M}{rA} \cdot \frac{ds}{E}. \qquad (108)$$

Comparing this equation with Eq. (99), we conclude that, if M and N

are numerically equal, the change in length $\Delta(ds)$ is numerically equal to the change in the angle $\Delta(d\phi)$ as it should be in virtue of the reciprocal theorem.

To finish the discussion of stresses in curved bars, we consider the action of a shearing force. If there is a shearing force Q acting in a cross section of the bar, we assume that the shearing stresses are distributed over the cross section in the same manner as in the case of straight bars.[1] In such a case, we can assume that the sliding of the cross section ad with respect to cross section bc (Fig. 453), due to shear action, is equal to
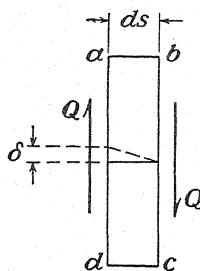
$$\delta = \frac{\alpha Q\,ds}{GA},$$

Fig. 453.

where α is a numerical factor depending on the shape of the cross section. In our subsequent calculations, we shall assume for a rectangular cross section

$$\frac{\alpha E}{G} = 3,$$

which gives

$$\delta = \frac{3Q\,ds}{AE}. \tag{109}$$

Concluding this discussion, we can state that the effect of curvature on angular changes [Eq. (105)] and on the magnitude of maximum stress [Eqs. (107)] is small and usually can be neglected in practical calculations.

73. Deflection of Curved Bars.—Let us consider an element, between two consecutive normal cross sections ad and bc, on which bending moment M, axial force N, and shearing force Q are acting (Fig. 454). We take the directions indicated in the figure as positive. Using the results of the preceding article we find that, owing to deformation, the initial angle $d\phi$ of the element diminishes [see Eqs. (104) and (99)] by an amount

$$\Delta(d\phi) = \frac{M\,ds}{EI'}\left(1 + \frac{I'}{Ar^2}\right) + \frac{N\,ds}{AEr}. \tag{110}$$

The length of the element ds of the center line diminishes [see Eqs. (99) and 108)] by the amount

$$\Delta(ds) = \frac{N\,ds}{AE} + \frac{M\,ds}{AEr}. \tag{111}$$

The cross section ad slides with respect to the cross section bc in the outward direction by an amount given in Eq. (109). In practical applica-

---

[1] A rigorous solution for a rectangular narrow cross section shows that this assumption is very accurate if $h < \frac{1}{3}r$ (see "Theory of Elasticity," p. 73).

tions the effect of curvature and the effect of shearing force are usually neglected, and, instead of Eqs. (110) and (111), the following simplified formulas are used:

$$\Delta(d\phi) = \frac{M\ ds}{EI}, \qquad \Delta(ds) = \frac{N\ ds}{AE}. \tag{112}$$

The accuracy of these simplified formulas will now be discussed by taking an example as shown in Fig. 455. It is required to find the horizontal displacement u and the vertical displacement v of a point C on the center line of the curved bar DCB fixed at D and loaded by a horizontal force H at the end B. These displacements are produced by deformation of the portion DC of the curved bar. Considering a cross section of the bar at a point K and taking as positive the directions of forces and moments indicated in Fig. 454 we find for this cross section

Fig. 454.

$$M = -H(f - y), \qquad N = H\cos\phi, \qquad Q = H\sin\phi. \tag{a}$$

Considering, now, an element of the bar between two adjacent cross sections at K and using the simplified formulas (112), we obtain

$$\Delta(d\phi) = -\frac{H(f - y)ds}{EI}, \qquad \Delta(ds) = \frac{H\cos\phi\ ds}{AE}. \tag{b}$$

The minus sign in the first of these formulas indicates that the angle between the two cross sections increases and the lower portion KCB of the bar rotates clockwise with respect to the point K. The corresponding small displacement of the point C is perpendicular to the direction KC and is of the magnitude

$$\frac{H(f - y)ds}{EI} \cdot t$$

where t denotes the distance between the points K and C.

The two components of this displacement in the directions of the coordinate axes, indicated in Fig. 455, are

$$\left.\begin{aligned} du &= -\frac{H(f - y)ds}{EI} \cdot t\sin\psi = -\frac{H(f - y)ds}{EI}(y_c - y), \\ dv &= \frac{H(f - y)ds}{EI} \cdot t\cos\psi = \frac{H(f - y)ds}{EI}(x_c - x). \end{aligned}\right\} \tag{c}$$
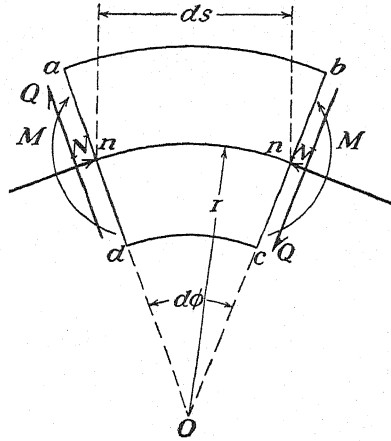
Considering now the shortening $\Delta(ds)$ of the element ds of the center line at K, we see that owing to this deformation the lower portion KCB of the curved bar moves toward point K in the direction of the tangent at K. The components of this displacement are

$$du_1 = -\Delta(ds) \cos \phi, \qquad dv_1 = -\Delta(ds) \sin \phi. \qquad (d)$$

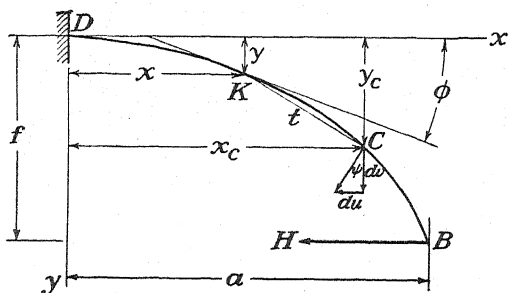Summing up the elemental displacements (c) and (d) produced by

Fig. 455.

deformations of all elements of the bar in the portion DKC, we obtain the required displacements of point C,

$$u = - \int_0^s \frac{H(f-y)}{EI} (y_c - y)ds - \int_0^s \frac{H \cos^2 \phi}{AE} ds, \qquad (113)$$

$$v = \int_0^s \frac{H(f-y)}{EI} (x_c - x)ds - \int_0^s \frac{H \cos \phi \sin \phi}{AE} ds, \qquad (114)$$

where s is the length of the arc DKC. To obtain the displacements of the end B of the bar, we have only to substitute for s in the foregoing equations the length of the arc DKB.

Let us assume, as an example, that the center line of the curved bar is a parabola given by the equation

$$y = \frac{fx^2}{a^2} \qquad (e)$$

and also that the cross-sectional areas and the moments of inertia of cross sections are inversely proportional to $\cos \phi$. Denoting by A_0 and I_0 these quantities at the cross section D we have, then, for any cross section,

$$A = \frac{A_0}{\cos \phi}, \qquad I = \frac{I_0}{\cos \phi}. \qquad (f)$$

Substituting these values in Eq. (113), we find that the horizontal dis-

placement of the end B of the bar is

$$u_b = - \int_0^a \frac{H(f-y)^2 dx}{EI_0} - \int_0^a \frac{H \cos^2 \phi \, dx}{A_0 E}. \qquad (g)$$

Substituting for y its value from Eq. (e) and observing that

$$\cos \phi = \frac{dx}{\sqrt{dx^2 + dy^2}} = \frac{1}{\sqrt{1 + (2fx/a^2)^2}},$$

we find from Eq. (g), after integration,

$$u_b = - \frac{8Haf^2}{15EI_0} \left(1 + \frac{15}{16} \frac{a}{f} \frac{k^2}{f^2} \arctan \frac{2f}{a} \right), \qquad (h)$$

where $k^2 = I_0/A_0$ represents the square of the radius of gyration of the cross section at D. The second term in parentheses on the right-hand side of this equation represents the influence of the compressive force N on the displacement u_b. This influence usually is very small. To show this we assume that the cross section is a rectangle of the depth h at point D, and take $h = a/5$. Then the above-mentioned N-term has the values given in the second column of Table XIII below.

TABLE XIII

$\dfrac{f}{a}$	N-term $\dfrac{h}{a} = \frac{1}{5}$	Values of β in Eq. (i)			
		$\dfrac{h}{a} = \frac{1}{5}$	$\dfrac{h}{a} = \frac{1}{10}$	$\dfrac{h}{a} = \frac{1}{15}$	$\dfrac{h}{a} = \frac{1}{20}$
$\frac{1}{6}$	0.2171	0.2247	0.0562	0.0250	0.0104
$\frac{1}{4}$	0.0927	0.0993	0.0248	0.0110	0.0062
$\frac{1}{2}$	0.0196	0.0232	0.0058	0.0026	0.0015
1	0.0035	0.0035	0.0009	0.0004	0.0002

The displacements u_b were also calculated by using the more accurate equations (110) and (111)* and by taking care of the shear deformation given by Eq. (109). The results of these calculations can be represented in the following form:

$$u_b = - \frac{8Haf^2}{15EI_0} (1 + \beta). \qquad (i)$$

The values of the constant β for various proportions of the curved bar are given in the last four columns of Table XIII. It is seen that in the case of thin bars, especially if f/a is not small, the displacement u_b is obtained with a very good accuracy by neglecting entirely the actions of the axial and shearing forces and also the effect of curvature on

---

* In this calculation I' was taken equal to I.

deformation. For thicker bars, having small values of f/a, a comparison of the values in the second and third columns of the table shows that a good accuracy is obtained by considering only the action of the longitudinal force N in addition to that of bending moment, and there is no necessity to have recourse to the more elaborate equations (110) and (111). In our subsequent discussion of arches, we shall always use the simplified equations (112) and shall indicate in only a few cases the magnitude of the errors that may result from this simplified analysis.[1]

74. Two-hinged Arches.—A two-hinged arch represents a structure with one redundant reactive force. Since the hinges at the supports
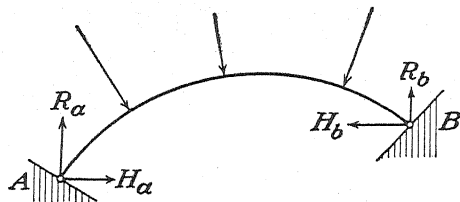

Fɪɢ. 456.

are immovable, the load acting on the arch (Fig. 456) produces at both ends not only vertical but also horizontal reactions and we have four unknown reactive forces, for the calculation of which there are only three equations of statics. For the derivation of the fourth equation, the deformation of the arch must be considered. Assume now that the arch is symmetrical and symmetrically loaded (Fig. 457a). In such a case, the two vertical reactions are equal and can be readily determined. The horizontal reactions are two equal and opposite forces H, called the *thrust* of the arch. To calculate H, we consider the deformation of the right-hand half of the arch (Fig. 457b), assuming that the cross section D is fixed. We remove first the force H and calculate the horizontal displacement u_b of the hinge B produced by the given loads and the vertical reaction R. Then we consider the action of a unit horizontal force applied at the hinge B (Fig. 457c) and calculate the horizontal displacement u_b' of this hinge. The required force H will then be found from the condition that hinge B is immovable. Hence,

$$u_b + Hu_b' = 0,$$

and we obtain

$$H = -\frac{u_b}{u_b'}. \tag{115}$$

To calculate u_b, we use the simplified equations (112), and proceeding

---

[1] The accuracy of the simplified methods of analysis of arches was investigated by Timoshenko in the paper Calcul des arcs élastiques, *Ciment*, Paris, 1922. In the subsequent discussion of arches, the results of that investigation are used.

as in the example of the preceding article we obtain

$$u_b = \int_0^{s_b} \frac{M(f - y)ds}{EI} - \int_0^{s_b} \frac{N \cos \phi \, ds}{AE}, \qquad (116)$$

where f is the rise of the arch and s_b is the length of the center line DB. For calculating u_b', we use Eq. (113), which gives

$$u_b' = - \int_0^{s_b} \frac{(f - y)^2 ds}{EI} - \int_0^{s_b} \frac{\cos^2 \phi \, ds}{AE}. \qquad (117)$$

Substituting expressions (116) and (117) in Eq. (115) we obtain the required thrust H for any symmetrical and symmetrically loaded arch.
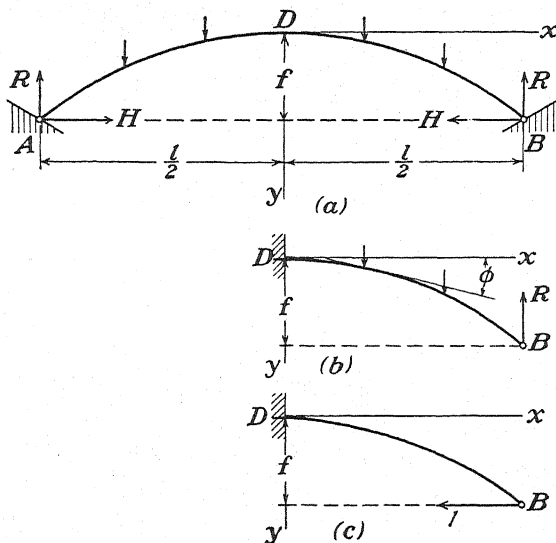

Fig. 457.

Let us consider, as an example, the case of a parabolic arch the variation of cross sections of which is given by Eq. (f) of the preceding article. Assume that the load is uniformly distributed along the horizontal projection of the arch. In such a case, the bending moment M in Eq. (116) has the same meaning as for a uniformly loaded beam, and with the origin of coordinates at D we obtain

$$M = \frac{q}{2}\left(\frac{l^2}{4} - x^2\right).$$

Observing that for a parabolic arch

$$f - y = f\left(1 - \frac{4x^2}{l^2}\right)$$

and that $I = I_0/\cos \phi$, we find that the first term on the right side of Eq. (116) is

$$\frac{qfl^2}{8EI_0} \int_0^{\frac{l}{2}} \left(1 - \frac{4x^2}{l^2}\right)^2 dx = \frac{1}{30} \frac{qfl^3}{EI_0}. \tag{a}$$

In calculating the second term, we observe that

$$N = \left[R - q\left(\frac{l}{2} - x\right)\right] \sin \phi,$$

which indicates that the axial force in this case is proportional to $\sin \phi$ and therefore is small for flat arches. For arches with a considerable rise $\sin \phi$ is not small, but from the discussion of the preceding article we know that for such arches the effect of axial force is negligible. We conclude, therefore, that the second term in Eq. (116) can be neglected in an approximate calculation of the thrust H. In calculating u_b', given by expression (117), we use Eq. (h) or Eq. (i)* of the preceding article. Equation (i) gives

$$u_b' = -\frac{4lf^2}{15EI_0}(1 + \beta). \tag{b}$$

Numerical values of β, depending on the proportions of the arch, can be taken from Table XIII (page 427) or from Eq. (h). Substituting (a) and (b) in Eq. (115), we obtain

$$H = \frac{ql^2}{8f} \cdot \frac{1}{1 + \beta}. \tag{118}$$

The first factor on the right-hand side of this equation represents the thrust for a three-hinged arch. This thrust, as we see, must be reduced in the ratio $1 : (1 + \beta)$ to obtain the thrust for the two-hinged arch.

Another example of symmetrical deformation of a symmetrical arch is that produced by a uniform temperature change. Assume that the temperature of the arch in Fig. 457a increases by t deg. Since the hinge B in Fig. 457b is free to move horizontally, the temperature change will produce the horizontal displacement of B equal to $\alpha tl/2$, where α is the coefficient of thermal expansion. Substituting this value of u_b in Eq. (115), we obtain for the thrust produced by the temperature change the value

$$H = -\frac{\alpha tl}{2u_b'}, \tag{119}$$

where u_b' is given by Eq. (117).

---

* In this latter equation, the small effects of shearing force and of curvature are taken into account.

Consider again the parabolic arch of the preceding example. Then u_b' is given by Eq. (b), and Eq. (119) gives

$$H = \frac{15EI_0}{8f^2} \cdot \frac{\alpha t}{1 + \beta}. \qquad (120)$$

The corresponding maximum compressive and maximum tensile stresses produced at the crown of an arch of a rectangular cross section is

$$\sigma_{\substack{\min.\\\max.}} = -\frac{H}{A_0} \mp \frac{6Hf}{A_0 h} = -\frac{15}{8}\frac{Eh^2}{12f^2}\frac{\alpha t}{1 + \beta}\left(1 \pm \frac{6f}{h}\right). \qquad (121)$$

It is seen that the importance of thermal stresses increases with the increase of the ratio h/f.
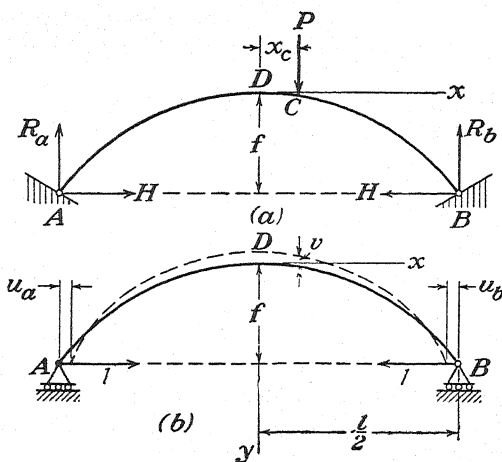

Fig. 458.

If there is a live load acting on an arch, influence lines can be used to advantage. To obtain the influence line for the thrust H of a symmetrical arch (Fig. 458a) we use the reciprocal theorem (see page 250). Comparing the two conditions of loading, shown in Figs. 458a and 458b, we conclude that

$$Pv + H(u_a - u_b) = 0, \qquad (c)$$

where the displacements u and v are taken positive when they are in the directions of the positive x- and y-axes. From Eq. (c) we obtain

$$H = -\frac{Pv}{u_a - u_b}. \qquad (122)$$

For calculating $u_a - u_b$, which represents the decrease in distance between the hinges A and B in Fig. 458b, we use Eq. (113), which gives

$$u_a - u_b = 2\left[\int_0^{s_b} \frac{(f - y)^2 ds}{EI} + \int_0^{s_b} \frac{\cos^2 \phi \, ds}{AE}\right]. \qquad (123)$$

In calculating v, we use Eq. (114). Observing that this equation was derived on the assumption that point D is fixed and point B is free to move vertically we conclude that the displacement v in Eq. (122) is obtained by subtracting the vertical displacement of point B in Fig. 455 from the expression (114), which gives

$$v = -\int_0^{s_b} \frac{f-y}{EI}\left(\frac{l}{2}-x\right)ds + \int_0^{s_c}\frac{(f-y)(x_c-x)}{EI}ds$$
$$+ \int_{s_c}^{s_b}\frac{\cos\phi\sin\phi}{AE}ds.$$

The last term on the right side of this equation represents the effect on v of the axial force. Usually it is very small and can be neglected. Then,

$$v = -\int_0^{s_b}\frac{f-y}{EI}\left(\frac{l}{2}-x\right)ds + \int_0^{s_c}\frac{(f-y)(x_c-x)}{EI}ds. \quad (124)$$

Substituting expressions (123) and (124) in Eq. (122) and performing the integration, we find the ordinates of the required influence line.

As an example, let us consider again a parabolic arch with $I = I_0/\cos\phi$ and $A = A_0/\cos\phi$. In such a case, we can use Eq. (b) and put

$$u_a - u_b = -2u_b' = \frac{8}{15}\frac{lf^2}{EI_0}(1+\beta). \quad (d)$$

In calculating v, we note that in our example

$$\int_0^{s_c}\frac{(f-y)(x_c-x)}{EI}ds = \frac{f}{EI_0}\int_0^{x_c}\left(1-\frac{4x^2}{l^2}\right)(x_c-x)dx$$
$$= \frac{fx_c^2}{EI_0}\left(\frac{1}{2}-\frac{1}{3}\frac{x_c^2}{l^2}\right).$$

For $x_c = l/2$ we obtain

$$\int_0^{s_b}\frac{f-y}{EI}\left(\frac{l}{2}-x\right)ds = \frac{5}{48}\frac{fl^2}{EI_0}.$$

Equation (124) then gives

$$v = -\frac{5}{48}\frac{fl^2}{EI_0} + \frac{fx_c^2}{EI_0}\left(\frac{1}{2}-\frac{1}{3}\frac{x_c^2}{l^2}\right). \quad (e)$$

Substituting the expressions (d) and (e) inEq. (122), we obtain

$$H = P\frac{15}{8(1+\beta)}\left(\frac{5}{48}\frac{l}{f}-\frac{x_c^2}{2lf}+\frac{x_c^4}{3l^3f}\right). \quad (125)$$

The factor by which the load P is multiplied gives us the ordinates of the

required influence line for H. In Fig. 459b, this line is given by curve $a_1d_1b_1$. With this line the influence lines for bending moment and axial force at any cross section C can be readily constructed. Denoting by M_0 the bending moments for a simply supported beam AB of the span l and defining the position of C by the distances a, b and c, we find that the
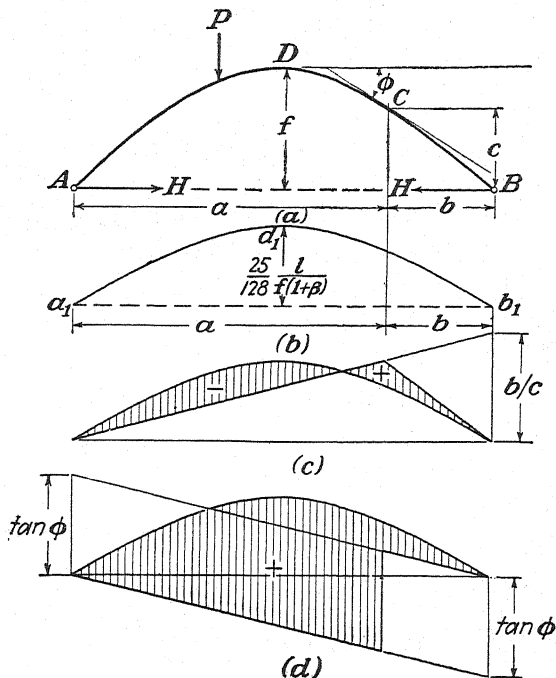

FIG. 459.

bending moment at the cross section C of the arch, for any position of the moving load P, is

$$M = M_0 - Hc = c\left(\frac{M_0}{c} - H\right).$$

It is seen that the moment M is obtained by multiplying by c the ordinates of the shaded area in Fig. 459c, which represents the differences of the ordinates of the M_0/c-influence line and the H-influence line.

The axial force for any position of the moving load is

$$N = H \cos \phi - V_c \sin \phi = \cos \phi \, (H - V_c \tan \phi),$$

where V_c is the shearing force at C for a simply supported beam. Hence, N is obtained by multiplying by $\cos \phi$ the ordinates of the shaded area in Fig. 459d, which represents the differences of the ordinates of the H-influence line and the $V_c \tan \phi$-influence line.

To inquire into the accuracy of the approximate equation (125), more elaborate calculations were made by using Eqs. (109), (110), and (111), which include the effects of shearing force, axial force, and curvature on the displacements u and v. The results of these calculations showed that in the most unfavorable case of a flat and very thick arch ($h/l = 0.1$, $f/l = \frac{1}{12}$) the error of the simplified equation (125) is only about 0.8 of 1 per cent. This justifies the use of Eq. (125) in practical applications. Similar calculations were made also for circular arches, and it was found that for such arches the error of the simplified formula is of the same order as in the case of parabolic arches.

75. Hingeless Symmetrical Arches.—A hingeless arch represents a structure with three redundant quantities. We can consider as redundants the bending moment, shearing force, and axial force at some chosen cross section of the arch. In a symmetrical arch (Fig. 460a) it is advantageous to take as unknowns the moment and the forces at the cross section D at the crown. In the calculation of these unknowns we need to consider the deformation of the arch. To find the components u_c and v_c of the deflection at any point C on the center line of the arch (Fig. 460a) and the angle of rotation θ_c of the cross section at C we have to consider the deformation of the portion CB of the arch. Taking an infinitesimal element cut out from this portion by two adjacent cross sections, we define the deformation of this element by the decrease $\Delta(d\phi)$ in its initial angle $d\phi$ and by the shortening $\Delta(ds)$ in the length ds of the center line. These quantities are given by the approximate equations (112)

$$\Delta(d\phi) = \frac{M\,ds}{EI}, \qquad \Delta(ds) = \frac{N\,ds}{AE}, \tag{a}$$

in which M and N are the bending moment and the axial force, respectively, acting on the element. Proceeding as in Art. 73, we find that the deformations (a) of an element of the arch result in the following infinitesimal deflections at C:

$$\left.\begin{aligned}
du_c &= \Delta(d\phi)(y - y_c) + \Delta(ds)\cos\phi, \\
dv_c &= -\Delta(d\phi)(x - x_c) + \Delta(ds)\sin\phi, \\
d\theta_c &= \Delta(d\phi),
\end{aligned}\right\} \tag{b}$$

where x and y are the coordinates of the center of the element under consideration and ϕ is the angle that the tangent to the center line at this point makes with the x-axis (Fig. 460a).

Summing up the elemental deflections (b) for all elements of the portion CB of the arch and using Eqs. (a), we obtain the total deflections at C,

$$u_c = \int_{s_c}^{s_b} \frac{M(y - y_c)ds}{EI} + \int_{s_c}^{s_b} \frac{N\cos\phi\,ds}{AE}, \tag{126}$$

$$v_c = -\int_{s_c}^{s_b} \frac{M(x - x_c)ds}{EI} + \int_{s_c}^{s_b} \frac{N \sin \phi \, ds}{AE}, \qquad (127)$$

$$\theta_c = \int_{s_c}^{s_b} \frac{M \, ds}{EI}. \qquad (128)$$

If point C coincides with the origin of coordinates at the crown D, we have $x_c = y_c = 0$, and the deflections at D are

$$u_d = \int_0^{s_b} \frac{My \, ds}{EI} + \int_0^{s_b} \frac{N \cos \phi \, ds}{AE}, \qquad (129)$$

$$v_d = -\int_0^{s_b} \frac{Mx \, ds}{EI} + \int_0^{s_b} \frac{N \sin \phi \, ds}{AE}, \qquad (130)$$

$$\theta_d = \int_0^{s_b} \frac{M \, ds}{EI}. \qquad (131)$$

Let us apply these equations to several specific cases that will be required in subsequent discussions. As the first example, we consider
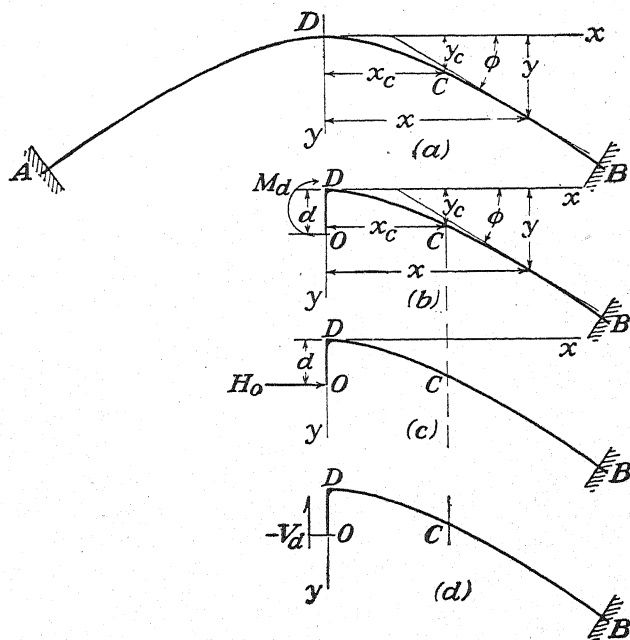

FIG. 460.

the right-hand portion of the arch fixed at B and loaded by a couple M_d at the free end D (Fig. 460b). In this case the bending moment M is constant along the length DCB of the arch, and the axial force N vanishes. Equations (126) to (128) then give

$$u_c = M_d \int_{s_c}^{s_b} \frac{(y - y_c)ds}{EI}, \qquad v_c = -M_d \int_{s_c}^{s_b} \frac{(x - x_c)ds}{EI},$$

$$\theta_c = M_d \int_{s_c}^{s_b} \frac{ds}{EI}, \quad (132)$$

and from Eqs. (129) to (131) we obtain

$$u_d = M_d \int_0^{s_b} \frac{y\,ds}{EI}, \qquad v_d = -M_d \int_0^{s_b} \frac{x\,ds}{EI}, \qquad \theta_d = M_d \int_0^{s_b} \frac{ds}{EI}. \quad (133)$$

It is seen that u_d and θ_d are both positive for the positive M_d indicated in Fig. 460b. This shows that the cross section D moves to the right and rotates clockwise. Imagine, now, an extension of the cross section D in the form of an absolutely rigid bar DO of a length d. It is evident that the horizontal displacement u_0 of point O depends on both the displacement u_d of point D and the rotation θ_d of the cross section D and is represented by the equation

$$u_0 = u_d - d \cdot \theta_d. \qquad (c)$$

It is seen that the length d of the assumed extension can be selected so as to make u_0 vanish. For this purpose we need only put

$$d = \frac{u_d}{\theta_d} = \frac{\int_0^{s_b} \dfrac{y\,ds}{EI}}{\int_0^{s_b} \dfrac{ds}{EI}}. \qquad (134)$$

Assume that the point O in Fig. 460b is selected in this manner. Then a couple M_d, applied at cross section D, does not produce any horizontal displacement of point O. In virtue of the reciprocal theorem we then conclude that a horizontal force applied at O (Fig. 460c) will not produce any rotation of the cross section D. In the subsequent discussion, point O will often be used and will be called the *elastic center*.

As the second example let us assume that a horizontal force H_0 is applied at the elastic center (Fig. 460c); it is required to find deflections at C produced by this force. In this case, the bending moment and the axial force at any cross section of the arch DCB are

$$M = H_0(y - d), \qquad N = H_0 \cos \phi.$$

Substituting these values in the general equations (126) to (128), we obtain

$$u_c = H_0 \int_{s_c}^{s_b} \frac{(y - y_c)(y - d)ds}{EI} + H_0 \int_{s_c}^{s_b} \frac{\cos^2 \phi\, ds}{AE}. \qquad (135)$$

$$v_c = -H_0 \int_{s_c}^{s_b} \frac{(x - x_c)(y - d)ds}{EI} + H_0 \int_{s_c}^{s_b} \frac{\cos \phi \sin \phi \, ds}{AE}, \quad (136)$$

$$\theta_c = H_0 \int_{s_c}^{s_b} \frac{(y - d)ds}{EI}. \quad (137)$$

For the cross section D, these equations give

$$u_d = H_0 \int_0^{s_b} \frac{y(y - d)ds}{EI} + H_0 \int_0^{s_b} \frac{\cos^2 \phi \, ds}{AE}, \quad (138)$$

$$v_d = -H_0 \int_0^{s_b} \frac{x(y - d)ds}{EI} + H_0 \int_0^{s_b} \frac{\cos \phi \sin \phi \, ds}{AE}, \quad (139)$$

$$\theta_d = H_0 \int_0^{s_b} \frac{(y - d)ds}{EI} = 0. \quad (140)$$

It is seen that rotation θ_d vanishes by virtue of Eq. (134).

Finally, let us consider the action of a vertical force V_d applied at the cross section D of the arch DCB (Fig. 460d). The bending moment and axial force at any cross section, in this case, are, respectively,

$$M = V_d x, \qquad N = -V_d \sin \phi.$$

Substituting these values in the general equations (126) to (128) for the deflections at C, we obtain

$$u_c = V_d \int_{s_c}^{s_b} \frac{x(y - y_c)ds}{EI} - V_d \int_{s_c}^{s_b} \frac{\sin \phi \cos \phi \, ds}{AE}, \quad (141)$$

$$v_c = -V_d \int_{s_c}^{s_b} \frac{x(x - x_c)ds}{EI} - V_d \int_{s_c}^{s_b} \frac{\sin^2 \phi \, ds}{AE}, \quad (142)$$

$$\theta_c = V_d \int_{s_c}^{s_b} \frac{x \, ds}{EI}. \quad (143)$$

For the cross section D, these equations give

$$u_d = V_d \int_0^{s_b} \frac{xy \, ds}{EI} - V_d \int_0^{s_b} \frac{\sin \phi \cos \phi \, ds}{AE}, \quad (144)$$

$$v_d = -V_d \int_0^{s_b} \frac{x^2 ds}{EI} - V_d \int_0^{s_b} \frac{\sin^2 \phi \, ds}{AE}, \quad (145)$$

$$\theta_d = V_d \int_0^{s_b} \frac{x \, ds}{EI}. \quad (146)$$

With the above obtained solutions of the auxiliary problems shown in Figs. 460b to 460d, the redundant forces in a symmetrical arch under any kind of loading can be calculated. We begin with the case of a symmetrical loading. From symmetry we conclude that the shearing force at the cross section D vanishes in this case, and we have only two

unknowns, the moment M_d and the axial force N_d shown in Fig. 461a. This system of forces can be replaced by the statically equivalent system consisting of the horizontal force $H_0 = N_d$ applied at the elastic center O and the couple $M_0 = M_d + H_0 d$ shown in Fig. 461b. The values of M_0 and H_0 will now be determined from the fact that in the case of a symmetrical loading the elastic center O does not move laterally and the
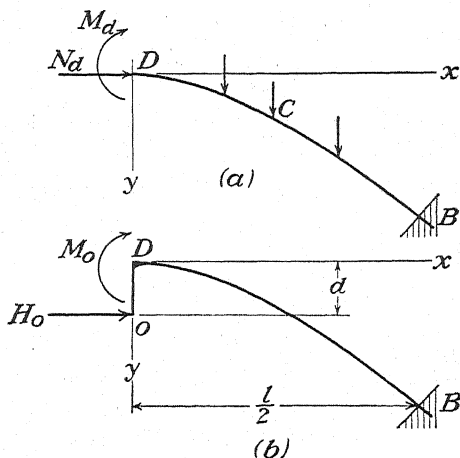

Fig. 461.

cross section D does not rotate. From Eqs. (129) and (131), which give the deflections produced at D by the load on the portion DCB of the arch, we find that the horizontal movement of point O is

$$u_0 = u_d - d \cdot \theta_d = \int_0^{sb} \frac{My\,ds}{EI} + \int_0^{sb} \frac{N\cos\phi\,ds}{AE} - d\int_0^{sb} \frac{M\,ds}{EI}.$$

For the deflections produced by M_0 and H_0 we use Eqs. (133) and (138). Then, from the conditions that point O does not move laterally and that the cross section D does not rotate, we obtain

$$\int_0^{sb} \frac{My\,ds}{EI} + \int_0^{sb} \frac{N\cos\phi\,ds}{AE} - d\int_0^{sb} \frac{M\,ds}{EI}$$
$$+ H_0\left[\int_0^{sb} \frac{y(y-d)ds}{EI} + \int_0^{sb} \frac{\cos^2\phi\,ds}{AE}\right] = 0, \quad (147)$$

$$\int_0^{sb} \frac{M\,ds}{EI} + M_0\int_0^{sb} \frac{ds}{EI} = 0. \quad (148)$$

From the first of these equations we calculate H_0 and from the second M_0, provided that the arch dimensions and load distribution are known.

As an example of a symmetrical deformation of an arch, let us take the case of a uniform change in temperature. To calculate H_0 and M_0

produced by a uniform change of temperature, we consider the right-hand side of the arch shown in Fig. 461b. Owing to a uniform rise in the temperature of t deg., the cross section D moves to the left, without rotation, by an amount $\alpha t l/2$. This displacement is counteracted by the thrust H_0 applied at O, which also does not produce rotation of the cross section D. The magnitude of H_0 is now found from the condition that the cross section D does not move laterally, which requires [see Eq. (138)] that

$$-\frac{\alpha t l}{2} + H_0 \left[\int_0^{sb} \frac{y(y-d)ds}{EI} + \int_0^{sb} \frac{\cos^2 \phi \, ds}{AE} \right] = 0. \qquad (149)$$

From this equation, the thrust produced by the temperature change can be calculated if t and the arch dimensions are known. The moment M_0 vanishes, in this case, since the temperature change and thrust H_0 both produce no rotation of the cross section D. Having H_0, we determine the bending moment M_d and the axial force N_d at the crown from the equations

$$M_d = -H_0 d, \qquad N_d = H_0. \qquad (150)$$

The application of Eqs. (149) and (150) to particular cases will be shown later.

Let us consider now the construction of influence lines for symmetrical hingeless arches. For this purpose we use the reciprocal theorem. To construct the influence line for the thrust H_0, we have to compare the actual condition of loading shown in Fig. 462a with the fictitious loading shown in Fig. 462b. In the first case, we have the vertical load P at the point C and the unknown redundant moment M_0 and forces H_0 and V_0 at the crown.[1] In the second case, the load P and the redundant quantities M_0 and V_0 are removed, and, instead of H_0, two opposite unit forces are applied. Owing to the specific choice of point O [see Eq. (134)] the unit forces will not produce any rotation of cross sections D. These cross sections will move apart only by an amount $2u_d$, without any relative rotation or relative sliding. Hence, the work of the redundant moment M_0 and of the redundant shearing force V_0 on the corresponding displacements produced by the unit forces in Fig. 462b vanishes, the reciprocal theorem gives

$$H_0 \cdot 2u_d + Pv_c = 0,$$

and we obtain

$$H_0 = -P \frac{v_c}{2u_d}, \qquad (151)$$

[1] To show these forces more clearly, a small distance between the extension bars OD is shown in Fig. 462a.

where v_c is the vertical displacement of point C taken positive if in the direction of the positive y-axis. The ordinates of the influence line are given by the ratio $-v_c/2u_d$ in which v_c and u_d are the previously calculated displacements given by Eqs. (136) and (138), for $H_0 = 1$, respectively.

Similar methods will be applied to obtain the influence lines for the redundant moment M_0 and the shearing force V_0. The fictitious loading
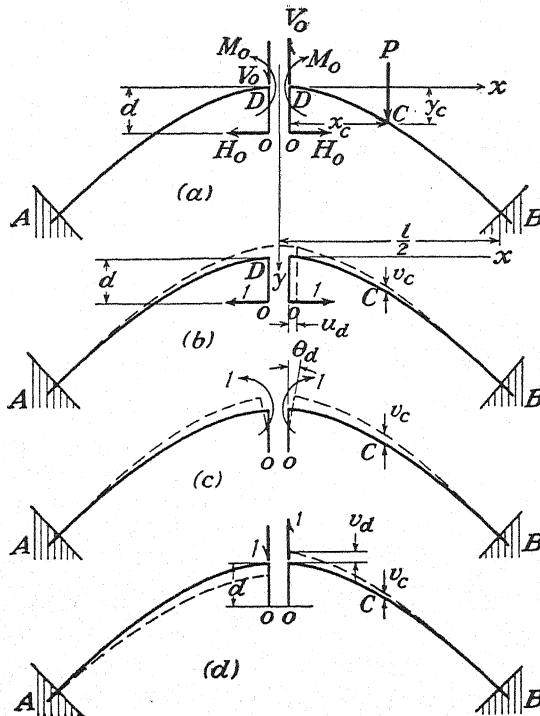

Fig. 462.

for the influence line of M_0 is shown in Fig. 462c. The unit moments shown in the figure do not produce relative movements of the points O and rotate the cross sections D one with respect to the other only by the amount $2\theta_d$. Hence, the work of V_0 and H_0 on the displacements produced by the unit moments vanishes, and the work of M_0 is $M_0 2\theta_d$. The reciprocal theorem then gives

$$M_0 2\theta_d + v_c P = 0,$$

and we obtain

$$M_0 = -P \frac{v_c}{2\theta_d}. \tag{152}$$

The required ordinates of the influence line are obtained by substituting

for v_c and θ_d the values given by the second of Eqs. (132) and the third of Eqs. (133), for $M_d = 1$, respectively.

The fictitious loading for V_0 is shown in Fig. 462d. We have only a relative sliding[1] of the amount $2v_d$ of the cross sections D, and the reciprocal theorem gives

$$-V_0 2v_d + Pv_c = 0$$

and

$$V_0 = P \frac{v_c}{2v_d}. \tag{153}$$

The ordinates of the required influence line are obtained by substituting in this equation the value of v_c and v_d, for $V_d = 1$, from Eqs. (142) and (145), respectively.

It is seen that, in all the cases considered, the ordinates of the required influence lines are proportional to the vertical deflections v_c produced in the arch by the unit loads shown in Fig. 462.

As soon as the values of the redundant quantities H_0, M_0, and V_0 at the cross section D are obtained by using the calculated influence lines, the values of the bending moment, the axial force, and the shearing force at any other cross section can be found from statics. If M_c and N_c at a cross section C are calculated, the magnitudes of the compressive stresses at the outermost upper and lower fibers will be given by the equations

$$\sigma_{\text{upper}} = \frac{N_c}{A_c} + \frac{M_c c_u}{I_c}, \qquad \sigma_{\text{lower}} = \frac{N_c}{A_c} - \frac{M_c c_l}{I_c}, \tag{154}$$

in which c_u and c_l are the distances to the outermost fibers (Fig. 463a). Introducing the notations

$$\rho_l = \frac{I_c}{A_c c_u}, \qquad \rho_u = \frac{I_c}{A_c c_l}, \tag{155}$$

where ρ_l and ρ_u are the core radii,[2] we obtain

$$\sigma_{\text{upper}} = \frac{N_c \rho_l + M_c}{A_c \rho_l}, \qquad \sigma_{\text{lower}} = \frac{N_c \rho_u - M_c}{A_c \rho_u}. \tag{156}$$

Observing that the bending moment M_c can be considered as produced by the eccentrically applied compressive force (Fig. 463b) we obtain $M_c = N_c a$, and Eqs. (156) become

$$\sigma_{\text{upper}} = \frac{N_c(\rho_l + a)}{A_c \rho_l} = \frac{M_l}{Z_u}, \tag{157}$$

$$\sigma_{\text{lower}} = \frac{N_c(\rho_u - a)}{A_c \rho_u} = -\frac{M_u}{Z_l}, \tag{158}$$

[1] The relative rotation and the relative horizontal movement of the cross section D evidently vanish in this case.

[2] See "Strength of Materials," vol. I, p. 235, 1940.

where

$$Z_u = A_c \rho_l = \frac{I_c}{c_u}, \qquad Z_l = A_c \rho_u = \frac{I_c}{c_l}. \tag{159}$$

and M_l and M_u are the moments taken with respect to the axes through
the lower and the upper core points
C_l and C_u, respectively (Fig. 463a).
It is seen that the calculation of the
maximum compressive stresses is
greatly simplified if the influence lines
for the *core moments* M_l and M_u, in-
stead of the line for the bending mo-
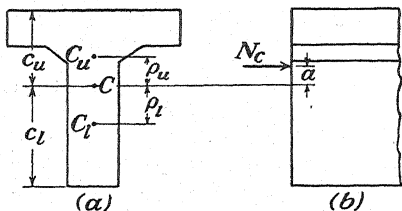ment M_c, are used.

(a)   (b)

FIG. 463.

76. Hingeless Symmetrical Parabolic Arches.—Stresses in a parabolic
arch produced by a load uniformly distributed along the span will be dis-
cussed later (see page 458). Here we shall consider the effect of tem-
perature change and the influence lines for parabolic arches.

Stresses produced by temperature changes may be of considerable
importance especially in cases of flat and comparatively thick arches.
The discussion of thermal stresses we begin with the application of Eq.
(149). Later on, by using the more complete equations (109), (110),
and (111) in analyzing deformations, we shall investigate the accuracy
of the results obtained from this approximate equation. If we take the
coordinate axes as shown in Fig. 461, the equation of the center line of
the parabolic arch becomes

$$y = \frac{4fx^2}{l^2}. \tag{a}$$

Assuming also that

$$A = \frac{A_0}{\cos \phi}, \qquad I = \frac{I_0}{\cos \phi}, \tag{b}$$

we find the position of the elastic center from Eq. (134), which gives

$$d = \frac{\int_0^{\frac{l}{2}} y \, dx}{\int_0^{\frac{l}{2}} dx} = \frac{f}{3}. \tag{160}$$

The integrals in Eq. (149) then are

$$\int_0^{sb} \frac{y(y-d) \, ds}{EI} = \frac{2}{45} \frac{f^2 l}{EI_0},$$

$$\int_0^{sb} \frac{\cos^2 \phi \, ds}{AE} = \frac{1}{8} \frac{l^2}{A_0 Ef} \arctan \frac{4f}{l},$$

and we obtain

$$H_0 = \frac{45}{4} \frac{EI_0 \alpha t}{f^2 \left(1 + \frac{45}{16} \frac{k^2 l}{f^3} \arctan \frac{4f}{l}\right)}, \tag{161}$$

where k is the radius of gyration of the cross section at the crown of the arch. The bending moment and the axial force at the crown are then obtained from Eqs. (150).

To show the effect of the variation in I on the magnitude of H_0 let us consider also the case in which

$$A = \frac{A_0}{\cos \phi}, \qquad I = \frac{I_0}{\cos^3 \phi}. \tag{c}$$

Equation (134) then gives

$$d = \frac{\int_0^{\frac{l}{2}} y \cos^2 \phi \, dx}{\int_0^{\frac{l}{2}} \cos^2 \phi \, dx} = \frac{l \left(1 - \frac{l}{4f} \arctan \frac{4f}{l}\right)}{4 \arctan \frac{4f}{l}}. \tag{162}$$

In the case of flat arches, we can put

$$\arctan \frac{4f}{l} = \frac{4f}{l} - \frac{1}{3} \left(\frac{4f}{l}\right)^3.$$

Then the value (162) coincides with that in Eq. (160). The first of the two integrals in Eq. (149) becomes

$$\frac{1}{EI_0} \int_0^{\frac{l}{2}} (y - d) y \cos^2 \phi \, dx = \frac{l^3}{32EI_0} \left[\frac{1}{3} + \frac{l}{4f}\left(\frac{l}{4f} - \frac{1}{\arctan \frac{4f}{l}}\right)\right].$$

The second integral remains unchanged, and we obtain

$$H_0 = m \cdot \frac{EI_0 \alpha t}{l^2} \tag{163}$$

where

$$m = \frac{16}{\frac{1}{3} + \frac{l}{4f}\left(\frac{l}{4f} - \frac{1}{\arctan \frac{4f}{l}}\right) + \frac{4k^2}{fl} \arctan \frac{4f}{l}}$$

The values of this coefficient for various proportions of the arch are given in the third line of Table XIV. The figures in the fourth line of the

same table are the values of the factor m in Eq. (163) calculated by assuming a rectangular cross section and using the more elaborate equations (109) to (111), instead of Eqs. (112), which take into account the effect on H_0 of the shearing forces and of the curvature. In the fifth line the errors in per cent of the approximate values of m are given. It is seen that the errors in H_0 due to the use of the approximate equations (112) may become of practical importance only in the case of arches of large thickness h.

TABLE XIV.—VALUES OF m IN EQ. (163)

	$f/l = \frac{1}{12}$			$f/l = \frac{1}{10}$			$f/l = \frac{1}{8}$			$f/l = \frac{1}{6}$			$f/l = \frac{1}{4}$		
h/l......	$\frac{1}{6}$	$\frac{1}{12}$	$\frac{1}{24}$	$\frac{1}{8}$	$\frac{1}{16}$	$\frac{1}{24}$	$\frac{1}{9}$	$\frac{1}{18}$	$\frac{1}{27}$	$\frac{1}{12}$	$\frac{1}{24}$	$\frac{1}{36}$	$\frac{1}{16}$	$\frac{1}{32}$	$\frac{1}{48}$
m.......	355.0	876.1	1,384	484.5	881.2	1,039	457.4	679.9	747.3	395.2	465.8	481.6	249.3	261.8	264.2
(m).....	327.2	832.5	1,356	444.1	846.1	1,016	415.6	655.4	733.6	366.4	455.2	476.6	237.5	258.4	262.7
%......	8.5	5.2	2.1	9.2	4.1	2.3	10.1	3.7	1.9	7.9	2.3	1.0	5.0	1.3	0.6
H'/H...	0.7567	0.4817	0.1962	0.5778	0.2753	0.1470	0.4272	0.1686	0.0839	0.2118	0.0659	0.0307	0.0773	0.0210	0.0095
δ/h_0.....	0.494	0.296	0.156	0.341	0.190	0.124	0.254	0.139	0.094	0.152	0.080	0.054	0.081	0.042	0.028
δ_1/h_1....	0.729	0.521	0.292	0.546	0.342	0.239	0.408	0.244	0.169	0.246	0.137	0.093	0.122	0.064	0.043

Equations (161) and (163) can be applied in investigating the effect of *shrinkage* of concrete in concrete arches on the magnitude of stresses. In such a case, the expected unit contraction due to shrinkage with negative sign must be substituted for αt in these equations.

The same equations can also be applied in analyzing stresses due to relative horizontal movement of the abutments of an arch. If, under the action of thrust, the distance between the supports of an arch increases by an amount Δ, the effect of this movement on the thrust will evidently be equivalent to that produced by a lowering of temperature of the arch. The equivalent change in temperature will be found from the equation

$$-\alpha t l = \Delta.$$

Hence, upon substituting $-\Delta/l$ instead of αt into Eqs. (161) and (163) the change in thrust, produced by the support movements, will be found.

Let us now calculate the ordinates of the influence lines for parabolic arches satisfying conditions (a) and (b). Beginning with the line for H_0 we use Eq. (151). In calculating the first approximation for H_0, the action of the axial force on the deformation is often neglected. Then, omitting the second term in Eqs. (136) and (138), we obtain

$$v_c = -\int_{x_c}^{\frac{l}{2}} \frac{(x - x_c)(y - d)dx}{EI_0} = -\frac{fl^2}{48EI_0}\left(1 - \frac{4x_c^2}{l^2}\right)^2,$$

$$u_d = \int_0^{\frac{l}{2}} \frac{y(y - d)dx}{EI_0} = \frac{2}{45}\frac{f^2 l}{EI_0}.$$

Substituting these values in Eq. (151), we find

$$H_0 = \frac{15}{64} \frac{Pl}{f} \left(1 - \frac{4x_c^2}{l^2} \right)^2. \tag{164}$$

Instead of measuring the horizontal distances of the moving load from the crown, we can take the distances $l/2 - x_c$ from the support. Introducing then the notation

$$\frac{l/2 - x_c}{l} = n, \tag{165}$$

we represent Eq. (164) in the following form

$$H_0 = \frac{15}{4} \frac{Pl}{f} n^2 (1 - n)^2. \tag{166}$$

It is seen that, if the effect of the axial force on deformation is neglected, the values of H_0 depend only on the ratio f/l and on the position of the load. To investigate the accuracy of the approximate Eqs. (164) and (166), calculations were made for arches of rectangular cross section in which the effect of the axial force and also the effect of shearing force, defined by Eq. (109), were considered. These calculations showed that the more accurate value of thrust can be represented by the equation

$$H_0 = m_1 \frac{15}{4} \frac{Pl}{f} n^2 (1 - n)^2, \tag{167}$$

where m_1 is a numerical factor depending on the proportions of the arch. Several values of this factor are given in Table XV. It is seen that the approximate equa-

TABLE XV.—VALUES OF FACTOR m_1 IN EQ. (167)

f/l	$\frac{1}{12}$			$\frac{1}{8}$			$\frac{1}{4}$			$\frac{1}{2}$		
h/l n	$\frac{1}{10}$	$\frac{1}{20}$	$\frac{1}{30}$	$\frac{1}{10}$	$\frac{1}{20}$	$\frac{1}{30}$	$\frac{1}{10}$	$\frac{1}{20}$	$\frac{1}{30}$	$\frac{1}{10}$	$\frac{1}{20}$	$\frac{1}{30}$
$\frac{1}{2}$	0.440	0.749	0.869	0.635	0.868	0.937	0.869	0.962	0.982	0.964	0.990	0.996
$\frac{3}{8}$	0.442	0.749	0.869	0.638	0.869	0.937	0.871	0.962	0.982	0.964	0.990	0.996
$\frac{1}{4}$	0.450	0.753	0.872	0.648	0.873	0.939	0.879	0.965	0.984	0.965	0.990	0.996
$\frac{1}{8}$	0.478	0.766	0.878	0.684	0.886	0.945	0.909	0.973	0.988	0.976	0.993	0.997

tions (164) and (166) are not accurate enough in the case of flat and comparatively thick arches and that the use of Eq. (167), instead of (166), is necessary in such cases.

In deriving the influence line for M_0, we use Eq. (152). From Eqs. (132) and (133) we obtain in this case

$$v_c = - \int_{x_c}^{\frac{l}{2}} \frac{(x - x_c)dx}{EI_0} = - \frac{1}{2EI_0} \left(\frac{l}{2} - x_c \right)^2,$$

$$\theta_d = \int_0^{\frac{l}{2}} \frac{dx}{EI_0} = \frac{l}{2EI_0},$$

and Eq. (152) gives

$$M_0 = \frac{P}{2l}\left(\frac{l}{2} - x_c\right)^2 = \frac{Pl}{2}\,n^2. \tag{168}$$

More elaborate calculations by using Eqs. (109) and (111), instead of Eq. (112), show that Eq. (168) is accurate enough in all practical cases and can always be used in calculating M_0. Having M_0 we find the bending moment M_d at the crown from the equation

$$M_d = M_0 - H_0 d. \tag{169}$$

In deriving the influence line for the shearing force, we use Eq. (153). Neglecting the effect of axial force, we obtain from Eqs. (142) and (145)

$$v_c = -\int_{x_c}^{\frac{l}{2}} \frac{x(x - x_c)dx}{EI_0} = -\frac{1}{EI_0}\left(\frac{l^3}{24} + \frac{x_c^3}{6} - \frac{l^2 x_c}{8}\right),$$

$$v_d = -\int_0^{\frac{l}{2}} \frac{x^2 dx}{EI_0} = -\frac{l^3}{24EI_0}.$$

Hence,

$$V_0 = \frac{P}{2}\left(1 + \frac{4x_c^3}{l^3} - \frac{3x_c}{l}\right). \tag{170}$$

Examples of influence lines, calculated from Eqs. (166), (168), and (170), are shown in Fig. 464. From the influence lines for H_0 and M_0 the influence line for the bending moment M_d at the crown will be obtained by using Eq. (169). This influence line is given by the shaded areas in Fig. 464d.

In the case of parabolic arches having

$$A = \frac{A_0}{\cos \phi}, \qquad I = \frac{I_0}{\cos^3 \phi},$$

the calculations show that Eqs. (167), (168) and (170) still can be applied with sufficient accuracy.

Comparisons of arches of various shapes indicate that considerable deviations from the shape of the arch, defined by Eqs. (a) and (b), produce only a small effect on the ordinates of influence lines. This means that the influence lines derived for parabolic arches can be used in an approximate analysis of arches of other shapes. The application of these lines, however, in the calculation of stresses produced by dead load or temperature change may result in errors of considerable magnitude. The reason for these errors is clearly seen from the influence line in Fig. 464d. If we assume, for example, that a dead load q is uniformly distributed along the span, the bending moment M_d at the crown is obtained by multiplying by q the algebraic sum of the three areas of the influence diagram. It is evident that the accuracy with which this sum is obtained will be much

lower than the accuracy with which the ordinates of the H_0- and M_0-influence lines are known.
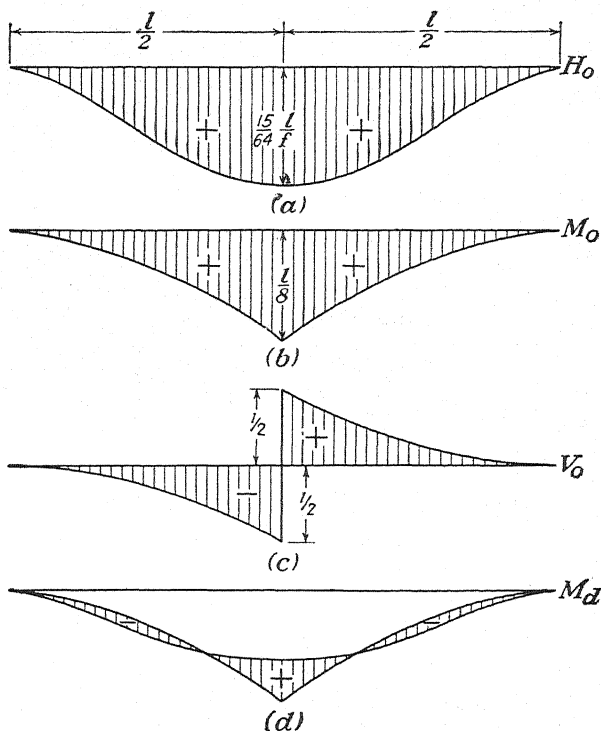

FIG. 464.

77. Hingeless Symmetrical Circular Arches.—If the center line of an arch is a circular segment (Fig. 465), we have

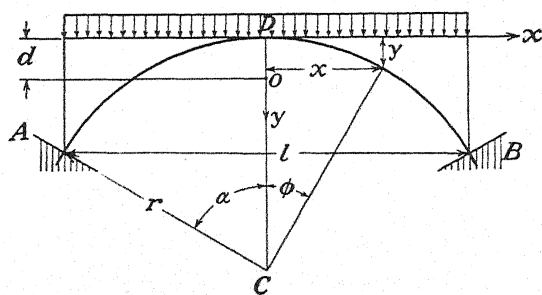$$x = r \sin \phi, \qquad y = r(1 - \cos \phi), \qquad l = 2r \sin \alpha. \qquad (a)$$

FIG. 465.

As a first example, let us consider an arch of constant cross section and assume that a load q is uniformly distributed along the span (Fig. 465). The distance d of the

elastic center in this case [see Eq. (134)] is

$$d = \frac{r}{\alpha}(\alpha - \sin \alpha). \tag{b}$$

For calculating H_0 and M_0, we use Eqs. (147) and (148). Substituting in these equations

$$M = -\frac{qx^2}{2} = -\frac{1}{2}qr^2 \sin^2 \phi, \qquad N = qx \sin \phi = qr \sin^2 \phi,$$

we obtain

$$H_0 = \frac{ql}{12 \sin \alpha} \cdot \frac{\sin \alpha(3\alpha - 3 \sin \alpha \cos \alpha - 2\alpha \sin^2 \alpha) - 4\dfrac{k^2}{r^2}\alpha \sin^3 \alpha}{\alpha^2 + \alpha \sin \alpha \cos \alpha - 2 \sin^2 \alpha + \dfrac{k^2}{r^2}(\alpha^2 + \alpha \sin \alpha \cos \alpha)}, \tag{171}$$

$$M_0 = \frac{ql^2}{16\alpha \sin^2 \alpha}(\alpha - \sin \alpha \cos \alpha). \tag{172}$$

The bending moment M_d at the crown is then obtained from Eq. (169). Representing H_0 and M_d in the form

$$H_0 = mql, \qquad M_d = nql^2, \tag{173}$$

we give the values of the factors m and $n \cdot 10^6$ for arches of rectangular cross section in lines 4 and 6, respectively, of Table XVI.

TABLE XVI.—VALUES ON CONSTANTS m, n, m_1, m_2 FOR CIRCULAR ARCHES

1	$\alpha =$	27 deg.			36 deg.			54 deg.			90 deg.		
2	$f/l =$	0.1200			0.1625			0.2548			0.5000		
3	$h/l =$	$\frac{1}{10}$	$\frac{2}{10}$	$\frac{3}{10}$	$\frac{1}{10}$	$\frac{2}{10}$	$\frac{3}{10}$	$\frac{1}{10}$	$\frac{2}{10}$	$\frac{3}{10}$	$\frac{1}{10}$	$\frac{2}{10}$	$\frac{3}{10}$
4	m	0.5758	0.8798	0.9701	0.6190	0.7339	0.7593	0.4821	0.5012	0.5048	0.2779	0.2795	0.2798
5	(m)	0.6149	0.8847	0.9710	0.6278	0.7342	0.7592	0.4811	0.5008	0.5047	0.2768	0.2792	0.2797
6	$n \cdot 10^6$	19,732	7,476	3,838	10,020	3,719	2,325	5,122	2,445	3,132	12,010	11,720	11,660
7	$(n) \cdot 10^6$	17,540	7,066	3,699	9,051	3,564	2,266	4,916	3,408	3,107	12,030	11,720	11,660
8	m_1	526.3	770.9	843.5	233.6	270.6	278.9	53.44	55.05	55.36	6.692	6.714	6.718
9	(m_1)	480.7	745.0	823.5	217.5	264.9	276.2	51.57	54.54	55.12	6.619	6.695	6.707
10	(m_2)	536	865	974	282.0	360.4	379.7	107.4	119.0	121.4	70.13	75.69	76.80

Equations (134), (147), and (148) used in these calculations were derived from the simplified equations (112). To investigate the accuracy of this simplified derivation, calculations were also made on a basis of the complete equations (109), (110), and (111). The results of these more elaborate calculations are given in lines 5 and 7 of the table. It is seen that Eq. (171) is accurate enough in all cases, except for very flat and thick arches, while the errors in values of M_d [Eq. (173)], are considerably larger. The reason for this has already been discussed in the preceding article (see page 446).

Let us consider now the magnitude of the thrust produced in a circular arch of constant cross section by a uniform temperature change. Substituting in Eq. (149) for y and d their expressions (a) and (b) and performing the indicated integrations,

we obtain

$$H_0 = m_1 \cdot \frac{EI_0 \alpha t}{r^2},$$ (174)

where

$$m_1 = \frac{2\alpha \sin \alpha}{\alpha^2 + \alpha \sin \alpha \cos \alpha - 2\sin^2 \alpha + \dfrac{k^2}{r^2}(\alpha^2 + \alpha \sin \alpha \cos \alpha)}.$$

The values of this factor are given in the eighth line of the table. In the ninth line, the values (m_1) were obtained by using Eqs. (109) to (111), instead of Eqs. (112). Again we see that more accurate calculations may be required in the case of flat and comparatively thick arches.

We give now some final results for a circular arch of variable cross section for which

$$A = \frac{A_0}{\cos \phi}, \qquad I = \frac{I_0}{\cos^3 \phi}.$$

The thrust produced by temperature change again is given by Eq. (174), but, instead of factors (m_1), factors (m_2) given in the tenth line of the Table XVI must be used. Comparing the values of (m_2) with those of (m_1) we see that, owing to increase in cross sections toward the supports, the thrust produced by temperature change increases.

Having the force H_0 produced by temperature change, we calculate the bending moment and axial force at the crown by using Eqs. (150). From statics, we find also the bending moment and axial force at the abutments. With these quantities, the thermal stresses can be calculated. Such calculations show that thermal stresses may become very large at the abutments of flat and thick arches. We arrive at the same conclusion also in analyzing stresses caused by shrinkage of the concrete or due to settlement of the abutments. In the case of materials that are weak in tension, these stresses may produce cracks at the abutments. This shows that it is advantageous, in the case of small values of f/l, to use three-hinged arches in which uniform temperature change and shrinkage do not produce stresses.

78. Numerical Calculation of Redundant Quantities in Arches.—The calculation of redundant quantities requires the evaluation of integrals such as we encounter in Eqs. (134), (147), (148), and (149). In the case of parabolic and circular arches, which were considered in the two preceding articles, these integrals can be readily evaluated. But often we have more complicated curves, or we have curves for which no analytical expression is known and only a system of ordinates is given. In all such cases, recourse must be had to an approximate calculation of integrals. For this purpose the arch will be divided into a finite number of segments and the integration replaced by a summation. In applying this numerical method of approximate integration, there arises the question regarding the number of subdivisions that must be used in order to obtain a required accuracy in the result. This question can be answered and the accuracy of calculations can be best demonstrated on particular examples. For this purpose, we select examples the rigorous solution for which is known; thus the errors of the approximate calculations can be readily seen.

Let us begin with a parabolic arch for which

$$\frac{f}{l} = \frac{1}{8}, \qquad A = \frac{A_0}{\cos \phi}, \qquad I = \frac{I_0}{\cos^3 \phi} \qquad (a)$$

and calculate the thrust H_0 produced by a uniform change in temperature. The position of the elastic center is determined from Eq. (162), which gives

$$d = \frac{l}{4 \arctan 4f/l} - \frac{l^2}{16f} = 0.03920l. \qquad (b)$$

The calculation of H_0 requires the evaluation of the two integrals in Eq. (149). The first of these integrals can be simplified by using the notation

$$y_1 = y - d \qquad (c)$$

and observing that, by virtue of Eq. (134), we have

$$\int_0^{s_b} \frac{(y - d)ds}{EI} = \int_0^{s_b} \frac{y_1 ds}{EI} = 0.$$

Then

$$\int_0^{s_b} \frac{y(y - d)ds}{EI} = \int_0^{s_b} \frac{(y_1 + d)y_1 ds}{EI} = \int_0^{s_b} \frac{y_1^2 ds}{EI}$$

$$= \frac{1}{EI_0} \int_0^{\frac{l}{2}} y_1^2 \cos^2 \phi \, dx. \qquad (d)$$

The second integral is

$$\int_0^{s_b} \frac{\cos^2 \phi \, ds}{AE} = \frac{1}{A_0 E} \int_0^{\frac{l}{2}} \cos^2 \phi \, dx. \qquad (e)$$

We now divide the length of the half span into eight equal parts and calculate for each subdivision or segment the quantities given in Table XVII by using for a parabola the known equations

$$y_1 = \frac{4fx^2}{l^2} - d, \qquad \cos^2 \phi = \frac{1}{1 + 64f^2x^2/l^4}.$$

TABLE XVII.—DATA FOR THE PARABOLIC ARCH GIVEN BY EQS. (a)

x/l	y_1/l	y_1^2/l^2	$\cos^2 \phi$	$y_1^2 \cos^2 \phi/l^2$	$\sin^2 \phi$
0	−0.03920	0.001537	1	0.001537	0
$\frac{1}{16}$	−0.03725	0.001388	$\frac{256}{257}$	0.001383	$\frac{1}{257}$
$\frac{1}{8}$	−0.03138	0.000984	$\frac{64}{65}$	0.000969	$\frac{1}{65}$
$\frac{3}{16}$	−0.02162	0.000467	$\frac{256}{265}$	0.000452	$\frac{9}{265}$
$\frac{1}{4}$	−0.00795	0.000063	$\frac{16}{17}$	0.000059	$\frac{1}{17}$
$\frac{5}{16}$	+0.00963	0.000093	$\frac{256}{281}$	0.000085	$\frac{25}{281}$
$\frac{3}{8}$	+0.03111	0.000968	$\frac{64}{73}$	0.000849	$\frac{9}{73}$
$\frac{7}{16}$	+0.05650	0.003192	$\frac{256}{305}$	0.002679	$\frac{49}{305}$
$\frac{1}{2}$	+0.08580	0.007362	$\frac{4}{5}$	0.005890	$\frac{1}{5}$

Now applying Simpson's rule to the integral (d), we obtain

$$\frac{1}{EI_0} \int_0^{\frac{l}{2}} y_1{}^2 \cos^2 \phi \, dx = \frac{l^3}{16EI_0} \cdot \frac{1}{3} [0.001537 + 4(0.001383 + 0.000452$$
$$+ 0.000085 + 0.002679) + 2(0.000969 + 0.000059 + 0.000849)$$
$$+ 0.005890] = 0.004929 \frac{l^3}{8EI_0}.$$

Proceeding in the same manner with the integral (e) and assuming a rectangular cross section, we obtain

$$\frac{1}{A_0 E} \int_0^{\frac{l}{2}} \cos^2 \phi \, dx = \frac{l}{2A_0 E} \cdot 0.9273 = \frac{lh_0{}^2}{24EI_0} \cdot 0.9273.$$

Substituting the calculated values of the integrals in Eq. (149), we obtain

$$\frac{H_0 l^3}{8EI_0} \left(0.004929 + \frac{1}{3} \frac{h_0{}^2}{l^2} 0.9273 \right) = \frac{\alpha t l}{2}. \tag{f}$$

The second term in the parentheses represents the influence of the longitudinal force N on the value of H_0. Let us consider the case of a very thick arch and assume $h_0/l = \frac{1}{9}$. Then Eq. (f) gives

$$\frac{H_0 l^3}{8EI_0} (0.004929 + 0.003816) = \frac{\alpha t l}{2},$$

and we obtain

$$H_0 = 457.4 \frac{\alpha t E I_0}{l^2}. \tag{g}$$

Taking $h_0/l = \frac{1}{27}$, we find

$$H_0 = 747.3 \frac{\alpha t E I_0}{l^2}. \tag{h}$$

The results obtained coincide exactly with the values given for our arch in Table XIV. This indicates that the subdivision of the half span into eight parts and the application of Simpson's rule give a very high degree of accuracy. If we divide the half span into only four parts, then Simpson's rule gives H_0, for the foregoing example, with an error of about 0.2 of 1 per cent. This shows that it is not necessary to divide an arch into many parts to obtain sufficiently good accuracy in applying Simpson's rule.

As a second example, let us consider the case of a circular arch of constant rectangular cross section and assume that the load is uniformly distributed along the span (Fig. 465). For calculating H_0 and M_0, we use Eqs. (147) and (148). The quantities entering into these equations are

$$x = r \sin \phi, \qquad y = r(1 - \cos \phi),$$

$$d = \frac{r}{\alpha}(\alpha - \sin \alpha), \text{ (see p. 448)},$$

$$M = -\frac{qx^2}{2} = -\frac{qr^2 \sin^2 \phi}{2},$$

$$N = qx \sin \phi = qr \sin^2 \phi.$$

Using again the notation $y_1 = y - d$, the integrals that we have to calculate become

$$\int_0^{sb} \frac{My\,ds}{EI} - d\int_0^{sb} \frac{M\,ds}{EI} = \int_0^{sb} \frac{y_1 M\,ds}{EI} = -\frac{qr^3}{2EI}\int_0^{\alpha} y_1 \sin^2 \phi\, d\phi,$$

$$\int_0^{sb} \frac{N \cos \phi\, ds}{AE} = \frac{qr^2}{AE}\int_0^{\alpha} \sin^2 \phi \cos \phi\, d\phi,$$

$$\int_0^{sb} \frac{y(y-d)ds}{EI} = \int_0^{sb} \frac{y_1^2 ds}{EI} = \frac{r}{EI}\int_0^{\alpha} y_1^2 d\phi,$$

$$\int_0^{sb} \frac{M\,ds}{EI} = -\frac{qr^3}{2EI}\int_0^{\alpha} \sin^2 \phi\, d\phi,$$

$$\int_0^{sb} \frac{\cos^2 \phi\, ds}{AE} = \frac{r}{AE}\int_0^{\alpha} (1 - \sin^2 \phi)d\phi = \frac{r}{AE}\left(\alpha - \int_0^{\alpha} \sin^2 \phi\, d\phi\right).$$

We take $\alpha = 36$ deg. and divide the semiarch into eight equal parts. Then

$$d = \frac{r}{\alpha}(\alpha - \sin \alpha) = 0.06451r,$$

and the quantities under the integral signs have the values given in Table XVIII.

TABLE XVIII.—DATA FOR A CIRCULAR ARCH HAVING $\alpha = 36$ DEG.

ϕ, deg.	y_1/r	y_1^2/r^2	$y_1 \sin^2 \phi/r$	$\sin^2 \phi$	$\sin^2 \phi \cos \phi$
0	−0.06451	0.004162	0	0	0
4.5	−0.06143	0.003774	−0.000378	0.00616	0.00614
9.0	−0.05220	0.002725	−0.001277	0.02447	0.02417
13.5	−0.03688	0.001360	−0.002010	0.05449	0.05299
18.0	−0.01557	0.000242	−0.001487	0.09549	0.09082
22.5	+0.01161	0.000135	+0.001700	0.14645	0.1353
27.0	+0.04448	0.001978	+0.009167	0.20611	0.1836
31.5	+0.08285	0.006864	+0.022620	0.27300	0.2328
36.0	+0.12647	0.015995	+0.043690	0.34549	0.2795

Using the values from this table and observing that an angle of 4.5 deg. is equal in radians to 0.07854, we obtain the following numerical values of all necessary integrals:

$$-\frac{qr^3}{2EI}\int_0^{\alpha} \sin^2 \phi\, d\phi = -\frac{qr^3}{2EI}\frac{0.07854}{3}[0 + 4(0.00616 + 0.05449 + 0.14645 + 0.27300$$

$$+ 2(0.02447 + 0.09549 + 0.20611) + 0.34549] = -\frac{qr^3}{2EI} \cdot 0.07639,$$

$$\frac{qr^2}{AE}\int_0^{\alpha} \sin^2 \phi \cos \phi\, d\phi = \frac{qr^2}{AE} \cdot 0.06769,$$

$$\frac{r}{EI}\int_0^{\alpha} y_1^2 d\phi = \frac{r^3}{EI} \cdot 0.002057,$$

$$-\frac{qr^3}{2EI}\int_0^{\alpha} y_1 \sin^2 \phi\, d\phi = -\frac{qr^4}{2EI} \cdot 0.003776.$$

Substituting these numerical values of the integrals in Eq. (147), we obtain

$$-\frac{qr^4}{2EI} \cdot 0.003776 + \frac{qr^2}{AE} \cdot 0.06769 + H_0\left(\frac{r^3}{EI} \cdot 0.002057 + \frac{r}{AE} \cdot 0.5519\right) = 0$$

and

$$H_0 = \frac{qr}{2}\frac{0.003776 - \cdot 2(h^2/12r^2)0.06769}{0.002057 + (h^2/12r^2)0.5519}.$$

Taking, for example, $h/r = 0.1$, we find

$$H_0 = \frac{qr}{2} \cdot \frac{0.003664}{0.002517} = 0.6191ql.$$

This coincides up to one unit in the last place with the value given in Table XVI.

Let us calculate now the bending moment M_d at the crown. From Eq. (148), we obtain

$$-\frac{qr^3}{2EI} \cdot 0.07639 + \frac{M_0 r}{EI} \cdot 0.6283 = 0,$$

which gives

$$M_0 = 0.04389ql^2,$$

and

$$M_d = M_0 - H_0 d = 0.04389ql^2 - 0.6191ql \cdot 0.06451r = 0.00992ql.$$

This moment differs by about 1 per cent from the value given in the sixth line of Table XVI. Since the bending moment M_d is obtained as a difference of the two quantities that do not differ much one from another, the accuracy of the result is much lower than that for H_0, but it is sufficient for practical applications.

We arrive at the same conclusion also in applying Simpson's rule in the calculation of influence lines. It can be stated in general that dividing the semiarch into eight equal portions and making the calculations to four significant figures we shall always obtain the redundant quantities with sufficient accuracy for practical applications. In our example of a circular arch all the quantities under the integral signs in Eqs. (147) and (148) given in Table XVIII were calculated from formulas for a circle. If we do not have an analytical expression for the center line and the curve is given graphically, then all necessary quantities must be taken from the drawing and a table similar to Table XVIII must be prepared before starting the calculation of the integrals in Eqs. (147) and (148).

In applying Simpson's rule we have to subdivide the center line of an arch into equal parts. Sometimes it is simpler to have unequal subdivisions, and in this case Simpson's rule cannot be applied. Then we replace the integrations by simple summations. We calculate the values of the quantities under the integral signs for the center of each portion and sum up these values. To show this kind of calculation let us determine the thrust produced by a uniform temperature change in the voussoir arch shown in Fig. 466. We begin with a calculation of the distance d of the elastic center of the arch. For this purpose we divide half the arch into eight portions with centers 1, 2, 3, . . . as shown in Fig. 466. The designation of these portions, their lengths Δs, and the cross-sectional dimensions at the centers are given in the first four columns of Table XIX. In the fifth column are given the moments of

inertia of the middle cross sections and in the sixth column the quantities $\Delta s/I$ at the centers of the portions. The summation of this column gives the approximate value of the denominator in Eq. (134) multiplied by E. The seventh column gives the ordinates of the centers 1, 2, 3,
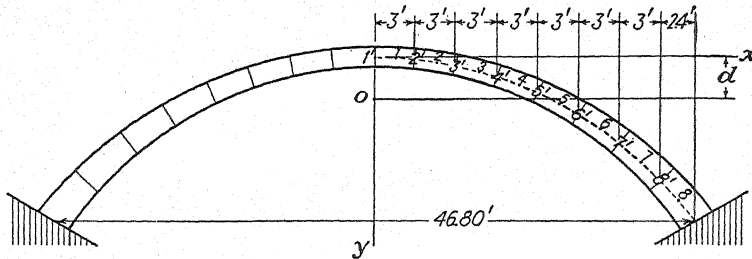

Fig. 466.

. . . , and the eighth column gives the moments of the quantities $\Delta s/I$ with respect to the x-axis. The summation of this column gives the approximate value of the numerator in Eq. (134) multiplied by E. The required distance d of the elastic center then is

$$d = \frac{10.9174}{3.2795} = 3.329 \text{ ft.} \qquad (i)$$

Table XIX.—Data for Arch in Fig. 466

(1)	(2)	(3)	(4)	(5)	(6)	(7)	(8)	(9)	(10)	(11)	(12)
Segment	Δs, ft.	b, ft.	h, ft.	I, ft.^{4}	$\dfrac{\Delta s}{I}$, ft.$^{-3}$	y, ft.	$\dfrac{\Delta s y}{I}$, ft.$^{-2}$	y_1, ft.	$\dfrac{\Delta s y_1{}^2}{I}$, ft.$^{-1}$	$\dfrac{\Delta s}{A}$	$\dfrac{\Delta s}{A}\cos^2 \varphi$
1	3.00	12	1.800	5.832	0.5144	0.045	0.0231	−3.284	5.548	0.139	0.138
2	3.06	12	1.830	6.132	0.4990	0.375	0.1871	−2.954	4.355	0.139	0.131
3	3.15	12	1.860	6.431	0.4898	1.050	0.5142	−2.279	2.544	0.141	0.123
4	3.27	12	1.945	7.241	0.4516	2.130	0.9618	−1.199	0.649	0.141	0.109
5	3.51	12	2.040	8.489	0.4135	3.720	1.5381	+0.391	0.063	0.143	0.097
6	3.93	12	2.190	10.506	0.3741	5.895	2.2052	+2.566	2.463	0.150	0.087
7	4.56	12	2.415	14.086	0.3237	8.835	2.8602	+5.506	9.814	0.157	0.078
8	4.20	12	2.700	19.683	0.2134	12.315	2.6277	+8.986	17.229	0.130	0.055
$\Sigma =$	....	..	.....	......	3.2795	......	10.9174	....	42.665	.....	0.818

In calculating the required thrust we now use Eq. (149), which gives

$$H_c = \frac{\alpha t l E}{2\left[\displaystyle\sum \frac{y(y-d)\Delta s}{I} + \sum \frac{\Delta s \cos^2 \phi}{A}\right]}.$$

Introducing the notation

$$y_1 = y - d$$

and observing that, by virtue of Eq. (i),

$$\sum \frac{(y - d)\Delta s}{I} = 0,$$

we obtain

$$H_0 = \frac{\alpha t l E}{2 \left(\sum \dfrac{y_1{}^2 \Delta s}{I} + \sum \dfrac{\Delta s \, \cos^2 \phi}{A} \right)}. \tag{j}$$

The summations in the denominator of this equation are given in columns (10) and (12) of Table XIX. Assuming now, for example, $\alpha = 6 \cdot 10^{-6}$, $t = 25°\mathrm{F}$., and $E = 432 \cdot 10^6$ lb. per sq. ft., we obtain

$$H_0 = 34{,}870 \text{ lb.}$$

This is the required thrust produced by the temperature change.

Let us now calculate the ordinates of the influence line for H_0. In this case we use Eq. (151) together with Eqs. (136) and (138). Neglecting the second term on the right side of Eq. (136), as a small quantity, we represent the ordinates η of the required influence line by the expression

$$\eta = \frac{\displaystyle\int_{s_c}^{s_b} \frac{(x - x_c)(y - d)ds}{I}}{2 \left[\displaystyle\int_0^{s_b} \frac{y(y - d)ds}{I} + \int_0^{s_b} \frac{\cos^2 \phi \, ds}{A} \right]}. \tag{k}$$

The denominator of this expression we have already calculated. The numerator, as we see, represents the moment of the quantities $y_1 \Delta s / I$ distributed on the portion CB of the center line (Fig. 462a) with respect to the vertical axis through point C, for which the ordinate η is to be calculated. Upon taking the points $8'$, $7'$, $6'$, . . . shown in Fig. 466, the corresponding values of the above-mentioned moments are as shown in the third column of Table XX. Dividing these moments by the value

TABLE XX.—DATA FOR H_0-INFLUENCE-LINE CALCULATION

Number	$\dfrac{\Delta s y_1}{I}$	$\sum (x - x_c) \dfrac{y_1 \Delta s}{I}$	η
$8'$	1.917	$1.917 \cdot 1.2 \qquad\qquad = 2.30$	0.026
$7'$	1.782	$2.300 + 1.917 \cdot 3 + 1.782 \cdot 1.5 = 10.72$	0.123
$6'$	0.960	$10.724 + 3.699 \cdot 3 + 0.960 \cdot 1.5 = 23.26$	0.266
$5'$	0.162	$\dotfill = 37.49$	0.430
$4'$	-0.541	$\dotfill$	$\dots$
$3'$	-1.116	$\dotfill$	$\dots$
$2'$	-1.474	$\dotfill$	$\dots$
$1'$	-1.689	$\dotfill$	$\dots$

of the denominator in expression (k), equal to $2(42.665 + 0.818) \approx 87.0$, we obtain the required ordinates of the H_0-influence line. Several of these ordinates are given in the last column of the table.

79. Funicular Curve as the Center Line of an Arch.—It is advantageous, in the case of a three-hinged arch supporting a distributed permanent load, to make the center line of the arch coincide with the funicular curve for that load. If this condition is fulfilled, the resultant
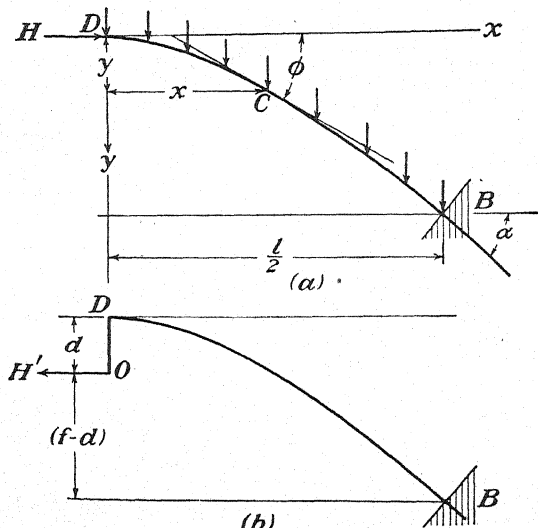
Fig. 467.

force on each cross section of the arch is tangent to the center line, producing only uniformly distributed compressive stresses (see page 27). In the case of a hingeless arch, the internal forces depend on the deformation of the arch, and we cannot entirely eliminate the bending stresses. But their magnitudes can be reduced by a proper selection of the shape of the center line. It is common practice to take as a first approximation for the center line of a hingeless arch the funicular curve constructed as for a three-hinged arch, having hinges at the centroids of the crown and abutment cross sections. Let H denote the thrust at the crown of such a three-hinged arch. Then the thrust in our hingeless arch will be smaller than H by a certain amount H' that can be readily calculated considering the deformation of the arch. Let DB represent one-half the hingeless arch (Fig. 467a), with the given load acting on it. If the thrust H is applied at the centroid of the cross section D, the resultant force acting on any cross section C produced by H and the load on the portion DC of the arch will be tangent to the center line. Assuming the

load vertical, the magnitude of the axial force will be

$$N = \frac{H}{\cos \phi}. \tag{a}$$

The compression of the element ds of the center line, produced by this force, is

$$\frac{H \, ds}{AE \cos \phi}.$$

Summing up the horizontal projections of such compressions, we find that the horizontal displacement at the cross section D is [1]

$$u_d = \int_0^{s_b} \frac{H \, ds}{AE}. \tag{b}$$

In the actual symmetrically loaded hingeless arch, there will be no lateral or rotational displacement of the cross section D. These conditions will be satisfied if to the forces considered in Fig. 467a we add the horizontal force H' (Fig. 467b) applied at the elastic center O and of such magnitude as to eliminate the displacement (b). This requires [see Eq. (138)] that

$$H' \left[\int_0^{s_b} \frac{y(y-d)ds}{EI} + \int_0^{s_b} \frac{\cos^2 \phi \, ds}{AE} \right] = \int_0^{s_b} \frac{H \, ds}{AE}.$$

Hence

$$H' = H \, \frac{\displaystyle\int_0^{s_b} ds/AE}{\displaystyle\int_0^{s_b} \frac{y(y-d)ds}{EI} + \int_0^{s_b} \frac{\cos^2 \phi \, ds}{AE}}. \tag{175}$$

Since the combined action of the forces shown in Figs. 467a and 467b satisfies the above-mentioned conditions for the symmetrically loaded hingeless arch, we conclude that the two forces H and H' together represent a system statically equivalent to the internal forces acting on the cross section D of the arch. This system can be reduced to the longitudinal force and the bending moment defined by the equations

$$N_d = H - H', \qquad M_d = H'd. \tag{176}$$

The axial force and the bending moment at the support B will then be found from statics by the equations

$$N_b = \frac{H}{\cos \alpha} - H' \cos \alpha, \qquad M_b = -H'(f-d). \tag{177}$$

It is seen that an analysis of a symmetrical and symmetrically loaded

[1] We neglect here the small angular changes produced by axial force N (see p. 420).

hingeless arch the center line of which coincides with the funicular curve reduces to calculation of the negative thrust H' defined by Eq. (175).

Let us apply this general discussion to particular cases and consider, as the first example, a parabolic arch of rectangular cross section having

$$A = \frac{A_0}{\cos \phi}, \qquad I = \frac{I_0}{\cos^3 \phi}. \tag{c}$$

In this case

$$\int_0^{sb} \frac{ds}{AE} = \frac{1}{A_0 E} \int_0^{\frac{l}{2}} dx = \frac{l}{2A_0 E}. \tag{d}$$

The denominator of expression (175) has already been calculated (see page 443) and is equal to

$$\frac{l^3}{2EI_0 m}, \tag{e}$$

where m is a numerical factor depending on the proportions of the arch. The values of this factor are given in the third line of Table XIV.

Substituting (d) and (e) in expression (175), we obtain

$$H' = mH \frac{I_0}{A_0 l^2}. \tag{178}$$

Observing that for parabolic three-hinged arches

$$H = \frac{ql^2}{8f}$$

and using for m the values from Table XIV, we can readily calculate the value of H'. The values of the ratio H'/H for arches of various proportions are given[1] in the sixth line of Table XIV. It is seen that the thrust of a hingeless arch may differ considerably from that of the corresponding three-hinged arch only in the cases of flat and very thick arches.

From Eqs. (176) we see that the internal forces at the crown can be represented by the compressive force $N_d = H - H'$ applied at the distance δ_0 above the centroid where

$$\delta_0 = \frac{M_d}{N_d} = \frac{H'd}{H - H'}. \tag{f}$$

In the same manner we find that at the abutments the point of application of the axial force moves from the centroid downward by the amount

$$\delta_1 = \frac{-M_b}{N_b} = \frac{H'(f - d) \cos \alpha}{H - H' \cos^2 \alpha}. \tag{g}$$

---

[1] The values given in the table were obtained by more elaborate calculations using Eqs. (109) to (111) in the analysis of the deformations. These calculations showed that the simplified equation (175) is accurate enough in all practical applications.

In the seventh and eighth lines of Table XIV are given the ratios of these displacements to the depths h_0 and h_1 of the corresponding cross sections.

We know that in the case of a rectangular cross section an eccentrically applied compressive force does not produce tensile stresses if the point of application is within the middle third of the depth of the cross section. The ratios δ_0/h_0 and δ_1/h_1 given in Table XIV indicate that it is likely that tensile stresses will be produced at the abutments during decentering in the case of flat and thick arches. To eliminate such stresses, thinner arches with larger values of f/l must be used.

As a second example we take a circular arch of constant rectangular cross section. The load distribution, for which the funicular curve is a circle, is found from the differential equation of funicular curves (see page 28)[1]

$$\frac{d^2y}{dx^2} = \frac{q}{H}. \qquad (h)$$

Observing that, for a circle (Fig. 467),

$$\frac{d^2y}{dx^2} = \frac{d}{dx}(\tan \phi) = \frac{1}{\cos^2 \phi}\frac{d\phi}{dx} = \frac{1}{r \cos^3 \phi},$$

we conclude that

$$q = \frac{q_0}{\cos^3 \phi}, \qquad H = rq_0, \qquad (i)$$

where q_0 is the intensity of the vertical distributed load at the crown.

The numerator in expression (175), in this case, is

$$\int_0^{s_b} \frac{ds}{AE} = \frac{r\alpha}{AE}.$$

The denominator of the same expression has already been calculated (see page 449) and is equal to

$$\frac{lr^2}{2m_1EI},$$

where m_1 is a numerical factor the values of which for arches of various proportions are given in the eighth line of Table XVI. Hence, from Eq. (175), we obtain

$$H' = 2m_1\alpha\frac{I}{lrA}H. \qquad (179)$$

Again, using Table XVI, we can readily calculate the displacements δ_0 and δ_1 of the *thrust line* at the crown and at the abutments. Calculations show that these displacements differ only slightly from those previously found for parabolic arches (see Table XIV).

Let us consider now a more general case in which the distributed vertical load varies from q_0 to q_1 (Fig. 468), following a parabolic law,

$$q = q_0 + (q_1 - q_0)\frac{4x^2}{l^2}. \qquad (180)$$

[1] Sign corresponds to coordinate axes in Fig. 467.

The total load on half the span consists, then, of a uniformly distributed load with the resultant

$$Q = \frac{q_0 l}{2}$$

applied at the distance $l/4$ from the crown and of a parabolically distributed load with the resultant

$$Q_1 = \frac{(q_1 - q_0)l}{6}$$

applied at the distance $3l/8$ from the crown.

Assuming that the center line of the arch coincides with the funicular curve for the given load, we find the thrust H from the moment equation with respect to point B, which gives

$$Hf = \frac{q_0 l^2}{8} + \frac{(q_1 - q_0)l^2}{48}. \tag{j}$$

Hence

$$H = \frac{5q_0 + q_1}{48} \cdot \frac{l^2}{f}. \tag{181}$$

The ordinate y for any point C of the center line is obtained by writing the moment equation with respect to point C. The load to the left of that point consists of the uniformly distributed load $q_0 x$ and of the parabolically distributed load

$$(q_1 - q_0) \frac{4x^2}{l^2} \cdot \frac{x}{3},$$

the resultants of which are at the distances $x/2$ and $3x/4$ from the crown D, respectively. Hence, the moment equation is

$$Hy = \frac{q_0 x^2}{2} + (q_1 - q_0) \frac{x^4}{3l^2}.$$

Substituting for H its value (181), we obtain

$$y = \frac{8f}{5q_0 + q_1} \left[3q_0 + 2(q_1 - q_0) \frac{x^2}{l^2} \right] \frac{x^2}{l^2}. \tag{182}$$

By taking various values for the ratio q_1/q_0, various shapes of the center line are obtained. For $q_1 = q_0$, we obtain the parabolic curve. By taking q_1 larger than q_0 and making the ratio q_1/q_0 larger and larger, we obtain funicular curves located above the parabolic funicular curve and at distances that increase as the ratio q_1/q_0 increases. For arches having the curve (182) as their center line, tables facilitating stress analysis

have been calculated.[1]   In preparation of these tables, it was assumed that the cross-sectional moment of inertia varies along the span in accordance with the equation

$$I = \frac{I_0}{\cos \phi [1 - \mu(2x/l)]},$$ (183)

in which, as before, ϕ is the angle that the tangent to the center line makes
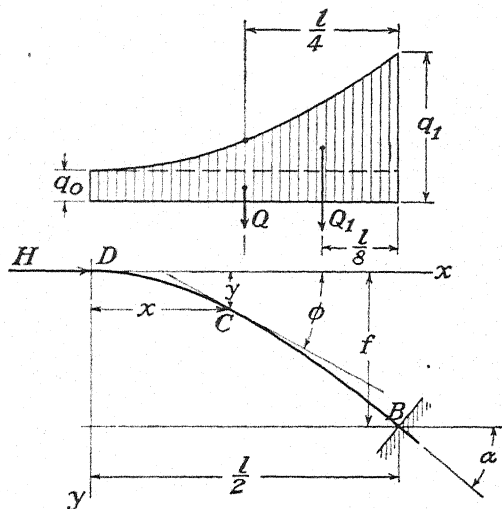
FIG. 468.

with the x-axis (Fig. 468), α is the value of ϕ at the abutment, I_0 is the moment of inertia at the crown, and μ is a numerical factor defined by the magnitude I_1 of the moment of inertia at the abutments.   Substituting $x = l/2$, $\phi = \alpha$, and $I = I_1$ in Eq. (183), we obtain

$$\mu = 1 - \frac{I_0}{I_1 \cos \alpha}.$$ (134)

For any given values of q_1/q_0 and f/l, we calculate the ordinates of the center line and the angles ϕ and α, using Eq. (182).   Then, upon taking a definite value for the ratio I_1/I_0, the value of I for each cross section of the arch is calculated from Eq. (183).   In this manner, a variety of arch proportions can be obtained.

Having the shape of the arch completely defined, we calculate now the magnitude of the negative thrust H' from Eq. (175).   The three integrals entering into this equation we represent in the following form:

$$\int_0^{sb} \frac{y(y - d)ds}{EI} = v \cdot \frac{f^2 l}{2EI_0},$$ (k)

[1] In our future discussion, we make use of the tables given in the book "Bogen-brücken, Handbuch für Eisenbetonbau," vol. XI.

$$\int_0^{s_b} \frac{\cos^2 \phi \, ds}{AE} = \frac{l}{2\beta A_0 E}, \tag{l}$$

$$\int_0^{s_b} \frac{ds}{AE} = \frac{l}{2\beta_1 A_0 E}, \tag{m}$$

where ν, β, and β_1 are numbers to be taken from Tables XXI to XXIII. Then the value of the negative thrust is

$$H' = \frac{k_0^2 / \nu \beta_1 f^2}{1 + k_0^2 / \nu \beta f^2} \cdot H. \tag{185}$$

In this equation the value of H is given by Eq. (181), $k_0^2 = I_0/A_0$, and the values of constants ν, β, and β_1 must be taken from the tables.

TABLE XXI.—VALUES OF $\nu \cdot 10^5$ IN EQ. (185)

q_1/q_0	$\mu = 0$	0.1	0.2	0.3	0.4	0.5	0.6	0.7	0.8	0.9
1.00	8,889	8,326	7,747	7,149	6,528	5,880	5,198	4,477	3,704	2,866
1.67	8,627	8,069	7,497	6,905	6,292	5,653	4,982	4,272	3,513	2,691
2.50	8,411	7,855	7,291	6,706	6,110	5,469	4,808	4,108	3,363	2,557
3.57	8,196	7,647	7,085	6,505	5,905	5,282	4,629	3,940	3,206	2,415
5.00	7,995	7,460	6,881	6,316	5,723	5,106	4,461	3,781	3,059	2,281
7.00	7,809	7,267	6,712	6,142	5,553	4,942	4,304	3,633	2,921	2,156
10.00	7,639	7,100	6,547	5,980	5,395	4,789	4,157	3,494	2,792	2,039
15.00	7,484	6,946	6,396	5,831	5,250	4,148	4,022	3,366	2,673	1,931

TABLE XXII.—VALUES OF β IN EQ. (185)

μ	$\frac{f}{l} = 0.10$	0.14	0.18	0.22	0.26	0.30	0.34	0.38
0.8	1.24	1.27	1.31	1.35	1.39	1.43	1.47	1.52
0.7	1.20	1.24	1.27	1.31	1.35	1.39	1.44	1.48
0.6	1.17	1.20	1.24	1.28	1.32	1.36	1.40	1.45
0.5	1.14	1.18	1.21	1.25	1.29	1.33	1.38	1.42
0.4	1.11	1.14	1.18	1.22	1.26	1.30	1.35	1.39
0.2	1.07	1.10	1.14	1.18	1.22	1.26	1.30	1.35
0	1.03	1.06	1.10	1.14	1.18	1.22	1.26	1.31

Take, for example, a parabolic arch with $f/l = 0.25$, $h/l = \frac{1}{32}$, and $I = I_0/\cos^3 \phi$. Then $\cos \alpha = 1/\sqrt{2}$, and $\mu = 0.5$, from Eq. (184). From the tables we then take $\nu = 0.0588$, $\beta = 1.28$, $\beta_1 = 1.01$. Equation (185) then gives $H'/H = 0.0215$, which is in satisfactory agreement with the value given in Table XIV.

As soon as the value of H' is found from Eq. (185), the values of the

axial force and of the bending moment at the crown of the given hingeless arch are obtained from Eq. (176). The distance d of the elastic center occurring in these equations is calculated by using Eq. (134) and is presented in the form

$$d = \gamma f, \tag{186}$$

in which values of γ for arches of various proportions are to be taken from Table XXIV.

TABLE XXIII.—VALUES OF β_1 IN EQ. (185)

μ	$\frac{f}{l} = 0.10$	0.14	0.18	0.22	0.26	0.30	0.34	0.38
0.8	1.19	1.18	1.16	1.13	1.11	1.08	1.06	1.04
0.7	1.15	1.14	1.12	1.09	1.07	1.04	1.02	1.00
0.6	1.12	1.10	1.08	1.06	1.04	1.01	0.99	0.96
0.5	1.09	1.07	1.05	1.03	1.01	0.99	0.96	0.94
0.4	1.06	1.05	1.03	1.01	0.98	0.96	0.94	0.91
0.2	1.02	1.01	0.99	0.96	0.94	0.92	0.90	0.87
0	0.98	0.97	0.95	0.93	0.91	0.89	0.86	0.84

TABLE XXIV.—VALUES OF γ IN EQ. (186)

q_1/q_0	$\mu = 0$	0.1	0.2	0.3	0.4	0.5	0.6	0.7	0.8	0.9
1.00	0.333	0.325	0.315	0.304	0.292	0.278	0.262	0.244	0.222	0.197
1.67	0.320	0.311	0.302	0.291	0.279	0.266	0.250	0.232	0.211	0.186
2.50	0.307	0.298	0.289	0.278	0.267	0.253	0.238	0.221	0.200	0.176
3.57	0.294	0.285	0.276	0.266	0.254	0.241	0.226	0.209	0.189	0.165
5.00	0.280	0.272	0.263	0.253	0.242	0.229	0.214	0.197	0.178	0.155
7.00	0.267	0.259	0.250	0.240	0.229	0.217	0.202	0.186	0.167	0.144
10.00	0.253	0.246	0.237	0.227	0.217	0.204	0.190	0.174	0.156	0.133
15.00	0.240	0.232	0.224	0.215	0.204	0.192	0.179	0.163	0.144	0.123

To calculate thermal stresses in an arch defined by Eqs. (182) and (183), we use Eq. (149) (page 439). With the notations (k) and (l), this equation gives

$$H_t = \frac{\alpha t l E I_0}{\nu f^2 l + \dfrac{l I_0}{\beta A_0}}. \tag{187}$$

It is seen that the thrust produced by temperature change can be readily calculated by using Tables XXI and XXII for ν and β. The same equation can be used also in discussing the effect of shrinkage of the

concrete, shrinkage being considered as equivalent to a certain lowering of the temperature.

The shortening of the axis of the arch due to dead load [see Eq. (b)], to lowering of the temperature, and to shrinkage of the concrete produces the reduction H' in the thrust H calculated as for a three-hinged arch. As a result of this, the thrust line of a hingeless arch is displaced upward at the crown and downward at the abutments from the assumed center line coinciding with the funicular curve for the dead load. Calculations made for parabolic and circular arches (see Arts. 76 and 77) show that the relative displacements δ/h are larger at the abutments and that at these places tensile stresses due to eccentric pressure are likely to occur. From Table XIV, it may be seen that the displacements are especially large in the case of flat arches and that the values δ_1/h_1 are approximately proportional to h/l. This indicates that in the case of thick and flat arches we must expect tensile stresses at the abutments; if the material is weak in tension, the only way to eliminate cracks is to use a three-hinged arch.

To reduce the above-mentioned displacements of the thrust line in large arch structures, such as bridges, various methods are used. Sometimes temporary hinges are put at the crown and at the abutments that permit free relative rotations at these points during decentering. In this manner, the displacements of the thrust line, which occur as a result of the compression of the center line by dead load, are eliminated. Filling up the gaps at the temporary hinges with concrete after decentering we obtain a hingeless arch the center line of which coincides with the funicular curve for the dead load. To take care of the thrust-line displacements due to shrinkage and lowering of the temperature, the temporary hinges must be placed with proper eccentricities. The eccentricities must be such that, after decentering and filling up the gaps, bending moments should be produced at the crown and the abutments, the signs of which are to be opposite to those we expect later from shrinkage and temperature drop. Sometimes hydraulic jacks are put in the temporary gap at the crown between the two halves of the arch.[1] By using these jacks, the thrust at the crown can be increased, and the arch is raised off the scaffolds. Later, by a proper distribution of pressures in the jacks, the most favorable position of the thrust line at the crown can be ascertained before filling up the gap with concrete.

The stress conditions in an arch can be improved also by introducing

[1] Such jacks were used, for example, in the construction of the large arch bridge over the Aar River at Bern, Switzerland. The description of the construction of that bridge is given in *Schweiz. Bauzeitung*, vol. 113, p. 91, 1939. The idea of using jacks to create a favorable stress distribution in arches belongs to E. Freyssinet. See his papers in *Génie civil*, vol. 79, p. 97, 1921; vol. 93, p. 254, 1928.

during construction residual stresses in the proper direction. In the case of concrete arches, this can be accomplished by making the arch in several layers and working on these layers in the proper sequence.[1]

Stresses produced in an arch by live loads are usually calculated by influence lines. The general method of constructing influence lines for symmetrical arches was described in Art. 75. For arches the shape of which is defined by Eqs. (182) and (183) the ordinates of influence lines for the redundant quantities are calculated for various values of q_1/q_0 and μ and are presented in Tables XXV to XXVII. By using these tables, the stresses produced by live loads can be readily calculated.
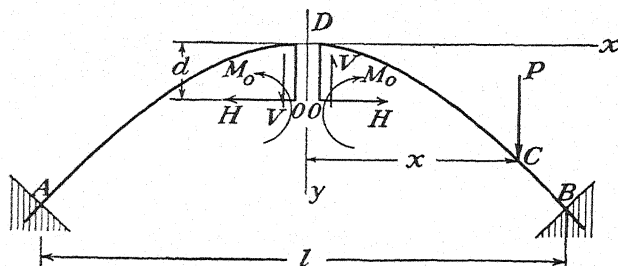
FIG. 469.

If a vertical load P is acting at the distance x from the crown (Fig. 469), the thrust produced by this load can be represented by the equation

$$H = \varphi \cdot \frac{Pl}{4f(1 + I_0/\nu\beta A_0 f^2)}. \tag{188}$$

The values of the quantities ν and β in this equation have already been given (see page 462); the values of φ are given in Table XXV.

The bending moment at the crown produced by the load P (Fig. 469) is

$$M_d = M_0 - Hd = M' - Hd - \varphi_1 \frac{Pl}{4}. \tag{189}$$

In this equation

$$M' = \frac{Pl}{4}\left(1 - \frac{2x}{l}\right)$$

is the bending moment at the middle of a simply supported beam of length l, and the constant φ_1 is to be taken from Table XXVI. Hence, by using the influence line for bending moment at the middle of a simply supported beam together with the constants φ and φ_1, given in the tables, the influence line for M_d can be constructed.

[1] The question of improving stress conditions by the introduction of residual stresses is discussed in the following papers: E. Baticle, *Compt. rend.*, vol. 177/II, p. 1006, 1923; A. Paris, *Bauingenieur*, 1928, p. 831.

TABLE XXV.—VALUES OF φ IN EQ. (188)

$q_1/q_0 = 1$

$2x/l$	$\mu = 0$	0.1	0.2	0.3	0.4	0.5	0.6	0.7	0.8	0.9
0	0.9375	0.9433	0.9505	0.9572	0.9658	0.9760	0.9892	1.0063	1.0299	1.0680
0.1	0.9188	0.9240	0.9300	0.9362	0.9439	0.9529	0.9646	0.9797	1.0008	1.0349
0.2	0.8640	0.8674	0.8716	0.8756	0.8790	0.8867	0.8948	0.9051	0.9195	0.9428
0.3	0.7764	0.7777	0.7792	0.7807	0.7824	0.7845	0.7878	0.7916	0.7972	0.8067
0.4	0.6615	0.6606	0.6596	0.6584	0.6570	0.6552	0.6535	0.6510	0.6471	0.6416
0.5	0.5273	0.5249	0.5223	0.5187	0.5149	0.5100	0.5046	0.4972	0.4867	0.4703
0.6	0.3840	0.3807	0.3773	0.3726	0.3676	0.3616	0.3540	0.3443	0.3304	0.3081
0.7	0.2438	0.2408	0.2375	0.2332	0.2284	0.2190	0.2155	0.2064	0.1930	0.1720
0.8	0.1215	0.1195	0.1173	0.1143	0.1111	0.1070	0.1023	0.0963	0.0872	0.0729
0.9	0.0339	0.0331	0.0326	0.0313	0.0302	0.0285	0.0270	0.0248	0.0216	0.0164

$q_1/q_0 = 1.67$

$2x/l$	$\mu = 0$	0.1	0.2	0.3	0.4	0.5	0.6	0.7	0.8	0.9
0	0.9418	0.9532	0.9605	0.9690	0.9789	0.9906	1.0056	1.0250	1.0527	1.0978
0.1	0.9233	0.9341	0.9406	0.9483	0.9569	0.9678	0.9811	0.9986	1.0236	1.0642
0.2	0.8694	0.8781	0.8826	0.8881	0.8943	0.9018	0.9114	0.9246	0.9419	0.9714
0.3	0.7826	0.7887	0.7907	0.7937	0.7962	0.7996	0.8041	0.8101	0.8187	0.8331
0.4	0.6688	0.6721	0.6716	0.6711	0.6707	0.6701	0.6694	0.6685	0.6675	0.6663
0.5	0.5352	0.5349	0.5334	0.5308	0.5275	0.5236	0.5189	0.5129	0.5041	0.4901
0.6	0.3914	0.3905	0.3872	0.3830	0.3784	0.3729	0.3650	0.3570	0.3438	0.3233
0.7	0.2498	0.2482	0.2448	0.2410	0.2365	0.2309	0.2240	0.2151	0.2021	0.1814
0.8	0.1247	0.1227	0.1215	0.1190	0.1154	0.1120	0.1072	0.1009	0.0919	0.0777
0.9	0.0350	0.0346	0.0337	0.0327	0.0316	0.0302	0.0285	0.0262	0.0231	0.0178

$q_1/q_0 = 2.5$

$2x/l$	$\mu = 0$	0.1	0.2	0.3	0.4	0.5	0.6	0.7	0.8	0.9
0	0.9511	0.9585	0.9660	0.9751	0.9841	0.9984	1.0143	1.0357	1.0648	1.1134
0.1	0.9330	0.9396	0.9465	0.9547	0.9623	0.9757	0.9900	1.0009	1.0364	1.0802
0.2	0.8791	0.8844	0.8907	0.8953	0.9001	0.9107	0.9210	0.9353	0.9551	0.9878
0.3	0.7935	0.7962	0.7985	0.8015	0.8038	0.8095	0.8147	0.8220	0.8325	0.8497
0.4	0.6801	0.6802	0.6803	0.6803	0.6803	0.6804	0.6805	0.6809	0.6814	0.6825
0.5	0.5461	0.5445	0.5450	0.5400	0.5363	0.5339	0.5297	0.5271	0.5169	0.5047
0.6	0.4011	0.3989	0.3953	0.3916	0.3869	0.3820	0.3754	0.3670	0.3546	0.3347
0.7	0.2575	0.2547	0.2514	0.2474	0.2429	0.2379	0.2317	0.2225	0.2099	0.1893
0.8	0.1289	0.1278	0.1255	0.1229	0.1196	0.1163	0.1113	0.1051	0.0961	0.0814
0.9	0.0366	0.0365	0.0351	0.0335	0.0325	0.0316	0.0297	0.0276	0.0242	0.0187

$q_1/q_0 = 3.57$

$2x/l$	$\mu = 0$	0.1	0.2	0.3	0.4	0.5	0.6	0.7	0.8	0.9
0	0.9557	0.9634	0.9719	0.9818	0.9934	1.0072	1.0246	1.0475	1.0805	1.1345
0.1	0.9379	0.9455	0.9526	0.9648	0.9723	0.9849	1.0008	1.0218	1.0520	1.1016
0.2	0.8853	0.8910	0.8967	0.9032	0.9111	0.9206	0.9327	0.9486	0.9747	1.0094
0.3	0.8005	0.8035	0.8083	0.8105	0.8149	0.8203	0.8272	0.8362	0.8493	0.8711
0.4	0.6882	0.6886	0.6900	0.6904	0.6909	0.6919	0.6933	0.6951	0.6980	0.7030
0.5	0.5548	0.5534	0.5517	0.5499	0.5480	0.5453	0.5421	0.5379	0.5320	0.5221
0.6	0.4095	0.4068	0.4038	0.4004	0.3964	0.3916	0.3855	0.3774	0.3656	0.3467
0.7	0.2660	0.2621	0.2591	0.2555	0.2516	0.2465	0.2403	0.2320	0.2199	0.2006
0.8	0.1340	0.1321	0.1298	0.1272	0.1243	0.1205	0.1158	0.1096	0.1004	0.0860
0.9	0.0381	0.0373	0.0364	0.0355	0.0343	0.0330	0.0312	0.0288	0.0252	0.0198

TABLE XXV.—VALUES OF φ IN EQ. (188).—(*Continued*)

$$q_1/q_0 = 5.0$$

$2x/l$	$\mu = 0$	0.1	0.2	0.3	0.4	0.5	0.6	0.7	0.8	0.9
0	0.9589	0.9683	0.9779	0.9871	0.9994	1.0145	1.0333	1.0584	1.0942	1.1543
0.1	0.9414	0.9473	0.9590	0.9674	0.9787	0.9925	1.0098	1.0331	1.0661	1.1217
0.2	0.8899	0.8945	0.9036	0.9099	0.9186	0.9293	0.9427	0.9607	0.9865	1.0301
0.3	0.8065	0.8089	0.8152	0.8185	0.8236	0.8302	0.8384	0.8495	0.8643	0.8921
0.4	0.6954	0.6966	0.6983	0.6992	0.7007	0.7028	0.7053	0.7090	0.7140	0.7231
0.5	0.5629	0.5621	0.5616	0.5596	0.5580	0.5562	0.5540	0.5513	0.5471	0.5450
0.6	0.4172	0.4146	0.4132	0.4096	0.4061	0.4019	0.3997	0.3896	0.3796	0.3631
0.7	0.2707	0.2675	0.2656	0.2609	0.2579	0.2531	0.2470	0.2392	0.2275	0.2082
0.8	0.1381	0.1360	0.1343	0.1316	0.1286	0.1250	0.1204	0.1145	0.1056	0.0850
0.9	0.0395	0.0387	0.0381	0.0370	0.0359	0.0345	0.0329	0.0305	0.0270	0.0213

$$q_1/q_0 = 7.0$$

$2x/l$	$\mu = 0$	0.1	0.2	0.3	0.4	0.5	0.6	0.7	0.8	0.9
0	0.9604	0.9691	0.9776	0.9904	1.0037	1.0199	1.0401	1.0670	1.1058	1.1716
0.1	0.9433	0.9515	0.9606	0.9711	0.9834	0.9984	1.0172	1.0421	1.0782	1.1395
0.2	0.8929	0.8993	0.9065	0.9148	0.9245	0.9364	0.9513	0.9711	0.9975	1.0498
0.3	0.8112	0.8152	0.8198	0.8253	0.8313	0.8389	0.8484	0.8612	0.8799	0.9118
0.4	0.7016	0.7032	0.7050	0.7072	0.7091	0.7125	0.7164	0.7215	0.7291	0.7564
0.5	0.5702	0.5697	0.5691	0.5684	0.5676	0.5666	0.5654	0.5639	0.5619	0.5586
0.6	0.4248	0.4229	0.4207	0.4181	0.4151	0.4115	0.4070	0.4010	0.3923	0.3860
0.7	0.2770	0.2746	0.2719	0.2688	0.2651	0.2606	0.2550	0.2475	0.2366	0.2322
0.8	0.1422	0.1404	0.1382	0.1358	0.1329	0.1276	0.1251	0.1192	0.1106	0.0960
0.9	0.0409	0.0402	0.0394	0.0384	0.0373	0.0359	0.0341	0.0318	0.0285	0.0226

$$q_1/q_0 = 10.0$$

$2x/l$	$\mu = 0$	0.1	0.2	0.3	0.4	0.5	0.6	0.7	0.8	0.9
0	0.9600	0.9691	0.9797	0.9917	1.0059	1.0231	1.0471	1.0736	1.1151	1.1864
0.1	0.9434	0.9520	0.9604	0.9730	0.9862	1.0026	1.0223	1.0491	1.0881	1.1548
0.2	0.8944	0.9012	0.9091	0.9181	0.9287	0.9312	0.9579	0.9797	1.0113	1.0658
0.3	0.8145	0.8176	0.8242	0.8342	0.8375	0.8460	0.8569	0.8717	0.8931	0.9303
0.4	0.7069	0.7090	0.7114	0.7141	0.7174	0.7215	0.7266	0.7336	0.7438	0.7618
0.5	0.5768	0.5767	0.5765	0.5764	0.5763	0.5763	0.5762	0.5762	0.5762	0.5762
0.6	0.4318	0.4302	0.4283	0.4262	0.4237	0.4208	0.4170	0.4121	0.4048	0.3926
0.7	0.2831	0.2809	0.2784	0.2755	0.2721	0.2681	0.2628	0.2561	0.2458	0.2283
0.8	0.1462	0.1445	0.1424	0.1402	0.1374	0.1342	0.1299	0.1242	0.1155	0.1015
0.9	0.0423	0.0417	0.0408	0.0399	0.0390	0.0375	0.0356	0.0334	0.0300	0.0241

$$q_1/q_0 = 15.0$$

$2x/l$	$\mu = 0$	0.1	0.2	0.3	0.4	0.5	0.6	0.7	0.8	0.9
0	0.9576	0.9672	0.9783	0.9910	1.0058	1.0239	1.0466	1.0769	1.1210	1.1973
0.1	0.9416	0.9507	0.9609	0.9728	0.9867	1.0037	1.0249	1.0533	1.0977	1.1666
0.2	0.8993	0.9053	0.9097	0.9194	0.9308	0.9448	0.9622	0.9857	1.0200	1.0797
0.3	0.8162	0.8213	0.8271	0.8338	0.8417	0.8514	0.8636	0.8801	0.9043	0.9466
0.4	0.7109	0.7134	0.7164	0.7199	0.7239	0.7290	0.7354	0.7441	0.7531	0.7796
0.5	0.5828	0.5828	0.5832	0.5837	0.5844	0.5855	0.5861	0.5876	0.5897	0.5939
0.6	0.4382	0.4369	0.4354	0.4338	0.4318	0.4296	0.4266	0.4227	0.4170	0.4073
0.7	0.2888	0.2868	0.2846	0.2820	0.2789	0.2753	0.2705	0.2643	0.2549	0.2387
0.8	0.1500	0.1468	0.1464	0.1442	0.1416	0.1385	0.1344	0.1260	0.1208	0.1067
0.9	0.0437	0.0429	0.0423	0.0413	0.0402	0.0389	0.0372	0.0349	0.0315	0.0250

The shearing force V at the crown is obtained from the equation

$$V = V' - \varphi_2 P, \qquad (190)$$

in which

$$V' = \frac{P}{2}\left(1 - \frac{2x}{l}\right)$$

is the shearing force at the middle of a simply supported beam and the constant φ_2 is to be taken from Table XXVII. Equations (188) and (189) can be used also for negative values of x when the load P is applied to the left of the crown, since the influence lines for M_d and H are symmetrical with respect to the middle of the span. The influence line for V is antisymmetrical, and the sign of its ordinates must be changed when we take $-x$ instead of x.

TABLE XXVI.—VALUES OF φ_1 IN EQ. (189)

$2x/l$	$\mu = 0$	0.1	0.2	0.3	0.4	0.5	0.6	0.7	0.8	0.9
0	0.2500	0.2544	0.2593	0.2647	0.2708	0.2778	0.2857	0.2949	0.3056	0.3182
0.1	0.2475	0.2518	0.2565	0.2618	0.2678	0.2745	0.2822	0.2911	0.3015	0.3138
0.2	0.2400	0.2439	0.2483	0.2532	0.2587	0.2649	0.2720	0.2802	0.2898	0.3011
0.3	0.2275	0.2310	0.2348	0.2390	0.2439	0.2493	0.2555	0.2627	0.2711	0.2810
0.4	0.2100	0.2128	0.2160	0.2195	0.2235	0.2280	0.2331	0.2391	0.2460	0.2542
0.5	0.1875	0.1897	0.1921	0.1949	0.1979	0.2014	0.2054	0.2099	0.2153	0.2216
0.6	0.1600	0.1615	0.1633	0.1652	0.1673	0.1698	0.1726	0.1758	0.1796	0.1840
0.7	0.1275	0.1285	0.1295	0.1307	0.1320	0.1335	0.1352	0.1372	0.1395	0.1422
0.8	0.0900	0.0905	0.0910	0.0915	0.0922	0.0929	0.0940	0.0947	0.0958	0.0971
0.9	0.0475	0.0476	0.0478	0.0479	0.0481	0.0483	0.0485	0.0488	0.0491	0.0494

TABLE XXVII.—VALUES OF φ_2 IN EQ. (190)

$2x/l$	$\mu = 0$	0.1	0.2	0.3	0.4	0.5	0.6	0.7	0.8	0.9
0	0	0	0	0	0	0	0	0	0	0
0.1	0.0248	0.0254	0.0262	0.0271	0.0282	0.0296	0.0314	0.0337	0.0369	0.0416
0.2	0.0480	0.0492	0.0506	0.0523	0.0544	0.0570	0.0602	0.0645	0.0704	0.0752
0.3	0.0683	0.0698	0.0717	0.0739	0.0767	0.0800	0.0843	0.0899	0.0977	0.1090
0.4	0.0840	0.0858	0.0878	0.0903	0.0933	0.0970	0.1017	0.1079	0.1164	0.1289
0.5	0.0938	0.0954	0.0974	0.0998	0.1027	0.1063	0.1108	0.1168	0.1250	0.1370
0.6	0.0960	0.0974	0.0991	0.1011	0.1035	0.1066	0.1104	0.1155	0.1224	0.1326
0.7	0.0893	0.0903	0.0915	0.0929	0.0946	0.0968	0.0996	0.1032	0.1081	0.1154
0.8	0.0720	0.0726	0.0732	0.0740	0.0750	0.0762	0.0777	0.0797	0.0824	0.0864
0.9	0.0428	0.0429	0.0431	0.0434	0.0437	0.0440	0.0445	0.0451	0.0459	0.0471

By using the tables given in this article, an analysis of a given arch can readily be made. From the tables we find the redundant forces produced by the dead load and temperature change, while the ordinates

of the influence lines give us a simple way of calculating redundant quantities produced by live loads.

In the preceding discussion, it has always been assumed that deflections of the arches are small and can be neglected.[1] It has also been assumed that the material follows Hooke's law and that there is no creep of the material under prolonged action of stresses.[2]

80. Unsymmetrical Arches.—In the case of an unsymmetrical arch, we take as the redundant quantities the bending moment M_a and the two components R_a and H_a of the reaction at the left support A (Fig. 470a). The magnitudes of these three quantities will be found from the condition that the end A is fixed, which requires that the two components u_a and v_a of the displacement of point A and the angle of rotation θ_a shall vanish. Using, for these deflections, Eqs. (129) to (131), we obtain

$$\int_0^{s_b} \frac{My\,ds}{EI} + \int_0^{s_b} \frac{N \cos \phi\,ds}{AE} = 0, \tag{a}$$

$$-\int_0^{s_b} \frac{Mx\,ds}{EI} + \int_0^{s_b} \frac{N \sin \phi\,ds}{AE} = 0, \tag{b}$$

$$\int_0^{s_b} \frac{M\,ds}{EI} = 0, \tag{c}$$

where s_b is the total length of the center line of the arch. In these equations M and N are bending moment and axial force, and ϕ is the angle that the tangents to the center line make with the x-axis. This angle is taken positive if measured clockwise from the horizontal axis, as shown in Fig. 470a. Taking the coordinates as shown in the figure and observing the previous sign rule (see page 424) for M and N, we obtain

$$M = M_a + R_a x + H_a y + M', \tag{d}$$
$$N = H_a \cos \phi - R_a \sin \phi + N', \tag{e}$$

where M' and N' are the moment and the axial force contributed by the load on the arch to the left of the cross section under consideration. If we substitute expressions (d) and (e) into Eqs. (a) to (c), we obtain for calculating the redundant quantities three equations each of which contains all three unknowns.

Such equations are not suitable for practical applications. A con-

---

[1] The influence of deflections of an arch on the magnitude of the redundant forces may become considerable in the case of arches of large spans. See articles by J. Melan, *Handb. Ingenieurwiss*, vol. 2, 1906, and *Bauingenieur*, 1925. See also S. Kasarnowsky, "Stahlbau," 1931 and B. Fritz, "Theorie und Berechnung vollwandiger Bogenträger," Berlin, 1934.

[2] Creep of concrete under load has been extensively studied in this country. See, for example, the papers by R. E. Davis, *Proc. A.C.I.*, vol. 24, 1928; vol. 27, 1931.

siderable simplification can be effected if, by the proper selection of the redundant quantities, we could obtain three equations each containing only one unknown. For this purpose we select the redundant quantities in such a manner that the displacements corresponding to one of them are not affected by the two other redundant forces. In Fig. 470a the couple M_a acting alone produces, not only rotation of the cross section A, but also some displacement. The reciprocal theorem then states that forces R_a and H_a will produce, not only displacement of point A, but also rotation of cross section A. To make the rotation of the cross section A
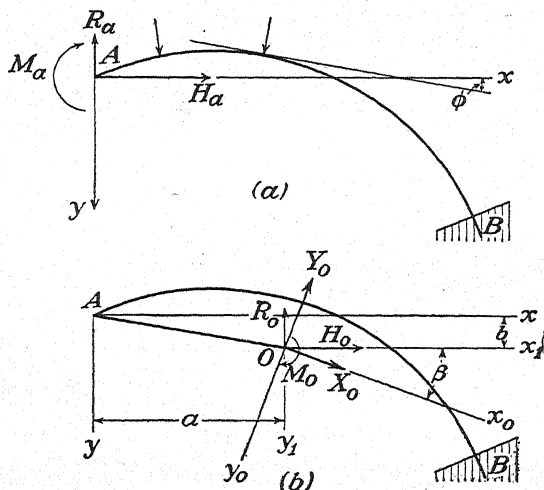
FIG. 470.

dependent only on the couple and unaffected by the forces, we replace the system of redundant forces, shown in Fig. 470a, by the statically equivalent system, shown in Fig. 470b. In this latter case, we assume that an absolutely rigid bar AO is rigidly attached to the end A of the arch and that the point O is selected in such a manner that it remains stationary when a couple is applied to the bar.[1] Then, from the reciprocal theorem, it follows that the forces R_0 and H_0 applied at O, will not produce any rotation of the cross section A. To make this new system of redundant forces statically equivalent to the previous one we have to satisfy the following equations:

$$R_0 = R_a, \qquad H_0 = H_a, \qquad M_0 = M_a + R_0 a + H_0 b. \qquad (191)$$

To find the proper coordinates a and b of the point O, we assume that a couple M_a alone is applied at the end A of the arch; then $M = M_a$, $N = 0$, and we obtain, from Eqs. (129) to (131),

[1] Such reasoning has already been used in the selection of the elastic center in Fig. 460.

$$u_a = M_a \int_0^{sb} \frac{y \, ds}{EI}, \qquad v_a = -M_a \int_0^{sb} \frac{x \, ds}{EI}, \qquad \theta_a = M_a \int_0^{sb} \frac{ds}{EI}. \quad (f)$$

To obtain the deflections of the end O of the bar AO, we must add to expressions (f) the displacements due to the rotation of the bar. Hence

$$u_0 = u_a - b\theta_a, \qquad v_0 = v_a + a\theta_a. \qquad (g)$$

These displacements vanish if we take

$$a = -\frac{v_a}{\theta_a} = \frac{\int_0^{sb} \dfrac{x \, ds}{EI}}{\int_0^{sb} \dfrac{ds}{EI}}, \qquad (192)$$

$$b = \frac{u_a}{\theta_a} = \frac{\int_0^{sb} \dfrac{y \, ds}{EI}}{\int_0^{sb} \dfrac{ds}{EI}}. \qquad (193)$$

The point O, defined by Eqs. (192) and (193), is the *elastic center* of the arch. Let us assume fictitious masses of an intensity $1/EI$ distributed along the center line of the arch. Then the point O, as seen from Eqs. (192) and (193), is the center of gravity of these masses. It is advantageous to take point O for the origin of the new coordinate system $x_1 y_1$ (Fig. 470b). If we substitute $x = x_1 + a$, $y = y_1 + b$, and

$$M = M_0 + R_0 x_1 + H_0 y_1 + M', \qquad (h)$$
$$N = H_0 \cos \phi - R_0 \sin \phi + N', \qquad (i)$$

into Eqs. (a), (b) and (c) and observe that for centroidal axes

$$\int_0^{sb} \frac{x_1 ds}{EI} = \int_0^{sb} \frac{y_1 ds}{EI} = 0,$$

we obtain equations for calculating the redundant forces in a simpler form. A further simplification of these equations is accomplished in the case of comparatively flat arches carrying vertical loads, since we can then neglect small terms containing $\sin \phi$ or N' as factors. With these simplifications, Eqs. (a), (b), and (c) become

$$R_0 \int_0^{sb} \frac{x_1 y_1 ds}{EI} + H_0 \left(\int_0^{sb} \frac{y_1^2 ds}{EI} + \int_0^{sb} \frac{\cos^2 \phi \, ds}{AE} \right) + \int_0^{sb} \frac{M' y_1 ds}{EI} = 0, \quad (j)$$

$$R_0 \int_0^{sb} \frac{x_1^2 ds}{EI} + H_0 \int_0^{sb} \frac{x_1 y_1 ds}{EI} + \int_0^{sb} \frac{M' x_1 ds}{EI} = 0, \quad (k)$$

$$M_0 \int_0^{sb} \frac{ds}{EI} + \int_0^{sb} \frac{M' ds}{EI} = 0. \quad (l)$$

The third of these equations gives us the redundant moment M_0. The first two equations each contain the remaining two unknown forces R_0 and H_0.

If the arch is symmetrical with respect to the vertical axis, the integral

$$\int_0^{sb} \frac{x_1 y_1 ds}{EI}$$

vanishes, and each of our equations will contain only one unknown. The same condition can be obtained also for unsymmetrical arches by a proper rotation of the coordinate axes. We observe that the integrals

$$\int_0^{sb} \frac{y_1{}^2 ds}{EI} = I_{x_1}, \qquad \int_0^{sb} \frac{x_1{}^2 ds}{EI} = I_{y_1}, \qquad \int_0^{sb} \frac{x_1 y_1 ds}{EI} = I_{x_1 y_1} \qquad (m)$$

in our equations represent the moments of inertia and the product of inertia with respect to x_1- and y_1-axes of the previously mentioned ficti- tious masses distributed along the center line of the arch. If, instead of the $x_1 y_1$-axes, we take the principal axes of inertia $x_0 y_0$, for which the product of inertia of the fictitious masses vanishes, and introduce the forces X_0 and Y_0 instead of H_0 and R_0 (Fig. 470b), the equations for calculating the redundant quantities become

$$X_0 \left[\int_0^{sb} \frac{y_0{}^2 ds}{EI} + \int_0^{sb} \frac{\cos^2 (\phi + \beta) ds}{AE} \right] + \int_0^{sb} \frac{M' y_0 ds}{EI} = 0,$$

$$Y_0 \int_0^{sb} \frac{x_0{}^2 ds}{EI} + \int_0^{sb} \frac{M' x_0 ds}{EI} = 0,$$

$$M_0 \int_0^{sb} \frac{ds}{EI} + \int_0^{sb} \frac{M' ds}{EI} = 0,$$

where β (see Fig. 470b) is the angle defining the directions of the principal axes. Each equation contains only one unknown, and we obtain

$$X_0 = - \frac{\displaystyle\int_0^{sb} \frac{M' y_0 ds}{EI}}{\displaystyle\int_0^{sb} \frac{y_0{}^2 ds}{EI} + \int_0^{sb} \frac{\cos^2 (\phi + \beta) ds}{AE}}, \qquad (194)$$

$$Y_0 = - \frac{\displaystyle\int_0^{sb} \frac{M' x_0 ds}{EI}}{\displaystyle\int_0^{sb} \frac{x_0{}^2 ds}{EI}}, \qquad (195)$$

$$M_0 = - \frac{\displaystyle\int_0^{sb} \frac{M' ds}{EI}}{\displaystyle\int_0^{sb} \frac{ds}{EI}}. \qquad (196)$$

The calculation of the redundant quantities M_0, X_0, Y_0 reduces to the evaluation of the integrals appearing in Eqs. (194) to (196).

We begin the analysis of an unsymmetrical arch with the determination of the elastic center from Eqs. (192) and (193). The next step is the determination of the principal axes, for which purpose we calculate the integrals (m). If the center line of the arch is given in a simple analytical form, we can make the integrations exactly. Otherwise, we use the approximate numerical integration method described in Art. 78. Having I_{x_1}, I_{y_1}, and $I_{x_1 y_1}$ and using the known equations for calculation of the principal moments of inertia and of the directions of the principal axes,[1] we obtain

$$I_{x_0} + I_{y_0} = I_{x_1} + I_{y_1}, \tag{197}$$

$$I_{x_0} - I_{y_0} = (I_{x_1} - I_{y_1}) \cos 2\beta - 2 I_{x_1 y_1} \sin 2\beta, \tag{198}$$

$$\tan 2\beta = \frac{2 I_{x_1 y_1}}{I_{y_1} - I_{x_1}}. \tag{199}$$

From these equations we find I_{x_0}, I_{y_0} entering into the denominators of Eqs. (194) and (195) and the angle β. To calculate the other integrals in Eqs. (194) to (196), we assume that fictitious masses of intensity M'/EI are distributed along the center line of the arch. Then the total mass and the moments of these masses with respect to x_0- and y_0-axes give us the integrals

$$\int_0^{s_b} \frac{M' ds}{EI}, \qquad \int_0^{s_b} \frac{M' y_0 ds}{EI}, \qquad \int_0^{s_b} \frac{M' x_0 ds}{EI}. \tag{n}$$

Finally, the second integral in the denominator of Eq. (194) representing the approximate expression for the displacement due to shortening of the axis of the arch can also be evaluated by numerical integration.[2] In this way all the integrals in Eqs. (194) to (196) can be evaluated, and we obtain the redundant quantities X_0, Y_0, and M_0.[*]

81. Frames and Rings.—Equations (194) to (196) derived for arches can be applied also for calculating redundant forces in frames. In such applications Eq. (194) can be simplified by omitting the second term in the denominator, which represents the action of the axial force. Such a simplification is reasonable if we observe that, in the case of arches under the action of dead load, the center line is usually very close to the line of pressure and the stresses produced by the axial force are of the same order

---

[1] See "Engineering Mechanics," 2d. ed., p. 502.

[2] This term is usually small, and a rough approximation is sufficient in its calculation.

[*] The ideas of elastic center and fictitious masses were introduced in the theory of structures by C. Culmann; see "Anwendungen der graphischen Statik" by W. Ritter, vol. IV, p. 197.

of magnitude as the maximum bending stresses. Hence the term representing the action of the axial force may be of practical importance. But, in the case of frames, the pressure line is usually far from coinciding with the center line, and the effect of the axial force is negligible in comparison with the effect of the bending moment.
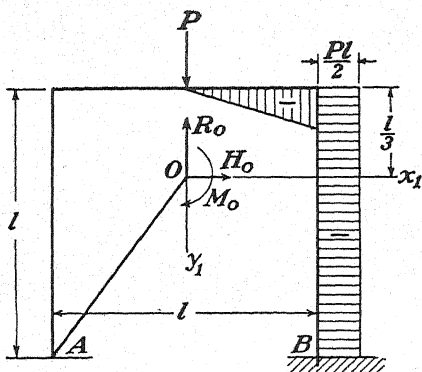
Fig. 471.

As a simple example, let us consider a square frame of constant cross section with a single load at the middle (Fig. 471). The redundant reactions at A we replace by the statically equivalent system of forces at the elastic center O, which, in this case, coincides with the center of gravity of the frame and lies on the axis of symmetry at the distance $l/3$ from the horizontal member. From symmetry we conclude that the principal axes of inertia for the fictitious masses ds/EI coincide with the x_1- and y_1-axes. The corresponding moments of inertia are

$$\left.\begin{aligned} \int_A^B \frac{y_1^2 ds}{EI} &= \frac{1}{EI}\left[l \cdot \frac{l^2}{9} + 2\left(\frac{l^3}{12} + l \cdot \frac{l^2}{36}\right)\right] = \frac{l^3}{3EI}, \\ \int_A^B \frac{x_1^2 ds}{EI} &= \frac{1}{EI}\left(\frac{l^3}{12} + \frac{l^3}{2}\right) = \frac{7l^3}{12EI}. \end{aligned}\right\} \quad (a)$$

The bending moments M' are shown in Fig. 471 by the shaded area, and we obtain

$$\left.\begin{aligned} \int_A^B \frac{M' ds}{EI} &= -\frac{1}{EI}\left(\frac{Pl^2}{8} + \frac{Pl^2}{2}\right) = -\frac{5Pl^2}{8EI}, \\ \int_A^B \frac{M' y_1 ds}{EI} &= -\frac{1}{EI}\left(-\frac{Pl^2}{8}\cdot\frac{l}{3} + \frac{Pl^2}{2}\cdot\frac{l}{6}\right) = \frac{Pl^3}{24EI}, \\ \int_A^B \frac{M' x_1 ds}{EI} &= -\frac{1}{EI}\left(\frac{Pl^2}{8}\cdot\frac{l}{3} + \frac{Pl^2}{2}\cdot\frac{l}{2}\right) = -\frac{7Pl^3}{24EI}. \end{aligned}\right\} \quad (b)$$

Observing that x_1, y_1 are the principal axes, we substitute the integrals (a) and (b) in Eqs. (194) to (196), from which, neglecting the effect of the axial force, we obtain

$$H_0 = \frac{P}{8}, \qquad R_0 = \frac{P}{2}, \qquad M_0 = \frac{5}{24}Pl.$$

As an example of an unsymmetrical frame, let us consider the frame in Fig. 472a. We assume a uniform cross section and take $l = 2h$ and $c = h$. Then, from Eqs. (192) and (193), we find that the coordinates

of the elastic center O are

$$a = \tfrac{2}{3}h, \qquad b = \tfrac{5}{6}h.$$

Taking the forces R_0, H_0 and the moment M_0 acting at this center (Fig. 472b) as the redundant quantities, we use Eqs. (j), (k), and (l) of the

(a)

(b)
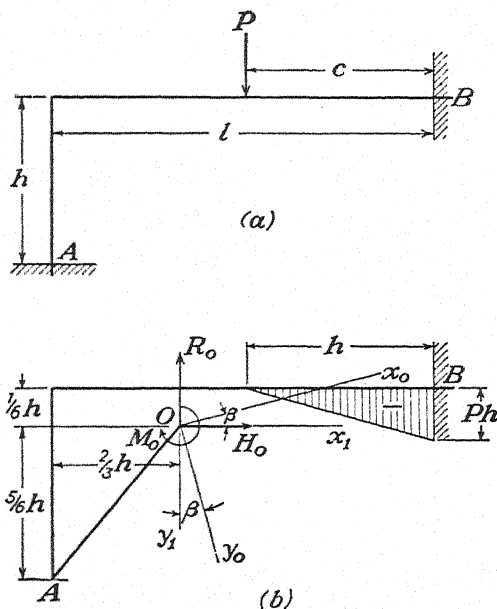
FIG. 472.

preceding article for calculating these quantities. The integrals occurring in these equations are readily evaluated, and we obtain

$$\int_0^{s_b} \frac{y_1^2 ds}{EI} = I_{x_1} = \frac{h^3}{4EI}, \qquad \int_0^{s_b} \frac{x_1^2 ds}{EI} = I_{y_1} = \frac{4h^3}{3EI},$$

$$I_{x_1 y_1} = \int_0^{s_b} \frac{x_1 y_1 ds}{EI} = -\frac{h^3}{3EI}.$$

We obtain also

$$\int_0^{s_b} \frac{ds}{EI} = \frac{3h}{EI}, \qquad \int_0^{s_b} \frac{M' ds}{EI} = -\frac{Ph^2}{2EI},$$

$$\int_0^{s_b} \frac{M' x_1 ds}{EI} = -\frac{Ph^3}{2EI}, \qquad \int_0^{s_b} \frac{M' y_1 ds}{EI} = \frac{Ph^3}{12EI}.$$

Substituting all these integrals in Eqs. (j), (k), (l) and neglecting the effect of the longitudinal force, represented by the second term in the parentheses of Eq. (j), we obtain

$$-4R_0 + 3H_0 + P = 0,$$
$$8R_0 - 2H_0 - 3P = 0,$$
$$6M_0 - Ph = 0,$$

from which

$$R_0 = \frac{7}{16}P, \qquad H_0 = \frac{P}{4}, \qquad M_0 = \frac{1}{6}Ph.$$

This result can be readily verified by using one of the previously discussed methods of analysis of frames (see Arts. 42, 61).

The directions of the principal axes x_0, y_0 are obtained from Eq. (199), which gives

$$\tan 2\beta = -\tfrac{8}{13} = -0.6154, \qquad 2\beta = -31° 36\tfrac{1}{2}',$$
$$\beta = -15° 48\tfrac{1}{4}'.$$

These axes are shown in Fig. 472b. Now, using Eqs. (197) and (198), we obtain

$$I_{x_0} + I_{y_0} = \frac{h^3}{EI}\left(\frac{1}{4} + \frac{4}{3}\right) = 1.5833\,\frac{h^3}{EI},$$
$$I_{x_0} - I_{y_0} = \left[\left(\frac{1}{4} - \frac{4}{3}\right)\cos 2\beta + \frac{2}{3}\sin 2\beta\right]\frac{h^3}{EI} = -1.2719\,\frac{h^3}{EI}.$$

Hence

$$I_{x_0} = 0.1557\,\frac{h^3}{EI}, \qquad I_{y_0} = 1.4276\,\frac{h^3}{EI}.$$

We calculate also

$$\int_0^{sb} \frac{M'y_0\,ds}{EI} = -\frac{Ph^2}{2EI}\left(-h\tan\beta - \frac{1}{6}h\right)\cos\beta = -0.0560\,\frac{Ph^3}{EI},$$
$$\int_0^{sb} \frac{M'x_0\,ds}{EI} = -\frac{Ph^2}{2EI}\left(h\cos\beta - \frac{1}{6}h\sin\beta\right) = -0.5038\,\frac{Ph^3}{EI}.$$

Substituting all these numerical values into Eqs. (194) and (195), we find

$$X_0 = 0.3597P, \qquad Y_0 = 0.3528P.$$

Projecting these forces on the vertical and horizontal axes, we again obtain the values of R_0 and H_0 that we have already calculated.

In the preceding examples of frames, we used Eqs. (194) to (197) derived for unsymmetrical arches; but if a frame is symmetrical and symmetrically loaded, these conditions should be used to simplify our calculation. This simplification will be shown for the previously discussed example shown in Fig. 471. In this case we conclude from symmetry that the vertical components of the reactions at the supports A and B are equal to $P/2$. Hence $R_0 = P/2$, and we have only two unknowns M_0 and H_0. Considering the vertical reaction at A as an

external force, we obtain the system of forces shown in Fig. 473. The bending moments M' now become positive and are represented in the figure by the shaded triangle. The integrals (a) remain unchanged; and, instead of the integrals (b), we obtain

$$\int_A^B \frac{M'ds}{EI} = \frac{Pl^2}{8EI}, \qquad \int_A^B \frac{M'y_1 ds}{EI} = -\frac{Pl^3}{24EI}, \qquad \int_A^B \frac{M'x_1 ds}{EI} = 0.$$

Substituting these values in Eqs. (j) and (l) of the preceding article, we find

$$H_0 = \frac{P}{8}, \qquad M_0 - \frac{Pl}{4} = -\frac{\int_A^B \dfrac{M'ds}{EI}}{\int_A^B \dfrac{ds}{EI}} = -\frac{Pl}{24},$$

which agrees with our previous result.

FIG. 473.

FIG. 474.

If the moment of inertia I of the members of a frame is variable, we can reduce the problem to that of members with constant moments of inertia I_0 by using the modified moments $M'I_0/I$ and the modified length $ds I_0/I$ of the elements in calculating the integrals (a) and (b) and the coordinates of the elastic center.

The theory developed in the preceding article can be used also in the analysis of rings. A ring, on which a system of known forces P_1, P_2, P_3 (Fig. 474) is acting, represents a structure with three redundant forces. We can take as the statically indeterminate quantities the axial force, the shearing force, and the bending moment at any cross section A of the ring. Then we assume that the ring is cut at this cross section and that an absolutely rigid bar AO is attached to the end A, while the end B is fixed as shown in Fig. 474. Assuming that the fictitious masses are

intensity $1/EI$ are distributed along the center line of the ring, we determine their center O by using Eqs. (192) and (193). Now, proceeding as before, we replace the forces acting on the cross section A by the statically equivalent system of forces applied to the bar AO at the elastic center O. Taking the forces X_0 and Y_0 in the directions of the principal axes of the fictitious mass system, we shall determine these forces and the moment M_0 from Eqs. (194) to (197). The integrals occurring in these equations in the simpler cases can be rigorously evaluated. In more complicated cases, the integrations will be replaced by summations as explained in Art. 78.
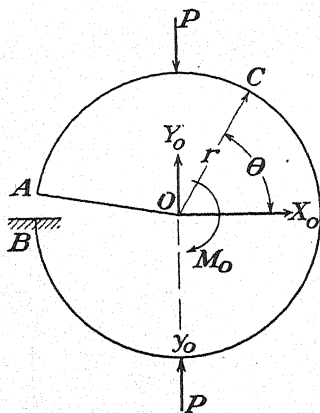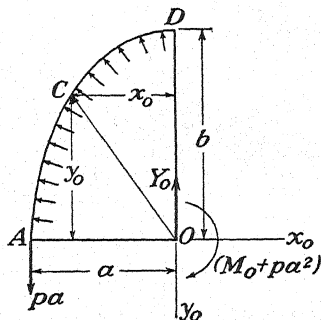
FIG. 475.   FIG. 476.

Let us consider as an example a circular ring of uniform cross section loaded by two equal and opposite forces acting along the vertical diameter (Fig. 475). From symmetry we conclude that in this case the elastic center O coincides with the center of the circle, and for the principal axes we can take any pair of perpendicular axes passing through O. Taking x_0 horizontal, we conclude, from symmetry, that $X_0 = 0$, $Y_0 = P/2$. For calculating M_0, we use Eq. (196). Since EI is constant, it cancels out, and the required integrals are

$$\int_0^{s_b} ds = 2\pi r, \qquad \int_0^{s_b} M' ds = -2 \int_0^{\frac{\pi}{2}} Pr^2 \cos\theta \, d\theta = -2Pr^2.$$

Hence

$$M_0 = \frac{Pr}{\pi} \quad \text{and} \quad M_a = \frac{Pr}{\pi} - \frac{Pr}{2} = -Pr\left(\frac{1}{2} - \frac{1}{\pi}\right).$$

For a ring of any shape and of uniform cross section, Eqs. (194) to (196) can be put in the following simplified form:

$$X_0 = -\frac{\int_0^{s_b} M'y_0\,ds}{\int_0^{s_b} y_0{}^2\,ds}, \qquad Y_0 = -\frac{\int_0^{s_b} M'x_0\,ds}{\int_0^{s_b} x_0{}^2\,ds}, \qquad M_0 = -\frac{\int_0^{s_b} M'\,ds}{\int_0^{s_b} ds}.$$

$$(200)$$

where s_b is the length of the center line of the ring.

We see that only the numerators in these equations depend on the forces applied to the ring. The denominators are independent of the load and represent the moments of inertia of the center line of the ring with respect to the principal axes x_0, y_0 and the length of the center line s_b. If the ring has two axes of symmetry, the axes x_0 and y_0 coincide with the axes of symmetry and the use of Eqs. (200) becomes especially simple.

Take as an example the case of an elliptical ring of uniform cross section submitted to the action of uniform internal pressure p. One-quarter of this ring is shown in Fig. 476. The elastic center coincides with the center of the ellipse, and the axes x_0 and y_0 are the axes of symmetry. From symmetry we conclude that $X_0 = 0$, $Y_0 = -pa$, and we have only one unknown M_0, which will be calculated from the last of Eqs. (200). To utilize the condition of symmetry, we proceed as was explained in the case of the frame shown in Fig. 473. We move the force Y_0 to point A and consider it as an external force. Then, instead of M_0, we shall have $M_0 + pa^2$ as shown in Fig. 476. The moment M' at any point C is then

$$M' = \frac{p}{2}(x_0{}^2 + y_0{}^2 - a^2),$$

and from the last of Eqs. (200) we obtain

$$M_0 + pa^2 = -\frac{\int_0^{s_b} M'\,ds}{s_b} = \frac{pa^2}{2} - \frac{p}{2s_b}(I_{x_0} + I_{y_0}), \qquad (c)$$

where s_b is the length and $I_{x_0} + I_{y_0}$ is the polar moment of inertia of the ellipse. Putting these quantities in the forms

$$s_b = \alpha b, \qquad I_{x_0} + I_{y_0} = \beta a^2 b,$$

we give in Table XXVIII the values of α and β for several values of a/b.

TABLE XXVIII.—VALUES OF α AND β FOR VARIOUS PROPORTIONS OF AN ELLIPSE

$a/b =$	1	0.9	0.8	0.7	0.6	0.5	0.4	0.3
$\alpha =$	2π	5.97	5.67	5.38	5.11	4.85	4.60	4.39
$\beta =$	2π	6.65	7.18	7.93	9.09	10.94	14.24	21.51

Using these numerical values, we readily calculate the bending moment at cross section A from Eq. (c).

If the center line of a ring is given graphically, we divide it into small portions and calculate for the center of each portion the values under the integral signs in Eqs. (200) by taking all the necessary information from the figure. Using summations, instead of integrations, we then obtain the required redundant quantities.
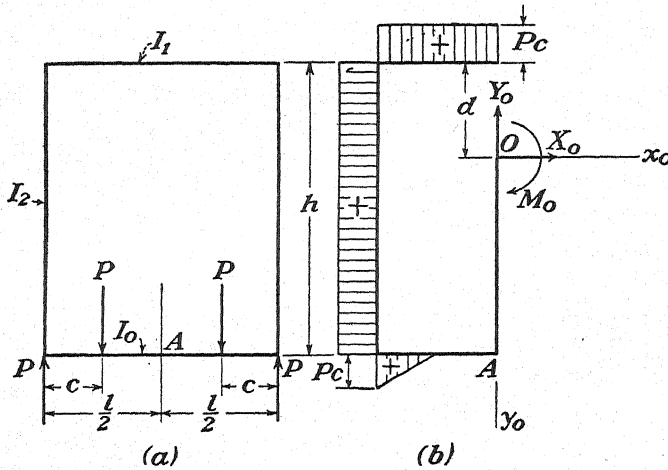
FIG. 477.

Let us consider now a symmetrical rectangular frame shown in Fig. 477a. We take for the redundant quantities the forces acting at cross section A. The elastic center O will be on the axis of symmetry at a distance d from the top of the frame. Using the notations

$$\frac{I_0}{I_1} = \alpha, \qquad \frac{I_0}{I_2} = \beta, \tag{d}$$

we find, from Eq. (193),

$$d = \frac{lh + \beta h^2}{l(1 + \alpha) + 2\beta h}. \tag{e}$$

The bending moments M' are shown in Fig. 477b.* From symmetry we conclude that $Y_0 = 0$, and we have remaining only two unknowns M_0 and X_0. From Eq. (196) we find

$$M_0 = -P \frac{c^2 + 2\beta ch + \alpha cl}{l(1 + \alpha) + 2\beta h}. \tag{f}$$

Equation (194) gives

---

* We continue to use, for the moments, the sign rule assumed for curved bars and take the moment positive if it produces tension on the inside.

$$X_0 = -\frac{\displaystyle\int_0^{s_1} \frac{M' y_0 ds}{I}}{\displaystyle\int_0^{s_1} \frac{y_0^2 ds}{I}} = P\,\frac{\alpha c\, ld - \beta ch(h - 2d) - c^2(h - d)}{l(h - d)^2 + \frac{1}{2}\beta(h - 2d)^2 + \frac{1}{6}\beta h^3 + \alpha l d^2}. \quad (g)$$

Take, for example, a square frame of uniform cross section. Then $\alpha = \beta = 1$, $h = l$, and we obtain

$$d = \frac{l}{2},$$

$$M_0 = -\frac{P}{4l}(c^2 + 2ch + cl),$$

$$X_0 = \frac{3}{4}P\,\frac{c(l - c)}{l^2}.$$

The tensile force at cross section A is equal to X_0, and the bending moment at that cross section is

$$M_a = \frac{X_0 l}{2} + M_0.$$

From the examples discussed, it will be appreciated that Eqs. (194) to (196) derived for nonsymmetrical arches also can be used to advantage in analyzing frames and rings.

INDEX